TRANSACTIONS

OF THE

AMERICAN INSTITUTE OF MINING AND METALLURGICAL ENGINEERS

(INCORPORATED)

Volume 154

IRON AND STEEL DIVISION
1943

Notice

This volume is the sixteenth of a series containing papers and discussions presented before the Iron and Steel Division of the American Institute of Mining and Metallurgical Engineers since its organization in 1928; one volume each year, as follows:

1928, Iron and Steel Technology in 1928 (later listed as Volume 80 of the TRANSACTIONS); 1929 (vol. 84), 1930 (vol. 90), 1931 (vol. 95), 1932 (vol. 100), 1933, 1934, 1935, 1936, 1937, 1938, 1939, 1940, 1941, 1942 and 1943, TRANSACTIONS of the American Institute of Mining and Metallurgical Engineers, Iron and Steel Division.

This volume contains papers and discussions presented at the meetings at Cincinnati, April 16–17, 1942; Cleveland, Oct. 12–14, 1942 and New York, Feb. 15–18, 1943.

Papers on iron and steel subjects published by the Institute prior to 1928 are to be found in many volumes of the TRANSACTIONS of the Institute; in Vols. 37 to 45, inclusive; 47, 50 and 51, 53, 56, 58, 62, 67 to 71, inclusive; 73 and 75. Vol. 67 was devoted exclusively to iron and steel.

Iron and steel papers published in the TRANSACTIONS before the year 1936 may be found by consulting the general indexes to Vols. 1 to 35 (1871–1904), Vols. 36 to 55 (1905–1916), Vols. 56 to 72 (1917–1925), and Vols. 73 to 117 (1926–1935).

FOREWORD

VOLUME 154 of the TRANSACTIONS is the sixteenth containing the publications of the Iron and Steel Division. It is made up of papers presented at the meetings of this Division following the annual meeting of 1942 and including the annual meeting of 1943.

It is perhaps worthy of comment that of the twenty-nine papers collected here, no less than nine are classified as dealing with the blast furnace and its raw materials, and two others, including the Howe Memorial Lecture by L. F. Reinartz, have to do in part with this field of metallurgy. This proportion is noticeably higher than it has been in recent years, which is not inappropriate, in view of the high iron charges employed in wartime steelmaking. Investigations of importance are reported in the papers in this classification, and that by Carl Hogberg should also be of interest because of its agreeably unorthodox approach to a difficult problem.

Under the remaining classifications are to be found contributions of value to workers in many fields. The Howe Memorial Lecture and the paper by W. C. Marshall and F. G. Norris are of more than usual importance to those who must consider the steelmaking process as an integrated whole, while those of more specific interests will appreciate the careful investigations to be found under the headings of Constitution and Thermal Treatment, and Properties, such, for example, as that of G. A. Roberts and R. F. Mehl on the austenite-pearlite reaction.

As is usual, the proceedings of the Division's Open Hearth and Blast Furnace Conferences are published as separate reports.

H. W. GRAHAM, *Chairman*,
Iron and Steel Division.

PITTSBURGH, PA.
October 11, 1943.

A.I.M.E. OFFICERS AND DIRECTORS

For the year ending February 1944

PRESIDENT AND DIRECTOR
C. H. MATHEWSON, New Haven, Conn.

PAST PRESIDENTS AND DIRECTORS
JOHN R. SUMAN, Houston, Texas
EUGENE McAULIFFE, Omaha, Nebraska

TREASURER AND DIRECTOR
H. T. HAMILTON, New York, N. Y.

VICE-PRESIDENTS AND DIRECTORS

ERLE V. DAVELER, New York, N. Y.
CHESTER A. FULTON, New York, N. Y.
PAUL D. MERICA, New York, N. Y.

HARVEY S. MUDD, Los Angeles, Calif.
LEROY SALSICH, Duluth, Minn.
L. E. YOUNG, Pittsburgh, Pa.

DIRECTORS

HOLCOMBE J. BROWN, Boston, Mass.
CHARLES CAMSELL, Ottawa, Ont., Canada
J. TERRY DUCE, San Francisco, Calif.
C. A. GARNER, Jeddo, Pa.
WILLIAM B. HEROY, Washington, D. C.
CHARLES H. HERTY, JR., Bethlehem, Pa.
O. H. JOHNSON, Denver, Colo.
IRA B. JORALEMON, San Francisco, Calif.

WILBER JUDSON, New York, N. Y.
RUSSELL B. PAUL, New York, N. Y.
LEO F. REINARTZ, Middletown, Ohio
FRANCIS A. THOMSON, Butte, Mont.
J. R. VAN PELT, JR., Chicago, Ill.
H. Y. WALKER, New York, N. Y.
F. A. WARDLAW, JR., Salt Lake City, Utah
CLYDE E. WILLIAMS, Columbus, Ohio

FELIX E. WORMSER, New York, N. Y.

SECRETARY
A. B. PARSONS, New York, N. Y.

DIVISION CHAIRMEN—Acting as Advisers to the Board

CYRIL STANLEY SMITH (Institute of Metals), Waterbury, Conn.
C. A. WARNER (Petroleum), Houston, Texas
HERBERT W. GRAHAM (Iron and Steel), Pittsburgh, Pa.
CADWALLADER EVANS, JR. (Coal), Scranton, Pa.
A. F. GREAVES-WALKER (Education), Washington, D. C.
HOWARD I. SMITH (Industrial Minerals), Washington, D. C.

STAFF IN NEW YORK

Assistant Secretaries
EDWARD H. ROBIE
CHESTER NARAMORE
FRANK T. SISCO
Assistant Treasurer
H. A. MALONEY

Assistant to the Secretary
E. J. KENNEDY, JR.

Business Manager
"Mining and Metallurgy"
WHEELER SPACKMAN

4

CONTENTS

Howe Memorial Lecture

Blast Furnace and Raw Materials

Steelmaking

Constitution and Thermal Treatment

Properties

The Howe Memorial Lecture

THE Howe Memorial Lecture was authorized in April 1923, in memory of Henry Marion Howe, as an annual address to be delivered by invitation under the auspices of the Institute by an individual of recognized and outstanding attainment in the science and practice of iron and steel metallurgy or metallography, chosen by the Board of Directors upon recommendation of the Iron and Steel Division.

So far, only American metallurgists have been invited to deliver the Howe lecture. It is believed that this lecture would gain in importance and significance were it possible to include metallurgists from other countries, but the Institute has not yet been able to do this on account of lack of special funds to support this lectureship.

The titles of the lectures and the lecturers are as follows:

1924 What is Steel? By Albert Sauveur.
1925 Austenite and Austenitic Steels. By John A. Mathews.
1926 Twenty-five Years of Metallography. By William Campbell.
1927 Alloy Steels. By Bradley Stoughton.
1928 Significance of the Simple Steel Analysis. By Henry D. Hibbard.
1929 Studies of Hadfield's Manganese Steel with the High-power Microscope. By John Howe Hall.
1930 The Future of the American Iron and Steel Industry. By Zay Jeffries.
1931 On the Art of Metallography. By Francis F. Lucas.
1932 On the Rates of Reactions in Solid Steel. By Edgar C. Bain.
1933 Steelmaking Processes. By George B. Waterhouse.
1934 The Corrosion Problem with Respect to Iron and Steel. By Frank N. Speller.
1935 Problems of Steel Melting. By Earl C. Smith.
1936 Correlation between Metallography and Mechanical Testing. By H. F. Moore.
1937 Progress in Improvement of Cast Iron and Use of Alloys in Iron. By Paul D. Merica.
1938 On the Allotropy of Stainless Steels. By Frederick Mark Becket.
1939 Some Things We Don't Know about the Creep of Metals. By H. W. Gillett.
1940 Slag Control. By C. H. Herty, Jr.
1941 Some Complexities of Impact Strength. By Alfred V. de Forest.
1942 Time as a Factor in the Making and Treating of Steel. By John Johnston.
1943 The Development of Research and Quality Control in the Modern Steel Plant. By Leo F. Reinartz.

IRON AND STEEL DIVISION

Established as a Division February 22, 1928

(Bylaws published in the 1939 TRANSACTIONS Volume of the Division)

Officers and Committees for Year ending February 1944

HERBERT W. GRAHAM, Chairman, Pittsburgh, Pa.

E. C. SMITH, Past-Chairman, Cleveland, Ohio

JOHN CHIPMAN, Vice-Chairman, Cambridge, Mass.

E. G. HILL, Vice-Chairman, Gary, Ind.

A. P. MILLER, Vice-Chairman, East Chicago, Ind.

F. T. SISCO, *Secretary*, 29 W. 39th St., New York, N.Y.

Past Chairmen

RALPH H. SWEETSER, 1928	JOHN JOHNSTON, 1933	J. T. MacKENZIE, 1938
G. B. WATERHOUSE, 1929	L. F. REINARTZ, 1934	J. HUNTER NEAD, 1939
W. J. MacKENZIE, 1930	A. B. KINZEL, 1935	FRANK T. SISCO, 1940
F. M. BECKET, 1931	C. E. WILLIAMS, 1936	C. H. HERTY, JR., 1941
F. N. SPELLER, 1932	FRANCIS B. FOLEY, 1937	E. C. SMITH, 1942

Executive Committee

1944	1945
A. L. BOEGEHOLD, Detroit, Mich.	C. E. MacQUIGG, Columbus, Ohio
W. E. BREWSTER, Chicago, Ill.	GILBERT SOLER, Canton, Ohio
JOSEPH WINLOCK, Philadelphia, Pa.	T. S. WASHBURN, Indiana Harbor, Ind.

1946

WALTER CRAFTS, Niagara Falls, N. Y.

C. D. KING, Pittsburgh, Pa.

W. J. REAGAN, Warren, Ohio

Blast Furnace and Raw Materials

J. C. MURRAY, *Chairman*
M. C. MORGAN, *Vice-Chairman*
F. B. CRONK, *Vice-Chairman*
CARL G. HOGBERG, *Secretary*

A. J. BOYNTON	C. D. KING
O. E. CLARK	R. A. LINDGREN
D. F. DOLAN	H. E. MCDONNELL
P. G. HARRISON	J. H. SLATER
W. A. HAVEN	G. E. STEUDEL
H. W. JOHNSON	H. A. STRAIN
T. L. JOSEPH	B. M. STUBBLEFIELD
C. L. WYMAN	

Open-hearth Steel

L. F. REINARTZ, *Chairman*
A. P. MILLER, *Vice-Chairman*
FRANK T. SISCO, *Secretary*

GEORGE S. BALDWIN	W. J. REAGAN
R. K. CLIFFORD	A. E. REINHARD
C. R. FONDERSMITH	E. A. SCHWARTZ
R. C. GOOD	C. E. SIMS
H. M. GRIFFITHS	GILBERT SOLER
C. H. HERTY, JR.	A. H. SOMMER
E. G. HILL	FRANCIS L. TOY
WILLIAM C. KITTO	DON N. WATKINS
L. A. LAMBING	T. T. WATSON
E. L. RAMSEY	M. F. YAROTSKY

Bessemer Steel

GORDON M. YOCOM, *Chairman*

H. M. BANTA	W. J. REAGAN
J. D. GOLD	G. A. REINHARDT
H. W. GRAHAM	E. C. SMITH
C. D. KING	L. B. THOMAS
R. E. PENROD	G. B. WATERHOUSE

Electric Furnace Steel

HARRY W. MCQUAID, *Chairman*
W. J. REAGAN, *Vice-Chairman*
H. A. SCHWARTZ, *Vice-Chairman*
FRANK T. SISCO, *Secretary*

C. W. BRIGGS	J. T. MACKENZIE
T. H. BURKE	H. E. PHELPS
W. M. FARNSWORTH	T. S. QUINN
C. A. SCHARSCHU	

Physical Chemistry of Steelmaking

T. S. WASHBURN, *Chairman*
KARL L. FETTERS, *Secretary*

R. S. ARCHER	A. E. MARTIN
H. M. BANTA	F. G. NORRIS
JOHN CHIPMAN	W. O. PHILBROOK
L. S. DARKEN	G. L. PLIMPTON, JR.
J. W. HALLEY	L. F. REINARTZ
C. H. HERTY, JR.	C. E. SIMS
E. R. JETTE	GILBERT SOLER
T. L. JOSEPH	R. B. SOSMAN
R. L. KULP	M. TENENBAUM
B. M. LARSEN	F. M. WASHBURN
J. S. MARSH	H. J. WIEGEL
H. K. WORK	

Alloy Steel

J. L. GREGG, *Chairman*

R. S. ARCHER	C. H. LORIG
G. R. BROPHY	R. M. PARKE
J. P. GILL	R. W. ROUSH
C. D. KING	JEROME STRAUSS
A. B. KINZEL	F. M. WASHBURN

Cast Ferrous Metals

HARRY A. SCHWARTZ, *Chairman*

J. W. BOLTON	R. F. HARRINGTON
H. BORNSTEIN	J. T. MACKENZIE
ROY A. GEZELIUS	S. C. MASSARI
JOHN HOWE HALL	E. K. SMITH

Metallography and Heat Treatment

G. R. BROPHY, *Chairman*

E. C. BAIN	MERRILL A. SCHEIL
C. Y. CLAYTON	DURAY SMITH
R. L. DOWDELL	A. M. STEEVER
A. J. HERZIG	W. P. SYKES
V. T. MALCOLM	A. B. WILDER

Membership

R. L. BALDWIN, *Chairman*

W. E. BREWSTER	T. L. JOSEPH
R. M. GARRISON	W. JOHN KING
J. L. GREGG	E. C. MILLER
E. G. HILL	R. M. PARKE
J. E. JACOBS	H. S. RAWDON
W. E. JEWELL	W. J. REAGAN
C. E. SIMS	

Mining and Metallurgy

A. B. KINZEL, *Chairman*

R. H. ABORN	T. S. FULLER
R. E. CROCKETT	G. M. YOCOM

Howe Memorial Lecture

H. W. GRAHAM, *Chairman*

E. C. BAIN	C. H. HERTY, JR.
A. V. DEFOREST	JOHN HOWE HALL

Robert W. Hunt Medal and Prize

H. W. GRAHAM, *Chairman*

E. S. DAVENPORT	J. HUNTER NEAD
F. B. FOLEY	C. E. WILLIAMS

J. E. Johnson, Jr. Award

B. J. HARLAN, *Chairman*

O. E. CLARK	P. V. MARTIN
T. L. JOSEPH	F. M. RICH

Programs

KARL L. FETTERS, *Chairman*

MORRIS COHEN	W. JOHN KING
H. B. EMERICK	C. H. LORIG
R. C. GOOD	J. S. MARSH

GILBERT SOLER

Publications

ERIC R. JETTE, *Chairman*

L. S. BERGEN	E. S. DAVENPORT
EARNSHAW COOK	JAMES L. GREGG

CARL M. LOEB, JR.

Nominating

E. C. SMITH, *Chairman*

JOHN JOHNSTON	J. T. MACKENZIE
A. B. KINZEL	J. HUNTER NEAD
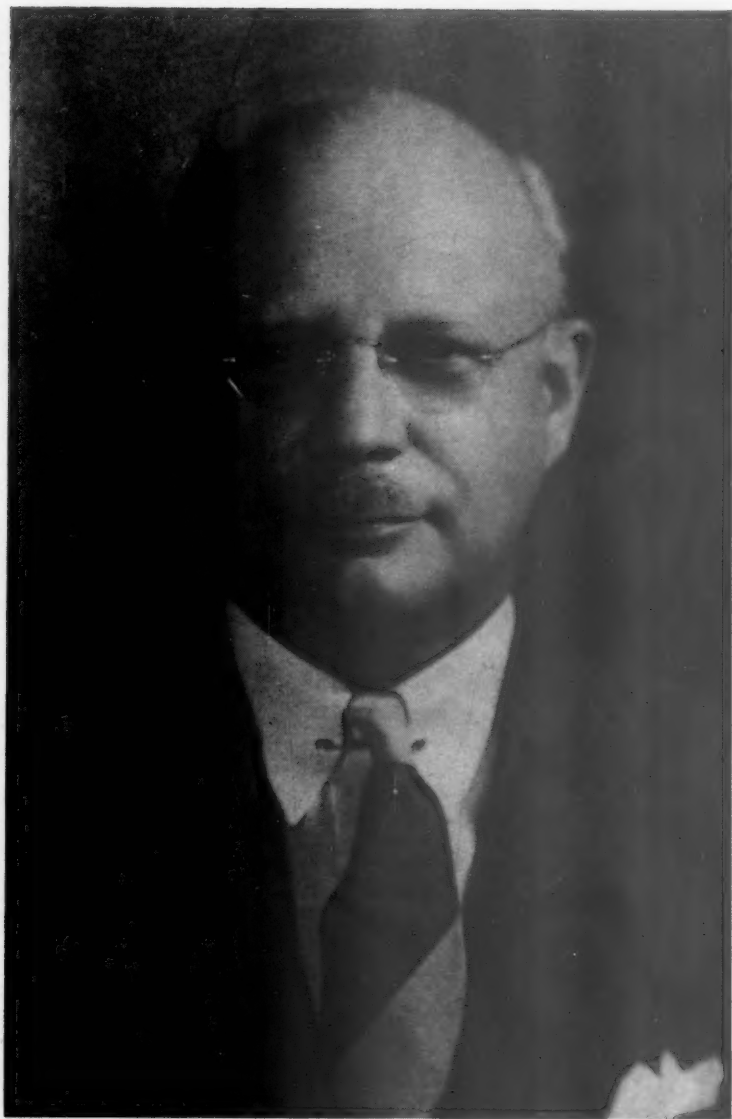
LEO F. REINARTZ
Henry Marion Howe Memorial Lecturer, 1943

The Development of Research and Quality Control in the Modern Steel Plant

By Leo F. Reinartz,* Member A.I.M.E.

The influence of a great man, be he philosopher or scientist, is beyond description.

Anon.

It was with humility that I accepted the invitation of the Board of Directors of our Institute to deliver the Twentieth Howe Memorial Lecture. Many previous lecturers could speak from personal experience of the great work done by Professor Howe. It was not my privilege to be one of his students but, indirectly, I came under the influence of his work many years ago. My mentor in Metallurgy at Carnegie Institute of Technology, Prof. Fred Crabtree, was an ardent admirer of Professor Howe and his work.

Professor Crabtree taught me early to appreciate Professor Howe's love of truth and keen desire to find a scientific reason for every metallurgical phenomenon. In this early search, Professor Howe encountered many unexplainable facts. Nevertheless, in the classic text, "The Metallurgy of Steel," published in 1891, he indicated that he believed Research could light the way.

Under the heading of "The Treachery of Steel" he said: "In the early use of Bessemer and Open Hearth Steel, many then unexplained and hence mysterious failures occurred. With our present knowledge, an easy explanation of most of them would probably have been seen. But even today certain unexplained and apparently inexpli-

cable failures occur in steel; inexplicable in spite of full and intelligent investigation."

Then Professor Howe continued to talk about "the trustworthiness of steel" in the following manner:

First, the steel-maker has learned by experience. He knows today far better the effects of a high percentage of carbon or of phosphorus; of cracks, pipes and blow-holes; of segregation and imperfect mixing; of over-heating; of finishing too hot or too cold. Knowing, he guards against them more effectually, and keeps *at home* much steel that he would formerly have sent into the market. Those who *would not*, or *could not learn* and *do*, have been driven out of the business; the conditions necessary for producing good sound steel by the acid Bessemer and the acid Open Hearth processes have been mastered.

By and by, the basic process came along with new conditions, new liabilities to unsoundness, a great hue and cry about mysterious fractures followed, and Lloyd's register provisionally forbade the use of basic steel. Much basic steel was irregular and brittle throughout; too much carbon, too much phosphorus, too cold teemings—imperfect mixing. Still there was little doubt that, with further experience, these difficulties of the basic process would be mastered as those of the acid process had been.

This shows that Professor Howe could not take anything for granted. Believing that careful research would find the answer to all mysterious phenomena, he was several generations ahead of the practical acceptance and adoption of this principle.

In the 1931 Howe Lecture, Francis F. Lucas said: "Professor Howe believed in controlling and regulating causes so as to produce specific effects, useful in serving mankind."

This definition indicates that Professor Howe was looking forward to the time when careful control of all factors in the manufacture of steel would produce products of such excellence that the lot of mankind would be improved.

Quality Control Ultimate Aim

A Chinese philosopher once said: "No theory has any value except in so far as it is translated into action."

Quality production is the ultimate aim of every progressive organization. Therefore, scientific methods must be used in such quality control because the "rule of thumb" or trial and error method is too slow and expensive for modern conditions.

Years ago, because of insufficient data as well as lack of care in compiling and correlating the results of experimental work, much time and effort were expended in useless repetitive work. Science must know not only that a certain thing is true, but must know why; otherwise, we do our experiments over and over again.

A research or operating steel-plant engineer must first realize his own lack of knowledge and, like a lawyer, study his problem so thoroughly that he is acquainted with every minute phase of the situation. Recently, I heard a successful lawyer say, "I check and recheck the evidence in every case to be sure I have not missed a single clue."

The scientific approach to a practical problem is one that pays attention to details that have been overlooked by the ordinary investigator, because the answer may often be found in some insignificant fact.

John Howe Hall, in the 1929 Howe lecture, while paying tribute to Professor Howe, indicated that "Henry Howe was a hard but fair taskmaster." He commented on Professor Howe's patient, never-failing attention to detail and accuracy of observation.

Recently I read this definition of practical quality control:

By positive control of quality is meant that form of management or direction which establishes the quality requirements, then sets up the organization, and selects the personnel capable of securing that quality. By continuous control of quality is meant the vigilant maintenance and direction of organization and personal set-up to make that control positive.

Love for, and almost fanatical zeal for quality by Management must precede any plant quality-control efforts. It has been said, "What we love, we do best."

Approach to Quality

In steel manufacture the engineer and operator must be sure of their facts. They must study and check all available data to be reasonably certain conclusions drawn from such facts are sound.

The manager of a steel plant must make a scientific and technical approach to the quality problem. He must also be keenly interested in the effect any given practice, be it quality or quantity control, may have on the customer, the stockholder, or the employee.

Striving for uniformity is very essential in the steel industry. In the mechanical world interchangeability and replacement of parts, as well as preventive maintenance, have been found to be valuable developments in helping to maintain continuity of operations. In steel-mill operations, it is also essential to control practices so that, in making heat after heat in metallurgical furnaces, the identical quality will be forthcoming. Modern metallurgy has been predicated on controls that will accomplish such results. Only by such controls could

the uniformity and quality of deep-drawing automobile steels have been assured.

IMAGINATION A FACTOR

The development and control of quality in steel manufacture has given the operator and engineer an opportunity to use their imaginations. Too often our practical men are willing to let well enough alone. Lord Beaconsfield described a practical man as: "One who practices the errors of his forefathers." *How often in the every day work in an industrial plant have we found that to be true.* It takes patient, constructive planning, and some ingenuity to win such an individual over to the proper approach to a practical problem so that an intelligent answer may be found.

In steel-mill quality control, the steps to be taken are:

1. *Get all the facts.*
2. *Keep accurate records.*
3. *Analyze them.*
4. *Check against previously set standards of procedure.*

The metallurgical engineer and practical operator must constantly strive, in these war times, to break "bottlenecks" and overcome obstacles and handicaps. These may be raw materials, equipment, or practices. All must be coordinated so that none interferes with the requirements of uniformity of operations, which has such a controlling influence on quality.

Shop arrangements and layouts must be studied because they may affect quality. Production engineers are called into consultation to assist in relocating equipment and machines to improve control of operations. We must remember that practice makes perfect. It is one thing to set a standard, and another thing to adapt it to actual practice in a steel plant. The training of intelligent workers in standard operations is an essential part of quality control, and cannot be accomplished in a few days or weeks. It can be attained only by painstaking, careful, and intensive teaching by technical, trained men.

QUALITY IN THE EARLY DAYS

During the early years of the twentieth century, a great many large steel corporations were organized. The drive for large tonnage output in the Bessemer and new open-hearth plants was on. Profits were high and enormous personal fortunes were made, and little attention was paid to the development of real quality controls in steel plants. Operations were in charge of practical steelmen who had very little knowledge of quality control, and who had little use for any ideas that might, in any way, affect large tonnage production.

Large steel corporations, despite careless and costly practices, could make satisfactory profits, whereas smaller concerns in the industry were not so fortunate. As time went on, owing to increasing and cutthroat competition, the managements of a number of such small concerns independently made up their minds that if their plants were to continue operations and make a profit they would have to enter into the manufacture of steels for special requirements. In changing over to such practice it was their hope that the spread between cost and selling price would be greater than for commodity steels.

Because of the higher cost, as well as special care and attention required in the manufacture of such specialty steels, the managements of companies operating on the basis of a large ingot tonnage had no desire to enter these fields.

SPECIALTY STEELS BROUGHT NEW KNOWLEDGE

The managements of companies making specialty steels early learned a great secret. Quality control was the starting point for economical and profitable operations. As time has gone on the entire steel industry has gradually learned that research and control are essential. Uni-

formity, which is secured through detailed exact quality control, is absolutely necessary to meet the exacting requirements of the present day. This is particularly true in the manufacture of steel, which requires accuracy and perfection in gauge, surface, physical and chemical constitution, as well as, in many cases, definite grain size and good internal structure.

In the early efforts of the managements of these small specialty companies to make new types of steel, it was discovered that many operating and technical problems faced them, not only in open-hearth practices but also in the rolling and processing of such steels.

As control studies proceeded and data began to accumulate, it became evident that the quality of raw materials, equipment, refractories and operations each had a vital bearing on results. Such problems could not be solved overnight. Now, no one in responsible charge of steel manufacture would question the vital need for uniformity and quality control.

GROWTH OF RESEARCH WORK

There is no steel company of any importance today that does not pay allegiance and homage to the need for research. Some companies spend large sums of money for pure research; others carry on such research by subsidizing independent research laboratories to work on definite problems; while still others combine the theoretical with the practical and carry on research investigations in special laboratories away from the operating plants. These companies then follow up with practical tests on a large scale in the operating departments.

Research and operating metallurgists and practical steelmen work together to develop new steels out of abstract metallurgical theories. In other words, the large modern plant becomes the laboratory for major experiments in metallurgy. Here, again, the managements that have built

small open-hearth or electric furnaces have been able to make greater experimental progress than the plants where original tests have had to be made in open-hearth furnaces of 150 to 200 tons capacity.

The management of the American Rolling Mill Co. more than 35 years ago began to realize that control of metallurgical processes in the plant alone was not the entire answer. Control could stabilize and standardize operations and quality, as it then existed, but without research work to improve the quality the steel industry would not keep pace with the expanding needs of a growing market. Armco, therefore, began to build up a Research Department, manned by scientific and technical men, to study ways and means to improve steel quality from a melting, processing, and metallurgical standpoint. A very definite decision was reached at an early date to carry on such research functions entirely apart from the plant metallurgical and operating functions, but to cooperate and collaborate very closely with them in their mutual problems.

Originally the research laboratory occupied a few rooms in the main plant offices and the plant chemical laboratory (Fig. 1). Research work increased by leaps and bounds. In 1912 a new two-story brick building was erected (Fig. 2). It was completely destroyed in 1935 by an explosion of unknown origin. This was a blessing in disguise, as the company then authorized the building of a modern research laboratory, which was dedicated in 1939 (Fig. 3).

This laboratory is really a combination of at least 12 laboratories, all adequately staffed and equipped to carry on scientific and practical research work in their respective fields (Figs. 4 to 7). Such experimental work includes delving into past practices of the industry; outside and home plant visitations and consultations; consultations with customers or prospective customers regarding their requirements, and very extensive laboratory research
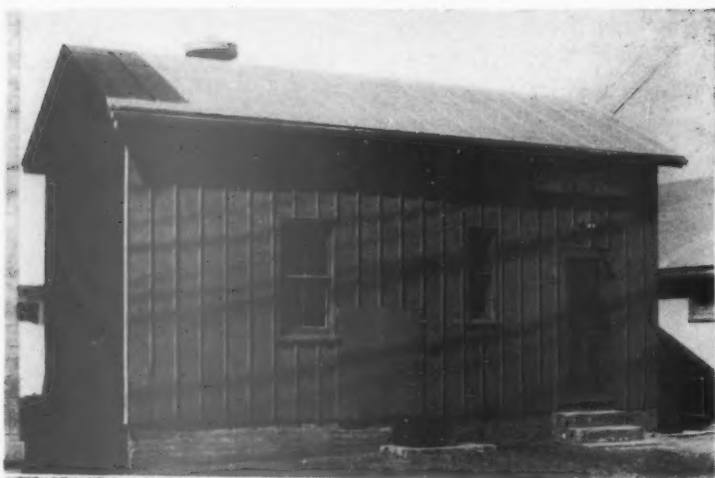
FIGS. 1-3.—RESEARCH LABORATORIES, AMERICAN ROLLING MILL COMPANY.
1, first laboratory; 2, laboratory built in 1912; 3, modern laboratory.

work. In many instances this work starts with the manufacture of the steel. A group of small electric furnaces, including a 40-lb. electric high-frequency induction furnace, are available in the research laboratories for such preliminary work.

TESTS ON PLANT SCALE

After the successful completion of the research phase of the work, the research metallurgists arrange with the operating management of the company to try out their theories on a modified plant scale. Experiments that are to be made jointly by research and operating men are authorized to be carried on in the plant in two 200-lb. electric induction furnaces. If these tests prove favorable, further heats are made in the 500-lb. furnace (Fig. 7) the 10-ton electric-arc furnace, or in the 10-ton open-hearth furnace. The heats in the larger electric furnaces or the small open-hearth furnace are poured into standard-size molds, so that the ingots can be rolled on modern 80-in. slabbing and hot strip mills.

If the results obtained prove promising, the research and operating metallurgists and the plant management make a joint recommendation to the General Management to proceed with the manufacture of one or more heats in 175-ton open-hearth furnaces. Such experimental work on a new grade, of course, means very close collaboration with the sales division, so that trial may be made in customers' plants. If the experimental steel proves to have commercial merit, its manufacture is then authorized by the management.

Research engineers continue to assist the operating divisions in perfecting their practices until the plant management agrees to accept the responsibility for manufacture as a commercial grade. Then the operating metallurgical staff writes up standard manufacturing and processing practices for each operation in all operating departments involved, and its control section proceeds to establish and standardize the quality control all along the line of manufacture.
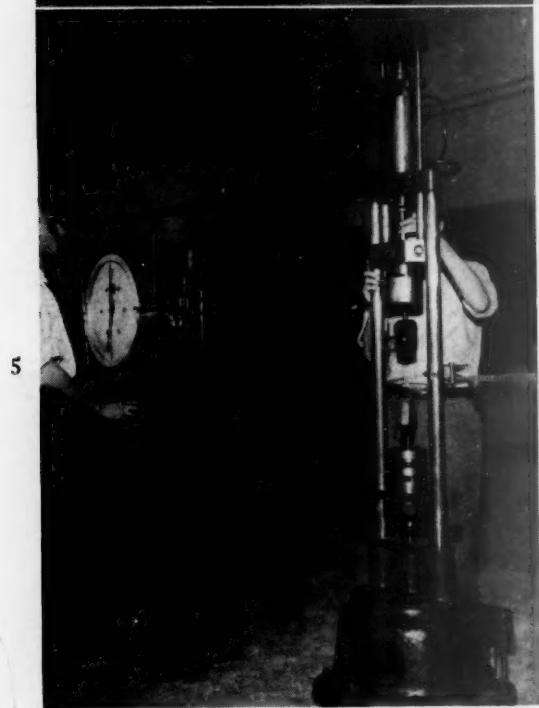
FIG. 4.—EXPERIMENTAL ENAMELING HEAT-TREATING FURNACE.
FIG. 5.—AMSLER TENSILE TESTING MACHINE.

In order to guarantee accuracy of results, the research laboratories make frequent checks of metallurgical testing equipment

and standards in all plant operations. Their chemists also control the accuracy of plant chemical determinations by routine check control of preliminary and final heat samples at *irregular* intervals. Many other companies—notably the Timken Roller Bearing Co., Canton, Ohio; The Allegheny-

FIG. 6.—EXPERIMENTAL COLD-REDUCTION MILL.
FIG. 7.—FIVE-HUNDRED-POUND ELECTRIC-ARC FURNACE.

Ludlum Steel Co., Brackenridge, Pa., and The United Alloy Co., now the Republic Steel Corporation, Canton, Ohio—have for many years carried on similar joint research and operating experimental work.

FIG. 8.—GOOD AND BAD METALLURGICAL COKE.

In recent years the Jones and Laughlin Co., Pittsburgh, Pa., has augmented its research facilities by the addition of a 5-ton experimental open-hearth furnace.

Today many manufacturers, technical men, and workmen are cooperating in improving the quality of modern steel. The quality that has made the products of our steel mills famous and efficient in the global conflict is the result of many years of painstaking search for better quality. It was also important during those hectic depression years from 1930 to 1935, when survival, particularly in the sheet-steel industry, depended on the production of quality steel sheets that showed virtually no rejections in the customers' blanking and forming operations.

CONTROL BY OPERATING DIVISION

Turning from the research angle, I am going to discuss those phases of quality control carried on mostly by the operating division of a company. During the early decades of the twentieth century, rich ores from the northern fields were plentiful and

comparatively little work was done in the classification of ores. About 15 years ago iron-mining companies found it necessary to work out plans together for producing more uniform ores, both chemically and physically, for blast-furnace practices. Accurate methods for mixing and analyzing ores were developed.

Ores from various deposits are blended at the American Rolling Mill plants for definite results in the blast furnaces. Attention must be paid to average silica, the phosphorus, the manganese, and the iron content of the ore, or mixture of ores.

mum delays. A correct mixture of high-volatile and low-volatile coals must be available to make a physically strong, but not too dense coke (Fig. 8). Control equipment must be available for accurately checking oven temperatures and gas analyses, as well as analysis of the resulting coke for shatter test, porosity, chemical constitution, and other qualities. At the metallurgical station the coke must be carefully screened and sized (Table 1).

Much depends on the cooperation of a loyal, intelligent working organization. The transportation department must be able to

TABLE 1.—*Coal and Coke Data for Record Month, August* 1942

Coal Mix	Moisture	Volatile Matter	Fixed Carbon	Ash	S	Wt. per Cu. Ft. Coal as Recd.	Percentage of Mixture
A.......................	5.0	36.6	57.4	6.0	0.88	50.3	27½
B.......................	3.0	34.6	59.9	5.5	0.72	53.0	27½
C.......................	4.0	35.0	60.2	4.8	0.72	50.0	25
D.......................	2.7	16.9	76.6	6.5	0.67	46.6	20
Mixed...................	3.7	31.7	62.6	5.7	0.75	43.8	100
Blast-furnace coke........	3.91	0.8	90.93	8.27	0.61	26.6	
Mixed coal..............	Pulverization: +½-in., 12.9 per cent, + ⅛-in., 13.6 per cent, − ⅛-in. = 73.5						

SCREEN TEST BLAST-FURNACE COKE, PER CENT

On 4 In.	On 3 In.	On 2 In.	Total on 2 In.	On 1½ In.	On 1¼ In.	On ⅞ In.	Through ⅞ In.
8	28.6	40.8	77.4	19.8	0.5	1.1	1.2

Particle size.............................	2.75	True specific gravity......................	1.83
Shatter test.............................	68.2	Degradation, per cent....................	15.2
Stability test............................	47.7	Cell space...............................	50.3
Apparent specific gravity.................	0.909		

In addition, in common with the practice of the steel industry, much time and effort of our plant engineers, working with the engineers of large construction companies and with the practical furnace operators, have been required to improve the designs of blast furnace and auxiliary equipment to ensure regularity of charging and the movement of the stock down through the furnace.

The coke plant plays an important and, we think, a controlling role in the maintenance of quality of pig iron or "hot metal." Quality coke results from proper design, and operation of the coke plant with mini-

move the large tonnages of materials to and from the coke plant and blast furnaces, and the maintenance men must have spares available to do preventive maintenance work and speed up repairs so as to minimize delays that are a serious handicap to metallurgical operations. It is self-evident that instruments must be accurately calibrated and charts must be intelligently interpreted by operators who must charge and operate the ovens and furnaces uniformly.

At the Armco Hamilton blast-furnace and coke plant, a joint Management and Employee (nonunion) War Production Committee was organized in March 1942.

Since then, seven consecutive monthly pig-iron tonnage records have been made in the two 650-ton blast furnaces. These results have been accomplished because of careful management planning, improved equipment, careful control of operations and practices by an enthusiastic organization.

GROWTH OF QUALITY CONTROL

Quality control in the open-hearth industry has had a slow and painful road to travel. In the early days, most open-hearth plants were operated on a rule-of-thumb basis. Prior to 1912, open-hearth furnaces were small, 25 to 35-ton solid-bottom basic-lined furnaces. Because of poor furnace design, poor refractories and silica brick, poor quality in the producer-gas fuel, and an untrained, unskilled personnel, many operating and metallurgical difficulties were encountered. Despite such handicaps as metal breakouts, lost heats, running stoppers, "cold" heats, roofs falling in prematurely, and scrap of very poor quality, two special grades of iron and steel were developed—ingot iron and Hadfield high-silicon steel.

About 1912, when research work was begun as a separate function, our company began the development of rimming steels for the automobile industry, which was still in its infancy.

In those days automobile manufacturers admitted they knew very little about the qualities or specifications they required in their sheet steel. The managements of several of these companies sent their metallurgists to steel plants to work with our management, embryo metallurgists, and operating men to try to develop the kind of sheets they needed.

NEW STRIP MILL

In 1926, Armco engineers announced a revolutionary new process for rolling iron and steel sheets. They designed and constructed the first successful continuous sheet-rolling mill—a notable page in the steel industry's book of research. This was the modest beginning of a revolution that led to the expenditure of hundreds of millions of dollars by the steel industry in the development of the amazing continuous hot and cold strip mills. The sheets and strips rolled on these mills are not only more accurate and uniform but have a denser, smoother surface to meet the more exacting and expanding requirements of the most dynamic industry of the twentieth century. This development was climaxed by the production of stabilized nonaging cold-rolled sheet steel in the years just prior to Pearl Harbor.

Since this momentous event, all energies and lessons learned in the manufacture of deep-drawing cold-rolled steels and other quality steels have been applied to the manufacture, for war purposes, of alloy and other steel sheets and plates having very exacting specifications. The lessons learned in the long school of experience have been helpful in obviating the many metallurgical mistakes of the first World War. Quality control has helped to put the manufacture of these new grades of steel on a practical basis within a period of three to six months.

EMPLOYMENT OF THE METALLURGIST

In the early days of the steel industry a new kind of investigator came into being to develop special grades of steel. He may have been a chemist assigned to the operating management to follow up some special tests; he may have been a man taken out of operations for a similar purpose; or he may have been a young college boy trained in the new way to be a so-called "metallurgist." No matter in which way these men were selected, they soon showed our management the benefits to be derived from special investigations. Such an investigator was assigned to each turn in the open-hearth department to observe and record everything that transpired in the charging, melting, refining, and casting of steel. At

Fig. 9.—QUALITY DATA SHEET, METALLURGICAL OPEN-HEARTH HEAT LOG.

first, this was limited to special heats, but later included all heats. This development was very slow. Quality-control data sheets are now used in all progressive steel plants

neers had to be enlisted in the job of designing and building furnaces that would rapidly melt pig iron or "hot metal" and steel scrap, and permit the furnaceman to
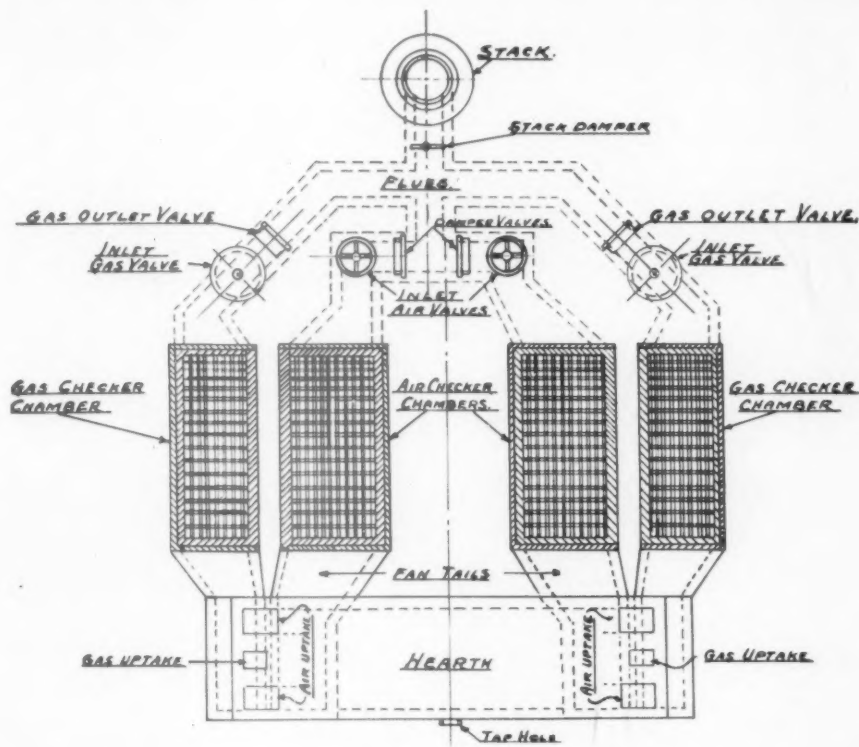
FIG. 10.—GENERAL ARRANGEMENT OF NATURAL-DRAFT OPEN-HEARTH FURNACE, 90 GROSS NET TONS, FIRED WITH PRODUCER GAS.

(Fig. 9). The control is so close that if there is a small deviation from the quality standard the place where the difficulty occurs can soon be determined by checking back over the records.

STANDARDIZATION INITIATED

As the idea of quality began to take root, it became increasingly evident that one of the paramount factors in such control was the standardization of conditions surrounding the manufacture, rolling and processing of steels. That has meant paying close attention to many details, especially in the open-hearth furnace and electric-furnace shops. It meant, in the first place, that just as in the blast-furnace practice, our engi-

control temperatures very closely during refining and tapping operations. This has taken many years and still is not completed. It has meant the improvement of furnace and auxiliary designs, improved refractory brick, better bottom-making materials, as well as a long, hard struggle to improve fuel-burning equipment and fuels themselves. Instruments have had to be developed for accurate control. Furnace hearths have been enlarged during the last 10 years at the Middletown works, so that the furnace would tap 180 net tons instead of 90 net tons—the original capacity of the eight basic open-hearth furnaces (Fig. 10). Isley stacks (Fig. 11) have helped the draft problem and auxiliary checker chambers

have been installed in place of the trouble-some reversing valves. (Steam jet blowers in the checker chambers and stack flues, in some plants, help keep these areas clean and

Water cooling is also used in doors and frames, skewback channels, port corners, and bridge walls to protect strategic parts of the furnace laboratory. Plastic refrac-
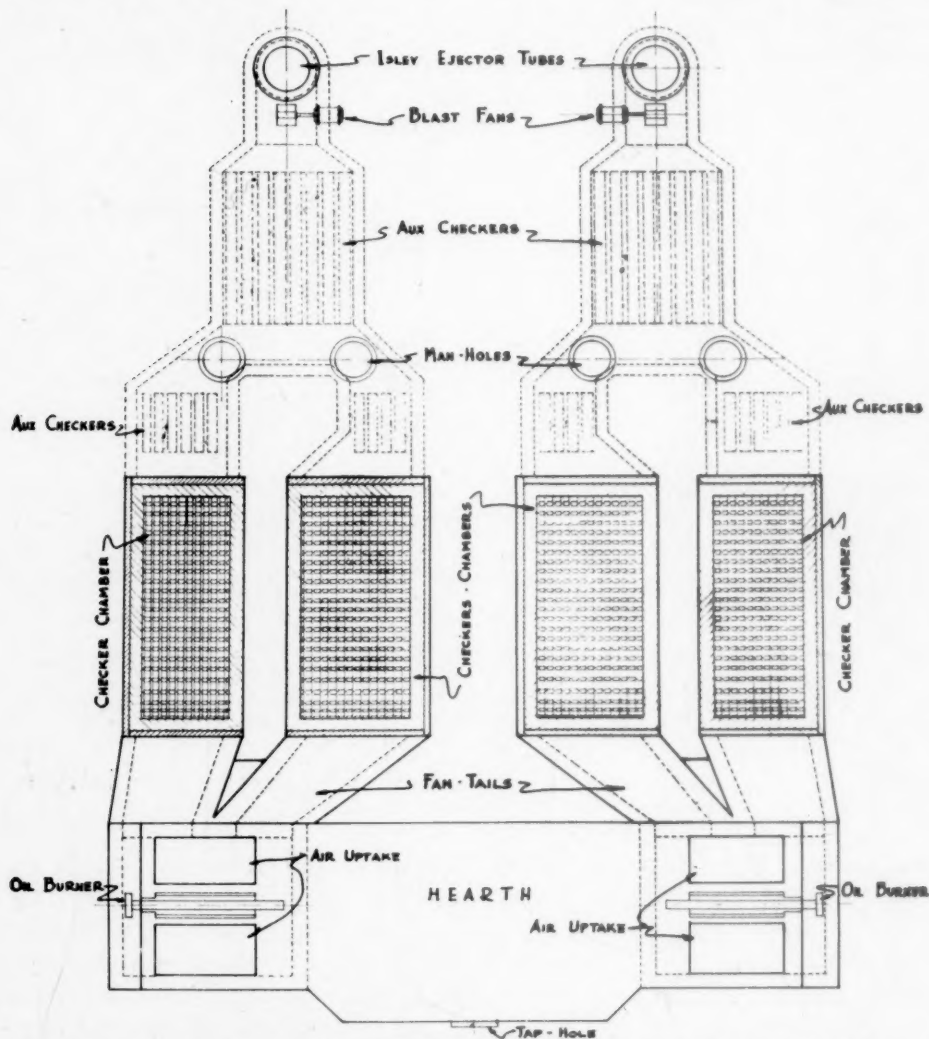
FIG. 11.—GENERAL ARRANGEMENT OF OIL-FIRED FURNACE, ISLEY CONTROL.

free from dust). Stronger slab buckstays, cast steel skewback channels, sloping back walls (Fig. 13), and in some places perma-nent solid bindings, have improved furnace life.

The use of basic refractory brick in the front walls, for lining the inside of the sloping back walls and for constructing the port ends of the furnaces down to the arches has helped prolong furnace life.

tories are used to cover basic brick and repair holes in banks and bottoms, as well as for monolithic linings of furnace doors.

In our plants, fuel oil as well as a combi-nation of oil and natural gas fuels, are relatively clean and efficient. All these improvements have increased the efficiency of the open-hearth furnaces and have helped quality control. It is an open-
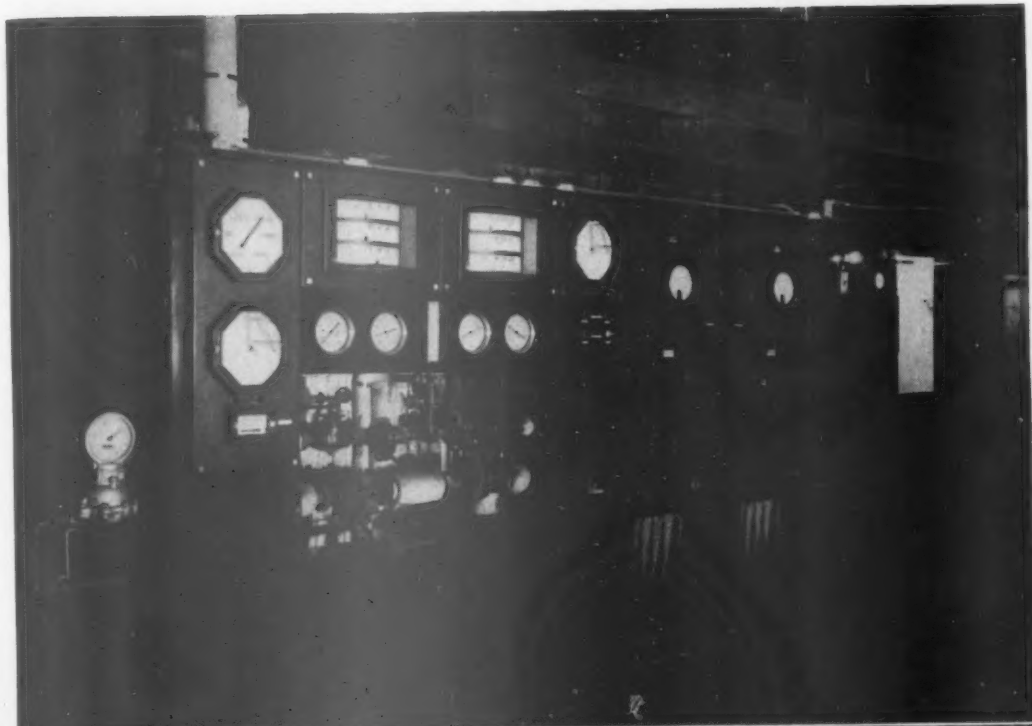
FIG. 12.—OPEN-HEARTH CONTROL PANEL.
FIG. 13.—CONSTRUCTION OF MODERN SLOPING BACK WALL.
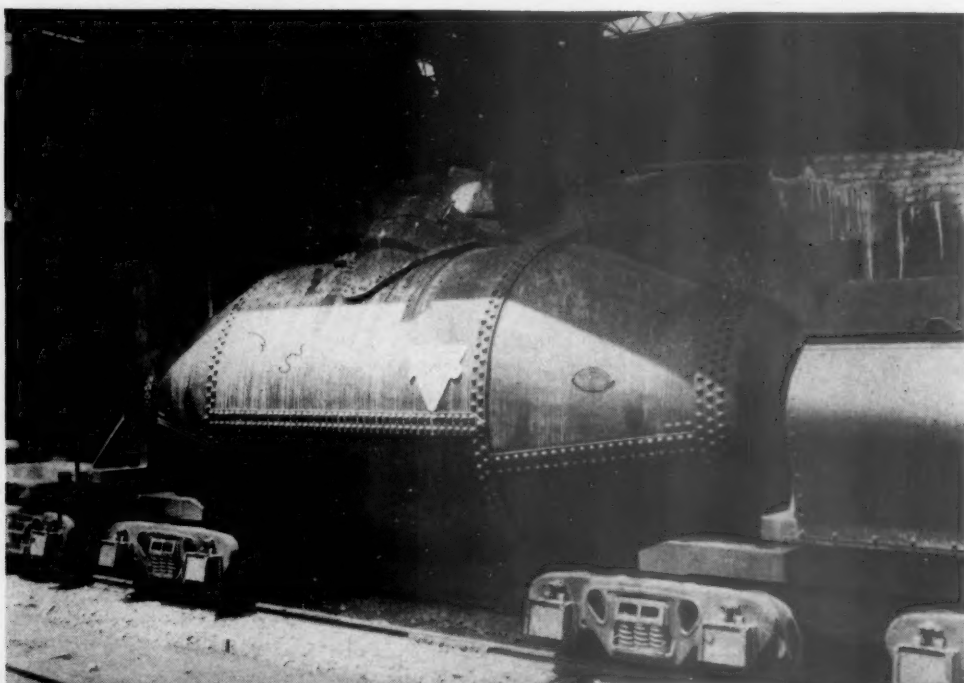
FIG. 14.—CASTING HOT METAL AT HAMILTON PLANT.
FIG. 15.—SCALE TREATMENT OF HOT METAL.

hearth maxim that "You can't make quality steels in a 'lazy' furnace." At the Middletown plant, the change from producer gas to fuel oil and natural gas as fuels has been helpful from both a tonnage and quality standpoint.

SCHEDULING HEATS

Then comes the problem of scheduling heats for the right type of furnaces. With the modern, high-powered furnace, it is seldom necessary to avoid charging special heats into certain furnaces because they are "old." Most furnaces can make quality heats to the end of their "run."

The proportioning and charging of open-hearth heats too often has been left in the hands of inexperienced weighmasters or stocker bosses, at most plants, leading to erratic melts requiring too many, or too few, iron-ore additions for best results, and often causing off-analysis heats.

Then gradually evolved the plan to standardize charges. In the first place, our blast-furnace organizations were asked to produce "hot metal" or pig iron of a constant and definite analysis. Much water ran over the dam before that was even partly accomplished. Many variables under the blast-furnace supervision had to be reduced or eliminated before much progress could be made.

USE OF HOT METAL

In our Middletown plant, where high percentages of "hot metal" must be charged into the open-hearth furnaces, it was found that low-silicon "hot metal" would improve operations, because it would be necessary to charge less ore and the resulting decreased slag volume would help in quality control and increased tonnages. Therefore, the blast-furnace supervision was asked to produce an iron having a silicon content as regularly as possible from 0.70 to 1.00 per cent. In addition, the sulphur content was kept under

0.030 per cent and the phosphorus under 0.300 per cent.

In addition, as a very important part of the specification, instructions have been

FIG. 16.—SCALE-TREATED METAL FLOWING INTO TRANSFER LADLE.

issued that the metal must be physically hot. At Hamilton the normal casting temperatures range from 2650° to 2750°F. About 50°F. is lost in transferring the "hot metal" in 175-net-ton cigar-shaped ladle cars to the Middletown works, a distance of 12 miles. Numerous tests in many steel plants have indicated, over a period of years, that so-called "cold-

bottom" basic pig iron is father of a progeny of troubles later on, such as long-time "cold" open-hearth heats and difficulties from laminations and blisters in the finished product (see Fig. 9).

metal ladle cars into the open-hearth transfer ladle (Fig. 16). By this method, the voluminous acid slag resulting from the oxidation of silicon and manganese can be removed easily from the top of the transfer
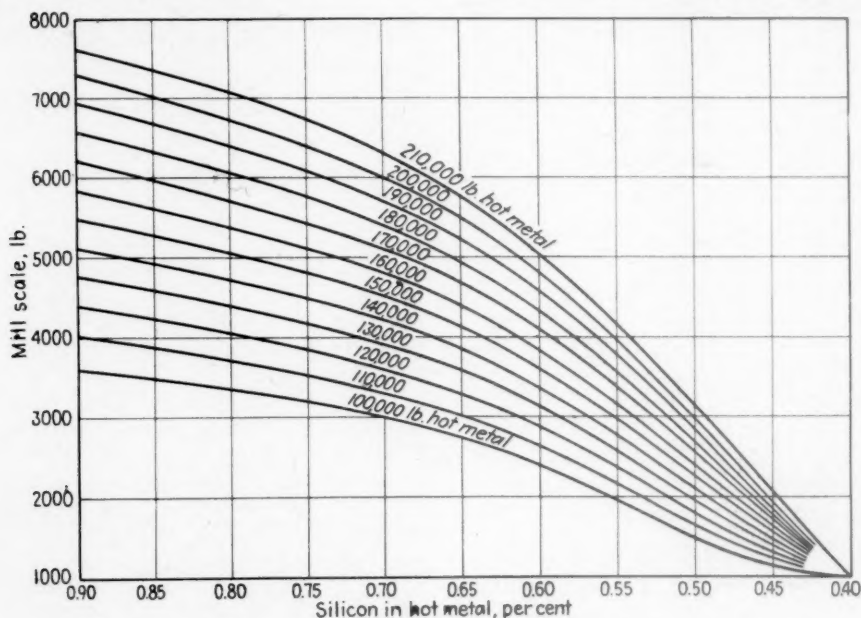
FIG. 17.—CHART FOR CONTROLLING SCALE ADDITIONS TO HOT METAL.

Table 2 shows the percentage of blisters by size of skull as taken from an open-hearth pit report. Heats weighed 180 net tons.

TABLE 2.—*Blisters*

Size of Skull, Lb.	Number of Heats	Number of Sheets Inspected	Percentage of Blistered Sheets Coated Stock
Clean ladle.....	179	437,026	1.01
500............	17	34,570	1.35
1000...........	42	115,986	3.33
2000...........	24	54,503	5.35
4000–8500......	11	21,235	11.42

In order to standardize "hot metal," which represents from 50 to 75 per cent of most open-hearth furnace charges, in one of the Armco plants this metal is being treated by the proportionate and regular addition of rolling-mill scale to the molten metal (Fig. 15), at the open-hearth department as it flows from 175-net-ton hot-

ladle. This process, if properly carried out (Fig. 17), delivers hot metal of uniform silicon analysis, say 0.40 to 0.70 per cent, to the open-hearth furnaces and therefore helps standardize this variable.

A typical analysis of hot metal before treatment is as follows: sulphur, 0.027 per cent; phosphorus, 0.282; silicon, 0.84; manganese, 1.42; copper, 0.052.

After treatment of one lot of 181,000 lb. of hot metal with 5600 lb. of rolling-mill scale, the analysis of the hot metal was as follows: sulphur, 0.026 per cent; phosphorus, 0.290; silicon, 0.49; manganese, 1.01; copper, 0.052.

The analysis of the resultant slag skimmed from the top of the treated metal, which represents about 2 per cent of the total weight of the iron, is as follows: SiO_2, 39.5 per cent; MnO, 23.6; sulphur, 0.12; phosphorus, 0.012.

FIG. 18.—A VICTORY-DRIVE SCRAP PILE.
FIG. 19.—AUTO GRAVEYARD.
FIG. 20.—HEAVY MELTING SCRAP NO LONGER AVAILABLE.
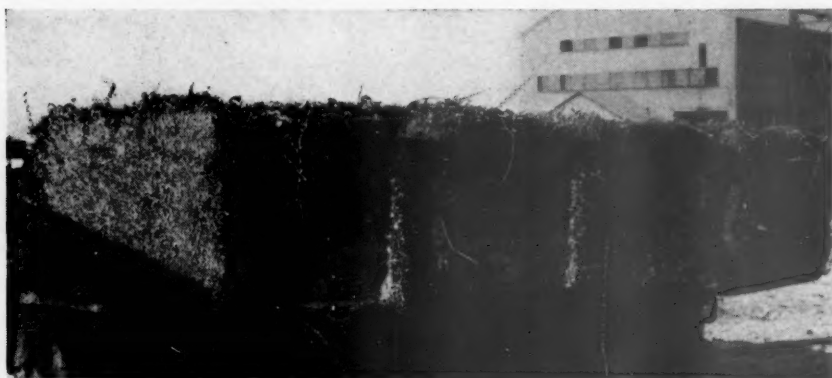
FIG. 21.—BUNDLES OF TURNINGS WEIGHING 2500 POUNDS.
FIG. 22.—BUNDLES OF BRITTLE ALLOY TURNINGS.
FIG. 23.—BRIQUETTES OF STEEL TURNINGS.

Scrap

During pre-war days, the preparation and selection of scrap for use in high-quality heats in the open-hearth depart-

sorting and classifying the motley array of scrap coming from nation-wide scrap drives.

The production of common or alloy turn-

FIG. 24.—MACHINE FOR MAKING IRON-ORE BRIQUETTES.

ment became standardized, so that consistent results, heat after heat, could be predicted. Now that war production requires such a large quantity of available suitable scrap, and has immobilized other tonnages in war materials, and decreased the turnover of used and obsolete equipment and machinery because of other war demands, this problem becomes very serious. (Figs. 18 to 20.)

National attention has been called to the need for better separation and segregation of scrap, particularly turnings (Figs. 21 to 23) and millings in fabricators' plants, as well as the elimination and salvage therefrom of such nonferrous metals as lead, brass, bronze, copper, tin, babbitt, not to forget rubber, all of which can be so detrimental to steel quality and proper open-hearth bottom maintenance. Scrap dealers must be encouraged or forced to carry on similar operations in their scrap yards by

ings has increased by leaps and bounds. To make them available for open-hearth or electric-furnace use they should be degreased, chemically or by burning, crushed and briquetted or bundled.

Charging

Limestone must be free of sulphur, low in magnesia, must go into solution easily, and physically not be too fine or in too large chunks. The ideal size is a chunk about 3 to 6 in. in diameter. A typical analysis of Bedford, Ind., limestone is as follows: $CaCO_3$, over 95 per cent; $MgCO_3$, under 1.50; S, trace; SiO_2, under 1.50; $Fe_2O_3 + Al_2O_3$, under 1.50.

After the right proportion of pig iron and scrap has been made for the open-hearth heat, the stock is charged into the furnace as rapidly as possible. Considerable control of future difficulties can be solved by the proper charging of various materials. In

ore-charged heats, great care must be taken to have dry ore charged on the bottom of the hearth. Formerly this was not difficult because good lump ore, low in moisture and silica, was available. Now, when larger quantities of hot metal are being used, many plants, because of inability to obtain lump ore, must use at least 50 per cent of the charge ore as fine ore, which is often high in combined moisture and high in silica. To charge such ore as this into an open-hearth furnace is dangerous and detrimental to furnace life and the quality of steel made. Therefore, many tests have

open-hearth furnace at the time of charging, so as to remove the combined moisture (Fig. 27). This practice helps from a safety standpoint but is erratic and causes some decrease in tons per hour.

We have recently built a briquetting machine similar to a concrete cinder-block machine (Fig. 24), and a continuous drying furnace is being constructed so that the moisture in the 35 to 50-lb. briquettes will be less than 2 per cent. Tests have indicated that this briquetted ore is very satisfactory, particularly for "feed" ore, and fills a vital need in quality control for

TABLE 3.—*Analyses of Ore*
PER CENT

Lump	Briquette	Sintered	Iron-ore Balls or Nodulized Ore, Dry
P.......... 0.096 to 0.111 Si.......... 8.72 to 10.36 Moisture.... 0.31 to 1.08 Fe, natural.. 56.77 to 63.2 S.......... trace	Fe.......... 61.00 P.......... 0.070 Si.......... 8.00 Mn.......... 0.53 Al$_2$O$_3$........ 1.38 Moisture.... 2.00	Fe.......... 61.00 P.......... 0.058 Si.......... 8.06 Mn.......... 0.63 Al.......... 2.75 CaO........ 0.80 MgO........ 0.40 Moisture.... 2.00	Fe.............. 66.04 S.............. 0.006 Mn.............. 0.19 P$_2$O$_5$............ 0.048 SiO$_2$.............. 2.75 Moisture and loss on ignition..... 1.20

been made to improve this practice, by such laboratories as the Minnesota School of Mines, and at the Carnegie-Illinois Steel Corporation's plants, where the ores have been nodulized in cement-clinker kilns. This type of substitute, we are told, gives better results than any other. In a number of other plants, the ores are sintered in the blast-furnace sintering plant. This is our present practice.

PREPARED ORE

Open-hearth sintered ore must be more lumpy and dense than blast-furnace sinter (Figs. 25 and 26). We have found that higher temperatures, and the additions of borings or turnings in quantities up to 15 per cent of the total sinter charge, will help solve this problem. ·

For years, we have briquetted "soft" ore in a jarring machine by the use of 2 per cent or less of cement as a binder. We then burn these briquettes for 20 to 30 minutes in the

the present type of high-hot-metal open-hearth charges.

Mixture of materials from which open-hearth sintered ore is made is: flue dust, 39.0 per cent; iron ore, 49.0; mill scale, 6.0; cast-iron borings, 5.0; extra coke, 1.0.

The open-hearth refining operation requires great skill in making additions of iron ore, fluorspar and burnt lime, as well as in control of bath temperatures.

For the manufacture of rimming steels of the best quality, a low-silica fluorspar is needed. Unfortunately this type of spar is becoming scarce. It has been found practical to use roll scale in the ratio of 6 lb. of scale to replace one pound of spar. This thins the slag and thus helps to conserve spar—a strategic commodity.

SLAG

The slag in the open-hearth furnaces must be kept basic enough to reduce the sulphur to the required limits, but must

FIG. 25.—LUMP ORE.
FIG. 26.—SINTERED ORE.
FIG. 27.—BRIQUETTED ORE.

contain enough oxides to ensure fluidity and removal of phosphorus. This is especially important in the manufacture of steel for deep drawing, and many metal

LABORATORIES

For a period of perhaps 50 years, the chemical laboratories were adjuncts of the open-hearth departments. Chemists had no

First Test   Second Test   Third Test

Fourth Test   Fifth Test
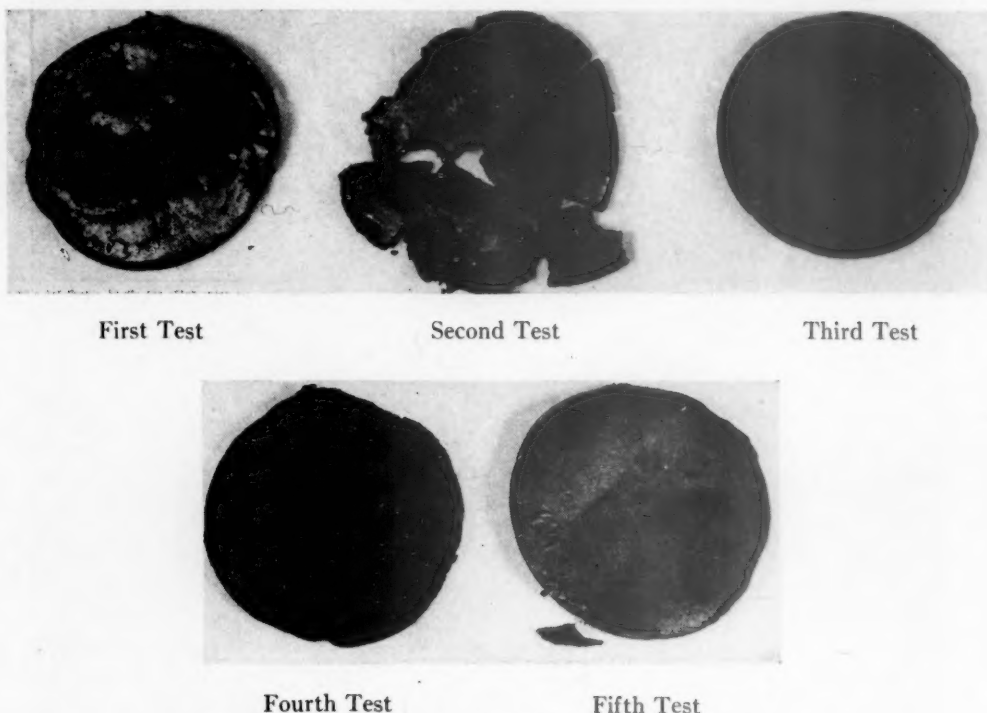
FIG. 28.—SLAG CAKES, LOW-CARBON RIMMING STEEL.

Analysis of slag cakes taken every half hour during the last two hours of the heat, as follows:

1:50. First test. Before any ore addition. Some lime-up. Fracture, carbon 0.50.
    SiO, 22.94 per cent; CaO, 38.21; MnO, 6.41; P_2O_5, 3.25; FeO, 14.8.
2:30. Second test. 40 minutes after first feed ore and spar. Heavy lime slag. Fracture, carbon 0.16.
    SiO, 19.04 per cent; CaO, 48.16; MnO, 4.45; P_2O_5, 2.76; FeO, 13.5.
3:00. Third test. 30 minutes after second shot of spar. Creamy slag. Fracture, carbon 0.12.
    SiO, 16.02 per cent; CaO, 50.00; MnO, 3.96; P_2O_5, 2.41; FeO, 16.2.
3:30. Fourth test. Heat melted. Final preliminary test to laboratory. Fracture, carbon 0.07.
        Good action, thin, creamy slag.
    SiO, 17.66 per cent· CaO, 48.94; MnO, 3.66; P_2O_5, 1.98; FeO, 22.5.
4:00. Fifth test. Just before tap.
    SiO, 12.12 per cent; CaO, 47.42; MnO, 3.95; P_2O_5, 1.77; FeO, 22.3.

and slag tests are taken to follow the progress of the refining. Slag may be tested chemically, by observation of solidified slag cakes, or by the fluidity test. Armco uses the chemical method.

For a heat analyzing carbon 0.065 per cent, manganese 0.30, phosphorus 0.008, sulphur 0.025 and copper 0.057, the analyses of the slag cakes were as shown under Fig. 28.

control of procedure, but merely recorded the results. In plants such as ours, where effort was being made to produce specialty steels, it became evident that for proper control of quality, accurate chemical analyses were essential. Every effort was made, therefore, to improve laboratory equipment and technique. In those days steel samples were drilled by hand power, and other equipment used by the chemists

was equally crude. But from these early beginnings came the urge to improve laboratory equipment and processes so as to make better steel. Our research laboratories' staff has been helpful in assisting the operating managements to make such improvements.

WORK OF THE CHEMIST

In the operation of the open-hearth department, the chemist must be sure that all raw materials and supplies meet the chemical specifications set up in our standard practices. He must analyze preliminary and final open-hearth heat tests quickly and accurately.

Additional aids have been installed recently in the operating chemical laboratories to assist the chemists in making their analyses accurately and rapidly.

From the sampling standpoint, the thimble test and nibbler (Fig. 29) have been of great help in speeding up the sampling of the alloy metal at the furnaces and in preparing samples at the laboratory for analysis. From 5 to 10 minutes can be saved by the use of these instruments.

Considered from the analytical angle, there are several instruments that are especially useful; for instance, the Burrell high-temperature furnaces (Fig. 30), Zircofrax tubes, Leco carbon and combustion sulphur determinators. The Burrell furnaces, in connection with Zircofrax or similar tubes, may be used to reach temperatures up to 2500°F., which are needed to secure accurate analysis of carbon and sulphur in certain kinds of alloy steels.

The Leco or similar combustion apparatus must be used in the analysis of alloy steels to guarantee accuracy in sulphur determinations. The combustion method is much faster than the evolution method. The former requires about 5 min. after sampling whereas by evolution $\frac{1}{2}$ hr. is required for analysis of the sample.

Ainsworth keyboard balances have helped a great deal in speeding up the weighing in the laboratory, as well as in decreasing balance upkeep cost.

The Klett-Summerson photoelectric colorimeter (Fig. 31) has speeded up the

FIG. 29.—THIMBLE TEST AND NIBBLER.

determination of molybdenum and titanium. Molybdenum can be determined in 12 to 15 min., which gives the melter a closer check of the molybdenum content in the heat. Titanium can be determined in about an hour.

The Telautograph enables the analyst to keep in close touch with the melter and open-hearth and mill managements. It eliminates the chance of error that may occur when results of analyses are given over the telephone, and, most important, it speeds up analysis of preliminary tests upon which quality depends.

I believe that the development of perchloric acid should be mentioned, as its use has been a time saver to chemists in the determination of chromium, columbium, manganese, silicon, and other elements in alloy steels, and because it saves hours in the determination of some of them, especially silicon in stainless steel.

CONTROL OF DETAILS IN MELTING

In the melt shop, quality control can be ruined in a few minutes at tapping time if the alloy and other additions, as well as deoxidizers, are not added in proper
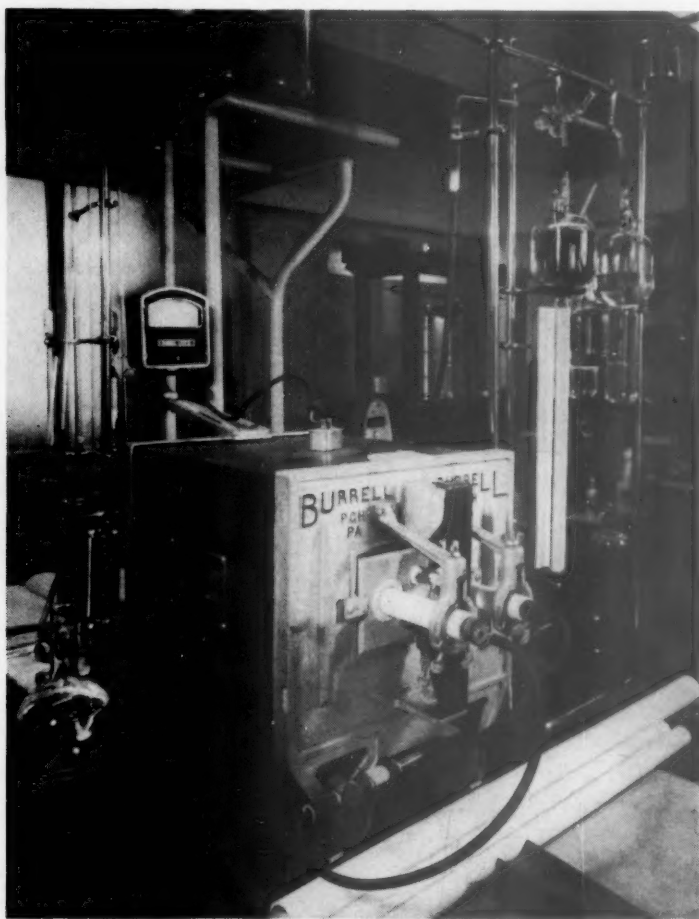
FIG. 30.—BURRELL HIGH-TEMPERATURE LECO SULPHUR AND CARBON APPARATUS.

FIG. 31.—KLETT-SUMMERSON PHOTOELECTRIC COLORIMETER.
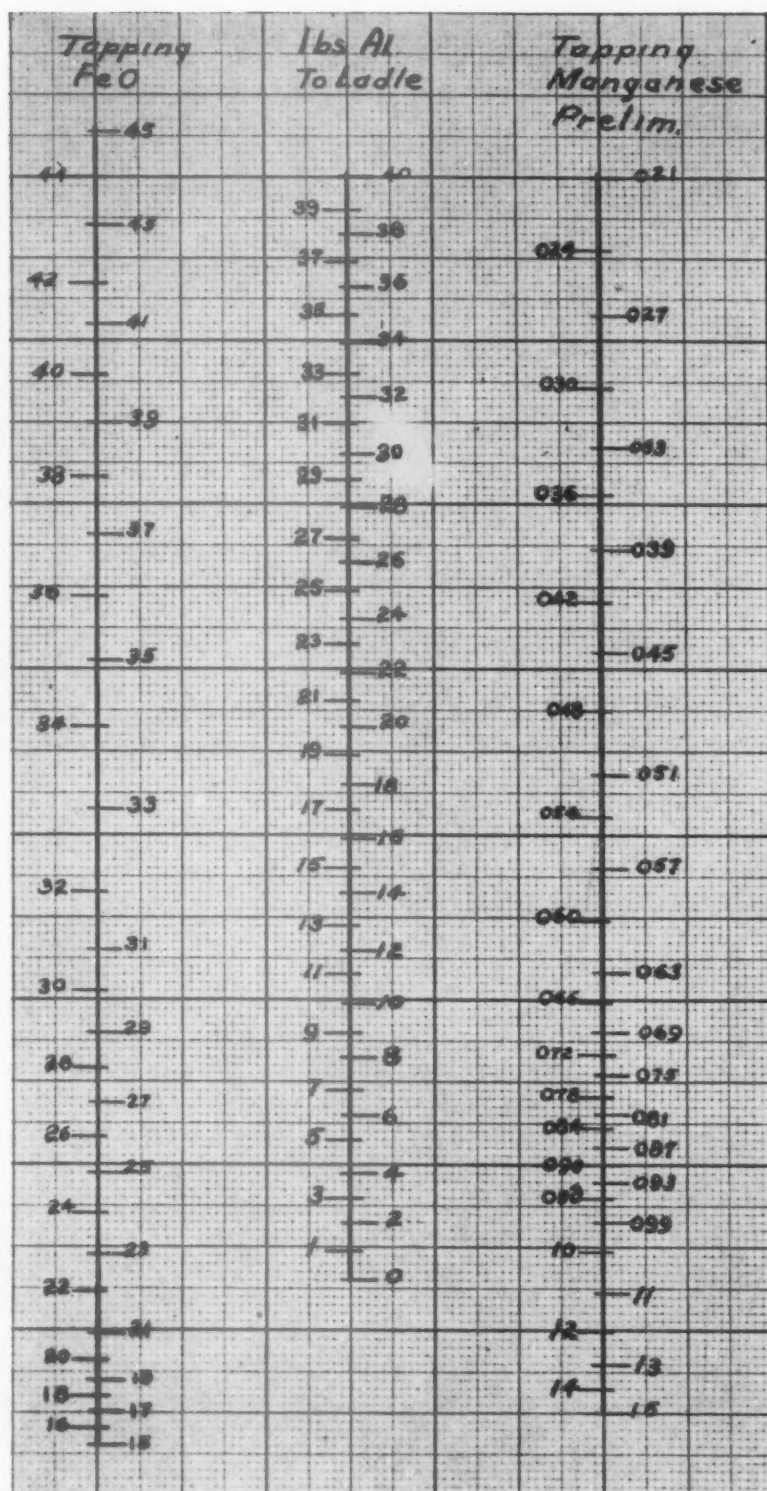
FIG. 32.—DEOXIDATION SCALE FOR LOW-CARBON RIMMING STEEL.

amounts and at the right time. Fig. 32 shows a deoxidation scale for low-carbon rimming steel. Similar charts are used for other types of steel.

manufacture of alloy steels, it is essential that steel be poured into big-end-up or big-end-down molds equipped with brick or other hot tops. For better surface, at times,

FIG. 33.—POURING HOT-TOP BIG-END-DOWN MOLDS BY BOTTOM-POUR METHOD.

In the open-hearth pit, more attention probably must be given to the control of small, apparently insignificant details than anywhere else in the steel mill; otherwise a quality open-hearth product may be ruined in the open-hearth pit.

The taphole must be made up carefully, so that it is the proper size. The runner or spout must be made up carefully and dried thoroughly. The ladle must be cleaned of all slag and metal accumulations after each heat. This practice is followed to eliminate inclusions in the steel. The nozzle must be properly burned in the brick plant, to withstand, without cracking or spalling, the terrific heat of the molten metal. It must be carefully set in the ladle and thoroughly heated through at the time the ladle is heated. The stopper-rod assembly is a job all by itself, and must be in exact accordance with standard instructions.

Molds must be carefully made and of the right sizes, analysis, and design selected for the type of product to be made. In the

molds are bottom-poured either on the ground or on heavy ingot cars (Fig. 33).

A number of mold washes are used in different steel plants. We spray graphite on the molds for ordinary steels, and apply aluminum mixed with powdered bituminous paint for stainless-steel ingots.

Teeming

Teeming an open-hearth heat is an art. The correct size of nozzle for the type of heat and the size of molds must be selected. Teeming must be carefully regulated, and splash must be avoided, and, on "killed" steels particularly, the hot tops on molds must be filled very slowly.

It is essential, in pouring any kind of quality steels, to have enough molds and buggies available so that molds can be poured at a hand-warm temperature. Aluminum dross was used for many years on top of hot tops to keep the metal in a molten condition as long as possible, to reduce internal piping; now, because of war

demands, rice hulls are used on some heats and ground cork on others.

Ingots should not be moved from the pouring platform until they have solidified. It is best to allow alloy steels to stand for $1\frac{1}{2}$ hours after pouring. After that, they should be stripped quickly and then charged into the soaking pits. For alloy steels, pits must be cooled down before the ingots are charged. It is desirable not to bank alloy steels; if ingots must be banked, they should be cooled very slowly in a holding pit. When used, they should be charged into an almost "black" soaking pit and heated very slowly with several "soaking" periods during the cycle.

STANDARDIZATION IN SHIPPING DEPARTMENT

From the open hearth on through to the shipping department, the same rigid mechanical and metallurgical control must be maintained if we are to be sure of consistent quality.

Written standard instructions are issued for heating all kinds of steel in the soaking pits. Rolling speeds and drafts, as well as temperatures of the ingots as they leave the soaking pits and the slabbing or blooming mills, as the case may be, must be carefully standardized. (Figs. 34 and 35.) This same practice is continued through succeeding mills. In order to standardize conditions, special pyrometers—often on mobile trucks—have been designed and installed to take temperatures at various strategic positions in the rolling operations (Fig. 36).

To improve the hot surface of slabs after ingots are rolled on the slabbing mill in the Middletown Division, a scarfing machine (Fig. 37) has been installed in line with tables to the slab-heating furnaces. This scarfer can remove from $\frac{1}{32}$ to $\frac{1}{8}$ in. of surface of the hot slab up to 75 in. in width —one side at a time—by the use of a series of oxyacetylene torches.

Finishing temperatures on bar mills, structural mills, or hot strip mills, are very

important and either the original temperature of the bar or slab as it enters the mill must be controlled or the temperature of the product, such as bars or strips, must be reduced below certain critical temperatures

FIG. 34.—TEMPERATURE CONTROLS FOR SOAKING PITS.

by cooling with water before coiling, or by slow air cooling before piling.

In the cold strip-rolling process, careful attention must be paid to standardizing conditions of temperature, speed of strip, and strength of acid in pickling the strip before cold-rolling. Then drafts on successive mills, roll contour, roll temperatures, proper alignment of guides and over-all speed of mills must be standardized to control quality of the surface. Modern cold strip mills are shown in Fig. 38.

From there on, processing operations require very close control; particularly in annealing. Furnace design and fuel controls, piling of stock, heating and cooling, as well as inert gas atmospheres must all be

FIG. 35.—TAKING TEMPERATURE OF INGOTS AT SOAKING PITS.
FIG. 36.—MOBILE PYROMETER FOR MEASURING BAR-MILL TEMPERATURE.
FIG. 37.—SCARFING WIDE SLABS BETWEEN SLABBING-MILL AND BAR-MILL REHEATING FURNACES.

FIG. 38.—MODERN 54-INCH AND 80-INCH COLD STRIP MILL.
FIG. 39.—FURNACE FOR ANNEALING COLD-REDUCED STEEL.
FIG. 40.—EQUIPMENT FOR TEMPERATURE CONTROL IN COLD STRIP PROCESSING ANNEALING
DEPARTMENT.

standardized and controlled within narrow limits from one lot to the next. (Figs. 39 and 40.)

Then comes skin passing, stretcher leveling, oiling, inspection, each with its own problems of control by standardized practice.

Inspectors check the quality of our sheets and plates from a surface and dimension standpoint from the hot strip mill to the inspection tables. We believe that a reputation for the quality performance of a product can be quickly ruined by careless and superficial inspections; so our inspectors are trained to protect our record by very careful, conscientious inspection.

The importance of correct stenciling, crating and shipping of steel sheets, for example, is at times overlooked, but it is just as important to standardize these details as to standardize any other operation in the history of an order. Some stencils are printed on the sheet with a machine, to ensure regularity and attractiveness. The first thing the customer observes, when an order arrives at his plant, is the appearance of the stock. After all, first impressions are the strongest.

Even there, the control of quality does not end. All wide awake steel-plant managements have found that it pays to service their sheets or other products in the customers' plants.

SUMMARY

Throughout the entire discourse it will be noted that in quality control as practiced at our plant—from the ore mines to the customer's plant—the emphasis is placed on standardization of processes, observation of deviations from such practices and methods of correction. All the way along, the need for an intelligent and efficient organization is indicated. Proper follow-ups must be maintained. Operators must know their jobs. Maintenance and service men must maintain equipment so

that delays may not interfere seriously with quality controls. Metallurgists must observe the operations in the steel plant from the blast furnace through the open-hearth department, the rolling mills, and the processing departments. In addition, the inspection department must double check on the physical and surface characteristics of the product as it goes through the mills, and on the inspection tables. Many accurate records must be kept so that there will be no "mix-ups," lost lifts, or improper schedules and treatments.

Mr. Andrew Carnegie is reported to have said, "You may take my mills, and my equipment, but if you will allow me to keep my organization, I will soon build a bigger and better business."

Quality production depends upon the interested cooperation of a loyal, efficient working organization. It is a responsibility of Management to make sure that the men understand the relationship between Quantity Production and Quality Control. They must realize that their own progress, as well as that of their company, depends upon the results obtained by working together to make products that meet the exacting requirements of present-day customers.

Quality is the only foundation stone upon which an enduring business can be built.

Essential Considerations in the Design of Blast Furnaces

By A. L. Foell*

(Cincinnati Meeting, April 1942)

The development of the modern blast furnace began more than one hundred years ago, with the abandonment of the small hillside furnaces. Its development, especially during the past 50 years, has been accomplished through a rapid succession of enlargements and improvements. The remarkable growth in furnace output during this period is a tribute to the engineers and operators who have constantly endeavored to build larger and more efficient blast furnaces. The blast-furnace operators and their mechanical and electrical maintenance staffs have originated most of the furnace improvements as a result of their practical operating experience.

Furnace Lines

About 50 years ago furnaces consisted of hearths about 11 ft. in diameter, which merged into rather high flat boshes, with no cylindrical section between the bosh and inwall and no cylindrical section at the stock line. Since then the lines of the furnace invariably have included a cylindrical section above the bosh and a cylindrical section at the stock line. Notable increases have been made in both hearth diameters and furnace heights. During the past 10 years hearth diameters in new and replaced furnace stacks have rather consistently fallen within the range of 25 to 28 ft. while their heights have varied be-

tween 100 and 106 ft. The lines of most large furnaces using Mesabi ores have followed a fairly uniform pattern (Fig. 1) in which the principal dimensions for 25-ft. hearth furnaces are as follows:

Hearth diameter..............	25 ft. 0 in.
Height of bosh................	10 ft. 0 in.
Bosh angle...................	$81\frac{1}{2}°$
Diameter top of bosh..........	28 ft. 0 in.
Inwall batter per foot..........	$1\frac{5}{16}$
Stock-line diameter...........	19 ft. 6 in.
Large-bell diameter...........	14 ft. 6 in.
Height from iron notch to top ring casting.....................	100 ft. 0 in.

In determining the size of a new furnace for the replacement of an existing stack or for an addition to productive capacity, it is not possible to formulate a procedure that can always be followed. Local conditions, requirements as to capacity, available raw materials and prospects for future expansion dictate the size of such proposed improvements or additions. However, where the immediate requirements indicate a stack or furnace of a certain productive capacity, and the future prospects indicate that more capacity can be utilized, it is well to consider building the furnace for the ultimate capacity rather than to install a smaller hearth with provision for future enlargement. The decision to build the larger hearth and stack for the ultimate capacity probably will require no greater initial investment, since the saving in the cost of brickwork will about offset the greater cost of the hearth jacket, tuyere breast and bosh bands. In the meantime, the furnace of larger hearth dimensions, while operating below its ultimate output, will yield a better coke rate and
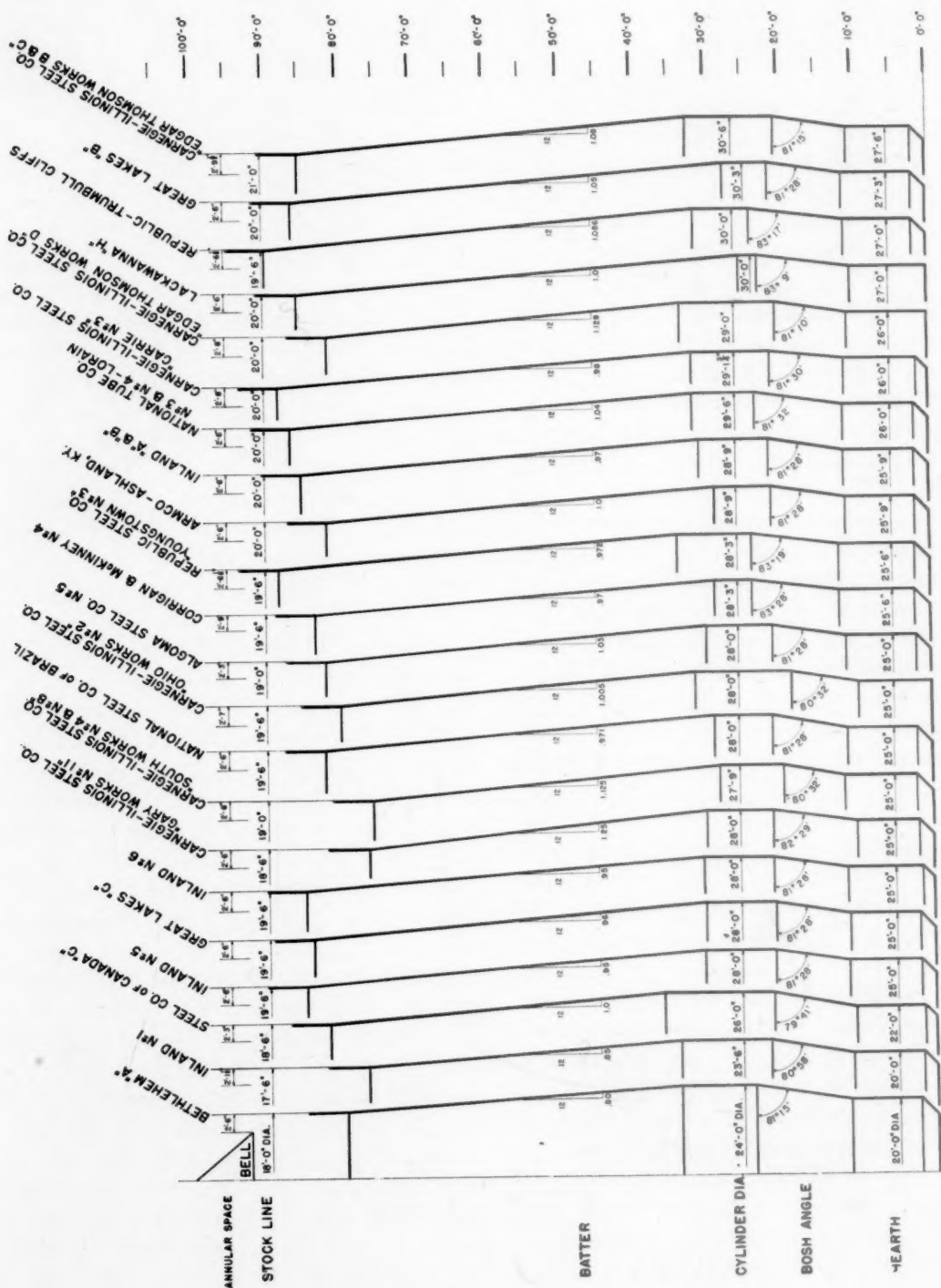
Fig. 1.—Typical lines of modern blast furnaces.

produce less flue dust than if it were lined-in to suit the smaller hearth.

HEARTH BRICKWORK AND COOLING

A great deal of disagreement among operators concerns hearth brickwork. The most commonly used hearth brick is the large 18 by 9 by 4½-in. block, but various smaller sizes, such as 13½ by 6 by 3 in. and 12 by 6 by 4 in., are still widely used. The large blocks have the definite advantage of presenting a smaller number of joints, thereby decreasing the probability of iron penetrating the joints and disrupting the hearth by floating the brickwork. Also, less time is required in laying the hearth when the larger blocks are used. The smaller blocks are less expensive and are truer in shape than the large sizes, and can be laid with a smaller amount of clay to fill the joints. Most hearth bottoms are laid with the blocks placed on end, arranged so as to break joints in various ways. These may be divided into two principal methods: (1) to lay the blocks so that the vertical joints are continuous and the horizontal joints are broken, and (2), the most widely used method, to lay all blocks of one course at the same level but to orient the blocks to preclude any continuous vertical joints.

The hearth construction in all furnaces incorporates means of cooling and retaining the hearth brickwork. This may be in the form of a water-cooled, cast steel jacket, or —a less expensive type of construction—of a rolled steel plate jacket surrounding a ring of cast-iron cooling staves. The cast steel jacket most frequently used consists of a number of water-cooled segments, 5 or 6 in. thick, assembled in the form of a large truncated cone with the large diameter at the base. In addition to being bolted together, the sections are held by a number of 12 by 1½-in. steel bands, which encircle the jacket and are tightened by wedges. The rolled steel plate jacket is fabricated from heavy (1½-in.) steel plates, riveted or welded into a cylindrical shell. The cooling staves used in conjunction with this jacket are iron castings 4 to 6 in. thick and approximately 14 ft. long. Two 4-in rows of staves inside the jacket have been used, but in most furnace hearths one heavy row with approximately 9-in. spacing of cooling pipes has given adequate protection. The hearth jacket may be exposed, or may be embedded in brick or concrete. The exposed construction is cheaper, and provides ready access to the jacket for inspection or for the installation of supplementary cooling if necessary, and also provides easier tapping of the salamander when removal of the salamander by this means can be undertaken.

The iron notch is without question the most vulnerable part of any hearth construction. As a rule, it is constructed to extend horizontally through the refractory hearth wall with its center line about 2 ft. above the hearth blocks. In opening the notch by drilling at the usual angle, it is necessary for the drill to pass through the refractories around the inner bottom of the notch. In order to meet all requirements of the tapping operation, the notch should be built of special shapes with its top surface on the horizontal and its bottom sloped to suit the maximum drilling angle.

BOSH CONSTRUCTION AND COOLING

Two important points in the design of the bosh, which should be given major consideration, are the number of tuyeres and the amount of bosh cooling to be installed. Experience with many furnaces has shown that 12 tuyeres in furnaces having 18-ft. 6-in. and 20-ft. 0-in. hearth diameters and 16 tuyeres in furnaces having 25-ft. 0-in. and 26-ft. 0-in. hearths have proved sufficient. This indicates that the tuyere spacing measured on the inner periphery of the hearth wall should fall between 4 ft. 10 in. and 5 ft. 2 in., and that the number of tuyeres for various hearth diameters should be as follows:

Hearth Diameter	Tuyeres
18'6" to 20'0"	12
20'6" to 23'0"	14
23'6" to 26'0"	16
26'6" to 28'0"	18

While these numbers must, of course, be predicated upon characteristics of raw materials and coke, it is safe to say that the figures given are perhaps the maximum number of tuyeres that should be considered for a given hearth, since numerous furnaces are operating successfully with fewer tuyeres.

Bosh cooling, while necessary for protection of bosh refractories, undoubtedly has a tendency to cool the combustion zone and decrease furnace efficiency. It is advisable, therefore, to limit the cooling-plate surface to the minimum amount sufficient for adequate protection. The tendency in most furnaces has been to overcool the bosh. The percentage of bosh-wall area exposed to combustion within the furnace that is taken up by cooling plates in most furnaces ranges from 8 to 11.2 per cent, while several furnaces that have had satisfactory bosh lives have been operated through normal campaigns with 25 to 45 per cent less exposed cooling.

Large Bells

Until the past few years, nearly all large bells were fastened to their bell rods through two hinged joints, so that the bell was free to adjust itself in any direction when seating. Most of the recent installations are of the rigid type, in which the bell is solidly connected to the rod through a bushed socket joint and a stiffening cone. By this means, and by directing the upper end of the rod in a straight line vertically, the axis and travel of the bell in opening is always plumb. When the bell and rod assembly is properly centered, accurate seating is at all times ensured, and wear against the small bell rod and distributor is largely eliminated. With the rigid bell connection, the large bell is also at all times concentric with the hopper and the dis-

tribution of material at the stock line at each bell dump is always the same, regardless of whether or not the material slides off the large bell uniformly at all points. Under such conditions the free type of bell will open first on one side and swing sufficiently to cause poor distribution. The rigid bell connection also makes possible positive opening of the bell, an operation for which the nonrigid type is not designed.

Bell Hoists

One of the debatable items of auxiliary equipment for moving the bell involves the suitability of the electric hoist versus that operated by air cylinder. Each has definite advantages and limitations. The air cylinder has the advantage of being both a bell hoist and counterweight, but because it fulfills both functions it must release tension on the bell cable in opening the bell. Air cylinders, therefore, are used in conjunction with bell beams, so that the raising of the cylinder lowers the bell. The power required to operate the air cylinders is very small. They are designed to operate on the pressure of the furnace cold-blast system or on plant compressed air in an emergency or failure of the cold blast. Complete failure of pressure from both sources will drop the load on both bells and reclose the empty bells. There is no necessity for counterweights at the top of the furnace. The air cylinder for the large bell has relief valves on each side of the piston, which allow the cylinder to move under extreme shock. In an explosion between bells, the large bell may be blown open without damage to either bell hoist. Speed of opening and closing can be controlled accurately and is easily adjusted. Smooth operation is assured by the cushioning effect of the air. The control does not necessitate the use of delicately adjusted limit switches to stop the bell hoists at the proper positions. In closing either bell, the cylinder lowers until the bell seats in the hopper with

sufficient force to counteract the force of the air on the bottom of the piston, and the pressure remains in the cylinder until the bell is to be reopened. The cables may stretch 5 or 6 in. without loss of seal on the bell. If positive opening of the bell is desired, an electric hoist should be used. An electric hoist combination as a single unit for the large and small bells is available for this purpose. This unit should be driven by a direct-current motor with variable-speed control, so that the speed of opening each bell can be varied to suit operating requirements. The bells are opened by application of tension to the operating cables by the hoist and are closed by means of counterweights located at yard grade. Either type of bell hoist can be operated automatically from the skip or charging control.

STRUCTURE OF FURNACE TOP

The structure of the furnace top is an important item among the considerations to be given the building of the furnace stack. The furnace top above the top platform includes the top gas-recovery system in the form of uptakes, bleeder stacks and downcomers and the filling equipment, comprising principally the revolving distributor, receiving hopper, bell beams or bell operator, skip sheaves and the dumping portion of the skip bridge. The arrangement and support of these parts should not be overlooked if an approach to perfection in furnace operation and low maintenance of top mechanism is to be attained. In the three types of top arrangements most commonly used in this country, the uptakes, bleeder stacks and downcomers are directly supported either by the furnace shell or top platform, and the distributor and revolving hopper by the furnace top ring. The distinguishing feature is the support of the remainder of the furnace-top mechanism. On older and smaller furnaces, this mechanism has frequently been supported by or attached to

the skip bridge (Fig. 2) and on all recently built furnaces either by a structure carried on the bleeder stacks (Fig. 3) or by an independent top structure separately supported on the top platform (Fig. 4).

An analysis of the advantages and disadvantages of these tops definitely indicates that the best arrangement for supporting the furnace-top mechanism is by an independent top structure such as is shown in Fig. 4. Regardless of whether the skip bridge is supported from the furnace stack or is self-supporting and independent of the stack, any settlement or differential settlement of foundations causes a perceptible movement of the top of the skip bridge horizontally in relation to the furnace center line and vertically in its relation to the furnace-top platform. Where the mechanism is supported by the skip bridge as in Fig. 2, such movement is sufficient to cause serious misalignment between the large and small bell rods and between bell rods and the revolving distributor, and will also cause vertical dislocations between the bells and their hoppers. Constant adjustments are necessary therefore to maintain bell and hopper seating relations. This objection, together with the inadequate space and limited platform room, has gradually eliminated the skip as a support for the top mechanism. Supporting the top on the bleeder stacks or on an independent top structure is far less objectionable from the standpoint of misalignment resulting from any settlement of the furnace stack.

In comparing the top supported by the bleeder stack (Fig. 3) with that of the independent top structure (Fig. 4) we find that the former requires four bleeder stacks and that these must be of heavier plate than is necessary when an independent top structure is used. The bleeder stacks or uptakes in an independent top structure are not dictated by structural requirements and therefore need not be more than two in number, nor need they be of heavier

material than $\frac{3}{8}$-in. plate. If the top is separately supported adjustments are not affected by expansion or contraction of the offtakes or bleeder stacks caused by changes in top temperatures or by differ-

mechanism in better alignment and in more accurate adjustment.

OFFTAKES, UPTAKES AND DOWNCOMERS

The present large furnace stacks with

FIG. 2.—GENERAL ARRANGEMENT

ences in gas flow in each bleeder stack. From the standpoint of design, the independent top structure can be more securely braced than can bleeder stacks, and this, together with the other features mentioned, makes it possible to maintain the top

relatively larger stock lines, greater working volumes and greater blast requirements, have made it necessary to scrutinize and bring into balance the furnace gas-recovery system. Offtakes, uptakes and downcomers have had to be enlarged in order to accom-

modate the larger volumes of gas to be
handled. To avoid irregular gas flow in the
stack of large furnaces, it is essential that
the resistance to gas flow at each offtake be
of equal value. The offtakes, therefore,
should be equally spaced, and if two down-

side of the furnace opposite the skip bridge.
To place the dust catcher in such a position
is seldom possible, therefore the single
downcomer has been developed recently
and has been applied to about 20 furnaces,
of which 13 are in operation and 7 in various
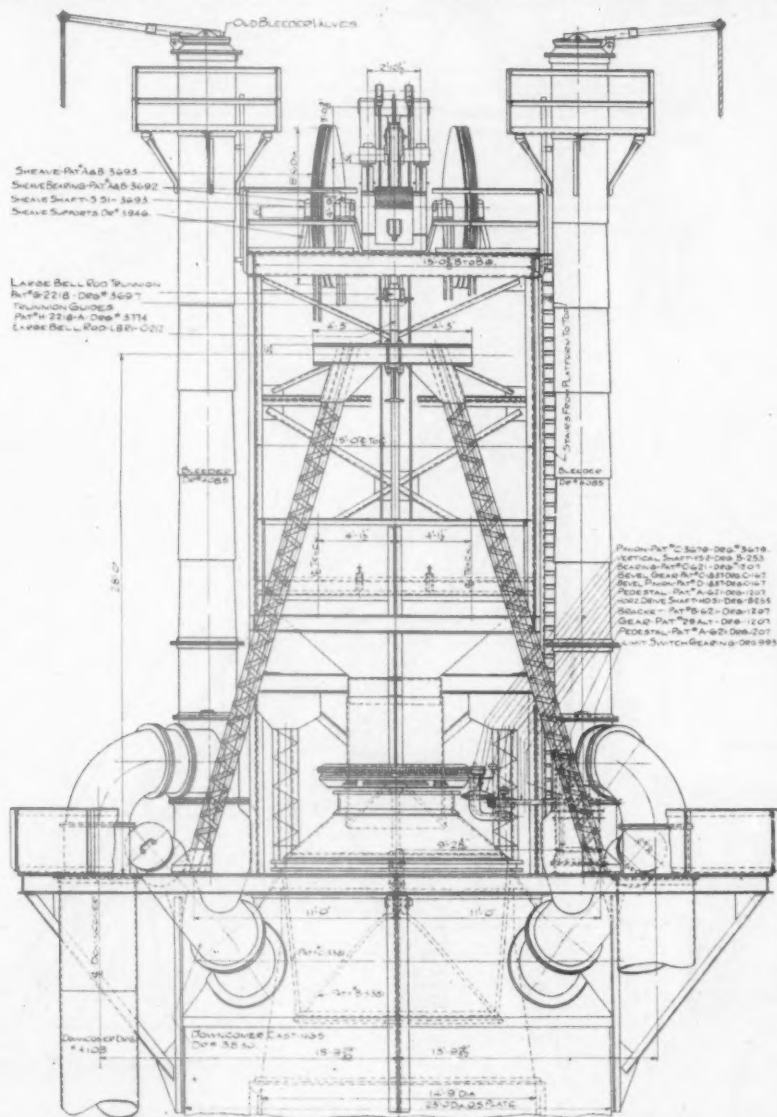
OF FURNACE TOP, SUPPORTED BY SKIP BRIDGE.

comers are used each should have as nearly
as possible the same length of gas travel
and offer the same resistance to gas flow.
This can be accomplished where two down-
comers are used only if the dustcatcher is
placed on the furnace center line on the

stages of construction. The single down-
comer arrangement, also shown in Fig. 4,
consists of four equally spaced offtakes and
uptakes, two pairs of which combine to
form two uptakes, one over each side of the
furnace, which in turn are joined into a

downcomer at a point above the center of the furnace. From this point the downcomer is brought to the top of the dust catcher, which can be placed anywhere

required in each, and also it allows the application of a desirable dust-catcher design, which cannot be used with the conventional two-downcomer arrangement.
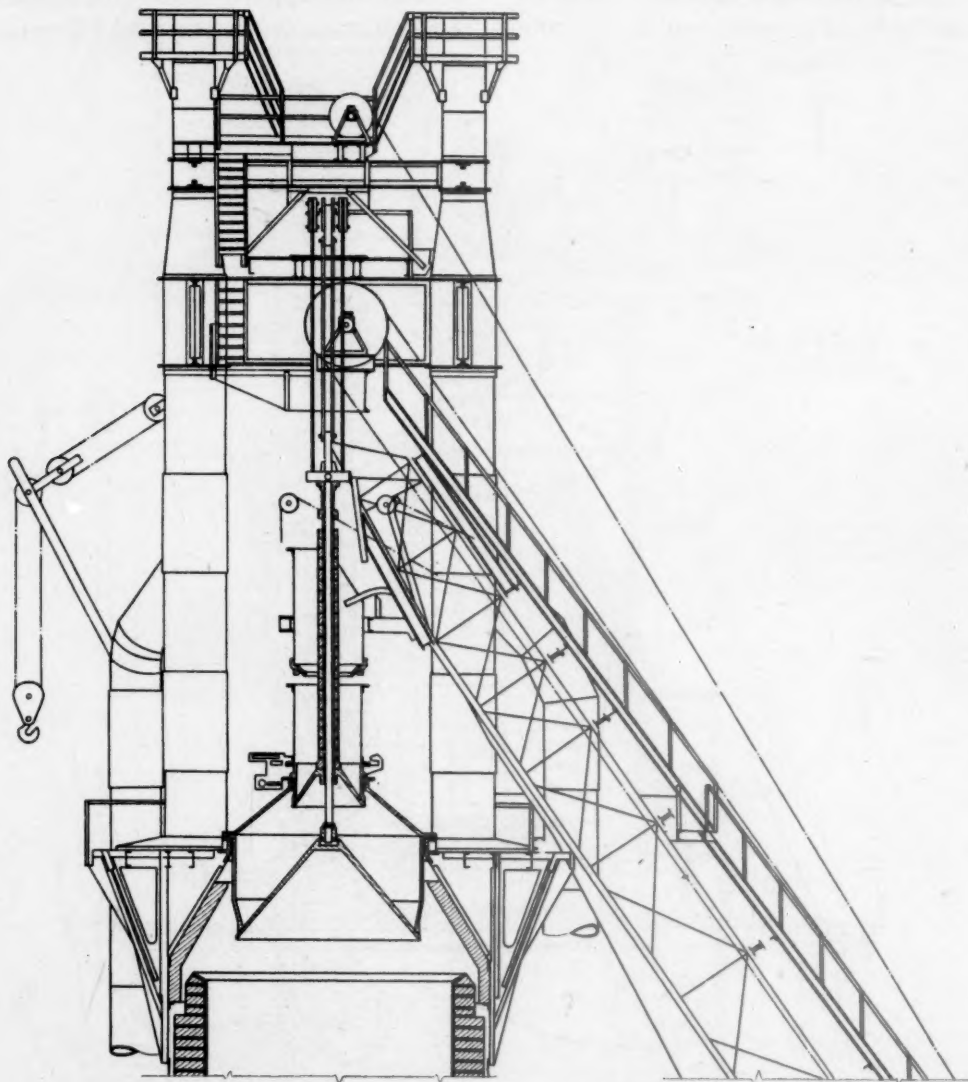
FIG. 3.—TYPICAL TOP STRUCTURE OF

adjacent to the cast house. The principal advantages of the single downcomer are apparent; it allows the choice of dust-catcher location to be determined entirely by the track and general plant layout, without the necessity of considering the effect of such location on the relative lengths of two downcomers or the number of bends

SKIP BRIDGE

Skip bridges for modern large furnaces are usually of trussed design, supported in one of two ways. The bridge is either self-supporting and free from the furnace stack or it is supported, through pin connections at its lower end, by foundations at the skip pit and, through a pin-connected link, at its

upper end by the furnace stack. The one has for its premise the idea that the furnace shell and stack foundations should not be encumbered with the extra loads entailed in supporting the skip bridge while

thus removing one of the forces tending to cause the furnace to lean, this can be accomplished only if the furnace and skip-bridge foundations can be installed as entirely independent units. This is seldom
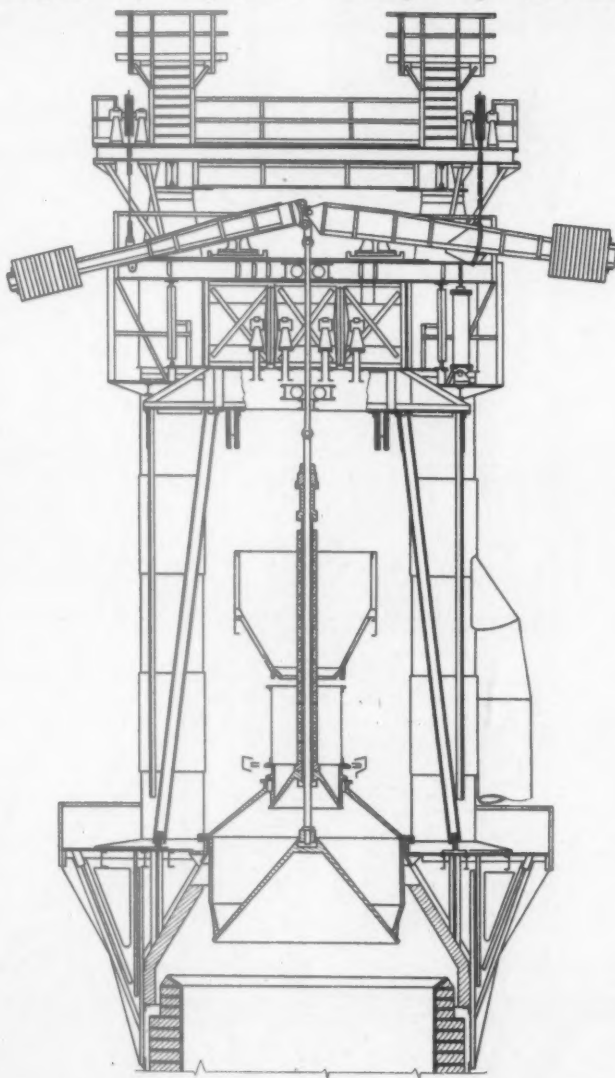
BLAST FURNACE SUPPORTED ON BLEEDERS.

the other is based on the premise that the maintenance of proper dumping relations between the skip and the furnace top requires the upper end of the skip bridge to be supported on the stack.

While the basic reason for independently supporting the skip bridge is to eliminate the lateral thrust against the furnace stack,

possible, since the angle of the skip incline usually is not flat enough to provide adequate room for supports without encroaching on the area required for the furnace foundation. Therefore it is generally necessary to position the shear leg for supporting the bridge within the cast house, in order to support it on the furnace foundation. The

effect on the foundation from the eccentric load applied thus by the shear leg is in most instances as great as the eccentric load advantage in independently supporting the skip bridge, whereas in addition to maintaining better skip-dumping relations by

NORTH ELEVATION
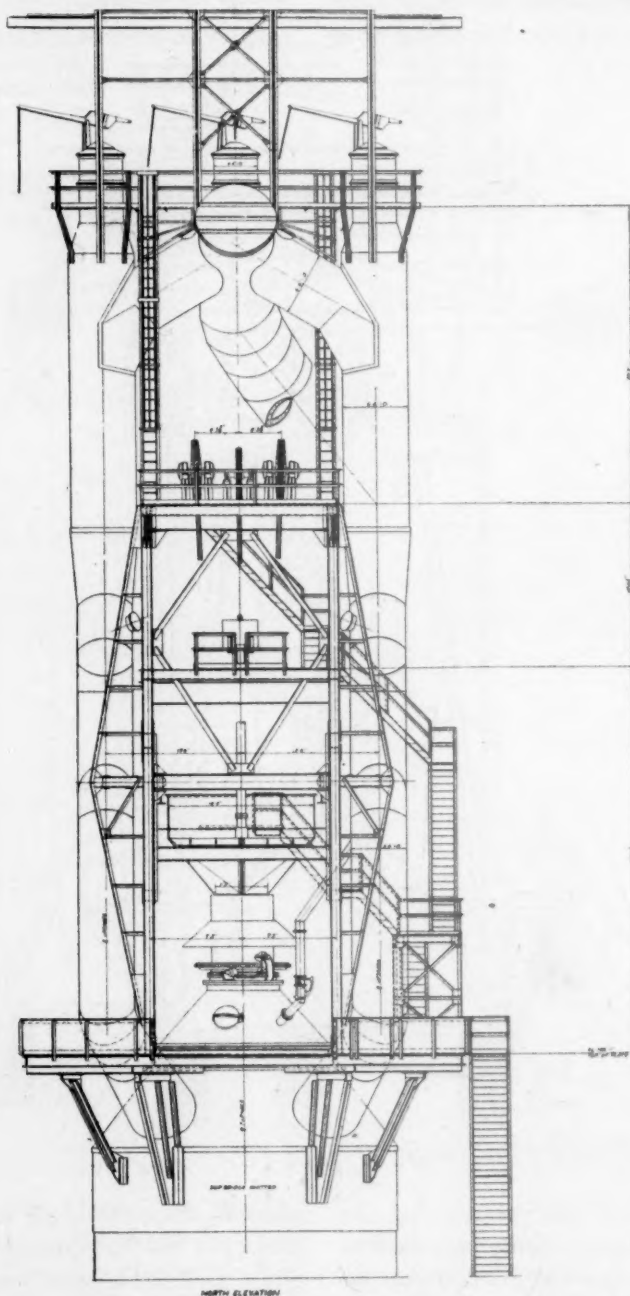
FIG. 4.—GENERAL ARRANGEMENT OF

transmitted to the foundation by the support of the skip bridge against the furnace stack. From the standpoint of furnace foundations, therefore, there is no great supporting the skip incline against the furnace stack it is possible also to reduce the cantilever at the upper end of the bridge, reduce the total weight of the structure for

an equally rigid bridge and eliminate the necessity of obstructing the cast-house floor with structural supports.

operation, in view of the fact that all materials except coke must be handled in this manner. To fill the present large fur-

SECTION LOOKING EAST
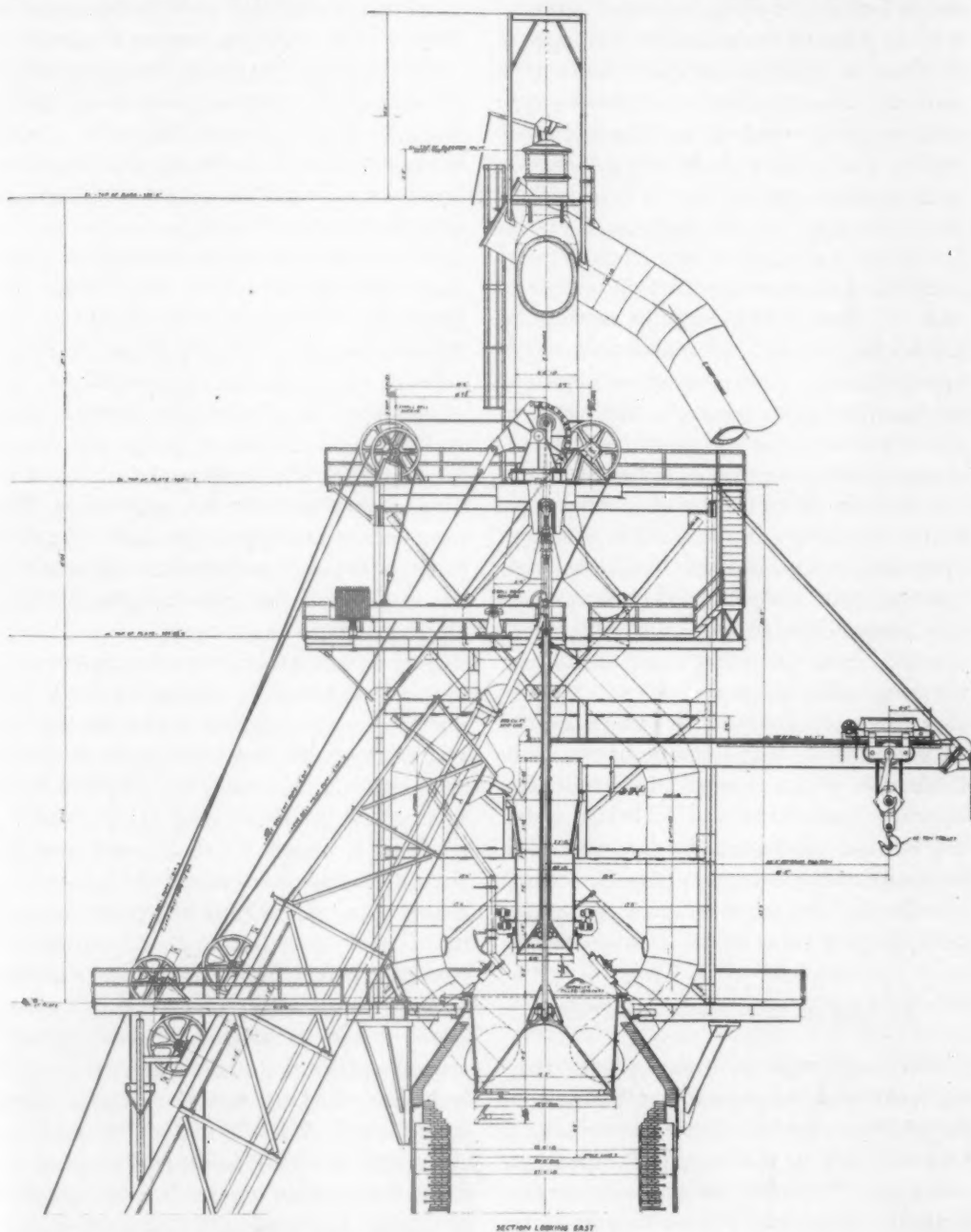
TOP STRUCTURE INDEPENDENTLY SUPPORTED.

STOCKHOUSE

The drawing of material from the stockhouse bins into the scale car is a major

naces, upward of 3000 tons of ore and stone is measured and charged in 24 hr. It is important that the equipment that handles

this material not only operates easily and quickly but is dependable and economical. To accomplish this objective, there is a choice between hand-operated and mechanical bin gates. A few miscellaneous types of mechanical gates are still in operation in some blast-furnace plants, but the only type that is widely used is the rotating drum feeder. The advantage of this gate over a hand-operated gate is that it involves less physical labor for the scale-car operator. In regard to speed of material handling and accuracy of measurement, there is little to choose between them, and the mechanical gates afford no saving in labor over hand-operated gates. The maintenance necessary on the mechanical gates is very high as compared with the maintenance on hand-operated gates. A motor or drive failure will incapacitate an entire stockhouse, whereas only a scale-car failure can slow down the operation of a stockhouse having a hand-operated gate. A recent development, which has improved the performance of the hand-operated gate on sticky ores, consists of the installation above the gate of a flexibly supported channel member, which can be deflected by a sharp opening of the gate. Deflection of the channel member breaks loose any material inclined to bridge across the bottom of the bin at the gate. The hand-operated gate makes possible a much roomier and cleaner stockhouse and causes less spillage while material is being drawn.

AUTOMATIC CHARGING OF COKE

Most large, modern furnaces where charging operations are entirely controlled from the scale car require automatic charging of coke to speed up the stockhouse operation and keep the furnace filled. There are two methods of automatic coke charging, the full automatic system and the preset system.

In the full automatic control, the skip sequence can be set up for any number of complete charges. The coke-charging pro-

gram is coordinated with the skip-hoist and bell-hoist controls to automatically weigh or measure by volume the proper amount of coke into any number of skips and dispatch them to the receiving hopper at predetermined points in the cycle. Operation under full automatic control requires no attention from the operator except the initial setting of the program to the desired charging cycle and the pushing of the skip start button to send up ore and stone skips.

The preset control is considerably simpler than the full automatic. It provides the possibility of automatically measuring the desired amount of coke by either weight or volume, and charging either one skip or two consecutive skips into the furnace. The setting of the control to charge coke must be done after the starting of the skip that immediately precedes the coke skips. The preset control does not include the charging program feature and therefore necessitates the pushing of the coke-charging buttons when coke is to be charged.

Both systems fulfill the primary purpose of automatic coke charging; in both the scale-car operator is free to operate the car and to draw ore and other material while coke charging is in progress. If more than two coke skips are to be charged consecutively it is necessary with preset control that the scale-car operator return to the charging panel and push the preset button or buttons again but with full automatic control it is possible to charge any number of consecutive coke skips. The full automatic system is somewhat more efficient than the preset system, but its original cost is higher and its control setup is more complicated. Without either system of automatic charging, comparable speed in filling the furnace requires a skip operator in a pulpit at the skip pit, to draw coke and to operate the skips. There is very little maintenance on either control, and since there is a saving of one man per turn the installation of such controls is fully justified on the basis of lower labor costs.

COKE HANDLING

The method of handling coke from the coke ovens, to and into the top of the furnace, provided that the ovens are at or near the furnace plant, is deserving of considerable study. After proper sizing and screening at the coke plant, furnace coke may be transported to the highline in one of three principal ways: (1) by hopper, or transfer cars, (2) by belt conveyor to transfer cars on the highline or (3) by belt conveyor systems through trippers or shuttle conveyors direct to the highline coke bins. The adaptability of one of these modes of transporting coke depends upon local conditions, relative location and distance between coke plant and the furnace plant, the number of furnaces to be served and the nature of the coke to be handled. Within limits, and in serving one or two furnaces, the conveyor system is generally the most economical method from the standpoint of initial and operating costs and from the standpoint of least injury to the coke. If more than two furnaces are to be served, the combination of conveyor and transfer cars, while somewhat higher in initial cost, provides an equally low operating cost with less dropping of coke at transfer points when coke is being carried to furnaces farthest from the coke plant.

Between the central coke bins at the skip pit and the top of the furnace, coke is generally dropped at six points of transfer, which add up to an initial height of approximately 58 ft., and as the weigh hopper, skip car and revolving hopper are filled to a total final height of about 23 ft., each piece of coke falls an average total of more than 40 ft., with six interruptions. To minimize these drops and avoid as much degradation of coke as possible, it is important that the weigh hoppers, skip cars and revolving hoppers be designed so as to obtain the largest possible cross-sectional areas and the shallowest possible heights. The capacity of the skip car should be no larger than is required for greatest flexibility in filling

and to keep the furnace full with reasonable speeds. If the physical properties of the coke to be used in a furnace make necessary careful handling to avoid breakage during filling, the usual heights through which it must drop should and can be reduced. At least one fourth of the drop can be eliminated if the foregoing observations are given careful consideration.

SKIP HOIST AND CONTROLS

There has been a great deal of difference of opinion in regard to the type of skip-hoist control best suited to the operation of the modern large furnace. Three types of controls are in use, generally referred to as rheostatic, variable voltage and series parallel controls. These differ principally in the type and arrangement of electrical apparatus used in driving the skip hoist and in the method of controlling its acceleration and deceleration during starting and stopping. Many furnaces are equipped with rheostatically controlled drives but the present trend is toward double-motor, double-generator variable-voltage drives. The selection of this type of drive in preference to the others has been dictated in some instances by the lack of sufficient direct current at the furnace site, and because of its rather marked inherent advantages. If it is necessary to install new generator and feeder capacity to furnish direct current for the blast-furnace hoist, the variable-voltage drive can be installed at little or no extra cost. The two-motor and two-generator arrangement offers no complications when applied to the variable-voltage control, and offers insurance against operating interruptions of the furnace if one unit becomes inoperable. With variable-voltage control the maximum torque is available with all speeds, smoother acceleration is obtainable, the top speed can be varied to fit any furnace production rate and more accurate speed control and consistent stopping are obtainable than with

other controls. This system also permits the use of relatively small standard 250-volt direct-current mill-type motors, which are used in all plants and which can be operated at higher voltages to obtain the required horsepower for skip operation.

The series parallel control for the operation of furnace skip hoists is a relatively new application and promises to become a close competitor to the variable-voltage control in respect of flexible operating characteristics and low maintenance costs.

SKIP CARS

Two types of skip cars are in common use today, the trailer type and the bail type. The bail type is the less expensive of the two and has many advantages over the trailer type. Its construction does not include the expensive castings that are used in a trailer skip, nor does it require the elaborate guide-rail system on the skip bridge. The trailer skip has several advantages over the bail type in that it requires fewer sheaves and less complicated reaving, thus permitting a lower top structure, and includes in its design simplified means of "taking up" the skip cable. However, both of these advantages are far outweighed by the fact that the trailer skip car requires a very much deeper skip pit. The higher construction costs of a deep pit, and the difficulty of keeping it dry and clean, has in most instances led to the choice of the bail skip car. For either, however, the skip wheels and axles should be designed so that each wheel of the skip car can revolve independently of the other wheels. Inaccuracies in machining the wheels and differences in their wearing qualities eventually cause discrepancies in the diameters of wheel treads, which causes them to slide on the skip rails when pairs are solidly pressed and keyed onto common axles. Such sliding accelerates wear of both wheels and rails and requires more frequent replacements of both wheels and rails.

STOVES

The number of stoves required for the operation of a furnace has long been a subject of controversy, and often rather fundamental concepts have been overlooked. The first of these is that the four-stove furnace plants have come down from the era during which dirty gas was used and frequent and regular shutdowns of one stove for cleaning were a necessity. The second is the fact that the total heating surface in a group of stoves used singly is not the determining factor. It is generally recognized that the maximum straight-line temperature available for any given blast volume is determined by the heating surface in one stove. If this statement is accepted at its face value, and it is assumed that a stove may be heated as rapidly as it is cooled, there is no reason why more than two stoves should be used. There are many practical considerations, however, that make three stoves necessary: (1) the time consumed in changing stoves, (2) the difficulties in burning gas at the rates necessary to fully heat the stove, and (3) the necessity for shutting down a stove for repairs. It would then appear that three stoves equipped with large burners and ample heating surface will satisfactorily take care of the furnace; and if one stove is down the two remaining stoves would be adequate to operate the furnace at somewhat lower blast temperatures than the maximum available with three stoves. This, at first glance, might seem an insufficient margin of reserve capacity, but when it is considered that all new stove installations are predicated on straight-line blast temperatures of from 1400° to 1500°F., and that most furnaces operate at below 1200°F., the penalty when operating with two stoves is not likely to be very great.

It is evident that the stove problem must be attacked primarily from the point of view of the performance capacities of a single stove and the ability to burn gas in that stove. With the present trend toward

decreased stack temperature, increased blast temperature and the use of clean gas, it has become impossible to use brick thicknesses of $2\frac{1}{2}$ and 3 in. and still maintain an economical balance between heating surface, brick mass and stove-shell dimensions. With the low stack temperatures and high blast temperature now demanded, it is necessary to reduce the average rate of heat transfer in a conventional stove to a figure below 10 B.t.u. per sq. ft. per min. The ability to heat a given blast volume to a given straight-line temperature while maintaining a limited stack temperature in a stove is determined therefore by its heating surface; or by the rate of heat transfer, which is determined by the exposed surface and not by brick mass or its heat-storage capacity. It is, of course, necessary that an adequate usable brick mass be available with this heating surface, so that the stove shall be able to carry the required heat for some specified period of time. This being the case, the heating surface of a single stove determines the maximum straight-line blast temperature that can be carried by any number of stoves; the active brick mass determines the length of time the stove can stay on the furnace; and the size of burner, combustion chamber and stack auxiliaries determine the amount of gas that can be burned and the time required to heat the stove.

In order that brick mass may be useful, it must be close enough to some exposed brick surface to allow its stored heat to reach the surface before the surface temperature falls below the required point. This distance appears to be about 1 in. Brick farther than 1 in. from the heating surface cannot be heated and cooled during the ordinary stove cycle. From this standpoint, considering only a single stove, the thickness of checker brick should not be more than 2 in. if economical use is to be made of the brick. If we now consider a group of three stoves designed to burn an ample supply of gas, and provided with enough heating surface to assure reasonably low stack temperatures, the checker-brick thickness should be materially less than 2 in. in order to obtain proper balance between heating surface, brick mass and maximum over-all economy from the stove installation. Checker-wall thicknesses of 1 to $1\frac{1}{4}$ in. are not uncommon in modern stoves. To obtain structural stability, the checkers must of necessity be laid up of special tile properly confined by a ring wall of stepped construction.

Checkers with 2-in. to $2\frac{1}{2}$-in. walls are in some instances considered necessary, in the belief that thin walls are more vulnerable than thicker ones to slagging and disintegration from alkalies in the blast-furnace gas. Neither of these difficulties, however, can be remedied by merely increasing checker-wall sizes. Slagging has been virtually eliminated by the fine cleaning of stove gas, and where alkaline conditions exist difficulties from this source are confined to the top 8 or 10 ft. of checkers. It is, therefore, a question either of applying special or superduty brick in this section of the checker chambers or occasionally replacing these checkers if failure from disintegration occurs.

CONTROL EQUIPMENT FOR HOT-BLAST TEMPERATURE

The mixing of hot and cold blast in order to maintain straight-line heats with modern stove equipment is worth some attention. The use of large and efficient small-checkered stoves burning clean gas has been productive of blast temperatures at the stove exits ranging from 1900° to 2000°F. By introducing cold blast through the mixing valve into the hot-blast main, the hot-blast valves, hot-blast trunk linings and their connections at the hot-blast main are subjected to these extreme temperatures. If cold blast for mixing is introduced at the end of the hot-blast main its lining is subjected to thermal shock, which is particularly severe at the hot-blast trunk con-

nections. Numerous lining failures have occurred at those places. This situation, combined with the necessity for installing larger hot-blast valves, trunks and mains to handle the greater volumes of blast for large furnaces, has been responsible for the more universal use of a system of blast mixing in which the mixing air is introduced at each stove into the lower part of the hot-blast trunk, where complete mixing is accomplished before the air reaches the hot-blast main. By thus limiting the temperatures in all parts of the hot-blast system to the temperature demanded by the furnace, obvious advantages are obtained. In most cases this temperature is well below 1400°F., stratification is eliminated and the hot-blast system is protected from sudden temperature changes. The additional cost of this system is not high, as the only extra equipment required is a valve at each stove and some mixer-line piping. Where this system has been used, maintenance cost of hot-blast valve lining has been greatly reduced.

Another innovation in blast-temperature control worthy of mention has been applied to a large furnace recently put into operation. In this two hot-blast controllers were used, one positioning the conventional mixer valve and the other controlling a butterfly valve in the cold-blast main between the mixer branch and the stoves. By the use of this second valve, cold air is automatically forced into the mixer line to further reduce the hot-blast temperature if a fully open mixer valve does not provide enough cold air to give the required straight-line heat of a low temperature. As the stove is cooled, the valve in the cold-blast main opens, forcing less cold air through the mixer line. When it is wide open, the valve in the mixer line takes over with the usual control sequence. The butterfly in the cold-blast main is not tight fitting, so that even though, through some fault in control, both the mixer valve and the cold-blast butterfly are closed at the same time, the blast will

not be off the furnace and no damage will be done to the cold-blast system. Such a control is advantageous in plants where, because of large stove capacities, it is necessary to manually throttle the cold-blast valves for a period in order to obtain low straight-line temperatures, since this practice usually imposes an unnecessarily high pressure on the blowing equipment.

DRY CLEANING OF GAS

The design of dust catchers has received considerable attention since the single downcomer has come into common use. With the single downcomer the dust catcher is built as a symmetrical unit, with the gas entering at the center of the top cone, where the velocity of the gas stream is reduced in an expanding nozzle that extends vertically into the dust-catcher chamber and has an included angle of from 8° to 10°. As the gas is released from the expanding nozzle it turns upward into the space between the dust-catcher shell and the nozzle and passes out of the top of the dust-catcher chamber through an annular passage around the expanding nozzle. The dust particles that are carried in the gas accelerate in their travel through the expanding nozzle and continue vertically to the bottom of the dust catcher. Separation of the heavier particles of flue dust from the gas stream takes place at the bottom of the nozzle, where the gas flow changes direction and is at its minimum velocity. Ample space is provided below the expanding nozzle to allow room for dust to accumulate in the bottom cone; the distance from the nozzle fo the bend line is about 18 ft. Dust catchers of this type now in successful operation on large furnaces (26-ft. dia. hearth) are from 30 to 35 ft. in diameter, with a straight side from 35 to 40 ft., and remove upward of 60 per cent of the flue dust from the furnace gas.

Dry centrifugal dust catchers have been used frequently for secondary cleaning of hot gas before it enters the boiler burners.

Efficiencies up to 90 per cent are obtained on some installations, and it appears safe to assume that an amount of dust equal to half that caught in the dust catcher can be removed in a centrifugal. Unless there is some need for additional dry dust, it is not necessary to install a centrifugal ahead of a wet washer where the sludge is being reclaimed from the washer overflow, as this dust is certain to be caught in the wet washer without adding to the load on the washer.

PRIMARY GAS WASHERS

Many attempts have been made to solve the problem of satisfactory wet washing in a single tower scrubber without excessive use of power. Many units have been highly successful at one plant but duplicate installations operating under different furnace conditions have produced decidedly poorer results. The original static tower washers designed to operate at low pressure differentials have in many instances given reasonably good results without excessive consumption of water. However, this type of primary gas washer serves principally as a gas cooler, in which contact between gas and water is brought about by the combined action of water sprays and hurdles through which pass the gas and sprayed water particles. Gas and water contact depends primarily upon the impingement of gas against the wetted surfaces of the hurdles, which are likely to plug unless gas and water distribution through the unit can be perfectly maintained. The introduction of one or two low-head recirculating pump units in the form of rotors in the bottom of the tower washer, to create a more intimate contact between gas and water before the gas reaches the hurdles or tile baffles, has in such installations virtually removed the difficulties from plugging of both hurdles and the washer bottoms. In many instances these rotor elements have made it possible to reduce the water consumption from 30 gal. to about 20 gal. per 1000 cu. ft. of gas.

FINE GAS CLEANERS

The choice between disintegrators and precipitators for fine cleaning of blast-furnace gas must in general be made on the basis of two main factors, the cost of capital and the cost of power. This statement is based on the fact that a disintegrator installation is generally considerably cheaper than a precipitator for the same work, but the power requirements are very much greater. There are, however, many other factors to be considered in choosing between these two types of equipment, each of which has very definite advantages and disadvantages. Aside from the lower initial costs, the disintegrator has the advantage of being capable of boosting, of flexibility in the matter of regulation of cleaning efficiency, of simple and easily maintained adjustments and of consistent performance under wide fluctuations of inlet loading. Offsetting these advantages are the disadvantages of higher operating costs, greater water consumption, higher maintenance costs and the possible dangers in producing a negative pressure in the gas system in case of a sudden loss of gas pressure at the disintegrator inlet. The precipitator, on the other hand, has the advantage of low operating costs, small water consumption, minimum of moving parts and very low gas-friction losses. However, its adjustments are somewhat difficult to maintain under some conditions, its efficiency is not constant under severe conditions of inlet loading, its flushing water must be relatively clean and the cost of protecting its wetted surfaces is high if corrosive water is to be used.

Space requirements in many plants have been and will continue to be more of a factor as furnaces and auxiliary equipments are enlarged on existing sites. In order to conserve ground space, precipitators have
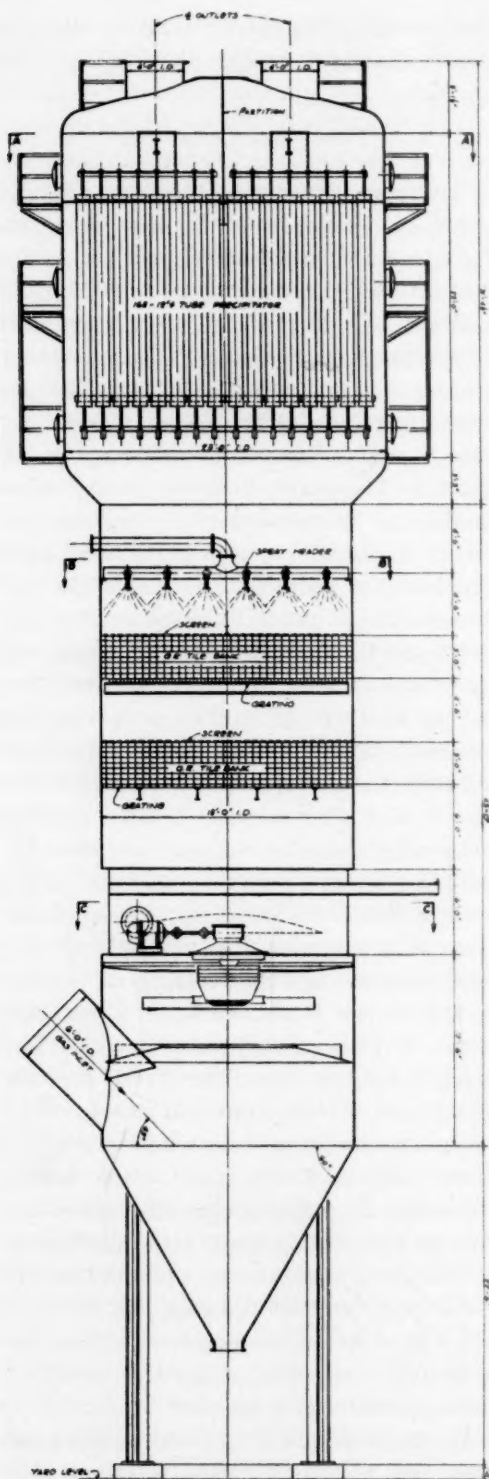
FIG. 5.—PRECIPITATORS SUPERIMPOSED ON PRIMARY GAS WASHER.

been and are being superimposed on the primary gas washer, with excellent results. This type of installation, as shown in Fig. 5, is not a great deal cheaper, if any, than one in which the precipitator is on the ground, but has the marked advantage of reducing the ground space required and simplifying the gas-main and sewer layouts. The number of valves is reduced and the operating hazards are diminished.

The degree of cleaning required for various plant uses of blast-furnace gas depends upon local conditions and the extent to which use is made of this gas. If the cleaning of gas for coke ovens and metallurgical purposes is eliminated from this consideration, the principal uses for this gas are in stoves and boilers. The modern high-efficiency stove should not be subjected to continued firing with gas containing more than 0.025 grain of dust per cu. ft. Gas cleaner than this can be justified in many cases, for as the dust content is allowed to rise, the life of the top checker brick is materially reduced by the fluxing action of the dirt on the checkers.

The gas for firing boilers can be considerably dirtier than that used on stoves if the steam-generating units are properly baffled and arranged for a wide tube spacing. In such boilers primary washed gas ranging from 0.15 to 0.30 grain per cu. ft. gives reasonably satisfactory results, although the burners and boiler tubes must be cleaned at frequent intervals. In some places, raw gas delivered from a secondary dust catcher or centrifugal, containing one to two grains of dust, is fired in combination with pulverized fuel and the slag formed by the dust merges with the fused ash in coal and is disposed of by the ash-handling equipment. Where, however, the surplus blast-furnace gas forms a large part of the boiler fuel, it is economical to clean all blast-furnace gas to the same cleanliness as is required for high-efficiency stoves. This simplifies the gas system and reduces to a minimum interruptions in boiler operation.

Each new furnace installation or new blast-furnace plant presents new and varying problems that affect both design and construction. Operating practices, raw materials and purposes for which the pig iron, slag and blast-furnace gas are to be used are items of first importance. Conditions at the site, space limitations, subsoil conditions, water supply, climatic conditions and operating requirements are factors that require that each furnace and its auxiliaries be "tailor made" to suit local conditions and the individual ideas of the operating staff.

Results Obtained from Surveys of Gas at Furnace Tops

By James M. Stapleton,* Member A.I.M.E.

It has long been recognized by blast-furnace men that correct top distribution of materials is very important in efficient and economical furnace operation. Thousands of experiments on top design, filling, sizing, and other operations have been carried out to improving furnace performance by securing uniform distribution. Many of these experiments have worked out satisfactorily and have been passed along to the industry. Many of them have been discarded and forgotten.

It has been the custom to judge the results of such experimentation by the results shown in improved or lowered furnace efficiency. While the effect on furnace practice will have to continue to be the final criterion of experimental changes, it has always been a desire of blast-furnace men to ascertain the reason for failure or success.

Efficiency in the blast furnace approaching the maximum can be measured in several ways: (1) by actual operating results as revealed in the coke rate and tonnage figures, and (2), in the degree to which the top gas approaches the limiting ratio of CO/CO_2 for the reduction of iron oxide by CO gas. This ratio is shown in the equilibrium curve in Fig. 1 for the system Fe-O-C and CO_2-CO-C. The closer the top gases approach this limiting ratio (set at 1.08 by Martin[1] because of the effect of limestone calcination) the more efficiently we may expect a furnace to operate. The fact that low CO/CO_2 ratios parallel efficient operating performance caused us to investigate the cause of good or poor distribution and the effect of filling and other changes on furnace operation.

Heretofore it has been possible to take a sample of furnace gas (usually from the dust catcher) and from it determine how closely the reducing gases were to the ideal or limiting value as set by the equilibrium diagram. However, to find just where in the top area the distribution was distorted and the top-gas CO/CO_2 ratios were distant from equilibrium values has been a difficult and expensive investigational procedure. In an effort to overcome this difficulty, apparatus was designed to take gas samples and temperatures across the top radius of the furnace. It was hoped that with the aid of this apparatus traverse sampling of the ascending gases could be simplified, and the cost of sampling substantially lowered. Routine experimenting could then be maintained and results checked with furnace operation. It must be emphasized that a traverse sampling is necessary for a true picture, as single samples at any one point are unreliable. This statement can be verified by an examination of Tables 3 to 6, showing results obtained at our furnaces in a large number of tests.

APPARATUS

The design of the equipment for taking the samples was governed by the need for providing a simple, routine test that could be performed fairly quickly without adversely affecting normal furnace operation.

Six holes were cut through the furnace shell and dome brickwork, and six guide tubes of $1\frac{1}{2}$-in. mild-steel pressure pipe, 4 ft. 10 in. to 6 ft. 6 in. long, were installed

was 90° from the iron notch while on No. 4 furnace it was on a radius to the iron notch. The arrangement of the gas-sampling apparatus for the furnace is
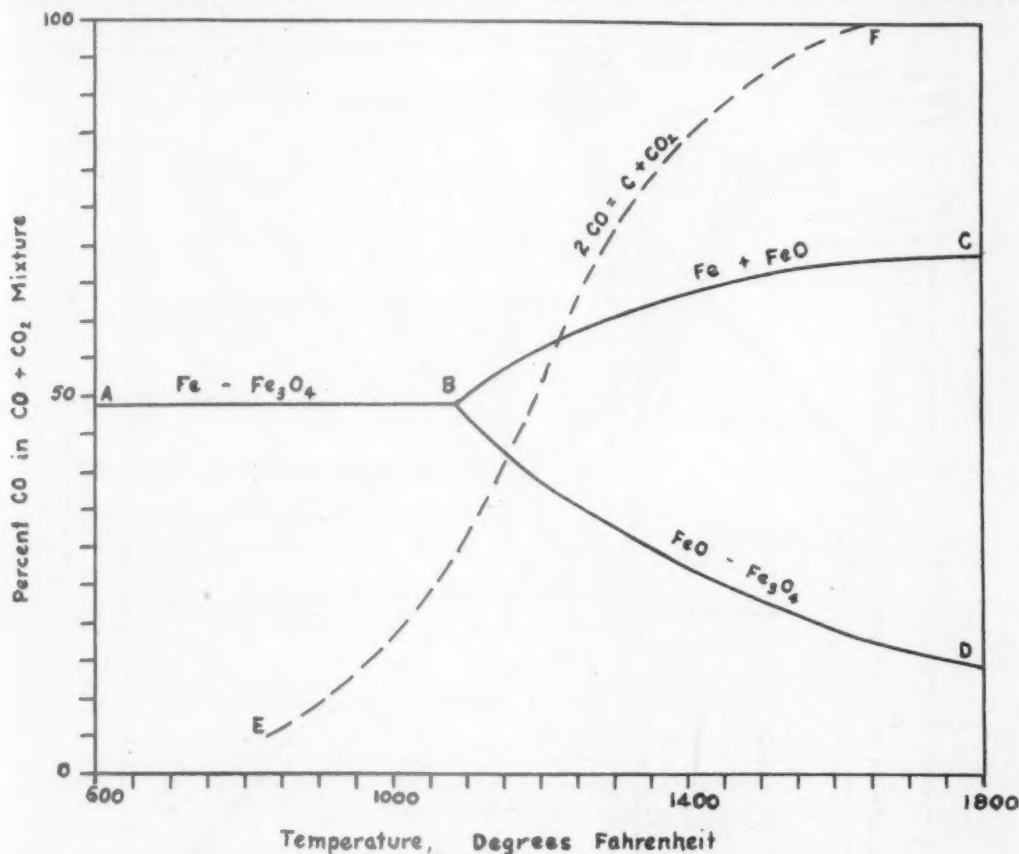

FIG. 1.—EQUILIBRIUM IN THE SYSTEM IRON-CARBON-OXYGEN.

in the furnace dome at angles ranging from 49° to 85° to the horizontal. The outer ends of these tubes extended 2 ft. 4 in. up from their intersections with the shell dome and were capped with gate valves. These valves are accessible through a trap door in the floor of the deck ring platform. This arrangement permitted the insertion of the sampling pipes into the interior of the furnace and was designed so that the points of intersections of the sampling pipes with a plane lying 8 ft. below the large bell (closed position) divided the furnace radius into segments of approximately equal length. The location of the line of sampling on Nos. 2, 5 and 10 furnaces

shown in Fig. 2. A rack for raising, lowering, and storing the gas-sampling pipes is shown in Fig. 3 and details of pipes in Fig. 4. Furnaces Nos. 2, 4, 5 and 10 were equipped for this experimental work in 1938 and 1939.

Before sampling is started, the furnace is filled approximately to the zero stock level (4 ft. below the large bell in closed position). During the sampling operation, gas samples are taken as nearly simultaneously as possible and the temperatures are observed consecutively. Time of sampling, exclusive of preliminary preparations, should take about 10 minutes.

INFLUENCE OF TOP AREA

Before discussing results at South Works it might be well to digress to quote some figures from Kinney's work,[2] to show how larger top diameters, as shown in Table 7. The dimensions of the 17-ft. furnace indicate that the outer foot and a half of the plane, which is the area normally covered
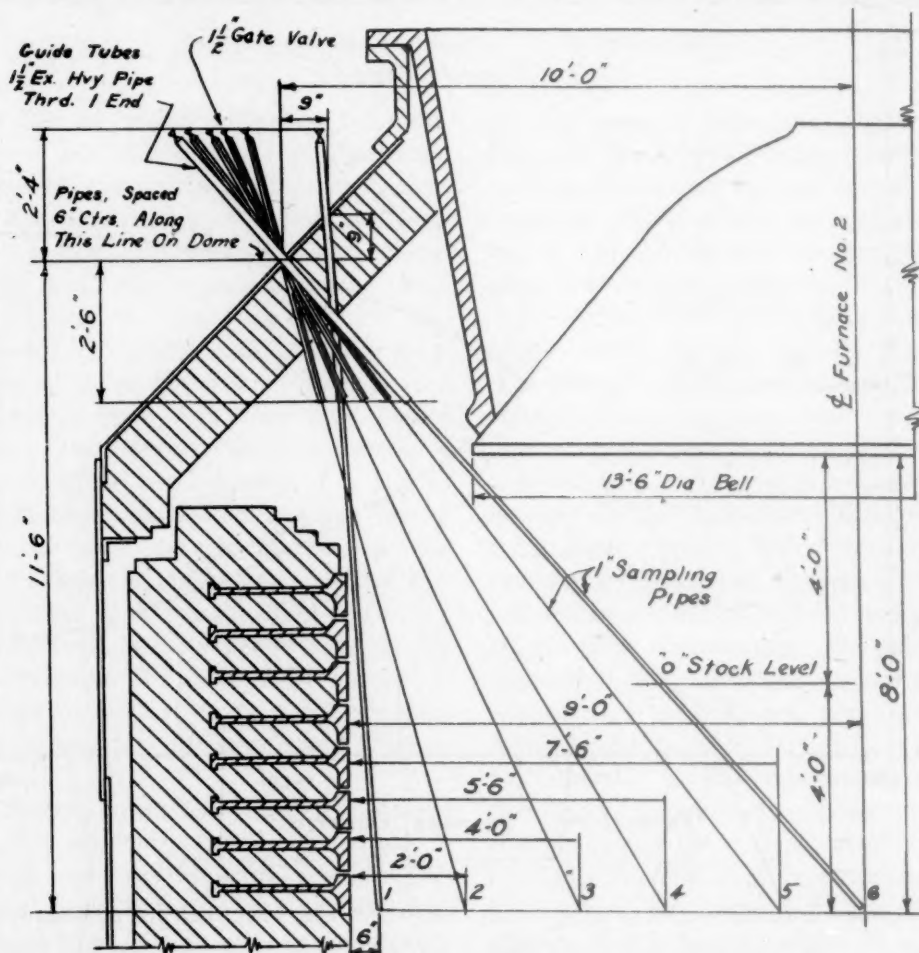

FIG. 2.—SAMPLING ARRANGEMENT, NO. 2 BLAST FURNACE.

important the outer rings of the furnace area are and how relatively unimportant the area represented by the central rings is to the whole.

Kinney took gas samples and temperatures across a plane 3 ft. below the level of the stock in a furnace measuring 17 ft. in diameter at this plane which was in the top straight section. The figures in Table 1 are taken from Kinney.[2]

The furnaces under consideration, Nos. 2, 4, 5 and 10, at South Works have even

by pipe No. 1, contains about 32 per cent of the area of the top section of the furnace. In furnaces with larger tops, the No. 1 pipe would still cover the same percentage of top area if the pipes are installed as on the furnaces at South Works. In Table 2 is shown the area relationship of the various concentric circles of an 18-ft. circle. It is obvious from these ratios that distribution in this outer area should be good and that a favorable CO/CO_2 ratio should be maintained.

Maintenance of such a favorable ratio is not always easy. In a furnace already built and operating it can sometimes be in stock level; variations in order of filling; a change in the physical character of raw materials; or combinations of several fac-
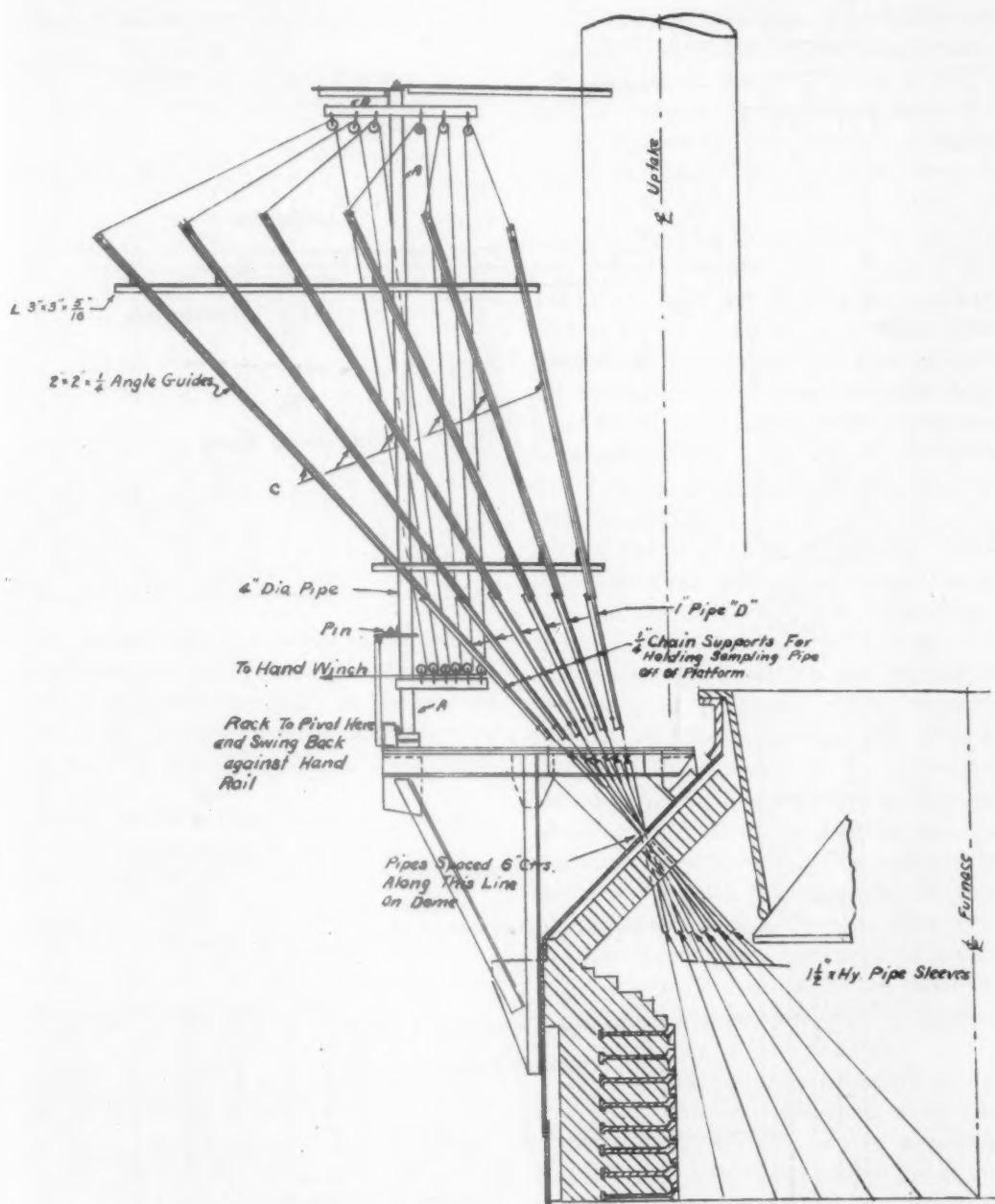

Fig. 3.—Sectional elevation showing gas-sampling pipe rack.

attained or approached by filling changes; by a change in the speed of lowering the bells, the large one in particular; a change tors. Tests made on an operating furnace where such changes have been tried and with which the desired results have not
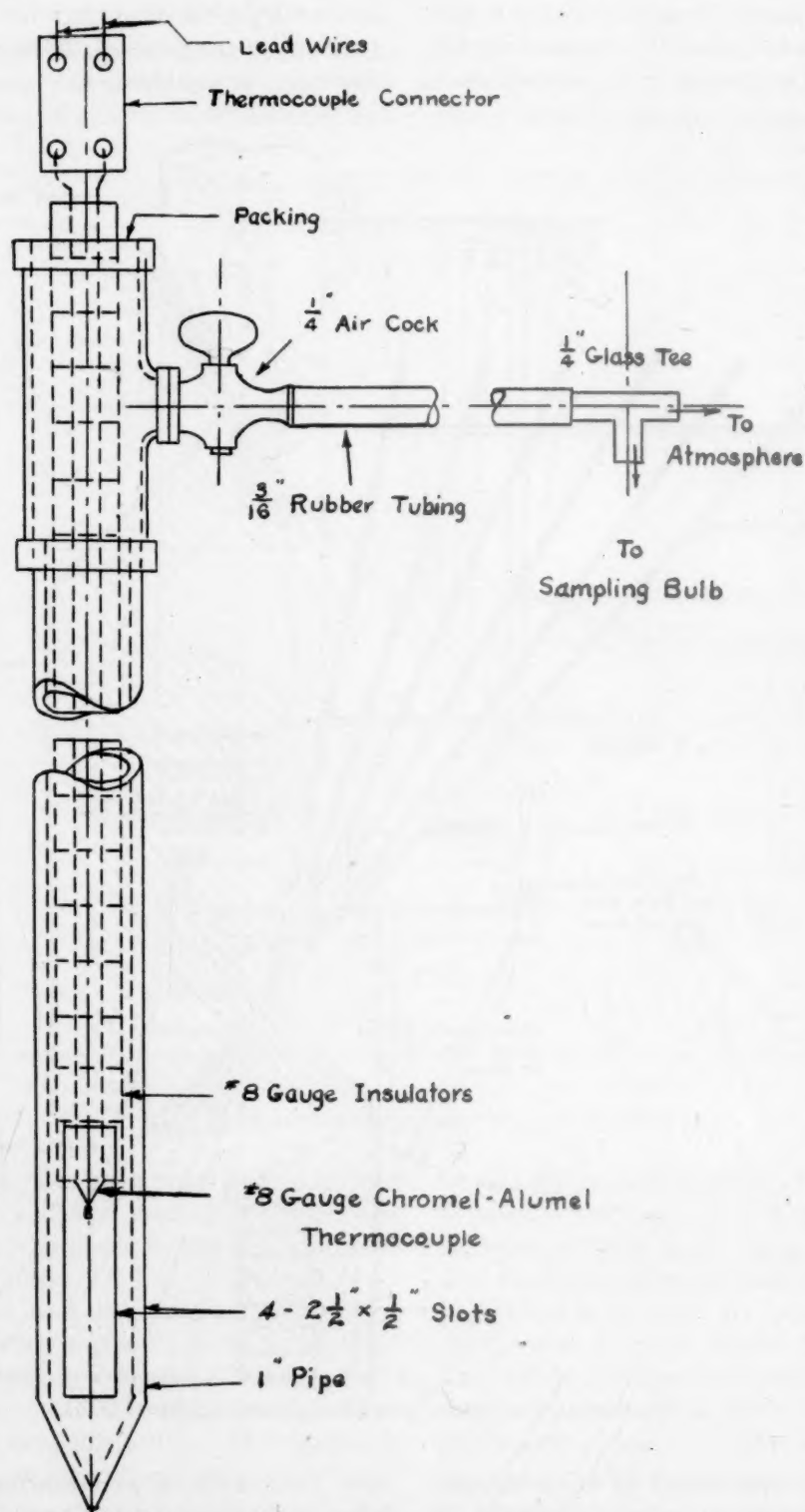
FIG. 4.—SAMPLING PIPE.

been obtained will aid in design of future furnaces, both in the lines and bell and hopper design.

In this paper, the importance of favorable gas ratios at the walls is stressed, with

TABLE 1.—*Kinney's Figures*

Annular Ring	From		To		Area	
					Sq. Ft.	Cumulative Per Cent
	Ft.	In.	Ft.	In.		
1	0	0	0	6	25.92	11.42
2	0	6	1	0	24.34	22.15
3	1	0	1	6	22.78	32.18
4	1	6	2	0	21.21	41.52
5	2	0	2	6	19.63	50.17
6	2	6	3	0	18.07	58.13
7	3	0	3	6	16.49	65.39
8	3	6	4	0	14.92	71.96
9	4	0	4	6	13.35	77.84
10	4	6	5	0	11.78	83.04
11	5	0	5	6	10.22	87.53
12	5	6	6	0	8.64	91.34
13	6	0	6	6	7.06	94.45
14	6	6	7	0	5.51	96.88
15	7	0	7	6	3.92	98.61
16	7	6	8	0	2.36	99.65
17	8	0	8	6	0.78	100.00

the thought that the ratios in the center of the furnace are relatively unimportant and their influence negligible. Aside from the small amount of area and gas flow represented, there is another serious factor,

TABLE 2.—*Area Relationship of Concentric Circles of an 18-foot Circle*

Annular Ring	Distance Wall to Center of Annular Ring		Area of Annular Ring, Sq. Ft.	Percentage of Total Area
	Ft.	In.		
1	0	6	53.30	20.9
2	1	6	47.00	18.5
3	2	6	40.96	16.1
4	3	6	34.70	13.6
5	4	6	28.24	11.2
6	5	6	22.00	8.6
7	6	6	15.71	6.2
8	7	6	9.45	3.7
9	8	6	3.14	1.2
			254.50	100.0

which was pointed out by Furnas and Joseph,[3] of the Bureau of Mines. They presented mathematical proof that "a bed in which the particle size is uniform over the whole cross-sectional area will offer more resistance to the flow of gas than a bed in which the sizes are segregated." Since bosh gas has a uniform composition, a uniform distribution of particle size throughout the entire furnace should manifest itself in a nearly constant CO/CO_2 ratio up through the shaft and across the whole top section. A furnace operating under these conditions would have a higher blast pressure, which might, in extreme cases, amount to three or four pounds per square inch. Furnas and Joseph[3] cite the layered filling of separate sizes at Provo, Utah, as a case where more uniform size distribution and more uniform gas distribution increased the blast pressure. Therefore, it might perhaps be better to sacrifice some efficiency at the place where it can be best sacrificed and most easily controlled.

It is not likely that changes in distribution or stock descent will revolutionize blast-furnace practice. If it is assumed that the conditions outlined by Kinney[2] are universally true, the rate and method of stock descent will have a minor effect on furnace efficiency. Furnas and Joseph[3] computed average particle size at various planes from the data collected by Kinney, which seem to show that particle size, and therefore the distribution, are uniform by the time the stock has descended to plane 3; that is, 24 ft. below the zero stock level. Further investigation of the kind undertaken by the Bureau of Mines should be carried out on other furnaces to establish the universality of their findings.

This condition of uniform distribution at this level, however, does not mean that distribution at the top can be neglected. Even though only 10 per cent of the reduction has been accomplished at the 24-ft. level, uniform heat transfer to the stock has been retarded and the amount of reduction has been held down if the distribution across the top was poor. The fact that the stock may descend by one method or rate

may have little influence below the 25-ft. level but probably does affect the reduction and heat transfer above this plane,

An excessive amount of direct reduction might be caused by unreduced materials entering the zone where direct reduction is

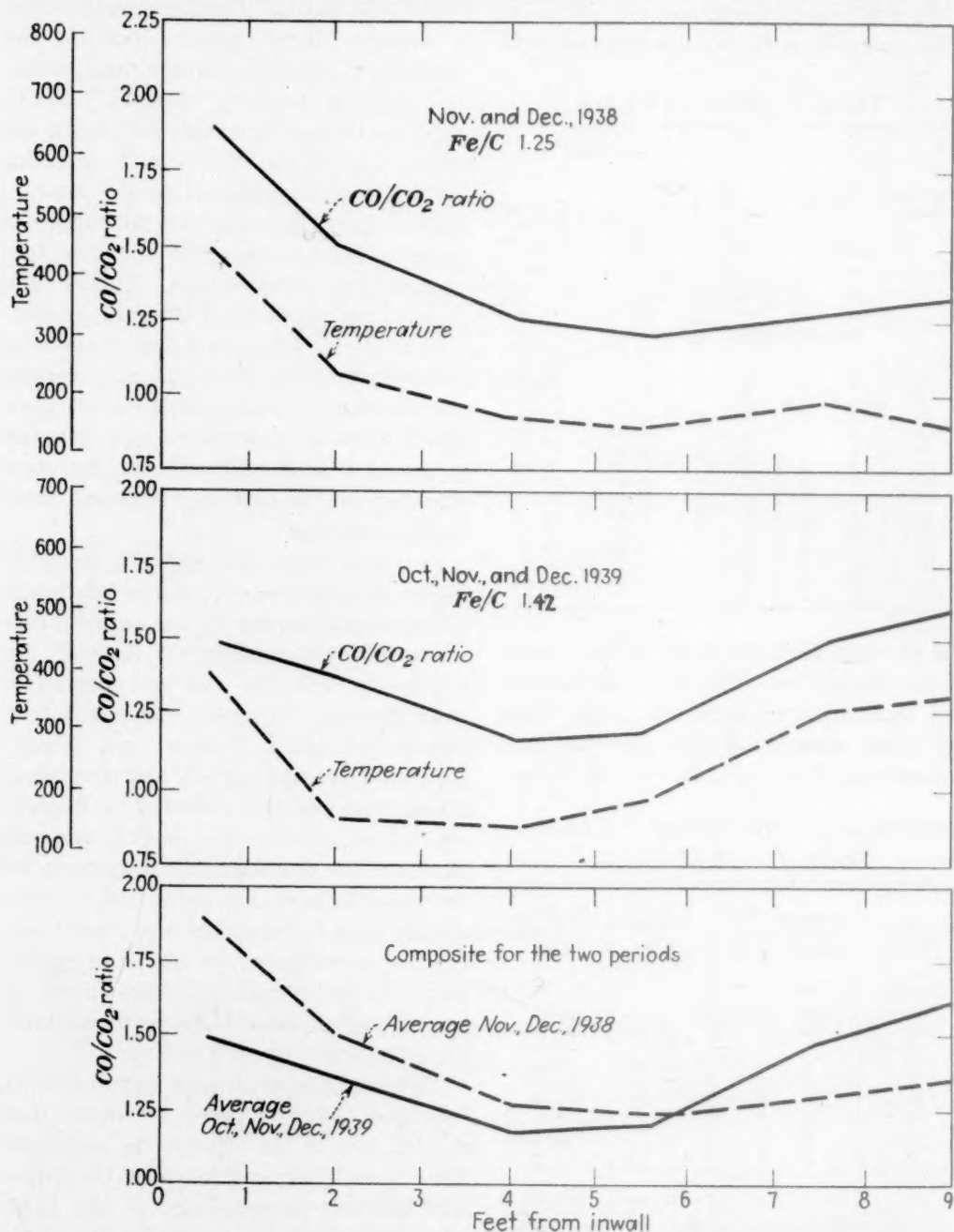

FIG. 5.—AVERAGE CO/CO₂ RATIO AND TEMPERATURE, NO. 2 FURNACE.

and it is conceivable that the distribution below this level might be adversely affected if the top distribution was poor.

dominant. In normal operation, direct reduction accounts for approximately 15 per cent of the total reduction, the heat

requirement (direct reduction, it is remembered, is endothermic) being supplied by the combustion of the coke, by indirect of insufficient temperature where the heat deficiency cannot be made up rapidly by external sources (blast heat). If this zone
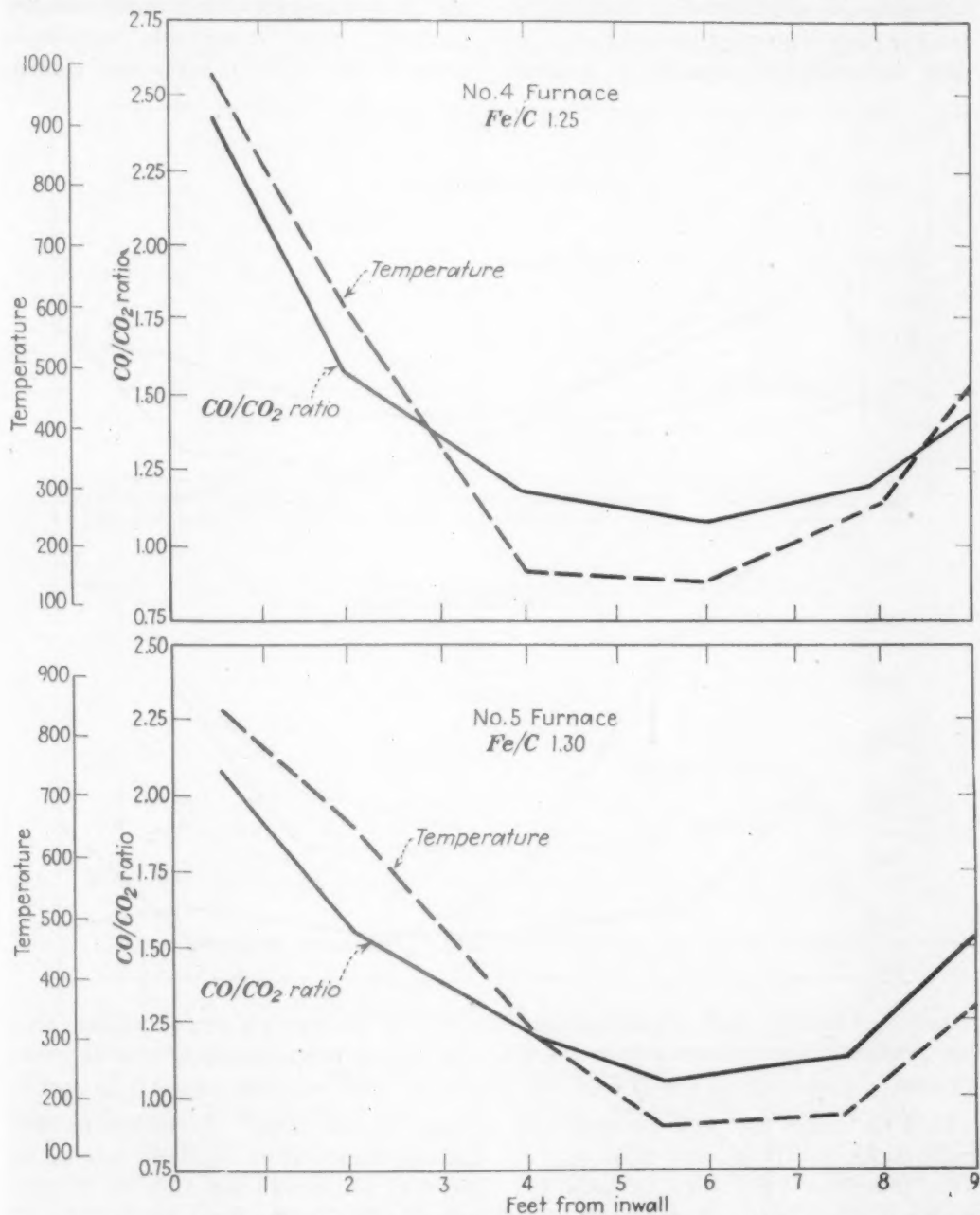

FIG. 6.—AVERAGE CO/CO_2 RATIO AND TEMPERATURE FOR 1938 AND 1939, NO. 4 FURNACE AND NO. 5 FURNACE.

reduction, and by the preheated blast. We may well reach a point where too much direct reduction will cause localized zones occurs in the hearth or bosh, furnace irregularities will be set up, causing loss of production or off-grade iron.

DISCUSSION OF RESULTS

Early Period

During the early period of sampling extending from September 1938 to June 1940, data were collected primarily to establish

took temperature readings while the gas samples were being taken. The graphs in Figs. 5 and 6 for furnaces 2, 4 and 5, showing the averages for all tests made on those furnaces, show remarkable correlation between the CO/CO_2 ratio and temper-
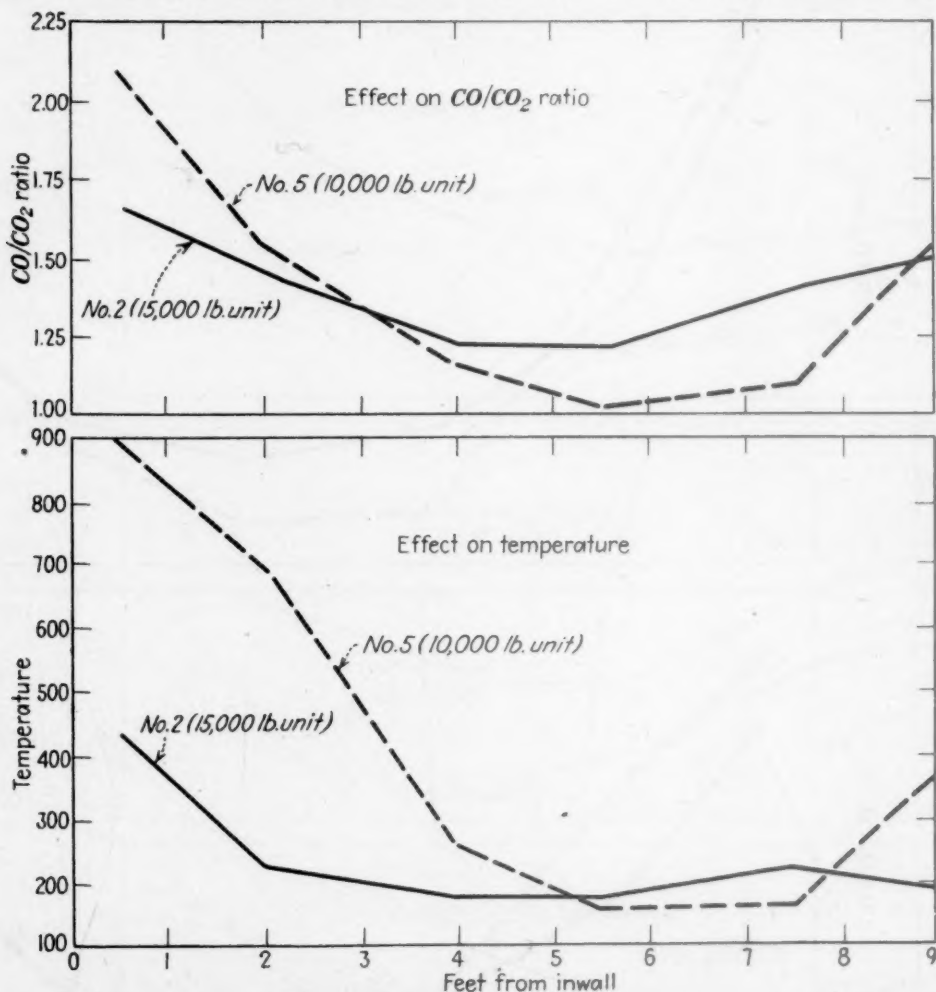
FIG. 7.—EFFECT OF COKE UNIT SIZE ON CO/CO_2 RATIO AND ON TEMPERATURE. COMPOSITE OF ALL TESTS ON NOS. 2 AND 5 FURNACES.

criteria for future use. Few changes were made, either in fillings, raw materials, or other practices. Figs. 5 to 10 show the results of these tests plotted from data given in Tables 3 to 5. Note that the wall ratios are usually high, an indication of distorted distribution or that the batter of the walls is excessive.

During the earlier part of our tests we

atures. In the future, we intend to take traverse temperature readings only as we feel they will serve adequately for investigation of distribution.

Fig. 10 represents the comparison of the CO/CO_2 ratios of the composite of all tests on Nos. 2 and 5 furnaces and the temperatures during the same period. These furnaces, as shown in Table 7, have tops

that are virtually identical, with an 18-ft. stock-line diameter and 13-ft. 6-in. bell. During the period under discussion No. 2 furnace was charged with a 15,000-lb. coke rate, and CO/CO_2 ratios obtained on No. 2 furnace, a 15,000-lb. unit was tried on No. 5 furnace, but the results were so unsatisfactory that a return to the 10,000-lb. unit
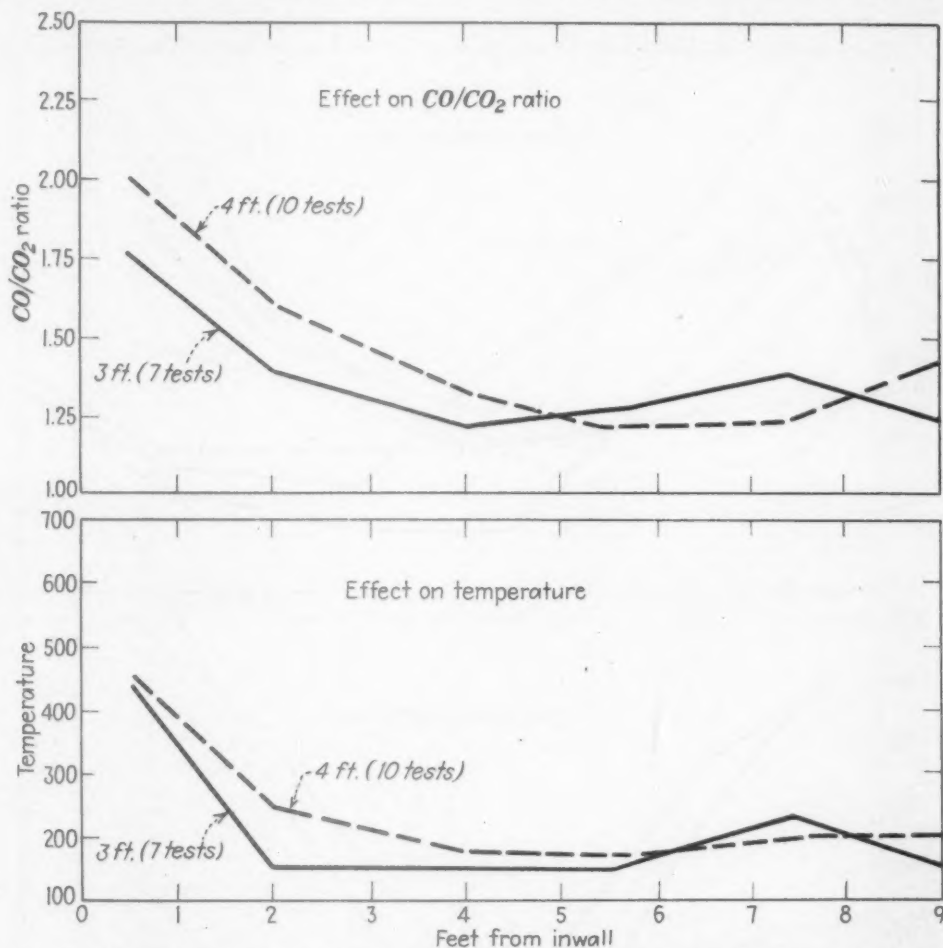

FIG. 8.—EFFECT OF VARIATION OF STOCK LEVEL ON CO/CO_2 RATIO AND ON TEMPERATURE, No. 2 FURNACE.

unit and No. 5 with a 10,000-lb. unit. The furnaces were not making the same grade of iron all the time, therefore they did not have the same burdens. The curve for No. 2 is more uniform throughout with a more favorable ratio in the outer areas. In Table 8 are shown representative burdens and charging sequence during this early period on Nos. 2, 4 and 5 furnaces. Chemical analyses of burden materials are shown in Table 9.

Because of the satisfactory tonnage, coke

was made before there was an opportunity to take any gas samples. This result may have been due to the difference in burdens, to the difference in the lines that each furnace had made for itself (both furnaces, though, were comparatively new, less than 1½ years old), or to some other obscure reason. A filling that works well on one furnace may work very poorly on another comparable furnace.

Figs. 8 and 9 show the effect of varying stock levels of Nos. 2 and 5 furnaces on the

CO/CO_2 ratios and the temperatures. On No. 5 furnace a difference of 2 ft. in the stock level made a marked change in distribution, as indicated in Fig. 9 by the furnace operators. The gas samples corroborate the observed change in furnace practice and the information obtained points the way toward further improve-
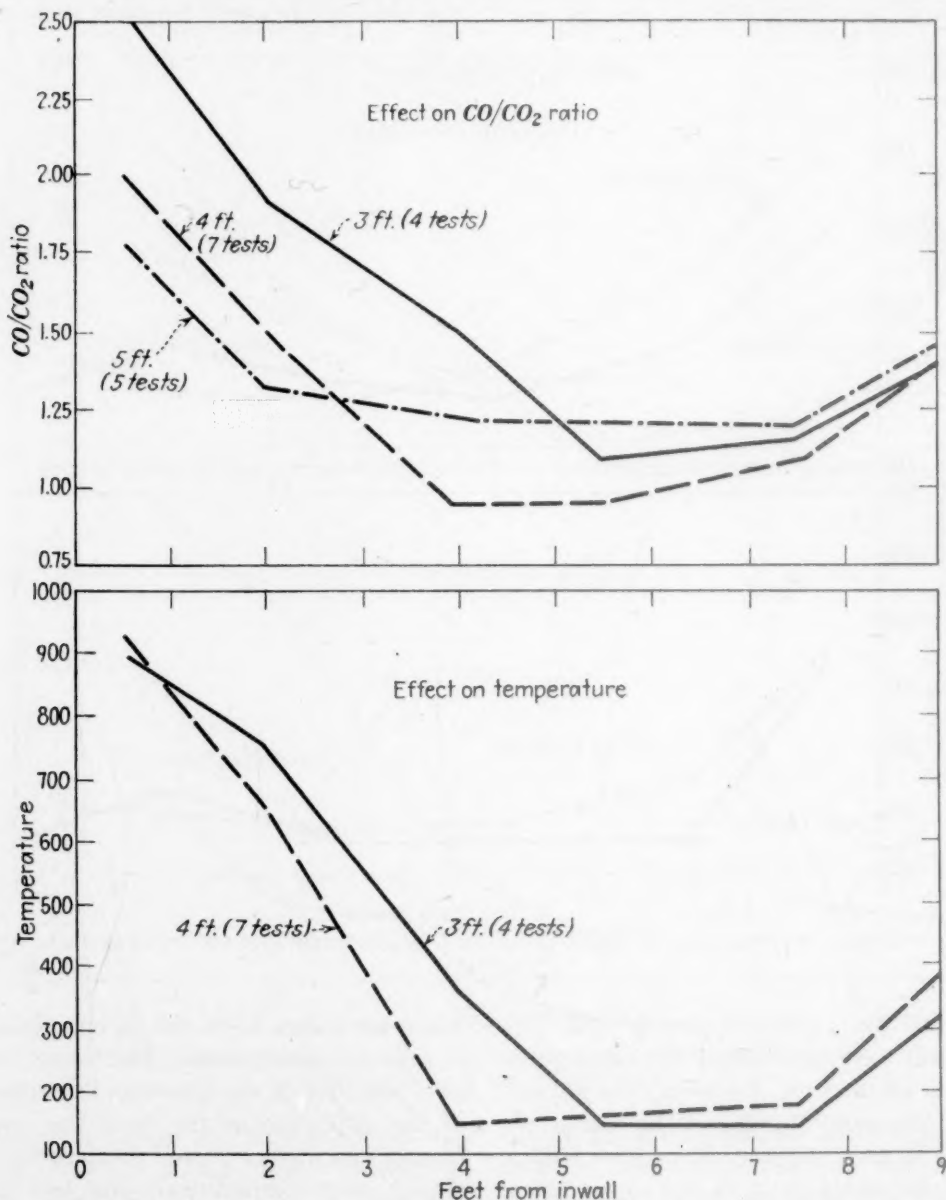

FIG. 9.—EFFECT OF VARIATION OF STOCK LEVEL ON CO/CO_2 RATIO AND ON TEMPERATURE, No. 5 FURNACE.

CO/CO_2 ratios. That so marked an improvement could be brought about by so small a change is not particularly new to ment. It must be remembered, however, that small changes in furnace lines or raw materials can upset any furnace, so that

the search for a correct stock level may have to be carried on from time to time as conditions change.

Wind rates should have some definite

that more favorable ratios were obtained with the higher wind rates. However, the number of tests is not sufficient for definite conclusions to be drawn. Correlation of
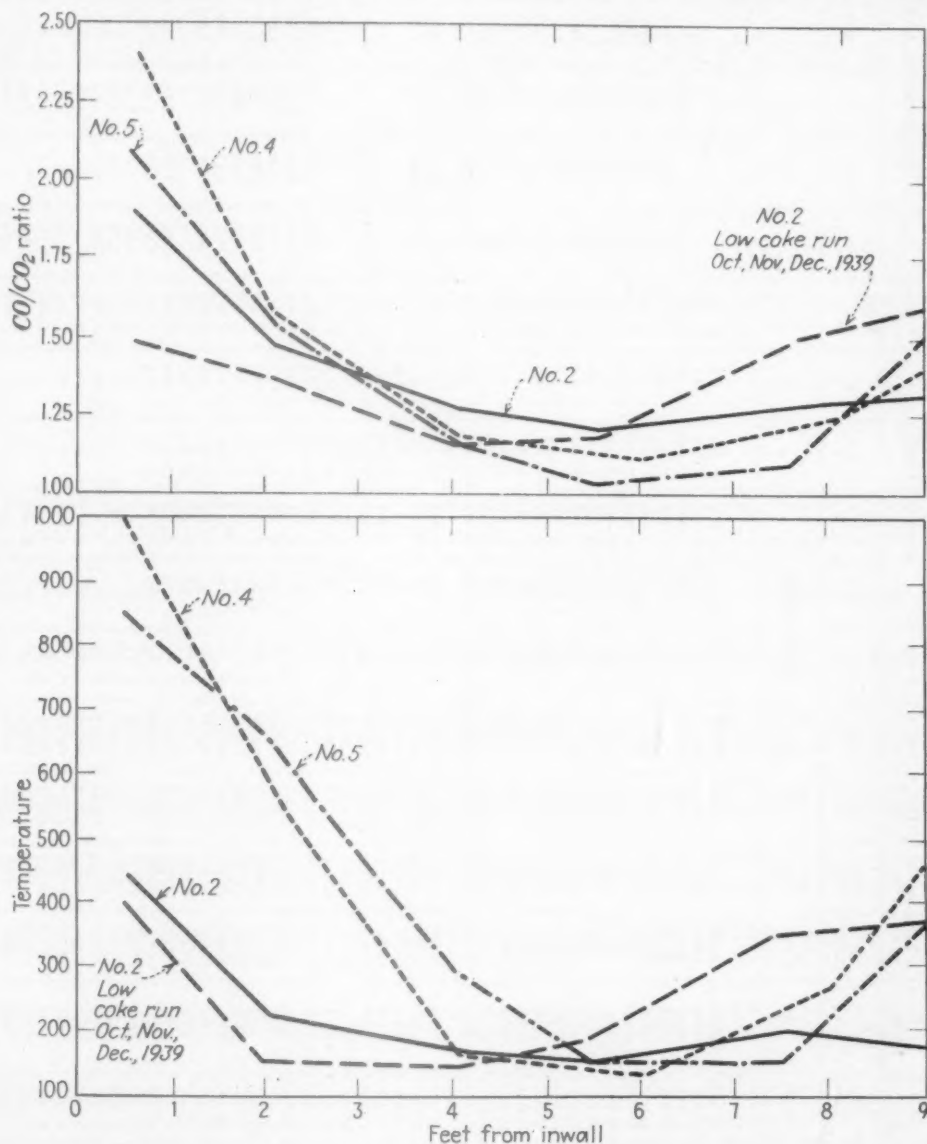
FIG. 10.—COMPOSITES OF THE AVERAGE CO/CO_2 RATIO AND THE AVERAGE TEMPERATURE FOR 1938 AND 1939—NOS. 2, 4, AND 5 FURNACES.

effect on gas distribution in the furnace. The figures shown in Tables 3 and 4 for furnaces 2 and 4 are plotted in Fig. 11. The samples were taken at periods when no other major changes were being made on the furnaces. The figures seem to indicate

wind rates with CO/CO_2 ratios at later periods has not yet been undertaken.

After this earlier period of accumulating test data, experimental work on furnaces Nos. 2, 4, 5 and 10 was carried on for some time. A discussion of the tests follows,

TABLE 3.—*Gas-sampling Data, No. 2 Blast Furnace*

Date	Time	Blast Temperature, Deg. F.	Fe/C	Slag Volume, Lb.	Tonnage D	Tonnage M	Coke D	Coke M	Ratio CO/CO₂ 1	2	3	4	5	6	Temperature 1	2	3	4	5	6
1938									**BASIC IRON**											
11-22	2P	1100	1.24	951	947	928	1470	1518	1.44	1.11	0.98	1.03	1.19	1.55	750				250	250
11-23	3P	1300	1.24	963	960	929	1464	1514	1.70	1.33	1.19	1.24	1.52	1.26	510				200	150
11-24	1P	1200	1.19	995	986	930	1440	1513	2.08	1.38	1.12	1.19	1.28	1.16	300	150	150	150	350	150
11-29	2P	1200	1.30	960	878	928	1438	1510	1.92	1.22	1.12	1.26	1.49	1.51	390	150	150	160	160	120
11-30	1P	1400	1.27	968	910	928	1416	1505	1.74	1.41	1.25	1.18	1.27	1.05	240	140	160	140	160	140
12-1	8A	1400	1.19	1,014	931	931	1545	1545	1.96	1.83	1.45	1.45	1.51	1.23	380	140	150	160	250	140
12-1	1P	1500	1.19	1,014	931	931	1545	1545	1.60	1.58	1.40	1.41	1.43	1.30	290	140	140	140	140	310
12-5	9A	1200	1.24	975	873	849	1593	1611	2.13	1.59	1.39	1.28	1.44	1.63	460	150	130	140	110	190
12-5	1P	1100	1.24	975	857	849	1605	1611	1.46	1.27	1.19	1.14	1.27	1.75	290	140	140	140	150	210
12-6	9A	1100	1.27	964	857	850	1605	1592	1.51	1.42	1.21	1.32	1.55	1.76	460	140	150	140	130	190
12-6	1P	1000	1.27	964	889	850	1568	1592	1.53	1.45	1.20	1.20	1.29	1.23	630	130	140	130	180	190
12-7	9A	1400	1.27	953	889	855	1568	1604	1.98	1.69	1.25	1.16	1.17	1.40	430	170	180	180	130	130
12-7	1P	1400	1.27	953	871	855	1507	1604	1.72	1.60	1.22	1.09	1.17	1.39	730	170	120	130	130	130
12-9	8A	1200	1.27	953	871	856	1507	1590	2.15	1.56	1.23	1.09	1.16	1.37	250	250	120	130	130	130
12-9	1P	1200	1.27	953	861	856	1507	1590	1.87	1.29	1.36	1.22	1.24	1.25	550	250	230	130	140	130
1939																				
1-3	10A	1200	1.26	887	782	792	1602	1580	2.48	2.03	1.94	1.10	1.10	1.13	690	190	190	290	490	200
1-3	2P	1200	1.26	887	782	792	1602	1580	3.44	2.25		1.54	1.30		240	940	350	240	240	210
10-19	10A	1000	1.43	762	1078	1060	1514	1511	1.39		1.03	1.15	1.20	1.50						
10-20	1P	1000	1.43	762	1110	1062	1448	1508	1.67	1.57	1.03	1.05	1.03	1.56						
10-21	10A	950	1.43	764	1052	1061	1483	1507	1.40	1.27	1.12	1.06	1.39	1.35						
10-23	10A	1000	1.43	764	1111	1064	1404	1505	1.20		1.12	1.21	1.18	1.96						
10-23	1P	1000	1.43	779	1111	1064	1404	1505	1.17	1.23	1.27	1.22	1.67	2.03						
10-24	10A	1250	1.43	779	1116	1066	1438	1502	1.39	1.41	1.26	1.36	1.85	1.82	470	360	150	150	200	220
10-24	1P	1050	1.43	783	1116	1066	1438	1502	1.31	1.36	1.57	1.56	1.92	1.55	500	200	150	150	400	150
10-25	1P	1200	1.44	795	1071	1065	1408	1499	1.19	1.16	1.18	1.18	1.73	2.36	150	150	150	150	220	170
10-26	10A	1200	1.44	795	1102	1067	1406	1496	1.28	2.09	1.09	1.42	2.83	1.73	150	120	170	510	690	600
10-31	10A	1350	1.44	789	1122	1076	1428	1480	2.07	1.23	1.17	1.19	1.16	1.65	200	130	140	100	400	270
11-1	1P	1200	1.41	795	1056	1056	1529	1529	1.39	1.32	1.03	1.09	1.28	1.73	790	130	120	80	400	510
11-2	1P	850	1.44	774	1104	1080	1390	1456	1.58	1.58	1.33	1.18	1.50	1.65	460	80	140	140	380	440
11-4	10A	1000	1.43	774	1046	1079	1511	1479	1.77	1.20	1.26	1.04	1.37	1.41						
11-6	1P	1150	1.43	789	1130	1092	1428	1468	1.33	1.20	1.30	1.22	1.30	1.36	230	120	130	140	160	220
11-7	1P	1200	1.43	848	1060	1088	1414	1461	1.79	1.65	1.28	1.11	1.13	1.63	180	120	120	230	250	270
11-8	9A	1300	1.40	792	1113	1091	1450	1458	1.41		1.13			1.63	180		110			180
11-9	10A	1200	1.43	763	1050	1086	1530	1466	1.59		1.26			1.23	550		140			150
11-13	1P	1250	1.43	763	1147	1092	1450	1465	1.46					1.85	300		180			880
11-14	1P	1150	1.43	790	1132	1095	1424	1464	1.19		1.07			1.31			130			340
11-15	1P	1200	1.43	774	1118	1098	1481	1465	1.72		1.08			1.63	650		150			650
11-16	1P	850	1.43	774	1124	1099	1419	1461	1.98		1.08			1.88	730		140			460
11-17	10A	1250	1.43	809	1115	1100	1436	1458	1.36		1.05			1.83	450		150			450.
11-21	1P	1050	1.43	783	1091	1097	1412	1453	1.35		1.00			1.71	330		140			310
11-22	1P	900	1.43		1044	1096	1462	1455	2.32		1.00			1.43			150			500
11-25	1P	1050	1.40	781	1061		1470	1453	1.14		1.17			1.28	600					

Date	Time														
11-27	IP	1115	1.40	795	1115		1482	1453	1.60	a	a	1.12	a	a	1.92
12-18	IOA	970	1.40	748	1014		1533	1502	1.96	a	a	1.01	a	a	1.36
12-19	IOA	969	1.48	720	967		1597	1506		1.67	1.00	1.26	a	a	
1940															
1-30	IIA	849	1.33	803	873	1047	1265	1566	1.77	a	a	1.41	a	a	1.42
6-11	IIA	1247	1.22	857	953	1047	1721	1575	2.50	a	a	1.14	a	a	1.10
6-12	4P	1247	1.22	857	953	1047	1721	1575	2.12	a	a	1.01	a	a	1.68
6-12	IIA	1194	1.22	839	1012	1044	1613	1578	1.79	a	a	1.04	a	a	1.55
6-13	4P	1194	1.24	839	1012	1044	1614	1578	1.51	a	a	1.13	a	a	1.29
6-13	IIA	1151	1.25	831	1010	1041	1648	1584	2.43	a	a	1.41	a	a	1.42
6-14	IIA	1165	1.25	826	1080	1041	1511	1578	1.54	a	a	1.20	a	a	1.81
6-14	3P	1165	1.25	826	1080	1043	1511	1578	1.34	a	a	1.26	a	a	1.61
6-15	IIA	1242	1.25	826	1079	1045	1524	1574	1.73	a	a	1.73	a	a	1.61
6-16	IOA	1148	1.28	816	1033	1045	1533	1572	1.72	a	a	1.50	a	a	2.89
6-17	3P	1097	1.31	803	931	1038	1701	1578	1.19	a	a	1.05	a	a	3.30
6-18	IOA	1073	1.31	803	1075	1041	1488	1572	1.62	a	a	0.99	a	a	3.04
6-18	3P	1073	1.31	803	1075	1041	1488	1572	1.97	a	a	1.12	a	a	1.91
6-19	4P	1063	1.33	781	1063	1042	1486	1568	1.48	a	a	1.12	a	a	2.22
6-20	IOA	1156	1.33	781	1041	1042	1507	1565	1.70	a	a	1.09	a	a	2.40
6-20	4P	1156	1.33	781	1041	1042	1507	1565	1.33	a	a	1.02	a	a	2.62

BLOWING IRON

Date	Time														
1940															
6-21	IIA	1293	1.21	553	1111	1045	1465	1561	1.43	a	a	0.95	a	a	1.63
6-24	IOA	1168	1.29	734	1039	1035	1506	1556	2.16	a	a	1.12	a	a	1.40
6-24	4P	1168	1.29	734	1039	1035	1506	1556	1.86	a	a	1.18	a	a	1.90
6-25	IOA	1293	1.29	751	1015	1034	1486	1562	1.90	a	a	1.05	a	a	1.33
6-25	4P	1293	1.26	755	1015	1034	1486	1562	2.04	a	a	0.94	a	a	1.21
6-26	IOA	1427	1.26	755	1043	1036	1568	1563	1.73	a	a	1.15	a	a	1.67
6-26	4P	1427	1.26	759	1036	1036	1568	1563	1.87	a	a	1.06	a	a	1.51
6-27	IOA	1387	1.23	759	981	1032	1700	1567	2.99	a	a	0.94	a	a	2.10
6-28	IOA	1285	1.23	759	1039	1033	1605	1569	2.68	a	a	1.06	a	a	1.57
6-28	4P	1285	1.21	747	1039	1033	1605	1569	1.83	a	a	1.05	a	a	1.58
7-1	IOA	1201	1.21	747	961	961	1731	1731	1.90	a	a	1.11	a	a	1.80
7-1	3P	1201	1.21	705	961	961	1731	1731	2.80	a	a	1.05	a	a	1.47
7-2	IOA	1052	1.13	705	1054	1007	1620	1674	2.07	a	a	1.12	a	a	1.73
7-2	4P	1052	1.13	717	1054	1007	1620	1674	2.12	a	a	0.97	a	a	1.84
7-6	3P	1015	1.23	717	1048	1102	1603	1709	1.86	a	a	0.95	a	a	1.67
7-6	3P	1015	1.23	731	1048	1102	1603	1709	1.48	a	a	0.89	a	a	2.97
7-7	3P	1174	1.23	731	1095	1095	1563	1673	2.09	a	a	0.95	a	a	1.72
7-7	3P	1174	1.23	726	1063	1095	1563	1673	2.01	a	a	1.06	a	a	1.42
7-10	IOA	1248	1.23	726	1048	1093	1622	1625	2.55	a	a	1.14	a	a	1.36
7-10	3P	1248	1.23	724	1048	1093	1622	1625	1.83	a	a	1.08	a	a	1.13
7-11	IOA	1251	1.24	724	1118	1095	1564	1618	1.56	a	a	1.16	a	a	1.74
7-11	3P	1251	1.24	726	1118	1095	1564	1618	1.60	a	a	1.36	a	a	1.12
7-12	3P	1138	1.26	726	1068	1092	1622	1618	2.57	a	a	1.05	a	a	1.53
7-12	3P	1138	1.26	736	1068	1092	1622	1618	1.51	a	a	1.04	a	a	1.29
7-15	IOA	1152	1.30	736	1048	1080	1659	1633	1.34	a	a	1.05	a	a	2.04
7-15	IP	1152	1.30	742	1080	1080	1659	1633	1.43	a	a	0.94	a	a	2.22
7-16	IOA	1051	1.30	758	1075	1079	1602	1625	1.95	a	a	0.93	a	a	1.30
7-17	IOA	1319	1.30	740	1020	1075	1672	1629	1.61	a	a	1.15	a	a	1.53
7-18	IOA	1325	1.30	740	1006	1070	1688	1632	1.81	a	a	1.16	a	a	1.45
7-19	IOA	1226	1.30	740	1097	1072	1528	1626	1.34	a	a	1.38	a	a	0.77

D indicates Daily.   M indicates Monthly.   a No samples taken at this point.

TABLE 3.—(Continued)

BLOWING IRON

Date	Time	Blast Temperature, Deg. F.	Fe/C	Slag Volume, Lb.	Tonnage D	Tonnage M	Coke, Lb. D	Coke, Lb. M	Ratio CO/CO₂ 1	2	3	4	5	6	Temp. Deg. F. 1	2	3	4	5	6
1940																				
7-19	1P	1226	1.30	740	1097	1072	1528	1626	1.62	a	0.76	a	a	1.67						
7-22	10A	1383	1.24	765	1060	1064	1581	1629	0.95	a	1.63	a	a	0.92						
7-22	1P	1383	1.24	765	1060	1064	1581	1629	1.49	a	1.07	a	a	1.67						
7-23	10A	1256	1.16	760	1007	1060	1713	1625	2.62	a	0.93	a	a	1.77						
7-23	1P	1256	1.22	760	1007	1060	1711	1636	1.89	a	0.88	a	a	1.50						
7-24	10A	1223	1.22	752	998	1057	1711	1636	1.55	a	1.78	a	a	1.03						
7-24	1P	1223	1.16	752	998	1057	1711	1635	2.18	a	1.14	a	a	1.75						
7-26	10A	1258	1.21	755	998	1053	1711	1645	1.74	a	1.02	a	a	1.43						
7-27	10A	1140	1.21	744	935	1048	1691	1645	1.84	a	0.87	a	a	1.36						
7-27	1P	1140	1.19	744	935	1048	1691	1646	2.62	a	1.04	a	a	1.96						
7-29	10A	1407	1.19	768	901	1038	1691	1646	1.58	a	1.07	a	a	1.42						
7-29	1P	1407	1.19	768	901	1038	1631	1631	1.65	a	1.01	a	a	1.40						
7-30	10A	1213	1.19	786	1009	1036	1274	1623	1.39	a	0.97	a	a	1.45						
7-31	10A	1215	1.20	786	964	1036	1274	1623	1.48	a	0.90	a	a	1.32						
7-31	1P	1215	1.20	786	904	1062	1586	1586	1.75	a	0.83	a	a	1.42						
8-1	10A	1255	1.20	783	1062	1062	1586	1586	0.99	a	1.14	a	a	1.31						
8-1	1P	1255	1.23	783	712	882	1781	1664	1.60	a	1.08	a	a	1.94						
8-2	10A	1266	1.14	796	987	925	1658	1673	1.11	a	1.51	a	a	1.73						
8-5	1P	1165	1.12	814	1010	939	1620	1664	1.30	a	1.02	a	a	1.73						
8-6	1P	1284	1.20	834	931	888	1802	1682	2.48	a	0.83	a	a	1.53						
8-7	1P	1413	1.20	790	807	916	1854	1702	1.67	a	0.82	a	a	1.68						
8-8	10A	1030	1.20	775	807	916	1854	1702	2.59	a	0.89	a	a	3.00						
8-8	3P	1030	1.17	787	962	921	1684	1700	3.11	a	0.81	a	a	2.20						
8-9	3P	1203	1.20	766	977	926	1074	1698	1.93	a	0.96	a	a	1.36						
8-10	10A	1268	1.20	766	923	929	1725	1994	2.61	a	1.02	a	a	2.01						
8-12	1P	1310	1.15	795	923	929	1725	1694	1.68	a	a	a	a	1.58						
8-12	10A	1310	1.15	795	1007	936	1621	1689	2.43	a	1.05	a	a	1.43						
8-13	10A	1348	1.17	791	1007	936	1621	1689	2.76	a	1.24	a	a	1.61						
8-13	1P	1348	1.20	791	938	937	1642	1686	2.86	a	1.37	a	a	1.67						
8-14	1P	1339	1.20	803	917	935	1862	1698	2.77	a	0.98	a	a	1.45						
8-15	10A	1172	1.17	803	917	935	1862	1698	1.16	a	1.05	a	a	1.91						
8-15	1P	1172	1.20	791	922	934	1700	1698	1.31	a	1.02	a	a	1.50						
8-16	10A	1321	1.17	791	922	934	1700	1698	2.24	a	0.97	a	a	1.67						

a No samples taken at this point.
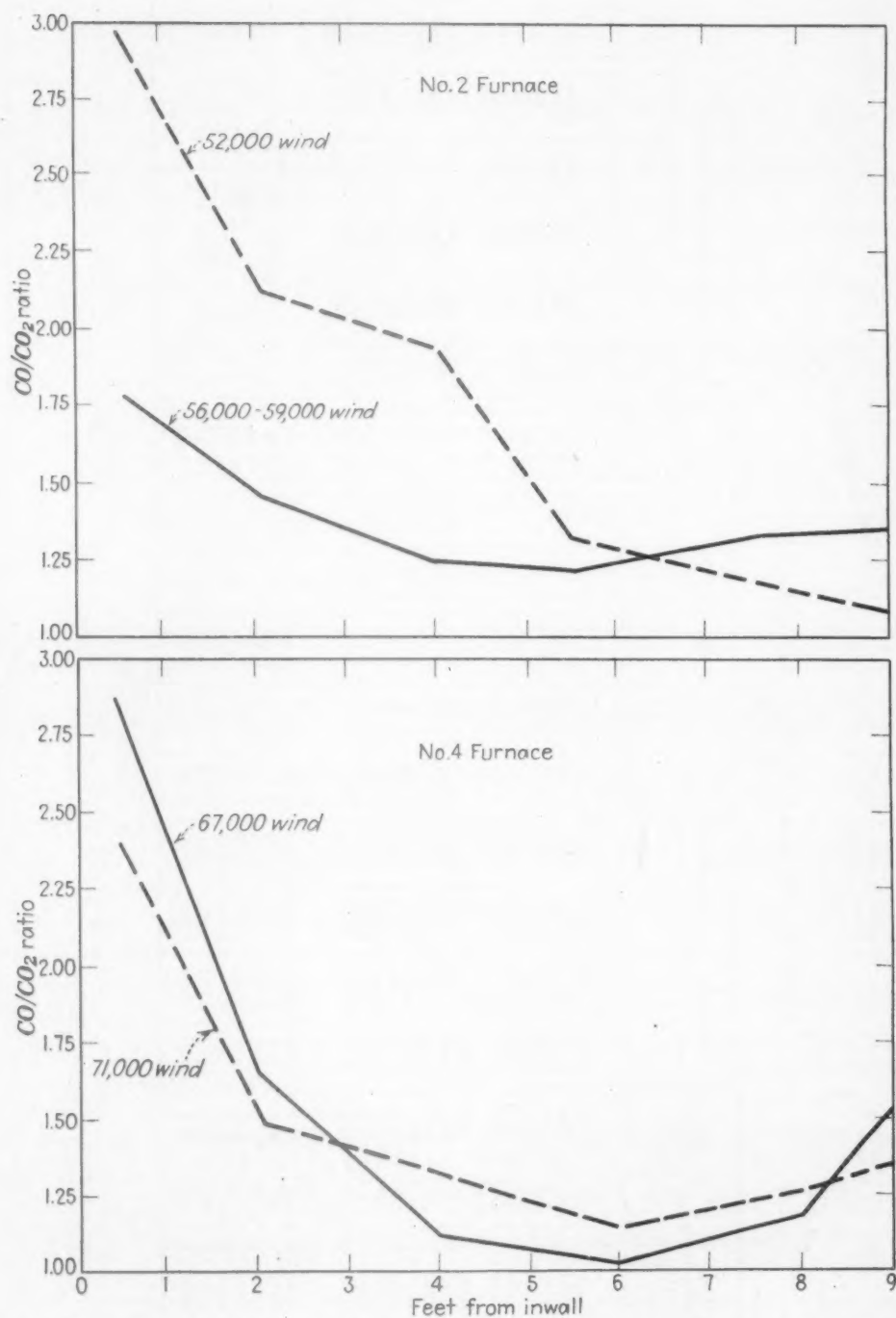
FIG. 11.—COMPOSITE GAS RATIO VARIATIONS IN WIND RATE, NO. 2 FURNACE AND NO. 4 FURNACE.

TABLE 4.—*Gas-sampling Data, No. 4 Blast Furnace*

BASIC IRON

Date	Time	Blast Temperature, Deg. F.	Fe/C	Slag Volume, Lb.	Tonnage D	Tonnage M	Coke, Lb. D	Coke, Lb. M	Ratio CO/CO₂ 1	2	3	4	5	6	Temperature, Deg. F. 1	2	3	4	5	6
1938																				
12-1	11A	1200	1.29	766	1252	1252	1404	1404	1.96	1.33	1.16	0.99	1.26	1.30	120	440	140	120	240	540
12-2	11A	1200	1.29	788	1133	1193	1510	1452	2.37	1.41	1.45	1.19	1.07	1.31	110	160	100	100	190	170
12-14	11A	1500	1.24	830	1270	1163	1421	1529	2.39	1.38	1.18	1.18	1.21	1.60	180	800	130	150	180	570
12-21	11A	1200	1.23	790	1230	1168	1452	1530		1.56	1.51	1.29	1.44	1.61	980	410	130	110	340	390
12-21	2P	900	1.23	790	1230	1168	1452	1530	2.84	1.63			1.55	1.41	1580	960	250	150	150	350
12-22	11A	1000	1.26	780	1035	1167	1530	1530		1.71	1.11	1.02	1.01	1.18	1110	530	120	110	170	430
1939																				
1-4	11A	1400	1.30	886	1065	1093	1607	1556	3.74	1.80	1.12	0.95	1.14	2.10	1260	450	120	120	380	710
1-4	2P	1500	1.30	886	1065	1093	1607	1556	1.98	1.46	1.10	1.08	1.23	1.58	980	440	120	110	190	470
6-21	8A	1300	1.25	862	1134	1071	1610	1657	1.88	2.06	1.09	1.00	1.22	1.70		250	210		640	840
6-21	1P	1200	1.25	854	1134	1071	1759	1659	1.83	1.59	1.20	1.06	1.03	1.42	1240	830	280	130	130	580
6-23	1P	1400	1.18	844	1076	1073	1550	1659	2.91	1.87	1.02	1.14	1.29	1.17	1280	980	180	180	240	800
6-28	8A	1500	1.18	844	1202	1087	1550	1659	2.91		1.07	1.03	1.19	1.91	1440	1130	220	210	340	650
6-28	1P	1500	1.27	804	1271	1107	1458	1584	2.19	1.74	1.04	1.01	1.54	1.97	1280	810	160	160	220	730
7-10	2P													1.70	1170	330	160	160	430	600
1940																				
4-1	1P	1005	1.24	821	1099	1099	1682	1682	2.01		0.94	1.51	1.29	1.24						
4-23	12N	1272	1.18	902	912	1135	1976	1636	2.64		1.40			1.87			Dust Catcher			
4-23	3P	1272	1.18	902	912	1135	1976	1636	1.28		1.12			1.93			2.30			
4-24	8A	1075	1.20	896	1155	1136	1550	1633	1.40		1.21			2.34						
4-24	2P	1075	1.20	896	1155	1136	1550	1633	2.13	1.74	1.29			1.74						
4-25	9A	1140	1.22	856	1135	1135	1618	1633	2.19		1.15			1.47						
4-27	1P	1053	1.25	852	1153	1134	1542	1630	3.05		1.10			1.64						

D indicates Daily.
M indicates Monthly.

TABLE 5.—*Gas-sampling Data, No. 5 Blast Furnace*

Date	Time	Blast Temperature, Deg. F.	Kind Iron	Fe/C	Slag Volume, Lb.	Tonnage		Coke, Lb.		Ratio CO/CO₂						Temperature, Deg. F.					
						D	M	D	M	1	2	3	4	5	6	1	2	3	4	5	6
1938																					
9-13	11A	1200	Blowing	1.33	761	965	1008	1605	1540	1.49	1.35	1.30	1.26	1.21	1.51						
9-21	10A	1000	In. mold	1.34	765	1013	1019	1606	1552	2.09	1.30	1.13	1.16	1.20	1.60		930				470
11-9	1P	850	In. mold	1.31	845	881	1008	1685	1537	1.85	1.93	1.00	0.98	1.00	1.54	1050	600	150	150	150	430
11-10	1P	900	In. mold	1.31	845	1080	1015	1415	1527	1.83	1.20	0.95	0.92	1.07	1.32	900	630	150	150	250	460
11-11	9A	1000	In. mold	1.33	820	1008	1013	1582	1530	2.33	1.89	0.92	0.86	1.00	1.06	900	500	150	150	200	310
11-16	9A	1100	In. mold	1.34	809	987	1024	1630	1536	2.00	1.24	0.77	0.74	0.77	1.51	930	650	170	180	150	300
11-17	1P	1400	In. mold	1.38	718	1106	1031	1473	1531	2.17	1.58	1.02	0.97	1.05	1.50	870			170	150	
11-18	1P	1000	Blowing	1.42	723	987	1031	1647	1537	1.79	1.29	0.96	0.98	1.23							
11-23	9A	800	In. mold	1.29	854	952	1036	1692	1539	2.07	1.42	1.06	1.18	1.26	1.64						
1939																					
1-13	2P	1400	In. mold	1.21	948	1017	972	1598	1611	1.61	1.58	1.56	1.28	1.06	1.54	380	330	200	200	200	280
1-17	9A	1200	Blowing	1.31	924	1005	968	1540	1610	3.49	2.07	1.98	1.07	1.13	1.84	1310	1240	970	120	100	310
1-20	9A	1100	In. mold	1.28	836	995	904	1582	1618	2.36	2.07	1.44	1.04	1.28	1.41	830	480	150	130	110	510
1-21	1P	1100	In. mold	1.26	836	959	963	1623	1618	2.72		1.05	1.01	1.12	2.01	1080	930	120	120	120	180
3-7	9A	1100	Blowing	1.20		879	928	1835	1790		1.19	1.18	1.16	1.07	1.25						
3-14	2P	1200	In. mold	1.26		947	938	1691	1738	1.67	1.49	1.31	1.25								
7-15	9A	1150	Blowing	1.25		904	926	1725	1732	2.03	1.79	1.17				280	280	780			380
1940																					
1-15	10A	915	Blowing	1.25	927	965	994	1699	1699	1.88			1.46		1.84						
6-17	10A	1160	In. mold	1.28	795	959	993	1707	1642	1.30			1.40								
6-18	10A	1121	In. mold	1.31	786	1038	995	1588	1640	1.24			1.20		1.52						
6-19	10A	1104	In. mold	1.28	795	1033	997	1595	1636	2.00			1.08		1.60						
6-19	2P	1104	In. mold	1.31	795	1033	997	1595	1636	1.89			1.06		1.41						
6-20	10A	995	In. mold	1.31	768	919	989	1792	1642	1.58			1.04		1.06						
6-21	10A	923	In. mold	1.31	800	972	992	1680	1642	1.81			1.21		1.44						
6-24	2P	1147	In. mold	1.31	800	1014	997	1590	1639	1.88			1.40		1.32						
6-24	10A	1147	In. mold	1.27	810	1014	998	1590	1639	2.02			1.08		1.42						
6-25	10A	1162	In. mold	1.27	810	1011	998	1622	1638	1.98			1.31		1.85						
6-26	10A	1116	In. mold	1.27	810	1007	998	1587	1636	2.01			1.10		1.17						
6-26	2P	1116	In. mold	1.29	802	1007	998	1587	1636	2.15			1.07		1.03						
6-27	10A	1062	In. mold	1.32	778	974	1102	1668	1636	1.57			1.03		1.15						
6-27	2P	1159	In. mold	1.32	778	1102	1102	1582	1582	1.56			1.10		1.37						
7-1	2P	1159	In. mold	1.32	936	1102	1082	1582	1582				1.20		1.75						
7-1	10A	1059	In. mold	1.23	770	1063	1066	1622	1602	1.73			1.10		1.23						
7-2	10A	1247	In. mold	1.33	797	1032	982	1364	1525	1.85			1.18		1.34						
7-3	2P	1124	In. mold	1.36	864	731	1069	2365	1681	1.83			1.22		1.58						
7-5	10A	1232	In. mold	1.23	812	1190	1088	1153	1637	1.84			1.08		1.17						
7-9	2P	1359	In. mold	1.36	812	1135	1082	1364	1565	1.88			1.46		1.84						
7-12	2P	1117	In. mold	1.26	838	1090	1082	1460	1544	2.21			1.22		1.31						
7-16	10A	1117	In. mold	1.26	840	1090	1085	1460	1544	2.17			1.13		1.48						
7-16	10A	1255	In. mold	1.26	840	1126	1081	1513	1542	1.55			1.26		1.24						
7-17	2P	1297	In. mold	1.26	800	1032	1081	1584	1544	3.14		1.08			1.14						
7-17	2P	1297	In. mold	1.30	856	1037	1081	1584	1544	1.52		1.07			1.06						
7-18	10A	1071	In. mold	1.30	800	1037	1060	1612	1588	1.18			1.03		1.42						
7-22	2P	1190	In. mold	1.32	856	1116	1074	1363	1561	1.55			1.21		1.19						
7-31	11A		In. mold																		

TABLE 6.—*Gas-sampling Data, No. 10 Blast Furnace*
BLOWING IRON

Date	Time	Blast Temperature, Deg. F.	Fe/C	Slag Volume, Lb.	Tonnage D	Tonnage M	Coke, Lb. D	Coke, Lb. M	Ratio CO/CO₂ 1	2	3	4	5	6	Dust Catcher
1940															
7-1	10A	1269	1.24	735	1105	1105	1705	1705	4.63			1.38	1.15		
7-1	2P	1269	1.24	735	1105	1105	1705	1705	5.41			1.13	1.14		
7-2	10A	1195	1.24	691	1243	1171	1544	1620		2.15		1.36	1.26		1.76
7-5	10A	988	1.24	724	1065	982	1698	1655		4.29		1.48	1.60		
7-5	2P	988	1.24	724	1065	982	1698	1655	3.31			1.73	1.64		
7-8	10A	1104	1.24	701	1033	1006	1798	1704		4.25			1.77		
7-15	10A	1193	1.29	716	1197	1065	1618	1703		2.81		1.35	1.22		
7-16	10A	1192	1.27	738	1208	1075	1614	1689		2.52		1.20	1.21		
7-16	2P	1192	1.27	738	1208	1075	1614	1689		2.85		1.45	1.08		
7-17	10A	1261	1.17	727	1180	1081	1629	1685		2.15		1.27	1.45		
7-18	10A	1235	1.25	668	1186	1088	1585	1679		2.85			1.15		
7-18	2P	1235	1.25	668	1186	1088	1585	1679		2.31		1.25	1.00		
7-19	10A	1223	1.22	646	1218	1095	1603	1685		2.81		1.42	1.27		
7-22	10A	1183	1.26	652	1221	1106	1626	1675		2.29		1.33	1.55		
7-23	10A	1183	1.26	652	1203	1110	1626	1675		1.55		1.29	1.23		
7-24	10A	1073	1.28	636	1080	1109	1767	1680	3.46	1.47	0.78		1.33	1.16	
7-30	10A	998	1.36	621	1119	1113	1862	1669	2.64	1.51	1.08		1.24		
8-1	10A	1085	1.25	668	1163	1163	1649	1649			1.40	1.12	1.12		
8-6	10A	1125	1.25	695	1198	1180	1651	1680			1.38	1.05	1.10	1.26	1.84
8-7	10A	1124	1.25	695	1176	1179	1616	1670			1.32	1.25	1.12	1.52	1.76
8-7	2P	1124	1.25	695	1176	1179	1616	1670			1.33	1.09		1.21	
8-8	2P	1200	1.25	682	1228	1183	1600	1609			1.25	0.88	0.97	1.24	1.85
8-13	10A	1168	1.28	653	1189	1162	1640	1659			1.62	1.35	1.11	1.69	1.63
8-14	10A	1190	1.28	640	1239	1181	1562	1653			1.20	1.50	1.18	1.32	1.63
8-16	2P	1178	1.31	638	1224	1184	1627	1648			1.19	0.95	1.17	1.56	
8-17	10A	1247	1.31	638	1274	1189	1574	1644				1.19	1.04		1.69
8-17	2P	1247	1.31	638	1274	1189	1574	1644			1.21	0.97	1.19	1.17	1.69
8-21	10A	1171	1.28	654	1255	1198	1559	1643			1.89	1.11	1.96	1.15	
8-22	2P	1185	1.28	654	1231	1199	1623	1642			1.69	1.20	1.13	1.13	1.65
8-26	10A	1247	1.28	650	1207	1200	1596	1633			1.67	1.52	1.22	1.30	1.70
8-26	2P	1247	1.28	650	1207	1200	1596	1633			1.54	1.41	1.15	1.08	1.69
1941															
1-3	2P	1041	1.21	739	1044	1110	1977	1815	2.01	2.05		1.62	1.66	1.64	1.89
1-7	2P	926	1.21	788	1163	1075	1711	1830	3.22	2.06	1.13	1.28	1.11		1.75
1-10	3P	773	1.27	745	1158	1079	1600	1804	2.91	4.15	1.33	1.03	1.44	1.27	1.87
1-15	2P	1068	1.27	745	1207	1095	1576	1758	3.46	2.36	1.37	1.21	1.11	1.22	1.74
1-21	2P	843	1.24	740	996	1075	1811	1763	4.65	1.51		1.27	1.33		2.13
1-23	2P	1003	1.22	740	718	2615	1782	1782	3.84	3.13	1.64	1.39	1.93		2.05
1-24	2P	1150	1.11	784	892	1067	1782	1782		2.35	1.17	1.15	1.21		2.06
1-27	2P	1049	1.19	741	1035	1055	1944	1781	2.17	3.60	2.24	2.06	1.55		2.02
1-28	2P	978	1.22	760	1166	1058	1775	1781	3.60	2.63	1.41	1.21	1.13		2.02

TABLE 7.—*Comparison of Nos. 2, 4, 5 and 10 Blast Furnaces, South Works*

Data	Furnace No. 2	No. 4	No. 5	No. 10
Rated capacity, tons per day	1,018	1,203	1,018	1,155
Height (large bell closed to iron notch), ft	81.0	84.8	85.7	83.4
Volume (large bell closed to iron notch), cu. ft.	31,320	37,450	33,460	35,425
Hearth diameter, ft	23	25	23	24.5
Stock-line diameter, ft	18	19	18	19
Large bell diameter, ft	13.5	14.0	13.5	14.0
Large bell angle, deg	50	50	50	50
Large bell drop, ft	2	2	2	2
Small bell diameter, ft	5.5	5.5	5.5	5.5
Small bell angle, deg	45	45	45	45
Number of tuyeres	12	14	12	12
Inwall batter, in. per ft	1 1/16	1 1/8	1 1/16	1 1/16

TABLE 8.—*Representative Burdens*

NO. 2 BLAST FURNACE
15,000-lb. coke unit
56 % Group 3 ore
29 % Group 7 ore
15 % Miscellaneous
6200 lb. limestone

NO. 4 BLAST FURNACE
15,900-lb. coke unit
78 % Group 3 ore
12 % Sinter
10 % Miscellaneous
5000 lb. limestone

NO. 5 BLAST FURNACE
10,000-lb. coke unit

40 % Group 2 ore	or 55 % Group 3 ore
17 % Group 3 ore	31 % Group 7 ore
8 % Group 5 ore	9 % Sinter
20 % Group 7 ore	5 % Miscellaneous
4100 lb. limestone	4300 lb. limestone

CHARGING SEQUENCE[a]

Furnace No. 2   O-O-C-C   lower large bell
             O-S-W-W   lower large bell, one charge
Furnace No. 4   O-O-C-C   lower large bell
             O-S-W-W   lower large bell, one charge
Furnace No. 5   O-O-S-W-W-W-W (one charge). Alternate use of weigh and chute coke
             O-O-S-C-C   (one charge)

[a] O = ore, S = limestone, C = chute coke, W = weigh coke. The same nomenclature is used throughout paper.

TABLE 9.—*Chemical Analysis of Burden Materials*
PER CENT

Material	Fe	P	Mn	SiO$_2$	Al$_2$O$_3$	CaO	MgO
Gary coke......................................	0.61	0.009		4.19	2.90	0.48	0.19
Joliet coke.....................................	0.75	0.006	0.010	4.06	2.38	0.63	0.13
Group 2 ore....................................	58.26	0.031	0.31	3.67	0.81	0.08	0.08
Group 3 ore....................................	51.92	0.054	0.71	5.64	1.57	0.10	0.10
Group 5 ore....................................	51.99	0.032	0.20	13.16	0.60	0.10	0.08
Group 6 ore....................................	55.05	0.049	0.30	4.22	1.09	0.06	0.09
Group 7 ore....................................	49.16	0.052	0.48	12.34	1.36	0.08	0.08
O. H. slag.....................................	27.60	0.64	8.08	16.47	2.20	27.25	6.85
Sinter...	56.42	0.056	0.69	10.64	2.27	2.87	0.33
Michigan limestone.............................	0.14	0.004		0.46	0.25	52.90	0.93

along with the results of the effect on furnace operation.

LOW-COKE, HIGH-TONNAGE RUN ON NO. 2 FURNACE

During the months of October, November and December, 1939, No. 2 furnace experienced a marked increase in output with a corresponding decrease in coke rate. It was one of those periods that most furnaces seem to exhibit at some time or other during their campaigns when distribution, lines, and the many other variables that affect them seem to hit on the one happy combination where everything "clicks" and records are broken. During this period we were fortunate enough to obtain a fairly complete record of gas samples to serve as a criterion for future tests and changes. Table 3 shows the data on gas and temperature gathered during the period with pertinent information, also the same information gathered at an earlier date (November-December 1938). Fig. 5 shows the gas and temperature data plotted for these periods and also a comparison of the two CO/CO$_2$ ratios plotted against one another.

These three graphs clearly indicate that the furnace operates more efficiently as revealed by the Fe/C ratio when the ratio of CO/CO$_2$ at the wall is lower than the ratio in the center of the furnace. Conversely, when the ratio is higher at the walls, the furnace seems to operate less efficiently. Samples of gas taken on other furnaces

seem to bear out this point, the reasons for which have already been discussed.

It will be noted from the various tables that ratios taken at points 3, 4 and 5, and, in most cases, also point 2, are usually favorable—well below the 2:1 ratio of Gruner[5] and in some instances below the practical minimum of 1.08 set by Martin[1]; in a few cases, even below the theoretical equilibrium mark of 0.96. It is obvious that if these favorable ratios can be maintained and at the same time a lower CO/CO$_2$ ratio can be secured at the furnace walls, the result should be an efficient furnace.

During this period on No. 2 furnace, it was found that the curve pattern of the CO/CO$_2$ ratios could be adequately determined by taking samples of gas at only three points instead of at six. Therefore we confined our further studies to the outer, or No. 1 point; the central, or No. 6 point; and one intermediate point.

VARYING STOCK LEVEL ON NO. 5 FURNACE

For several months during 1940, it was noted that whenever charging had been interrupted on No. 5 furnace with a consequent lowering of stock level and refilling to the normal level, the furnace became hot two casts later, as evidenced by an increase in silicon. At first it was assumed that the furnace made a much larger amount of flue dust due to higher top temperatures during the time it was not being charged, but the quantity of dust drawn from the dust catcher failed to substantiate this

theory. In May 1940, the stock level was deliberately lowered to 10 ft. several times and the effect on furnace operation was carefully gauged. The results verified the effects noted previously during involuntary stock-level lowerings and it was decided to make this a regular practice. Starting on May 28, 1940, the stock level was allowed to drop to 10 ft. every 4 hr., after which it was gradually raised over a period of 2 hr. to the normal level.

The response of the furnace to this filling was marked. Since maximum production was being demanded, it was necessary to raise the wind, thus a tonnage comparison could not be made definitely. However, the figures on coke per ton of iron (Table 10) are very interesting.

4 ft. on May 8. There was 2500 lb. of sinter in the burden half of the time during both of the periods March-April-May and June-July. No scrap was used at any time. Top temperatures were moderate, a gradual rise of 200° to 300° being noted during the time charging was stopped. There was little or no increase in flue-dust production. No gas samples were taken during the period March-April-May but samples were taken at intervals during June and July. The results are shown in Table 5, and the CO/CO_2 ratios are plotted in Fig. 12.

For comparison, the CO/CO_2 ratios of No. 5 taken in 1938-39 are shown on the same graph. A more favorable ratio is shown at the wall during June and July 1940 than in 1938-39. Operating per-

TABLE 10.—*Coke per Ton of Iron*
YEAR 1940

Month	Average Fe/C Ratio	Average Slag Volume, Lb.	Average Coke per Ton Iron, Lb.	Wind, Cu. Ft. per Min.	Number of Tests
June	1.28	790	1,636	65,000	12
July	1.32	785	1,561	65,000	14
March	1.25	837	1,689	55,000	
April	1.21	823	1,727	55,000	
May	1.24	832	1,720	62,000	

AVERAGE CO/CO_2 RATIOS

	1	2	3	4	5	6
All tests up to March 1939	2.10	1.57	1.16	1.04	1.13	1.56
June-July, 1940	1.84		1.07	1.18	1.57	1.36

The filling sequence in March and until April 13 was:

O-O-S-C-C
O-O-S-W-W-W-W

On April 13 the chute coke charge was changed to:

O-C-O-S-C

The weigh coke charge was left unchanged. This sequence was subsequently followed during the period under discussion. The regular stock level was changed from 3 to

formance in March-April-May indicate that the CO/CO_2 ratios would have been no better than in the 1938-39 period. We have continued the practice of regularly lowering the stock level on this furnace and the satisfactory results obtained are apparent in the tonnage, coke figures, and regularity of operation. The tonnage is consistently above rated capacity and the coke rate is usually 100 to 200 lb. per ton of iron less than in comparable furnaces.

The success of this type of filling opens a new field of experimentation in distribution and improved gas-solid contact. It is logical to assume that under the varying

and irregular conditions obtaining in the blast furnace, a filling that involves only one stock level may not be satisfactory. If the ores and coke are not distributed uni-

would also improve the practice on other furnaces. But blast furnacing is not so easy. We have tried this method of filling on several furnaces, some working successfully,
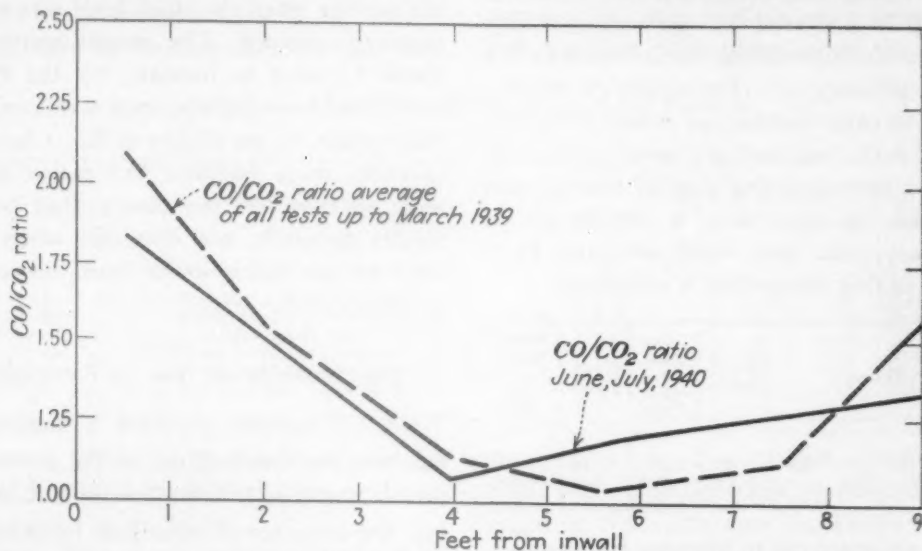
FIG. 12.—COMPOSITE OF ALL TESTS UP TO MARCH 1939 AND TESTS IN JUNE AND JULY, 1940, ON NO. 5 FURNACE.

formly over the top area of the furnace (and we may suppose that they never are from results obtained in gas sampling wherever such samples have been taken), an attempt to remedy this condition may be made by trying a different size of charge, a different stock level, a different rate of lowering the large bell, different sizes of raw materials, and so forth. Perhaps not one of these measures will cause appreciable improvement, but a combination of two or more of them may cause the furnace to show a decided change for the better. One way to obtain a combination of such factors is to lower the big bell at varying stock levels. It may be that not one of the levels at which the bell is dropped will, in itself, give satisfactory results, but the combination of a number of levels will tend to throw the distribution of ores and coke uniformly across the furnace top.

From the results observed on No. 5 furnace with a varying stock level, it is natural to suppose that what worked so well there

others showing no improvement or even a loss in efficiency. Several of the furnaces at South Works have Venturi tops, and when this type of variable stock-level filling was put on them, they would usually begin to slip so much, and showed such an increase in flue-dust production, that any gains in gas-solid relationship in the furnace were offset by losses incurred in the irregular operation. Furnaces with straight top sections usually showed improvement of varying degrees in their efficiency when this type of filling was tried. The experimental work on No. 2 furnace in this regard is related elsewhere in this paper.

Variable stock-level filling was tried without success on Nos. 1 and 10 furnaces, which have Venturi tops. No. 1 was not equipped to take gas samples but operating results did not warrant continuance of this filling. The slipping, while the level was down, was pronounced but could be compensated for. The results on No. 10 are discussed later.

VARIATIONS IN STOCK LEVEL ON NO. 2 FURNACE

During January and February 1940, some change had occurred in No. 2 furnace, which had altered her performance from that of an outstanding furnace to that of a very ordinary one. The ability of the furnace to carry burden, as evidenced by the Fe/C ratio, had declined from 1.39 to 1.27, with a corresponding drop in tonnage and increase in coke rate. A comparison of tonnage, coke rate, wind rate, and Fe/C ratio during this period is as follows:

Period	Fe/C Ratio	Coke Rate, Lb. per Ton	Tons Daily	Wind Rate, Cu. Ft. per Min.
Oct.-Nov.-Dec. 1939..	1.39	1,482	1,059	62,000
Jan.-Feb. 1940.......	1.27	1,595	940	59,000

In an endeavor to improve the practice, a series of experiments on stock-level variations was carried out. The regular practice had been to carry a stock level of 4 ft. Before the experiments were started, samples were taken at the regular 4-ft. level, and also during the course of the tests, from Aug. 5 to 16. This same level was carried

During the period there were no coke changes and the quality of coke was substantially the same. There was no appreciable change in flue-dust production during the periods when the stock level was being regularly lowered. The results shown in Table 12 seem to indicate, by the Fe/C ratio, that lowering the stock level periodically results in the ability of No. 2 furnace to carry more burden. The ratios again seem to bear out the theory that better results generally are obtained when the ratio at the wall is lower than the center of the furnace.

EXPERIMENTS ON NO. 10 FURNACE

No. 10 furnace presents a somewhat different problem because of the construction of the top. It is built with a Venturi top, the only one of these four furnaces so designed.

This design has given some unusual and, we believe, somewhat unreliable gas samples from the pipe next to the wall. The furnace was blown in in May 1940 and test data were collected in July and August 1940. Again, in January 1941, a number of

TABLE 11.—*Summary of Gas Tests No. 2 Furnace*
YEAR 1940

Month	Summary Average, Fe/C	Average Slag Volume, Lb.	Average Coke, Lb.	Wind, Cu. Ft. per Min.	Number of Tests
June............................	1.26	828	1,569	62,000	25
July............................	1.27	743	1,608	62,000	35
August.........................	1.21	786	1,648	62,000	40
				8-14-40 63,000	
				8-15-40 65,000	

as a check on the results being obtained, and because the grade of iron being made, blowing iron, was different from that at the beginning of the test, standard basic. Blowing iron is a low-manganese iron (0.60–0.80) with 1.50 per cent silicon. A summary of the results of the gas tests made during this period is given in Table 11; CO/CO₂ ratios and pertinent information in Table 3.

tests were made for purposes of comparison while the furnace was not acting so well. Table 13 shows pertinent operating data and average CO/CO_2 ratios during these periods.

During July 1940, the furnace was not performing satisfactorily, with moderate tonnage and indifferent coke rate. The average CO/CO_2 ratio of the gas samples

taken during the month show the ratio uniformly high at the wall, much higher, in fact, than any of the other furnaces on which we had taken samples. The furnace however did not operate as poorly as these results would indicate. Indeed, the sample of gas taken at the dust catcher at one time

that the samples of gas gathered by the outer pipe are gases that have traveled up the walls and have taken little or no part in the reduction process. From the rapidity with which the CO/CO_2 ratio descends as samples are taken farther away from the wall, together with the values of the ratio

TABLE 12.—*Summary of Gas Tests, No. 2 Furnace*
YEAR 1940

Dates	Filling	Average CO/CO_2 Ratios			Fe/C Ratios	Kind of Iron
		1	2	3		
6-1 to 6-13...........	Regular; 4-ft. stock level	2.21	1.17	1.44	1.26	Basic
6-14 to 6-20.........	Stock level 4 ft. Drop to 7 ft. every 4 hr.	1.55	1.16	2.24	1.29	Basic
6-21 to 6-26.........	Stock level 4 ft. Drop to 7 ft. every 4 hr.	1.93	1.08	1.50	1.26	Blowing
6-27 to 7-27.........	Stock level 4 ft. Drop to 6 ft. every 3 hr.	1.94	1.05	1.60	1.24	Blowing
7-28 to 8-5..........	Stock level 3 ft. Drop to 6 ft. every 3 hr.	1.57	1.04	1.57	1.20	Blowing
8-5 to 8-16..........	Regular; 4-ft. stock level	2.24	1.00	1.76	1.18	Blowing

showed a ratio of 1.76, which was not far out of line for a furnace with the performance shown in the table.

Since these outer points encompass so much of the area of the furnace, it is, of course, to be presumed that furnace performance would suffer from such an un-

revealed in the dust-catcher sample, it would seem that the outer gas sample collected on No. 10 furnace represents but a very small portion of the ascending gases.

During July 1940, variable stock-level filling was tried on one day (July 9) but the furnace started to slip violently and the test

TABLE 13.—*Pertinent Operating Data and Average* CO/CO_2 *Ratios, No. 10 Furnace*

Month	Year	Average Fe/C Ratio	Average Slag Volume, Lb.	Average Coke, Lb.	Average Tonnage	Wind, Cu. Ft. per Min.	Number of Tests
July....................	1940	1.25	721	1,680	1,115	67,000	17
August.................	1940	1.28	661	1,619	1,205	67,000	14
January................	1941	1.21	752	1,781	1,066	65,000	9

AVERAGE CO/CO_2 RATIO

Month	Year	1	2	3	4	5	6	Dust Catcher
July....................	1940	3.89	2.57	0.93	1.36	1.31	1.16	1.76
August.................	1940	2.31[a]	1.80[a]	1.44	1.18	1.19	1.30	1.73
January................	1941	3.23	2.32	1.47	1.36	1.32	1.38	1.95

[a] Calculated.

favorable ratio. The fact that the furnace performance did not always deteriorate is attributed to the unreliability of the ratios obtained from these outer areas because of the Venturi top construction. This construction evidently distorts the gas flow and the distribution. It is quite probable

was discontinued. This confirmed earlier experience with this phenomenon on other furnaces equipped with Venturi tops and it has occurred again. As soon as the stock level gets below the bend line of the Venturi, regular slipping or "blowing through" occurs.

From July 21 to 31, 1600 lb. of coke per charge was weighed with the ore. Fig. 13 shows a comparison of the CO/CO₂ ratios taken before and during the time this

(Fig. 13) seems to indicate considerably better distribution.

For the month of August 1940, several changes were made in the filling of No. 10
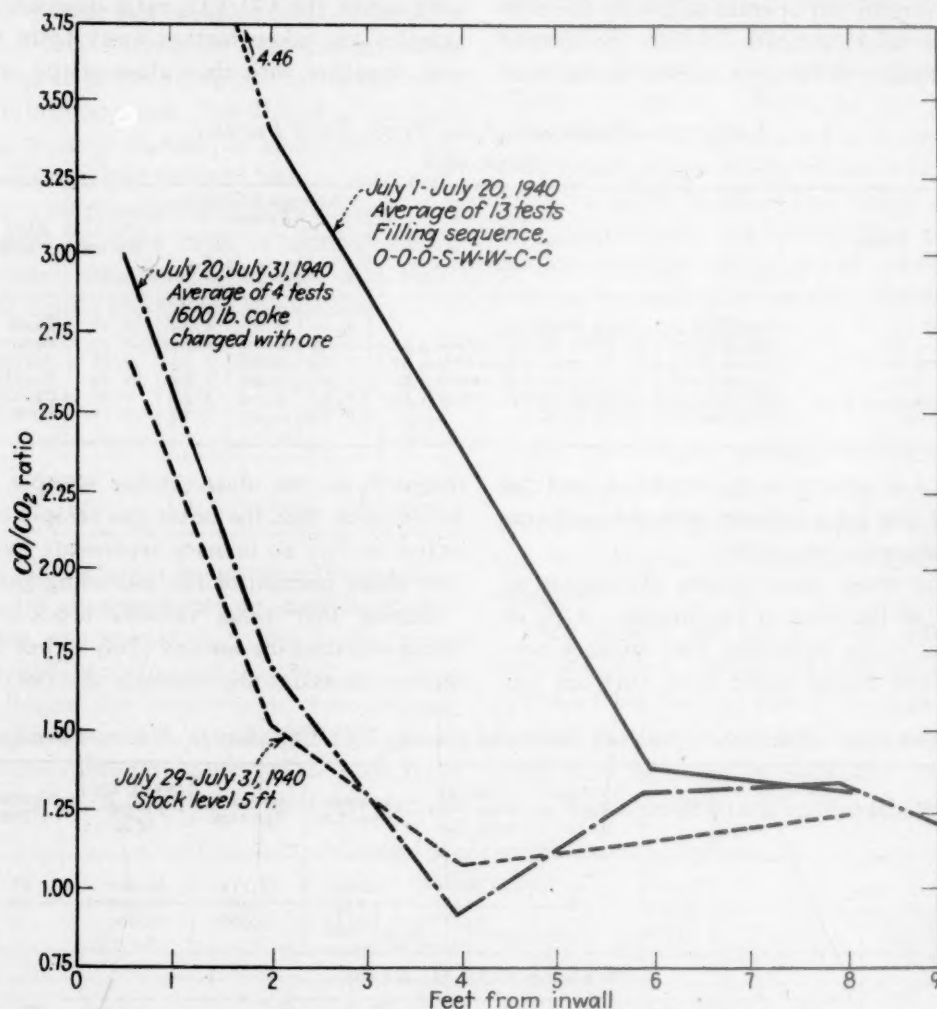
FIG. 13.—CO/CO₂ RATIOS, No. 10 FURNACE, DURING DIFFERENT TESTS.

experiment was tried. Apparently more favorable ratios were obtained when mixing some of the coke with the ore but there was little discernible difference in practice. The coke rate and tonnage were the same as before.

On July 27 the normal stock level was lowered from 3 to 4 ft. and on July 29 from 4 to 5 ft. There was again no appreciable difference in performance, although the single gas sample taken during this period

furnace. The coke unit was changed from 10,500 to 15,000 lb. per charge, a constant stock level of 2 ft. was maintained, and no coke was weighed with the ore after July 30. On Aug. 8 the filling sequence was changed from O-O-O-S-W-W-C-C to O-O-W-W-O-S-C-C, accompanied by one dumping of the large bell (No. 10 furnace is the only one built with a hopper large enough for a coke unit of this size).

The furnace had a good month, with greatly increased tonnage and lowered coke, but unfortunately pipes Nos. 1 and 2, points. In Fig. 14, however, the curves have been extrapolated by calculation from known ratios in the furnace and dust
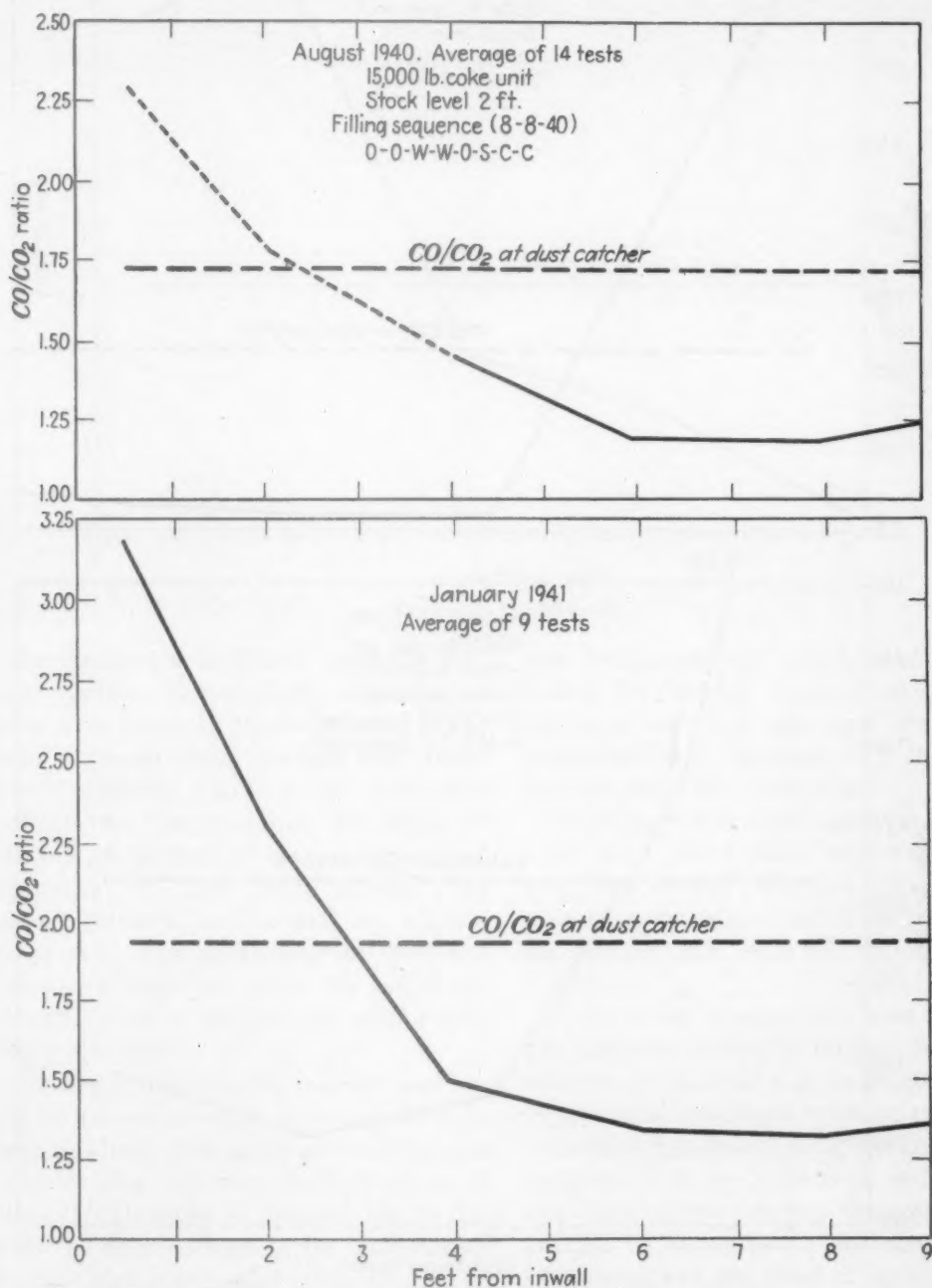
FIG. 14.—CO/CO₂ RATIOS, No. 10 FURNACE, AVERAGE OF 14 TESTS IN AUGUST 1940 AND AVERAGE OF 9 TESTS IN JANUARY 1941.

which sample the outer area, were out of service and no samples were made at these catcher. That figure shows also a composite of all tests for the month of January 1941.
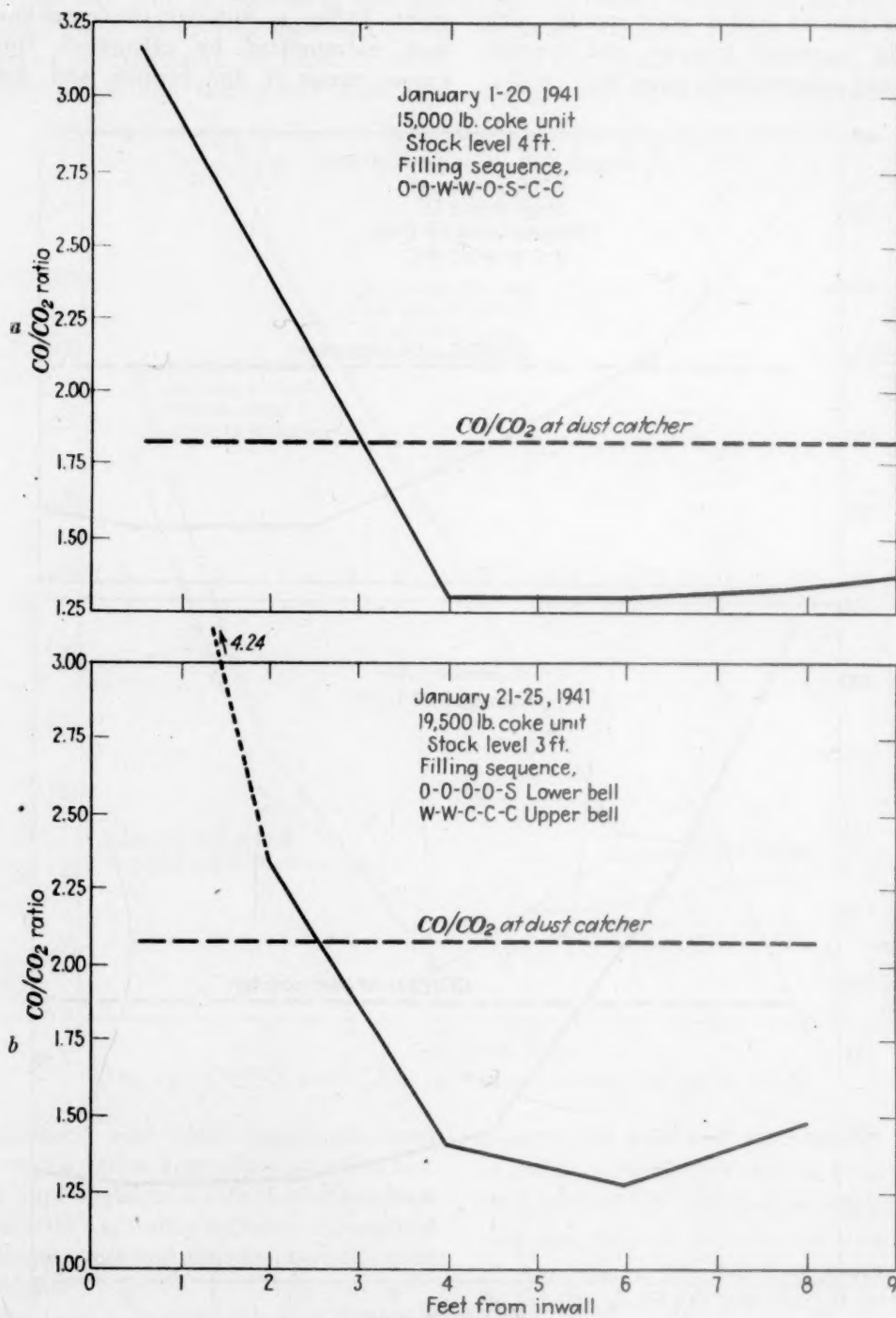
FIG. 15.—CO/CO₂ RATIOS, No. 10 FURNACE, IN THREE TESTS DURING 1941.
(Third part on next page.)
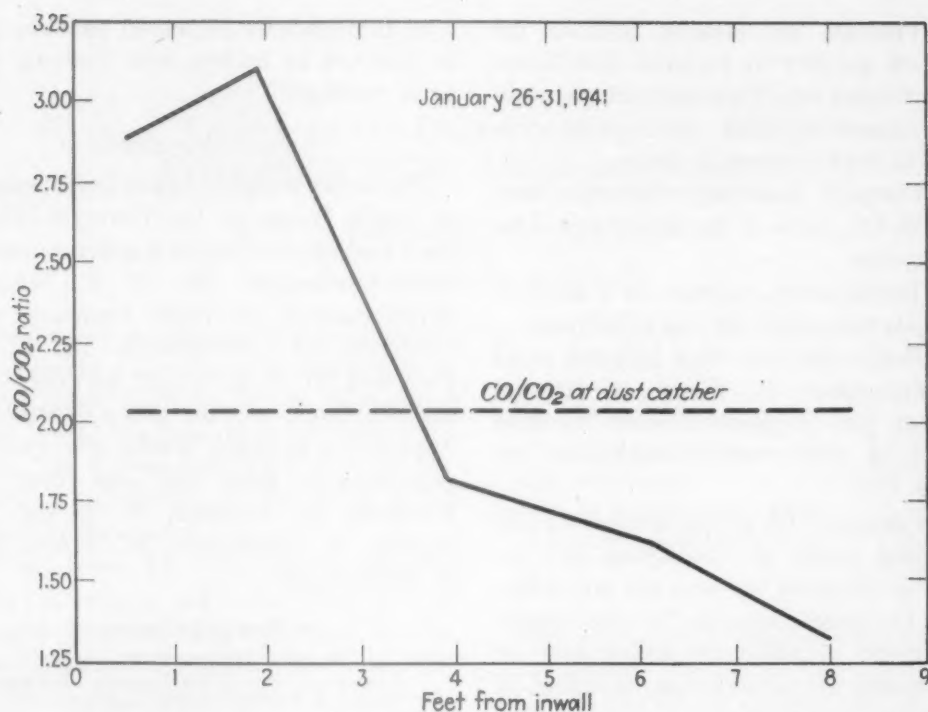
FIG. 15.—(*Continued*)

In January, a month in which the furnace operated rather poorly, a number of tests were made. In the latter third of the month several filling changes were tried, with indifferent results as far as furnace performance was concerned. The results of the test are plotted in Fig. 15 for the period preceding the first filling change, the period between Jan. 20 and 25, when a large unit with a split filling was tried and the period from Jan. 26 to the end of the month, when a smaller unit with a split filling was used.

During this period the tonnage was low for the amount of wind blown and the coke rate was high. The graph of the composite samples (Fig. 14) show the high values of the CO/CO_2 ratios at the wall, but in this case the values shown in the dust catcher are also high, a very good indication that all was not well with the furnace.

The three samples taken in the period between Jan. 20 and 25 show even worse ratios at the walls, while the dust-catcher ratios were considerably higher. The fur-

nace performed very poorly during this period, the tonnage dropping off over 10 per cent and the coke rate increasing correspondingly. Slipping and increased flue dust were also noticeable.

The filling was changed again on Jan. 25, after which the furnace improved somewhat, the tonnage rising and the coke rate decreasing to values near those at which the furnace had operated earlier in the month.

Many filling changes have been tried on the furnaces at South Works, involving material, stock level and mechanical aids. These experiments have not been recorded, because of insufficient data, but they have contributed to our knowledge and experience concerning practice changes to be effected by variations in the distribution of material and the effect of such changes upon the gas flow through the stock.

CONCLUSIONS

The conclusions to be drawn from this investigation are:

1. Traverse gas samples indicate the effect on gas flow by material distribution in the furnace top. These samples may indicate corrective filling changes or even point to improvement in design.

2. Furnaces operating efficiently have low CO/CO_2 ratios in the outer rings of the furnace top.

3. Temperature readings are a guide to CO/CO_2 ratios and may be substituted.

4. Single traverses may indicate trend brought about by filling or material changes, but a series of such traverses should be made before conclusions are drawn.

5. Furnaces with similar dimensions and operating under like conditions but far apart in operating performance may sometimes be brought into line by some simple adjustment of which the nature may be determined by traverse gas sampling or temperature readings.

6. From the results of the studies at South Works, a 1-in. batter of the inwall is considered sufficient for furnaces of the height of those in the plant.

7. While unquestionably the mechanical top has benefited distribution in every major way, it has not, as yet, given all of the answers.

8. Undoubtedly improved practice can be attained by making and studying traverse readings.

REFERENCES

1. P. V. Martin: Effect of the Solution-loss Reactions on Blast-furnace Efficiency. *Trans.* A.I.M.E. (1940) **140**, 31.
2. S. P. Kinney: The Blast Furnace Stock Column. U. S. Bur. Mines *Tech. Paper* 442 (1929).
3. C. C. Furnas and T. L. Joseph: Stock Distribution and Gas-solid Contact in the Blast Furnace. U. S. Bur. Mines *Tech. Paper* 476 (1930).
4. P. H. Royster and T. L. Joseph: Effect of Coke Combustibility on Stock Descent in the Blast Furnaces. *Trans.* A.I.M.E. (1924) **70**, 224.
5. M. L. Gruner: Blast Furnace Phenomena. Translation by L. D. B. Gordon. Philadelphia, 1874. Henry Carey Baird Co.

Physical Aspects of the Dust Catcher, Gas Washer and Precipitator on No. 3 Furnace at Carrie

By C. P. Clingerman* and C. J. Fleisch*

(Cincinnati Meeting, April 1942)

THE recent installation of a combination dust catcher, gas washer and precipitator at Carrie blast furnaces of the Homestead Steel Works has given very satisfactory results. The following description of the gas-cleaning installation is based on actual operating experience.

When Carrie blast furnace No. 3 was rebuilt the decision was made to fine-clean all the gas produced by the furnace, because the management wanted fine-cleaned gas for fuel in the stoves and boilers. In order to keep the installation cost as low as possible, the gas-cleaning system was streamlined. All by-pass lines and goggle valves for by-pass lines were eliminated from the system. A radical departure from the use of 8-in. tubes in the Cottrell-type precipitators was made by using 12-in. diameter tubes in a single compartment, the single compartment being divided into two units by a single partition wall in the top header.

THE FURNACE PROPER

A few of the characteristic points and dimensions of the furnace proper are:

Hearth diameter	26 ft. 0 in.
Bosh diameter	29 ft. 1¾ in.

Stock-line diameter	20 ft. 0 in.
Large-bell diameter	14 ft. 8 in.
Small-bell diameter	6 ft. 6 in.
Height of furnace from center of iron notch to bottom of large bell, closed	94 ft. 4 in.
Height of furnace from center of iron notch to main platform	105 ft. 0 in.

The furnace top is equipped with a McKee revolving distributor, the operation of which is electrically interlocked with the skips, bell hoists, and coke-weighing and charging apparatus through a Freyn automatic charging control.

The gas leaves the furnace first through four offtakes, 5 ft. 9 in. in diameter, then through uptakes that are approximately 85 ft. high, which feed into a single downcomer that is 9 ft. in diameter.

DUST CATCHER

The primary dust catcher installed (Fig. 1) may be described as a single-cone type. The inlet pipe at the top of the dust catcher is 9 ft. in diameter; it is flared to a conical shape as it extends down inside the dust-catcher shell, which is 35 ft. in diameter, 37 ft. high on the straight side, and has a conical top and bottom. The slope of the bottom is 50° with the horizontal. The cone-shaped pipe inside the dust-catcher shell is 42 ft. high and is 19 ft. 7 in. in diameter at its bottom lip where it releases the gas inside the dust catcher. The ratio of the area of the inside cone at its bottom lip to the

annular area between the bottom lip and the dust-catcher shell is 1.0 to 2.0.

The gas enters the top of the dust catcher, passes down through the inside cone, makes a 180° change in direction around the bottom lip of the cone and passes up through the dust catcher to an outlet, 8 ft. in diameter, on the dust-catcher dome. The velocities of the gases under normal operating conditions of 110,000 cu. ft. (standard at 60°F. and 30 ft. Hg) per minute at a temperature of 300°F. are as follows:

	FT. PER SEC.
Through the inlet	50.1
At outlet from inside cone	9.6
Through annular space between bottom lip of inside cone and dust-catcher shell (where direction is changed)	4.8
Through outlet pipe	64.9

Numerous tests have shown the dust catcher to have an efficiency of 80 per cent under normal operating conditions. Tests made have shown the following average results: dust-catcher inlet, 12.73 grains per cu. ft. at 60°F. and 30 in. Hg; dust-catcher outlet, 2.39 grains, and dust-catcher efficiency, 81.30 per cent.

The dust caught in the dust catcher is removed at the bottom by a pug mill. An auxiliary valve is provided on the bottom cone for dumping the dust if the pug mill is out of service.

TOWER WASHER

The tower washer (Fig. 1), which has four banks of spiral tile, is designed to clean all the gas produced by the furnace (110,000 cu. ft. per min. at standard conditions of 60°F. and 30 in. Hg) to 0.25 grains per cu. ft. The washer is 20 ft. in diameter and 45 ft. 2 in. high on the straight side. The cone bottom has a slope of 50° with the horizontal. The inlet at the bottom is 7 ft. 3 in. in diameter and the outlet at the top is 7 ft. in diameter.

The washer is packed with four banks of spiral tile so placed that the spiral passage is continuous in each bank. The first bank has six layers of 6-in. tile; the second bank has four layers of 6-in. tile and each of the third and fourth banks has four layers of 3-in. tile. There is one set of sprays above the bottom banks of 6-in. tile and one set above the two top banks of 3-in. tile. Water is fed to the spray nozzles at a pressure of 10 lb. per sq. inch.

The gas enters at the bottom on the side of the washer. First, it passes up through a perforated baffle ($1\frac{1}{8}$-in. holes on 4-in. center), then continues up through the four banks of spiral tile and out of the top through the outlet pipe.

The dust-laden water from the washer is carried off at the bottom through a water seal to a Dorr thickener.

Data accumulated since the tower washer has been in operation gives the following average results:

Gas cleaned per minute, 110,000 cu. ft. at 60°F. and 30 in. Hg

Average gas-inlet temperature, 300°F.

Dust content before washer, 2.39 gr. per cu. ft. at 60°F. and 30 in. Hg

Dust content after washer, 0.074 gr. per cu. ft. at 60°F. and 30 in. Hg

Gas-pressure drop through washer, 17 in. H_2O

Water consumption per 1000 cu. ft. gas at 60°F. and 30 in. Hg, 20 gal.

DORR THICKENER

The Dorr thickener is of the four-stage type. It is built in a steel tank 55 ft. in diameter and 28 ft. high. The dust-laden water is fed into a central inlet box. The clean overflow water is removed at four outlet boxes evenly spaced around the circumference, while the thick underflow sludge is removed by three Dorrco diaphragm pumps. The sludge is pumped to a tank adjacent to the thickener and from there is pumped to a central settling basin, 500 ft. away, by a pneumatic sludge-handling system. The pneumatic system consists of

two tanks that are fed by gravity from the sludge tank and are arranged to fill and discharge by a float and air-control mechanism.

12-in. tubes, the gas leaves the top of the precipitator through two outlet pipes, 6 ft. in diameter, which merge into a main of
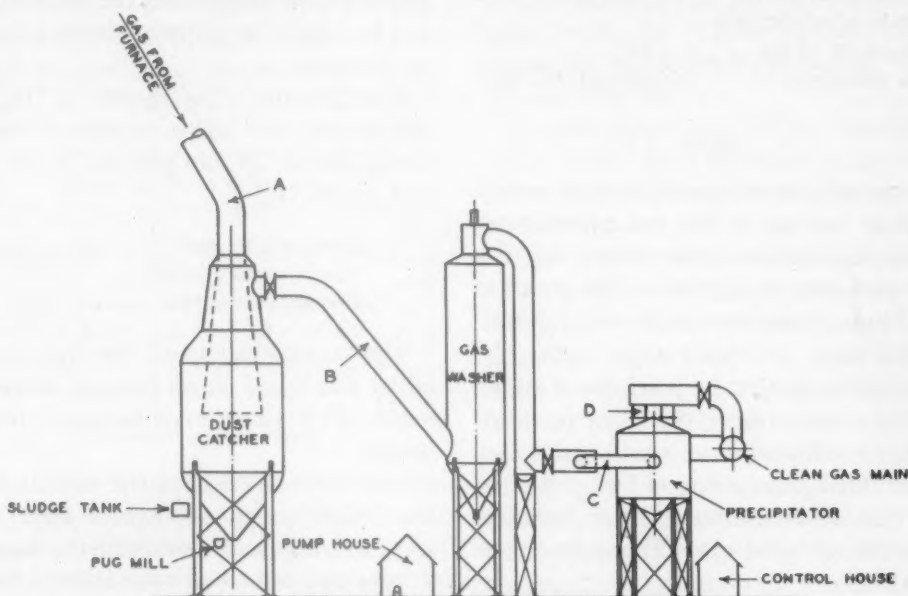
FIG. 1.—GAS-CLEANING SYSTEM, NO. 3 BLAST FURNACE.
A, dust-catcher inlet. C, washer outlet.
B, dust-catcher outlet. D, precipitator outlet.

PRECIPITATOR

The precipitator (Fig. 1), consisting of 224 tubes, each 12 in. in diameter and 15 ft. long, is of the wet Cottrell type as built by the Research Corporation. A single partition wall in the top header divides it into two units of 112 tubes each. The precipitator was designed to clean 110,000 cu. ft. of gas (standard at 60°F. and 30 in. Hg) to a dust cleanliness not to exceed 0.025 grains per cu. ft. and to be free of entrained moisture. This guarantee was based on the following conditions: Dust content of the inlet gas not to exceed 0.25 grains per cu. ft., inlet gas temperature not to exceed 100°F., and gas pressure not to exceed 20-in. water column positive pressure.

After leaving the tower washer, the gas goes to the precipitator. The gas main leaving the washer branches into a Y, 5 ft. in diameter, and enters the precipitator on opposite sides. After passing up through the

7-ft. diameter. The gas then goes to the points of consumption. Approximately 15 per cent goes to the stoves and 85 per cent to the boiler houses. No blast-furnace gas at Carrie furnaces is used as metallurgical fuel.

The electrical equipment consists of one Westinghouse single-phase transformer with a high voltage of 75,000 volts and low-voltage taps at 320, 360, 400, 440 and 480 volts. The precipitator is run at 320 on the low-voltage side, which gives 50,000 volts on the unit. For the rectification, there are two mechanical rectifiers driven by $\frac{1}{2}$-hp. G.E. three-phase synchronized motors. One rectifier is used at a time, the two units being switched daily.

River water is used in the operation of the precipitator. Silt accumulates in the water pans at the top, which are cleaned every three or four months.

Some average results of tests made on the precipitator are as follows:

Dust concentration be- 0.074 gr. per cu. ft. at
    fore precipitator.   60°F. and 30 in. Hg
Dust concentration aft- 0.015 gr. per cu. ft. at
    er precipitator.   60°F. and 30 in. Hg
Power required per mil-
    lion cu. ft. of gas.... 1.4 kw.
Water consumed....... 250,000 gal. per day

TESTS

Many tests have been made to determine
the dust content of the gas entering and
leaving the various units during the time
they have been in operation. The points at
which tests have been made are: (1) dust-
catcher inlet; (2) dust-catcher outlet; (3)
tower-washer outlet; (4) precipitator outlet.
Typical of these tests is the following report
of results collected on a series of tests con-
ducted during the period of Dec. 2 to Dec.
18, 1941, and reported by the Fuel and
Power Department of the Homestead Steel
Works.

Test Method Used.—The test procedure
was the same as that used on previous tests.
The method of taking the samples was an
adaptation of the "Brady method," which
consists essentially of filtering a quantity of
gas through a paper thimble. The thimble
was dried and weighed before and after
each test and the increase in weight was
converted to grains. The gas that passed
through the thimble passed through a meter
that recorded volume, gas temperature and
pressure. This meter volume was then cor-
rected to dry gas at standard condition of
60°F. and 30 in. Hg.

Test Equipment.—Two different types of
sampling equipment were used, in order to
check the results: (1) the type that had been
used on previous tests, which is standard
equipment at numerous plants, including
Carrie furnaces; (2) a Research Corporation
(Cottrell precipitator) type of thimble
holder.

The Carrie-furnaces thimble holder was
electrically heated and remained outside
the gas main. Only the sampling nozzle was
inserted in the main. The length of the noz-

zle varied with the size of the gas main that
was being tested. The Research Corpora-
tion type of holder was equipped with a
steam-heated jacket and the nozzle was 2
to 3 in. long. The entire holder was inserted
in the main.

Test Results.—The results of the tests
showed the dust concentrations at the fol-
owing points (grains per cu. ft. at 60°F.
and 30 in. Hg):

> Dust-catcher outlet..... 2.39
> Tower-washer outlet.... 0.074
> Precipitator outlet...... 0.0145

The concentration at the dust-catcher
outlet was based on an average of six tests
made with the Carrie-furnaces thimble
holder.

The concentration at the washer outlet
was based on an average of eight tests,
seven of which were made with the Research
Corporation holder and one with the Carrie-
furnaces holder.

The concentration at the precipitator
outlet was based on an average of seven
tests, all made with the Research Corpora-
tion thimble holder.

Discussion of Test Results

A comparison of the tests made in August
and September 1941, with a Carrie-furnaces
thimble holder, and the tests made in
December 1941 (using average concentra-
tion at dust-catcher inlet as determined by
previous tests) is shown in Table 1.

During the tests in August and Septem-
ber, the average wind on the furnace was
about 72,500 cu. ft. per min. During the
tests in December the wind was increased
until it reached 75,000 to 80,000 cu. ft. per
min. This indicated an increase in gas
volume of from 3 to 10 per cent over that
handled on the previous tests.

In view of this, a slight increase in dust
concentration throughout the system was
to be expected. In order to check the results
obtained by the two types of sampling
equipment, two sets of simultaneous tests

TABLE 1.—*Comparison of Tests*

Point of Test	August, 1941, Gr. per Cu. Ft.	September, 1941, Gr. per Cu. Ft.	Average, Gr. per Cu. Ft.	Average Efficiency, Per Cent
Dust-catcher inlet.	14.49	10.97	12.73	
Dust-catcher outlet	2.26	1.59	1.92	84.9
Washer outlet.....	0.068	0.075	0.071	96.3
Precipitator outlet.	0.0033	0.0045	0.0039	94.5

TESTS IN DECEMBER 1941

Point of Test	Gr. per Cu. Ft.	Point of Test	Per Cent Efficiency
Dust-catcher inlet...	12.73[a]	Dust catcher.	81.3
Dust-catcher outlet..	2.39	Washer......	96.9
Washer outlet.......	0.074	Precipitator..	80.4
Precipitator outlet...	0.0145		

[a] Average of previous tests.

were made on the precipitator outlet. Duplicate test setups were made and each test was run independently. Samples were drawn from the main at a point where the sampling nozzles were approximately 6 in. apart and the same sampling rates were used. The results were as shown in Table 2.

TABLE 2.—*Tests on Precipitator Outlet*, Dec. 12, 1941
GRAINS PER CUBIC FOOT

Time of Test	Research Corporation Holder	Carrie Holder
Morning..............	0.0111	0.0048
Afternoon.............	0.0105	0.0062
Average...............	0.0108	0.0055

The dust concentration obtained on the precipitator outlet by the Research Corporation type of thimble holder was double that obtained by the Carrie-furnace holder, and was more in line with expected results. When the increased gas volume was taken into account, the results were in line with those reported on previous tests.

Seven tests were made at the precipitator inlet, using the Research Corporation thimble holder. The average dust concentration at this point with this holder was 0.077 gr. per cu. ft., compared with an average concentration of 0.071 gr. per cu. ft. at the same point with the Carrie-furnace thimble holder. At this point, both thimble holders checked very well.

No tests were made at the dust-catcher outlet with the Research Corporation holder because there were no 4-in. openings in the main.

The thimble holders checked each other at the precipitator inlet but showed different results at the precipitator outlet. This difference might have been caused by the ionized condition of the gas discharging from the precipitator. As each dust particle carried an electrical charge, they collected on any ground that offered, which in this case was the nozzle. Since the nozzle of the Carrie-furnace holder is 36 in. long, it is reasonable to suppose that a large proportion of the dust collected on the inside of the nozzle instead of filtering out into the thimble. Therefore, the test results with the Carrie-furnace holder showed a very clean gas. The nozzle of the Research Corporation holder is very short (2 to 3 in. long). It is safe to assume that the results with the Research Corporation type of holder were more accurate than the others.

CONCLUSION

The performance of the dust catcher, gas washer and precipitator installation on Carrie blast furnace No. 3 has been much better than had been guaranteed. The use of 12-in. tubes in the precipitator was a radical departure from the standard 8-in. tubes previously installed in similar installations. In view of the results obtained, it is felt that this report of the installation should be of unusual interest to blast-furnace operators.

Slag Control by Introduction of Flux through Blast-furnace Tuyeres

By Carl G. Hogberg,* Junior Member A.I.M.E.

During recent months, the acute shortage of steel scrap has necessitated the use of higher percentages of hot metal in the open-hearth charge. With these higher percentages, the sulphur content of hot metal has become an increasingly important factor in the control of the quality of steel. Thus, the blast-furnace operator is faced with a demand not only for more output but for a higher quality of product.

More than 90 per cent of the sulphur charged into the blast furnace is contained in the coke. With the tremendously increased demand, the trend of coke quality has been toward higher sulphur, higher and more variable ash, and poorer physical characteristics. This has been brought about by less selective coal mining, increased production rates in coke plants and resumption of operations of many beehive ovens. In a single month last year, one blast-furnace plant in the Pittsburgh district operated with coke obtained from 52 sources.

The effect of variability and quantity of coke ash on blast-furnace operation is well known. The improved results obtained with furnaces operating on coke made from washed coals compared with results on coke made from raw coals is ample proof of the effectiveness of low and uniform ash. Coal-washing plants, however, require a large capital expenditure, and are impractical for most of the large number of small producers, whose operations are confined chiefly to periods of abnormally high demand. Furthermore, not all coals are physically adaptable to washing.

Principles of Iron Desulphurization in Furnace

Although investigations of the blast-furnace process have not clearly revealed the detailed mechanism of iron desulphurization within the furnace, they have been sufficiently extensive to permit a postulation of the following general principles:

1. Iron, in its travel from furnace top to hearth, continues to pick up sulphur until it has reached tuyere level. The zone of iron desulphurization is relatively narrow, being confined to a vertical distance extending approximately from tuyere level to the iron-slag interface in the hearth.[1]

2. Combustion of coke is confined to spherical zones extending approximately 40 in. from the nose of each tuyere.[2] Coke ash is released as the coke burns in these combustion areas.

3. With a constant amount of sulphur in the charge, the sulphur content of the metal product is a function of hearth temperature, final slag analysis, slag viscosity, and slag volume. Both hearth temperature and slag analysis affect slag viscosity. For a slag of constant analysis, viscosity always decreases with an increase in temperature;

[1] References are at the end of the paper.

in the range of blast-furnace slags, an increase in lime generally will increase viscosity and raise the melting point.[2-4]

In a paper presented in 1939, G. E. Steudel[5] said that two distinctly different types of slag are made in the blast furnace: (1) the final slag drawn from the furnace hearth, and (2) the bosh slag, which differs from the final slag in that it is not diluted by the highly siliceous oxides in the coke ash and is, therefore, high in lime and extremely viscous. McCaffery[6] has said (1) that bosh slags high in lime probably contain calcium ferrites, which are decomposed in the hotter zone lower in the bosh, with a reaction absorbing considerable heat, and (2) that the limy bosh slags are not conducive to utilization of uniformly high blast temperatures.

Steudel suggested that an improved type of bosh slag could be obtained if part of the lime normally charged into the furnace top were blown into the tuyeres, thus attaining the desirable high-lime final slag required for proper desulphurization.

The success attained with the use of acid slag at the Corby plant in England is well known,[6] but there increased production and decreased coke consumption were obtained at the expense of higher sulphur in the iron.

Variation in Coke Ash

Coke ash may vary daily as much as 2 per cent above and below the average, particularly when coke is obtained from several sources. The blast-furnace operator normally has at his disposal several means of adjusting his operations to compensate for the thermal and chemical effects of these variations. Within limits, the thermal effect may be controlled by variation in blast temperatures, the chemical effect by a constant excess slag volume or by frequent adjustments in the amount of limestone and ore burden charged. These methods of control all require either a reserve in blast temperature or operation at an ore-coke ratio lower than the optimum

that would obtain if the ash were uniform in analysis. Obviously, production and coke rate suffer in this practice.

Data shown on Table 1 illustrate the effect of variation in coke ash on theoretical final and bosh slags for a typical standard basic iron burden and coke containing ash in which the slag-forming oxides analyze 61.9 per cent SiO_2, 34.4 per cent Al_2O_3, 2.8 per cent CaO and 0.9 per cent MgO. These data were calculated on the basis that limestone required for each change in ash would be charged into the furnace top and would be timed to compensate for variations in coke ash exactly when needed. Table 1 shows that while final slags are relatively constant in analysis, the bosh slags vary considerably. Considering magnesia as lime, a plot of slag compositions on the ternary diagram SiO_2-CaO-Al_2O_3 (Fig. 1) indicates for each increment of ash variability a considerable change in melting points ($A'B'C'D'E'F'G'$) of bosh slag, but only a minor change in the melting points of the final slag (A–G). If limestone additions could be timed perfectly, this practice would not be objectionable as far as final slags are concerned. However, a sudden change in ash is usually detected only after its ill effect on slag composition and hearth temperature has become a reality, and subsequent changes in burden do not become effective until from 7 to 12 hr. later. If, in the meantime, there were a reversion of ash content to the original figure, the result would be a dual action on slag chemistry—the furnace then swings too far in the opposite direction.

Table 2 shows the effect of variations in coke ash on final slag analyses when the amount of limestone charged is left unchanged at the amount required to flux the ash in a coke containing 9 per cent ash. Theoretical slag analyses plotted on Fig. 1 for these data indicate a wide range in final slag analysis (a, b, c, d, e, f, g). For the coke used in the example, this range in final slag analysis is very undesirable, particularly

for slag *d*, which lies on a mineralogical phase boundary. A slag of this type theoretically is more undesirable than the

spaced isotherms in the region of slags *a*, *b* and *c*—and these are the slags obtained when the coke ash is low—may partly ex-
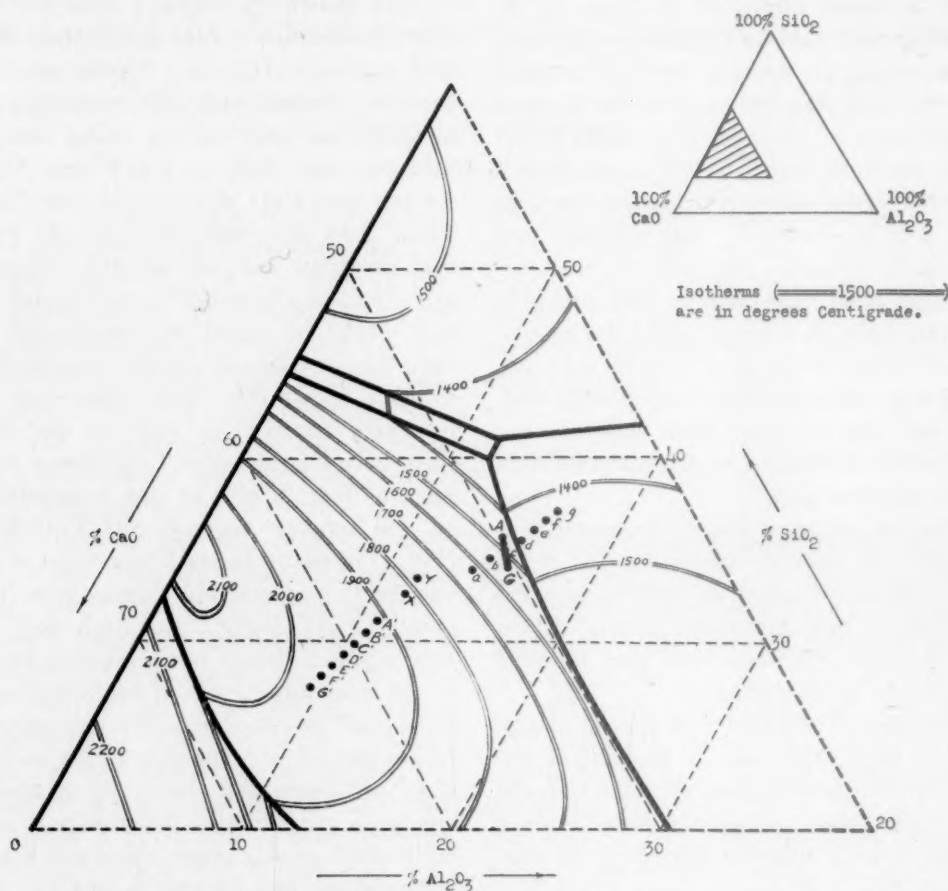
FIG. 1.—EFFECT OF VARIATION IN COKE ASH ON COMPOSITION AND MELTING POINT OF FINAL AND BOSH SLAGS.

Percentage of Coke Ash	Final Slag		Bosh Slag	
	Stone Burden Adjusted for Ash in Coke	Stone Burden Not Adjusted for Ash in Coke	Stone Burden Adjusted for Ash in Coke	Stone Burden Not Adjusted for Ash in Coke
7	A	a	A'	C'
8		b	B'	C'
9		c	C'	C'
10		d	D'	C'
11		e	E'	C'
12		f	F'	C'
13	G	g	G'	C'

X and *Y* denote bosh slags at flux injection rates of 15 and 20 per cent, respectively.

higher-ash coke slag *f* or *g*, because very slight changes in chemistry would have a comparatively greater effect on mineralogical content and viscosity. The closely

plain the contention of some operators that variations of ash content in low-ash coke have a greater effect on furnace operation than do the same variations in high-ash

TABLE 1.—*Effect of Variation in Coke Ash on Theoretical Final and Bosh Slags*
(Flux quantities based upon amount required to maintain a 1.00 bases = acids ratio in final slag)

Material	Pounds in Burden (Excludes Coke and Flux)	7 Per Cent Coke Ash			8 Per Cent Coke Ash			9 Per Cent Coke Ash			10 Per Cent Coke Ash			11 Per Cent Coke Ash			12 Per Cent Coke Ash			13 Per Cent Coke Ash		
		Coke	Flux	Total	Coke	Flux	Total	Coke	Flux	Total	Coke	Flux	Total	Coke	Flux	Total	Coke	Flux	Total	Coke	Flux	Total
Coke and flux, lb......		12,000	4,116		12,000	4,349		12,000	4,566		12,000	4,794		12,000	5,014		12,000	5,236		12,000	5,464	
Fe........	13,184	98	26	13,308	98	28	13,310	98	29	13,311	98	30	13,312	98	32	13,314	98	34	13,316	98	35	13,317
P.........	32.79	1.28	1.23	35.30	1.28	1.30	35.37	1.28	1.36	35.43	1.28	1.44	35.51	1.28	1.50	35.57	1.28	1.57	35.64	1.28	1.64	35.71
Mn........	359.3	0.8	1.6	361.7	0.8	1.7	361.8	0.8	1.8	361.9	0.8	1.9	362.0	0.8	2.0	362.1	0.8	2.1	362.2	0.8	2.2	362.3
SiO_2......	1,608	527	87	2,222	601	92	2,301	676	96	2,380	750	100	2,458	823	105	2,536	900	110	2,618	973	115	2,696
Al_2O_3.....	470	293	35	798	334	37	841	376	39	885	418	41	929	458	43	971	499	45	1,014	541	47	1,058
CaO.......	389	24	2,090	2,503	28	2,208	2,625	30	2,320	2,739	34	2,437	2,860	37	2,543	2,969	40	2,660	3,089	43	2,777	3,209
MgO.......	123	7	90	220	8	95	226	10	100	233	11	105	239	12	110	245	13	115	251	14	120	257
Slag......	2,372	875	2,370	5,617	998	2,507	5,877	1,122	2,632	6,126	1,247	2,765	6,384	1,370	2,885	6,627	1,494	3,020	6,886	1,619	3,150	7,131
Flux required...	2,554	1,562		4,116	1,795		4,349	2,012		4,566	2,240		4,794	2,460		5,014	2,682		5,236	2,910		5,464
Flux required, lb. per net ton pig...		600			633			666			699			732			765			798		
Slag volume, lb. per net ton pig...		819			858			895			932			967			1,005			1,040		
Final slag... SiO_2, per cent		35.4			35.3			35.2			35.1			34.9			34.8			34.7		
Al_2O_3, per cent		14.6			14.7			14.8			14.9			15.1			15.2			15.3		
CaO, per cent		46.0			46.1			46.1			46.2			46.2			46.3			46.3		
MgO, per cent		4.0			3.9			3.9			3.8			3.8			3.7			3.7		
Base-acid ratio		1.00			1.00			1.00			1.00			1.00			1.00			1.00		
Melting point		1480°C. = 2695°F.			1485°C. = 2705°F.			1490°C. = 2715°F.			1495°C. = 2720°F.			1500°C. = 2730°F.			1505°C. = 2740°F.			1510°C. = 2750°F.		
Ref. on Fig. 1		A			B			C			D			E			F			G		
Bosh slag[a]... SiO_2, per cent		31.6			30.8			30.1			29.5			28.9			28.3			27.7		
Al_2O_3, per cent		10.8			10.6			10.3			10.1			9.9			9.7			9.5		
CaO, per cent		53.1			54.1			55.1			55.9			56.7			57.5			58.3		
MgO, per cent		4.5			4.5			4.5			4.5			4.5			4.5			4.5		
Melting point		1900°C. = 3450°F.			1920°C. = 3490°F.			1940°C. = 3525°F.			1955°C. = 3550°F.			1966°C. = 3570°F.			1973°C. = 3580°F.			1980°C. = 3595°F.		
Ref. on Fig. 1		A'			B'			C'			D'			E'			F'			G'		

[a] Final slag based upon 1 per cent silicon in iron, remaining oxides balanced to 100 per cent; bosh slags based upon 0.75 per cent silicon in iron.

coke. The composition and melting point of the bosh slag would not change because of variations in coke ash, but would remain
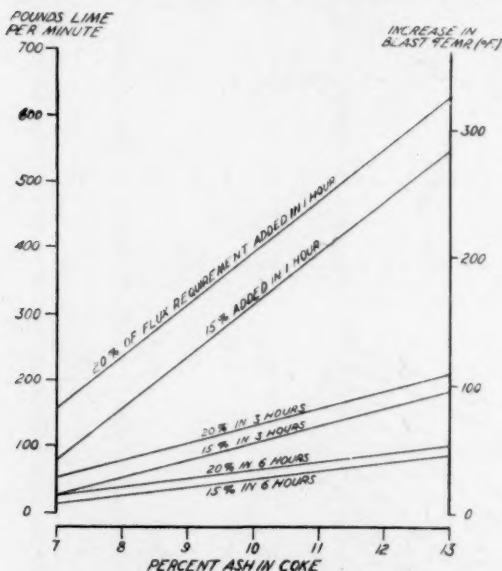
FIG. 2.—THEORETICAL RATE OF LIME ADDITION AND INCREASE IN BLAST TEMPERATURE REQUIRED UNDER VARIOUS CONDITIONS OF ASH IN COKE, FLUX REMOVED FROM BURDEN, AND DURATION OF ADDITION THROUGH TUYERES.

the same as that for the coke of 9 per cent ash content (C').

INTRODUCTION OF LIME THROUGH TUYERES

On Table 2 is indicated the excess or deficiency in limestone caused by variations from the normal 9 per cent coke ash. In this case it is 33 lb. per net ton of iron per 1 per cent variation in coke ash. Table 3 shows that if 15 per cent of the normal limestone for a 9 per cent ash coke were introduced through the tuyeres instead of into the furnace top it would be equivalent to a reduction of 100 lb. of flux per ton of iron. In the example cited, the actual amount of lime injected would vary from 19 to 132 lb. per ton of iron, dependent upon the requirement of the furnace as determined by the ash content of the coke. The bosh slag at a 15 per cent limestone injection rate would be of the composition indicated by X in Fig. 1, and would not vary, be-

cause the amount of limestone charged into the furnace top would be held constant. By injection of various amounts of limestone through the tuyeres, the final slags could be held at almost any desired composition; their uniformity in analysis would be limited only by the time required for injection.

If 20 per cent limestone were removed from the burden, the composition of the bosh slag would be as indicated by Y on Fig. 1. This slag theoretically would have a melting point 72°F. lower than that of the bosh slag in the 15 per cent stone reduction. The only difference in operation under the 20 per cent practice would be the higher amounts of blown flux required.

In practice, burnt lime instead of limestone will be injected through the tuyeres, since limestone by calcination would probably unduly lower the hearth temperature. This feature would make additional heat available in the stack to the extent of that required to calcine the amount of limestone replaced, and would increase the reducing power of the stack gas to the extent of the carbon dioxide contained in the limestone removed from the burden.

The theoretical increase in blast temperature required to raise the added lime to hearth temperature is calculated as follows:

A furnace making 1000 net tons per day will produce

$$\frac{1000}{60 \times 24} = 0.694 \text{ net ton iron per minute.}$$

90,880 cu. ft. air was required per net ton iron for a typical plant during January 1942:

90,880 × 0.694 = 63,071 cu. ft. air required per minute.

0.07661 × 63,071 = 4832 lb. air required per minute.

0.248 × 4832 = 1198 B.t.u. per minute = heat content of 4832 lb. or 63,071 cu. ft. air per 1°F.

TABLE 2.—*Effect of Variation in Coke Ash on Final Slag Analyses*

(Flux quantity constant at amount required to maintain 1.00 base-acid ratio in final slag when using 9 per cent ash coke)

Material	Pounds in Burden (Includes 4,566 Flux but Excludes Coke)	7 Per Cent Coke Ash Coke	Total	8 Per Cent Coke Ash Coke	Total	9 Per Cent Coke Ash Coke	Total	10 Per Cent Coke Ash Coke	Total	11 Per Cent Coke Ash Coke	Total	12 Per Cent Coke Ash Coke	Total	13 Per Cent Coke Ash Coke	Total
Coke............		12,000		12,000		12,000		12,000		12,000		12,000		12,000	
Fe............	13,213	98	13,311	98	13,311	98	13,311	98	13,311	98	13,311	98	13,311	98	13,311
P............	34.15	1.28	35.43	1.28	35.43	1.28	35.43	1.28	35.43	1.28	35.43	1.28	35.43	1.28	35.43
Mn............	361.1	0.8	361.9	0.8	361.9	0.8	361.9	0.8	361.9	0.8	361.9	0.8	361.9	0.8	361.9
SiO₂............	1,704	527	2,231	601	2,305	676	2,380	750	2,454	823	2,527	900	2,604	973	2,677
Al₂O₃............	509	293	802	334	843	376	885	418	927	458	967	499	1,008	541	1,050
CaO............	2,709	24	2,733	28	2,737	30	2,739	34	2,743	37	2,746	40	2,749	43	2,752
MgO............	223	7	230	8	231	10	233	11	234	12	236	13	237	14	238
Slag............	5,004	875	5,879	998	6,002	1,122	6,126	1,247	6,251	1,370	6,374	1,494	6,498	1,619	6,623
Flux required............	2,554	1,562	4,116	1,795	4,349	2,012	4,566	2,240	4,794	2,460	5,014	2,682	5,236	2,910	5,464
Flux used, lb. per net ton pig............		666		666		666		666		666		666		666	
Flux required, lb. per net ton pig............		600		633		666		699		732		765		798	
Excess (+) or deficit (−) in flux............		+66		+33		0		−33		−66		−99		−132	
Slag volume, lb. per net ton pig............		857		875		895		911		929		947		965	
Final slag: SiO₂, per cent		34.0		34.6		35.2		35.6		36.1		36.7		37.1	
Al₂O₃, per cent		14.1		14.5		14.8		15.3		15.7		16.0		16.4	
CaO, per cent		47.9		47.0		46.1		45.2		44.4		43.6		42.8	
MgO, per cent		4.0		3.9		3.9		3.9		3.8		3.7		3.7	
Base-acid ratio		1.08		1.04		1.00		0.96		0.93		0.90		0.87	
Melting point		1625°C. = 2955°F.		1570°C. = 2855°F.		1490°C. = 2715°F.		1440°C. = 2625°F.		1435°C. = 2615°F.		1430°C. = 2605°F.		1425°C. = 2595°F.	
Desulphurizing power[a]		12.0		9.0		7.7		6.7		5.8		5.0		4.2	
Ref. on Fig. I		a		b		c		d		e		f		g	
Bosh slag: SiO₂, per cent		30.1		30.1		30.1		30.1		30.1		30.1		30.1	
Al₂O₃, per cent		10.3		10.3		10.3		10.3		10.3		10.3		10.3	
CaO, per cent		55.1		55.1		55.1		55.1		55.1		55.1		55.1	
MgO, per cent		4.5		4.5		4.5		4.5		4.5		4.5		4.5	
Melting point		1940°C. = 3525°F.		1940°C. = 3525°F.		1940°C. = 3525°F.		1940°C. = 3525°F.		1940°C. = 3525°F.		1940°C. = 3525°F.		1940°C. = 3525°F.	
Ref. on Fig. I		C_1		C_1		C_1		C_1		C_1		C_1		C_1	

a Desulphurizing power as determined on Fig. 9 appearing in reference No. 4.

Heat content of 1 lb. CaO at 2900°F. = 611 B.t.u.

$611/_{1198} = 0.510°F.$ increase in hot-blast temperature required per pound CaO injected per minute.

of lime addition and blast-temperature requirements for various ash contents of coke and under conditions of various intervals of addition and various base increments of flux removed from the burden.

TABLE 3.—*Flux Requirement for 15 and 20 Per Cent Flux Equivalent Blown through Tuyeres*

Material	7 Per Cent Coke Ash	8 Per Cent Coke Ash	9 Per Cent Coke Ash	10 Per Cent Coke Ash	11 Per Cent Coke Ash	12 Per Cent Coke Ash	13 Per Cent Coke Ash
15 Per Cent Flux Equivalent Blown through Tuyeres							
	Lb. per Net Ton Pig	Lb.	Lb.	Lb.	Lb.	Lb.	Lb.
Flux required for 9 per cent ash coke.	666	666	666	666	666	666	666
Flux required for 15 per cent injection	0.15 × 0.666 = 100	100	100	100	100	100	100
Excess (+) or deficit (−) in total flux	+66	+ 33	0	− 33	− 66	− 99	−132
Blown flux required to maintain 1.00 base-acid ratio in final slag.......	100 − 66 = 34	67	100	133	166	199	232
Equivalent lime required..........	34 × 0.57 = 19	38	57	76	95	113	132
Bosh slag analysis and melting point.	SiO₂, 32.9 per cent; Al₂O₃, 11.3; CaO, 52.9; MgO, 2.9. Melting point 1820°C. = 3310°F.						
20 Per Cent Flux Equivalent Blown through Tuyeres							
Flux required for 9 per cent ash coke.	666	666	666	666	666	666	666
Flux required for 20 per cent injection	0.20 × 0.666 = 133	133	133	133	133	133	133
Excess (+) or deficit (−) in total flux	+66	+ 33	0	− 33	− 66	− 99	−132
Blown flux required to maintain constant final slag analysis..........	133 − 66 = 67	100	133	166	199	232	265
Equivalent lime required..........	67 × 0.57 = 38	57	76	95	113	132	151
Bosh slag analysis and melting point.	SiO₂, 33.7 per cent; Al₂O₃, 11.5; CaO, 51.8; MgO, 3.0. Melting point, 1780°C. = 3235°F.						

Table 3 indicates that addition through tuyeres of 57 lb. of lime per net ton of iron would be required when using a 9 per cent ash coke at a 15 per cent reduction in limestone charged into the furnace top. For a furnace of 1000 net tons, this requires an addition through the tuyeres of

$$\frac{1000 \times 57 \times 6}{24 \times 60} = 238 \text{ lb. lime per minute}$$

for a period of one hour to satisfy the slag requirements for the iron made in a 6-hr. casting interval and would necessitate an increase of 120°F. in blast temperature for the period of addition. If the same requirements were uniformly added over the entire 6-hr. period, only 40 lb. per min. need be added, at an increase in blast temperature of only 20°F. Fig. 2 shows the rate

In practice, the rate of addition will be determined by the actual chilling effect of the injected lime on the hearth. While sudden increases in blast temperature for short injection periods may not be desirable from an operating standpoint, if the lime were injected immediately after cast, the higher-lime slag would tend to stratify immediately above the metal bath in the hearth and might prove much more effective as a desulphurizer than the more acid slag formed as the siliceous oxides from the coke ash progressively dilute the slag during the 6-hr. interval.

In summary, the introduction of flux through tuyeres offers a solution to the problem of immediate control of iron analysis under conditions of widely fluctuating coke ash. The adjustment of bosh slags to

a lower thermal and a more uniform chemi-
cal range also offers possibilities of increased
production and decreased coke rate in-
herent in operation with leaner bosh slags
and utilization of higher and more uniform
blast temperatures.

ACKNOWLEDGMENTS

The author wishes to thank Messrs.
Harry A. Strain, R. M. Lloyd, and M. E.
Gaebe, of the Carnegie-Illinois Steel Corpo-
ration, Pittsburgh, Pa., for their helpful
suggestions.

REFERENCES

1. S. P. Kinney: Composition of Materials
   from Various Elevations in an Iron Blast
   Furnace. U. S. Bur. Mines *Tech. Paper* 397
   (1926).
2. S. P. Kinney, P. H. Royster and T. L.
   Joseph: Iron Blast Furnace Reactions.
   U. S. Bur. Mines *Tech. Paper* 391 (1927).
3. R. S. McCaffery and Co-workers: Determi-
   nation of Viscosity of Iron Blast-furnace
   Slags. *Trans.* A.I.M.E. (1932) **100**, 86.
4. W. F. Holbrook and T. L. Joseph: Relative
   Desulphurizing Powers of Blast-furnace
   Slags. *Trans.* A.I.M.E. (1936) **120**, 99.
5. G. E. Steudel: Effect of Volume and Proper-
   ties of Bosh and Hearth Slag on Quality
   of Iron. *Trans.* A.I.M.E. (1940) **140**, 65.
6. R. S. McCaffery: A Study of Blast-furnace
   Slags. *Blast Furnace and Steel Plant* (June
   and July, 1938).

The Electrical Conductivity of Molten Blast-furnace Slags

By A. E. Martin,* Junior Member, and Gerhard Derge,† Member A.I.M.E.

If the molecular constitution of molten slags were better known, the nature of chemical reactions in slags and between slags and metals could be better understood and as a consequence might be better controlled. Constitutional information can be obtained by studies on either the molten or the solidified slags. Valuable as the studies on solidified slags admittedly are for many purposes, especially as control methods in steelmaking, they are always of questionable value in giving information on the molecular constitution of liquid slags. However, the characteristics of molten slags such as viscosity, rates of diffusion, and electrical conductivity can be determined experimentally and interpreted along with other knowledge on slag-metal and slag-gas reactions so as to provide direct information on liquid slags.

Metallurgists are accustomed to regard reactions in molten slags as involving only neutral molecules, whereas it is quite possible that ionic constituents are actually involved. For example, the dissociation of calcium silicate usually is represented as

$$Ca_2SiO_4 = 2CaO + SiO_2$$
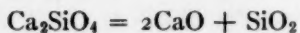
although a reasonable alternative would be to write

$$Ca_2SiO_4 = 2Ca^{+2} + SiO_4^{-4}$$
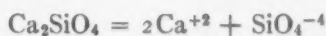
Such ionic dissociation has been suggested frequently without adequate experimental proof.

This paper deals especially with electrical conductivity measurements on slags of the blast-furnace type. These measurements were made to determine whether or not slags are ionized and, if so, to provide a qualitative estimate of the extent of ionization. Electrolysis experiments that indicate the identity of the ions present are also reported. Since the presence of ions has not been considered carefully in modern slag studies, the relevant literature will be reviewed.

Review of Literature

In 1906 Aiken[1] obtained a patent for a continuous process of producing iron electrolytically by passing a direct current through a bath of $FeO \cdot SiO_2$ to which iron oxide was added periodically to maintain a uniform concentration. The patent also included the addition of CaO and MgO to the bath to lower its melting point. The silicate melts involved were thus in the same system as basic open-hearth slags but with higher FeO and lower CaO contents.

Electrical conductivity measurements were made on some molten silicates by Doelter[2] in 1907. Natural silicates, such as

labradorite, diopside, hornblende, and augite were used. The melts were sufficiently good conductors to convince Doelter that these silicates were ionized when molten. A

of many fused salts. Measurements were limited to 1500°C.

In papers published in 1925, 1928 and 1932, Sauerwald and Neuendorff[5] described
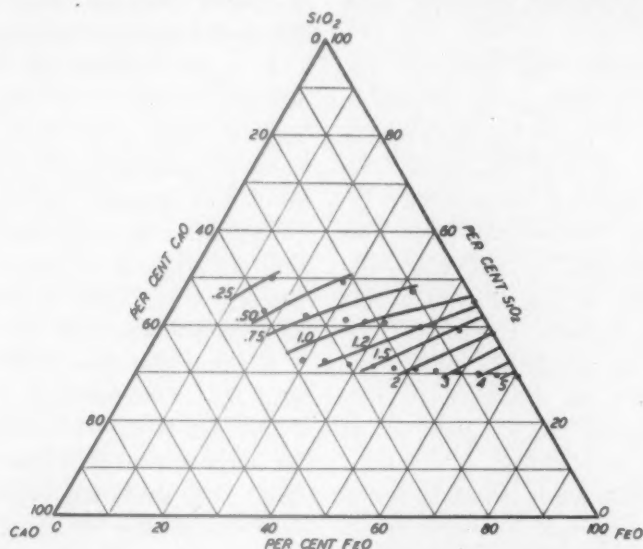
FIG. 1.—ISOELECTRICAL CONDUCTIVITY LINES OF MELTS IN CaO-FeO-SiO$_2$ SYSTEM AT 1500°C. Based on Wejnarth's data.

marked increase in the conductivity of the silicates with increasing temperature was observed. This he interpreted as the effect of increased fluidity of the melt or of increased ionization. The silicates that he investigated are not unlike some steelmaking slags if the low percentage of Na$_2$O is disregarded.

In 1910 Beckman[3] patented a method of plating out iron on a cathode from a molten bath of CaO-Fe$_2$O$_3$, in which a slight excess of iron oxide was maintained. An unidentified gas was evolved at the anode. This experiment showed the presence of iron ions in the melt.

In 1924, Farup, Fleischer and Holtan[4] measured the electrical conductivity of melts in the CaO-SiO$_2$ system and in the high-silica portion of the CaO-Al$_2$O$_3$-SiO$_2$ system. A few compositions approximating blast-furnace slags were included but not enough to indicate the relation between conductivity and chemical composition. The conductivities were higher than those

a number of experiments dealing with the electrolysis of several silicates, the majority of them in the iron oxide-silica system. In one series of experiments, the molten silicate was contained in an iron crucible, which also served as one of the electrodes. The other electrode, usually the cathode, consisted of either an iron or a graphite rod placed concentrically in the crucible. Iron went into solution at the anode and a very pure form of iron was deposited in a spongy form at the cathode. A typical composition of the molten silicate was 75 per cent iron oxide and 25 per cent silica. In another cell, a refractory-lined crucible was used. The cathode consisted of an iron rod that pierced the bottom of the crucible. A carbon rod, which dipped into the molten bath from above, served as the anode. The electrolyte was composed of commercial iron ores, both with and without additions of silica. When the cell was operated at temperatures above the melting point of iron, the electroplated metal collected

as a molten pool at the bottom of the crucible. When iron ores high in manganese were used in the electrolysis, an iron-manganese alloy containing as much as 68 per cent manganese was deposited from the molten bath.

Wejnarth[6] measured the electrical conductivity of a large number of silicates in the $FeO-SiO_2$, and $FeO-CaO-MnO-Al_2O_3-SiO_2$ systems. In the $FeO-SiO_2$ system, he found that the electrical conductivity increased with the concentration of iron oxide. The results for the $FeO-CaO-SiO_2$ system are shown in Fig. 1, which was constructed from his data. The conductivities are given in reciprocal ohms per centimeter, as are all conductivities reported in this paper. This diagram shows that the partial substitution of CaO for FeO results in a decrease in conductivity though not as large as is obtained by partly substituting SiO_2 for FeO. When Wejnarth substituted MnO for part of the FeO in this system, an increase in conductivity was obtained. Wejnarth found an abrupt change in conductivity of the silicates at the temperature of primary crystallization. The effect was so sharp that it proved to be a good method of determining melting points of silicates. He collected many data on freezing points of slag systems by this method.

In 1931[7] Tammann cited as proof of the ionic dissociation of slags some experiments made in 1924 involving slag-metal interchanges. For example, in one test, an iron-aluminum alloy was added to an $FeO-CaO-2SiO_2$ melt at 1500°C. After 10 min. it was found that iron had been precipitated from the silicate and replaced by an equivalent amount of aluminum. Other experiments involved the precipitation of iron both by manganese and by nickel from the same silicate mentioned above, and the precipitation of nickel by iron added to a $NiO-CaO-2SiO_2$ melt. These experiments do not appear to constitute proof of the ionization of the melts

to the authors of this paper, although it is considered noteworthy that Tammann believed that slags were ionized. McCaffery[8] mentioned that electrical conductivity work on slags ought to be an important field for future research.

In 1933 Koerber and Oelsen[9] listed as further evidence of the ionization of molten slags some facts concerning the color of quenched acid slags in the $FeO-MnO-SiO_2$ system. Such slags are green in color, the same color possessed by ferrous ions in aqueous solution. Moreover, the density of the color is deeper with higher concentrations of iron oxide in the slag.

Koerber and Oelsen also mentioned the fact that the reaction generally written $FeO + Mn = Fe + MnO$ had the same equilibrium constant in silicate as in phosphate slags. One would not expect that FeO and CaO would have the same activities in the two slag types. This was taken as indicating that the actual reaction is $Fe^{++} + Mn = Mn^{++} + Fe$. With complete ionization, it seems likely that the activities of Fe^{++} and Mn^{++} would not be influenced much by other ions present. (This is somewhat analogous to the discovery made many years ago, that the reaction between a strong base and a strong acid always involved the same simple reaction: $H^+ + OH^- = H_2O$. This became apparent when the heats of the reactions for different pairs of reactants were compared and found to be identical.)

Herasymenko[10] was so completely won over to the ionic theory of slags that he made many calculations based on the assumption that ionic dissociation was complete; i.e., that no electroneutral molecules were present. In 1940 Geller,[11] apparently unaware of the work of Sauerwald and Neuendorff, repeated many of their experiments, with identical results. Iron was plated out from iron silicate melts. In the same year, D. E. Babcock, in a discussion of a paper by Wood, Barrett, and Holbrook,[12] suggested that a satisfactory

explanation of desulphurization of iron by slag might be obtained from the ionic theory of slags. In 1941 Martin, Glockler and Wood,[13] made use of the ionic theory of molten slags to explain the stability of some colloidal sulphides which they had observed in $CaO-Al_2O_3-SiO_2$ slags.

In 1941 Hellbrugge and Endell[14] investigated the viscosity of a number of silicates and concluded that the variations of viscosity with composition could be well explained on the basis of ionization of slags. They found that viscosity was related to ionic valence and ionic size. A method of calculating viscosity from chemical composition was developed and was found to check well with experimental values for blast-furnace slags. The method is not applicable to open-hearth slags, as it does not hold at a basicity greater than 2. It was suggested that a critical change occurs at this basicity.

PURPOSE OF INVESTIGATION

Much of the work that has been reviewed appeared to be good evidence of ionization in molten slags. However, a systematic experimental study of this question seemed to be lacking in slags of interest to ferrous metallurgists.

The blast-furnace range of compositions in the $CaO-Al_2O_3-SiO_2$ system was selected for study for several reasons. First, graphite crucibles and electrodes could be used. Second, correlations could be made with the data on desulphurization of Holbrook and Joseph[15] and with the viscosity data of McCaffery[8] and of Feild and Royster.[16] The aim of the research, then, was to determine whether or not these slags are ionized by measuring the electrical conductivity in this system as a function of composition and temperature, supplementing these measurements with some electrolysis experiments in an attempt to identify the ions present.

ELECTRICAL CONDUCTIVITY MEASUREMENTS

The conductivity experiments were carried out in an enclosed induction furnace through which a steady stream of high-purity nitrogen was passed. The slag was contained in a graphite crucible, which also served as the heater. Temperatures of the slag were measured with an optical pyrometer, which was calibrated for the conditions of the experiment by means of a noble-metal thermocouple. Fuming did not interfere with the measurement of temperatures under 1620°C.

Synthetic slags were prepared from C.P. aluminum oxide, C.P. silica, and calcined C.P. calcium carbonate. A sufficient quantity of slag was taken for each test so that a depth of about one inch of molten slag would be obtained in the crucible. After a slow melting period, the temperature of the slag was raised to 1620°C. for homogenization and elimination of bubbles. The temperature was then lowered to 1500°C. Two parallel graphite rods of $\frac{1}{16}$-in. dia., spaced $1\frac{1}{8}$ in. apart, were immersed vertically a distance of $\frac{3}{16}$ in. into the melt, by a rack and pinion mechanism. The temperature was then raised to about 1620°C. and held for 5 to 10 min. at that temperature. The power to the furnace was then decreased slowly, so that the temperature fell at the rate of about 1° to 2°C. per minute. Simultaneous readings of resistance and temperature were taken at approximately 5°C. intervals. When a temperature of 1420°C. was reached, the electrodes were withdrawn and the melt was allowed to cool.

The electrical resistance of the melt was measured with a Wheatstone bridge. The point of balance was determined by a sound minimum in a pair of earphones. The noise accompanying the operation of the high-frequency unit did not seriously interfere with the detection of the sound minimum in the earphones because of the

difference in (sound) pitch involved. At constant temperature, the same conductivity reading was obtained when the power was on as when it was off. Standardization
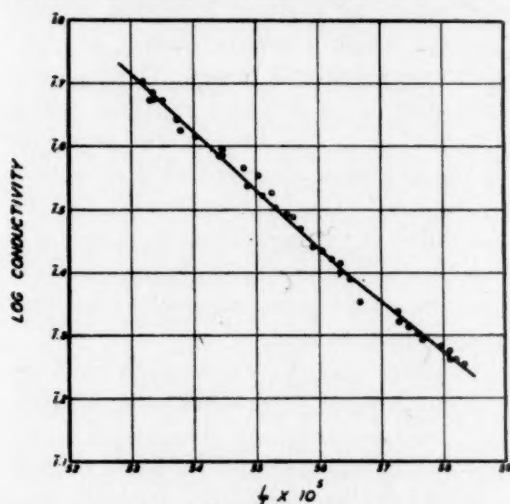
FIG. 2.—DATA ON CONDUCTIVITY VS. TEMPERATURE FOR SLAG NO. 8.

was made at room temperature with a solution of potassium chloride of known

TABLE 1.—*Conductivity Measurements for Slag No. 8*

Temperature, Deg. C.	Conductivity, Reciprocal Ohms per Cm.	Temperature, Deg. C.	Conductivity, Reciprocal Ohms per Cm.
1607	0.503	1526	0.308
1601	0.472	1522	0.295
1603	0.470	1515	0.275
1601	0.483	1511	0.270
1599	0.472	1506	0.264
1596	0.470	1502	0.260
1588	0.440	1502	0.251
1586	0.423	1497	0.245
1578	0.413	1492	0.225
1565	0.383	1473	0.217
1563	0.393	1475	0.217
1563	0.384	1473	0.209
1552	0.367	1468	0.206
1552	0.366	1463	0.200
1550	0.344	1461	0.196
1544	0.358	1452	0.191
1542	0.333	1448	0.188
1537	0.336	1445	0.182
1535	0.319	1448	0.182
1529	0.311	1441	0.180

conductivity. A correction, obtained by experiment, was applied for the change of resistance of the graphite electrodes between room temperature and the temperature of the conductivity measurements.

On plotting the logarithm of the conductivity versus the reciprocal of the absolute temperature, the data were found to form approximately straight lines in most cases. To illustrate the nature and accuracy of the measurements, all of the data for slag No. 8, which was typical, are recorded in Table 1 and plotted as the logarithm of the conductivity versus the reciprocal of the absolute temperature in Fig. 2.

TABLE 2.—*Electrical Conductivities of* CaO-Al_2O_3-SiO_2 *Slags*

Sample No.	Slag Composition, Per Cent			Electrical Conductivity, Reciprocal Ohms per Cm.			
	SiO_2	Al_2O_3	CaO	1600°C.	1550°C.	1500°C.	1450°C.
1	41.7	11.6	46.7	0.817	0.671	0.551	0.442
2	40.1	14.8	45.1	0.785	0.538	0.361	0.236
3	40.05	9.9	50.05	0.762	0.587	0.447	0.337
4	45.0	5.0	50.0	0.730	0.560	0.424	0.327
5	50.0	5.0	45.0	0.671	0.543	0.459	0.350
6	36.1	14.8	49.1	0.637	0.434	0.290	0.188
7	43.3	8.3	48.3	0.563	0.423	0.311	0.225
8	50.05	9.9	40.05	0.479	0.352	0.256	0.188
9	45.05	9.9	45.05	0.469	0.358	0.251	0.146
10	43.0	14.0	43.0	0.439	0.289	0.197	0.138
11	35.15	19.7	45.15	0.383	0.290	0.194	0.129
12	45.15	19.7	35.15	0.333	0.218	0.140	0.099
13	40.15	19.7	40.15	0.297	0.209	0.144	0.098
14	50.1	14.8	35.1	0.282	0.203	0.144	0.101
15	45.1	14.8	40.1	0.248	0.175	0.135	0.090

Similar plots for all slags are shown in Fig. 3. It was considered impractical to show the experimental points in this plot because there were from 30 to 50 values for each of the 15 slags. Values of the conductivities at 50°C. intervals from 1600° to 1450°C. taken from this figure are presented in Table 2, together with the compositions of the slags.

The conductivities of the slags at 1600°C. range from 0.24 to 0.82 reciprocal ohms per centimeter. The following conductivities of well-known ionic media are given for comparison purposes. A 1.0 N. KCl solution has a conductivity of 0.11 at room temperature. Sulphuric acid at a concentration corresponding to its maximum

conductivity, 31 per cent H_2SO_4, has a conductivity of 0.82 at room temperature. Fused ionic salts usually have conductivities ranging from 0.1 to 2.0, dependent on

and 1600°C. varies from 1.46 to 2.36 for the 15 slags studied, the average value being 1.93. The conductivities at 1600°C. are thus 93 per cent greater on the average
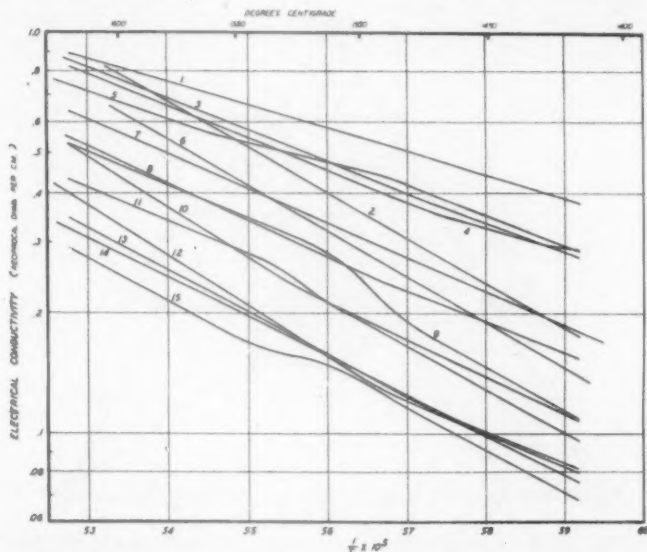
FIG. 3.—LOG OF ELECTRICAL CONDUCTIVITY VS. RECIPROCAL OF ABSOLUTE TEMPERATURE FOR FIFTEEN CaO-Al$_2$O$_3$-SiO$_2$ SLAGS.
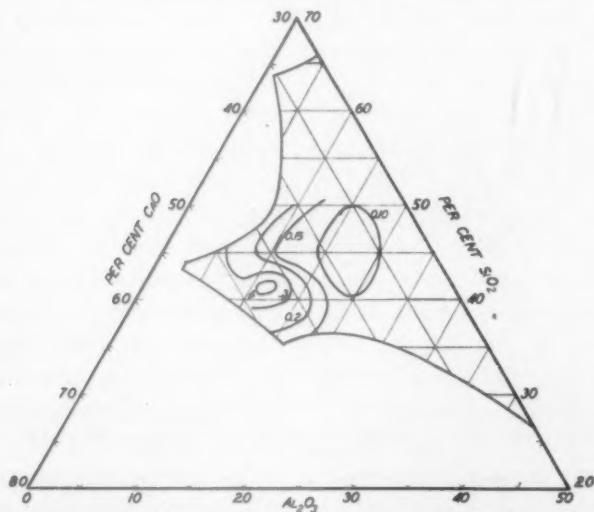
FIG. 4.—ISOELECTRICAL CONDUCTIVITY LINES OF SLAGS IN CaO-Al$_2$O$_3$-SiO$_2$ SYSTEM AT 1450°C.

the salt and the temperature. It is apparent from these figures for highly ionized media that the slags are also ionized to a large extent, although the actual amount cannot be deduced from the data.

The temperature coefficient of conductivity for the 100° interval between 1500°

than those at 1500°C. This increase of conductivity with temperature is characteristic of ionic conductance and is definite proof of the ionic nature of these slags. Materials such as metals that have electronic conductance show a decrease in conductivity with increase in temperature.

The conductivity data for 1450°, 1500°, 1550°, and 1600°C., are plotted on ternary diagrams in Figs. 4, 5, 6, and 7 to show the effect of chemical composition of the

other compositions physical effects might be confused with chemical effects; i.e., the abrupt increase of viscosity accompanying the entrance into a two-phase field would
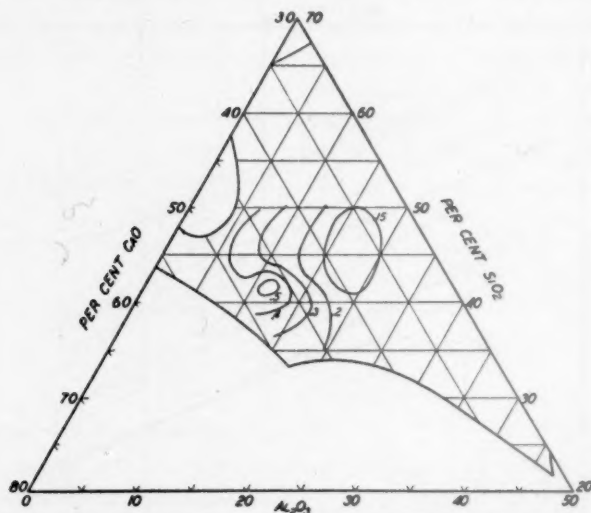
FIG. 5.—ISOELECTRICAL CONDUCTIVITY LINES OF SLAGS IN CaO-Al$_2$O$_3$-SiO$_2$ SYSTEM AT 1500°C.
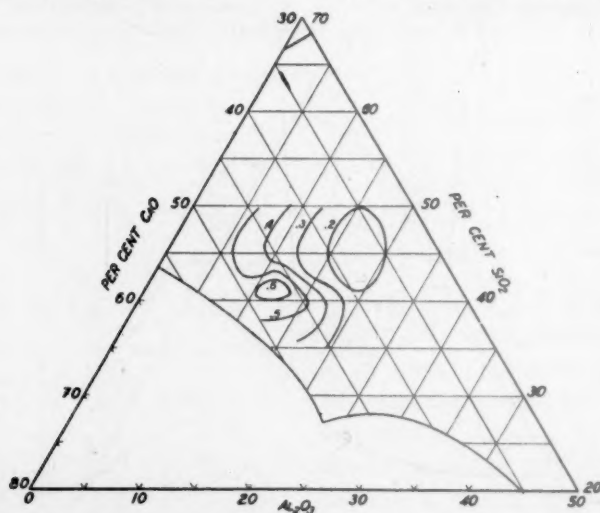
FIG. 6.—ISOELECTRICAL CONDUCTIVITY LINES OF SLAGS IN CaO-Al$_2$O$_3$-SiO$_2$ SYSTEM AT 1550°C.

slags on conductivity at constant temperature. Contour lines are shown for compositions of equal conductivity. In these diagrams the fields of compositions above the liquidus surface on the CaO-Al$_2$O$_3$-SiO$_2$ diagram are clearly distinguished from the fields of those that are not. Only compositions above the liquidus surface were investigated, as it was felt that by taking

result in a marked lowering of the electrical conductivity, which might be construed by some as a chemical effect.

The curves show a maximum in conductivity occurring in the region 38 to 43 per cent SiO$_2$, 44 to 50 per cent CaO and 10 to 15 per cent Al$_2$O$_3$. The peak appeared to be close to the composition: 42 per cent SiO$_2$, 47 CaO and 11 Al$_2$O$_3$. This composi-

tion is close to a ternary eutectic in the $CaO-Al_2O_3-SiO_2$ system located at approximately 41 per cent SiO_2, 47.3 CaO and 11.7 Al_2O_3. A region of minimum conduc-

searches are not in good agreement. The electrical conductivity data do not seem to correlate any better with one than with the other but general trends of increasing
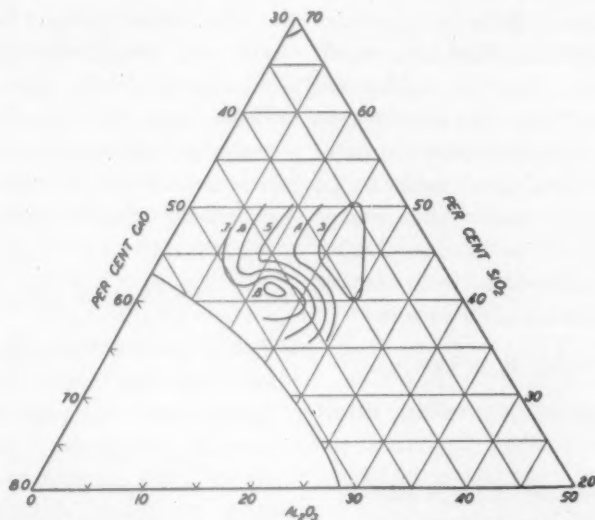
FIG. 7.—ISOELECTRICAL CONDUCTIVITY LINES OF SLAGS IN $CaO-Al_2O_3-SiO_2$ SYSTEM AT 1600°C.

tivity was observed at about 46 per cent SiO_2, 37 CaO and 17 Al_2O_3.

Aside from the maximum and minimum regions, there appears to be a general trend of increasing conductivity with increasing basicity. In this respect there is a correlation with the isodesulphurization curves of Holbrook and Joseph.[15] They observed a continuous increase of desulphurization power with increase of lime up through the region of maximum conductivity. They did, however, encounter a decrease in desulphurizing power at higher lime contents when they entered a two-phase field.

It would not be surprising if a close correlation between electrical conductivity and viscosity were found to exist in slags, since with high ionization both electrical conductivity and viscosity should depend on the number and size of the ions in the melt. The viscosity in the $CaO-Al_2O_3-SiO_2$ system has been reported on twice; first by Feild and Royster[16] and later by McCaffery.[8] The data of these two re-

conductivity with decreasing viscosity can be observed. Feild and Royster show several minima in viscosity; one at about 14 per cent Al_2O_3, 46 CaO, 40 SiO_2, which is within the field of maximum conductivity. McCaffery also shows a minimum in viscosity but this is not apparent if only his compositions above the liquidus surface of the ternary system are plotted. Incidentally, when this is done, McCaffery's data show a good correlation with Holboook and Joseph's[15] data on desulphurizing power; i.e., desulphurizing power increases with decreasing viscosity.

In slags it is to be expected that the decrease of viscosity observed with rising temperature will lead to an increase in conductivity. The amount of this increase might be estimated by a comparison with fused salts of the ionic type, where it is believed that all the increase of conductivity with temperature is due to the change of viscosity, and Lorenz and Kalmus[17] found that in such salts a 79 per cent decrease in viscosity is associated

with a 55 per cent increase in conductivity. However, in these slags in the temperature range from 1500° to 1600°C. the viscosity decreases 79 per cent according to McCaffery,[8] while the electrical conductivity increases 93 per cent. This is a greater increase than the work on fused salts would predict. The reason for the additional increase of conductivity is not certain but the presence of more ions or smaller ions at higher temperatures seems to be indicated. This could result from higher ionization of neutral molecules, higher dissociation of silicate ions into smaller ions or lower solvation of silicate ions.

EXPERIMENTS WITH ELECTROLYSIS

Electrolysis experiments using direct current were also carried out with the

TABLE 3.—*Analyses of Slags after Electrolysis with Direct Current at 1450°C.*
PERCENTAGE BY WEIGHT

Slag	Place of Test	SiO₂	Al₂O₃	CaO
A	Anode	40.00	12.40	47.13
	Cathode	39.69	12.40	48.03
B	Anode	44.06	20.30	36.22
	Cathode	43.37	20.44	36.42
C	Anode	48.44	11.10	40.39
	Cathode	48.11	11.20	40.49

same equipment. The temperature was maintained at about 1450°C. for the duration of the electrolysis, usually one hour. Currents of the order of 1.4 amp. were obtained with a 6-volt storage battery. A gas could be observed evolving at the anode. After the electrolysis a great difference was found to exist in the physical appearance of the solidified slag adjacent to the two electrodes. (In these experiments the slag was solidified without withdrawing the electrodes.) A white deposit was found on the anode. Analyses of sections of the slag near the electrodes are given in Table 3. It is apparent from these analyses that the slag near the anode is richer in silica and poorer in lime than the slag near the

cathode. Although the differences in analysis are not great, it is believed that much larger differences existed but were not apparent because the sections analyzed were too large (5 to 10 grams).

The results indicate that silicon migrates with the negatively charged groups and calcium with the positively charged groups. These, and other considerations[13] make it probable that calcium is present as calcium ions and silicon as silicate ions. It is suggested that the reaction that occurs at the anode is:

$$(SiO_4)^{-4} = SiO_2 + O_2 + 4e.$$
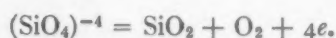
This would account for the gas evolved and for the white deposit. Since the deposit was analyzed with the slag adjacent to the anode, it also accounts for the higher silica content of this region of the melt.

THEORY OF SLAG CONSTITUTION

A theory of slag constitution can be developed on the basis of this research and the recent papers dealing with the structure of glasses,[18] which are in most cases supercooled liquid silicates and therefore similar to fused slags.

A silicon ion is much smaller than most ions. The aluminum ion is also fairly small. Calcium, magnesium and iron ions are larger, though not as large as the oxygen ion. Silicon and aluminum ions also have larger charges than the other cations. The result is that silicon and aluminum ions are able to attract oxygen ions much more strongly than other cations because of their greater charge and smaller size.[19] Silicon and aluminum, therefore are largely combined with oxygen in the form of silicates, aluminates and silicoaluminates. What is said in the following about silicon applies also to aluminum if present in moderate amounts. The simplest silicate ion is $(SiO_4)^{-4}$. This can be pictured as a tetrahedron with a silicon ion at the center and oxygen ions at the corners. Larger silicate

groups exist, made up of tetrahedra that share corners through a common oxygen ion. Thus $(Si_2O_7)^{-6}$ consists of two tetrahedra having one common oxygen. Two tetrahedra never share more than one corner together, though a tetrahedron can share all four corners with four other tetrahedra. In larger silicate groups, the chains of tetrahedra may be closed to form rings. Silicate ions with many rings are the equivalent of sheets; i.e., two-dimensional networks. Still larger silicate groups may consist of three-dimensional networks. The size of the silicate groups is dependent on the availability of oxygen ions in the melt. This can be shown by reactions that can be written between the silicate ions and the oxygen ions; e.g.:

$$2(SiO_4)^{-4} = (Si_2O_7)^{-6} + O^{-2}$$
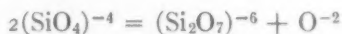
Thus, with a plentiful supply of oxygen ions, the tendency is toward the smaller silicate ions; e.g., $(SiO_4)^{-4}$, resulting in low viscosity and high electrical conductivity. With a less plentiful supply of oxygen ions, the tendency is toward larger silicate groups, resulting in high viscosity and low electrical conductivity.

The supply of oxygen ions in the slag is dependent primarily on the atomic ratio of oxygen to silicon, which can be roughly represented by the basicity of the slag, and secondarily on the presence of other ions such as Fe^{++} and Ca^{++}. The latter ions have considerable difficulty in removing oxygen ions from silicate ions in acid slags where the oxygen to silicon ratio is small, but as the basicity of the slag is increased, it becomes easier for them to do so.

At a basicity corresponding to a lime-silica ratio of 2, the smallest silicate ion, $(SiO_4)^{-4}$, is present in high concentration with only a small amount of larger silicates present in equilibrium with the oxygen ions. As the basicity is further increased, the larger silicate groups virtually disappear. Silicon is then saturated with oxygen and for the first time it is possible for other oxygen combinations, such as CaO, FeO and ferrites, to exist in high concentrations. This theory explains, then, why frequently there is a marked change in the properties of silicates at a lime-silica ratio of 2.

It is suggested that calcium and iron exist in acid or moderately basic slags largely as the ions Ca^{++} and Fe^{++}. Neutral molecules such as Ca_2SiO_4, CaO and FeO are present probably to some extent. The concentration of free CaO and FeO increases with increasing basicity, as already brought out, and ferrites probably are present in very basic slags.

Large silicate groups may entrap cations such as Ca^{++} and Fe^{++} as well as neutral molecules. Furthermore, it is possible that the silicate groups may be more or less solvated; in other words, enveloped by neutral molecules.

SUMMARY

1. Molten blast-furnace slags have high electrical conductivities and a high positive temperature coefficient of conductivity, which indicate high degrees of ionization.

2. At a given temperature, electrical conductivity in the $CaO-Al_2O_3-SiO_2$ system is somewhat related to viscosity; the former increasing, the latter decreasing with increasing basicity. This probably means that in the more basic slags either ionization is higher or the ions are smaller and therefore more mobile.

3. Silicon migrates with the negatively charged groups during electrolysis; calcium, with the positively charged groups.

4. A theory of slag constitution based on the results of this research and modern knowledge of glasses assumes that as the atomic ratio of oxygen to silicon in a slag increases the number of small silicate ions of the type $(SiO_4)^{-4}$ and $(Si_2O_7)^{-6}$ will increase, and that constituents such as CaO, FeO and ferrites become stable in basic slags because it is only under these conditions that unsaturated silicate com-

plexes will not tend to attract all available oxygen ions.

ACKNOWLEDGMENT

Mr. D. A. Russell, of The Youngstown Sheet and Tube Co., kindly furnished some of the chemical analyses.

REFERENCES

1. R. H. Aiken: U. S. Patent 816142 (March 27. 1906).
2. C. Doelter: *Monatsch.* (1907) **28**, 1313–1379.
3. J. W. Beckman: *Trans.* Amer. Electrochem. Soc. (1911) **19**, 171–181. U. S. Patent 973336, Oct. 18, 1910.
4. F. Farup, W. Fleischer and E. Holtan: *Chem. und Industrie* (1924) **12**, 11–15.
5. F. Sauerwald and G. Neuendorff: *Ztsch. Elektrochem.* (1925) **31**, 643–646; (1928) **34**, 199–204 (1932) **38**, 76.
6. A. Wejnarth: *Trans.* Amer. Electrochem. Soc. (1934); **65**, 177–187; **66**, 329–343. *Archiv Erzaufbereit Metallhuttenw.* (1931) **1**, 191–208. *Jernkontorets Ann.* (1933) **117**, 21–43.
7 G. Tammann: *Archiv Eisenhuttenw.* (1931) **5**, 71–74.
8. R. S. McCaffery: *Trans.* A.I.M.E. (1932) **100**, 64–121.
9. F. Koerber and W. Oelsen: *Mitt.* K. W. I.: Eisenforschung (1933) **15**, 293.
10. P. Herasymenko: *Trans.* Faraday Soc. (1938) **34**, 1245–1254.
11. W. Geller: *Ztsch. Elektrochem.* (1940) **46**, 277.
12. C. E. Wood, E. P. Barrett and W. F. Holbrook: *Trans.* A.I.M.E., **140**, 105 (1940).
13. A. E. Martin, G. Glockler and C. E. Wood: U. S. Bur. Mines *R. I.* 3552 (1941).
14. H. Hellbrugge and K. Endell: *Archiv Eisenhuttenw.* (1941) **14**, 307–315.
15. W. F. Holbrook and T. L. Joseph: *Trans.* A.I.M.E. (1936) **120**, 99–120.
16. A. L. Feild and P. H. Royster: U.S. Bur. Mines *Tech. Pubs.* 187 and 189 (1918).
17. R. Lorenz and H. T. Kalmus: *Ztsch. Physik und Chem.* (1907) **59**, 244.
18. W. H. Zacharaisen: *Jnl.* Amer. Chem. Soc. (1932) **54**, 3841–3852; *Jnl. Chem. Physics* (1935) **3**, 162–163.
    G. Hagg: *Jnl. Chem. Phys.* (1935) **3**, 42–49.
19. N. V. Sidgwick: The Electronic Theory of Valency. Oxford Univ. Press, 1927.

DISCUSSION

(B. M. Larsen presiding)

M. A. BREDIG,* New York, N. Y.—I should like to draw attention to recent additional, though somewhat indirect, evidence for the simple ionic nature of the dissociation products of calcium orthosilicate in slags. The crystal

* Vanadium Corporation of America.

structure, as derived from X-ray patterns, of a solid solution of calcium phosphate in Ca_2SiO_4 occurring in open-hearth furnace slags,[20] was shown[21] to be entirely analogous to that of the high-temperature modifications of simple salts of the general type A_2XO_4, such as Na_2SO_4 and K_2SO_4. Small additions, other than calcium phosphate, such as $Na_2O + Al_2O_3$ (or Fe_2O_3)[22] also produce in calcium orthosilicate the same simple hexagonal structure, which is believed to be that of the individual compound Ca_2SiO_4 at its melting point. The above alkali sulphates have not been assumed to be dissociated to any appreciable degree, at their melting points, into constituents other than simple cations A^+ and anions $XO_4{}^{2-}$.

B. M. LARSEN,* Kearny, N. J.—This paper is one of the best that has yet appeared on this subject, and the evidence for a large degree of ionization in liquid slags seems quite convincing. At the present stage of development, it is difficult to see whether or not such data will be useful in understanding the chemistry of slag-metal reactions. Perhaps this will not result until we can somehow learn much more about the kinds of ionic units that are present in the liquid slags. We have been moderately successful in interpreting slag-metal equilibria in terms of oxide units, more or less associated into silicate and phosphate molecules with changing "acid-base ratios," etc., and it seems to increase rather than diminish the clarity of such pictures when we have to consider the slags more or less completely dissociated into ionic units. For example, the rapid decrease in residual Mn in the metal phase with CaO/SiO_2 ratios dropping below the 2 to 1 mol proportions, as caused apparently by a decrease in the *effective* MnO/FeO ratio due to silicate formation, the efficient removal of P from steel by basic slags as related presumably to the stability or small degree of dissociation of lime-phosphate compounds, and the effect of "free"

20 G. Nagelschmidt: *Jnl.* Chem. Soc. (1937) 865.
21 M. A. Bredig: *Jnl.* Amer. Chem. Soc. (1941) **63**, 2533; *Jnl. Phys. Chem.* (1942) **46**, 747.
22 Personal communication from Dr. Kenneth T. Greene, Research Associate, Portland Cement Association Fellowship at the National Bureau of Standards, Washington, D. C.

* Research Laboratory, U. S. Steel Corporation.

CaO and MnO on the concentration of S; how are these effects to be explained in terms of an ionized slag phase? When a slag is *diluted* by SiO_2 from a lime-silica ratio of say 3.5 to one of 2.5, the apparent concentration of iron oxide is *increased* (at least its activity appears to be increased). It is doubtful that this is related to changes in lime ferrite concentration and more likely that the effect is as though the total number of molecular (or ionic) units in a unit weight of slag is decreased by the added silica. There is much of guesswork in such interpretations, however, and we need to know very much more about the true constitution of liquid slag phases. The authors certainly deserve unstinting praise and encouragement to continue their studies on this difficult subject.

A. E. MARTIN AND G. DERGE.—The example cited by Dr. Bredig of the ionic nature of calcium phosphate dissolved in Ca_2SiO_4 is an interesting study of the nature of solidified slags and does indicate that this constituent is also ionized when molten.

The chairman has pointed out some of the slag problems that still require study. We feel that the argument presented in that part of the paper dealing with the Theory of Slag Constitution throws enough light on these problems to justify additional study of these conditions through measurements of conductivity or other slag properties related to the ionization of the slag.

Additional work on the electrical propertise of molten slags is in progress in the Metals Research Laboratory, but the experimental technique becomes much more difficult when it is no longer possible to use graphite electrodes and crucibles.

Some Physical Characteristics of By-product Coke for Blast Furnaces

By Charles C. Russell* and Michael Perch†
(Cincinnati Meeting, April 1942)

Nearly 75 per cent of the total coke production in the United States in 1940 was consumed in blast furnaces. In 1939 the percentage was 69.9, and in 1938 it was 61.3. To produce a net ton of pig iron 1757 lb. of coke was required in 1940 and 1760 lb. in 1939. These figures indicate how dependent the production of pig iron is upon the production of coke. The rate of iron production is in some measure influenced by the physical and chemical characteristics of the coke. Blast-furnace operators believe that the physical properties of coke profoundly influence the operation of the furnace. Although it is true that coke of a wide variety of physical properties is used in American blast furnaces, the periodic fluctuation of these properties is one of the causes of irregularity of blast-furnace operation.

The purpose of this paper is to present a broad picture of the physical properties of by-product coke that are generally considered to be important by coke-oven and blast-furnace operators. Effects of the kind of coal used, the preparation of the coal, the rate of coking, and other factors will be considered. Of all these variables, the kind of coal used is by far the most important. In this discussion use will be made of the method of coal classification by rank[1] standardized by the American Society for Testing Materials. Although this method of classification has been an American standard for several years, it has not been given the attention it deserves, especially in connection with the selection of coal for production of coke. Despite the fact that many producers of blast-furnace coke are limited to some particular source or sources of coal, a good understanding of the principles involved in setting up the standard method of classification may lead to a better appreciation of the causes of changes in coke characteristics. Furthermore, where it is necessary to select new coals as a substitute for the original supply, this method of classification can be of great assistance.

The data presented have been gathered from many sources, but no attempt has been made to cover the vast literature. Instead, some of the more important data have been selected to show how coals and their carbonization affect some of the physical properties of coke. It must be emphasized that generalizations concerning the behavior of coking coals are presented and that individual coals may vary widely from the specific behavior depicted. Nevertheless, it is believed that the data illustrate certain typical behaviors. Neither was it possible to cover completely all the factors involved; for example, the macroscopic constituents of coal are believed to have important effects on the physical properties of coke, but since there is little information available for such study, and since vitrain, clarain, and durain are neither

chemical entities nor have constant composition throughout the realm of coal seams, their effects cannot be satisfactorily evaluated at this time.

supplies virtually all the requirements of the Pittsburgh, Youngstown, Cleveland, and Chicago districts. Alabama coals supply the Birmingham district. Other fields that
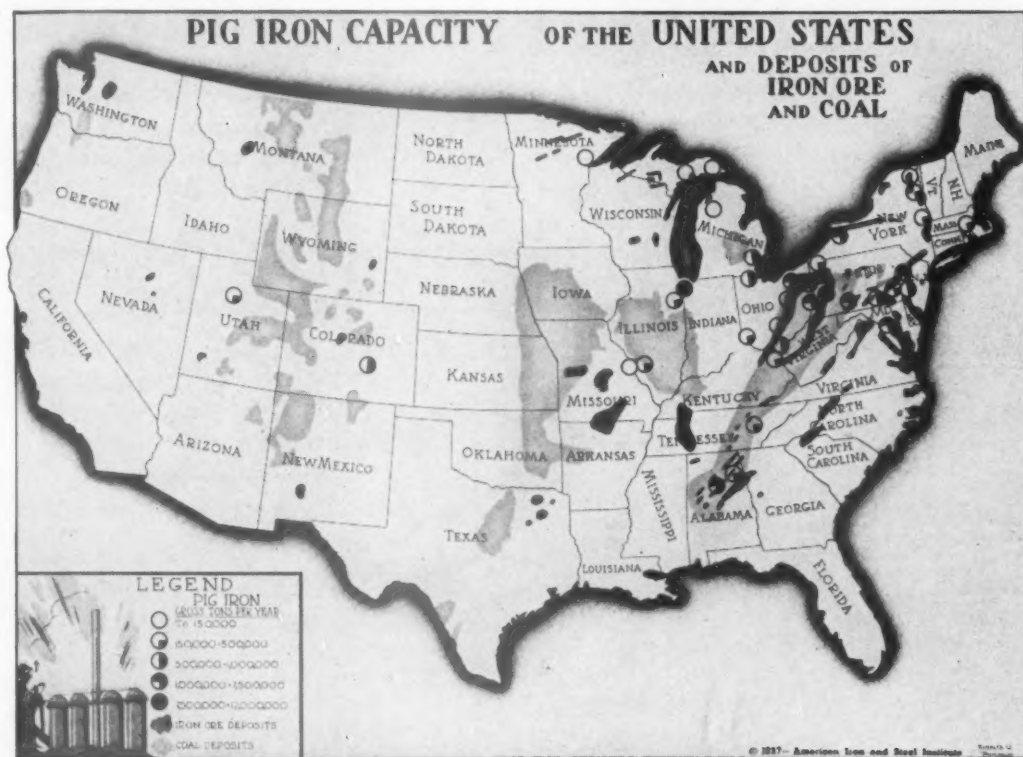
FIG. 1.—PIG-IRON CAPACITY OF THE UNITED STATES AND DEPOSITS OF IRON ORE AND COAL.
Copyright, American Iron and Steel Institute.

KINDS OF COAL USED FOR BY-PRODUCT COKING

Fields of Origin

More than 76 million net tons of coal was carbonized in by-product ovens in the United States in 1940. This tonnage represented 17 per cent of the bituminous coal mined during that year. A map showing pig-iron capacity of the United States in 1937 and deposits of iron ore and coal is shown in Fig. 1.[2] This map indicates the geographical location of the coal deposits. By far the largest quantities of coking coals are produced in the Appalachian region of western Pennsylvania, West Virginia, Virginia, and eastern Kentucky. This field

produce or contain smaller amounts of coking coals are found in southern Illinois, Colorado, Utah, and Washington.

In general, coals used for coking are selected from the fields most advantageously situated in respect to the coke-oven plants. A detailed summary of all districts producing coking coals in 1940 and the areas in which the coal was used is presented in Table 1.[3]

Rank

Because coal is a natural material produced from plant remains by progressive metamorphism, its chemical and physical properties vary over a wide range. The various ranks of coal that are recognized

are not separated by sharp lines of demarcation, but have been defined until recently according to a variety of schemes, none of which was generally accepted. It remained for the committees of the American Society for Testing Materials to establish an acceptable method of classification in which the boundaries of the various coal ranks are specifically defined. This work required more than 10 years of study by the country's foremost coal technologists.

The method finally adopted is simple in that it requires the determination of only the proximate analysis and heating value, both of which can be readily determined in any coal laboratory. For the actual classification, the fixed carbon is calculated to the dry mineral-matter-free basis, and the heating value to the moist mineral-matter-free basis. Mineral matter is the ash-forming material as it exists in the coal before the coal is burned. It is the inorganic

TABLE 1.—*Coal Purchased for Manufacture of By-product Coke in the United States in 1940*[3]

State and District Where Coal Was Produced	Total Purchased, Net Tons	States Where Coal Was Consumed—in Order of Importance
Alabama	6,716,803	Alabama
Colorado:		
Canon, Crested Butte and Walsen	126,890	Colorado
Trinidad	719,543	Colorado
Georgia	14,423	Tennessee
Illinois: Southern	214,845	Illinois
Kentucky, Eastern:		
Elkhorn (including Hazard)	2,067,341	Indiana, Ohio, New York, Illinois, New Jersey, Michigan, Minnesota, Wisconsin
Harlan	4,254,922	Indiana, Illinois, Ohio, Minnesota, Michigan, New York, Wisconsin
Kenova-Thacker	1,709,299	Michigan, Ohio, Wisconsin, and West Virginia
Miscellaneous	181,716	Indiana, Missouri
New Mexico	4,413	Colorado
Ohio	962	Ohio
Pennsylvania:		
Central Pennsylvania:		
Medium-volatile	574,035	New York and Pennsylvania
Low-volatile	1,738,156	Pennsylvania, New York, Maryland
Connellsville	17,868,048	Pennsylvania, Ohio, West Virginia, New York, Illinois, Minnesota, Indiana, Michigan
Freeport	1,982,018	Ohio, West Virginia, Michigan, New York, Pennsylvania
Pittsburgh	9,627,541	Pennsylvania, New York, Ohio, Michigan, Illinois, Wisconsin
Somerset	662,302	Pennsylvania, West Virginia
Westmoreland	915,380	Pennsylvania, New York, Minnesota, Ohio, Wisconsin, Maryland
Miscellaneous	32,905	Pennsylvania
Tennessee	116,138	Tennessee
Utah	369,145	Utah
Virginia: Southwestern[a]	671,527	Michigan, New York, New Jersey, Ohio, Illinois
West Virginia:[a]		
Coal and coke	85,044	Pennsylvania
Kanawha-Logan	8,529,353	Massachusetts, Ohio, Indiana, New Jersey, Illinois, New York, Kentucky, West Virginia, Michigan, Wisconsin, Pennsylvania, Connecticut, Rhode Island, Missouri, Minnesota
New River:		
High-volatile	486,874	New York, Massachusetts, Connecticut
Low-volatile (including Winding Gulf)	2,245,900	Massachusetts, New York, New Jersey, Michigan, Missouri, Rhode Island, Pennsylvania, Illinois, West Virginia, Connecticut, Kentucky, Maryland, Minnesota, Ohio
Northern	3,666,260	Maryland, Pennsylvania, Ohio, Michigan, West Virginia
Pocahontas (including Tug River)	11,578,864	Indiana, Ohio, Illinois, New York, Michigan, Maryland, Wisconsin, Pennsylvania, Minnesota, Kentucky, Connecticut, Alabama, Massachusetts, Tennessee, West Virginia
Webster-Gauley	182,586	Pennsylvania, New York
Total	77,343,243	

[a] Coal from extension of the Pocahontas field in Virginia is included under Pocahontas district, West Virginia.
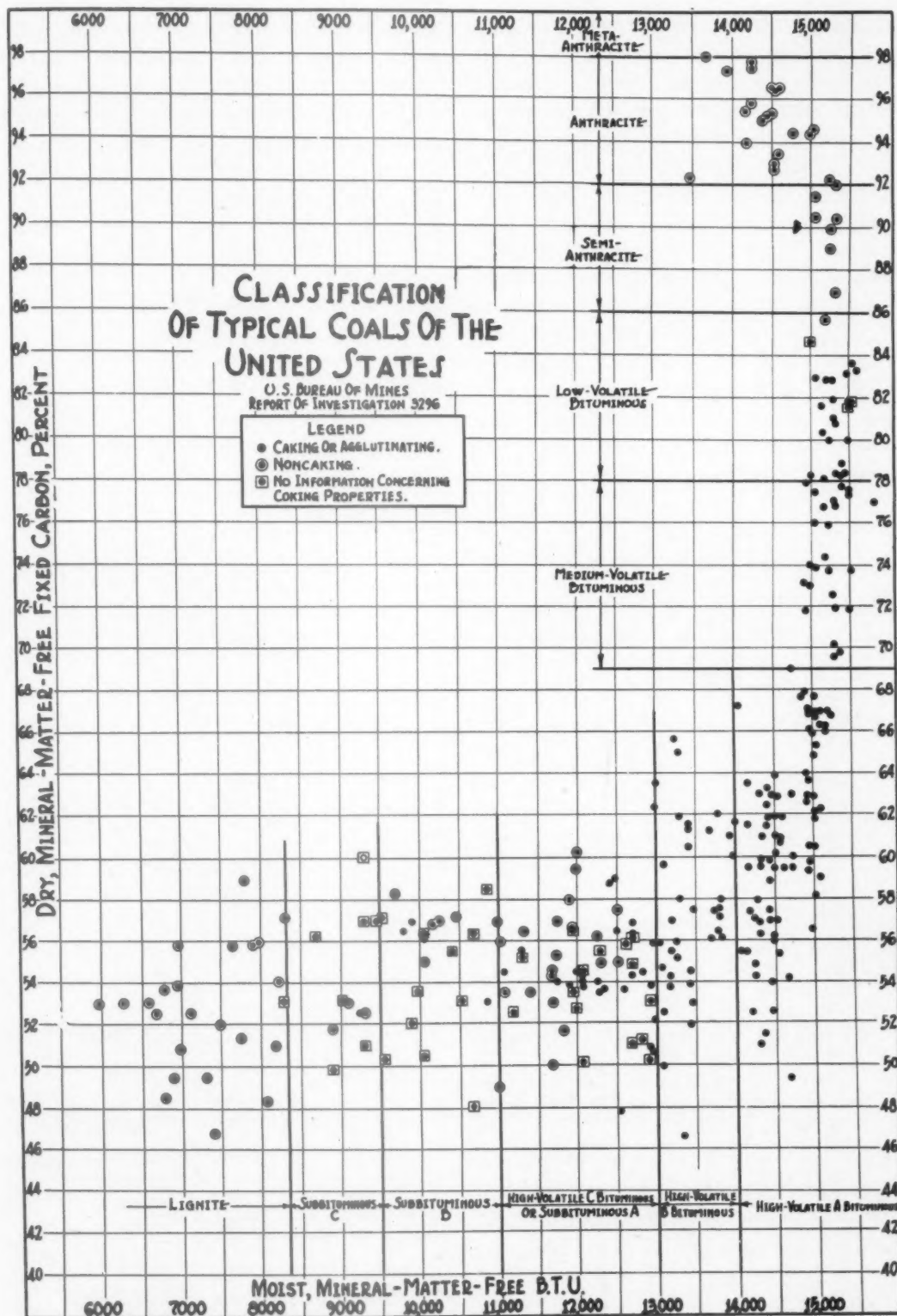
FIG. 2.—CLASSIFICATION OF TYPICAL COALS OF THE UNITED STATES.
U. S. Bureau of Mines *R.I.* 3296.

diluent of the coal. For example, when coal is burned, the iron pyrites are converted to the heavier Fe_2O_3; the water of hydration of the shale or slate is volatilized, and so the composition of the ash is different from that of the original mineral matter of the coal. Simple formulas[1,4] were developed for converting the ash of coal, as weighed, back to the original mineral matter of the coal. Further study of these formulas has shown that with certain modifications they are applicable to virtually all coals within satisfactory limits of accuracy. The natural-seam moisture is used for correction of the heating value, and not the moisture of the coal "as received." The values of typical coals of all ranks are shown in Fig. 2.[5] After thus plotting the coals, the major task was to define the actual limits for each class of coal. There are also several changes in the naming of each rank; thus, for example, the old term "semibituminous" has been dropped and "low-volatile bituminous" has been selected in its stead.

According to the standard method, coal is divided into four classes, and each of these classes is subdivided into two or more groups. Table 2 shows the outline form of the specifications for classification of coals by rank. For more detailed considerations, reference should be made to the A.S.T.M. standard.

TABLE 2.—*Classification of Coals by Rank*

Class	Group	Limits of Fixed Carbon or British Thermal Units, Mineral-matter-free Basis[a]	Requisite Physical Properties
I. Anthracite	1. Meta-anthracite...............	Dry F.C., 98 per cent or more (dry V.M., 2 per cent or less)	
	2. Anthracite....................	Dry F.C., 92 per cent or more and less than 98 per cent (dry V.M., 8 per cent or less and more than 2 per cent)	
	3. Semianthracite...............	Dry F.C., 86 per cent or more and less than 92 per cent (dry V.M., 14 per cent or less and more than 8 per cent)	Nonagglomerating
II. Bituminous	1. Low-volatile bituminous coal.....	Dry F.C., 78 per cent or more and less than 86 per cent (dry V.M., 22 per cent or less and more than 14 per cent)	
	2. Medium-volatile bituminous coal.	Dry F.C., 69 per cent or more and less than 78 per cent (dry V.M., 31 per cent or less and more than 22 per cent)	
	3. High-volatile A bituminous coal..	Dry F.C., less than 69 per cent (dry V.M., more than 31 per cent); and moist B.t.u. 14,000 or more	
	4. High-volatile B bituminous coal..	Moist B.t.u., 13,000 or more and less than 14,000	
	5. High-volatile C bituminous coal..	Moist B.t.u., 11,000 or more and less than 13,000	Either agglomerating or nonweathering
III. Subbituminous	1. Subbituminous A coal..........	Moist B.t.u., 11,000 or more and less than 13,000	Both weathering and nonagglomerating
	2. Subbituminous B coal..........	Moist B.t.u., 9,500 or more and less than 11,000	
	3. Subbituminous C coal..........	Moist B.t.u., 8,300 or more and less than 9,500	
IV. Lignitic	1. Lignite......................	Moist B.t.u., less than 8,300	Consolidated
	2. Brown coal..................	Moist B.t.u., less than 8,300	Unconsolidated

[a] F.C., fixed carbon; V.M., volatile matter.

Coking Properties

Coal forms coke when heated because the coal softens and fuses into a solid mass. The degree of softening of coal determines

the Gieseler method[6,7] and the Davis plastometer.[8] The Gieseler apparatus, used by the Research Department of Koppers Company, measures both the degree of
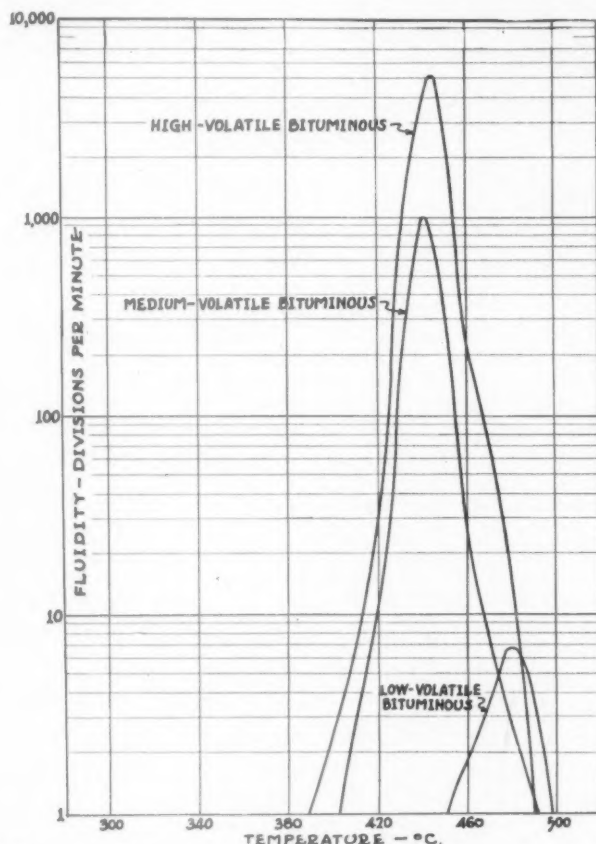
FIG. 3.—GIESELER FLUIDITY OF THREE TYPICAL COALS.

in part the character of the coke that is produced. In general, low-volatile coal becomes fluid only to a small degree, while most of the high-volatile A coals become very fluid. The fluidity of high-volatile B coals, however, is low. Since coal is a hetero-geneous mixture, the various components which make up the coal have a profound effect on the fluid characteristics. Thus, a coal that contains considerable noncoking material may have a low fluidity due simply to the diluent effect of the component material inert to coking.

There are several methods of determining the degree of fluidity. Among those most commonly used in the United States are

fluidity attained by the coal during heating and the temperature range in which the coal is fluid. It operates much like a Stormer viscosimeter and is sensitive to small changes in consistency. Fig. 3 shows typical Gieseler fluidity curves for the three classes of coking coals; namely, high-volatile A, medium-volatile and low-volatile bituminous. The Davis plasto-meter measures the resistance of the plastic coal at the beginning and at the end of the temperature range in which the coal is plastic. The values are the opposite of those obtained by the Gieseler apparatus.

All coals when coked in by-product ovens exert some pressure on the oven walls at some stages of their conversion to coke, depending on the kind of coal and the con-

The subject of measuring these pressures is relatively new and one of great interest and importance. Two such apparatus in use at present are the movable-wall oven
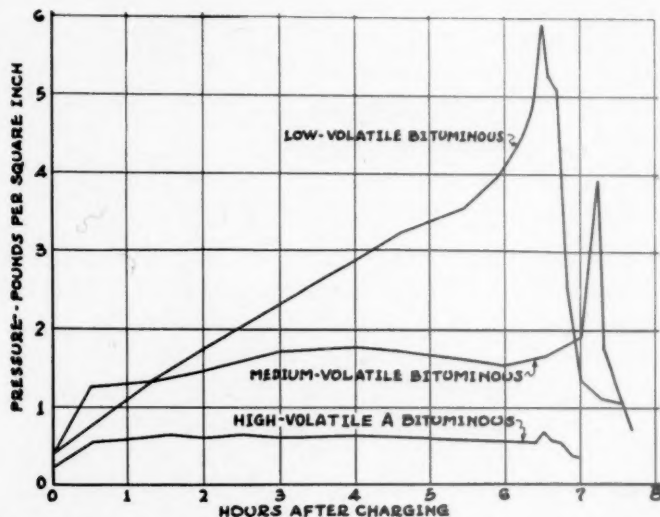
FIG. 4.—PRESSURES DEVELOPED BY THREE TYPICAL COALS DURING COKING IN MOVABLE-WALL EXPANSION OVEN.

ditions of carbonization. In a very general way, high-volatile coals develop low wall pressure, of the order of 0.5 lb. per sq. in., while low-volatile coals exert dangerous maximum pressure, of the order of 6 to 8 lb. per sq. in. or more—dangerous in that enough force is developed to distort or destroy oven walls. By the examination of coals in the Koppers movable-wall test oven, it has been found that coals or mixtures known to have caused damage to ovens create pressures of more than 2.0 lb. per sq. inch.

The first methods developed for the assessment of the safety of coals involved the measurement of the expansion or contraction of coal when carbonized under a load of 2.0 to 2.2 lb. per sq. in. Apparatus developed by V. J. Altieri[9] and W. T. Brown[10] were widely used and continue to be of value. However, the methods that measure the pressure developed are now receiving more attention.

of the Research Department of Koppers Company, designed by one of the authors,[11] and that of the U. S. Bureau of Mines, developed by Auvil and Davis.[12] These are large apparatus requiring from 250 to 500 lb. of coal for each test. Fuchs, Sandhoff, Taylor and Gauger[13] have described a laboratory-scale method for measuring pressures developed by coal during coking, and Altieri[9] obtains the pressure developed in one of his small apparatus by examination of his stress-strain diagrams. In Fig. 4 are shown typical pressure curves obtained in the movable-wall oven for high-volatile A, medium-volatile, and low-volatile bituminous coals.

So far, there is no satisfactory way of predicting what pressures will be created by a coal mixture; therefore it is imperative that a determination of its expanding properties be made before a coal or blend of unknown characteristics is selected for regular plant use.

METHODS OF TESTING COKE FOR PHYSICAL CHARACTERISTICS

Method of Sampling

Samples of coke to be used for the determination of physical properties must be obtained with great care so that they may be representative. Run-of-oven coke comprises a mixture of sizes, and the various procedures in pushing, depositing on the wharf, and running from the wharf onto the belt all tend to increase the difficulties of obtaining representative samples. Furthermore, breakage of large pieces that contain fractures occurs with each act of handling the coke. To obtain a fairly accurate estimate of the size consist of coke, the procedure for obtaining the sample must be carefully worked out. The American Society for Testing Materials recommends that a sample of not less than 500 lb. be obtained of run-of-oven coke. Russell and Rose[14] studied the accuracy that may be expected from samples of various sizes. It was concluded that 1000 lb. or more of sample is necessary for satisfactory accuracy.

Physical Tests of Coke of Interest to Blast-furnace Operators

The physical characteristics of coke that usually are determined and that are of the most interest to blast-furnace operators are listed in Table 3. Test methods for all

TABLE 3.—*Physical Characteristics of Coke*

CHARACTERISTIC	TEST METHOD USED
Size	Screen test
Strength	Shatter test
	Tumbler test
Apparent specific gravity	Water displacement of full-length pieces or specially sized pieces
True specific gravity	Hogarth bottle 200-mesh sample Water displacement
Porosity	Calculated from apparent specific gravity and true specific gravity
Weight per cubic foot	8-cubic-foot box
Cell structure	Comparison with arbitrary standards

those listed except cell structure have been standardized by the American Society for Testing Materials. It should be noted that

the A.S.T.M. designates the porosity determination as "Volume of Cell Space of Lump Coke." Because most of these methods are empirical, they must be followed precisely in order to obtain comparable results. No doubt many liberties are taken with the standard methods of testing in various localities, therefore great care should be taken when comparing data from various sources.

Physical properties are used most frequently in correlations with blast-furnace behavior. In general, most attempts at correlation have not met with great success.[15,16,17,18] At least it can be said that there is no general scheme by which blast-furnace operation can be predicted accurately from the values of the physical properties of coke. Undoubtedly the most important justification for thorough and frequent coke testing is the knowledge of the changes that occur. Factors that affect the physical properties of coke in coke-oven operation are fairly well understood and, providing the samples tested represent the coke produced, certain adjustments can be made to bring back the coke properties, at least in part, to the desired values. Since it is partly the purpose of this paper to discuss the physical properties of coke and the factors that cause variations, a brief discussion of each one is presented in the following paragraphs.

Size

The size of coke is measured by the sieve analysis. Since sieve-analysis results are reported by showing the percentage of the aggregate that is found to remain on the various sieve sizes, it has been customary among coke-oven and blast-furnace operators to use a single number as an index of size. The usual figure used is the cumulative total of all sizes 2 in. and over. In some instances the weighted-average size, as calculated from the sieve analysis, has been used, but the "total on a 2-in." index remains most popular.

The size and shape of run-of-oven by-product coke depends to a large extent on the coal used for its manufacture. Other factors, such as rate of coking, degree of

Only small quantities of this class are used and, so far as is known, no coal of high-volatile C class is used.

Fig. 5 shows the effects of addition of
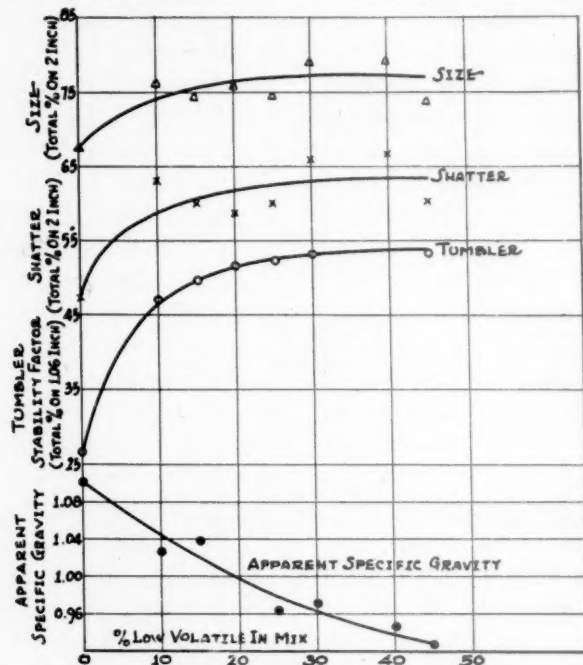
FIG. 5.—EFFECT OF LOW-VOLATILE COAL ON PHYSICAL PROPERTIES OF COKES.

overcoking or undercoking, and oven width, have important effects on the size of coke produced from a given coal. Admixture of low-volatile coal with a high-volatile coal usually leads to larger coke, and the use of finely divided inert material such as coke breeze also increases coke size under certain conditions discussed later.

High-volatile A coals are used in the largest quantities for coke production. These coals when coked alone produce coke that is often small and fingery in shape. It should not be inferred that all coals in the high-volatile A class produce coke of the same general character. Coals that are near the medium-volatile class have coking characteristics approaching those of that class; at the other end of the A class, the coking characteristics approach those of the high-volatile B coals. High-volatile B coals produce coke that is small, fragile, and very fingery under conditions generally used for producing blast-furnace coke.

increasing amounts of low-volatile Pocahontas No. 3 seam coal to a high-volatile A coal of the Powellton seam. These results are illustrative of the behavior of mixtures of these two types of coals, but various kinds of coal will exhibit this trend in different degrees. Not every coke-oven plant is so located that advantage can be taken of the use of low-volatile coal. In such cases, modification of oven operation is undertaken to produce coke best suited to the blast-furnace operation in keeping with satisfactory economic considerations.

English coal technologists have published considerable information concerning the use of inert material mixed with coal to improve coke size, strength, and other qualities. Although there is a good deal of interest in this subject in the United States, there is not much published information. Pfluke and Sedlachek[19] presented a paper before the American Gas Association discussing the carbonization of coal

admixed with breeze. Fig. 6 presents some of their results. This study consisted of the addition of 1 to 5 per cent of breeze, graded in various sizes up to ¼ in., to a blend of
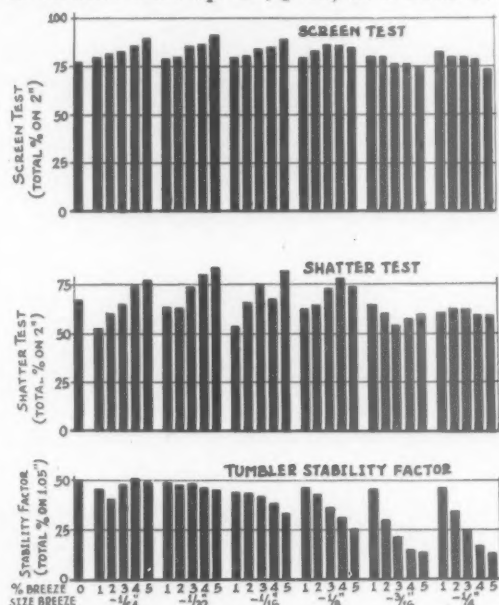
FIG. 6.—EFFECT OF COKE BREEZE ADMIXTURE TO COAL ON SIZE, SHATTER AND TUMBLER OF RESULTANT COKE.

80 per cent Powellton seam and 20 per cent Pocahontas seam, and also to a straight high-volatile Pittsburgh-seam coal. In general, the data show that the addition of the smallest sizes of breeze—i.e., minus ¼₄-in., ⅓₂-in., and ⅟₁₆-in.—to the blend tends toward increase in the size of the resultant coke; but the coarsest breeze admixtures cause smaller sizes. The coke produced by the addition of the coarsest breeze was found to be weaker than others, and broke easily on handling because of the number of fractures formed.

The data shown in Fig. 7 indicate that the degree of pulverization of the coal before carbonization has only a small effect on the size of the run-of-oven coke produced. However, other coals or coal mixtures may be affected to a greater extent, dependent upon the composition of the coal or coals. If coal contains a considerable amount of slate, coarse pulverization leaving large pieces of slate may have the effect

shown in Fig. 9. Coke made from clean coal, hand-picked free of slate, is shown in Fig. 8 and coke made from the same coal to which a quantity of slate has been
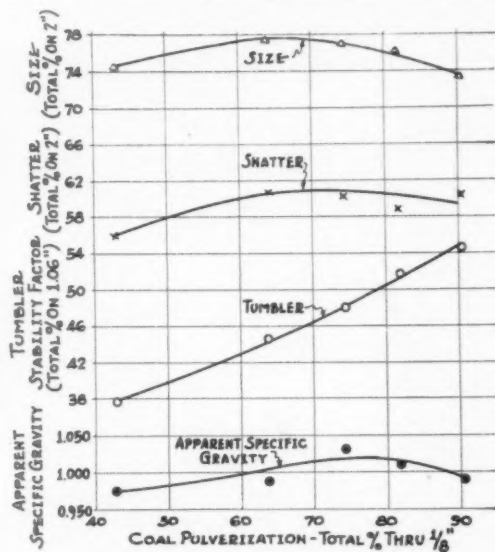
FIG. 7.—EFFECT OF PULVERIZATION OF COAL ON PHYSICAL PROPERTIES OF RESULTANT COKE.

added is shown in Fig. 9. Both cokes were made under the same carbonizing conditions. Fracture lines emanating from each piece of slate are indicative of the deleterious effect.

Rate of coking has an important bearing on size. Coke made at low temperatures is usually large and blocky whereas with higher temperatures the coke pieces are smaller. With a given flue temperature, the effect of leaving coke in the oven for longer periods of time is to produce smaller average-sized coke. When flue temperatures are lowered and the coking time is proportionately increased, larger coke results. Fig. 10 shows some of the data presented recently by Mr. H. W. Johnson,[15] and Fig. 11 shows similar data on coke made from a mixture of 80 per cent Powellton seam and 20 per cent Pocahontas No. 3 seam. The U. S. Bureau of Mines has reported results of the B.M.-A.G.A investigation of American coals in laboratory retort tests.[20] These data indicate that cokes made above 800°C. decrease rapidly in size as the temperature of coking is increased.

FIG. 8.—COKE MADE FROM CLEAN COAL.
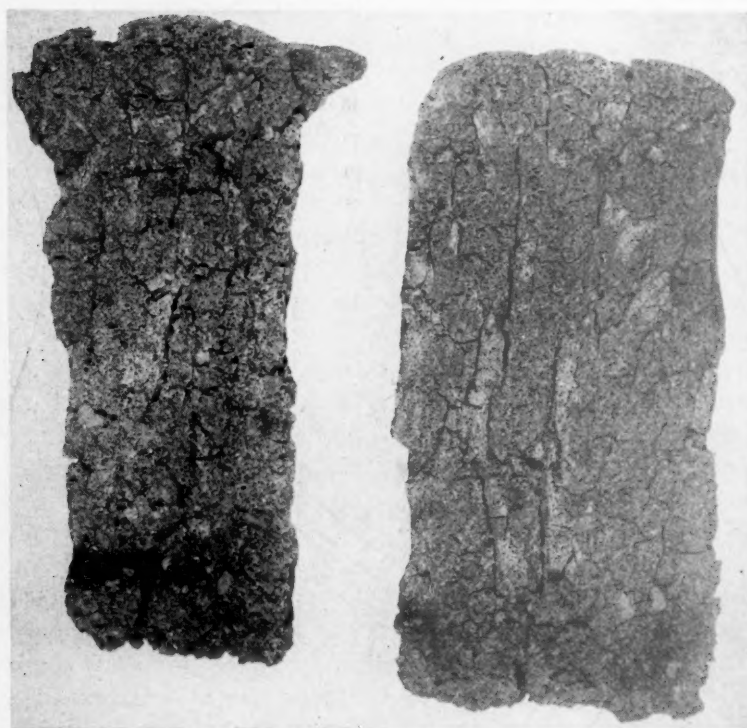
FIG. 9.—COKE MADE FROM COAL CONTAINING A CONSIDERABLE AMOUNT OF SLATE.

Strength

Coke strength probably is the most important physical property, next to size, desired by coke consumers, for it is the oldest of the A.S.T.M. standard methods for the determination of that property.[21] More recently the tumbler test was devised and adopted by the A.S.T.M.[22] Other
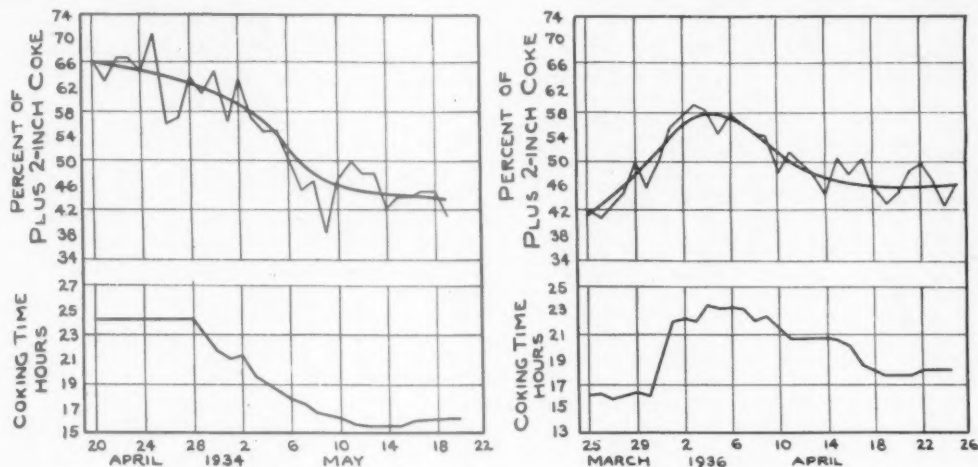
FIG. 10.—RELATION OF SIZE OF COKE TO COKING TIME. (FROM H. W. JOHNSON.[18])
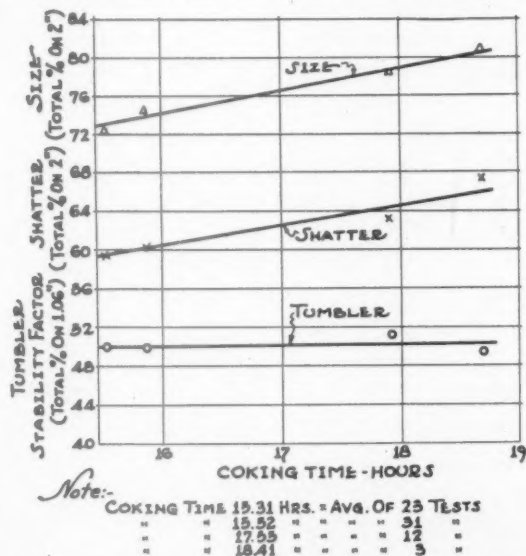
FIG. 11.—EFFECT OF COKING TIME ON PHYSICAL PROPERTIES OF COKES.

measure of the ability of coke to retain its size during handling. Both blast-furnace and foundry men prefer coke of high strength, since one of its principal functions is to support heavy burdens and allow easy flow of air upward through the charge. Various tests have been devised to measure the strength of coke. The shatter test is perhaps the most generally used and is the

methods have been proposed and used, principally in Europe, to measure strength and qualities related to strength.

The shatter test actually measures the resistance to impact and is indicative of the amount of fracturing of the coke. The results depend to a large extent on how and where the sample was taken. Duplicate determinations are difficult to

check and differences may be as high as 5 per cent.[23] Under such conditions, great care must be exercised in the procedure if coke strengths are to be compared on the

weathering will render the coal noncoking. These effects probably occur with high-rank high-volatile coals only. Coals in the lower rank of the high-volatile A class and
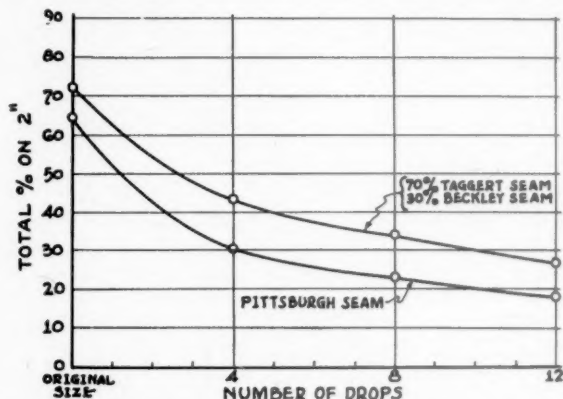
FIG. 12.—EFFECT OF REPEATED SHATTER ON SIZE OF COKE.

basis of shatter index. The main factors affecting shatter-test results, assuming satisfactory sampling conditions, are kind of coal, coking time, and temperature of carbonization.

Cokes made from high-volatile coals, particularly those at the lower end of the high-volatile A class and the high-volatile B class, shatter easily. The addition of a small amount of low-volatile coal, however, increases considerably the resistance to shatter as illustrated in Fig. 5. Further additions have a less pronounced effect. Admixtures of coke breeze of specified sizes in proper amounts may also increase the shatter index as indicated in Fig. 6. In general, the breeze of large particle size decreases the shatter index. All coals are not affected to the same degree by the admixture of breeze, and investigation of the size and amount of breeze is necessary for each coal or mixture to determine how the satisfactory effects can be obtained.

Coal pulverization also affects strength in a manner similar to the effect on size (Fig. 7). In addition, a small amount of data indicate that slight weathering of certain coals increases the shatter index slightly. Further weathering will eventually weaken the coke obtained and still further

the coals of the high-volatile B class are adversely affected by slight weathering.

There seem to be few published data on the effects of oven operation on shatter-test results, especially for American coals. Mott and Wheeler[24] show that an increase in shatter index occurs up to a maximum and then decreases as the coking time is lengthened. The U. S. Bureau of Mines shows a similar effect with cokes made in its laboratory B.M.-A.G.A. retort tests.[20]

Repeated shatter tests provide interesting and valuable information on the rate of degradation of coke. The data in Fig. 12 illustrate results that were calculated from repeated shatter tests. Run-of-oven coke was separated into the plus 2-in. size, and minus 2-in. and plus ½-in., by standard sieve-test procedure. Each of these size increments was subjected to a standard shatter test of 4 drops. The resultant coke was then sieved and subjected to four more drops, and so on. By calculation, the data were reassembled so that they represent the size of run-of-oven coke resulting from 4 drops, 8 drops, and 12 drops. Data are shown for coke made from 70 per cent Taggart-seam and 30 per cent Beckley-seam coals and from 100 per cent Pittsburgh-seam coal. Both cokes were made

in the same ovens under substantially the same oven conditions. It is indicated that considerable breakage occurs during the first four drops, and that the

stability factor. Stability factors range from 15 to 20 per cent for poorly coking high-volatile B coals to upward of 60 to 65 per cent for very strong cokes from high-rank
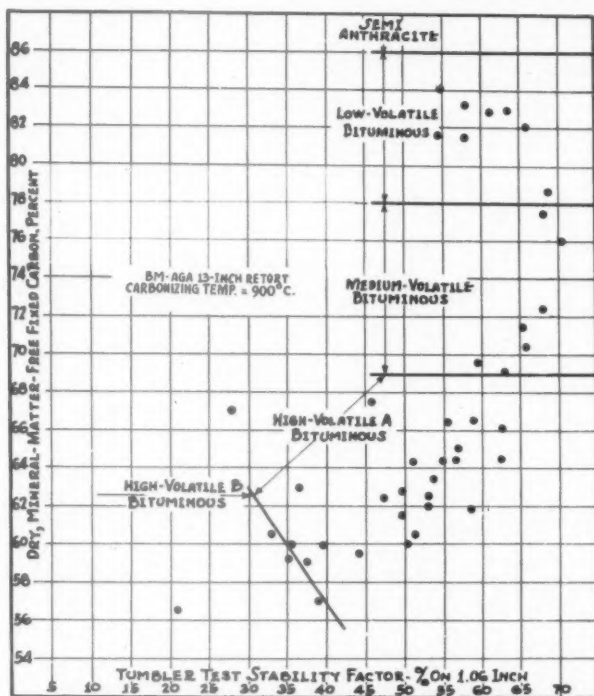
FIG. 13.—EFFECT OF RANK OF COALS ON COKE. TUMBLER-TEST STABILITY FACTOR.
Data from U. S. Bureau of Mines.[20]

increment of breakage becomes less with further dropping.

The tumbler test standardized by the A.S.T.M. was designed by W. A. Haven.[25] The test measures both breakage and abrasion of coke and appears to possess the ability to be duplicated with relatively small differences. The stability factor (total remaining on a 1.06-in. sieve) is more generally used than the hardness factor (total remaining on a 0.265-in. sieve). However, the hardness factor is sometimes important. Blast-furnace men generally prefer to maintain a uniform stability factor rather than to aim for some particular value of that index. If the sample is representative, duplicate determinations may agree within 1.4 per cent.[23]

The rank of coal used for carbonization has the most important bearing on the

coals or coal mixtures. Fig. 13 shows the variation of tumbler-test stability factors with rank of coals from data of the U. S. Bureau of Mines investigations of American coals in B.M.-A.G.A. retort tests.[20] In general, the configuration is the same as the coal-classification diagram of Fig. 2, and the coals occupy approximately the same position in relation to other coals that they do in the classification scheme. It should be remembered, however, that coke made in the B.M.-A.G.A. retort is not identical with oven coke, and care should be used in translating the figures to practical use.

Fig. 5 shows how the stability factor is affected by increasing amounts of low-volatile Pocahontas No. 3 seam coal added to high-volatile A Powellton seam coal. A considerable increase results from the addition of just 10 per cent low-volatile coal

and further additions have a less marked effect. The degree of pulverization appears to have a considerable effect on the stability factor of coke made from mixtures of the cific gravity. The porosity value is used principally in connection with blast-furnace coke, although users of foundry coke also consider the figure significant. While po-
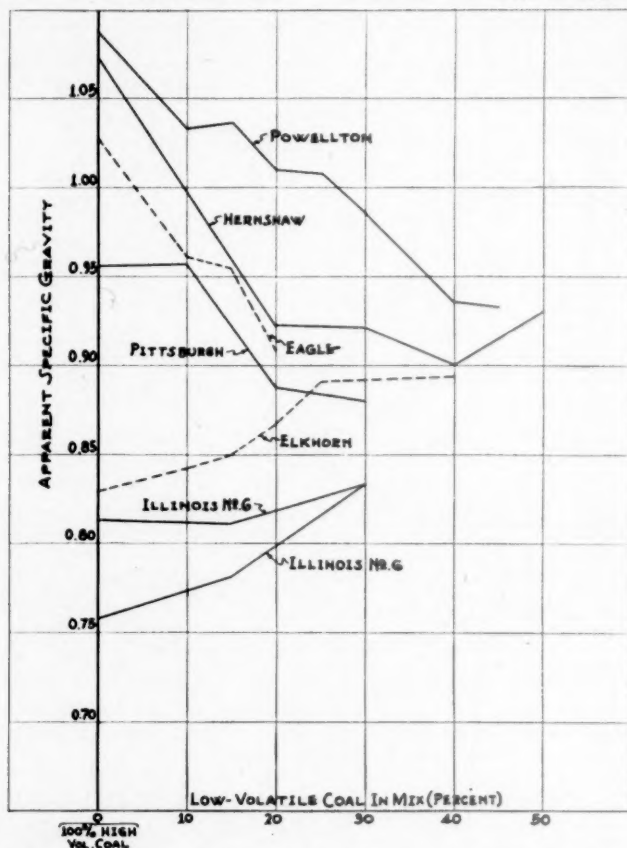
FIG. 14.—EFFECT OF ADDING LOW-VOLATILE COAL ON APPARENT SPECIFIC GRAVITY OF COKE MADE FROM HIGH-VOLATILE COAL.

two coals, as illustrated in Fig. 7. The work of Pfluke and Sedlachek[19] indicates that no increase in the stability factor was obtained by additions of breeze in any quantity or size used for their tests (Fig. 6). Hardness factor, it is believed, generally decreases with addition of coke breeze to coal. In the data presented in Fig. 11, no important changes in the stability factor are found with change in coking time.

Porosity

Porosity is the term commonly used in discussing the volume of cell space in coke. It is a value obtained by calculation from the apparent specific gravity and true spe-

rosity actually expresses the percentage of the volume of pieces of coke that is void space, the numerical value does not necessarily indicate cell size. Because the true specific gravity of coke made in by-product ovens at usual coking speeds does not vary through a wide range, the porosity is dependent chiefly on the apparent specific gravity.

The apparent specific gravity of coke varies with the kind of coal, bulk density of the coal charge, coking temperature and/or coking time. An attempt to show the relation between the rank of coal and the apparent specific gravity of coke was unsuccessful. In a very broad way, with constant conditions of carbonization, it has

been the experience of the authors that the high-volatile B coals produce coke of low apparent specific gravity and the high-volatile A coals produce cokes of relatively

suggest that the degree of pulverization of coal has only a slight effect on the apparent specific gravity for the coal under consideration. Doherty[26] also supports this and
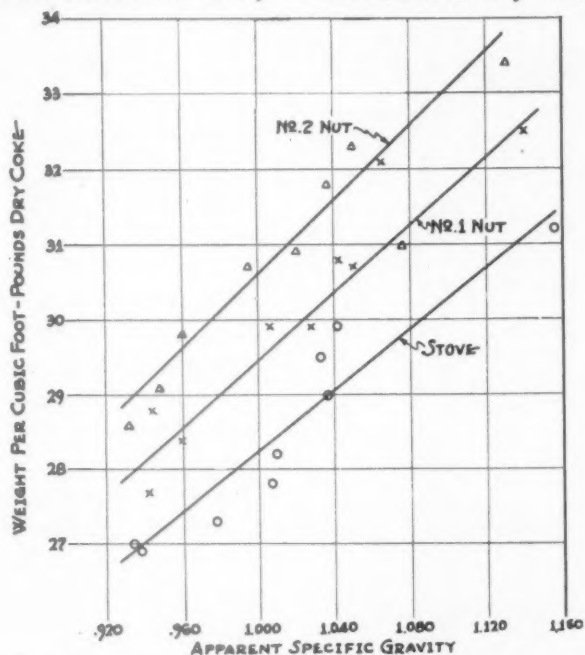
FIG 15.—RELATION BETWEEN WEIGHT PER CUBIC FOOT OF DRY COKE AND ITS APPARENT SPECIFIC GRAVITY.

high apparent specific gravity. Cokes made from low-volatile coals in box tests have apparent specific gravities lower than those from high-volatile A coals but higher than cokes made from high-volatile B coals. There may be exceptions to these findings.

J. D. Doherty[26] has shown the effect of addition of low-volatile coal to high-volatile coals of various seams. His data (Fig. 14) show that blending with a low-volatile coal tends to reduce the apparent specific gravity if the high-volatile coal alone produces a coke of 0.95 apparent specific gravity or higher. However, the apparent specific gravity is increased by the addition of low-volatile coal to the high-volatile coals that give cokes of less than 0.85 apparent specific gravity.

Precise relationship of apparent specific gravity of coke to various factors that affect it are not evident, consequently it is necessary to consider the data as indicative of trends. The data presented in Fig. 7

states that the apparent specific gravity can be lowered appreciably by adding moisture to pulverized coal. However, increasing moisture in the coal generally tends to decrease its bulk density, and finer pulverization, especially of moist coal, tends to decrease bulk density. In consequence, individual factors such as coal pulverization, for example, cannot be considered for correlation without some knowledge of attendant effects of other related variables.

The true specific gravity is not generally considered to be a significant factor aside from its application in computing the volume of cell space of lump coke. It is chiefly affected by the temperature of carbonization, but ash content and coking time also have a slight effect.

Weight per Cubic Foot

In the blast furnaces that charge coke by volume rather than by weight, the vari-

ations in the weight per cubic foot of coke alters the ratio of coke to ore. Such variations may be the cause of irregular blast-furnace operation. The main factors

FIG. 16.—COKE STANDARDS USED BY KOPPERS COMPANY FOR EVALUATION OF CELL SIZE.

affecting the weight per cubic foot of coke are the apparent specific gravity, size, and moisture. Moisture, however, is purely additive in its effect on the bulk density of lump coke and it does not cause the effect of "fluffing" in coke as it does in pulverized coal. The effect of apparent specific gravity

and size on the weight per cubic foot of dry coke are shown in Fig. 15 for three nominal sizes of coke prepared for domestic purposes.

Cell Size

A great deal of importance has been attributed to the cell structure of coke, by blast-furnace men, foundry men, and producers of domestic coke. Variations in cell structure have been used as the basis for explanation of peculiarities in combustion of coke. Attempts have been made to evaluate this characteristic by setting up standards of comparison[27,28] but there is no generally accepted procedure for evaluating cell size. The standards used by Koppers Company consist of flat coke sections arbitrarily selected and numbered from 1 to 4 with increasing cell size. A photograph of the standards is shown full size in Fig. 16.

Cell structure apparently is dependent upon the plastic state of coal and the degree of fluidity attained during the plastic stage, together with the rate of decomposition of the coal. Low-volatile coals, which become only slightly fluid, produce in most cases, coke with uniform small cells and thin walls. High-volatile B coals that often have similar fluid characteristics form the same type of cells. Cokes from high-volatile A coals produce coke with large cells and often have thick cell walls. The medium-volatile coals produce cells that are often semispherical in shape, the flat side being toward the center of the oven.

Many of the high-volatile A coals when coked without admixture of low-volatile coal produce sponge, which is found at the top of the charge. The formation of sponge is characteristic of many coals, principally those that shrink excessively so that the charge slumps in the oven. High-volatile B coals that also shrink during coking do not form sponge because they do not become sufficiently fluid. On the other hand, some of them produce pebbly seam, which apparently is caused by the same phenomena as sponge formation. Careful examination of

the position of sponge and its connection with solid coke in the oven has disclosed that it is due to the pulling apart of the plastic coal by the slumping of the charge. Sponge may be reduced or eliminated by minimizing the shrinkage of the charge; i.e., by increasing the bulk density of the charge or by addition of low-volatile coal. It might be added that the old idea that sponge was due to a distillation of bituminous material that condensed at the center of the charge has been disproved in the cases examined, by the fact that sponge contains substantially the same ash content as the solid coke.

CONCLUSION

In this review of the physical characteristics of coke, the results of the accepted methods of testing have been used as the basis for the discussion. There are, undoubtedly, large quantities of unpublished data in the files of various organizations that manufacture or use coke. Such data may contravert some of the relationships discussed herein. It was not possible, or desirable, to cover the entire field of coal technology related to the physical characteristics of coke, nor was it the purpose of the paper to cover the entire literature on the subject. In presenting a discussion of the standard method of coal classification, together with some of the factors that are responsible for the physical characteristics of coke, the writers hope that a little better understanding of the coking phenomena will result.

ACKNOWLEDGMENT

The writers are indebted to Mr. Fred Denig, Vice President, Koppers Company, Research Department, and Dr. A. R. Powell, Assistant Director of Research, for their helpful suggestions and for permission to publish some of the data.

REFERENCES

1. A.S.T.M. Standards (1939) D388-38.
2. Pig Iron Capacity of the United States and Deposits of Iron Ore and Coal. *Steel Facts* No. 19 (May 1937). Amer. Iron and Steel Inst.
3. U. S. Bur. Mines, Minerals Yearbook (1940) 877, Table 24.
4. S. W. Parr: Chemical Study of Illinois Coal. Illinois Coal Mining Investigations, State Geol. Survey *Bull.* 3 (1916) 35.
5. A. C. Fieldner, W. A. Selvig and W. H. Frederic: Classification Chart of Typical Coals of the United States. U. S. Bur. Mines *R.I.* 3296.
6. K. Gieseler: Measurement of the Plastic Properties of Heated Coal. *Glückauf* (1934) 70, 178–183.
7. R. E. Brewer and J. E. Triff: Measurement of Plastic Properties of Bituminous Coals. *Ind. and Eng. Chem.*, Anal. Ed. (1939) 11, 242–247.
8. J. D. Davis: The Plastometer. *Ind. and Eng. Chem.*, Anal. Ed. (1931) 3, 43–45.
9. V. J. Altieri: *a.* Coal Expansion. Amer. Gas Assn. Prod. and Chem. Conf. (1935). *b.* Measurement of Expansion of Coal during Carbonization. *Proc.* Amer. Gas Assn. (1935) 812. *c.* Coal Expansion during Carbonization in Engineering Models of a Coke Oven. Amer. Gas Assn. Prod. and Chem. Conf. (1938).
10. W. T. Brown: Coal Expansion. *Proc.* Amer. Gas Assn. (1938) 20, 640.
11. C. C. Russell: Measurement of Pressures Developed during the Carbonization of Coal. *Trans.* A.I.M.E. (1940) 139, 313.
12. H. S. Auvil and J. D. Davis: Determination of the Swelling Properties of Coal during the Coking Process. U. S. Bur. Mines *R.I.* 3403 (1938).
13. W. Fuchs, H. G. Sandhoff, J. A. Taylor and A. W. Gauger: Studies Concerning the Pressure Developed during the Carbonization of Coal. Pennsylvania State College *Bull.* 34 (1941).
14. C. C. Russell and H. J. Rose: Sampling Run-of-oven Coke. *Proc.* Amer. Gas Assn. (1928) 1071–1074.
15. H. W. Johnson: Correlations of Some Coke Properties with Blast-Furnace Operations. *Blast Furnace Proc.*, A.I.M.E. (1941) 1, 12; also *Trans.* A.I.M.E. (1942) 150.
16. M. A. Mayers and H. G. Landau: Relation of Coke Properties to Blast-furnace Performance—an Application of Statistical Methods of Correlation. Presented at A.I.M.E. Annual Meeting, Feb. 1941.
17. F. W. Wagner and R. W. Campbell: Physical Testing of Coke and Correlation with Furnace Operation. Unpublished manuscript received from authors, 1936.
18. E. C. Evans and F. J. Bailey: Blast-furnace Data and Their Correlation. *Jnl.* Iron and Steel Inst. (1928) 117.
19. F. J. Pfluke and A. C. Sedlachek: Coke Strength and Structure as Affected by Coke Breeze Admixtures to Coal. *Proc.* Amer. Gas Assn. (1936) 18, 771–785.
20. A. C. Fieldner and J. D. Davis: Gas-, Coke-, and Byproduct-making Properties of American Coals and Their Determination. U. S. Bur. Mines *Monograph* No. 5 (1934).
21. A.S.T.M. Standards (1939) D141-23 (p. 70).
22. A.S.T.M. Standards (1939) D294-29 (p. 73)

23. A. R. Powell and D. W. Gould: Coke
    Tumbler Tests. *Ind. and Eng. Chem.*
    (1928) **20**, 725–728.
24. R. A. Mott and R. V. Wheeler: The Quality
    of Coke. London, 1939. Chapman and
    Hall Ltd.
25. W. A. Haven: Notes on Coke Testing.
    Yearbook Amer. Iron and Steel Inst.
    (1926) **171–210**.

26. J. D. Doherty: Coal for Byproduct Coking.
    Amer. Gas Assn. Prod. and Chem. Conf.
    (1941).
27. C. J. Ramsburg and F. W. Sperr, Jr.:
    Byproduct Coke and Coking Operations.
    Jnl. Franklin Inst. (1917) **183**, 391–431.
28. O. O. Malleis: Byproduct Coke Cell Struc-
    ture. *Ind. and Eng. Chem.* (1924) **16**,
    901–904.

Pyrometry at the Coke Oven

BY ROBERT B. SOSMAN,* MEMBER A.I.M.E.

(Cincinnati Meeting, April 1942)

THE relative temperature distribution within a coke oven and among the ovens in a battery can be obtained automatically for the operator's guidance by sighting a total-radiation pyrometer on the face of the coke as it is pushed out, and recording the surface temperature. Keeping the instrument clean and keeping its view of the coke unobstructed by smoke and dust are the principal problems. Typical records from three plants are presented in this paper, showing that the temperature patterns are reproducible.

DEVELOPMENT OF METHOD

The method of coke pyrometry described in this paper was introduced in 1936 by E. A. Lee, then Assistant Superintendent, now Superintendent, of the Coke Plant at Lorain Works, National Tube Co., Lorain, Ohio. At the request of the Coke Committee of the United States Steel Corporation, the Research Laboratory of the Corporation undertook to adapt the method to the somewhat different conditions met with at the Gary Works of the Carnegie-Illinois Steel Corporation, Gary, Ind., and at the Clairton Works of the same Corporation at Clairton, Pa. This work was done in cooperation with the Leeds and Northrup Co. of Philadelphia and later with the Brown Instrument Co. Division of Minneapolis-Honeywell Regulator Co., Philadelphia. We of the Research Laboratory wish to express our appreci-

ation of the courtesies extended by Mr. Lee, by A. N. Cole, Superintendent of the Gary coke plant, and by D. P. Finney, Assistant General Superintendent in charge of coke-plant operations at Clairton. We are also indebted to the instrument companies for the loan of a part of the equipment. At Gary and Clairton the instruments were installed and various experiments were made by J. W. Bain, of the Research Laboratory of the United States Steel Corporation.

PYROMETRY OF COKE

The coke inside a by-product oven is almost completely inaccessible to pyrometric instruments. The temperature in the walls can conceivably be measured with thermocouples, but the atmosphere is usually strongly reducing, a condition well known to be destructive to the accuracy of the customary high-temperature couples.

In some plants, periodic readings are taken with an optical pyrometer sighted into the top of the combustion flues. This is a useful measure for safety and general control, as it tends to prevent the damage that would result from overheating of the ovens. It does not, however, tell much about the temperature of the coke itself, because of the continually changing gradient in the wall between the coke and the combustion chamber.

The best indication of the temperature of the coke itself must therefore be obtained by observation of the product as it is pushed out of the oven. The human eye is very sensitive to variations in brightness of a surface, and particularly to differences in brightness over a continuous hot surface.

The experienced operator needs no measuring instrument to tell him whether the coke at one end of the oven is colder than at the other end, or whether oven No. 10 averages about 100° hotter than No. 40. The great drawback to these visual estimates is that there is no continuous record for the superintendent or anyone else to inspect and no carry-over of quantitative information from one operating turn to the next.

OPTICAL PYROMETRY OF COKE

The optical pyrometer provides an easy and precise method of reading the surface temperature of any solid. If the coke surface is "black" in the sense of radiational physics—i.e., if it absorbs and emits like a theoretically perfect radiator[1]—the optical reading gives the true temperature, not, as for liquid steel, an apparent temperature that must be corrected for emissivity. Although the true emissivity of oven coke has not been measured, the surface is so rough and porous that probably it can be considered for pyrometric purposes to be a perfect radiator.

But the optical reading also has its drawbacks. First, the observation is subjective and no automatic record is made. The observer can therefore inspect the reading and reject it if it does not seem correct, or if he thinks it may not look good to the boss. This influence can be felt without any implication whatever of dishonesty. Second, a cloud of smoke or steam may sweep over the face of the coke and dull the apparent brightness of the surface, and the observer, with his eye at the telescope and his attention concentrated on the matching of the filament, can never be quite sure that his reading was not interfered with in this manner. Third, it takes several seconds to make a satisfactory optical reading; but the coke is moving fast and there is insuffi-

cient time to survey the surface with a series of readings, or even to concentrate satisfactorily on one selected point so that a series of ovens or a series of days will be comparable. For all these reasons, optical pyrometry of the coke has not proved satisfactory, although several plants take routine optical readings on the coke for the operating record.

TOTAL-RADIATION PYROMETRY OF COKE

A device that has proved satisfactory for pyrometry of coke as it comes out of the oven is the total-radiation pyrometer. This pyrometer consists of two parts: a radiation receiver and an automatic recorder. In the type of receiver used in this study, an objective lens receives the whole of the radiant energy, visible and invisible, from as much of the coke surface as lies inside the cone of vision of the lens, the angle of the cone being limited by a diaphragm. The lens reflects or absorbs some of this energy, but, being made of fused quartz (vitreous silica) or of a highly siliceous glass, it transmits most of the energy and focuses it on a small group of thermocouples connected in series. The electromotive force so produced is measured automatically by a potentiometer, which records it as temperature on a chart.

For radiation receiver and recorder we have used the two instruments available from American manufacturers; namely, the Leeds and Northrup "Rayotube" (lens type No. 8841) with a "Micromax" automatic potentiometric recorder with strip chart; and the Brown Instrument Company's "Radiamatic" with its "Continuous Balance" electron-tube potentiometric recorder with strip chart.

For readers unfamiliar with the design of by-product coke ovens, a word of description should be added. The ovens are vertical slots about 40 ft. long and 10 to 14 ft. high, but only about 18 in. wide, assembled into a battery. The whole structure is built almost entirely of silica brick.

---

[1] See R. B. Sosman: Pyrometry of Solids and Surfaces (Amer. Soc. for Metals, 1940), p. 15; or any textbook or manual of pyrometry.

Between the ovens are vertical flues in which the gas is burned to heat the ovens. Each oven is closed at each end by a refractory-lined metal door. At the end of the coking period—about 18 hr.—the two doors of an oven are removed and set to one side, and a ram is driven horizontally from the "pusher" side through to the discharge or "coke" side, pushing the mass of coke out between the steel walls of a guide into a car. The coke side of a battery, therefore, is provided with a traveling door-lifting machine and a traveling coke guide, usually combined into a unit. The pyrometer is most conveniently mounted on this traveling mechanism.

The general disposition of the radiation pyrometer and its recorder as set up at plant A is shown in the plan of Fig. 1 and the perspective sketch of Fig. 2. These are not working drawings or scaled drawings but should give a better idea of the arrangement than a detailed dimensioned drawing.

CONDITIONS TO BE MET

The car on the discharge side of a battery of coke ovens is about as difficult a place as could be found in which to set up a recording pyrometer. When the coke is discharged, there is a shower of coke dust together with smoke of residual hydrocarbons and some fume, such as volatile chlorides. Even when all ovens are closed there is likely to be smoke from leaky doors, and from the open charging holes in the top of the oven while it is being recharged with coal. If the lens of the receiver is accessible to this dust and smoke, it quickly becomes clouded and the readings are falsified.

The ideal way to prevent this clouding would be to use piped clean air to keep clear the atmosphere in front of the receiver lens. This plan has not been feasible at the plants mentioned, so near-by air has been drawn through a filter by means of a fan blower and driven past the receiver.

There is no filter that will take smoke completely out of air that is being transmitted at low pressure, but the dust can be stopped.
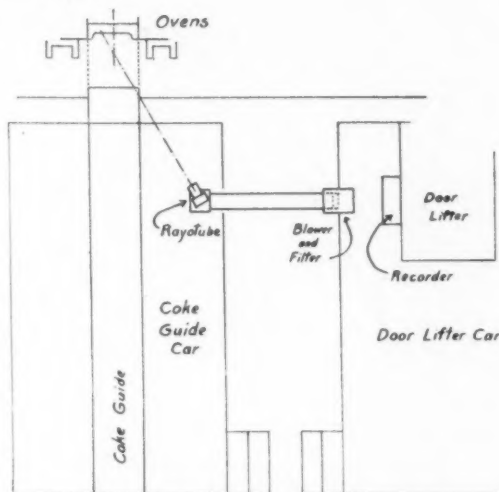
FIG. 1.—PLAN OF ARRANGEMENT OF COKE PYROMETER AND ACCESSORIES.

Another troublesome condition is the almost constant vibration of the door machine and guide. This is more easily taken care of than the dust and smoke, as spring suspension devices are available with which to absorb and eliminate the effects of vibration.

The temperature around the pyrometer receiver and recorder is likely to be abnormally high at times, especially in summer. While the coke is being pushed, the radiation receiver gets much radiant heat besides that which enters the lens opening. Forced circulation of air to keep back the dust also helps to keep the receiver cool. With receivers built to stand a working temperature of 250°F. there has been no need of water cooling, which would be impracticable.

To make a record that is easily interpreted, the chart must travel at a fairly high speed, as the total time of pushing is only 30 to 40 sec. The recorder must therefore be started and stopped in synchronism with the pushing, either automatically, or manually by one of the operators.

The following paragraphs will give details to show how these conditions have been met.

in the radiation head to the recorder. The guide car has no electrical connections and a plug-and-socket connection between the
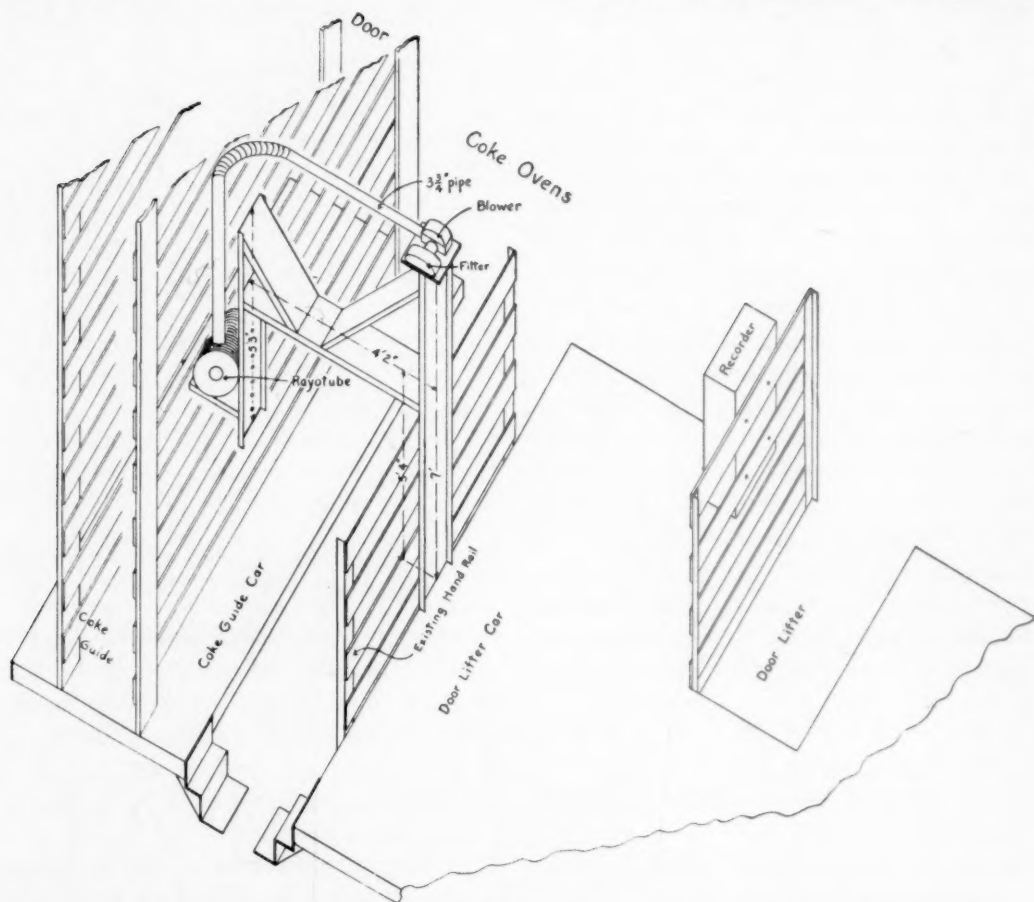
FIG. 2.—PERSPECTIVE SKETCH OF ARRANGEMENT OF COKE PYROMETER AND ACCESSORIES.

DETAILS OF DESIGN AND CONSTRUCTION

A troublesome feature at plant A, in which it differed from the other two installations, was the separation of the door-lifter car from the coke-guide car. The recorder must be carried on the door-lifter car, while the receiver must be in a fixed position with respect to the guide. Now the door-lifter is frequently uncoupled from the guide, and in their comings and goings the distance between the two cars may vary by several inches. Furthermore, there must be electric power for both recorder and fan, and a good independent electrical connection must lead from the thermocouples

two cars is not practicable. The radiation receiver, therefore, must be mounted on an arm attached to the door-lifting car, in such a position that it comes into the right relation with the coke guide and the door when the cars are coupled, yet can never come so close to the guide as to be damaged.

Plant A has a Leeds and Northrup Rayotube receiver and Micromax potentiometric recorder. The usual model of recorder has automatic standardization, occurring at regular intervals. This is not wanted in the present application, because the instrument is at rest most of the time, and because it would be undesirable to have

the machine interrupt an oven record in order to make the automatic adjustment.

The Rayotube is sighted between two of the slats of the coke guide and aimed toward the left of the center line of the oven opening, as one views the oven door from the door-lifter car (Fig. 1). Therefore it receives radiant energy first from the front of the mass of coke and then at an angle from the side of the coke as the charge is being pushed past it. It can be set at various heights to read the temperature at different levels, but reads on only a single level during one discharge. The advantages of setting the receiver at an angle to the line of discharge are that it stands a little farther away from the front of the ovens than would otherwise be possible, and also that it receives some preliminary heating from the front of the coke before pushing begins.

At plant B the door-lifting machine and the coke guide are built into a single car, and all parts can be permanently connected electrically. The air-circulation system also is simpler than that shown in Fig. 1. Air is drawn by a fan blower through a removable filter consisting of a pack of sheets of wire gauze, about 1 in. thick and 8 in. square. About 2 ft. above the blower is a T in the 4-in. air pipe. The Rayotube receiver is inserted in the open end of this T and the end is capped. One or two turns of the cap exposes the Rayotube for easy removal for examination and wiping of the lens, the whole operation taking less than one minute.

The air passing by the Rayotube goes horizontally through the 4-in. pipe, which extends about 3 ft. to the slots of the guide, and ends there at a flange. This makes almost a sealed connection from the Rayotube to the face of the passing coke, although there should be considerable outward leakage of air between the coke and the flange, enough to ensure a constant current of air to drive back smoke.

Experience with this setup shows that the prevailing wind direction is the im-portant variable. With certain wind directions the lens soon becomes clouded and must be cleaned several times during a turn. With other wind directions there is no interference from smoke and dust. If the lens is kept clean the results appear to be reliable and reproducible enough for use in studying the temperature distribution from day to day. The air current seems to have no very marked effect on the face of the coke. It might heat it by combustion or cool it by convection. As a rule, the surface of a solid mass of coke is cooled rather than heated by exposure to air.

The same types of receiver and recorder are used at plant B as at plant A.

At plant C, although the guide car and the door-lifter car can be uncoupled, they are seldom separated, and a bolted electrical connection can be made between the radiation receiver permanently mounted on the coke guide and the recorder mounted on the door-lifter car. This arrangement also makes it possible to mount the blower on the floor of the guide car with only a short connecting pipe to carry the air to the radiation receiver. Advantageous consequences are that a smaller blower can be used than in plant A and there is much less trouble from clogged dust filters.

The pyrometric equipment tried at plant C consists of one Rayotube-Micromax combination similar to those at A and B; also a Brown Instrument Co. Radiamatic receiver connected with a Continuous Balance electron-tube recorder with strip chart.

BLOWERS AND AIR FILTERS

The blower used at plant A is an ILG direct-current blower, type 15P, 230 volt, 1720 r.p.m. with enclosed antifriction bearing. At plant B the blower equipment is similar to that at plant A. One of the two blowers at plant C is a Marvel blower, type 40, 250-volt direct current.

At plant A the air is conducted across between the cars and down to the receiver
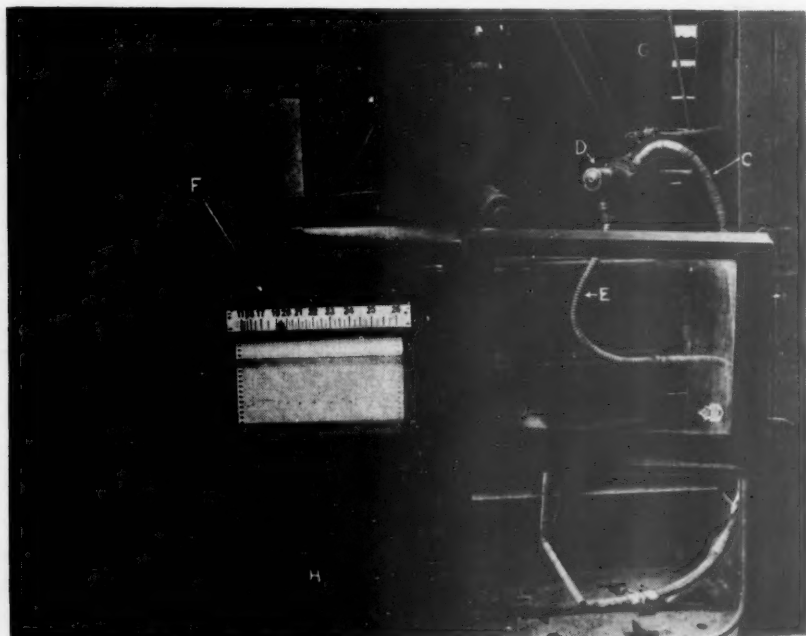
FIG. 3.—BROWN INSTRUMENT COMPANY RADIAMATIC PYROMETER AT PLANT C.

FIG. 4.—LEEDS AND NORTHRUP COMPANY RAYOTUBE PYROMETER AT PLANT C.

A, air filter.
B, blower case.
C, air hose.
D, radiation receiver.
E, electrical leads from radiation receiver to recorder.
F, automatic potentiometric recorder.
G, slats of coke guide.
H, rotary converter, 250-volt direct-current to 110-volt alternating current.

(Fig. 1) by two straight lengths and one jointed length of 3¾-in. tinned pipe. Part of the air blows past the Rayotube and out while the remainder follows along the sighting tube of the pyrometer toward the coke face.

At plant A steel wool was tried as a filter but was not satisfactory. When dry it was not sufficiently dense and when moistened with oil it caused a slight clouding of the lens. Glass wool was effective but after a week of service it had accumulated so much carbon that when the deposit was accidentally ignited the glass wool was melted and destroyed. Changing the position of the filter diminished the amount of dust, but it is necessary to recharge the filter at intervals as part of the regular maintenance.

It was obvious from inspection that the screen-wire pack at plant B is not a good filter. Dependence here is placed on frequent inspection and cleaning of the lens rather than on efforts to obtain clean air.

Fig. 3 shows the arrangement of blower and Brown pyrometer at plant C, and Fig. 4 is a similar view of the Leeds and Northrup equipment. The latter has about 2 lb. glass wool in the filter box. This has seldom needed replacing because the air is drawn from a point where there is not much dust. The Brown is supplied by a Marvel blower (not seen in Fig. 3) through a T-joint inlet carrying glass wool.

OPERATION

At all of the plants, after the door on the discharge side has been lifted out and the coke guide has been brought into place, the operator on that side blows a whistle signal. Pushing of the coke begins on this signal, and at most plants is then almost immediately interrupted for 4 or 5 sec., so that the discharge operator may make sure that everything about the door and guide is in order. At a second signal pushing of the coke proceeds. The total pushing time at plant A is 34 to 35 sec. An auto-matic stopping and restarting device was tried at plant B, but was not successful.

STARTING THE RECORD

As the record paper travels fast (2 in. per minute in the Micromax record reproduced in Fig. 5) the recorder cannot economically be left operating continuously but must be started and stopped in synchronism with the coke. Such a recorder can be made to start itself whenever the temperature read by the radiation receiver exceeds a set value, but this method calls for a relay and starting device, with possibilities of trouble from interruptions due to dusty contacts.

Plant B has a mechanical electrical starter, consisting of a wheel of about 18-in. diameter on an arm. The wheel rolls on the face of the passing coke and is thus pushed aside, closing a switch in the power circuit of the recorder. Such a device proved unsatisfactory at plant A because of the variable position of the instrument combination on the door-lifter car with reference to the coke guide on its separate car. The best method at both plants A and C proved to be the closing of a switch by the operator on the discharge side as part of his regular routine of movements. At plant C the recorder is started by a switch interlocked with the switch of the signal to the pusher. As the guide car cannot be moved until the signal switch is again opened, this interlock system takes care of both the starting and the stopping of the recorder. At plant A the door-lifter operator closes the instrument switch at the same time that he gives the signal, and opens it again after the coke is out. This is not as good as an interlock system, because there is a possibility that the record of one or more ovens may be omitted, and there will be nothing on the record to show which ones are missing.

CALIBRATION

A total-radiation pyrometer is influenced by several external variables, therefore

generally reliance is not placed on its original calibration with reference to a "black body" or holoradiator. The customary procedure is to sight it on a surface

brightness temperature seen on the flat face of the coke at the level of the radiation pyrometer as the coke passed by, and this reading was correlated with the maximum
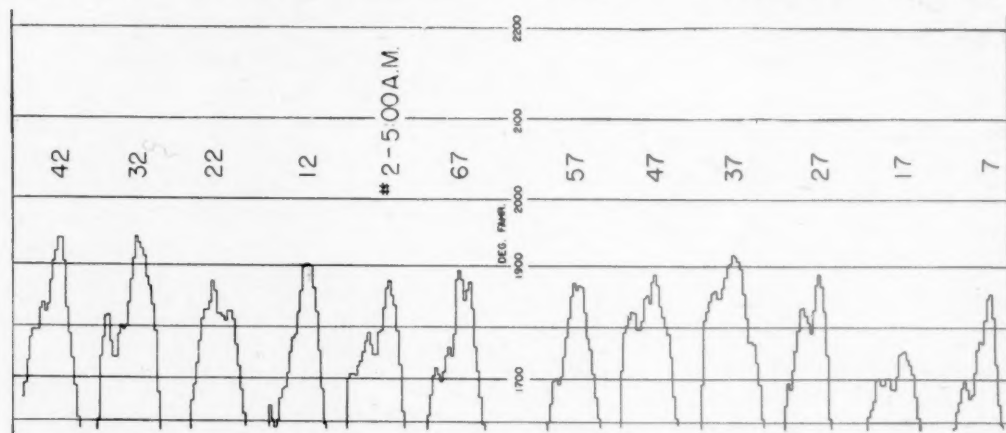
FIG. 5.—TYPICAL COKE PYROMETER RECORD, MADE WITH LEEDS AND NORTHRUP RAYOTUBE AND MICROMAX RECORDER.

whose true temperature is determined independently in some other way (for instance, by an embedded thermocouple), and then set the indicating or recording instrument scale to match.

The optical pyrometer can be used for this calibration. As mentioned before, the coke surface is a holoradiator and no correction is necessary for emissivity. The coke surface, however, is far from uniform. It is crisscrossed by bright lines, which are the cracks between blocks of coke. Optical settings can be made either on the bright lines or on the darker face, but the latter is the more representative of what the radiation receiver sees.

At plant B the optical readings were so irregular that the calibration was made by means of an Ardometer (a German total-radiation pyrometer) sighted first into a holoradiator furnace and then on a coke surface simultaneously with the coke pyrometer, the electromotive force of the Ardometer being read with a portable potentiometer.

At plants A and C the calibration was made by means of optical pyrometer readings. The observer matched the maximum

recorded by the radiation instrument. A series of such readings gives an average difference by which the radiation pyrometer can be reset and again tested.

As the Rayotube and Radiamatic undergo little change provided the lens is kept clean, frequent recalibrations are hardly worth while, particularly since it is the relative distribution of temperature, rather than its absolute value, that is of most interest to the operator.

THE TEMPERATURE RECORD

Fig. 5 is a reduced reproduction of a sample Rayotube record from plant A; the temperature line in the original is in red ink.

The recorder has a suppressed zero and no record is made of any temperature below 1100°F. Temperatures between 1100° and 1550° also are not recorded, because a special pen lifter comes into action when the temperature falls past 1550°, taking the pen off the paper. The necessity of this device (invented by E. A. Lee) arises from the fact that when the record paper is standing still and no coke is in view the vibration of the instrument causes the pen to wear a hole in the paper at the place

where it has been kept wet by the ink. On starting again, the pen is likely to tear the paper.

The Micromax recorder has a cam speed

is also partly illusory, because the heating-up curve of the thermopile is asymptotic and the time gained is far from being proportional to the temperature attained.
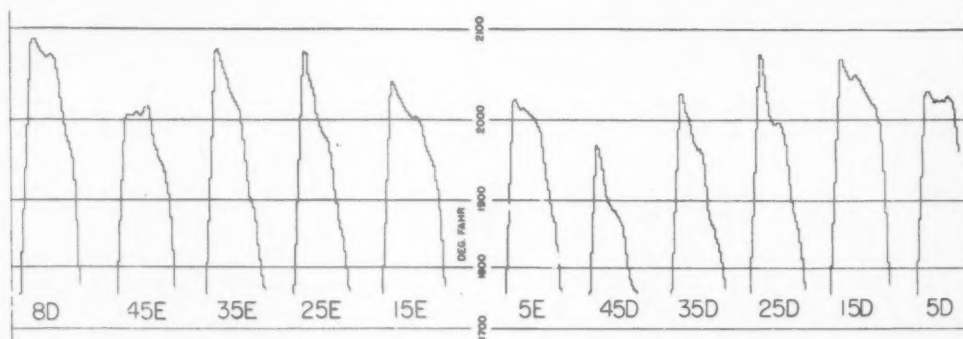
FIG. 6.—COKE PYROMETER RECORD MADE WITH A GALVANOMETER HAVING TOO STIFF A SUSPENSION.

of 27 r.p.m.; that is, a cycle of about 2.2 sec. The heating-up period of the Rayotube to 98 per cent of full value is 6 sec. The maximum travel of the pen at each stroke when the recorder galvanometer is not in balance is one inch. which is equivalent to about 140°F. starting from 1600°, and 105° starting from 1800°F.

With these facts in mind, it is easy to interpret a record such as that reproduced in Fig. 5. The Rayotube is exposed to hot coke as soon as the guide car, with its attached door-lifter car and overhanging pyrometer frame, comes into place. The end of the mass of coke, however, is not fully up to temperature. and the full reading will not be attained until the side of the coke comes into view of the Rayotube. If the side of the charge were at a uniform temperature of 1900°F. and the Rayotube attained its corresponding temperature instantly, the recorder would require 5 cycles of 2.2 sec. each (total 11 sec.) before it would be recording the correct temperature. The speed can be doubled, to 54 r.p.m., but as the Rayotube itself takes 6 sec. to heat up there would be little real gain in speeding the record. The apparent gain in time due to the preliminary exposure of the Rayotube to the end and side of the coke during the initial pause

In most of the records, therefore, I believe the temperature can be considered correct with a precision of 20°F. after the first two steps that appear on the record. This is assuming that there has been no variable interference by smoke, dust, or gases. It does not mean that the true temperature is known with any such accuracy as 20°F. On the other hand, it does mean, for example, that if oven No. 7 has a maximum reading that is 100° higher than the maximum of oven 17, the real difference between the hottest spots of ovens 7 and 17 is at least +80° but may be as much as +120°.

Any step that has a straight rise of a full inch below it (or a drop of a full inch above it if the temperature is falling) may be considered to be without meaning, because this one-inch step is evidence that the recorder has not been able to catch up with the Rayotube. A continuous curve drawn through the middle points of the successive smaller steps consequently gives a fairly exact picture of the variation of temperature along the side of the coke, beginning perhaps 10 ft. in from the front end, through to the rear end.

Inspection of the records in Fig. 5 brings out such facts as the following:

1. Oven 37 is the hottest in the series comprising Nos. 7, 17, 27, 37, 47, 57, 67, with a maximum of 1920°F., and oven 17 is the coldest with a maximum of 1750°F.

instead of its normal 2.5-mil, and its response was only one third as fast as it should have been, consequently the temperature irregularities of the oven were not
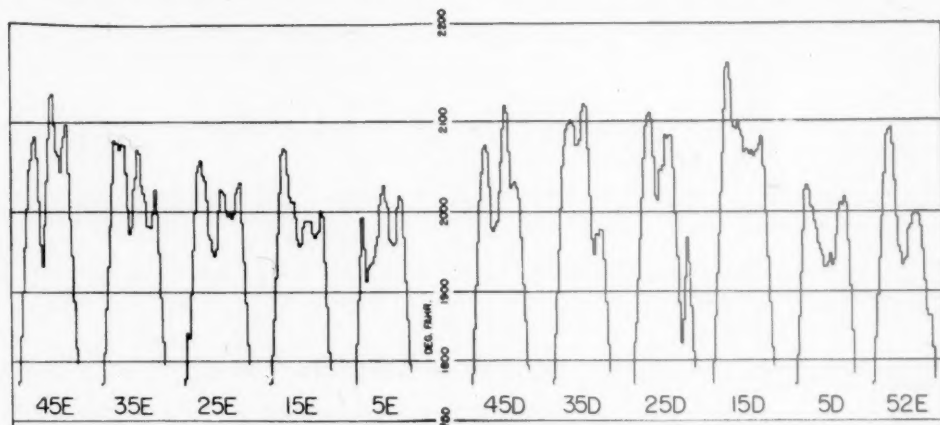
FIG. 7.—COKE PYROMETER RECORD ON SAME OVENS AS FIG. 6, BUT WITH A GALVANOMETER OF SUITABLE SENSITIVITY.
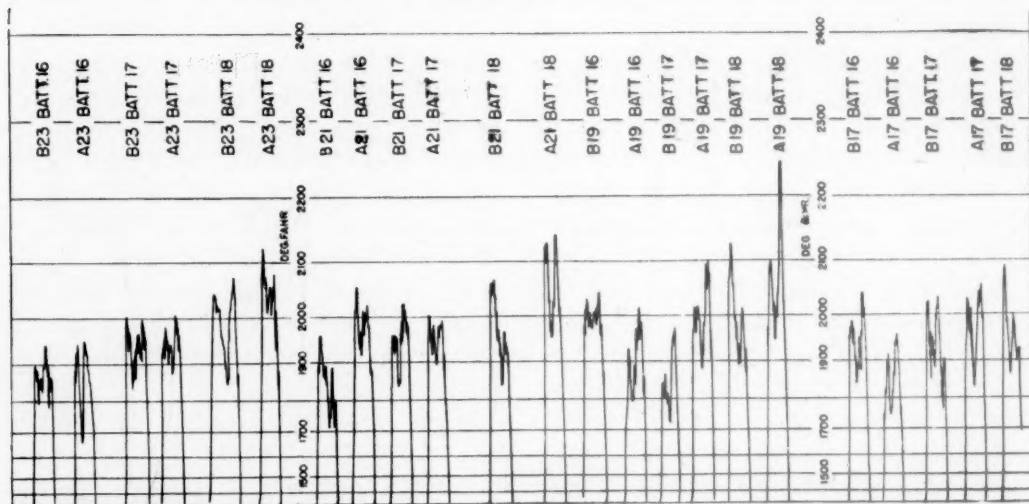
FIG. 8.—COKE PYROMETER RECORD MADE WITH BROWN RADIAMATIC AND ELECTRON-TUBE CONTINUOUS BALANCE RECORDER.

2. Ovens 7 and 27 are the most unsymmetrically heated.

3. Ovens 7, 27, and 47 have spots near the middle that are colder than at either side of the middle.

Figs. 6 and 7 are reduced reproductions of records from plant B. When the record of Fig. 6 was being made the galvanometer of the recorder had inadvertently been provided with a 4-mil suspension ribbon

recorded. The record of Fig. 7, made on the same group of ovens, is normal, and shows the position of the cold spots known to exist in the coke charge, together with their relative magnitude.

The disadvantage of the lightweight suspension is that it is too easily broken by vibration of the car, or during transportation of the recorder from one battery to another. Care in mounting should take

care of the vibration problem, but if the recorder must be moved from place to place the galvanometer needle should be clamped in position.

Fig. 8 is a record from plant C made by the Radiamatic receiver and the Brown Continuous Balance potentiometric recorder. Not being dependent on a mechanical cycle with fixed period, this record does not have the series of steps seen in Figs. 5, 6 and 7. The record is believed to follow the temperature of the coke surface somewhat more closely than the record in Figs. 5 to 7, first because the heat capacity of the thermocouple junctions of the receiver is less than in the Rayotube and, second, because the response of the recorder is faster. The sample shown is not entirely satisfactory, for two reasons: (1) the range was wrongly selected (maximum 2600°F. instead of 2200°) causing the record to be crowded into the lower quarter of the paper; (2) the paper speed is too slow, compressing the record too much in length.

This is not the place for an extended discussion of the characteristics of various types of recording radiation pyrometers, but to round out the picture it should be stated that the Brown Continuous Balance recorder operates on the same principle as the Leeds and Northrup Speedomax recorder. The Speedomax is more elaborate and is faster, but is needlessly fast for the coke-oven application. Both instruments depend upon electron tubes, are therefore less familiar and more of a problem in maintenance than the long-established mechanically operated recorders, now made in the potentiometric type by at least five American instrument manufacturers.

Effect of Carbon Dioxide

One possible source of error in both relative and absolute temperatures remains to be mentioned. Oxidation on the face of the coke will produce a layer of carbon dioxide, which probably would be very thin if a strong wind were blowing against the side observed by the pyrometer but might be of appreciable thickness if the air were still or if the wind came from the opposite direction. Its effect would arise from the following facts. Most of the energy received by the pyrometer is in the invisible infrared region of the spectrum. The lens of the Rayotube receiver is made of vitreous silica (fused quartz), which is transparent to a large part of the infrared. Carbon dioxide has absorption bands in this same portion of the infrared and therefore a thick layer of the gas would act like a partly opaque screen or like a cloud of smoke between the coke and the pyrometer, causing low readings.

In principle, this effect of carbon dioxide can be partly neutralized by using a lens of Pyrex instead of vitreous silica, as Pyrex absorbs some of the infrared that would be absorbed by CO_2 if present. In the calibration of the instrument, therefore, the part of the infrared that is absorbed both by CO_2 and by Pyrex is not effective, and it makes relatively little difference to the pyrometer whether or not it is looking through a layer of carbon dioxide. The Radiamatic regularly employs a Pyrex lens for temperatures above 2300°F., and this was the type used at plant C. The Rayotube can be provided with a Pyrex instead of a silica lens, if slidewire and scale of the recorder are changed to correspond. Whether the effect at the coke surface would be large enough to be observed is still open to question; we hope to have opportunity to investigate this point with one of the instruments at plant C.

Use of the Record

Too much confidence should not be placed in the absolute value of the coke temperature as recorded. It would be easy to take a series of records like those in Figs. 5 to 8 and deduce that the average coking temperature at plant A is x and its maximum x'; that the average for plant B is y, etc., but the deductions might be

misleading. The comparison would be reliable only if the method of calibration and the conditions of cooling during pushing of the coke were strictly comparable.

time the operator has no choice but to raise the oven temperature.

While the absolute value of the coke temperature is thus so difficult to define

Apr 14, 1940
" 15, "
" 16, "
" 17, "

67   57   47   37   27   17   7
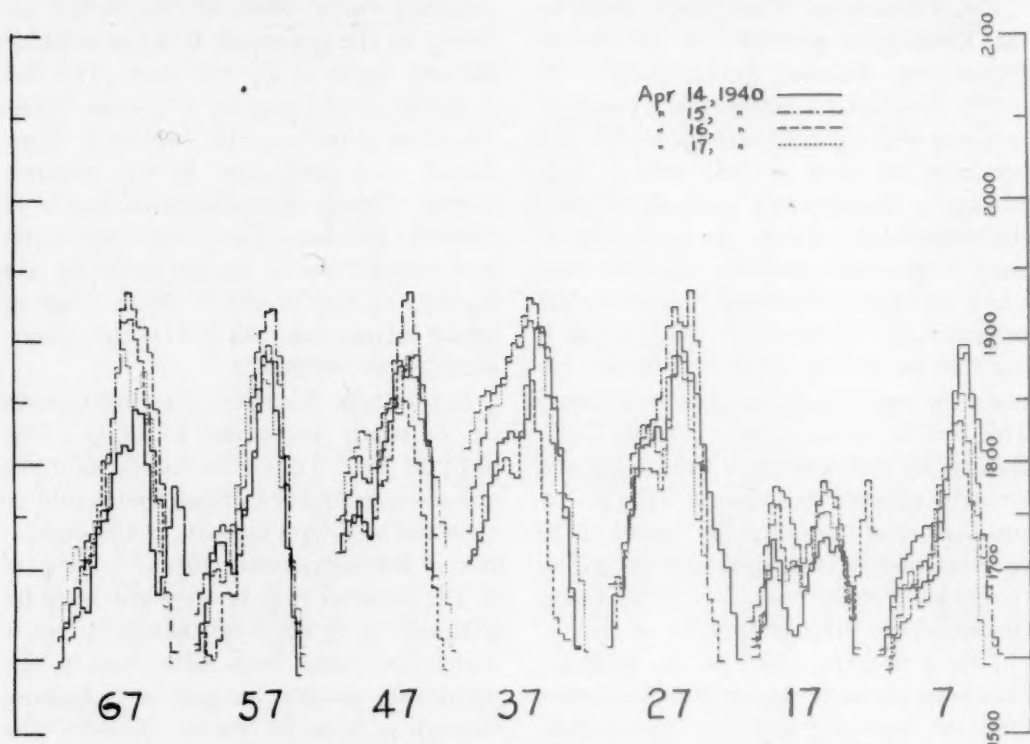
FIG. 9.—COMPARSION OF TEMPERATURE PATTERNS OF COKE OVENS ON SUCCESSIVE DAYS.

It must be remembered that there is always a gradient of temperature within the mass of coke, because both coal and coke are poor conductors of heat and the heat can be introduced only through the two parallel side walls of the oven.

The apparent coke temperature is influenced also by the coking time, for the reason that the coking time affects the width and frequency of the bright cracks. If cracks are wider, or if they are more closely spread across the face of the coke, the galvanometer receives more upward impulses and the average temperature appears higher. Dr. Lowry, furthermore, directs attention to the fact that the effective variable actually is temperature, not time, because in order to obtain reasonably satisfactory coke in a shorter

and to measure that the readings of the radiation pyrometer cannot be directly interpreted, the *relative* distribution of temperature within any oven or among the ovens of a battery, as seen on the record, are quite significant. The variations seen in the typical record are not haphazard. This is proved by comparing the records of the same oven for several successive coking periods at a time when no readjustments are being made. Such a comparison is presented in Fig. 9, made by tracing a series of four records over one another. With such records before him, the operator can make adjustments toward securing uniform coking, with assurance that there will be some tangible evidence as to whether or not he is succeeding in his efforts. He can also see whether any progressive

changes have been taking place that began
in an earlier operating turn, such as are
suggested in oven 37 of Fig. 9. The superin-
tendent, familiar with his batteries and
viewing the entire record for a day or a
week, can recognize other facts that are
not obvious to casual inspection.

VERTICAL VARIATION OF TEMPERATURE

If horizontal variations such as are
recorded in Fig. 5 are persistent in an oven,
are there not vertical variations that are
likewise significant? There are, and it has
been proposed to examine them by placing,
say, three radiation receivers at different
levels on the coke-guide car. The consensus,
however, is that the horizontal pattern, as
seen in Fig. 5, both for the single oven and
for the battery, tends toward reproduction
at higher and lower levels and not to inde-
pendent variation. Good reason for this
can be found in the fact that the combus-
tion flues are vertical and are supplied
from a common main, hence a change in
the pressure or calorific value of the fuel
gas might raise or lower the average tem-
perature of the battery without having
much effect on the relative horizontal
distribution.

Calcination Rates and Sizing of Blast-furnace Flux

By T. L. Joseph,* Member A.I.M.E., H. M. Beatty† and Gust Bitsianes‡

Successful blast-furnace operation depends upon securing an optimum balance between a number of important variables. This balance will vary somewhat from furnace to furnace in the same plant and with raw materials available in different plants. It is difficult to isolate the effect of any one variable unless it has a rather pronounced effect upon the efficiency of operation. The physical properties of iron ore and coke are known to affect the process, yet it is difficult to set up any definite yardstick by which these differences can be appraised.

In recent years, whenever practicable, operators have taken steps to obtain better control over the absolute size and uniformity of size of the ore and coke. The size and physical character of the stone, however, have received comparatively little attention, emphasis being placed upon chemical composition, fluxing efficiency, and action as a desulphurizing agent. Since the stone occupies only about 10 per cent of the volume of the stock column, its influence upon permeability is less than that of the ore and the coke. The large pieces now used have a tendency to roll to the center and thus increase the permeability of this part of the stock column. Smaller pieces would be more effective in promoting the permeability of denser portions of the stock.

The size and physical properties of blast-furnace stone are important also for reasons best understood by considering the results obtained by the crushing and the sizing of iron ore. Crushing ore to about 2 in. at Provo, Utah, and to about 1 in. in Alabama produced material somewhat less permeable to gases, even though sized. In spite of some sacrifice in permeability, the efficiency of the process was improved by crushing and sizing the ore, as indicated by a substantial saving in fuel and increased output. This saving in fuel is due in large measure to more thorough reduction of ore in the upper part of the furnace and to a corresponding decrease in the amount of carbon consumed prematurely above the tuyeres by the reaction

$$CO_2 + C = 2CO - 70,080 \text{ B.t.u.} \quad [1]$$

The physical properties of stone, its size and rate of calcination are important because they influence the rate at which CO_2 is released and the completeness of calcination before reaching a level in the furnace where the temperature does not exceed 1050°C. (1920°F.). Briefly, carbon dioxide from the limestone or from the reduction of ore may cause premature combustion of carbon above the tuyeres.

Assuming that 1000 lb. of limestone is used per ton of pig iron, about 435 lb. of CO_2 will be liberated during calcination of a good grade of stone. If all this CO_2 from the stone were to oxidize carbon prematurely, about 120 lb. would be consumed above the tuyeres in a heat-absorbing reaction. The amount of carbon thus consumed when a

particular grade of stone is used will depend largely upon its size and rate of calcination. These characteristics of the stone, together with the time for the stock to travel from

rate of calcination of limestone. Furnas[1] passed hot gases through a bed of broken pieces of limestone and found the extent of calcination by the loss in weight. The dis-
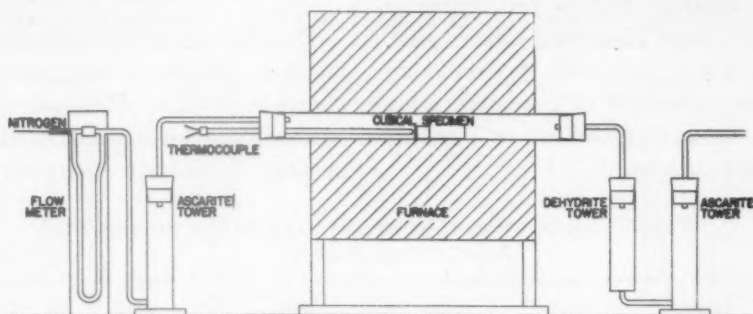
FIG. 1.—APPARATUS USED IN CALCINATION TESTS.

the stock line to a level near the top of the bosh, determine the amount of CO_2 liberated above 1025°C. and the effect of the stone on the amount of carbon oxidized above the tuyeres.

COMPARATIVE RATES OF CALCINATION

At 800°C. (1470°F.) flux stone calcines very slowly, but at 885°C. (1625°F.) the rate is rapid enough to permit reasonable speed in testing and yet slow enough to detect accurately the differences in the time required to attain varying degrees of calcination. To determine whether a number of stones calcined at substantially different rates, comparative tests were made at 885°C. (1625°F.), using ½-in. cubes. While the results of such tests permit a comparison of several stones, it is necessary to know the rate of calcination over the temperature range of 800° to 1100°C. (1470° to 2010°F.), before any attempt can be made to apply the data in determining the degree of calcination attained at various levels in the blast furnace. Three stones were calcined at temperatures of 800°C. (1470°F.), 900°C. (1625°F.), 1000°C. (1830°F.), 1100°C. (2010°F.).

TEST PROCEDURE

Various investigators have used somewhat different methods for observing the

tance the line of calcination had penetrated was determined by measuring the width of the calcined band. Conley[2] heated 1.5 by 2.0-in. test cylinders in a resistance-wound furnace and measured the volume of CO_2 evolved at a pressure of one atmosphere. Kinzell, Holmes and Withrow[3] heated 4-mesh samples in porcelain crucibles and observed the loss in weight. Although the results of tests made on such small pieces showed differences in rates of calcination of different stones, the data cannot be applied to the blast-furnace process.

The apparatus used in the present study is shown in Fig. 1. Specimens closely approaching ½-in. cubes were cut with alundum wheels from lumps of each lot of stone tested. After drying, weighing, and measurement of their volume, the cubes were heated about 3 min. in the end of the quartz tube and then inserted. The temperature dropped slightly but soon was restored to the level selected for a particular test. The weights and volume of the cubes as determined by mercury displacement gave a good check on the uniformity of the size of the cubes.

As soon as the specimen was moved into the hot zone, the stopper at the outlet end of the quartz tube was placed in position. As the CO_2 evolved, it was flushed from the

[1] References are at the end of the paper.

furnace by nitrogen, which was passed through the central tube at the rate of about 300 c.c. per minute. The CO_2 was first dried and then absorbed in a tower containing ascarite. During the course of the test, alternate absorbing towers were weighed at 5-min. intervals. Accumulated weights gave the total CO_2 evolved from which the amount given off at various intervals was calculated.

ture and the end of the thermocouple and the test specimen were kept well within this zone of uniform temperature.

STONES TESTED

The first series of calcination tests was made on samples of eight flux stones from quarries in Ohio, Michigan and Pennsylvania. These tests, made to determine the ·average calcination characteristics of the

TABLE I.—*Analyses of Material Used in Calcination Tests*
PER CENT

Sample	Loss	SiO$_2$	R$_2$O$_3$	CaO	MgO	S	CaCO$_3$	MgCO$_3$
Lot 1	44.40	1.50	0.40	45.14	8.56	0.064	80.56	17.90
Lots 1-4	44.22	1.14	0.24	48.94	5.52	0.038	87.34	11.54
Lot 2	43.68	0.50	0.32	54.65	0.69	0.063	97.53	1.44
Lot 3	47.14	0.24	0.18	30.52	21.82	0.023	54.46	45.63
Lot 4	47.30	0.34	0.16	30.31	21.88	0.019	54.09	45.75
Lot 5	41.76	3.12	2.14	51.97	0.66	0.093	92.75	1.38
Lot 6, light	44.82	0.60	0.64	46.84	6.96	0.128	83.59	14.55
Lot 6, dark	43.98	0.24	0.24	54.95	0.30	0.077	98.06	0.63
Lot 6	44.10	0.38	0.24	53.51	1.68	0.049	95.50	3.51
Lot 7	43.52	1.42	0.32	52.96	1.56	0.060	94.51	3.26
Lot 8	43.60	0.94	0.44	54.30	0.92		96.9	1.92

In order to calculate the porosity, true density determinations were made on minus 100-mesh particles corresponding as closely as possible to the material in the cube calcined. The apparent density was calculated from the weight of each cube and its volume obtained by the weight of the mercury it displaced. An accurate determination of the volume was useful in calculating the average length of each cube. The percentage of porosity was calculated from the following equation:

Percentage of porosity =
$$\left(1 - \frac{\text{Apparent Density}}{\text{True Density}} \right) \times 100$$

As shown later, rates of calcination are very sensitive to changes in temperature. Before the equipment described (which is very similar to that used in making a combustion carbon determination) was used the temperature along the length of the tube was checked to locate a section where the temperature was uniform. A central section about 2 in. long was constant in tempera-

samples submitted, showed that the rate of calcination depends largely upon the magnesia content and the porosity. In tests discussed later, specimens were selected to cover a wide range in magnesia and percentage of porosity for correlation of these properties with rates of calcination. Because of variations in the magnesia and rate of calcination observed on cubes cut from the same lump, each cube was analyzed after it had been calcined.

From the eight lots of stone representative samples were selected for calcination. The appearance of cross sections of 2 to 6-in. lumps cut in half revealed differences in color and texture, which were good guides in selecting specimens for calcination. The eight lots of stone cover material ranging from high-calcium stone to dolomites (Table 1).

Substantial differences in the rates of calcination of cubes cut from the same lump and of cubes from different lumps of the same stone prompted a separate analysis of lump 4 from lot No. 1 and of the light and

dark portions of lump 1 in lot 6. The analyses reported in Table 1 show substantial differences in the percentage of magnesia in parts of the same piece. For example, the

This seems to be true for some stones but does not hold rigorously for others.

In some stones, there is little contrast between the calcined and uncalcined areas;

TABLE 2.—*Physical Properties and Time Required for 95 Per Cent Calcination* (885°C.)

Stone No.	Weight, Grams	Volume, C.C.	Apparent Density	True Density	Porosity, Per Cent	Minutes for 95 Per Cent Calcination
1	5.591	2.176	2.569	2.760	6.9	47.0
2	5.730	2.178	2.630	2.707	2.8	62.3
3	5.331	2.173	2.453	2.855	14.1	29.8
4	5.052	2.144	2.356	2.857	17.5	28.8
5	5.845	2.172	2.691	2.722	1.1	48.7
6	5.677	2.177	2.609	2.708	3.7	49.5
7	5.653	2.165	2.611	2.725	4.2	52.5
8	5.788	2.201	2.629	2.709	3.0	58.2

light layer in lump 1 of lot 6 contained 6.96 per cent MgO, compared with only 0.30 per cent in a well-defined dark layer running through the same lump.

PHYSICAL PROPERTIES

The eight lots of stone cover a rather wide range in color, physical texture, and porosity. The color ranged from a dove gray or black to a pure white. In general, the high-magnesia stones were the most porous. For example, stones 3 and 4, which are true dolomites, averaged 14.1 and 17.5 per cent porosity. Lot 5, with 0.66 per cent MgO, is a dense stone with a porosity of 1.1 per cent. The true density of the stones of low magnesia content was about 2.71 per cent compared with 2.86 for the two dolomites (Table 2). Some of the stones were uniform in every respect from one lump to the next. Others, such as No. 6, showed a marked variation within the same lump with respect to rates of calcination as well as in magnesia content.

MECHANISM OF CALCINATION

Calcination takes place at the boundary of two solid phases, one composed of lime and the other of calcium carbonate. Furnas[1] and Shafor[4] concluded that calcination of a lump of stone is confined to a definite boundary plane, which progresses from the surface toward the center at a definite rate.

moreover, there is definite evidence that calcination occurs beyond the zone of
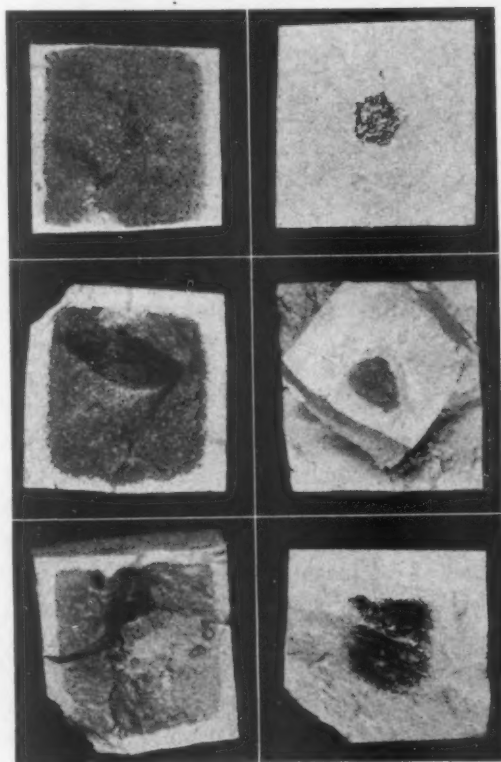
FIG. 2.—PARTLY CALCINED CUBES SHOWING ZONE OF CALCINATION.

complete calcination, giving a mottled appearance on the interior. As calcination proceeds, the sharp corners outlining the shape of the piece disappear from the contour of the zone of calcination. This feature

of calcination is brought out in the work of Conley (ref. 2, p. 339).

Notwithstanding the fact that calcination is not completely restricted to a well-

FIG. 3.—PENETRATION OF CALCINATION ZONE BASED UPON EXTERIOR VOLUME EQUIVALENT TO THE CARBON DIOXIDE EVOLVED.

defined zone, it appears, nevertheless, to proceed largely along a rather definite boundary. The rate of progress of this boundary, which represents a dividing line between partially and completely calcined material, is a useful means of following rates of calcination.

In the present tests, the amount of total CO_2 evolved during successive 5-min. periods was determined. Assuming that the CO_2 is expelled from a series of outer shells representing definite percentages of the total volume of the cubes, the progressive penetration of the zone of calcination can be determined from the equation:

Depth of Penetration

$$= \frac{L}{2}\left(1 - \sqrt[3]{1 - \frac{V}{100}}\right) \quad [2]$$

where

L = length of cube,

V = percentage of total volume calcined (from percentage of CO_2 evolved)

$1 - \dfrac{V}{100}$ = fraction of original volume remaining uncalcined

$\sqrt[3]{1 - \dfrac{V}{100}}$ = length of uncalcined portion

$1 - \sqrt[3]{1 - \dfrac{V}{100}}$ = fraction of total length calcined

Using Eq. 2, the accumulative depth of penetration was calculated for stones 1, 2 and 3 from the results of calcination tests at 885°C. For example, Fig. 5 shows that 20.2 per cent of CO_2 was expelled from stone 1 in the first 5 min. of heating at 885°C. This amount is equivalent to an outer layer 0.047 cm. thick. At the end of 10 min., 38.7 per cent of the total CO_2 was expelled and the depth of the calcined layer had increased to 0.098 cm. The results of similar calculations for stones 1, 2 and 3 are shown graphically in Fig. 3.

For the first minute or two, the rate is a little slower because the exterior of the cube is not up to temperature. There follows a period during which the rate of CO_2 evolved is somewhat more rapid. It does not necessarily follow, however that the zone of calcination is traveling more rapidly. In this stage of heating the shape of the calcination zone follows the exterior contour and has more area than it has during a later period when the zone approaches a spherical shape. That is, the corners of the cubes contribute to a more rapid evolution of CO_2 during this period. For an intermediate period, when the uncalcined area approaches a spherical shape, the two lower curves in Fig. 3 are close to a straight line. Near the end of the calcining period, the heat wave is converging toward the center from all sides and apparently

increases the rate of heating and the speed of calcination. For all practical considerations, it may be concluded that, regardless of particle size, the zone of calcination

dioxide evolved during regular periods. From such curves, the time to reach 95 per cent calcination can be determined. For comparing the rates of calcination, the
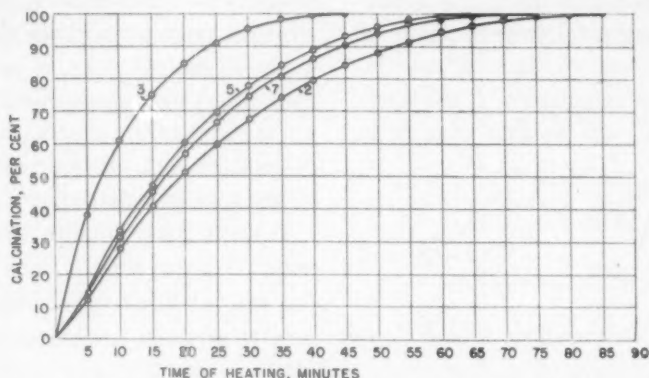
FIG. 4.—TYPICAL CURVES SHOWING PERCENTAGE CALCINATION WITH TIME.

advances at a constant linear rate depending upon the character of the stone and the temperature.

RESULTS OF CALCINATION TESTS AT 885°C.

In order to compare rates of calcination, the amount of CO_2 evolved during 5-min.

time to reach 95 per cent calcination has been used throughout, as there is always some uncertainty as to the exact moment of complete calcination.

Although the time for reaching 95 per cent calcination serves as a basis of comparison, the rate of penetration of the
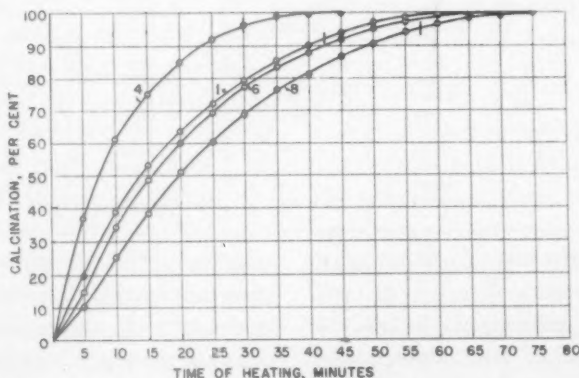
FIG. 5.—TYPICAL CURVES SHOWING PERCENTAGE CALCINATION WITH TIME.

intervals was determined. Average results of 43 calcination tests on eight stones are shown graphically in Figs. 4 and 5. The time required to completely calcine ½-in. cubes at 885°C. ranged from 45 min. for two dolomites, 3 and 4, to 85 min. for the high-calcium stone No. 2. These curves show the regularity with which calcination can be followed by weighing the carbon

calcination zone is more useful in applying the data. When the specific rates are thus expressed for any temperature, the time for complete calcination at this temperature and the degree of calcination at the end of a given time can be determined for lumps of various sizes. In other words, the zone of complete calcination proceeds at a definite linear rate from the outside to the

center of the piece, independent of its size or shape but dependent upon the character of the stone and the temperature.

The zone of calcination penetrates only one half of the length of the linear dimension, since it progresses inward from all sides. If D equals the distance of penetration for 95 per cent calcination, L, the linear dimension, and V, the volume of a cube, then

$$D = \frac{L}{2} - \sqrt[3]{0.05 \times \frac{V}{2}}$$

$$D = \frac{L}{2} - \frac{0.368L}{2}$$

$$D = 0.50L - 0.184L \text{ or } 0.316L \qquad [3]$$

The volume of each cube tested was determined accurately, to obtain its apparent density. Knowing the volume and

ture upon the rate of calcination, three stones were calcined at 800°, 900°, 1000°, and 1100°C. A high-calcium limestone, a a dolomitic limestone and a dolomite were selected for these tests. An effort was made to select from each of the three stones four cubes as nearly alike as possible. Table 3 shows the pronounced effect of temperature on the minutes required for 95 per cent calcination and on the rate of penetration of the zone of calcination.

For the high-calcium stone, the rate of penetration at 1100°C. was about 23 times the rate at 800°C. The effect of temperature is greatest between 800° and 900°C. (Table 3 and Fig. 6).

Equilibrium pressures as determined by Johnson[5] for calcium carbonate are the best

TABLE 3.—*Effect of Temperature on Rate of Penetration of Zone of Calcination*

Type of Stone	Temperature, Deg. C.	Length of Cube, Cm.	Penetration for 95 Per Cent Calcination, Cm.	Minutes for 95 Per Cent Calcination	Rate of Penetration, Cm. per Hr.
High-calcium................	800	1.299	0.4105	263.7	0.093
	900	1.299	0.4105	60.3	0.408
	1000	1.299	0.4105	24.3	1.014
	1100	1.299	0.4105	11.6	2.123
Dolomitic limestone..........	800	1.297	0.4099	177.8	0.138
	900	1.297	0.4099	37.8	0.651
	1000	1.297	0.4099	15.8	1.556
	1100	1.297	0.4099	9.7	2.535
Dolomite....................	800	1.297	0.4099	83.1	0.296
	900	1.297	0.4099	24.3	1.012
	1000	1.297	0.4099	11.9	2.067
	1100	1.297	0.4099	7.2	3.416

the average linear dimension of the cube, the distance of penetration for 95 per cent calcination can be calculated. From the distance of penetration thus determined and the time required for 95 per cent calcination, the average rate of penetration of the zone of calcination is calculated in centimeters per hour. A series of such calculations may be seen in Table 3, which shows the effect of temperature upon the rate of penetration of the calcining zone.

EFFECT OF TEMPERATURE UPON
RATES OF CALCINATION

In order to observe the effect of tempera-

measure of the driving force of temperature upon calcination. The effect of temperature on the rate of calcination should be proportional to its effect in raising the equilibrium pressure of carbon dioxide. All three curves in Fig. 6 are similar in shape to Johnson's curve in which equilibrium pressures of CO_2 are plotted against temperature. Magnesium carbonate begins to dissociate at a lower temperature than calcium carbonate. The more rapid rates of calcination of the dolomitic limestone and the dolomite are to be expected, therefore. At the higher temperatures, the three

curves are farther apart, which shows that the temperature effect becomes more pronounced as the magnesia increases.

lated the volume of stock charged per minute and the thickness of the layer it formed in the cylindrical section at the
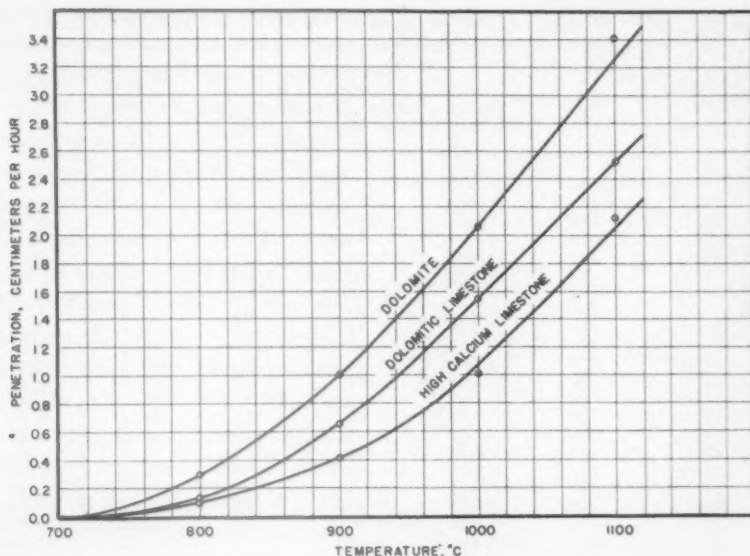
FIG. 6.—EFFECT OF TEMPERATURE ON RATE OF CALCINATION.

RATE OF STOCK TRAVEL AND TEMPERATURE GRADIENT BETWEEN THE STOCK LINE AND BOSH

Several factors govern the progress of calcination of a given flux in the blast furnace. With normal rates of driving, the time of stock travel between the stock line and the top of the bosh will vary with furnace height. In shorter furnaces, the stock is heated more rapidly or it remains in various temperature zones a shorter time. Additional height means a flatter temperature gradient between the stock line and the top of the bosh and a proportionately longer time in the wider portion of the shaft just above the bosh.

Several operators were consulted regarding the time required for the charge to reach the top of the bosh under normal conditions in furnaces varying in height. This information checked very well with results obtained by a method used by Kinney[6] to calculate the rate of stock descent. After determining the weight per cubic foot of the charge, Kinney calcu-

stock line. For example, the 3610 lb. of stock charged per minute occupied a volume of 37.8 cu. ft. On a 17-ft. stock line with an area of 228 sq. ft., this volume of stock would form a layer 0.166 ft., or 1.99 in. thick $\left(\dfrac{37.8}{228} = 0.166 \text{ ft.}\right)$.

As the stock moves down below the bend line, or the level at which the batter begins, the area increases and the stock accordingly settles at a slower rate. With a batter equal to one inch per foot, the diameter increases 0.5 ft. for each 3 ft. of vertical height. By dividing the furnace into 3-ft. sections, the average rate of stock travel through each section can be determined. The result of applying the method to a furnace with a 19.5-ft. stock line and a diameter of 28.5 ft. at the top of the bosh is given in Table 4. A decrease in rate of flow from 2 in. per min. at the stock line to 0.94 in. at the top of the bosh shows the effect of furnace batter in progressively decreasing the rate of stock descent. The last column shows the time for the stock to reach various elevations in the furnace down

to the bosh. From such data the time that the stock remains in various zones can be readily determined.

presentation of the results, distances have been expressed in percentage of height from the stock line to the bosh as shown in

TABLE 4.—*Rate of Flow of Stock in Modern 1000 to 1100-ton Blast Furnace*

Distance below Stock Line, Ft.	Diameter, Ft.	D^2	Area Factor	Rate of Stock Flow, In. per Min.	Average Rate for Zone, In. per Min.	Time in Zone, Min.	Time in Zone, Hr.	Time in Furnace, Hr.
0	19.5	380	1.000					
4	19.5	380	1.000	2.00	2.00	24.0	0.400	0.400
7	20.0	400	0.950	1.90	1.95	18.5	0.318	0.718
10	20.5	420	0.904	1.81	1.86	19.4	0.324	1.040
13	21.0	441	0.862	1.72	1.76	20.2	0.337	1.38
16	21.5	462	0.823	1.65	1.69	21.3	0.355	1.73
19	22.0	484	0.785	1.57	1.61	22.4	0.374	2.11
22	22.5	506	0.751	1.50	1.54	23.4	0.390	2.50
25	23.0	529	0.718	1.43	1.46	24.6	0.410	2.91
28	23.5	552	0.688	1.37	1.40	25.7	0.428	3.34
31	24.0	576	0.660	1.32	1.35	26.6	0.443	3.78
34	24.5	600	0.633	1.27	1.29	27.9	0.465	4.24
37	25.0	625	0.608	1.22	1.25	28.8	0.480	4.72
40	25.5	650	0.585	1.17	1.19	30.2	0.506	5.23
43	26.0	676	0.562	1.12	1.15	31.3	0.522	5.75
46	26.5	702	0.541	1.08	1.10	32.7	0.545	6.30
49	27.0	729	0.521	1.04	1.06	34.0	0.567	6.86
52	27.5	756	0.503	1.01	1.03	35.9	0.596	7.46
55	28.0	784	0.485	0.970	0.98	36.7	0.612	8.07
58	28.5	812	0.468	0.940	0.96	37.5	0.625	8.70
61	28.5	812	0.468	0.940	0.96	37.5	0.625	9.32
64	28.5	812	0.468	0.940	0.96	37.5	0.625	9.95
67	28.5[a]	812	0.468	0.940	0.96	37.5	0.625	10.57
Total..						633.6		10.57

[a] Top of bosh.
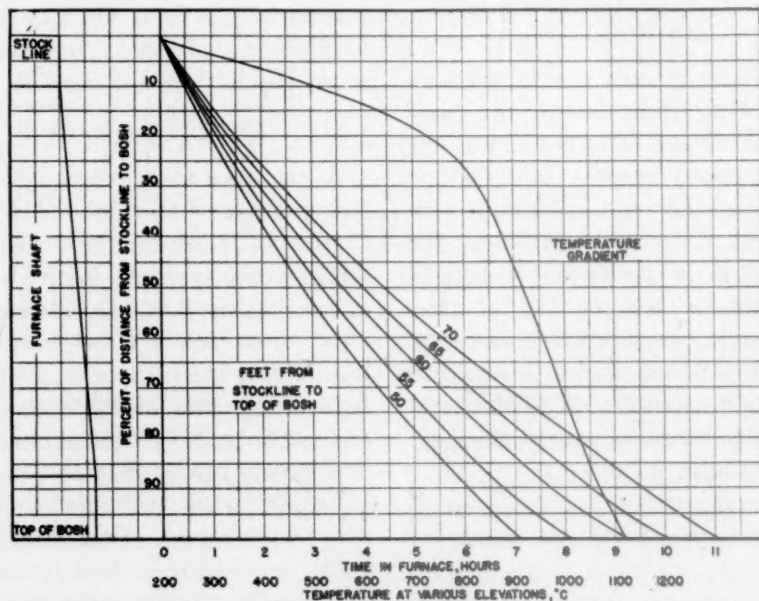
FIG. 7.—STOCK TRAVEL AND TEMPERATURE GRADIENT BETWEEN STOCK LINE AND BOSH.

Calculations similar to those in Table 4 were made for furnaces with distances from the stock line to the bosh of 50, 55, 60, 65, and 70 ft. In order to simplify

Fig. 7. The time for the stock to reach the top of the bosh ranges from 7.10 hr. for a stock-line bosh height of 50 ft. to 11.10 hr. for a similar height of 70 ft. This seems to be

consistent with observations on the normal time for burden changes to work through furnaces of varying size.

In order to follow the progress of calcination of a given stone in the blast furnace, it is necessary to know the rate of calcination of the stone at various temperatures and the time it remains in various temperature zones as it travels through the furnace. It is well known that the temperature across the blast-furnace shaft varies from the inwall to the center. Moreover, there are differences in the rate of stock descent at the wall and at the center. To consider variations in the time-temperature history of stock in different parts of the furnace would greatly complicate the problem. The alternative is to proceed on the basis of the best information available on the average time of stock in the furnace and the average temperature across various levels between the stock line and the bosh.

Kinney's work for the Bureau of Mines has been used in formulating the temperature gradient shown in Fig. 7. The temperature rises rather rapidly for the first 25 per cent of the distance from the stock line to the bosh but more slowly thereafter.

TIME OF STOCK IN VARIOUS TEMPERATURE ZONES

Fig. 7 shows that the stock reaches a temperature of 1050°C. in 9.05 hr. and a temperature of 1000°C. in 7.20 hr. in the 70-ft. furnace; that is, the stock is at an average temperature of 1025°C. (1875°F.) for 1.85 hr. Similarly, in the 50-ft. furnace, the stock comes up to a temperature of 1050° and 1000°C. in 5.70 and 4.55 hr., respectively. In the short furnace the stock is at an average temperature of 1025°C. for only 1.15 hours.

The temperature range of 800° to 1050°C. is of interest in connection with the calcination of limestone in the blast furnace. Below 800°C., calcination proceeds at very slow rates and it is desirable to complete the decomposition below 1050°C. Using Fig. 7

in the manner indicated above, Table 5 was prepared to show the time the stock remains in six temperature zones.

TABLE 5.—*Time of Stock in Various Temperature Zones*

Temperature		Feet from Stock Line to Bosh				
Deg. C.	Deg. F.	70	65	60	55	50
		Time for Stock to Reach Temperature, Hr.				
1050	1920	9.05	8.25	7.30	6.50	5.70
1000	1830	7.20	6.60	5.80	5.20	4.55
950	1740	5.50	5.00	4.45	4.00	3.50
900	1650	4.00	3.55	3.20	2.90	2.60
850	1560	2.75	2.45	2.25	2.00	1.80
800	1470	2.00	1.85	1.65	1.50	1.35
750	1380	1.65	1.50	1.35	1.20	1.10
		Hours in Temperature Zone				
1025	1870	1.85	1.65	1.50	1.30	1.15
975	1780	1.70	1.60	1.35	1.20	1.05
925	1690	1.50	1.45	1.25	1.10	0.90
875	1600	1.25	1.10	0.95	0.90	0.80
825	1510	0.75	0.60	0.60	0.50	0.45
775	1420	0.35	0.35	0.30	0.30	0.25

PROGRESS OF CALCINATION IN FURNACES OF VARIOUS HEIGHTS

As the pieces of limestone descend in the blast furnace, the zone of calcination progresses inward at rates depending upon the character of the flux and the time it remains in various temperature zones. Table 6 shows the advance of the zone of calcination of high-calcium limestone, a dolomitic limestone, and a dolomite. The second column gives the rate of penetration taken from the proper curve in Fig. 6. For the high-calcium stone the rate of penetration at 1025°C. is 1.32 cm. per hour. According to Table 5, the stock is in the temperature zone from 1000° to 1050°C. for 1.85 hr. in a 70-ft. furnace. During this time the zone moves in 2.44 cm. from all exterior faces. In the 50-ft. furnace the time is only 1.15 hr. and the penetration 1.52 centimeters.

By reading from top to bottom of the columns showing the penetration, it be-

comes evident that most of the calcination takes place above 850°C. The summation of the distance penetrated in all the temperature zones must be doubled to obtain the diameter of a piece that would be completely calcined before reaching 1050°C. For the high-calcium stone in the 70-ft.

calcined before reaching 1050°C. in the 70-ft. furnace. For the 50-ft. furnace, the indicated size is about 5.2 in. for dolomite.

In order to get a general picture of the maximum size of various types of stone that can be completely calcined before reaching

TABLE 6.—*Progress of Calcination in Furnaces of Various Heights*

Temperature, Deg. C.	Rate of Penetration, Cm. per Hr.	Feet from Stock Line to Top of Bosh									
		70		65		60		55		50	
		Hours in Zone	Penetration, Cm.	Hours in Zone	Penetration, Cm.	Hours in Zone	Penetration, Cm.	Hours in Zone	Penetration, Cm.	Hours in Zone	Penetration, Cm.
HIGH-CALCIUM STONE											
1050											
1000	1.32	1.85	2.44	1.65	2.18	1.50	1.98	1.30	1.72	1.15	1.52
950	0.89	1.70	1.51	1.60	1.42	1.35	1.20	1.20	1.07	1.05	0.93
900	0.55	1.50	0.83	1.45	0.80	1.25	0.69	1.10	0.61	0.90	0.50
850	0.31	1.25	0.39	1.10	0.34	0.95	0.29	0.90	0.28	0.80	0.25
800	0.15	0.75	0.11	0.60	0.09	0.60	0.09	0.50	0.07	0.45	0.07
750	0.06	0.35	0.02	0.35	0.02	0.30	0.02	0.30	0.02	0.25	0.02
Inches of penetration..........			5.30 4.17		4.85 3.82		4.27 3.36		3.77 2.98		3.29 2.59
DOLOMITIC LIMESTONE											
1050											
1000	1.75	1.85	3.24	1.65	2.89	1.50	2.63	1.30	2.28	1.15	2.01
950	1.29	1.70	2.19	1.60	2.06	1.35	1.74	1.20	1.55	1.05	1.35
900	0.83	1.50	1.25	1.45	1.20	1.25	1.04	1.10	0.91	0.90	0.76
850	0.47	1.25	0.59	1.10	0.52	0.95	0.45	0.90	0.42	0.80	0.38
800	0.24	0.75	0.18	0.60	0.14	0.60	0.14	0.50	0.12	0.45	0.11
750	0.09	0.35	0.03	0.35	0.03	0.30	0.03	0.30	0.03	0.25	0.02
Inches of penetration..........			7.48 5.89		6.84 5.39		6.03 4.75		5.31 4.18		4.63 3.65
DOLOMITE											
1050											
1000	2.35	1.85	4.35	1.65	3.88	1.50	3.53	1.30	3.06	1.15	2.70
950	1.78	1.70	3.03	1.60	2.85	1.35	2.40	1.20	2.14	1.05	1.87
900	1.27	1.50	1.91	1.45	1.84	1.25	1.59	1.10	1.40	0.90	1.14
850	0.78	1.25	0.98	1.10	0.86	0.95	0.74	0.90	0.70	0.80	0.62
800	0.42	0.75	0.32	0.60	0.25	0.60	0.25	0.50	0.21	0.45	0.19
750	0.20	0.35	0.07	0.35	0.07	0.30	0.06	0.30	0.06	0.25	0.05
Inches of penetration[a]........			10.84 8.54		9.75 7.68		8.57 6.75		7.57 5.96		6.57 5.17

[a] Calcination zones move in from all sides. Inches of penetration $= \dfrac{10.84 \text{ cm.} \times 2}{2.54} = 8.54$.

furnace, the depth of penetration is 10.6 cm., or 4.17 in. Under the same conditions the depth of penetration for a dolomitic limestone is 5.89 in. The dolomite calcines still more rapidly, giving a depth of penetration of 8.54 in.; that is, a piece of dolomite 8.54 in. in diameter would be completely

1050°C., the results given in Table 6 have been summarized graphically in Fig. 8. It appears that high-calcium limestones should be crushed to about 4 in., or possibly smaller, depending upon the furnace height. Although lumps of dolomitic limestone and dolomite larger than 4 in. can be calcined

before reaching 1050°C., small sizes or lumps more nearly the size of the coke would promote permeability of the stock where it is needed most.

The indicated size that will permit calcination below 1050°C. can then be determined from Fig. 7 by the procedure previously outlined.
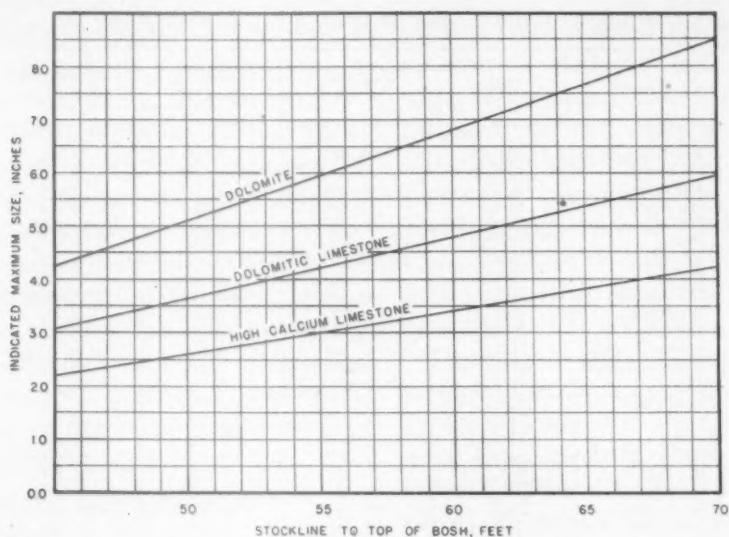
FIG. 8.—INDICATED SIZE OF STONE FOR FURNACES OF VARIOUS HEIGHTS.

APPLICATION OF CALCINATION TESTS ON SPECIFIC FLUXES

Calcination tests have shown that portions of the same lump will calcine at substantially different rates. A careful study of a specific flux requires a study of the appearance of the stone and its physical texture, followed by tests at about 900°C. to determine the calcination characteristics of portions differing materially in color or physical texture. Differences in color sometimes indicate differences in magnesia content. Such differences can be observed by cutting slices from the centers of lumps. A little work of this sort will indicate whether the stone is homogeneous, and the different portions that should be tested for calcination characteristics.

Once the average calcination characteristics have been determined at about 900°C., the relative position of the stone on Fig. 6 can be fixed. By drawing a curve similar in shape to one of the three curves, rates at other temperatures can be approximated.

Care must be taken to control the temperature in all calcination work. It is essential to know the temperature gradient in the furnace, the calibration of the thermocouple used and to hold the temperature at the level set for the tests. Normally, no difficulty is experienced with the cracking of cubes during calcination, providing there is no evidence of a crack in the cube before heating. Only cubes that are free from cracks should be used in calcination tests.

EFFECT OF POROSITY AND MAGNESIA CONTENT UPON RATES OF CALCINATION

A series of 24 cubes was calcined under the same conditions to determine whether porosity and magnesia content can be used to predict calcination rates accurately. Each cube was analyzed after calcination and its composition computed on the basis of its original weight. The type of stone, magnesia content, percentage of porosity, and calcination rates are given in Table 7.

In general, the more porous specimens were higher in magnesia and calcined more

rapidly. There are, however, too many exceptions to this general relationship to predict calcination rates accurately from either porosity or magnesia content. Some

When arranged in order of increasing rates of calcination, the first 13 samples are all of the high-calcium type (Table 7). Samples that calcine at intermediate rates

TABLE 7.—*Effect of Porosity and Magnesia Content on Rates of Calcination*

No.	Source	Type	Magnesia, Per Cent	Porosity, Per Cent	2 × Porosity plus MgO	Penetration, Cm. per Hr.
1-19	West Virginia	H-C.[a]	0.27	0.70	1.67	0.277
2-21	Colorado	H-C.	0.77	0.88	2.53	0.324
3-5	Michigan	H-C.	0.23	1.81	3.85	0.329
4-14	Michigan	H-C.	0.46	0.88	2.22	0.377
5-9	Michigan	H-C.	0.57	5.20	10.97	0.382
6-18	Utah	H-C.	0.51	1.36	3.25	0.388
7-15	Michigan	H-C.	0.91	2.08	5.07	0.422
8-11	Ohio	H-C.	0.84	3.42	7.68	0.430
9-12	Michigan	H-C.	0.34	2.03	4.40	0.448
10-7	Michigan	H-C.	0.37	1.44	3.25	0.475
11-10	Michigan	H-C.	0.66	1.48	3.62	0.476
12-24	Pennsylvania	H-C.	0.54	0.84	2.22	0.483
13-6	Pennsylvania	H-C.	0.62	1.06	2.74	0.500
14-2	Ohio	D. L.[b]	8.40	6.37	21.14	0.524
15-23	Michigan	H-C.	0.37	2.00	4.37	0.548
16-17	Utah	Dol.[c]	18.22	3.22	24.66	0.563
17-1	Ohio	D. L.	7.48	5.89	19.26	0.564
18-3	Ohio	D. L.	5.32	7.51	20.34	0.581
19-16	Michigan	H-C.	0.56	6.29	13.14	0.600
20-8	Michigan	D. L.	6.30	9.49	25.28	0.629
21-13	Michigan	Dol.	21.39	4.61	30.61	0.749
22-22	Colorado	Dol.	20.59	6.95	34.49	0.780
23-4	Ohio	Dol.	21.51	12.20	45.91	0.826
24-20	Michigan	Dol.	20.80	8.14	37.08	0.904

[a] High-calcium.
[b] Dolomitic limestone.
[c] Dolomite.
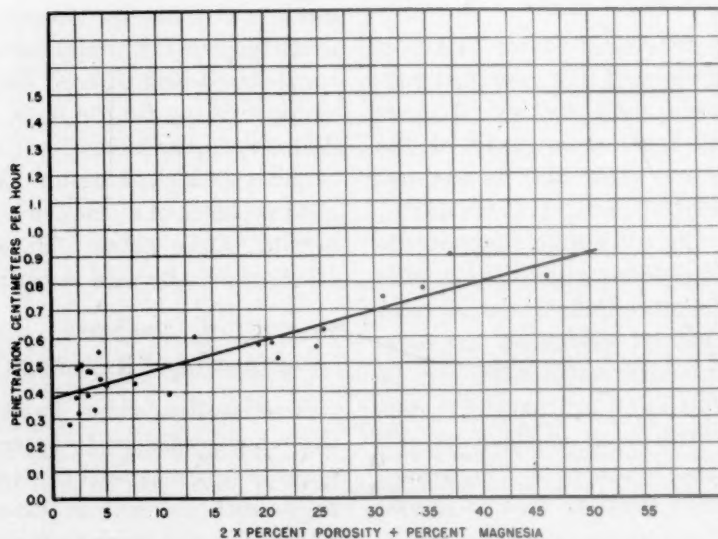
FIG. 9.— EFFECT OF POROSITY AND MAGNESIA CONTENT UPON RATES OF CALCINATION.

porous high-calcium stones calcined at an unusually high rate for this type of material. Although magnesium carbonate dissociates more rapidly than calcium carbonate, dense dolomites calcined slowly.

consist of dolomitic limestones, some rather dense dolomites and the more porous high-calcium stones. Most of the dolomites are at the end of the list, with the highest rates of calcination.

In attempting to work out the best correlation between porosity, magnesia content, and rate of calcination for the data as a whole, it was found that the effect of porosity was about double that of magnesia content. Unless the material is porous, a high magnesia content does not mean a high rate of calcination. The closest correlation obtained is shown in Fig. 9, in which rates of calcination are plotted against double the percentage of porosity plus the percentage of magnesia. The greatest spread in the points occurs in the high-calcium stones. Viewing the data as a whole, it is obvious that all the factors affecting calcination have not been taken into consideration. Thus it becomes necessary to measure the rate of calcination to get accurate information.

Summary and Conclusions

Comparative tests on a wide variety of fluxes, ranging from dolomite to high-calcium stones, disclosed differences of about three to one in rates of calcination. The more porous stones were, in general, higher in magnesia and calcined at faster rates. High-calcium stones calcined at the slowest rate, dolomitic limestone at intermediate rates and dolomites at the most rapid rate. However, unusually porous limestones and exceptionally dense dolomites calcined at intermediate rates. Differences observed in the rates of calcination of high-calcium stone cannot be accounted for by comparatively small differences in porosity and magnesia content.

Up to about 50 per cent calcination, the rate of evolution of carbon dioxide is closely related to the amount of magnesia in dolomitic limestone and dolomites. This may be due to the decomposition of magnesium carbonate throughout the specimen in the early stages rather than in a definite or restricted zone of calcination.

Until a more definite relation is established between physical properties, composition and rates of calcination, comparative tests will be necessary to obtain accurate information. By conducting such tests at a fixed temperature, accurate comparisons can be made.

In order to apply the results of laboratory tests to the sizing of blast-furnace flux, a study was made of the time the stock remains in different temperature zones when the distance from the stock line to the top of the bosh varies from 50 to 70 ft. Calcination that begins at about 800°C. should be completed below 1050°C., to avoid solution loss. In taller furnaces, the stock remains in this temperature zone for a longer time, thus permitting complete calcination of larger pieces.

Dependent upon furnace height, the results indicate that high-calcium stone should be crushed to from 3 to 4 in., dolomitic limestone from 4 to 6 in. and porous dolomites from 6 to 8 in. Although larger pieces of material higher in magnesia can be calcined before solution loss occurs, smaller sizes would be more effective in promoting the permeability of denser portions of the stock column.

Acknowledgments

References

1. C. C. Furnas: The Rate of Calcination of Limestone. *Ind. and Eng. Chem.* (1931) **23**, 534.
2. J. E. Conley: Calcination Conditions for Limestone, Dolomite and Magnesite. *Trans.* A.I.M.E. (1942) **148**, 330.
3. H. K. Kinzell, M. E. Holmes and J. Withrow: The Loss in Weight of Limestone as a Function of Time and Temperature of Burning. *Trans.* Amer. Inst. of Chem. Eng. (1926) **18**, 249–281.
4. W. R. Shafor: Lime Problems in the Beet Sugar Industry. A Symposium on Lime. Ohio State Univ. *Bull.* 35 (1927) 86.
5. J. Johnson: The Thermal Dissociation of Calcium Carbonate. *Jnl.* Amer. Chem. Soc. (1910) 32–938.
6. S. P. Kinney: The Blast Furnace Stock Column. U. S. Bur. Mines *Tech. Paper* 442 (1929) 34.

The Low-temperature Gaseous Reduction of a Magnetite

By M. C. Udy,* Junior Member, and C. H. Lorig,† Member A.I.M.E.

(Cleveland Meeting, October 1942)

Through the years much interest has been centered in attempting to develop a direct method of iron-ore reduction, to replace or supplement the present indirect blast-furnace process. It would not be difficult to produce a list of more than 500 patents dealing with the direct production of iron and steel, but the few of this type of process that have proved successful do not produce in competition with the blast furnace; they produce special products.

A survey of the literature reveals that the equilibrium conditions for the reduction reactions (iron oxides with carbon monoxide and with hydrogen) have been fairly well established but that data on the rate of reaction are discordant, although the general effects of the variables are known.

This dissertation deals with the rate of reduction of a magnetite concentrate with hydrogen. The following variables have been studied: bed depth, gas velocity, particle size and temperature. The behavior of a single particle was also studied.

Literature

Two general factors should be considered in a study of reduction of iron oxide:

(1) equilibrium relations, and (2) rate of reaction.

The first factor, equilibrium, has received the attention of many investigators and the equilibria Fe_3O_4-FeO-H_2-H_2O, Fe_3O_4-FeO-CO-CO_2, FeO-Fe-H_2-H_2O, FeO-Fe-CO-CO_2 are fairly well established.

Of the second factor, the rate of reaction, much less is known. Data are comparatively scarce and there is very little concordance. The discordance probably results from the large number of variables influencing the reactions. However, the general effect of the variables is known.

Among these variables are temperature, gas velocity, particle size, porosity, gas composition (distance from equilibrium), presence of impurities, greater or less prevalence of side reactions, and even design of the apparatus itself.

Wetherill and Furnas[1] published an excellent paper in 1934. They point out that any one or more of five processes (the chemical reaction, diffusion of the reactant through the gas film, diffusion of the reactant through the solid phase, diffusion of the reaction product through the solid phase, or diffusion of the reaction product through the gas film) may be the slow process, and thus the rate-controlling process. It is regretted that the work of these authors was limited to experiments at one temperature, and that the range of gas compositions was limited.

Langmuir[2] has shown that heterogeneous reactions take place at phase boundaries.

[1] References are at the end of the paper.

Wetherill and Furnas draw the conclusion that, inasmuch as solid solution takes place between FeO and Fe, the reaction zone is a narrow band of finite thickness.

products, and the adsorption of gases on reacting surfaces.

Joseph[7] in 1936 discussed the effect of porosity on reducibility. His experiments
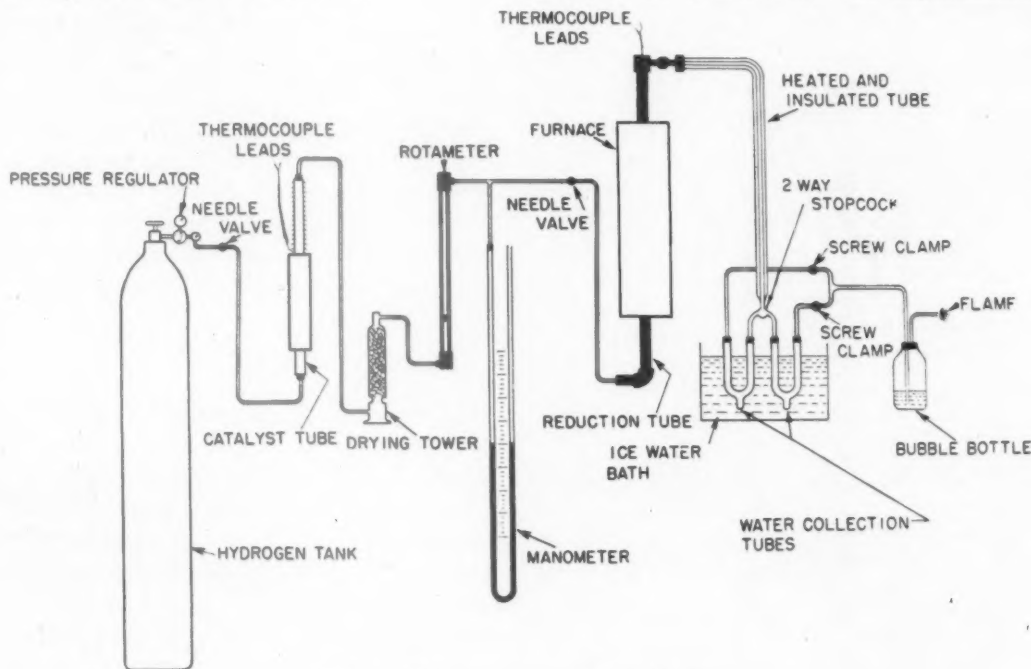
FIG. 1.—LINE DIAGRAM OF APPARATUS.

It is claimed[3] that for all particles under about one centimeter in diameter, no ferric iron is present when metallization begins.

Evidence[4] points to the fact that the reaction zone advances radially at a constant rate from the surface to the center of the particle.

Tenenbaum and Joseph[5] discuss the effect of pressure on the rate of reduction by hydrogen. They also discuss the process of diffusion and its effect on reaction rate.

Tenenbaum and Joseph have also investigated the reduction of iron ores under pressure by carbon monoxide.[6] The rate of diffusion depends on molecular weight, pressure, temperature, and concentration gradient. The rate of reaction will depend not only on the specific reaction rate but also upon the available surface of unreduced iron oxide, the rate of diffusion of reducing gas, the rate of effusion of gaseous

were with hydrogen, using cubes cut from ore.

Meyer[8] studied the rates of reduction of magnetite and of minette in hydrogen, carbon monoxide, and mixtures of the two. He quotes a paper by K. Hoffman[9] which discusses the effect of temperature. In general, increasing temperature increases rate of reaction, but Hoffman showed a minimum in the reaction rate between 750° and 950°C. Sintering of the formed iron and the alpha-gamma transformation were given as the causes of the minimum.

Meyer showed faster rate of reduction with hydrogen than with carbon monoxide and intermediate values for mixtures of the two gases.

Joseph, Scott, and Kalina[10] claim that certain types of material form a continuous skin of ferrite around the outside of the particle, and that under some conditions this outer layer of metallic iron is relatively

impervious to gases, thus making it difficult to attain a high degree of reduction.

Williams and Ragatz[11] have investigated the effect of foreign materials on the

FIG. 2.—SECTION OF CENTRAL PORTION OF REDUCTION TUBE.

rates of reduction. Their investigations show that Na_2CO_3, K_2CO_3, and $BaCO_3$ act as promoters, that SiO_2 will decrease the effect of the promoters, and that many other substances are indifferent.

Side reactions may present a difficulty. For example, below 800°C. the reaction $2CO \rightleftharpoons CO_2 + C$ interferes with the CO reduction reaction, even to its actual exclusion at lower temperatures.

At higher temperatures sintering is a difficulty. It is greatly enhanced by the presence of sulphides or of silica. Silica may form relatively impervious silicate layers on the surface.

For a complete understanding of the rate of reaction, a large number of variables needs to be considered.

It was the purpose of the present investigation to study further the rate of reduction

of iron oxide with hydrogen, and the effects of the several variables thereon.

MATERIALS

The magnetite used in the present investigation was a concentrate from the Scrub Oaks mine (furnished by the Alan Wood Steel Co., of Dover, N. J.). The major impurity present was about 2.25 per cent of silica.

Commercial electrolytic hydrogen, from which traces of oxygen were removed with platinized asbestos, was the reducing gas.

APPARATUS

Fig. 1 is a line diagram of the apparatus used for the majority of the experiments. Hydrogen from the cylinder passed in turn through the platinized asbestos tube (kept at 575° to 625°C.), a drying tower containing anhydrous magnesium perchlorate, a flowmeter, the reaction tube, the tube for collecting the water formed in the reaction, and finally a bubble bottle. The hydrogen leaving the bubble bottle was burned.

Gas velocities were measured to ± 0.003 cu. ft. per minute.

The reaction tube was heated in a tube-type electric furnace, designed to have an 8-in. section of uniform temperature at the middle. Temperature was controlled with a Foxboro potentiometer controller to better than ± 5°C. A Chromel-Alumel thermocouple was used.

The reaction tube was a length of 1-in. double-strength iron pipe. Through the center ran a $\frac{1}{4}$-in. steel tube for protection of the thermocouple; thus, the reduction zone was an annular space.

Fig. 2 shows a section of the reaction tube. The tube was charged from the bottom and the load of magnetite particles (to be reduced) was supported between a lower and an upper bed of $\frac{1}{8}$-in. porcelain beads, and separated from these beds by 120-mesh iron screens. The function of the beads was threefold: to support the charge,

to preheat the gas, and to prevent excess heat loss through the top of the tube.

Connections to the reduction tube were made with standard pipe fittings sealed with Glyptal lacquer.

The water-collection tubes were fitted with rubber stoppers, through which the branches of the stopcock passed. Fig. 3 shows the setup of the furnace and the water-collection apparatus.
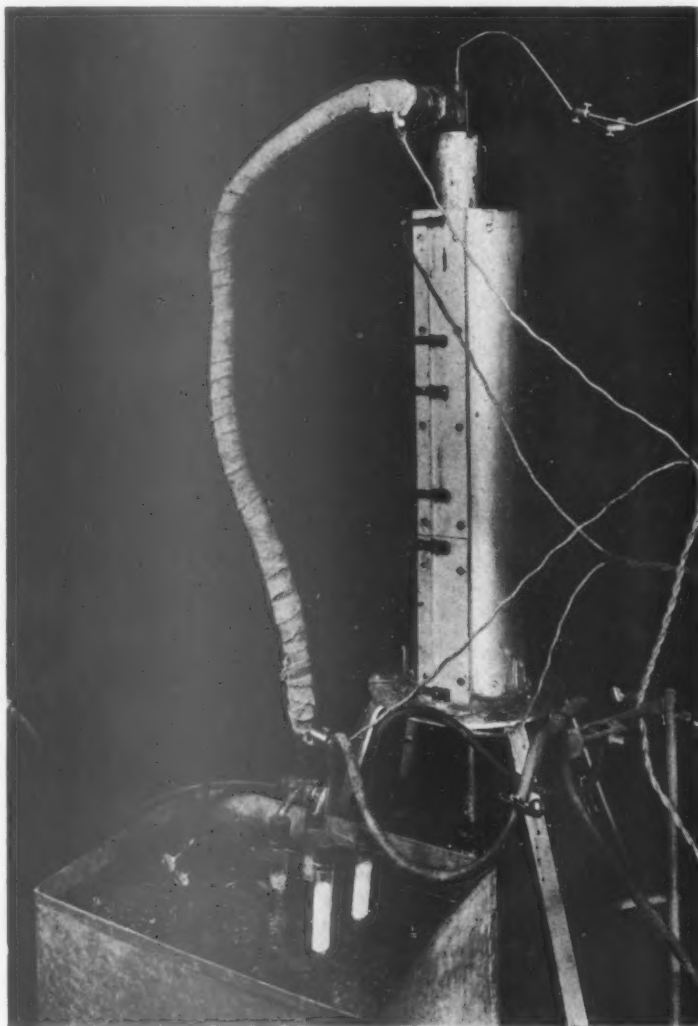
FIG. 3.—FURNACE AND WATER-COLLECTION APPARATUS.

In some of the experiments at higher temperatures, the iron tube was found to have an effect on the results obtained, and these experiments were repeated with a fused silica reaction tube.

Leading from the top of the reaction tube was a $\frac{3}{8}$-in. i.d. copper tube, which was heated electrically to prevent condensation of water. A twoway stopcock was connected to the lower end of the copper tube.

Fig. 4 shows a water-collection tube, which consisted of a U-tube ($\frac{3}{4}$-in. i.d.) with a water trap sealed to the bottom of the U. Glass beads supported on a perforated porcelain plate were placed in the entry arm of the tube. The beads offered a large surface for condensation. The exit arm contained granular anhydrous magnesium perchlorate, also supported on a perforated porcelain plate. In use, the

TABLE 1.—*Data for Run No. 14, February 7, 1941*

| Tube No. | Weight, Grams | | Δ Wt., Grams | Δ Time, Min. | Total Time, Min. | Total Wt., Grams | Percentage of Total Oxygen Removed |
	Before	After					
1	7.6570	8.1223	0.4653	3	3	0.4653	9.5
2	18.8124	19.4451	0.6327	3	6	1.0980	22.9
3	12.7780	13.1406	0.8626	5	11	1.9606	41.2
4	15.2902	15.6496	0.3594	5	16	2.3200	48.6
5	8.1174	8.3003	0.1829	5	21	2.5029	52.4
6	14.9482	15.0876	0.1394	5	26	2.6423	55.3
7	11.4136	11.5182	0.1046	5	31	2.7469	57.5
8	13.0440	13.1344	0.0904	5	36	2.8373	59.3
9	20.5697	20.6438	0.0741	5	41	2.9114	60.9
10	16.8904	17.0738	0.1834	15	56	3.0948	64.8
11	19.2898	19.4250	0.1352	15	71	3.2300	67.7
12	11.7832	11.8997	0.1165	15	86	3.3465	70.1

Bed depth, ½-inch magnetite concentrate (−28+35 mesh)
Gas velocity, 0.200 cu. ft. per min. hydrogen (O_2 removed)
Temperature, 700°C. Rotameter setting, 38 mm.
Back pressure, 1-inch Hg

FIG. 4.—WATER-COLLECTION TUBE.

tubes were immersed in an ice-water bath. The efficiency of these tubes proved to be excellent.

Some of the experiments were made with single particles. In these the reaction tube was Pyrex. A smaller furnace was used and the water-collection apparatus discarded. The particle was packed in a supporting bed of crushed porcelain of the same grain size. The particle was weighed, before and after reduction, on a microbalance to determine the degree of reduction.

EXPERIMENTS IN BEDS

The reaction tube was charged as described and placed in the furnace. Connections were made and sealed. Then the furnace, the catalyst tube, and the tube leading from the furnace were brought to their respective proper temperatures. Next, a stream of nitrogen was passed through the apparatus for about five minutes. After this, the first two water-collection tubes were put in place and the hydrogen flow was started and adjusted to the proper velocity. When the hydrogen flow began, a stop watch was started. Then, at timed intervals, the gas stream was switched to new collection tubes. In a run, 12 tubes were used. These were weighed before and after collection of the water. Before weigh-
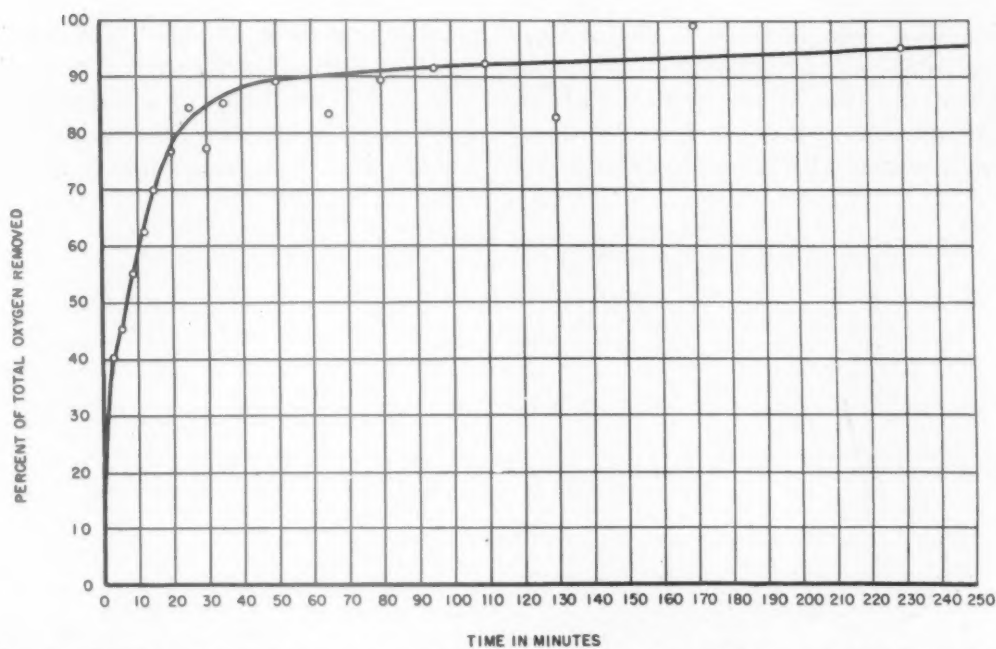
FIG. 5.—SINGLE PARTICLES REDUCED BY HYDROGEN, 700°C. AND 0.298 CUBIC FEET PER MINUTE PER SQUARE INCH, CORRECTED TO PARTICLE DIAMETER OF 2.35 MILLIMETERS.
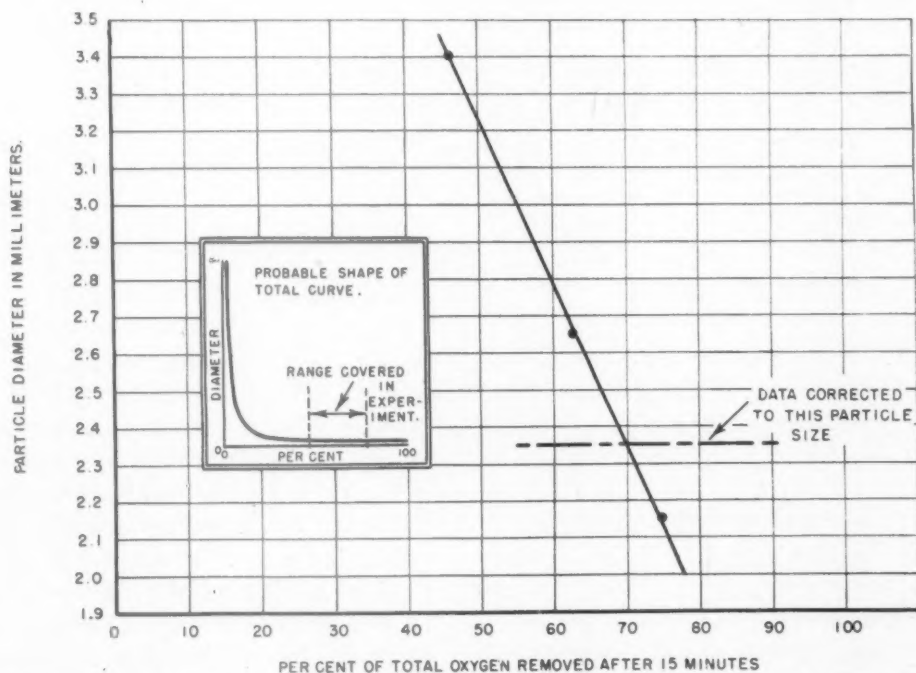
FIG. 6.—SINGLE PARTICLES REDUCED BY HYDROGEN 15 MINUTES AT 700°C., 0.298 CUBIC FOOT PER MINUTE PER SQUARE INCH.

ing, they were purged with dry nitrogen and wiped on the outside with an absorbent cloth wet with alcohol. After the 12 tubes had been used, the hydrogen was turned off and the system purged with nitrogen, thus

pure dry hydrogen at 700°C. Gas velocity was kept at 0.298 cu. ft. per min. per sq. in. (the same as was later used for experiments in the bed). At the end of the desired time, the reaction was stopped with nitrogen.
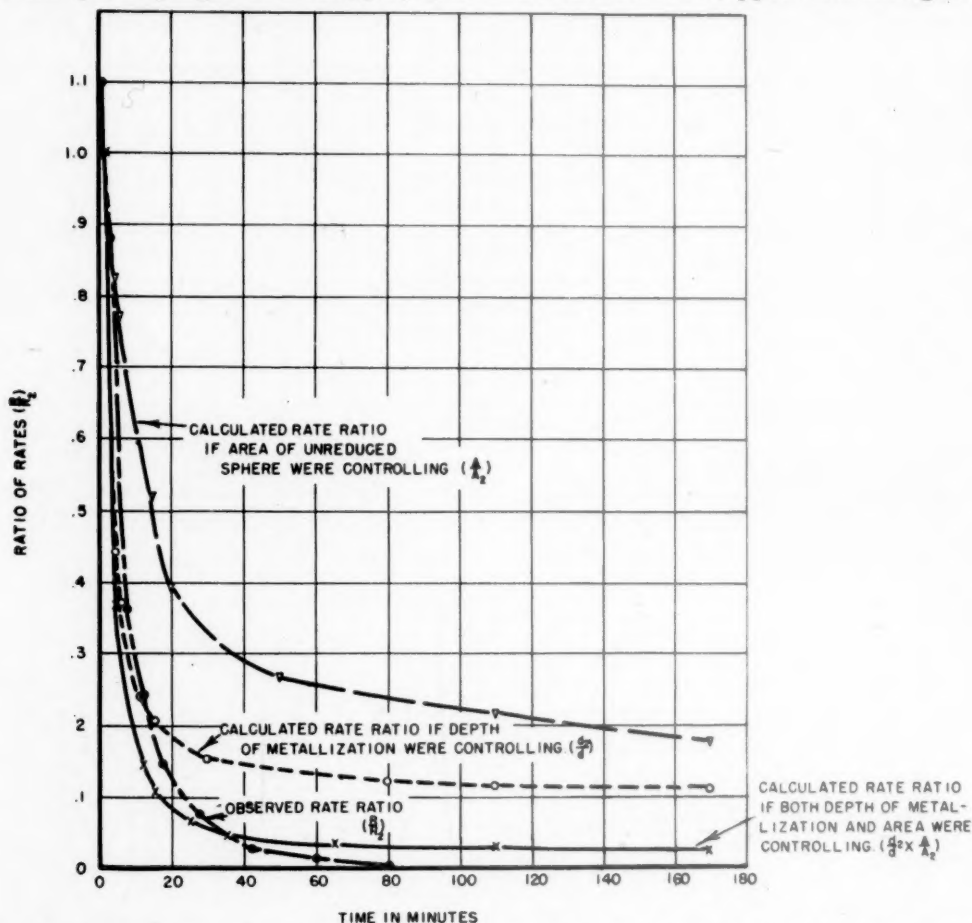
FIG. 7.—COMPARISON OF CALCULATED AND OBSERVED RATE RATIOS, SINGLE PARTICLE, 0.235-CENTIMETER DIAMETER, 700°C. AND 0.298 CUBIC FOOT PER MINUTE PER SQUARE INCH.

quickly terminating the reaction. A typical set of data for a run is given in Table 1.

RESULTS AND DISCUSSION
Behavior of Single Particles

The magnetite particles for this experiment were hand-picked for uniformity in size, from the −6+10 mesh fraction of the ore sample. They were weighed separately on a microbalance both before and after being exposed separately for increasing lengths of time to the action of a stream of

Fig. 5 shows the results. Percentage loss of oxygen is plotted against time. Corrections were made to a common particle diameter of 0.235 cm., using Fig. 6 as a calibration curve. To obtain Fig. 6, three particles of different size were reduced for 15 min. each, and the percentage loss of oxygen plotted against particle diameter.

While this correction may not be strictly applicable over the whole time interval, it does bring points that originally were scattered into good order along the curve of Fig. 5. Experimental errors may arise, not

only from small variations in the control of factors governing the rate, but also from variations in porosity and composition of the particle, and from the loss of small fragments in the handling.

if the situation is idealized. Suppose that the particle is a sphere of 0.235-cm. diameter. Then, since the percentage loss of oxygen is known at various time intervals, all the information required to calculate the
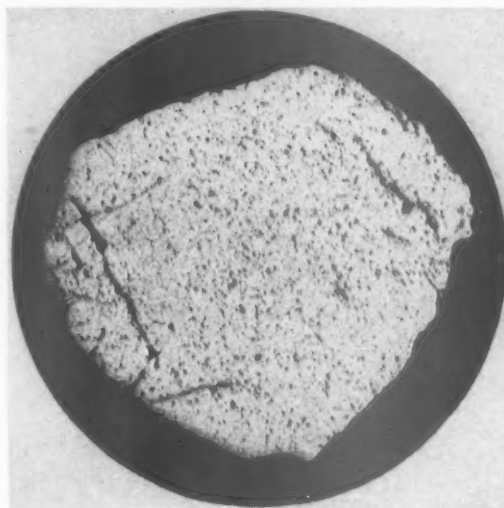
FIG. 8.—UNREDUCED GRAIN OF MAGNETITE.

FIG. 9.—GRAIN OF MAGNETITE REDUCED 3 MINUTES AT 700°C. IN HYDROGEN.

Original magnification of both, × 20; reduced ¼ in reproduction.

Fig. 5 shows that the original rate of reaction is many times larger than that near the last. Because the water formed in the reaction is continually being swept away with fresh hydrogen, it would seem difficult to explain the behavior in terms of anything happening in the gas phase or on the surface of the particle. Some of the particles used in the experiments were sectioned, polished, and photographed. From these photographs (Figs. 8–16), it is clear that a shell of metallization advances from the outside of the grain toward the interior with increasing time. Possibly the increasing resistance of the metallized jacket to diffusion of water and hydrogen could offer a satisfactory explanation of the shape of the curve of Fig. 5. Probably also to be included is another factor—the ever-decreasing surface area of the magnetite core as the amount of metal increases.

The degree to which this conception of the controlling factors accounts for the observed rate of reduction can be tested

surface area of the inner sphere of reduced magnetite and the depth of the metallized shell is available.

It is convenient to take the observed rate of the first few minutes (R_2) as a basic rate and express later rates as the fraction $\dfrac{R}{R_2}$. Similarly, the decreasing areas are expressed as fractions, $\dfrac{A}{A_2}$. Inversely, the depth is expressed as a decreasing fraction, $\dfrac{d_2}{d}$. Plots of these ratios against time are compared in Fig. 7.

The conclusions are further borne out by consideration of Fig. 6. There the *percentage* loss of oxygen in 15 min. is greater for a small particle than for a large particle, and naturally so, because the ratio of surface to volume is larger for the smaller particle. But the *actual weight* of oxygen lost is greater for the larger particles. This is to be expected, because the larger particle with the larger absolute surface area would

react faster with the hydrogen, and would require metallization to a shallower depth for the reduction of a given quantity of magnetite.

depth of metallization would be expected in the smaller particle than in the larger in the same time.

If the hypothesis that both the depth of

FIGS. 10-12.—GRAINS OF MAGNETITE RE-
DUCED AT 700°C. IN HYDROGEN.   × 20.
Fig. 10, reduced 6 minutes; Fig. 11, re-
duced 12 minutes; Fig. 12, reduced 20 min-
utes.

Calculations from the data of Fig. 6 show that the depth of metallization in 15 min. is greater for the smaller than for the larger grain. If the reduction were proceeding vertically into flat pieces of different thick-nesses, the depth of metallization in a given time would be the same. But where spherical particles are involved, the diffu-sion lines of the entering hydrogen converge more rapidly and the diffusion lines of the escaping water vapor diverge more rapidly the smaller the sphere. Therefore, a greater

the metal jacket and the area of the inner sphere are the rate-controlling factors is correct, it follows that the total loss in oxygen in 15 min. divided by the product of the average depth $(r_1 - r_2)$ and the average area $(4\pi r^2)$, should give a value that is constant for three particles of different sizes. Results of such a calculation are: for the large particle, 2.71; for the medium particle, 2.81; for the small particle, 2.70.

Figs. 8 to 16 show sections of grains of magnetite reduced under various conditions.

Effect of Bed Depth

The effect of bed depth was studied by subjecting −28+35-mesh particles of magnetite in beds of ½-in., 2-in. and 4-in.

ducibility). As might be expected on *a priori* grounds (since the upper portion of the bed receives hydrogen already more or less loaded with water vapor, the exposure

13   14
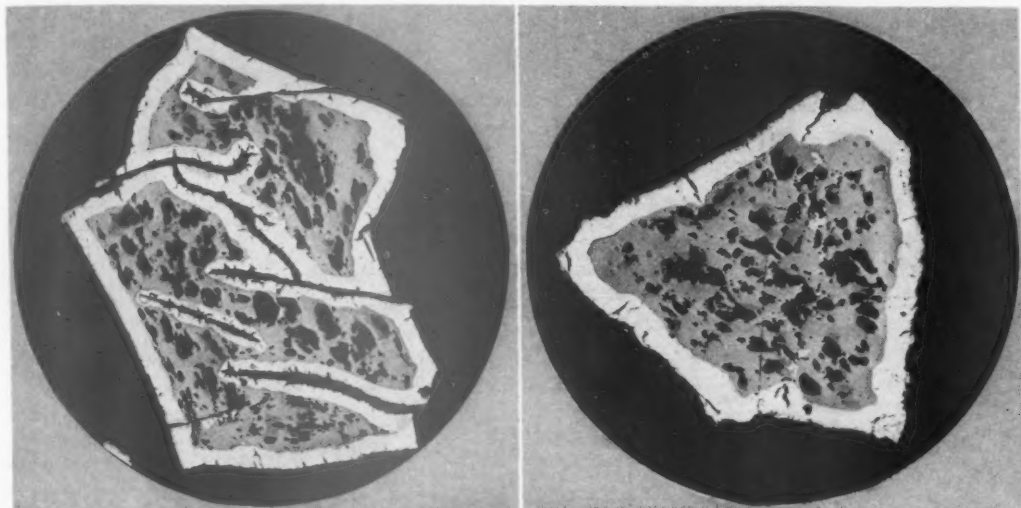
FIGS. 13 AND 14.—GRAINS OF MAGNETITE REDUCED 1½ HOURS AT 400°C. IN HYDROGEN. Original magnification × 100; reduced ⅕ in reproduction.
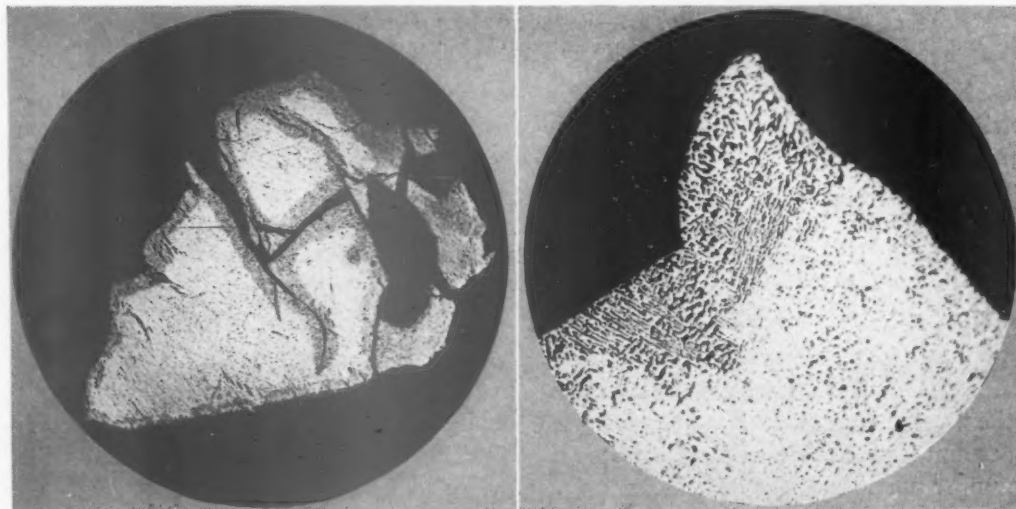
FIG. 15. GRAIN OF MAGNETITE REDUCED COMPLETELY AT 650°C. IN HYDROGEN (SHOWING REOXIDATION).

Original magnification, × 100; reduced ⅕ in reproduction.

FIG. 16.—SAME AS FIGURE 15 BUT AT HIGHER MAGNIFICATION TO SHOW EUTECTOID STRUCTURE.

Original magnification × 500; reduced ⅕ in reproduction.

to reduction at 700°C. with hydrogen at 0.298 cu. ft. per min. per sq. in. Results are presented in Fig. 17 (duplicate runs were made at each bed depth to determine repro-

of the particle to the hydrogen is lower than that of a single grain, because of packing, shielding, and channeling effects, and water vapor that might tend to accumulate in

pockets would not be removed instantly), there is an appreciably smaller rate of oxygen removal (expressed as a percentage of the total oxygen in the charge) for a

water would increase at increasing bed depths, if the rate in the initial thin layer were maintained throughout the entire bed. The horizontal line drawn at 29.8 per cent
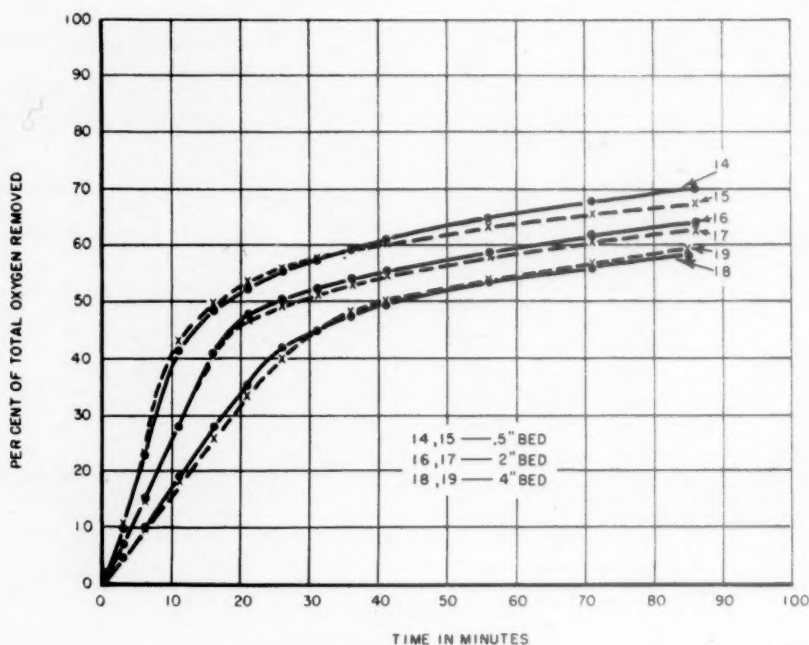
FIG. 17.—EFFECT OF BED DEPTH.
Magnetite, $-28+35$ mesh, 700°C., 0.200 cu. ft. per minute.

bed of particles as compared with a single particle. Also, the rate for a thick bed is lower than for a thin bed.

It can be shown that distance from equilibrium is not adequate to explain the slowing down in the upper portions of the bed. It is well known that "distance from equilibrium" is a controlling factor with respect to chemical reaction rates in general. It does not, however, govern the rates in the present setting, for it is not adequate to account for the observed slowing down in the upper portions of the bed.

The percentage of water in the gas can be ascertained from the amount of water found in the collector tubes, and from the rate of gas flow. Line E of Fig. 18 is a plot of the observed percentage of water against bed depth for the conditions of one of the experiments. The slope of line A, which is drawn tangent to E at a small bed depth, indicates the rate at which percentage of

water represents the equilibrium concentration. While the distance of E from equilibrium is clearly decreasing as the bed grows deeper, the rate of this decrease is not adequate to explain the much faster decrease in the slope of line E.

To pursue the matter in a somewhat different manner, curve B in Fig. 18 shows what the gas composition would be at various bed depths if the distance from equilibrium were the controlling factor. The calculations involved are based on the rate of reaction observed for a $\frac{1}{2}$-in. bed at $4\frac{1}{2}$ min. after the reaction had started, and were made in the following manner:

It was assumed that the only difference, at any instant, in the factors controlling the reaction in the various layers of the bed was the distance from equilibrium $(2[H_2O]_E - \%[H_2O])$; i.e.,

$$\frac{\Delta[H_2O]}{\Delta t} = k(\%[H_2O]_E - \%[H_2O]) \quad [1]$$

From the data on the ½-in. bed depth at 4½ min. $\frac{\Delta[H_2O]}{\Delta t} = 0.21$. Substituting the appropriate values in Eq. 1 (i.e., $\%[H_2O]_E = 29.8$, $\%H_2O = 0$, $\frac{\Delta[H_2O]}{\Delta t} = 0.21$), we obtain $k = 0.007$.

The gas leaving the first ½-in. section of

For the third ½-in. section:

$$\frac{\Delta[H_2O]}{\Delta t} = 0.007(29.8 - 9.1)$$

$$= 0.15 \text{ gram per min. } H_2O$$

$0.38 + 0.15 = 0.53$ grams per min., or 12.6 per cent water in the gas leaving this section.
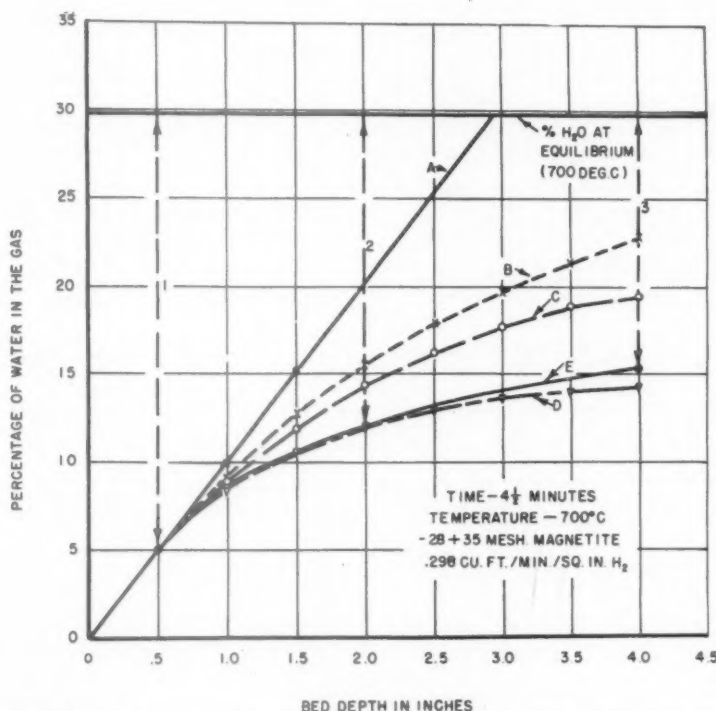
FIG. 18.—COMPARISON OF OBSERVED VALUE OF WATER CONTENT OF GAS STREAM AT DIFFERENT BED DEPTHS, WITH VALUES OBTAINED BY CALCULATION, MAKING CERTAIN ASSUMPTIONS.

A, assuming reaction in each layer is a duplication of that in first layer.

B, assuming distance from equilibrium is controlling factor.

C, assuming diffusion of water is controlling factor and that 75 per cent equilibrium concentration of water is maintained at seat of reaction.

D, same as *C* but assuming that 50 per cent of equilibrium concentration of water is maintained at seat of reaction.

E, observed values.

the deep bed has 0.21 grams per min. of water. At 0.200 cu. ft. per min. gas velocity, this amounts to 5 per cent water.

For the second ½-in. section:

$$\frac{\Delta[H_2O]}{\Delta t} = 0.007(29.8 - 5.0)$$

$$= 0.17 \text{ gram per min. } H_2O$$

$0.21 + 0.17 = 0.38$ grams per min., or 9.1 per cent water in the gas leaving this section.

Similar calculations for the other sections give the following results:

WATER, PER CENT	IN GAS LEAVING
15.8	Fourth ½-in. section
17.9	Fifth ½-in. section
19.7	Sixth ½-in. section
21.4	Seventh ½-in. section
22.8	Eighth ½-in. section

These results are plotted as line *B*, Fig. 18, and show approximately the slackening of rate that could be attributed to the "distance from equilibrium" effect.

But some other, more potent factor must   leads one to believe, just as with the single
be operating. The search for an explanation   particle, that something occurring *within*
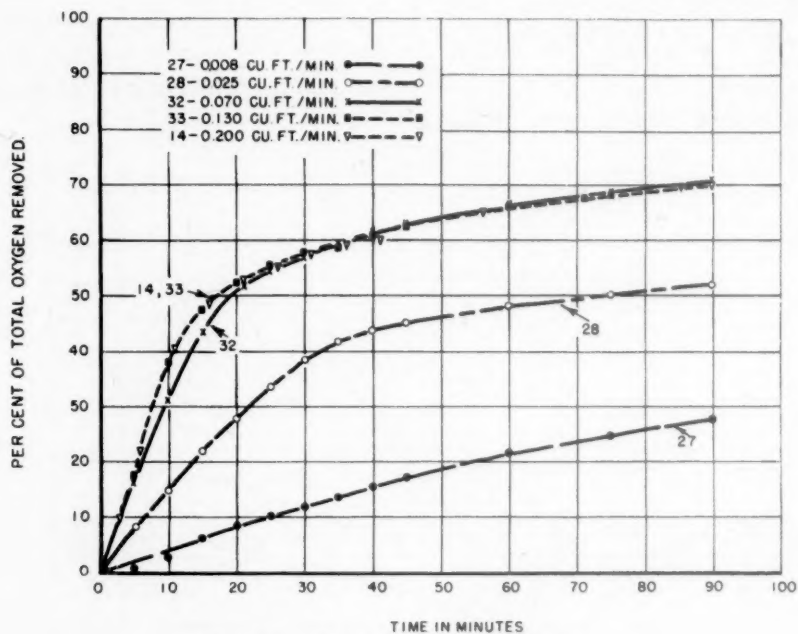
FIG. 19.—EFFECT OF GAS VELOCITY.
15.6 grams magnetite (½-in. bed), −28+35 mesh, 700°C.
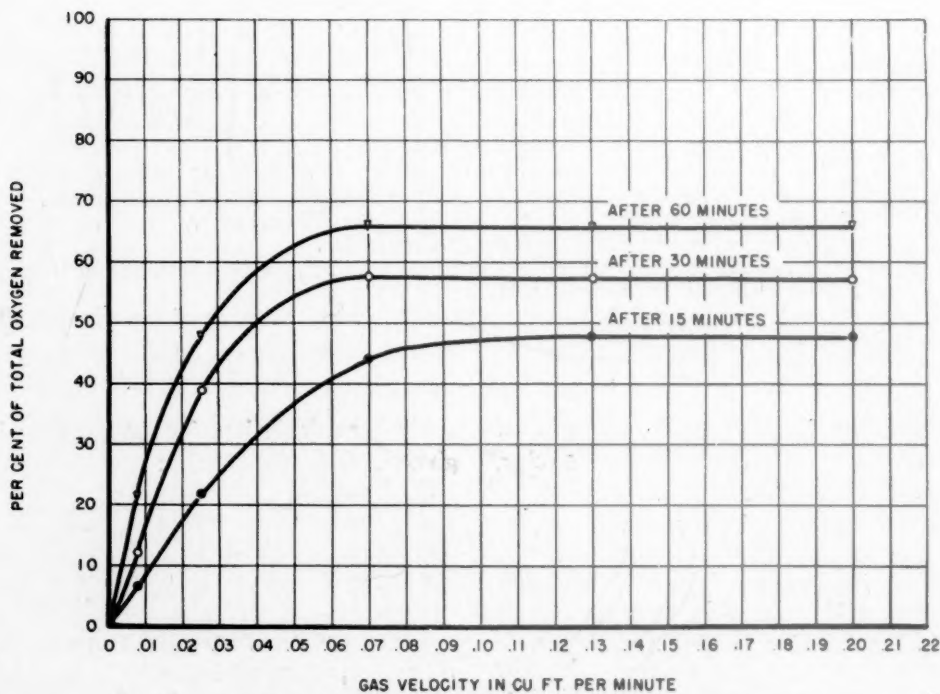
FIG. 20.—EFFECT OF GAS VELOCITY ON DEGREE OF REDUCTION.
15.6 grams magnetite (½-in. bed), −28+35 mesh, 700°C.

the particle itself is the controlling factor. Probably the most plausible suspicion is phase is responsible. In the study of the single particle where diffusion rate was also
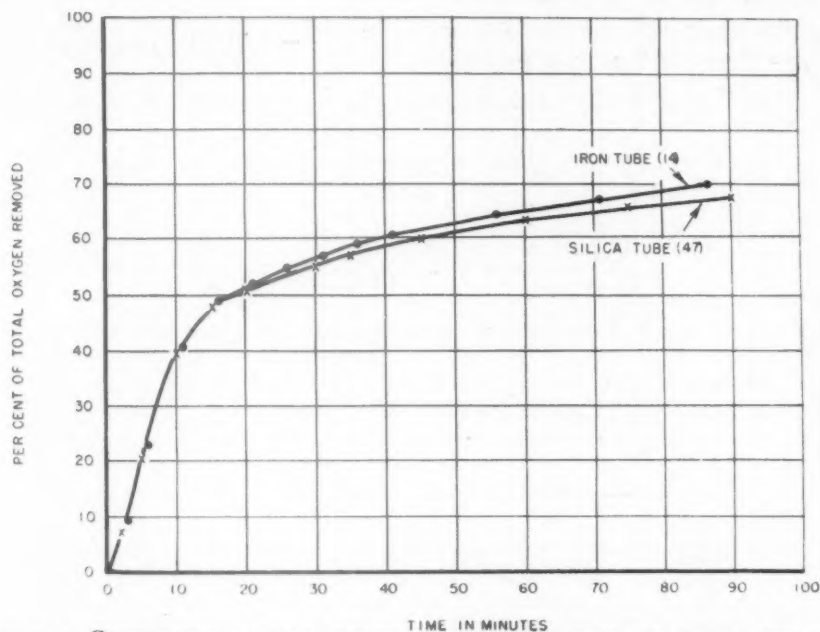
FIG. 21.—COMPARISON OF DATA OBTAINED WITH SILICA TUBE AND WITH IRON TUBE.
15.6 grams magnetite, $-28+35$ mesh, 700°C., 0.298 cu. ft. per min. per sq. inch.
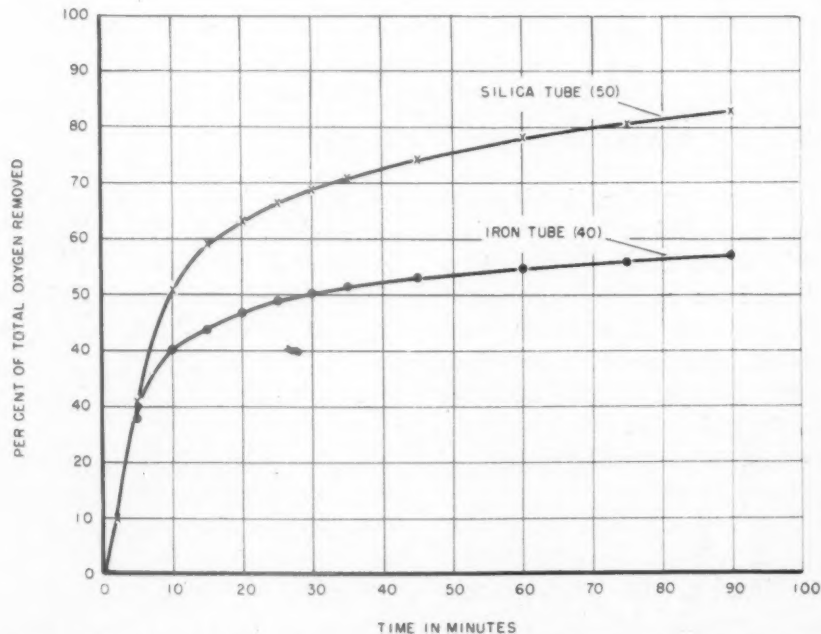
FIG. 22.—COMPARISON OF DATA OBTAINED WITH SILICA TUBE AND WITH IRON TUBE.
15.6 grams magnetite, $-28+35$ mesh, 800°C., 0.298 cu. ft. per min. per sq. inch.

that the rate of diffusion of water vapor out from the seat of reaction to the gas important, the governing factors were the distance and area through which diffusion

was taking place. Since hydrogen travels more rapidly than water vapor, three times faster by Graham's law, it is the rate of diffusion of the water that probably controls the over-all rate of the whole process.

the water gradient in the grain. The equation used is of the form:

$$\frac{\Delta H_2O}{\Delta t} = k([H_2O]_{\text{seat of reaction}} - [H_2O]_{\text{gas}})$$
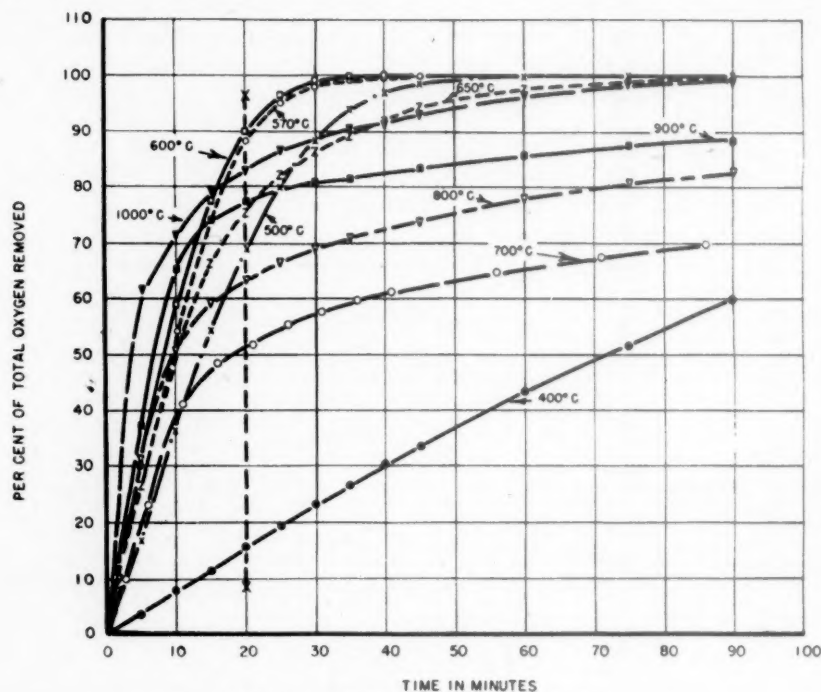
FIG. 23.—EFFECT OF TEMPERATURE.

15.6 grams magnetite (½-in. bed), −28+35 mesh, reduced by hydrogen, 0.298 cu. ft. per min. per sq. in.; 800°, 900° in silica tube, all others in iron tube.

In a bed, however, the situation is somewhat altered. Instead of having the surface of the particles continually bathed in a stream of fresh hydrogen, we find that the concentration of water builds up as the gas passes through the bed. Under these circumstances, it might well be that the factor controlling diffusion rate is the concentration gradient between the seat of reaction and the gas phase.

Neglecting the geometrical factor that makes radial diffusion in a grain different from linear diffusion, and assuming that the depth of metallization is the same throughout the entire bed depth (permissible as an approximation), it is possible to make a rough calculation of the rate of outward diffusion of the water as a function of

This equation has the same form as the one employed in the discussion of "distance from equilibrium" but there is a real point of difference. The concentration of water vapor at the seat of the reaction cannot be the equilibrium concentration. It must be less. Otherwise, the reaction would not proceed.

Let us now arbitrarily assume that 75 per cent of the equilibrium concentration of water is maintained at the seat of reaction. With calculations similar to those carried out for the "equilibrium factor," we obtain:

WATER, PER CENT	IN GAS LEAVING
5.0	First ½-in. section
8.8	Second ½-in. section
11.9	Third ½-in. section
14.3	Fourth ½-in. section
16.2	Fifth ½-in. section
17.6	Sixth ½-in. section
18.8	Seventh ½-in. section
19.5	Eighth ½-in. section

These data are plotted as curve C, Fig. 18. While it is an improvement over curve B, it is still not good enough.

Assuming that 50 per cent of the equilib-

mesh magnetite concentrate were subjected to reduction at 700°C. by hydrogen at a series of gas velocities from 0.008 to 0.200 cu. ft. per min. (0.012 to 0.298 cu. ft.

TEMPERATURE DEG. C
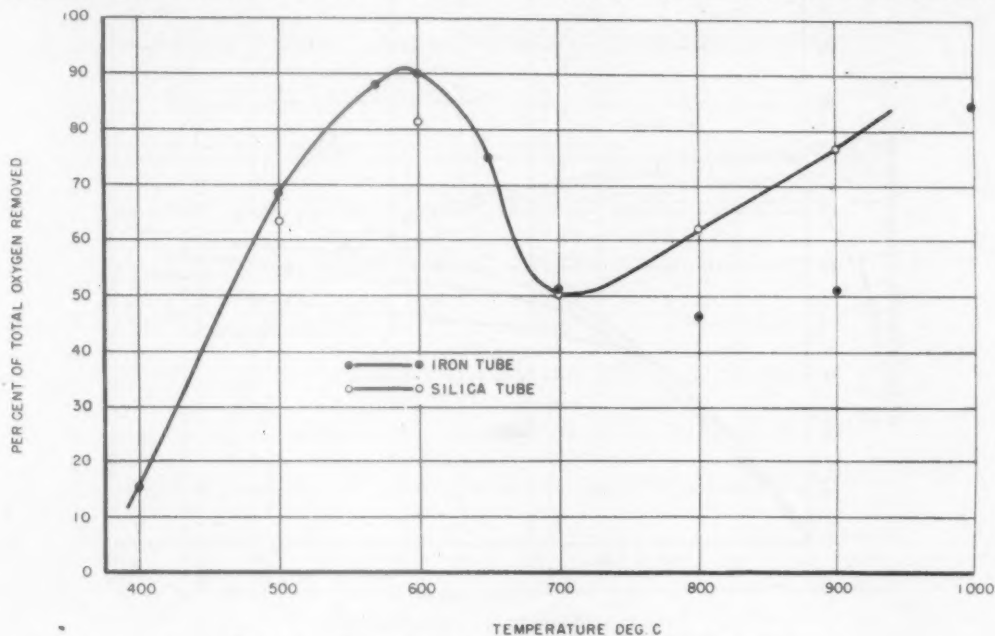
FIG. 24.—DEGREE OF REDUCTION AFTER 20 MINUTES.

Magnetite (½-in. bed), −28+35 mesh, reduced by hydrogen, 0.298 cu. ft. per min. per sq. inch.

rium concentration of water is maintained at the seat of reaction, we obtain:

WATER, PER CENT	IN GAS LEAVING
5.0	First ½-in. section
8.3	Second ½-in. section
10.5	Third ½-in. section
11.9	Fourth ½-in. section
12.9	Fifth ½-in. section
13.6	Sixth ½-in. section
14.0	Seventh ½-in. section
14.3	Eighth ½-in. section

These data are plotted as curve D, Fig. 18, which lies not far from the experimental curve E.

These calculations are rough, but they suggest the possibility of explanation of the effect of bed depth in terms of the rate of egress of water from the grain, against the increasing partial pressure of water vapor at deeper and deeper portions of the bed.

Effect of Gas Velocity

To study the effect of gas velocity on the rate of reduction, ½-in. beds of −28+35-

per min. per sq. in.). Results are shown in Figs. 19 and 20.

At the relatively slow rates of flow, the rate of percentage reduction increases with increasing rates of flow, but eventually a critical rate of flow can be reached beyond which no further increase in reaction rate is noted. This critical rate of flow is, more than likely, a function of the other variables such as bed depth, temperature, and particle size.

Effect of Temperature

To study the effect of temperature on the rate of reduction, ½-in. beds of −28+35-mesh magnetite concentrate were subjected to reduction by hydrogen at a velocity of 0.298 cu. ft. per min. per sq. in. and at the following temperatures: 400°, 500°, 570°, 600°, 650°, 700°, 800°, 900°, and 1000°C.

Because it was found that at higher temperatures the gas leaving the ore bed con-

tained sufficient water to be oxidizing to the upper portion of the iron tube (and the temperature of that upper portion was

ing tubes, runs were made in a fused silica tube at the following temperatures: 500°, 600°, 700°, 800°, and 900°C. For 700°C. and
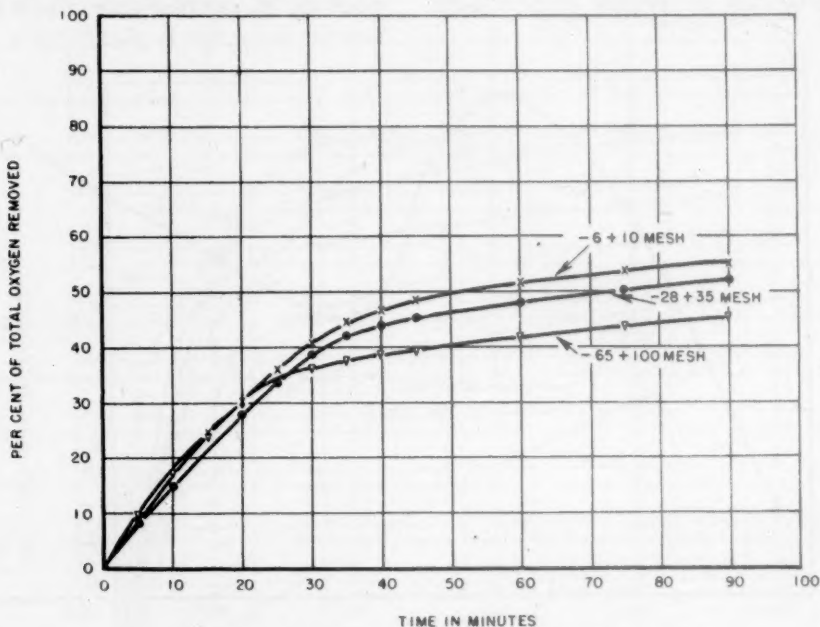
FIG. 25.—EFFECT OF PARTICLE SIZE.
Magnetite (½-in. bed), 700°C., 0.025 cu. ft. per minute.
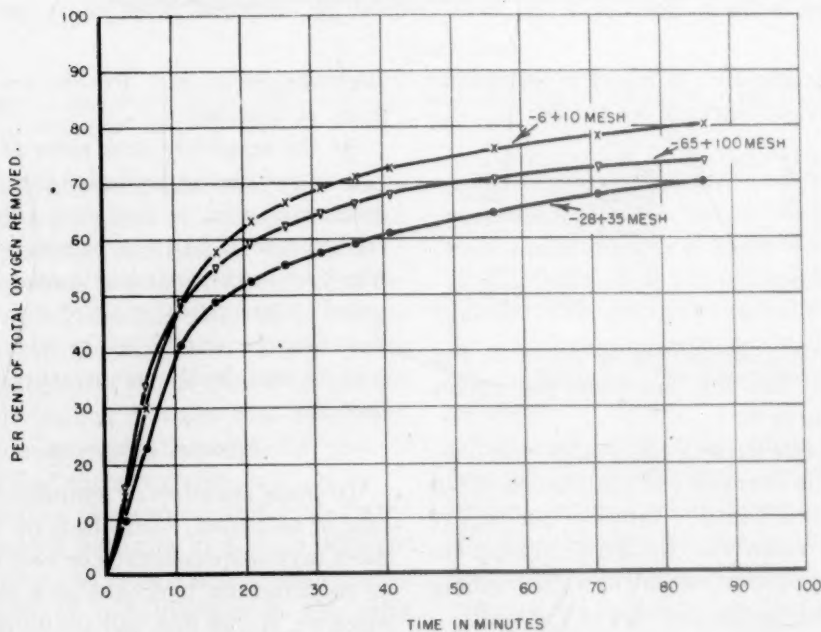
FIG. 26.—EFFECT OF PARTICLE SIZE.
Magnetite (½-in. bed), 700°C., 200 cu. ft. per minute.

sufficiently high to favor oxidation) and therefore less water collected in the weigh-

below, a good check was obtained between results in the iron and silica tubes. but the

results at 800° and 900° were much lower for the iron tube. Figs. 21 and 22 show examples of these check runs.

Results are plotted in Fig. 23. The curves

jected to reduction at 700°C. in a stream of hydrogen at two different gas velocities, 0.037 and 0.200 cu. ft. per min. per sq. in. Further runs were made with the three
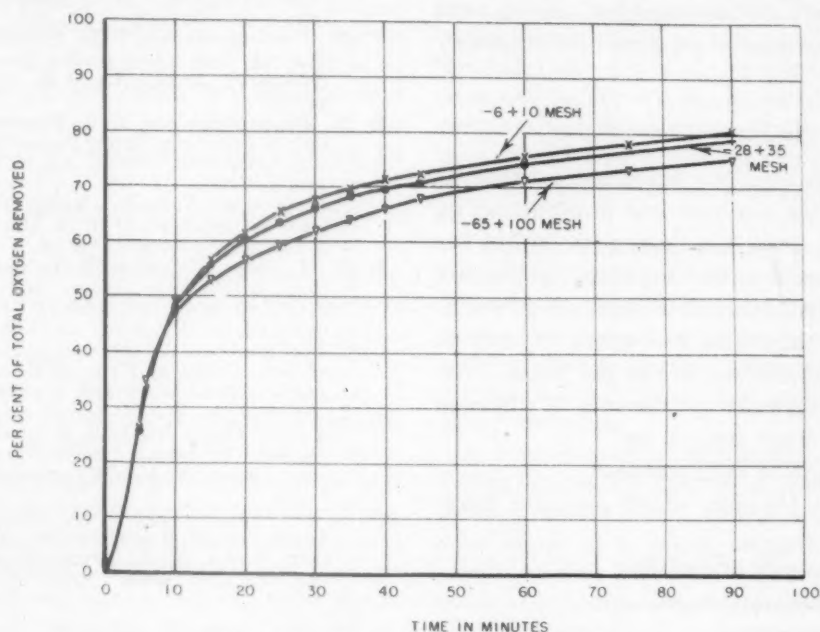
FIG. 27.—EFFECT OF PARTICLE SIZE.
15.6 grams magnetite diluted 3:1 by volume with crushed porcelain; 2-in. bed; 700°C.; 200 cu. ft. per minute.

do not arrange themselves in order with respect to temperature, but seem to be very much mixed up. The percentage of reduction at the 20-min. interval (along line x-x of Fig. 23) is plotted against temperature in Fig. 24.

A possible explanation of the sudden downward inflection of the curve between 600° and 700°C. is the sintering and consolidation of the metallized zone to give a body much more resistant to penetration by hydrogen and especially by water vapor. Then, further rise in temperature results in a restoration of diffusion, but at a greatly reduced rate.

Effect of Particle Size

To study the effect of particle size on the rate of reduction, ½-in. beds of the following sizes: −6+10, −28+35, −65+100-mesh magnetite concentrate were sub-

sizes mentioned above, but with the charges diluted 3 to 1 by volume with crushed porcelain of the same size. Gas velocity = 0.200 cu. ft. per min. The results of this study are presented in Figs. 25, 26 and 27.

The effect of particle size with a single particle has already been discussed and a plausible explanation presented. However, no such explanation can be presented for the effect of particle size in the bed. The results are so complex that little success has been achieved in an attempt to interpret them. This is not surprising, for the experimental setting is complex. Although within the three ranges the sizes were fairly uniform, there was probably enough variation in size and shape of the grains to give highly unpredictable types of contacting, packing, shielding, eclipsing, pocketing, and channeling. Further, it is not unlikely that

the different sized grains possessed slightly different porosities and surface textures, simply because they were crushed to different degrees.

Because of this complex setting, the results are merely presented for their face value.

GENERAL CONCLUSIONS

From this study it would appear that, at least for the ore used and in reduction by hydrogen, something going on within the particle is the controlling factor in the rate of reduction. More than likely, this "something" is the diffusion of water vapor from the seat of reaction to the gas phase. Controlling influences on the rate of diffusion of water vapor seem to be:

1. Length of diffusion path.

2. Area through which diffusion takes place.

3. Geometry of particle.

4. Concentration gradient.

5. Temperature.

6. Nature of medium through which diffusion takes place (and variables affecting this nature, and thus indirectly the over-all rate).

ACKNOWLEDGMENTS

The authors wish to express their appreciation to the Battelle Memorial Institute for providing the fellowship that made this study possible. Special thanks are due Prof. D. J. Demorest and Dr. Edward Mack, Jr., for their counsel and encouragement. Thanks are expressed to the Alan Wood Steel Co., Dover, N. J., which furnished the magnetic concentrate used in the experiments.

REFERENCES

1. W. H. Wetherill and C. C. Furnas: Rate of Reduction of Iron Ores with Carbon Monoxide. Effect of Particle Size, Gas Velocity, and Gas Composition. *Ind. and Eng. Chem.* (1934) **26**, 983–992.
2. I. Langmuir: The Constitution and Fundamental Properties of Solids and Liquids, Part I. Solids. *Jnl.* Amer. Chem. Soc. (1916) **38**, 2221–2295.
3. F. Weinert: Die Reduktion von Eisenerzon mit Wasserstoff und Kohlen oxide. *Archiv Eisenhüttenwesen* (1933) **7**, 275.
4. B. Stahlhane and T. Malmberg: Untersuchen uber den Verlauf der Eizererz-Reduktion (reviews of the original paper). *Stahl und Eisen* (1929) **49**, 1836; (1930) **50**, 967; (1931) **51**, 216.
5. M. Tenenbaum and T. L. Joseph: Reduction of Iron Ores under Pressure by Hydrogen. *Trans.* A.I.M.E. (1939) **135**, 59–71.
6. M. Tenenbaum and T. L. Joseph: Reduction of Iron Ores under Pressure by Carbon Monoxide. *Trans.* A.I.M.E. (1940) **140**, 106–123.
7. T. L. Joseph: Porosity, Reducibility, and Size Preparation of Iron Ores. *Trans.* A.I.M.E. (1936) **120**, 72–98.
8. H. H. Meyer: Speed of Reduction of Iron Ores in Flowing Gases. *Mitt.* K.W.I. Eisenforschung Dusseldorf (1928) **10**, 107–116.
9. K. Hoffman: On the Reduction Mechanism of Iron Oxide in Flowing Gases. *Ztsch. angew. Chem.* (1925) **38**, 715–721.
10. T. L. Joseph, W. F. SCOTT and M. H. Kaline: Oxide Analysis in Iron Ore Reduction Problems. *Blast Furnace and Steel Plant.* (1940) **28**, 975–978, 1073–1077.
11. C. C. Williams and R. A. Ragatz: Low Temperature Reduction of Magnetite Ore. Effect of Catalytic Compounds. *Ind. and Eng. Chem.* (1938) **28**, 130–133.

DISCUSSION

(*A. B. Kinzel presiding*)

C. Q. PAYNE,* N. Y.—After reading the paper by M. C. Udy and C. H. Lorig, I think that the authors are entitled to congratulations, not only for their skill in devising a new method of attack but also for their frankness in presenting results that are not conclusive or convincing. This seems to invite cooperation and to make the final solution of the problems quite hopeful. While they cite ample references showing that the equilibrium relations in the reduction of magnetite with CO as well as with hydrogen are well established, they wisely limit themselves to that area of uncertainty which they define as the "rate of reaction," in which they include temperature, gas velocity, particle size, porosity, gas composition and presence of impurities.

Roughly, the tests show that only about 70 per cent of the oxygen is removed from the magnetite even when finely crushed material ($-28+35$ mesh) is exposed, in small quantities, to hydrogen preheated to 700°C. for periods varying from 3 min. to over an hour. The

---

* Consulting Engineer.

authors gather from these unexpected results that "something" is occurring within the particles themselves, which hampers the reducing action. They assume from this that the rate of the diffusion of the water vapor from the seat of reaction to the gas phase is delayed by the gradual metallization of the ore particles. This may be true but does not seem to go to the root of the problem. It is also true that since sponge iron is actively formed at the temperature at which alpha iron changes its properties—viz., 760°C., which is an endothermic reaction—the temperature of reduction should have been increased from 700° to about 850° to 900°C. This would greatly speed up the reduction, especially if the charge were actively vibrated to assist the release of the gases and to avoid sintering.

Moreover, nearly all the magnetite ores of New Jersey contain about 0.25 to 0.5 per cent titanium. This impurity is an added reason for raising the temperature of reduction as suggested, since titanium renders these ores somewhat refractory. By a curious coincidence, I was able to test the concentration of a sample of a New Jersey magnetite ore from the Mount Hope mine, with Mr. Leonard Peckitt's cooperation about a year or two ago. This is a non-bessemer ore. At present, by coarse crushing and dry magnetic separation, it is raised to about 65 per cent metallic iron, and is then utilized as a foundry ore. My object was to see whether it could be so highly enriched that it could be converted into sponge iron and sold without briquetting on the basis of scrap-iron

prices. I found that this ore contained a small amount of titanium. It is also quite finely mineralized, and in order to enrich it as much as possible I crushed a sample quite fine (−80 mesh) and with a special magnetic separator, which could exert a considerable centrifugal force upon the ore while passing through the field, I was able to bessemerize the concentrate, but the iron in it was raised only to 70.82 per cent. A partial analysis by Ledoux and Co. gave the following result: metallic iron, 70.82 per cent; silica, 0.48; sulphur, 0.07; phosphorus, 0.03.

I did not carry my investigation of utilizing this ore any further, as I did not have facilities at hand for converting the concentrate into sponge iron. I am, however, strongly inclined to believe that the further improvement of this process offers a hopeful future for all our New Jersey iron mines.

Another ground for encouragement which I find in this paper is that the authors were able to carry out their tests on a laboratory scale even down to a single magnetite particle (−6+10 mesh). This is a great advantage, and will enable them to test other ores without great expense. I would suggest that their next trial test be made with a hematite iron ore, both with hydrogen and with CO as the reducing agent. Such ores contain little or no titanium, and they are also somewhat less refractory than the magnetites. Hematites from the Lake Superior district comprised about 80 per cent of all the iron ores mined in this country in 1940.

Problems of Total Operation in Steelmaking

BY WILLIAM C. MARSHALL* AND FRANK G. NORRIS,* MEMBER A.I.M.E.

(New York Meeting, February 1943)

THE term "total operation" is meant to include problems that cannot be answered from the standpoint of either the blast furnace or the open hearth separately but must be studied by considering the interrelations of these two processes. There are other ways of expressing this idea, such as reference to the blast furnace and the open hearth as an integrated process or by emphasizing the interrelation and interaction of the two processes.

Much progress has been made in metallurgy and other fields by breaking complicated processes and reactions into simpler parts and studying each of these intensively. This intensive study frequently is done under the controlled conditions of the laboratory experiment. The entire process is understood better by this specialized study of each of its parts. This procedure is so satisfactory that an understanding of unit operations is a fundamental requirement of chemical engineering.

Much discussion of the open-hearth process is in terms of one heat or one furnace. By this is meant that the conclusions apply to one furnace, wherever it may be. Furnaces seldom occur singly; they are located in groups and these groups are located in steel plants having characteristic blast-furnace equipment. Problems that are affected by the number of furnaces operating, by the number of blast furnaces in the plant and by the fact that the open-

hearth shop is dependent on the blast-furnace capacity rather than on its own needs for the amount of iron available are among those which, in contrast to "unit operations," we have chosen to call "total operations."

Many of these problems, such as charging delays and the general mechanical problem of material handling, are so familiar that merely to define "total operations" brings them to mind. These problems are of such importance that already they have received careful thought and study and probably will merit further study.

As will be shown later, these mechanical problems are so intimately related to metallurgical problems of total operations that the effect of certain changes cannot be ascribed with certainty to either a mechanical or a metallurgical cause entirely.

Although the problems coming under the general term of "railroading" are included in the problems of total operations, two others are selected for the discussion of this paper. One of these is strictly a problem of composition; the other is strictly a problem of tonnage production.

The problem of phosphorus is present whenever basic open-hearth slag is used in the blast-furnace burden. This practice has not secured universal acceptance chiefly because of difference in preference for high-manganese or low-manganese pig iron. If high-manganese (2.00 per cent) iron is to be made, open-hearth slag as a source of manganese is usually cheaper than man-

Manuscript received at the office of the Institute Dec. 1, 1942. Issued in METALS TECHNOLOGY, April 1943.

* Wheeling Steel Corporation, Steubenville, Ohio.

ganiferous ores. Ordinarily the problem could be decided on the comparative cost of various sources of manganese within the limitations of the phosphorus tolerance specification. At present, however, the question of manganese conservation must also be considered. We must decide not how much manganese we can recover from open-hearth slag but rather how little manganese we must throw on the dump as open-hearth slag.

The slag analysis and percentage of open-hearth slag in the burden furnish a description of the phosphorus problem, which is incomplete because it considers one blast furnace as a unit. The viewpoint of the total operation considers all blast furnaces and all the open-hearth furnaces receiving iron from them as one unit. A phosphorus balance can be worked out for this large unit in much the same way that a burden sheet is made for one furnace. It is recognized in the operation of one furnace that a change does not have an immediate effect but takes a little time to come through. This same time effect is found in the phosphorus cycle of the plant with the advantage of additional information because samples can be taken at various stages during the change.

Over a sufficiently long period or during any short period when no change is going through the system, the weight of phosphorus entering the system is equal to the weight of phosphorus leaving the system.

The sources of phosphorus into the system are:

1. Blast-furnace burden, including ore and coke.

2. Ferrophosphorus additions to open-hearth ladle.

3. Phosphorus content of purchased scrap or other open-hearth materials.

4. Cold iron charged to open hearth.

Phosphorus leaves the system in the following forms:

1. Open-hearth slag going to the dump.

2. Phosphorus content of iron pigged.

3. Phosphorus content of finished steel.

Most of these items remain essentially constant and are enumerated merely so that the effect of occasional changes will not be overlooked.

If no high-phosphorus steel is made, the phosphorus content of purchased scrap and that of the finished steel are compensating and may be neglected. Let:

P = percentage of phosphorus in the iron.

p = the weight of new phosphorus in the burden; i.e., from ore and coke.

i = the iron production, lb.

s = the fraction of the open-hearth slag production that is used in the blast-furnace burden.

With no open-hearth slag in the burden, the weight of phosphorus introduced equals the weight in the iron, or $p = Pi$. This weight of phosphorus ultimately leaves the cycle in the open-hearth slag.

With open-hearth slag on the burden, the pounds of phosphorus in the iron is $p\left(\dfrac{1}{1-s}\right)$, which is the limiting value of the series $p(1 + s + s^2 + s^3 + s^4 + s^5 \ldots)$. In this case the analysis of both the iron and open-hearth slag increases until the weight of phosphorus leaving the cycle is equal to the new phosphorus introduced.

TABLE 1.—*Effect of Open-hearth Slag in Blast-furnace Burden*

New phosphorus per 24 hours, P = 4000 lb.

Iron production per 24 hours, i = 1600 tons = 3,200,000 lb.

Total materials consumed by blast furnace, 6,000,000 lb.

Total slag produced by open hearth, 1,000,000 lb.

s Fraction O.H. Slag Used by B.F.	P in Iron, Per Cent	P in O.H. Slag, Per Cent	O.H. Slag in B.F. Burden, Per Cent
0	0.125	0.400	0
0.25	0.167	0.533	4.17
0.50	0.250	0.800	8.33
0.75	0.500	1.600	12.50

An example of these relations is given in Table 1. The controlling consideration is proportion of open-hearth slag returned to the blast furnace; what part of the blast-furnace burden is made up by this weight of open-hearth slag is incidental.

The effect of changing the slag volume, as by cutting or raising the lime charge in the open hearth, is disclosed by this relation. It is not proper in this case to consider that blast-furnace conditions are constant simply because the pounds of open-hearth slag on the burden is not changed.

Open-hearth Production

At various times the desired goal of open-hearth operation changes, dependent on the influence of factors that are well known. Now the object is to produce the greatest number of tons of ingots with the pig iron, scrap and equipment that is available. The information that more tonnage could be made with more pig iron or with better scrap is of only academic interest. The problem is to make the most effective use of the materials available. As an approach to this problem, a study was made to evaluate the effect of some of the factors that determine open-hearth production. Early in this study it was seen that the problem to determine what factors have most influence on open-hearth production can be stated correctly only in terms of the total operation of both the blast-furnace and open-hearth shop, rather than in terms of the effect of various factors on the time of one heat or on the production of one open-hearth furnace.

The method chosen to show the inter-relation of several factors is that of multiple regression. For simplicity, the open-hearth production is stated in number of heats per day, which is selected as the dependent variable. The production in tons was converted to number of heats, using an average heat size rather than the number of heats with no regard to variation in heat weight.

It is well recognized that accidental influences may have an effect on the production of a single day. For example, a few minutes difference in tapping time may determine to which day the production of one entire heat is credited. Also, there is a certain lag in the effect of some influences on open-hearth production. For example, part of today's blast-furnace production affects tomorrow's open-hearth production, the exact interval being dependent, at least in part, on such accidental causes as bunched heats. A convenient and fairly satisfactory way of eliminating the effect of these and other accidental influences is to study the relation among averages of a 5-day interval rather than daily figures.

The factors studied and values of the coefficients in the regression equation are listed in Table 2. The value of the beta coefficients, which are simply the regression coefficients when each variable is expressed in standard deviation units, is also shown.

The beta coefficients offer a means of estimating the relative importance of the influence of each independent variable. This is also shown in Table 2.

These four factors naturally fall into two groups—two of the greatest and about equal importance, and the other two of secondary, but again about equal importance. It is not considered especially original or startling to disclose that the more furnaces in operation, the more heats will be tapped. This factor is included because it must be taken into account in order to study the effect of other, perhaps less obvious, variables.

The direct effect of blast-furnace operation on open-hearth production is perhaps not always realized. This regression equation shows that aside from putting another furnace into operation, the most effective way to increase open-hearth production is to increase blast-furnace production.

It may seem paradoxical that the percentage of hot metal has a negative coefficient. This, of course, is not true with respect to an individual heat because in this

treatment of the problem it is assumed (often without realizing it) that there is an unlimited supply of hot metal available. The problem from the standpoint of total operation is not what percentage of hot metal to use in one furnace to make the best heat time but rather how best to proportion the charge, including charge ore, so as to make the best production. In other words, as large an amount as possible of metal should be as small a percentage as possible of the total daily charge. This is simply the

Because of the almost uncanny potency of the regression method, there frequently arises the temptation to attempt to glean from the equation more information than is there. The equation shows the quantitative effect of the factors studied for the group studied. The answers to the questions, Why? or How?, or any theorizing as to mechanism must come from other sources. The best way to compare two groups of data is to study each group by the same method. If similar studies have

TABLE 2.—*Regression of Various Factors on the Average Number of Heats per Day for a Five-day Period*

$N = 36$. $R = 0.9118$. $\sigma = 0.838$

Independent Variable	Standard Deviation	Regression Coefficient	Beta Coefficient	Relative Importance	Change in Variable to Result in One More Heat per Day	Variation in Heats per Day Due to Direct Effect of Variable
Number of furnaces........	0.405	0.98	0.473	0.340	1.02	22.4
Tons of metal to O.H......	57.07	0.00665	0.453	0.325	150.4	20.5
Metal in O.H. charge, per cent...	2.23	−0.088	0.235	0.169	−11.4	5.5
Weight of boxes of scrap, lb.....	78.17	0.0025	0.231	0.166	400	5.3

relation that a greater weight is charged during 5-day periods when more heats are tapped.

The fourth independent variable is a means of expressing the beneficial influence of heavy scrap.

A word of caution is in order regarding the interpretation and application of the results. Extrapolation of a regression equation beyond the limits for which it is derived can, and probably will, yield misleading results. Another possible source of inaccuracy is that the method of treatment assumes that the relations are linear. By this is meant that an increase of one unit of any variable has the same effect whether it be at the low end of the range studied, near the middle, or at the high end. There is some reason to believe that this may not be true outside the range of some of the variables reported in this study, but within the scope of the data, significant departures from linearity have not been disclosed.

disclosed more important factors influencing production of the open-hearth shop (as distinguished from heat time or production of a single furnace) at other plants, the results have not come to our knowledge.

Extension of the data to another period of time is fairly satisfactory provided the values are restricted to those for which the relation is derived. Regardless of the limitations of this particular equation, the proposed method of considering the blast-furnace and open-hearth operation as a whole is believed to be sufficiently general that it can be applied to any plant or to any time period.

A few typical values of the regression illustrating the effect of changes among the variables are computed for illustration as shown in Table 3.

The correlation between pairs of variables is shown in Table 4.

The correlation of 0.91 is still low enough so that an attempt was made to improve

it by including the effect of other variables. A complete account of this study will not is masked by the practice of putting a slow furnace on oil to finish out a run.

TABLE 3.—*Effect of Various Factors on Open-hearth Production*

X_1 No. of heats $= +0.98$ X_2 (Number of furnaces operating)
$+0.0066X_3$ (Tons hot metal delivered to open hearth)
-0.088 X_4 (Percentage hot metal in open-hearth charge)
$+0.0025X_5$ (Average weight per box scrap)
-0.667

Number of Furnaces	Average Weight per Box, Lb.	1400 Tons Iron		1500 Tons Iron		1600 Tons Iron		1700 Tons Iron	
		Per Cent Hot Metal		Per Cent Hot Metal		Per Cent Hot Metal		Per Cent Hot Metal	
		50	45	50	45	50	45	50	45
HEATS PER DAY									
9	1,000	15.50	15.94	16.16	16.60	16.83	17.27	17.49	17.93
	1,300	16.24	16.68	16.91	17.34	17.58	18.01	18.24	18.67
10	1,000	16.48	16.92	17.14	17.58	17.81	18.25	18.47	18.91
	1,300	17.22	17.66	17.88	18.32	18.55	18.99	19.21	19.65
11	1,000	17.46	17.90	18.12	18.56	18.79	19.23	19.45	19.89
	1,300	18.20	18.64	18.86	19.30	19.53	19.97	20.19	20.63
TONS PER DAY									
9	1,000	2,403	2,471	2,505	2,573	2,609	2,677	2,711	2,779
	1,300	2,517	2,585	2,621	2,688	2,725	2,792	2,827	2,894
10	1,000	2,554	2,623	2,657	2,725	2,761	2,829	2,863	2,931
	1,300	2,669	2,737	2,771	2,840	2,875	2,943	2,978	3,046
11	1,000	2,706	2,775	2,809	2,877	2,912	2,981	3,015	3,083
	1,300	2,821	2,889	2,923	2,992	3,027	3,095	3,129	3,198

be given, but one result is so striking that it may be of interest.

The effect of fuel was included by break-

The correlation and the value of the coefficients are virtually unchanged, which shows that the net effect of type of fuel is

TABLE 4.—*Description of Variables and Total Correlation between Pairs*

Variables	Mean	Standard Deviation	Highest Value	Lowest Value	X_3	X_4	X_5	X_1
X_2 furnaces................	10.3	0.405	11.0	9.2	+0.294	−0.524	−0.066	+0.714
X_3 tons hot metal...........	1,537.6	57.07	1,694	1,413		+0.042	+0.298	+0.651
X_4 percentage hot metal......	46.58	2.23	51.23	41.09			−0.107	−0.489
X_5 average weight box of scrap, lb....................	1,179.25	78.17	1,350	959				+0.360
X_1 number heats in 24 hours..	18.4	0.838	20.3	16.1				

ing up into two parts the total number of furnaces operating; viz., the number of furnaces on oil and the number of furnaces on producer gas. The beneficial effect of oil relatively slight compared with the effect of the other factors considered (Table 5).

The question may be asked, What is the best use to make of No. 1 scrap? Should a

limited amount be used in the blast furnace even at the sacrifice of robbing the open hearth of this good grade of scrap? The regression equation offers a definite answer to such questions.

Assume that current practice is 2600 boxes of scrap at an average of 1200 lb. per box, or a daily consumption by the open hearth of 3,120,000 lb. of scrap and take an extreme case of using 200,000 lb. of heavy scrap, averaging 3,000 lb. per box, in the blast furnace. Assume that the only scrap

Study of Table 3 reveals that for a given weight and percentage of hot metal the best 9-furnace operation can never equal the production of the poorest 10-furnace operation. In taking off furnaces, the percentage of hot metal would probably be increased, but would further decrease the open-hearth output.

The indication of the mathematical expression may be rationalized as follows:

Suppose 10 furnaces (or any given number) are using all the iron available. It is

TABLE 5.—*Effect on the Regression Equation of Considering the Type of Fuel*
X_1 = Average number of heats per day made by the open hearth

Constant	Coefficients				R
	Number of Furnaces Operating	Hot Metal Received by O.H., Tons	Hot Metal in O.H. Charge, Per Cent	Scrap Wt. per Box., Lb.	
−0.67	+0.978	+0.0066	−0.088	+0.0025	0.9118
	Furnaces on				
	Oil Gas				
−0.67	+0.934 +0.985	+0.0066	−0.091	+0.0025	0.9118

available to replace this good scrap is 200,000 lb. of light scrap weighing 500 lb. per box. After this change, the new average is 1064 lb. per box, or a decrease of 136 lb. per box.

A companion study of the effect of scrap in the blast-furnace burden shows that the increase in hot metal resulting from this scrap addition is 80 tons per day.

80 × 0.0066 = 0.53 heats per day due to increase in pig iron.
136 × 0.0025 = 0.34 decrease due to light scrap.

———

0.19 heats per day net increase.

The effect of scrapping the blast furnace without robbing the open hearth is obvious. Sometimes the statement is considered that with so many charging delays it would be just as well to take off one furnace so that those remaining in operation could make better time.

decided to put on one more furnace without damaging the 10-furnace operation. This eleventh furnace would get only very poor scrap and would not be allowed to interfere with the rest of the shop by any delays. Once in a while—say every two or three days—this extra furnace would tap a heat which, of course, would benefit the total shop production. The lower average heat time, etc., should not obscure the fact that more steel is made by operating more furnaces.

In times when efficiency of operation rather than total production is the sole objective, regression methods are just as effective, but the action dictated by the results will be very different.

SUMMARY

Attention is drawn to a class of problems that cannot be solved either in the blast-furnace or open-hearth department alone, but must be considered as joint problems

of both departments. Two problems of this type are discussed. One is the use of open-hearth slag in the blast-furnace burden. The other is a study by multiple linear regression of some factors affecting the production of the open-hearth shop.

1. The two typical problems selected illustrate the thesis that the blast-furnace department and the open-hearth department are coordinate members of a production team.

2. The problem of the phosphorus cycle within a plant using open-hearth slag in the blast furnace is stated briefly to show the total effect of both operations on the iron analysis. Phosphorus build-up in the iron is not continuous, but levels off at a constant value, so that the weight of phosphorus leaving the cycle is equal to the weight of phosphorus entering the cycle.

3. For the period studied the average daily production of steel is shown to be dependent on the number of open-hearth furnaces in operation, the weight of hot metal delivered to the open hearth, the percentage of hot metal in the open-hearth charge, and the quality of the scrap as expressed by the average weight per box. The relative importance of each of these factors is expressed by a regression equation and is discussed briefly.

ACKNOWLEDGMENTS

APPENDIX

DESCRIPTION OF COMPUTATIONS

The method of computation is largely a combination of the methods described by Snedecor[1] and by Ezekiel.[2] Any one of a number of procedures is correct, and the one used is primarily a matter of personal preference. The first step in studying a group of data by regression methods is to get the total of the squares and cross products of the original observations.

TABLE 6.—*Data for Regression Equation*

X_1	X_2	X_3	X_4	X_5
20.3	10.4	1,694	46.98	1,347
19.7	11.0	1,575	44.03	1,220
18.7	10.6	1,591	46.70	1,173
19.2	10.4	1,620	47.33	1,220
18.5	10.2	1,586	46.38	1,139
19.5	10.5	1,584	46.81	1,195
19.1	10.4	1,559	46.44	1,212
18.1	10.0	1,553	47.01	1,139
18.2	10.2	1,598	48.37	1,258
18.8	10.2	1,600	46.95	1,176
18.9	10.4	1,604	49.16	1,155
20.3	11.0	1,605	43.33	1,207
18.3	10.2	1,563	42.04	1,256
18.3	10.0	1,550	46.79	1,155
19.4	10.6	1,541	45.71	1,220
18.6	10.6	1,485	41.09	1,118
19.1	10.8	1,513	41.23	1,286
18.7	10.2	1,547	46.12	1,350
17.7	10.0	1,512	48.27	1,174
17.6	9.4	1,541	49.44	1,173
17.7	10.4	1,541	46.51	1,065
18.6	10.8	1,530	47.94	1,093
18.2	10.0	1,481	44.65	1,089
18.0	10.8	1,496	47.47	959
17.8	10.8	1,535	47.56	1,115
18.3	10.4	1,563	48.65	1,113
18.1	10.2	1,519	46.58	1,150
18.0	10.0	1,539	48.74	1,171
18.1	10.0	1,487	47.90	1,237
18.8	10.8	1,497	45.76	1,125
16.8	9.6	1,462	48.61	1,107
18.6	10.4	1,468	46.33	1,306
16.1	9.2	1,444	51.23	1,222
17.5	10.0	1,507	49.33	1,229
18.1	10.4	1,413	45.40	1,192
17.9	10.0	1,442	44.20	1,107
Sum..663.6	370.9	55,345	1,677.04	42,453
$\bar{X}$.....18.433	10.303	1,537.361	46.584	1,179.25

Table 7 follows the pattern of Snedecor's Table 13.13. The sum of the items and their average are recorded from Table 6. The figures on the diagonal of the table are based on squares of each variable and will be referred to as squared items. The figures in the body of the table are based on products between pairs of variables. The sums of squares (or products) are entered in line 1.

Line 2 is the correction term (or, by Ezekiel's nomenclature, the correction item). It is the product of two sums divided by N the number of items in the correla-

tion. For example, in line X_2 No. 2, col. X_3, 570207.2 is $\dfrac{370.9 \times 55345}{36}$. This, of course, is the same as 370.9×1537.361 or as 55345×10.303, provided no figures are dropped to round the average.

Line 2 of the squared items is simply a special case:

3821.30 is 370.9×10.303 or $(370.9)^2/36$.

In the body of the table, line 5 is the correlation coefficient and is found by dividing line 3 by line 4.

On the diagonal of the table, the standard deviation of each variable is entered in line 5. In this case it is found by multiplying line 4 by the reciprocal of the square root of N. If r is to be calculated, this is the efficient way in which to obtain the stand-

TABLE 7.—*Computation of Correlation between Pairs of Variables*

		X_2	X_3	X_4	X_5	X_1
Sum.........		370.9	55,345	1,677.04	42,453	663.6
Average.......		10.303	1,537.361	46.584	1,179.25	18.433
X_2	1	3,827.21	570,451.8	17,261.149	437,309.1	6,845.65
	2	3,821.30	570,207.2	17,278.170	437,383.8	6,836.92
	3	5.91	244.6	−17.021	−74.7	8.73
	4	2.431	832.5	32.478	1,140.1	12.22
	5	0.405	0.294	−0.524	−0.066	0.714
X_3	1		85,202,505	2,578,406.74	65,313,424	1,021,313.2
	2		85,085,251	2,578,216.08	65,265,591	1,020,192.8
	3		117,254	190.66	47,833	1,120.4
	4		342.45	4,575.13	160,609	1,721.2
	5		57.07	0.042	0.298	0.651
X_4	1			78,302.6176	1,976,975.88	30,880.58
	2			78,123.9767	1,977,649.42	30,913.44
	3			178.6409	−673.54	−32.86
	4			13.36	6,265.84	67.147
	5			2.23	−0.107	−0.489
X_5	1				50,282,677	783,399.7
	2				50,062,700	782,550.3
	3				219,977	849.4
	4				469	2,357.2
	5				78.17	0.360
X_1	1					12,257.62
	2					12,232.36
	3					25.26
	4					5.026
	5					0.838

Line 3 is line 1 minus line 2. It is always positive for the squared items, but may be positive or negative for the products. It is called the corrected sum of squares (or products). For the squared items, line 3 is the sum of the squares of the deviations of the items from their mean and is numerically identical with the result of subtracting each item from the mean, squaring the differences and taking the total of these squared deviations.

For the squared items, line 4 is the square root of line 3. In the body of the table, line 4 is the product of two square roots; e.g., in line 4 of row 3, col. 5, 160609 is 342.45×469.

ard deviation. If desired, the standard deviation can be secured directly from line 3 by dividing line 3 by N and extracting the square root. This method is used if a value of the variance is desired. Either of these methods is preferred to the equally correct method of finding the variance by subtracting the square of the average from the average square.

A series of simultaneous linear equations is now set up from the data in line 3, following the pattern in Table 8 (Ezekiel's formulas 40 and 41). These equations can be solved by any one of several methods. If there is not much of this work to be done, the usual algebraic method of

TABLE 8.—*Simultaneous Equations Leading to the Regression Coefficients*

	X_2	X_3	X_4	X_5	X_1	ΣX
X_2	X_2^2	X_2X_3	X_2X_4	X_2X_5	X_2X_1	$X_2\Sigma$
X_3	X_2X_3	X_3^2	X_3X_4	X_3X_5	X_3X_1	$X_3\Sigma$
X_4	X_2X_4	X_3X_4	X_4^2	X_4X_5	X_4X_1	$X_4\Sigma$
X_5	X_2X_5	X_3X_5	X_4X_5	X_5^2	X_5X_1	$X_5\Sigma$
	5.91	244.6	-17.021	-74.7	8.73	167.519
	244.6	117,254	190.66	47,833	1,120.40	166,642.66
	-17.021	190.66	178.6409	-673.54	-32.86	-354.1201
	-74.7	47,833	-673.54	219,977	849.40	267,911.16

Solving the above:
$b_2 = 0.978349$
$b_3 = 0.006648$
$b_4 = -0.088463$
$b_5 = 0.002477$

$$R^2 = \frac{b_2X_1X_2 + b_3X_1X_3 + b_4X_1X_4 + b_5X_1X_5}{X_1^2}$$

0.978349×8.73 .... 8.54 $\dfrac{21.00}{25.26} = 0.8314$
0.006648×1120.4 .... 7.45
-0.088463×-32.86 .... 2.91
0.002477×849.4 .... 2.10

                  21.00 $R = 0.9118$

Standard error of estimate is standard deviation of X_1 times the square root of 1 minus R^2:
$0.837656 \times 0.4106 = 0.344$

Beta coefficients:
$\text{Beta}_{1.2}$ is $b_2 \times \text{sigma}_2/\text{sigma}_1$

$0.978349 \times 0.405/0.838 = 0.473$

eliminating variables is satisfactory. Certain short cuts are possible because of the symmetry of the equations. If much of this work is to be done, the time spent in learning Crout's[4] method will be repaid. Peters and Van Voorhis[3] (pp. 225–235) have a good discussion and example of the Doolittle method of solving such equations.

The most arduous part of the computations is now finished. Having determined the various b's R is found by Ezekiel's formula 46, shown in Table 8. It may be desirable to correct for the number of items and the number of variables as follows where N is the number of observations and m is the number of constants in the equation:

$$\bar{R}^2 = 1 - (1 - R^2)\frac{(N-1)}{(N-m)}$$

The formula for the beta coefficients and one example is given in Table 8.

It is equally correct to set up the linear equations to give the beta coefficients first and find b from them.

REFERENCES

1. G. W. Snedecor: Statistical Methods. Ames, Iowa. Collegiate Press, Inc.
2. M. Ezekiel: Methods of Correlation Analysis. New York. John Wiley and Sons.
3. C. C. Peters and W. R. Van Voorhis: Statistical Procedures and Their Mathematical Bases. New York. McGraw-Hill Book Co.
4. P. D. Crout: A Short Method for Evaluating Determinants and Solving Systems of Linear Equations with Real or Complex Coefficients. Amer. Inst. Elec. Engrs. Summer Convention, Toronto, Ontario, Canada. Also published as Marchant Method, MM-182, MM-183, Marchant Calculating Machine Co., Oakland, California.

DISCUSSION

(*H. K. Work presiding*)

K. L. FETTERS[*] AND E. G. OLDS,[*] Pittsburgh, Pa.—The authors are to be congratulated on a timely and very interesting paper exemplifying one of the newer methods of investigation. In addition to the operating conclusions present, which are of interest in these days of high production, the statistical methods they have used appear to have wide applicability for the solution of metallurgical and production problems. The manner of presenta-

[*] Carnegie Institute of Technology.

tion is such, however, that it is a little difficult for anyone not completely familiar with the methods used to understand fully the import of their correlation factors and to understand the possible application of these methods to similar problems.

We feel, therefore, that the authors should give an example of their method of calculation in their discussion of this paper, in order to clarify this point. One might also remark in this connection that whereas statistical methods are a very useful tool to the metallurgist, he is still forced to go to references where all the examples are in terms of such things as bushels of corn per acre of ground, or even less evidently analogous biological data. This is a plea, then, for someone to bring together before this society in paper form, or to present in book form, the statistical methods of principal applicability to metallurgical problems with examples that we can use readily without terror of unknown quantities and difficultly understood formulas.

The authors show that as the percentage of metal in the open-hearth charge increases, the tendency is for a decrease in daily production. This apparent anomaly is explained when we note the nature of the other independent variables. If the number of furnaces, the tons of metal to the open hearth, and the weight of boxes of scrap are held constant, a decrease in the percentage of hot metal in the open-hearth charge can be accomplished only by an increase in the total charge. It is to be expected, of course, that, within a certain range, as the total charge increases, the production will do likewise.

This comment suggests the further remark that a problem of this kind requires exceeding care in the choice of independent variables. As far as possible, quantities that are fundamental causes of variation in the production rate are preferable to those that are, in a measure, determined by the smoothness of furnace operation.

Silicon-oxygen Equilibria in Liquid Iron

By C. A. Zapffe* and C. E. Sims,* Members A.I.M.E.

An investigation of the behavior of inclusions in steel several years ago[1] led to the conclusion that some of the commonly occurring inclusions in steel have

FIG. 1.—FRONT VIEW OF APPARATUS USED FOR DETERMINING CHEMISTRY OF SILICON AND OXYGEN IN LIQUID IRON.

appreciable solubilities, particularly in liquid steel. In the belief that further study

and clarification of this matter was warranted, a laboratory study of oxides in liquid steel was started. These oxides are generally the result of deoxidation treatment, and the basis of an understanding of their behavior must be, therefore, the behavior of the deoxidizer in liquid iron. The Fe-Si-O system was selected for the first study, and the apparatus used and experiments conducted are described herein.

APPARATUS

The apparatus is shown in Fig. 1 and the system is shown by diagram in Fig. 2.

Furnace Atmosphere

Commercial hydrogen (1) passes through an orifice (2) into a manometric system that measures the tankside pressure (3) and the back pressure (4) in the system. A water trap (5) guards against excess tankside pressure. A by-pass with stopcocks (6 and 7) is provided, so that the hydrogen can be routed directly from the tank to the furnace if desired. When stopcock 7 is closed and stopcock 6 is open, the gas proceeds through the conditioning train, of which the first unit is a furnace (8) that contains platinized asbestos at 350°C. The temperature is measured by a thermocouple and potentiometer (9) and is controlled by a slidewire resistance (10). In this furnace free oxygen is converted to water vapor. The exiting gas passes over a water bath (11) kept slightly below boiling temperature by an auxiliary heating unit (12). This unit also heats a surrounding copper coil (13) containing water, and the heated water rises through a collar (14)
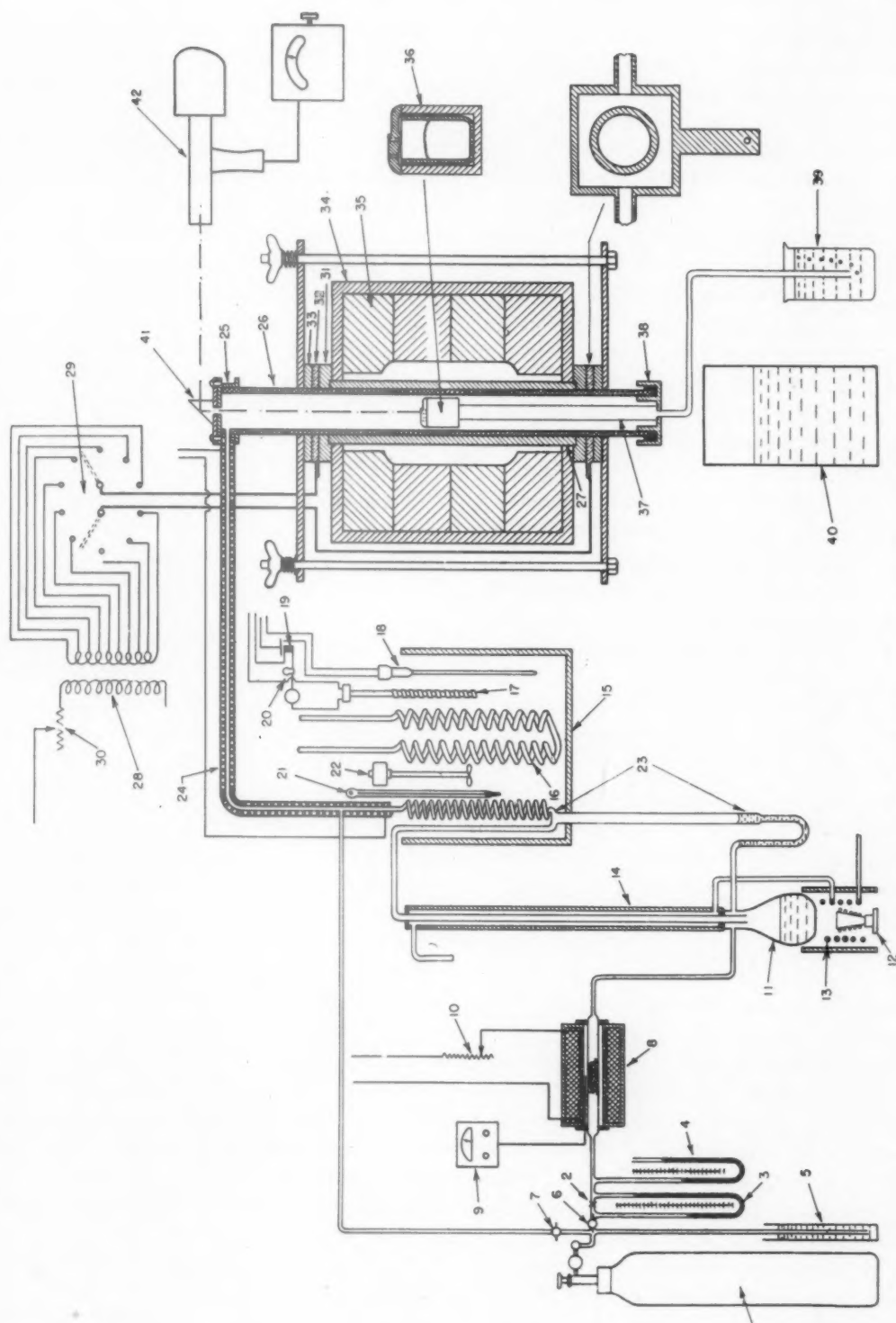
FIG. 2.—DIAGRAMMATIC SKETCH OF APPARATUS.

that surrounds the exit gas tube. This collar prevents cooling of the water-laden hydrogen until the gas passes into a large water bath (15) that is carefully thermostatted by using a double copper coil containing cooling water (16) and a bimetallic strip thermoregulator (17) connected with a knifeblade heating element (18), a relay (19), and a 2-watt lamp signal (20). The incoming gas serves as another source of heat, and auxiliary heating units are inserted when necessary. A thermometer (21) and a mechanical stirrer (22) complete the equipment for this bath. The temperature control under most conditions is ±0.05°C.

In this bath the water vapor in excess of the carefully controlled dew point is condensed and refluxed (23) to flask No. 11. The exit gas of known composition passes from the bath into the furnace through a tube (24) that is heated to some temperature greater than that of the gas by a wire resistance set in asbestos, Alundum cement, and water glass. The gas enters a brass head (25) soldered to the top of a vertical 30-in., 1½-in. i.d. Sillimanite tube (26). which stands within a 12-in., 2-in. i.d., cylindrical Globar heating unit (27). Thus, an atmosphere of known oxygen content is provided.

Temperature Control

A 5-kva. current transformer (28), operating on 220 volts, supplies the current for this Globar. A knifeblade switchboard in the secondary (29) affords 3-volt steps from 20 to 92 volts; and a 25-ampere, 1.2-ohm slidewire resistance (30) in the primary adjusts the voltage between these steps so that exceedingly close control of the heating is afforded.

The electrode ends of the Globar are fitted in graphite blocks (31), which in turn are faced with water-cooled copper plates (32), and they in turn with transite spacers (33). The furnace (34) is a steel case 11 in. on a side and is lined with insulating silica brick (35) cut away to provide an air space around the Globar. Inside the Sillimanite tube, in the center of the furnace, is placed an Alundum crucible containing a pure silica crucible in which the charge is placed (36). The crucibles are supported on a section of Alundum brick (37), which in turn is supported by a porcelain rod; and the assemblage rests on the bottom of a mercury well (38), which seals the bottom of the furnace tube but permits the gas stream to exit through a water bubbler (39). The bubbler is used to regulate the back pressure in the system.

Preservation of Equilibrium Composition

At the expiration of the test period, the mercury well is removed and the supports and crucibles are allowed to drop directly into a water bath (40).

Temperature Measurement

A prism (41) placed over a glass window in the brass head (25) permits temperature measurement of the melt to be made by an optical pyrometer (42).

Avoidance of Thermal Diffusion

The gas mixture must be at the temperature of the melt when reaching the melt, or error will result. In a static system a thermal gradient would cause the water molecules in an H_2O-H_2 mixture to concentrate in the cold end of the tube; whereas in a dynamic system like this, if the gas contacted the melt without being properly preheated, the water molecules would be proportionately less effective chemically than the hydrogen molecules—that is, their thermodynamic activity would be less than the normal for the temperature of the melt. In either case, the activity of the hydrogen at the melt would be disproportionately high.

Induction melting, commonly used in this type of investigation, requires special conditions for preheating the gas; but the 12-in., 1.5-in. i.d. Globar unit was found

to provide ample preheating when the rate of gas flow was not excessive. Besides the long heated zone and the wide passageway, the crucible cover, which was vented only on the sides, except for two small holes for temperature measurement, exerted an additional restriction to unheated gas entering the crucible.

Avoiding Error from Physical Diffusion of Gas through Furnace Tube

As the back pressure in the system is increased, the porosity of the refractory furnace tube becomes more important in changing the composition of the gas phase; that is, hydrogen will diffuse preferentially through the tube according to Graham's law, and the remaining gas will become enriched with water vapor. Several identical melts were made using various back pressures; and it was found that when the back pressure was of the order of several centimeters of mercury, silicon analyses tended to be low, indicating an enrichment of H_2O in the system. The back pressure was thereafter maintained at only 2 mm. of mercury, which was just enough to provide a positive pressure in the system and could hardly lead to measurable error by leakage through the tube.

The Sillimanite tube was sufficiently impermeable so that several minutes were required after cutting off the gas flow at 1600°C. to reduce appreciably the back pressure; and, of course, chemical action in the furnace would account for some of the gas loss.

Adjusting Rate of Gas Flow

If the gas flows at too rapid a rate, errors from thermal diffusion may arise. On the other hand, to approach equilibrium by oxidation of silicon, a certain minimum quantity of gas, dependent upon the amount of silicon to be oxidized, must be available to the melt during the course of the experiment.

Accordingly, a rate was chosen that compromised these limiting conditions. A tankside pressure of 1 cm. of mercury was used throughout the work, from which a constant rate of flow of approximately 2 c.c. of gas per second was obtained.

Catalyst for Removing Free Oxygen from Gas Stream

The catalyst was prepared from Italian washed and shredded asbestos and chlorplatinic acid. Even at room temperature this catalyst was so effective that to prevent an explosion it was necessary to flush the tube with nitrogen before hydrogen could be admitted. The catalyst was kept at 350°C. during the experiment to assure its best performance, and polished stainless-steel sheet heated in the exit gas stream developed no discoloration.

Controlling Dew Point of Gas Mixture

The thermostatted bath is depicted in Fig. 2. To ensure against supersaturation with water vapor, the incoming gas was given a sufficient excess so that water was continually condensing into the reflux tube.

Numerous periodic measurements of the dew point were made at the entrance to the furnace tube. It was found that at all bath temperatures the error in the dew point lay within the error of the bath thermometer, which in tests at temperatures below 50°C. was calibrated in tenths of a degree. The control of oxygen pressure, upon which the study was based, was thereby accurate far beyond requirement.

Obtaining Black-body Conditions in Crucible

Accurate temperature measurement was a prime consideration. The crucible cover was formed from Alundum brick and was cut to fill quite closely the cross section of the tube, thereby reducing heat losses from the melt and at the same time reducing reflection losses that are so important in determining emissivity. In addition, gas

could not freely by-pass such a crucible and cover, but must pass throughout it. Two 0.1-in. holes were drilled through the cover, one in the center and the other halfway to the edge. The crucible thereby approached an evenly heated, hollow black body whose temperature may be measured through a pinhole. In addition, the hole toward the side overlay the meniscus of the melt so that the wedge effect also contributed to the attainment of black-body conditions. The purpose of the two holes was to provide some criterion for emissivity by offering a comparison of apparent temperatures. Throughout the work the rim hole uniformly showed a temperature 5° higher than the center hole, regardless of the presence or absence of a slag on the surface. The difference of 5° may possibly be a true temperature difference between rim and center with external Globar heating, representing the heat flow compensating for heating the gas stream and for reflection to the cold ends of the tube.

The crucible was centrally placed, and no important gradient is likely to exist through the distance equal to the depth of the melt (about $\frac{1}{2}$ in.). The under edges of the crucible cover were serrated to permit gas to enter the crucible, but reflection could occur through those openings only to the equally heated adjacent wall. The crucible thereby had the conditions of equalized and external heating that characterize the "black body."

To assure even greater accuracy of temperature measurement, both a red and a green filter were calibrated, and periodically checked, with a Bureau of Standards lamp; and temperature readings were alternately made using each filter. No discrepancies between the readings could be detected. If the emissivity of the melt were not unity, some disagreement would sometime have been noted. The melting point of the electrolytic iron was frequently observed to be 1530°C. using either filter, by noting the pause in the temperature rise.

The calibration was made through the actual sighting system, which comprised a quartz prism and a glass window; and care was taken that no film or dust deposited on the glass faces during the experiment. The window was so high above the melt that metallic vapors, which also would have had to proceed against the gas stream, never reached the glass.

Temperature changes of about 3° were detectable. It seems probable that the readings as a group are within 10°C. of the true, or absolute, temperature.

Precautions Necessary during Heating of Charge

About two hours were required for heating the charge to the desired temperature, principally because the refractory furnace parts give better service when treated moderately. During that two hours precautions were necessary to prevent reactions in the charge that might subsequently confuse the results. The amount of metallic silicon added to most of the charges was very small; and the oxygen pressure of SiO_2 decreases so rapidly with decreasing temperature that oxidation of Si to SiO_2 might occur during heating in an atmosphere that at higher temperatures is reducing to SiO_2. It was therefore found advisable to by-pass dry hydrogen directly from the tank to the furnace throughout the heating period, to protect the metallic silicon until the temperature was reached at which its reaction was to be studied.

Error from the opposite effect—reduction of SiO_2 by the H_2—was not found; nevertheless, at temperatures near the melting point the stream of dry hydrogen was kept slow as a precaution; and, shortly after melting, the controlled atmosphere was admitted.

In spite of these precautions, some silicon often oxidized before the charge melted, probably from rust on the iron or from air remaining in the crucible walls; perhaps from oxygen or moisture in the unpurified

hydrogen (the catalytic furnace was by-passed). It was necessary to know the degree of this oxidation, or it would be impossible to determine from the analyzed value for silicon whether oxidation or reduction had occurred while the charge was at temperature. Accordingly, several melts were made with different charges of silicon, and each melt was quenched at the moment the temperature reached 1600°C.—at which point the thermostatted gas would ordinarily be admitted. The results are shown in Table 1.

TABLE 1.—*Melts with Different Charges of Silicon*
PER CENT BY WEIGHT

Weight Charged	Analysis of Charge				Silicon Recovered by Analysis of Ingot	Silicon Loss, Per Cent
	Al	Ca	Fe	Si		
2.50	0.021	0.015	0.07	2.40	2.25	6.3
2.00	0.014	0.011	0.06	1.92	1.70	11.5
1.00	0.007	0.005	0.03	0.96	0.88	8.3
0.40	0.003	0.002	0.01	0.38+	0.31	19.
					Average	11.3

Therefore, in tests approaching equilibrium by oxidation, to ensure that any apparent loss of silicon from oxidation occurred during the constant temperature test, and not during heating, it was necessary to charge some quantity of silicon safely greater than about 110 per cent of the desired value. The fate of the aluminum and calcium can only be surmised, but the great preponderance of silicon in all cases should permit postponing their consideration as far as the present work is concerned.

Obtaining Proper Quenching Conditions

After equilibrium in the liquid iron is attained at some constant temperature, that iron must be cooled so rapidly that its components are unable to change in any way that might affect the analytical results. Errors could result during slower cooling from levitation of silica or silicates that might escape to the slag. A rapid quench was used in the hope of ensuring retention of all silicon components.

At the termination of the 2 to 5-hr. test period, during which the melt was at a carefully controlled constant temperature under a closely regulated atmosphere, the mercury well at the bottom of the furnace tube was removed; and the crucible and supports were allowed to fall directly into a water bath in which an immersed towel served as a parachute to prevent spilling.

Materials Charged

The charge consisted only of electrolytic iron, obtained from the National Radiator Castings Co., analyzing: C, 0.01 per cent; Si, 0.003; P, 0.002; Mn, 0.002; S, 0.001; and silicon analyzing: Si, 97.2 per cent; Fe, 0.48; Al, 0.72; Ca, 0.56.

Crucibles

Silica crucibles were used, except in early, unsatisfactory runs in alumina crucibles. A score of melts were made in transparent silica crucibles of high purity that were made in England. No changes in results were found, however, when Vitreosil crucibles were used, so the latter were adopted. The Vitreosil was reported to be 99.8 per cent SiO_2.

ANALYTICAL METHODS

Determining Silicon.—After quenching, the ingots were etched with hydrofluoric acid to remove surface entrapments of slag and crucible, if any were present. To assure further the absence of mechanically entrained impurities, a binocular microscope was used during the sectioning and cleaning of each ingot. A fragment of SiO_2, of course, would invalidate the total silicon analysis. Total silicon analyses were made by double dehydration methods, followed by volatilization with hydrofluoric acid.

Determining FeO.—The [FeO] values used are simply expressions for [O], the activity of the oxygen dissolved in the iron, and are

calculated from the H_2O-H_2 ratios of the atmosphere, which determine the true chemical activity of the oxygen in the system. The accuracy of the computed values for [FeO], therefore, depends on the control of the dew point. This was controlled so precisely that calculated oxygen pressures are probably within a tenth of a per cent of the actual.

Oxygen determinations by direct analysis were considered highly desirable as checks on the calculated values, of course; and some samples at the very outset of the work were analyzed for total oxygen by vacuum fusion under the direction of Dr. Chipman at the Massachusetts Institute of Technology. The results are shown in Table 2.

TABLE 2.—*Total Oxygen*

Run No.	Calculated[a] O as FeO, Per Cent	Total O by Analysis, Per Cent	Ratio: O by Vac. Fus. / O calculated	Condition of Ingot
10	0.0011	0.0066	6	No record of solidity
11	0.0016	0.0046	3	No record of solidity
12	0.0022	0.0045	2	Solid ingot
2	0.0036	0.0060	1⅔	Solid ingot
5	0.0036	0.0236	6⅔	Porous ingot
6	0.0036	0.0229	6⅓	Porous ingot
7	0.0039	0.0074	2	Solid ingot
3	0.0043	0.0177	4	Porous ingot
4	0.0051	0.0123	2½	Solid ingot
8	0.0060	0.0087	1½	Solid ingot
				Calculated Total O[b]
103	0.0016	0.0071, 0.0091	5	0.2086
104	0.0016	0.0060, 0.0040	3	0.2086
106	0.0352	0.054	1½	0.047

[a] Calculated from Chipman's equation, which he deduced from this same type of test.
[b] Total O includes that present as FeO, SiO and SiO$_2$, and is calculated from constants obtained in these experiments. See Fig. 10 and page 21.

Because those early runs were made in Alundum crucibles, samples from three of the later runs were analyzed at Battelle by the vacuum-fusion method. The results are shown also in Table 2.

In all of the early samples the total O by analysis greatly exceeded that computed to be present as FeO, the discrepancy being greater in the more porous ingots and in those having higher silicon. The total O by analysis in two of the later tests (103 and 104) was from 3 to 5 times that of the computed FeO, but was much less than the calculated total O. For test 106, the total O by analysis and by computation are in close agreement. FeO alone falls far short of accounting for the total oxygen analyses in all cases.

Vacuum-fusion analysis of silicon and ferrosilicon, on the other hand, gave the following results:

SI CONTENT, PER CENT	TOTAL O, PER CENT
97.2	0.039, 0.015
77	0.024
51	0.010
40	0.005
15	0.004, 0.006

These have no direct bearing on the present work other than to indicate that materials high in silicon content do contain oxygen, even by vacuum-fusion analysis, which will be shown in a later publication to be inefficient for such tests.

Further analyses for total oxygen were abandoned; and the work was returned to its original premise that, in determining a principle, absolute values for oxygen pressure were preferable to total oxygen analyses. Hence, the only means of estimating the oxygen contents was to calculate them according to Chipman's equation.[2,8]

SUMMARY OF EXPERIMENTAL PROCEDURE

The stepwise experimental procedure was as follows:

1. Compute 25-gram charge to necessitate either oxidation or reduction. Place iron in silica crucible and add silicon. Tap lightly to distribute silicon about the surface of the iron. Assemble crucibles, cover, and supports and place in furnace.

2. Flush furnace with dry hydrogen for 15 min. Turn on Globar cooling water

3. Begin Globar heating. Turn on catalyzing furnace, heating coils, water circuits, stirrer and other bath accessories. Make necessary adjustments.

4. Bring furnace to temperature in about two hours. Admit thermostatted gas.

5. Hold at temperature for 2 to 5 hr., depending upon the temperature and other factors. Maintain catalyzing furnace at 350° ± 25°C., tankside gas pressure at 1 cm. of mercury, back pressure at 2 mm. of mercury, rate of gas flow at about 2 c.c. per second. Make certain that condensation is continually occurring in the thermostatted coils.

6. At termination of test, drop melt directly into water. Record barometric pressure. (This affects the back pressure upon the exit gas.)

7. Scrub ingot. Dissolve in hydrofluoric acid silica from the crucible mechanically held on the surface. Saw into sections and analyze.

EXPERIMENTATION

Validity of Data

The data of all heats used in developing the hypothesis of the present paper are included in Table 3. Many of the runs made were discarded for one reason or another. Some were only trial heats made while developing the apparatus and the operating technique. Others were rendered useless because of failure of the apparatus or controls, or because of accidents in quenching. Runs charged too far from the equilibrium content could not reach equilibrium in the time allowed. If subsequent runs, charged at the end point of the first, proved this to be true, the data were discarded for final tabulation, although they were useful in pointing the direction of equilibrium.*

Some 55 early tests were run in alumina crucibles with an addition of powdered

SiO₂ to the charge when equilibrium was to be approached from the side of reduction of SiO₂. Run 24 (not listed), held 2 hr. and 20 min. at 1550° with an oxygen pressure to give 0.00491 per cent FeO, duplicating run 99, gave a final Si analysis of only 0.37 per cent. The fluxing between the SiO₂ and the crucible evidently depleted the available SiO₂ supply. In other cases, there was evidence of contamination from the powdered silica, even though the silica had been previously levigated to a size 30 times greater than that which would rise out of the melt in the time of the test, according to Stokes' law. The tests in alumina crucibles gave good experience, but the results were considered unreliable and none were tabulated. All data not excluded for reasons given above are included in Table 3.

At 1550°, reactions are relatively slow, and at 1650° the life of the furnace is materially shortened. The temperature of 1600°, consequently, was found to be most favorable for experimentation.

Attention was paid to securing more points for plotting the curves rather than the exact duplication of the oxygen pressure and initial silicon content in repeat tests. But where the conditions were practically duplicated, the results show reasonable agreement. In fact, all of the data of Table 3 are in good agreement with the exception of runs 110, 111, and possibly 105 at 1600°. These are anomalous, for no known reason, but may be in error because of extraneous silica from the crucible.

*An example of the method of approaching equilibrium values stands in the following list of data. In Table 3, heats such as the first five listed below are often omitted because their data are obviously incomplete.

Speci-men No.	H₂O-H₂ Ratio	Calculated [FeO]	Si, Per Cent		Time	
			Charged	Analyzed	Hr.	Min.
49	0.0061	0.00491	0.25	0.36	1	40
51	0.0061	0.00491	0.36	0.42	2	
53	0.0061	0.00491	0.50	0.60	2	30
57	0.0061	0.00491	0.70	0.74	2	20
58	0.0061	0.00491	0.70	0.85	4	0
99	0.0061	0.00491	0.90	0.95	3	0 ⎫ equil.
71	0.0061	0.00491	1.02	0.945	2	0 ⎭

TABLE 3.—*Experimental Data for Relations of Calculated [FeO] Activity to [ΣSi] in Liquid Iron at Temperatures of 1550°, 1600°, and 1650°C., Respectively*[a]

Specimen	H_2O/H_2	[FeO][b]	Silicon Charged[c]	Silicon Analyzed[d]	Time at Temperature Hr.	Min.
1550°C.						
56	0.0440	0.0353	0.12	0.10, 0.10	1	20
58	0.00613	0.00492	0.70	0.76, 0.84, 0.86	4	
61	0.01735	0.01392	0.25	0.25, 0.25	1	35
62	0.0240	0.01925	0.18	0.15, 0.17	2	45
65	0.0449	0.0360	0.08	0.086, 0.067	2	45
68	0.141	0.113	0.036	0.008, 0.010	2	30
69	0.081	0.065	0.063	0.028, 0.029, 0.036	2	15
71	0.0621	0.00498	1.02	0.93, 0.96	2	
73	0.0124	0.0099	0.40	0.24, 0.36	2	15
74	0.0328	0.0263	0.10	0.076, 0.086, 0.090	2	30
78	0.0446	0.0358	0.06	0.066	3	30
80	0.0803	0.0645	0.02	0.019, 0.028	1	45
83	0.1435	0.1155	0.00	0.005, 0.006	3	15
88	0.0240	0.0193	0.12	0.11, 0.10	2	15
91	0.01745	0.0140	0.20	0.273, 0.288	2	30
95	0.01255	0.0101	0.40	0.503, 0.469	3	
99	0.00615	0.00493	0.90	0.947, 0.962	3	
1600°C.						
76	0.0328	0.0371	0.12	0.119, 0.129	1	30
77	0.0445	0.0504	0.08	0.082, 0.092	1	
81	0.0805	0.0911	0.03	0.035, 0.035, 0.036	1	45
84	0.1416	0.1605	0.00	0.026	2	
89	0.0241	0.0273	0.18	0.167, 0.209, 0.226	1	45
92	0.0174	0.0197	0.30	0.377, 0.378	2	
96	0.0125	0.0142	0.45	0.491, 0.523, 0.550	2	
100	0.0062	0.0054	1.00	1.06	2	
103	0.00625	0.00708	1.11	1.30	3	30
104	0.00622	0.00705	2.00	2.01	5	30
109	0 0062	0.00702	2.50	2.29, 2.30, 2.30	5	
105	0.0332	0.0269	0.20	0.33, 0.34	5	30
106	0.1396	0.1582	0.00	0.022, 0.037	5	30

TABLE 3.—(*Continued*)[a]

Specimen	H_2O/H_2	[FeO][b]	Silicon Charged[c]	Silicon Analyzed[d]	Time at Temperature Hr.	Min.
107	0.625	0.707	0.00	0.003, 0.006, 0.007	5	
110	0.0443	0.0502	0.40	0.34, 0.36	4	
111	0.0239	0.0271	0.50	0.45, 0.50, 0.45	4	
112	0.0328	0.0371	0.50	0.45, 0.38	5	30
113	0.0174	0.0197	0.60	0.66, 0.71, 0.68	5	30
1650°C.						
59	0.00612	0.0096	0.90	1.02, 1.05	1	15
60	0.0173	0.0271	0.35	0.38, 0.39	1	50
63	0.0241	0.0378	0.27	0.21, 0.22, 0.24	2	
64	0.0450	0.0705	0.143	0.11, 0.11	1	10
66	0.0795	0.1248	0.065	0.010, 0.077	1	35
67	0.1402	0.2202	0.03	0.047, 0.069	1	30
70	0.0062	0.00973	1.25	1.15, 1.16	1	30
72	0.0126	0.0197	0.56	0.61, 0.64	2	15
75	0.0328	0.0515	0.15	0.175, 0.193, 0.203	1	45
79	0.0446	0.0701	0.08	0.118, 0.135, 0.145	1	30
82	0.0810	0.1272	0.04	0.049, 0.059	1	45
85	0.1413	0.222	0.02	0.015, 0.027	1	45
86	0.1402	0.220	0.08	0.020, 0.023	2	
95	0.0125	0.0196	0.55	0.66, 0.65, 0.66	1	45
90	0.0241	0.0378	0.18	0.225, 0.237, 0.259	1	15
93	0.0174	0.0273	0.42	0.37, 0.33, 0.26	1	30
98	0.0125	0.0196	0.70	0.755, 0.760, 0.762	2	

[a] FeO and Si are expressed in weight per cent.
[b] Activity calculated according to Chipman's equation.[2,3]
[c] Refer to Table 1.
[d] Decreases in Si over the course of the experiment signify loss of [Si] by oxidation, and increases indicate that reduction of the SiO₂ crucible occurred.

Formation of Inclusions

If the silicon analyses are to mean anything in regard to equilibrium conditions, the Si determined must be only that in the melt when it is at equilibrium. Any silicate slag or any previously separated droplets of slag that have not risen to the surface would lead to high values for Si.

The quiescent period of 1 to 5 hr. at temperature facilitates that separation, and

care was taken to clean the ingots from adhering slag or particles of the crucible. The frozen ingots, however, did contain inclusions. If these inclusions resulted from chemical processes, they should be included in the analyses as part of the dissolved entities that have been at equilibrium in the melt.

That the inclusions did result from chemical processes and did not represent a pre-existent suspension is borne out by direct observations. Total dissolved silicon could be diminished at will to about 0.001 weight per cent, depending upon the temperature, merely by increasing [FeO] toward saturation; and that entire 0.001 weight per cent is readily accounted for by known chemical reactants. Furthermore, when the temperature increased, the residual total silicon increased, which is contrary to the behavior of suspensions.

Calculations based on Stokes' law show that inclusions as large as those found could hardly have remained in the melt for more than a small fraction of the time of the test.

The inclusions were far from being of colloidal dimensions; yet, no distribution of sizes from top to bottom could be detected in any of the melts examined.

The appearance of the inclusions conformed with that to be expected from reaction products corresponding to the respective FeO-Si ratios.

The inclusions found in the present work are assumed to represent components that were in solution during the test. The various steps in the development of a silica inclusion are shown at 3000 diameters in the micrographs of Fig. 3. The specimen is that from No. 105, Table 3.

In the upper photograph, four inclusions have been frozen so instantaneously by the rapid quench that they may give stepwise indication of the process of their formation. As numbered, these inclusions seem to show: (1) a collection of distinct, minute droplets in the very first stage of coalescence, but without a discernible common nucleus; (2) the incipient formation of a common nucleus; (3) a partially formed, spherical inclusion in the late stages of coalescence; and (4) a completely formed, spherical inclusion.
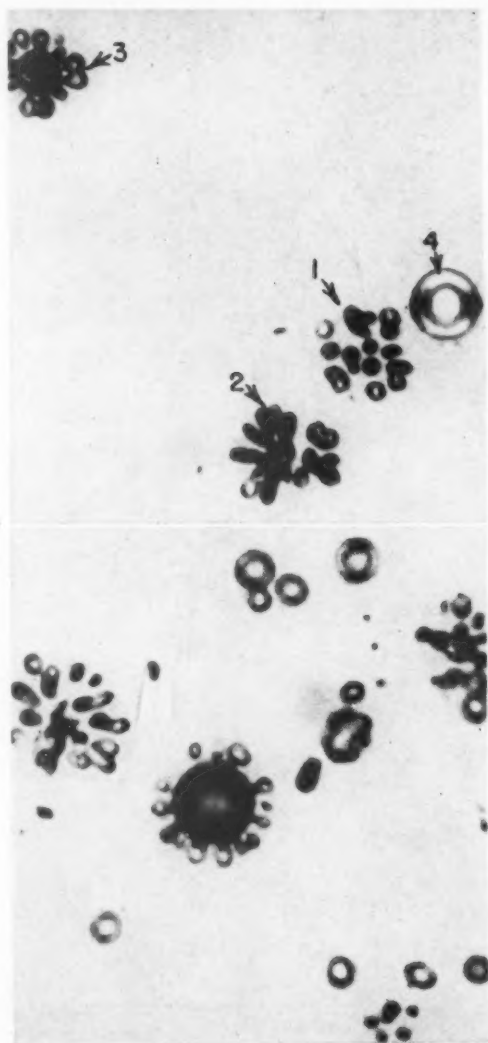
FIG. 3.—INCLUSIONS IN SPECIMEN INSTANTANEOUSLY QUENCHED FROM EQUILIBRIUM MELT AT 1600°C.
Showing arrested forms in process of developing ordinary inclusions in steel. Above, inclusions numbered with respect to their stage of development; below, similar field showing an even greater diversity of forms.
Original magnification 3000; reduced ⅓ in reproduction.

In the lower photograph an even more complete series can be found. The smallest droplets shown in the micrograph may have

themselves agglomerated from even smaller particles; and, with slower cooling, the completed spherical inclusions resulting from the above-listed steps would again coalesce

Another explanation for the inclusions of Fig. 3 is suggested by Sosman's discussion of the work of Sims and Lillieqvist.[1] The symmetrical distribution of the satellite
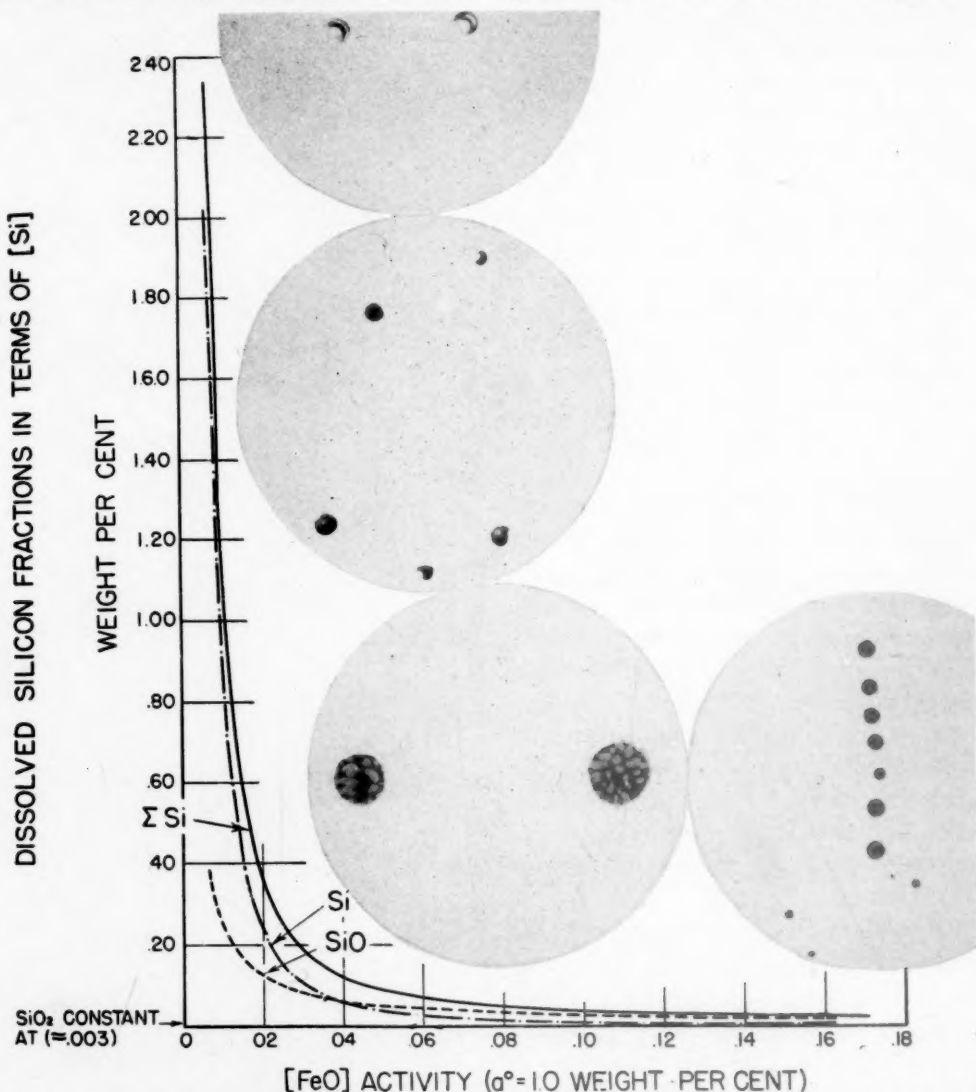
FIG. 4.—COMPOSITE SHOWING VARIATION OF INCLUSION TYPE WITH RESPECT TO FeO-Si EQUI-LIBRIUM AT 1600°C.
Original magnification of inclusions, 3000; reduced ⅓ in reproduction.

to form larger inclusions. One such instance is observable in the lower photograph. These results seem to corroborate the original observation by Sims and Lillieqvist[1] that the size of inclusions depends upon the rate of cooling, and is consistent with their postulate that systematically occurring inclusions in steel are formed from dissolved components.

inclusions around the larger ones, the uniformity of their size and the absence of small background inclusions suggest that this may be a case of dispersion rather than coalescence. This would indicate a chemical or physical reaction producing a very low surface tension. Such a reaction might be the decomposition of precipitated

SiO to Si and SiO$_2$, according to Eq. 4 on page 215.

In Fig. 4 a composite is arranged to show how the inclusions in the ingots of the

principally blue-gray iron oxide and often delineated the grains by exuding to the boundaries.

The data of Table 3 are based on an
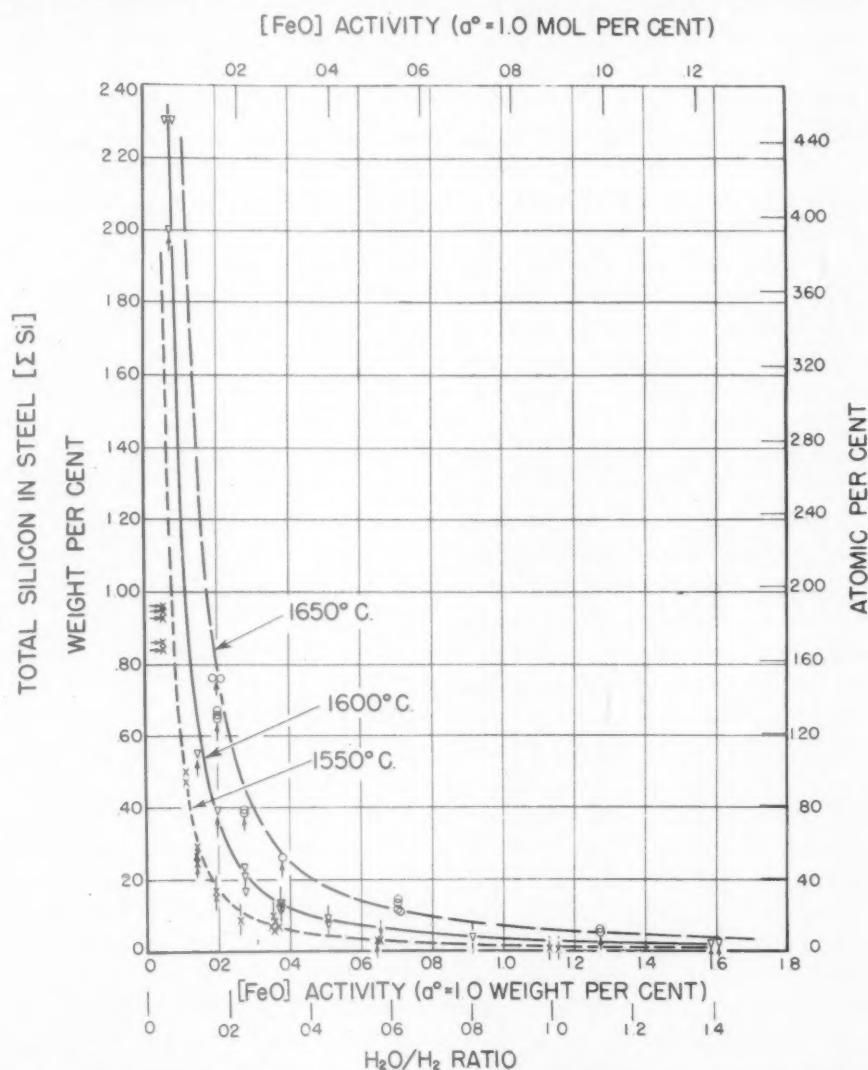
FIG. 5.—PLOT OF EXPERIMENTAL VALUES IN TABLE 3 SHOWING VARIATION OF TOTAL DISSOLVED
SILICON WITH ACTIVITY OF DISSOLVED OXYGEN EXPRESSED AS FeO.

present research corresponded in type to the FeO-Si ratio. Specimens high in silicon content contained glassy inclusions of nearly pure silica, which generally were spherical and showed sharp optical crosses under crossed Nicols. With increasing FeO, these spherical inclusions darkened; then a duplex structure appeared; and finally, at high [FeO] values, the inclusions were

indirect evaluation of the oxygen content according to accepted equations for oxygen solubility and upon silicon analyses that may or may not include suspended slag droplets. They are not presented with any claim to absolute accuracy. Rather, they are presented as the results of a systematic series of tests carried out under the controlled conditions that have been described.

It will, however, be necessary, in discussing the results, to speak as though the tabulated oxygen and silicon values were established beyond cavil. The discussion should be read with the understanding that that premise is made.

The data are plotted in Fig. 5 as calculated [FeO] activity versus total silicon. Small arrows indicate the direction of the change in composition that occurred during the test. Vertical arrows signify oxidation of the charged metallic Si (downward) or reduction of SiO_2 from the crucible (upward). The several horizontal arrows express a probability that in those particular tests [FeO] was higher than calculated because of a temporary difficulty in obtaining a dew point of $0.0°C$.

Determining Activity of [FeO]

The oxygen pressure of the system, though fundamentally the key entity in the present problem, is in itself of little immediate use to the steelmaker. Oxygen concentrations are the values that must be known to translate theory into practice, and for their determination under certain conditions the careful researches of Fontana and Chipman[2] and Chipman and Samarin[3] are fortunately available. Those investigators established the relationship between the actual concentration of [FeO] in the Fe-O-H system and the ratio of H_2O to H_2 in the atmosphere; but, more important, they showed also that the ratio of the *activity* of [FeO] to its *concentration* was unity nearly to saturation with oxygen.

The present study concerns a system that has an additional component, Si, as solute; and it cannot be assumed that the same 1:1 relationship exists between activity and concentration of [FeO] as in the simpler system Fe-O-H. Values for oxygen *concentration* cannot be supplied with certainty from existing knowledge. However, the usefulness of *activity* remains inviolate, when the oxygen pressure of the system is known; and for solving chemical systems,

in truth, only activities are validly used. Consequently, for present purposes the *activity* of [FeO] will be used. The applicability of the work of Fontana,[2] Chipman and Samarin[3] to deriving actual numerical activities in the present research follows from simple reasoning:

The oxygen pressure (P_O) is the controlling and thermodynamically useful factor in all the experiments and is directly proportional to the H_2O-H_2 ratio, according to the equations for the dissociation of water vapor:

$$H_2O = H_2 + \tfrac{1}{2}O_2$$
$$\tfrac{1}{2}O_2 = O$$
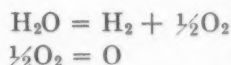
The atomic oxygen, in which form the gas dissolves in the iron, has a partial pressure:

$$(P_O) = k \times H_2O/H_2$$

and solution of the gas in the iron:

$$(O) = [O]$$

may be expressed as

$$(P_O) = k' \times [FeO]$$

whereupon

$$[FeO] = k'' \times H_2O/H_2$$

This equation is identical to Chipman's equation:

$$[FeO] = 1/K_{FeO} \times H_2O/H_2$$

The constant k'' relates the oxygen pressure directly to its activity in the iron and is therefore equal numerically to the reciprocal of Chipman's constant. Now, at saturation values for [FeO] in the system Fe-Si-O-H the total dissolved silicon does not exceed a few thousandths weight per cent. Chipman's constant K_{FeO} must therefore be valid for that portion of the Fe-Si-O-H system within the negligible percentage error that could be introduced by such a small impurity.

The equation $[FeO] = k'' \times H_2O/H_2$, just listed, then shows that Chipman's K_{FeO} must likewise be valid for all other values of [FeO], regardless of the presence of silicon, for expressing the *activity* of [FeO].

In the following discussion, activity values for [FeO] will be calculated from the H_2O-H_2 ratios according to the equation of Chipman and will be expressed in terms of an activity whose standard state is 1.0 per cent by weight, or by mol, as specified. Any deviation in the *activity coefficient* that may occur as the silicon content increases will only affect the total *oxygen concentration*. The advantage of the procedure is that the numerical values for the activities are those of established work on the iron-oxygen system and may be substituted for concentrations where desirable until proof is developed that the activity coefficient of [FeO] in the iron-silicon system is not unity.

Determining Activity of [Si]

For silicon, no direct method is yet known for determining either its activity or its distribution in dissolved compounds. The variation of the total silicon as a function of whatever its individual fractions may be, however, is rigorously controlled by the oxygen pressure ([FeO] activity) of the system.

The work of Körber and Oelsen[4] on the system Fe-Si-O has been widely accepted and was adopted as a preliminary guide in calculating the charge. For the equilibrium constant

$$K'_{Si} = [FeO]^2[Si]*$$

---

* The equation $K'_{Si} = [FeO]^2[Si]$ is derived from the chemical reaction:

$$2Fe + SiO_2 = 2FeO + Si$$

which takes place within the liquid iron phase, and for which the mass action constant is

$$K = \frac{[FeO]^2[Si]}{[Fe]^2[SiO_2]}$$

[Fe] may be eliminated from this expression without introducing important error because

these investigators quote the following values:

TEMPERATURE	K'_{Si}
1550°	2.5×10^{-4}
1600°	7.1×10^{-4}
1650°	$21. \times 10^{-4}$

A test was made at 1600° using a dew point of 20°C. From Chipman's equation:

$$\log K_{FeO} = \log \frac{(H_2O)}{(H_2)[FeO]} = \frac{10,200}{T} - 5.50$$

FeO could be calculated as follows:

$$[FeO] = \frac{(H_2O)}{(H_2)K_{FeO}} = \frac{(17.54)}{(728.5)(0.883)}$$
$$= 0.0273 \text{ weight per cent}^{*,\dagger}$$

Substituting [FeO] = 0.0273 in Körber and Oelsen's expression for K'_{Si} requires that 0.95 weight per cent of silicon be the corresponding equilibrium value. Accordingly, 0.95 weight per cent of silicon was added to the charge.

Upon analyzing the resulting ingot, however, only 0.70 weight per cent silicon was found; and it was necessary to make four subsequent melts, charging each at the progressively diminished silicon analysis of

---

its activity is in most cases practically unity; and [SiO_2] may be eliminated similarly if the reaction takes place in the presence of excess SiO_2, for then the solubility of SiO_2 is a constant at constant temperature and the activity of [SiO_2] is unity. The resulting expression is usually written

$$K'_{Si} = [FeO]^2[Si]$$

* H_2O-H_2 ratios for all the tests were obtained from the following typical data:

	MM. HG
Corrected barometric pressure..	(744.0)
Back pressure.................	(2.0)
Total pressure................	(746.0)
P_{H_2O} (at dew point).........	(17.54)
P_{H_2}......................	(728.5)

Van der Waal's corrections for the nonideality of the gases were found unnecessary because in all cases the corrections lay within the experimental error.

† As has been explained, this value for [FeO] is now the activity based upon a standard state of a 1 per cent solution in liquid iron. In the early parts of this discussion it may also be regarded occasionally as representing concentration because previous investigators, whose work is being compared, have assumed that the two are numerically identical.

the preceding melt, before an end point was finally reached at 0.20 weight per cent. The equilibrium constant accordingly became:

$$K'_{Si} = [FeO]^2[Si] = [0.0273]^2[0.20]$$
$$= 1.49 \times 10^{-4}$$

which is exactly that value given by Herty and Fitterer.[5] It is also considerably nearer

To check the validity of that assumption, a melt was made using a dew point of 50°C. to compare with the preceding test. With the resulting changed [FeO], the silicon should have adjusted itself to 0.006 weight per cent so that [FeO]²[Si] would remain constant at the value just determined. Instead, a value of 0.026 weight per cent

TABLE 4.—*Values for Equilibrium Constant* $K'_{Si} = [FeO]^2[Si]$ *According to Different Investigators*

Investigator	Year	Tempera-ture, Deg. C.	$K'_{Si} \times 10^4$, Wt. Per Cent	Remarks
Feild[6]	1925	(1530)	0.17	Calculated from Stoughton's data on one basic open-hearth heat, using Tritton and Hansen's values for [FeO]
McCance[7,8]	1925	1600	0.56	Calculated from early thermochemical data
Herty and Fitterer[5]	1928	1600?	1.49	Laboratory experiment; no dependable temperature measurement and no control of atmosphere; [FeO] by hydrogen reduction; [Si] by subtracting Si inclusions (electrolytic method) from Si total
Herty, Fitterer, and Christopher[9]	1931	1600?	2.07	Plant data; same technique
Herty, Fitterer, and Christopher[9]	1931	1600?	1.65	Accepted value; average of plant and laboratory values
Schenck[10]	1931	1600 (1527)	0.28 (0.044)	Calculated by extrapolating oxygen dissociation pressures for FeO and SiO₂, using Nernst's law
Schenck[11]	1932	1600	5.6	Acid open-hearth plant data; total oxygen and total silicon
Schenck[12]	1934	1600	2.5	Same, revised
Körber and Oelsen[4]	1933	1600	7.1	Laboratory experiment; no control of atmosphere nor attempt to attain equilibrium; total [FeO] obtained by vacuum fusion at 1600°; [Si] is total Si; high Si always accompanied by high Mn
Portevin and Perrin[13]	1933	1600?	6.	Calculated by present authors from reported 0.29 per cent Si found with 0.05 FeO
Chipman[14]	1934	1600	0.48	Calculated from thermochemical data, not necessarily reliable
Oelsen and Kremer[15]	1936	1600	11.	Calculated from some values of Körber and Oelsen (FeO = 0.47, Si = 0.005)
Schenck and Brüggemann[16]	1936	1600	3.55	Total Si and FeO by modified Al method
Herasymenko[17]	1938	1600	11.5	Constant reported as (FeO)²[Si] converted to K'_{Si} by present authors using Körber and Oelsen's constant [FeO]/(FeO) = 0.0095
Darken[18]	1940	1600	6.1	Calculated from summation of published results and some plant data

the theoretical values than is Körber and Oelsen's, which may be significant because the present constant is calculated on the basis of [FeO] activity and is therefore free from aggravation by extraneous oxides or changes in activity coefficients.

According to the mass-action constant, when [FeO] is varied silicon must vary inversely with the square of [FeO]. It is generally assumed that the total silicon analysis of steel, perhaps corrected for mechanically suspended inclusions, is valid for insertion in the mass-action expression.

silicon was found. Furthermore, no metallic silicon had been placed in the charge, so 0.026 is very likely a minimum value, being obtained by reduction of SiO₂. As the calculated [FeO] was 0.1603 weight per cent, the equilibrium constant became

$$K'_{Si} = [0.1603]^2[0.026] = 6.7 \times 10^{-4}$$

which value is almost exactly that of Körber and Oelsen's and is four times greater than the previously determined constant which agreed with Herty's value.

Tests were next made using the dew point of ice. The bath was kept at 0.0°C. by actively stirring a mixture of ice and water. Experimental runs lasting from 2 to 5 hr. at 1600° indicated the equilibrium value for [Si] as 2.30 weight per cent (obtained both

theoretical.* It seems to be the lowest experimentally determined constant ever recorded.

A dew point of 75°C. was then used, and K'_{Si} was found to be 25×10^{-4}, which *exceeds* every recorded constant.
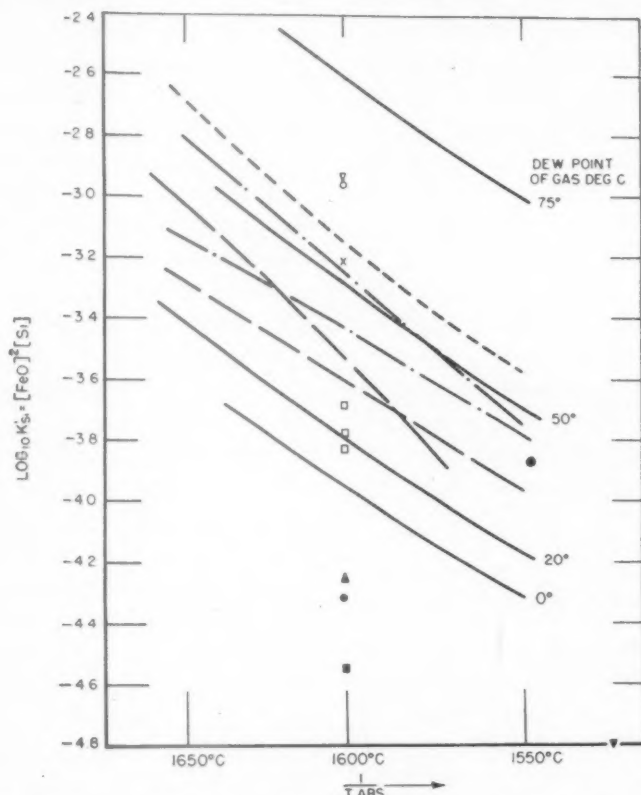
FIG. 6.—PLOT OF DATA IN TABLE 4 WITH SOME PRELIMINARY RESULTS OF PRESENT RESEARCH SUPERIMPOSED TO SHOW THAT EACH OF THE DIVERGENT PUBLISHED CONSTANTS CAN BE REPRODUCED SIMPLY BY SELECTING PROPER OXYGEN PRESSURE.

—————— Values of present research for [FeO activity]² × [ΣSi]
— — — — — Körber and Oelsen
—— · —— Schenck and Brüggeman
—— — —— Schenck
☐ Herty
▽ Herasymenko

○ Oelsen and Kremer
✕ Portevin and Perrin, Darken
◼ Schenck
● Chipman
▲ McCance } theoretical
▼ Feild

by oxidation and by reduction), for which [FeO] was calculated to be 0.0070 weight per cent. The equilibrium constant then became:

$$K'_{Si} = [0.0070]^2[2.30] = 1.1 \times 10^{-4}$$

which is appreciably less than Herty's value and even more closely approaches the

Further tests were made using other dew points and other temperatures. The results

---

* Comparison of experimental with theoretical values is not made on the assumption that theoretical values *per se* are necessarily the more accurate. Theoretical values are lower because of arbitrary assumptions, but it is to be shown shortly that the significance attached to the low values is justifiable.

that were obtained are illustrated in Fig. 6. The data of previous investigators, as listed in Table 4, are plotted there in the familiar form of log K'_{Si} versus $1/T$, and superimposed are some results from the present research. For each different H_2O-H_2 ratio a different K'_{Si} was obtained and the values encompassed the entire range of experimental values reported by other investigators. By selecting a proper H_2O-H_2 ratio, therefore, any of the published experimental results can be exactly duplicated. Some theoretical values are yet lower, but there is every indication that with dew points less than 0°C. even they might be attained.

From these few preliminary tests two conclusions must be drawn:

1. The variation in published values for K'_{Si} results principally from the fact that $[\Sigma FeO]^2[\Sigma Si]$ is not a constant.

2. $[FeO]^2[\Sigma Si]$ also is not constant, but varies with FeO.

Inapplicability of ΣSi Values for Mass Action Calculations

The first conclusion should not be surprising, because a total analysis for one component in a system containing four components (Fe-O-Si-H) with all their chemical interrelationships may have but little relation to the activity of that component.

The second conclusion is important, because the variation of $[\Sigma Si]$ is plainly not inversely proportional to the square of the oxygen activity in the system, as would accord with the accepted constant. Nor can the inconstancy be corrected by any simple adjustment of an activity coefficient for ΣSi. Total dissolved silicon therefore apparently comprises more than one silicon-containing component having appreciable magnitude.

The inapplicability of ΣSi values to mass-action calculations is illustrated in Fig. 7. Two sets of the most dependable data obtained at 1600° were selected—one for a low value of [FeO] and the other for a high value. From each set of data, K'_{Si} was separately calculated in the usual manner; and two values were obtained that differed about fivefold. Each value for K'_{Si} was then used to plot a curve showing the equilibrium relationships of [FeO] and [Si] based upon that respective single value and the currently accepted X^2Y relationship. These curves are shown in Fig. 7 along with the experimental curve for 1600°C.

It seems that some fundamental and as yet unidentified factor invalidates the usefulness of K'_{Si} of any magnitude as long as the total concentration of [Si] is substituted for its activity. The calculated curves are symmetrical and of the common X^2Y type, but the experimental curve is skew and intersects both of the others.

These curves have interest for the steelmaker, because the upper curve is approximately that of Darken[18] and contemporary investigators. For example, to reduce FeO to 0.03 weight per cent, a residual silicon of 0.60 weight per cent would be required according to the upper curve; whereas by experiment it was found that 0.18 weight per cent Si is sufficient. Again, to reduce [FeO] to 0.007 weight per cent, a residual silicon content of 11.4 weight per cent would be required according to the upper curve; whereas only 2.30 weight per cent is necessary, according to experiment. In a similar manner, the upper curve shows that one tenth per cent of residual silicon signifies that [FeO] has been reduced only to 0.075, but experiment shows that FeO is reduced instead to 0.045.

Silicon might conceivably exist dissolved in the melt (1) as the element, (2) as iron silicide, (3) as silicon hydride, or (4) as a silicate or oxide of silicon.

Iron Silicide.—The most logical form, *iron silicide, can very fortunately be dismissed immediately*, because the quantity of silicide would necessarily increase with increasing

silicon content in the iron. But, the curve would then trend toward ΣSi contents that are higher, not lower, at low [FeO] contents than is required by the mass-action expres-

Because all melts were made in the presence of excess silica, the solubility of SiO_2 must have been a constant for a given temperature. The unimportance of SiO_2
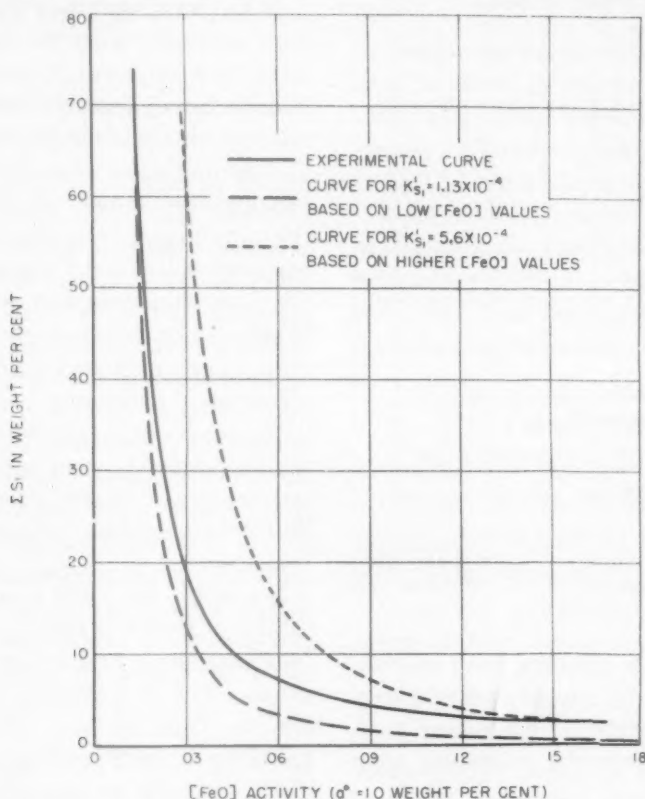
FIG. 7.—SECTION OF 1600° CURVE FROM FIG. 5 WITH TWO SUPERIMPOSED CURVES BASED ON K'_{Si} CONSTANTS CALCULATED FROM EITHER END OF EXPERIMENTAL CURVE, ILLUSTRATING INAPPLICABILITY OF ΣSi VALUES FOR MASS-ACTION CALCULATIONS.

sion. This effect is exactly opposite to the one required. As a matter of fact, the results of the present research may dispute the measurable existence of iron silicide in liquid iron.

Silicon Hydride.—Nothing has been found to justify the assumption of dissolved silicon hydride.

Silica.—Silica is occasionally regarded as being insoluble in liquid steel. That is, of course, incorrect, for some solubility is demanded by simple chemical principles. The question is rather whether the solubility has sufficient magnitude to warrant consideration.

solubility then immediately follows from the fact that total silicon analyses, which must include the $[SiO_2]$ increment, became less than 0.01 weight per cent at all temperatures investigated when [FeO] neared saturation.

Silicates.—Oxide complexes can hardly account for the discrepancy under consideration. The equation for the formation of the most common of these complexes

$$\cdot\ 1,2[FeO] + [SiO_2] = [(FeO)_{1.2}(SiO_2)]$$
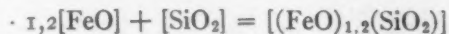
demands that the solubility of the complex increases with increasing [FeO] if the $[SiO_2]$ is kept constant. No such increment can

exist with a maximum value of more than a few thousandths of a weight per cent, because the experimental curve *decreases* with increasing FeO to a *total* silicon value of that amount.
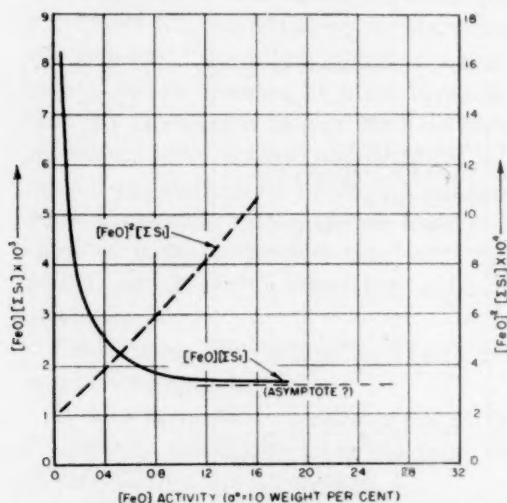
FIG. 8.—PLOT SHOWING VARIATION WITH [FeO] OF THE PRODUCTS $[FeO]^2[\Sigma Si]$ AND $[FeO][\Sigma Si]$.

Silicon Monoxide.—There is no thermodynamic reason why oxygen in liquid steel cannot be considered as [O] rather than [FeO], in which case the commonly used equation:

$$2[Fe] + [SiO_2] = 2[FeO] + [Si]$$

becomes

$$[SiO_2] = 2[O] + [Si]$$
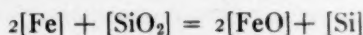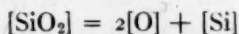
This equation represents the dissociation of SiO_2 dissolved in steel. In the presence of excess SiO_2, $[SiO_2]$ is constant at constant temperature and $[O]^2[Si]$ must be a constant, which proves the validity of the constant K'_{Si}. However, the dissociation of dissolved SiO_2, in a strictly chemical sense, may be expressed alternatively as two equations:

$$[SiO_2] = [SiO] + [O]$$
$$[SiO] = [Si] + [O]$$
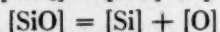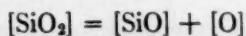
somewhat analogous to the dissociation of

sulphuric acid in water, wherein HSO_4^- is produced. This, of course, implies at least a transitory existence for the compound silicon monoxide.

It has been explained that $[\Sigma Si]$ does not vary inversely with the square of [FeO]. According to the equations for the stepwise dissociation of dissolved SiO_2, a square-root relationship could not be expected. Instead, a combination of square-root and linear relationships should obtain, representing the two stages in the oxidation of Si to SiO_2; and predomination of one relationship over the other should depend upon the range of oxygen pressures being considered. Calculations based on various exponents and combinations of exponents to correspond with numerous possible suboxides and protoxides of silicon failed to show agreement with the experimental values except when the simplest assumption—that of the monoxide—was used.

However, the first-power product of $[\Sigma Si]$ and [FeO] was found to be very nearly constant over a long range of high oxygen values. The calculations are plotted in Fig. 8. There it may be seen that the solubility product based upon the square of [FeO] changes continually and without indication that an end point will ever be reached. On the other hand, products based upon the first power of [FeO] rapidly approach what appears to be an asymptote; and over a long range of high oxygen values a monoxide relationship seems to predominate sufficiently so that the product of total silicon and [FeO] is approximately a constant.

The hypothesis is therefore advanced that SiO may exist in steel at steelmaking temperatures. That it does not exist at room temperature, but decomposes according to

$$2SiO = SiO_2 + Si$$
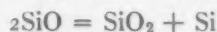
as indicated by the work of Baumann,[19] is no argument against its existence at higher temperatures.

Indeed, metallurgists freely recognize that the oxides of Fe and Mn dissolved in the steel bath are FeO and MnO. It seems logical to admit the possibility that Si, also, may be there in a lower state of oxidation than SiO_2.

Resolution of the Silicon-oxygen Equilibria in Liquid Iron

Fractionation of $[\Sigma Si]$.—The close inverse relationship between $[\Sigma Si]$ and the first power of [FeO] shown in Fig. 8 seems to imply that silicon monoxide is concerned exactly as predicated by the foregoing equation for stepwise dissociation of SiO_2 in iron. Such an approximately linear relationship could result from a concentration range wherein the silicon increment in the form of the monoxide predominated, for SiO would require only one more oxygen atom to form SiO_2 instead of the two required to oxidize Si. That the constancy occurs in the high-oxygen range carries an obvious significance, for the monoxide is a semi-oxidized form. The equation for oxidation of the monoxide would be:

$$[SiO] + [O] = [SiO_2]$$

or

$$[SiO] + [FeO] = [SiO_2] + [Fe]$$
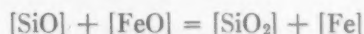
If such a reaction takes place, and if it is the only important reaction besides the oxidation of Si to SiO_2, the system can be solved mathematically by simultaneous equations, as will now be shown.

In the present work, $[SiO_2]$ is a constant at constant temperature, for reasons already given. Then the product of [SiO] and [FeO] must be a constant:

$$[SiO][FeO] = K_{SiO}$$

Total silicon values, which are determined experimentally, can then be considered to comprise for the most part several fundamental fractions:

$$[Si], [SiO], [SiO_2]$$

The Si_{SiO_2}* increment has been proved negligible in comparison with the other two. Therefore

$$[\Sigma Si] \approx [Si] + [Si_{SiO}]$$

As will be shown, the SiO_2 increment can later be solved by approximation after [Si] and [SiO] have been obtained; consequently, all three components [Si], [SiO], and $[SiO_2]$ can ultimately be known

Mathematical Analysis for [Si] *and* [SiO]. Mathematically, the problem is to divide a summation $[\Sigma Si]$ into two components [Si] and [SiO] whose functions are expressed by the following equations:
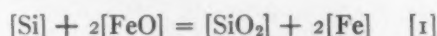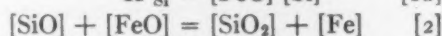
$$[Si] + 2[FeO] = [SiO_2] + 2[Fe] \quad [1]$$
$$K'_{Si} = [FeO]^2[Si] \quad [1a]$$
$$[SiO] + [FeO] = [SiO_2] + [Fe] \quad [2]$$
$$K_{SiO} = [FeO][SiO] \quad [2a]$$

Equilibrium values for [FeO] and [Si] + [SiO]($= [\Sigma Si]$) are known from the research.

From Eq. 2a an expression for [SiO] in terms of [FeO] can be derived:

$$[SiO] = \frac{K_{SiO}}{[FeO]}$$

Accordingly, for each $[FeO]_i$ there must be an $[SiO]_i$ such that:

$$[FeO]_a[SiO]_a = [FeO]_b[SiO]_b$$
$$= \cdots [FeO]_i[SiO]_i = K_{SiO}$$

and from this relationship K_{SiO}^x, which is unknown, may be eliminated by expressing ith values of [SiO] in terms of one voluntarily selected [SiO] value—$[SiO]_a$—and the corresponding known value of [FeO]:

$$[SiO]_i = \frac{[SiO]_a[FeO]_a}{[FeO]_i} \quad [2b]$$

By the arbitrary definition of $[\Sigma Si]$, Eq. 1a may be written:

$$K'_{Si} = [FeO]^2[[\Sigma Si] - [Si_{SiO}]]$$

* In the following discussion these compounds having silicon increments will always be expressed in terms of Si, or as mol per cent. In either case the expression for Si_{SiO}, for example, will be numerically equal to SiO, and the two may be used interchangeably.

The following equations can then be arranged to incorporate the experimental data obtained at different positions along the curve:

$$[FeO]_a^2[[\Sigma Si]_a - [Si_{SiO}]_a] = K'_{Si}$$
$$[FeO]_b^2[[\Sigma Si]_b - [Si_{SiO}]_b] = K'_{Si}$$
$$\cdots\cdots\cdots\cdots\cdots\cdots$$
$$[FeO]_i^2[[\Sigma Si]_i - [Si_{SiO}]_i] = K'_{Si}$$

These equations can be solved simultaneously by inserting the respective values for [FeO] and [ΣSi] and by substituting for [Si$_{SiO}$] according to Eq. 2b.

The value for [Si$_{SiO}$]$_a$ is thereby obtained, and from that basic value all other values for [SiO] immediately follow from Eq. 2b.

When [SiO] values are known, corresponding [Si] values follow from the arbitrary definition for [ΣSi].

Solubility of SiO$_2$.—The relationships of [Si] and [SiO] just postulated permit obtaining extrapolated or interpolated values for [ΣSi] at any point up to the solubility limit of [FeO]. If an extrapolation is made toward that limit, the difference between the extrapolated value, which represents the sum of [Si] and [SiO], and the corresponding experimental value for [ΣSi] may be used as an approximation for the solubility of SiO$_2$ in liquid steel.

On this assumption the following values for [SiO$_2$] result:

Approximate Solubility of SiO$_2$ *in Terms of* Si

1550°	0.001 weight per cent
1600°	0.003 weight per cent
1650°	0.005 weight per cent

Equilibrium Constants.—The total silicon analyses have now been broken down into three components: [Si], [SiO], and [SiO$_2$], of which only the first two are quantitatively important.

From the data plotted in Fig. 5, the equilibrium constants in Eqs. 1a and 2a can be calculated. They are:*

---

* Calculations are based upon weight per cents because no additional accuracy can be gained by using mol per cents when the solution is so dilute. Accuracy greater than ±10 per cent is not claimed.

Equation	1550°	1600°	1650°
$K'_{Si} =$ $\dfrac{}{[FeO]^2[Si]}$	0.42×10^{-4}	0.95×10^{-4}	2.15×10^{-4}
$K_{SiO} =$ $\dfrac{}{[FeO][SiO]}$	13×10^{-4}	25×10^{-4}	48×10^{-4}

From these figures, silicon appears to be a much stronger deoxidizer than is commonly supposed.

Equilibrium Curves.—The integrated silicon-oxygen relationships in liquid iron at 1550°, 1600°, and 1650°C. are presented in Figs. 9, 10, and 11, respectively. The solid lines are the experimental curves for total silicon; and the total silicon is in turn subdivided into the fractions of silicon that exist in the steel as Si, SiO, and SiO$_2$. The solubility of SiO$_2$ is comparatively so negligible that it can only be indicated by an arrow at the side of the graph. The corresponding curves of Körber and Oelsen are also shown for comparison. The curves coincide with Körber and Oelsen's at high oxygen values. In fact, in the range of oxygen contents common in steelmaking, most work agrees closely. The most serious discrepancy exists in the low [FeO] range.

If the erroneous assumption is made that [ΣSi] = [Si], then, because [FeO]^2[Si] must be a constant, other equilibrium values can be extrapolated along an X^2Y-type of curve. The disagreement at low [FeO] values has usually been obtained, but overlooked.

Equilibrium among Si, SiO, and SiO$_2$.—Examination of the [Si] and [SiO] curves in Figs. 9, 10, and 11 reveals a logical behavior. Both Si and SiO are reduced forms, so both must increase as [FeO] decreases. Because Si is a more reduced form than SiO, one should expect low oxygen pressures to favor Si over SiO, just as either form would be favored over SiO$_2$. Accordingly, under highly reducing conditions [ΣSi] comprises principally [Si], in spite of the fact that [SiO] is also at its maximum. With increasing oxygen pressure, both [Si] and [SiO] decrease, but [Si] decreases so much more rapidly that at high values for

FIG. 9.—SILICON-OXYGEN EQUILIBRIA IN LIQUID IRON AT 1550°C.

FIG. 10.—SILICON-OXYGEN EQUILIBRIA IN LIQUID IRON AT 1600°C.

[FeO] the relationship between [Si] and [SiO] has reversed and [SiO] is the predominating form. Quantitative curves for

might be interesting to speculate on this in relation to the amount of silicon necessary to kill a steel.

FIG. 11.—SILICON-OXYGEN EQUILIBRIA IN LIQUID IRON AT 1650°C.
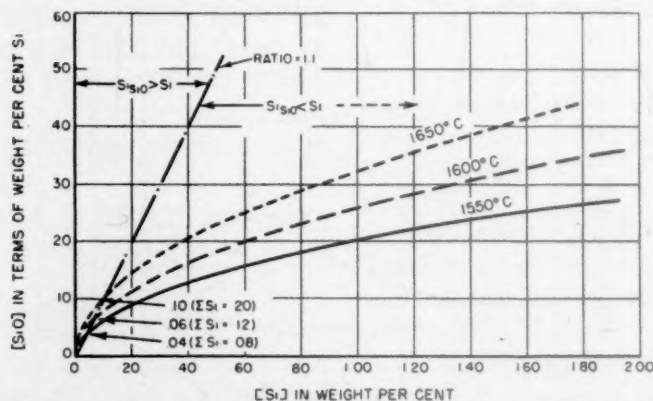
FIG. 12.—PLOT OF QUANTITATIVE RELATIONSHIPS BETWEEN [Si] AND [SiO] ACCORDING TO PRESENT INVESTIGATION.

[Si] and [SiO] therefore cross, as illustrated in Fig. 12. It is interesting to observe in that figure that silicon-killed steel containing 0.10 to 0.20 residual silicon probably has about half of that silicon in the semi-oxidized state—that is, as silicon monoxide —according to the present calculations. It

These relationships of [Si] and [SiO] can be expressed in the form of an equation:
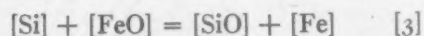
$$[Si] + [FeO] = [SiO] + [Fe] \qquad [3]$$

which is an equilibrium expression and represents the first stage in the oxidation of [Si] to $[SiO_2]$. The equilibrium constant:

$$K'_{SiO} = \frac{[Si][FeO]}{[SiO]} \qquad [3a]$$

can be calculated directly from the constants K'_{Si} and K_{SiO} by the relationship:

$$K'_{SiO} = \frac{K'_{Si}}{K_{SiO}}$$

Another expression for this equilibrium does not involve [FeO]:

$$[Si] + [SiO_2] = 2[SiO] \qquad [4]$$
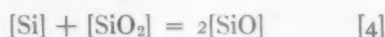
and depicts directly the balance among the reduced and oxidized forms of silicon dissolved in liquid iron. That equation is a direct analogue of the one for the carbon-oxygen equilibrium:

$$[C] + [CO_2] = 2[CO]$$
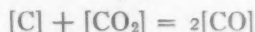
Carbon and silicon are two of the best known analogues in the Periodic Table.

The mass-action constant for Eq. 4

$$K_{Si\text{-}O} = \frac{[Si]}{[SiO]^2} \qquad [4a]$$

can also be calculated from the constants K'_{Si} and K_{SiO} by the relationship:

$$K_{Si\text{-}O} = \frac{K'_{Si}}{(K_{SiO})^2}$$

The values for these two constants are as follows:

Equation	1550°	1600°	1650°
$K'_{SiO} = \frac{[Si][FeO]}{[SiO]}$	0.032	0.038	0.045
$K_{Si\text{-}O} = \frac{[Si]}{[SiO]^2}$	25	15	9

Consideration of Silicon Monoxide

The agreement of the present hypothesis with so many experimental observations of silicon and oxygen in steel can hardly be fortuitous. Although silicon monoxide has not been considered in steelmaking reactions, the compound has been discussed, prepared, and then identified over a period of more than half a century.[20] The evidence for the existence of SiO at steelmaking temperatures seems deserving of full consideration.

The position of the present research in regard to SiO may be presented in three statements:

1. The data necessitate, for their use in the mass-action expressions, the presence of an unidentified increment of silicon in the steel; and that increment must increase with decreasing [FeO].

2. The relation of that increment to [FeO] is linear and inverse and corresponds to the thermodynamic requirements for dissolved silicon monoxide.

3. Based on the assumption that the increment is SiO, calculations immediately provide a solution that is unique and that requires no adjustment of activity coefficients.

Thermodynamic Properties of the System

In the present research four principal equations depict the reactions of greatest interest:

$$[Si] + 2[FeO] = [SiO_2] + 2[Fe] \qquad [1]$$
$$[SiO] + [FeO] = [SiO_2] + [Fe] \qquad [2]$$
$$[Si] + [FeO] = [SiO] + [Fe] \qquad [3]$$
$$[Si] + [SiO_2] = 2[SiO] \qquad [4]$$
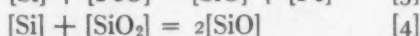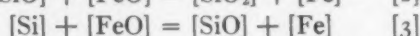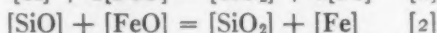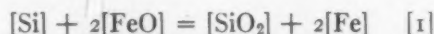
These are listed in the order in which they have already been discussed. The first equation is commonly discussed and synoptically expresses the oxidation of [Si] to [SiO_2]. Eqs. 2 and 3 treat the process in its two integral steps: [SiO] to [SiO_2] and [Si] to [SiO]. The last equation delineates the dissociation of silicon monoxide in liquid iron and shows the relationship among the three dissolved components of silicon.

The equilibrium constants for these reactions have been determined for 1550°, 1600°, and 1650°C.; they are plotted in Fig. 13 as functions of temperature. These constants can also be expressed mathematically as functions of temperature:*

---

* T in all these equations refers to deg. K.

$K'_{Si} = [FeO]^2[Si]$:

$$\log K'_{Si} = -\frac{25{,}250}{T} + 9.46 \quad [1a]$$

$K_{SiO} = [FeO][SiO]$:

$$\log K_{SiO} = -\frac{20{,}690}{T} + 8.46 \quad [2a]$$

Information in those figures permits several conclusions to be drawn. First, the reaction of metallic silicon with dissolved FeO is the most energetic of the group. Secondly, dissolved silicon monoxide likewise reacts strongly with [FeO], but with
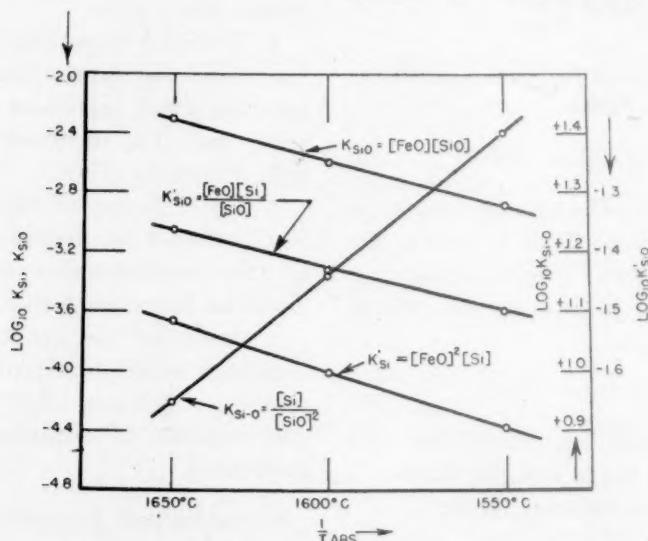
FIG. 13.—PLOT SHOWING VARIATION OF EQUILIBRIUM CONSTANTS WITH TEMPERATURE.

$K'_{SiO} = \dfrac{[FeO][Si]}{[SiO]}$:

$$\log K'_{SiO} = -\frac{4{,}560}{T} + 1.00 \quad [3a]$$

$K_{Si-O} = \dfrac{[Si]}{[SiO]^2}$:

$$\log K_{Si-O} = +\frac{16{,}130}{T} - 7.45 \quad [4a]$$

From the relationship:

$$\Delta F^\circ = -RT \ln K = -4.575 T \log K$$
$$= \Delta H - T\Delta S^\circ$$

the thermodynamic properties of the system, shown in Table 5, can be obtained.

less vigor than does metallic silicon. Such an observation is consistent with the difference to be expected from consideration of the two forms. Thirdly, metallic silicon reduces [FeO] more avidly than the iron reduces [SiO]. Phrased differently, [SiO] has a lower dissociation pressure than does [FeO] and is therefore more stable and less easily affected by deoxidizers in the liquid iron than is [FeO]. Lastly, at 1600°C. [SiO] dissociates to form a predominance of [Si] and [SiO₂]. Higher temperatures favor [SiO], and at about 1900°C. K_{Si-O} becomes unity.

Note on Total Oxygen Content of Steels

The conception of a dissolved monoxide carries with it an implication not recognized in the literature on steelmaking, yet one that seems of some practical importance. Thus, Eq. 2 states that, when oxygen dissolved as [FeO] diminishes, oxygen dissolved as a monoxide of the deoxidizing element increases. If this is correct, the

TABLE 5.—*Thermodynamic Properties*

Equation	ΔF°	ΔF° at 1600°C., Cal.	ΔH,[a] Cal.	ΔS°[a] Cal. per Deg.
1	$-115{,}500 + 43.3\,T$	$-34{,}500$	$-115{,}500$	-43.3
2	$-94{,}650 + 38.7\,T$	$-22{,}000$	$-94{,}600$	-38.7
3	$-20{,}860 + 4.58\,T$	$-12{,}300$	$-20{,}900$	-4.58
4	$+73{,}800 - 34.1\,T$	$+10{,}000$	$+73{,}800$	$+34.1$

[a] Values assumed constant 1550° to 1650°C.

total oxygen content of "deoxidized" steels cannot decrease regularly to some end point near zero, but instead must follow some type of reversed curve. That curve would decrease from high [FeO] values to some minimum, beyond which it would

cast iron, pig iron, and steel high in Mn, Si, and C. Chipman's vacuum-fusion analyses, listed earlier, show regularity on a plot except for Nos. 3, 5, and 6; and, when plotted as total oxygen versus the oxygen activity as determined by the atmosphere
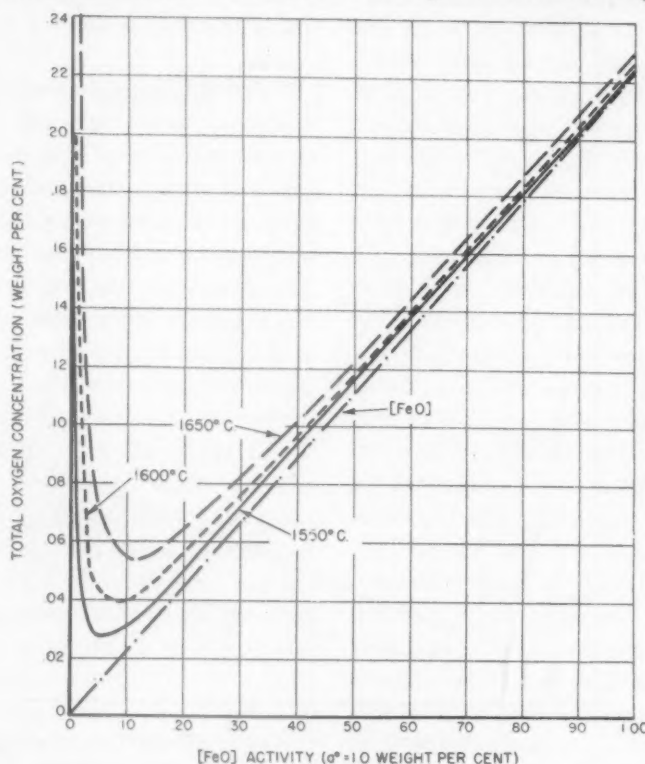
FIG. 14.—CALCULATED CURVES FOR SYSTEM Fe-Si-O-H SHOWING VARIATION OF TOTAL DISSOLVED OXYGEN IN STEEL WITH OXYGEN PRESSURE, OR ACTIVITY OF [FeO].

Total oxygen concentration:

$$c_O = \gamma_1 a_{FeO} + \gamma_2 a_{SiO} + 2c_{SiO_2}$$

where $\gamma_1 = 1$ (known),

$\gamma_2 = 1$ (assumed),

$c_{SiO_2} =$ constant for each temperature (values approximated)

again ascend, and in degree depending upon such factors as activity coefficients and solubility limits. Total oxygen curves calculated for the present system are shown in Fig. 14.*

Although these curves lack direct verification, they may account for many observations regarding so-called "anomalous analyses" showing large oxygen values for

for the experiment, they lie along a curve of the type shown in Fig. 14. In addition, the Battelle analyses of ferrosilicon and silicon extend the reversed curve as postulated, though to a lesser degree. (See Fig. 15.)

One wonders whether vacuum-fusion values may not perhaps be faulty for steels and irons having low oxygen pressures. One might question whether vacuum fusion in a graphite crucible extracts all the oxygen from certain steels; for, once an alloying element such as carbon or silicon is added to

* One must recognize that the curves in Fig. 14 are calculated equilibrium values for the particular system Fe-Si-O-H, and need not apply to steels made under other conditions.

the iron, the solvent is no longer iron, but an alloy of iron with an element that has a high affinity for oxygen.

Vacuum-fusion analysis depends on the reaction of carbon with oxygen and oxides mated by cast iron, give off appreciable CO when melted in a graphite crucible? Its activity is the same as that of the crucible in respect to carbon. The only CO that would effuse would be that which diffused
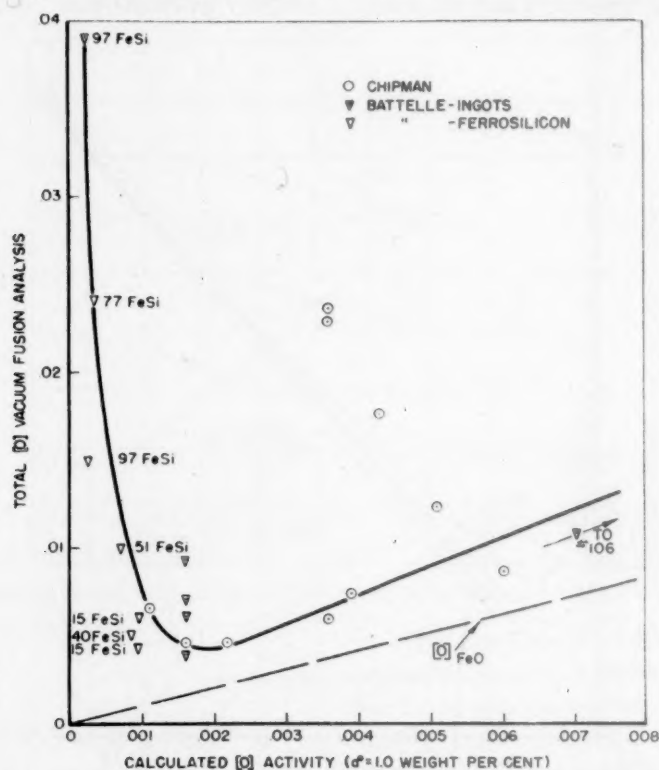
FIG. 15.—PLOT OF VACUUM-FUSION ANALYSES FOR OXYGEN, SHOWING CONFORMATION TO REVERSED CURVE POSTULATED IN PREVIOUS FIGURE.
Ferrosilicon analyses assigned estimated [FeO] activities.

in the sample. The vacuum *per se* is extremely inefficient in removing dissolved gas if a bubble, or gas phase, does not form within the specimen. The idea of "sucking" out a dissolved gas is a misconception. A dissolved atom can only respond to a concentration gradient; consequently, the only effect of a vacuum, in the absence of a gas-forming reaction in the specimen, is to decrease the surface concentration so that diffusion to the surface will be more rapid. In vacuum-fusion analysis it has been observed that little gas is obtained after the visible reaction ceases.

If a carbon reaction is necessary, why should a carbon-saturated iron, approxi-

through the surface; and the known high capacity of graphite for carbon oxide gases necessitates a "blank" correction in spite of extended degassing at temperatures above 2000°C.

The upswing at the left of the curve in Fig. 15, which gives a rough qualitative confirmation of the conclusions of this paper, can probably be explained on the basis that these data were obtained on iron-silicon alloys. In such specimens, the oxygen, after solidification, may exist partly as SiO_2,[19] which can be reduced by carbon at 1600°C. The chemical and residue methods have shown such high oxygen values for iron and steel high in carbon,

silicon, and manganese that they have been discredited in favor of vacuum fusion. There has always been the suspicion, of course, that the higher values obtained by extraction methods were caused by oxidation of Si or Fe during extraction. Perhaps they should be re-examined before they are discarded.

The foregoing discussion is intended in no wise to discredit vacuum fusion as a useful tool for steel analysis. There is no reason to believe, for example, that oxygen analyses for steels containing 0.10 per cent or more of FeO (to the right of the low point of the curve in Fig. 14) are not consistent and reproducible. The reservation is held, however, that there may be a small residue that is not extracted. For absolute values, then, a small, and possibly constant, correction would be necessary. On the other hand, there is some reason to question the validity of vacuum-fusion results on irons containing large quantities of deoxidizing elements; and, until these doubts are resolved, such results can hardly be held adequate either to verify or to refute the main premise of this paper.

Note on Equilibria of Other Systems

The line of thought in the discussion may point a way to settling difficulties in the study of systems of other deoxidizers. The product [FeO][C] is notably variable, just as is its analogue [FeO]^2[Si]; but an adjustment for the solubility of CO similar to that for SiO could possibly meet the difficulties.

Similarly, the system Fe-Mn-O seems in need of clarification. The distribution ratio, widely discussed in relation to slag-metal equilibria, as (MnO)/[Mn], would be more properly applied to (MnO)/[MnO], possibly with interesting consequences in view of the present results.

Conclusions

From the foregoing, the authors draw the following conclusions:

1. Previous investigations on the system Fe-O-Si at steelmaking temperatures have produced data that are in disagreement. This appears to be because the equilibria cannot be expressed simply as [FeO]^2[Si].

2. Uncorrected total analyses for oxygen and silicon in steel are inapplicable to mass-action calculations. Furthermore, by controlling the silicon-oxygen equilibria by oxygen pressures, or activities, one may reproduce any result previously reported for this system, for [FeO]^2[ΣSi] is also not a constant. The reported magnitude of K'_{Si}, consequently, has depended principally upon the range of oxygen pressures in which each investigator worked.

3. Expressing [FeO] in terms of activities is not sufficient in itself; and [ΣSi] must in turn be corrected before it can be applied to mass-action calculations. A direct method for determining the activity of Si, however, is not yet available.

4. Simple graphical and mathematical manipulations indicate that there is only one important increment of silicon in the steel besides [Si]. That increment must vary linearly and inversely with [FeO]. Iron silicide as a factor is quickly eliminated. SiO$_2$ must dissolve in the steel, but its importance from a quantitative standpoint seems minor.

5. On that basis, the equation [FeO] + [SiO] = [SiO$_2$] + [Fe] fulfills the requirements of the increment and satisfies the data. No corrective activity coefficient need be applied. Furthermore, the explanation is unique. No alternative explanation involving silicides, hydrides, silicates or other oxides is either necessary or acceptable, as can be shown. The equation is reasonable, for it expresses the solution of SiO$_2$ in liquid steel as a stepwise process: [SiO$_2$] = [SiO] + [O] and [SiO] = [Si] + [O], which has common analogies in other chemical reactions. The analogy to the carbon-oxygen equilibrium is especially significant because carbon and silicon are so similar chemically.

6. The existence of silicon monoxide in liquid iron is accordingly a plausible assumption. The only alternative is that the activity coefficient of silicon in liquid iron is some complicated function introducing a corrective factor that is both rapidly variable with concentration and unreasonably large in magnitude.

7. SiO has been discussed and identified by electrochemists and physicists over the course of half a century, but the compound seems to have received no mention in metallurgical literature.

8. Based upon the assumed existence of [SiO], the equilibria for the Fe-O-Si system have been redetermined. The constant K'_{Si} is a smaller value than those previously determined by experiment and closely approaches some previously derived theoretical values. Silicon diminishes [FeO] to a value that is only a small fraction of that ordinarily assumed and approaches aluminum as a deoxidizer, from the standpoint of oxygen pressures. Conversely, to reduce [FeO] to some given value, roughly only a tenth of the residual [Si] usually thought to be required becomes necessary on this basis. (The distinction between Si and ΣSi must be noted here.)

9. For the four more important reactions:

$$[Si] \ + 2[FeO] = \ [SiO_2] + 2[Fe]$$
$$[SiO] + \ [FeO] = \ [SiO_2] + \ [Fe]$$
$$[Si] \ + \ [FeO] = \ [SiO] \ + \ [Fe]$$
$$[Si] \ + \ [SiO_2] = 2[SiO]$$
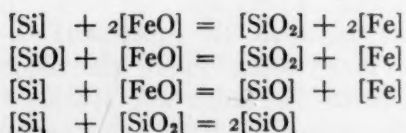
equilibrium constants, free-energy changes, heats of reactions, and entropy changes have been calculated for the temperature range of $1550°$ to $1650°C$., in a form that allows extrapolation to other steelmaking temperatures.

10. These results lead to an unusual interpretation of many steelmaking phenomena. For example, the total oxygen content of steels cannot be regarded as representing FeO, but must also be reckoned for suboxides of the alloying and deoxidizing elements. As the content of the extraneous element increases, the total oxygen content of the steel will increase, after some minimum has first been reached. The nature and degree of the increase probably depends largely upon such factors as activity coefficients and solubility limits.

11. The product [FeO][C] in the analogous system Fe-O-C may perhaps be brought into adjustment by assuming a similar variable solubility for CO.

12. The ability of vacuum-fusion analysis to obtain reliable figures for oxygen in steels containing appreciable Mn, Si, C, etc., is questionable.

13. These concepts of oxygen and oxides in steel lead to a re-evaluation of the importance of pure chemical processes in forming inclusions. Microscopic examination of specimens quenched directly from the liquid state after a long test period at $1600°C$. gave plausibility to an earlier theory that systematically occurring inclusions in steel vary in size with the rate of cooling and represent formerly dissolved components. The reservoir of oxygen afforded by the dissolved monoxide may offer an explanation for the otherwise unwarranted presence of oxide inclusions in some alloy steels or cast irons of notably low oxygen pressures.

Acknowledgment

REFERENCES

1. C. E. Sims and G. A. Lillieqvist: Inclusions —Their Effect, Solubility and Control in Cast Steel. *Trans*. A.I.M.E. (1932) **100**, 154-175; discussion, 176-195.
2. M. G. Fontana and J. Chipman: Equilibrium in the Reaction of Hydrogen with Ferrous Oxide in Liquid Iron at 1600°C. *Trans*. Amer. Soc. Metals (1936) **24**, 313-333; discussion, 333-336.
3. J. Chipman and A. M. Samarin: Effect of Temperature upon Interaction of Gases with Liquid Steel. *Trans*. A.I.M.E. (1937) **125**, 331-345.
4. F. Körber and W. Oelsen: Basic Principles of Deoxidation by Means of Manganese and Silicon. *Mitt*. K.W.I. Eisenforschung (1933) **15**, 271-309.
5. C. H. Herty, Jr. and G. R. Fitterer: The Physical Chemistry of Steel-Making: Deoxidation with Silicon and Formation of Ferrous-Silicate Inclusions in Steel. Carnegie Inst. Tech., U.S. Bur. Mines, Min. and Met. Invest. *Coop*. *Bull*. 36 (1928). 92 pages.
6. A. L. Feild: Physico-Chemical Phenomena from Melt to Ingot. *Trans*. Faraday Soc. (1925-1926) **21**, 255-267; discussion, 268-292.
7. A. McCance: Balanced Reactions in Steel Manufacture, *Trans*. Faraday Soc. (1925-1926) **21**, 176-201.
8. A. McCance: Application of Physical Chemistry to Steel-Making. Symposium on Steel-Making. Iron Steel Inst., London, Special Report No. 22 (1938) 331-371.
9. C. H. Herty, Jr., G. R. Fitterer and C. F. Christopher: Deoxidation of Steel with Silicon. U.S. Bur. Mines *Tech*. *Paper* 492 (1931). 42 pages.
10. H. Schenck: Investigations on the Chemical Reactions in the Acid Steel-Making Process and the Deoxidation of Steel with Manganese and Silicon. *Archiv Eisenhüttenwesen* (1930-1931) 4, 319-332. Also *Stahl und Eisen* (1931) **51**, 292-294.
11. H. Schenck: Physical Chemistry of the Iron-Making Processes, I. Berlin, 1932. Julius Springer. 306 pages.
12. H. Schenck: Physical Chemistry of the Iron-Making Processes, II. Berlin, 1934. Julius Springer, 274 pages.
13. A. M. Portevin and R. Perrin: Contribution to the Study of Inclusions in Steel, *Jnl*. Iron and Steel Inst. (1933) **128**, 153-172; discussion, 173-187, 443-450.
14. J. Chipman: Application of Thermodynamics to Deoxidation of Liquid Steel. *Trans*. Amer. Soc. Metals (1934) **22**, 385-435; discussion, 435-446.
15. W. Oelsen and G. Kremer: Behavior of Liquid Iron, Nickel, and Manganese in Contact with their Molten Silicates and Solid Silica at 1600°C., *Mitt*. K.W.I. Eisenforschung (1936) **18**, 89-108.
16. H. Schenck and O. Brüggemann: Investigations on the Chemistry of Acid Open Hearth Practice, *Archiv Eisenhüttenwesen* (1936) **9**, 543-553.
17. P. Herasymenko: Electrochemical Theory of Slag-Metal Equilibria, I—Reactions of Manganese and Silicon in Acid Open Hearth Furnace, *Trans*. Faraday Soc. (1938) **34**, 1245-1254.
18. L. S. Darken: Equilibria in Liquid Iron with Carbon and Silicon. *Trans*. A.I.-M.E. (1940) **140**, 204-221.
19. H. N. Baumann, Jr.: The X-ray Diffraction Examination of Material having the Composition SiO. Electrochem. Soc. Preprint No. 8-9 (1941). 3 pages.
20. C. A. Zapffe and C. E. Sims: Silicon Monoxide. *Iron Age* (1942) **149** (4), 29-31; (5), 34-39.

DISCUSSION

(Karl L. Fetters presiding)

C. B. POST AND D. G. SCHOFFSTALL,* Reading, Pa.—This paper directs attention to a perplexing problem in the melting of high-silicon steels. Steels with silicon contents over 2.00 per cent and carbons greater than 0.25 per cent have a tendency to ingot blowiness when certain precautions are not exercised during the melting of these steels. A prerequisite for sound high-silicon steels is that the bath must not be overheated at any time during the melting process, and must be tapped as cold as possible consistent with other metallurgical factors. These effects have been interpreted by steelmakers to imply that silicon loses its deoxidation properties when added in large amounts at conventional steelmaking temperatures (1550° to 1600°C.).

During the summer of 1939 we were interested in studying the equilibrium between iron, carbon, silicon and oxygen at 1550°C. Preliminary experiments were conducted in a gas-fired forced-pressure furnace, using plumbago crucibles. The melting charges averaged about 5 lb. The raw materials included electrolytic iron and ferrosilicon. Charges containing various percentages of silicon were melted down with a graphite cover on the crucible and held at a temperature of 1550°C. for ½ hr. to 1 hr. Samples of slag were balled off the surface of the melt before tap, and immediately on lifting the crucible from the furnace, an excess of aluminum wire was added, and the melt cast in a small test mold. Temperatures were held constant at 1550°C. ± 15° by means of an optical pyrometer sighted on the crucible wall when the gas was turned off. This procedure was standardized by means of a platinum-platinum rhodium thermocouple in a quartz

* Metallurgical Department, The Carpenter Steel Company.

sheath in the melt. The metal samples were analyzed for C, Si, Mn and Al_2O_3,* and the slag analyses included SiO_2, FeO, Al_2O_3 and CaO. The oxygen, analyzed as Al_2O_3 in the metallic

agreement with the data of Körber and Oelsen (referred to by Zapffe and Sims) at this temperature. At silicon contents of about 0.60 per cent the deoxidizing power of silicon reaches its
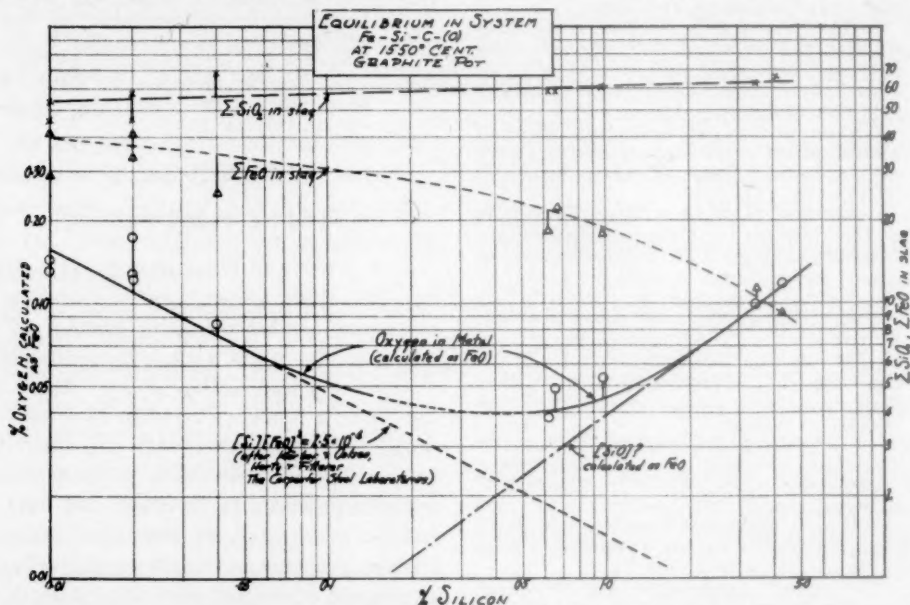
FIG. 16.—EQUILIBRIUM IN SYSTEM Fe-Si-C-(O) AT 1550°C., GRAPHITE POT.

samples, was considered to exist as FeO before the aluminum was added, and it is understood that the so-called FeO content of the metal samples was obtained only from the total Al_2O_3 content of the metal. These preliminary results are shown in Table 5, and are shown graphically in Fig. 16.

Fig. 16 shows that at low silicon contents the "equilibrium constant" $K'_{Si} = [Si][FeO]^2$ has the value 2.5×10^{-4} at 1550°C., which is in

maximum, and for silicon contents greater than this value the oxygen content increases with the silicon content.

We wish to emphasize again that these data were obtained under highly reducing conditions in a graphite crucible and are not at all indicative of what one would expect in a basic pot, such as magnesite, or in carbon-free alloys, etc.

In treating these data to find a possible explanation for this effect, the assumption can be made that the constant $K'_{Si} = [FeO]^2[Si] = 2.5 \times 10^{-4}$ holds for *ferrous oxide* and silicon in these melts, throughout a range of FeO and Si contents in liquid iron at 1550°C., and to attribute the excess oxygen, when found, to some other source of oxygen than FeO. In line with the argument of Zapffe and Sims, we can calculate this excess oxygen to SiO, as shown in Table 6.

If this excess oxygen is due to SiO, a possible chemical reaction for its formation would be

$$[Si]_{metal} + (SiO_2)_{slag} = 2[SiO]_{metal} \qquad [1]$$

and the mass-action expression for this reaction would be

$$K_{SiO} = \frac{[SiO]^2}{[Si](SiO_2)} \qquad [2]$$

---

* The Al_2O_3 content of these melts was determined in two ways:

One method is based on the color reaction of aluminum with the ammonium salt of aurintricarboxylic acid. The Al_2O_3 residue from a small sample was purified by fusion and electrolysis over a mercury cathode cell, so that the "pink" lake of the "aluminon" solution could be obtained without interference by any other element. Measurement was made by a Cenco-Sheard-Sanford photelometer.

All samples were analyzed a second time by a gravimetric method involving solution of a large sample in weak HCl. The Al_2O_3 residue was purified of hydrolyzed silicic acid and occluded aluminum by treating with a 5 per cent sodium carbonate, 10 per cent sodium citrate solution. The residue from the first filtration was stirred in this mixture for 1 hr. at 80°C. The resulting residue was purified by conventional methods before weighing as Al_2O_3.

The results of the two methods were in good agreement.

Letting $(SiO_2) = 1$ because of the silica-saturated slags in this experiment, [SiO] (as computed) should be proportional to $\sqrt{Si}$. This method of plotting the results of Table 6 is

work is needed to present an unambiguous answer to this question. It is to be emphasized that Körber and Oelsen did not find the effect in their experimental melts in silica crucibles.
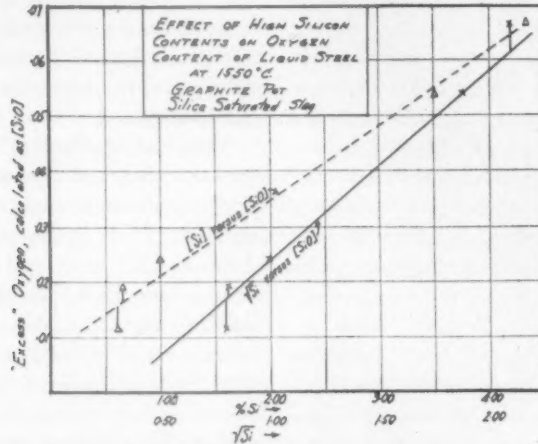
FIG. 17.—EFFECT OF HIGH SILICON CONTENTS ON OXYGEN CONTENT OF LIQUID STEEL AT 1550°C., GRAPHITE POT, SILICA-SATURATED SLAG.

shown in Fig. 17 (curve A). These preliminary data in Fig. 17 show that [SiO] (as computed) is indeed proportional to $\sqrt{Si}$, but the straight line does not pass through the origin. A linear relation also exists between [Si] and [SiO] (as calculated), as shown in Fig. 17 (curve B).

Furthermore, we believe Zapffe and Sims' comments on the vacuum-fusion method are not justified, since they call on the vacuum-fusion method to justify their conclusions in one instance (see Fig. 15) and then condemn it in other instances. We further question the prudence of resorting to thermodynamic calculations on such limited data.

TABLE 5.—*Slag-metal Analyses; Graphite Pot, Temperature 1550°C.*

Trial	Metal Analyses, Per Cent					Slag Analyses, Per Cent			
	C	Mn	Si	$\sqrt{Si}$	FeO[a]	SiO_2	FeO	Al_2O_3	CaO
1	0.116	Nil	0.01	0.10	0.142	46.2	41.3	11.7	
2	0.105	Nil	0.02	0.14	0.175	46.2	41.6	11.7	
3	0.129	Nil	0.04	0.20	0.085	64.9	24.7	8.9	
4	0.162	Nil	0.02	0.14	0.127	45.3	33.9	13.6	3.97
5	0.132	Nil	0.01	0.10	0.130	54.3	27.2	13.7	
6	0.100	Nil	0.02	0.14	0.123	58.4	20.8	17.4	
7	0.132	Nil	0.62	0.79	0.038	58.5	18.1	19.4	
8	0.120	Nil	0.66	0.81	0.049	57.4	22.2	15.9	
9	0.154	Nil	0.99	0.995	0.054	60.0	18.0	19.1	
10	0.49	0.07	4.36	2.09	0.118	65.1	9.2	15.0	7.9
11	0.24	0.03	3.52	1.88	0.098	61.5	11.5	16.9	4.5

[a] Oxygen calculated as FeO from Al_2O_3 content of metal samples.

These data lend support to the contention of Zapffe and Sims regarding the existence of SiO in liquid steel, but we are not entirely convinced that the existence of SiO is the only explanation of these effects, especially when highly reducing conditions are not present, as in iron-silicon alloys in a silica crucible. Further

TABLE 6.—*Calculation of Excess Oxygen at High Silicon Contents to SiO*

Trial	Metal Analyses, Per Cent					Calculations, Per Cent		
	[C]	[Mn]	[Si]	$\sqrt{Si}$	[FeO]	[FeO][a] from K Si at 1550°C.	Excess [FeO]	[SiO]
7	0.132	Nil	0.62	0.79	0.038	0.019	0.019	0.0117
8	0.120	Nil	0.66	0.81	0.049	0.018	0.031	0.019
9	0.154	Nil	0.99	0.995	0.054	0.015	0.039	0.024
10	0.49	0.07	4.36	2.09	0.118	0.008	0.110	0.067
11	0.24	0.03	3.52	1.88	0.098	0.009	0.089	0.054

[a] Oxygen calculated as FeO from Al_2O_3 content of metal samples.

Zapffe and Sims give the impression that their method of determining the activity of ferrous oxide in liquid steel is beyond reproach, but the *possibility* exists that the composition of the gas could be different in the high-temperature tube from that expected from dew-point measurements made only on the entry

side. The existence of possible reactions in the Sillimanite tube could be ascertained by repeating the experiment in other types of tubes, such as quartz, and making dew-point measurements on both the entry and exit sides of the high-temperature tube.

The experimental fact to date is that *sometimes* high-silicon irons and steels will show oxygen contents in excess of that to be expected from the FeO-Si equilibrium in liquid iron, and this excess oxygen increases as the silicon content increases. Further work is needed to give a clear reason for this effect, which will also enable the conditions for its existence to be specified.

H. B. FLANDERS, Hammond, Ind.—I merely wish to explain an experiment that was done while I was at the American Rolling Mill Co., which may have a bearing on the subject under discussion. In this experiment a low-carbon iron containing approximately 0.08 per cent oxygen content was treated with approximately 4 per cent silicon as ferrosilicon. The liquid iron-silicon alloy was held at approximately 2900°F. in a silica crucible and samples were taken at 5-min. intervals by allowing the metal in the furnace to run over coiled aluminum wire held in an iron spoon that was dipped into the liquid alloy. Chemical analyses for oxygen content were made by simply determining the aluminum oxide present. These oxygen contents gradually decreased from approximately 0.03 per cent at 5 min. to 0.007 to 0.008 per cent in 20 min., after which the oxygen content remained constant. Later the samples were analyzed for inclusions and found to contain 0.014 per cent SiO_2. The test was repeated with almost identical results.

G. DERGE,[*] Pittsburgh, Pa.—So much interest has been shown in the major subject of this paper that I would like to call attention to some of the side lines, which also are very important and interesting.

The photomicrographs of Fig. 3 illustrate very clearly that careful metallographic work can throw a good deal of light on the mode of formation and behavior of nonmetallic inclusions. Studies similar to those of the authors on various types of common deoxidation products

would appear desirable. The authors point out that their photomicrographs can be interpreted as indicating either the conventional coagulation theory for the formation of inclusions or the dispersion theory suggested by Sosman. I believe that a series of samples taken under various controlled rates of cooling should enable us to distinguish between these two interpretations.

The vacuum-fusion analyses reported for various grades of ferrosilicon represent a new application of vacuum fusion. I would like very much to know just what experimental procedure was followed and how reproducible the results were. In my own limited experience with similar work I found that silicon carbides formed rapidly in the vacuum-fusion crucible. This led to cracking of the crucible and distillation of silicon vapor on to the oxide refractories, and finally to high oxygen values. The difficulty can be avoided by first reducing a large amount of relatively pure iron, such as ingot iron, and dropping the ferrosilicon into this reservoir of iron.

Another important source of error is the SiO_2 formed on the surface of silicon-rich grades and the H_2O absorbed by such a surface. Reproducible results could be obtained from two samples if the surface area and surface treatment were carefully controlled. These errors could account for the results reported. If they were not considered by the authors, I do not believe the data should be used, as in Fig. 15, to support the reversed oxygen-curve argument. If these errors have been avoided, I am sure that other investigators would like to learn about the methods used.

N. F. DUFTY,[*] Wrexham, Wales.—The authors must be congratulated on their brilliant paper, which may well prove to be a landmark in the published literature on the physical chemistry of steelmaking. The aspect the writer would like to discuss is the effect of the oxygen remaining in the steel after deoxidation on the surface tension and fluidity during the pouring of the cast.

It has long been known that aluminum added to the ladle has an effect on the appearance of the steel in the molds, making it sluggish. This was formerly attributed to the formation of

* Metals Research Laboratory, Carnegie Institute of Technology.

* Assistant Manager, Electric Furnace Melting Shop, Brymbo Iron and Steel Company.

alumina by reaction either with the oxides in the steel or by atmospheric oxidation. However, on basic electric-arc furnaces it has been found that a strongly carbide slag has a similar effect. It is noticeable in the United States that ingot-steel makers favor carbide slag practice because of its supposedly superior deoxidizing properties whereas the maker of steel castings, where fluidity of the metal is of prime importance, will work under a white or neutral slag.

When making steel containing 0.7 per cent C, 0.3 Mn, 0.2 Si, 2 Cr and 0.4 Mo, the addition of aluminum or the carrying of a carbide slag has no effect early in the heat. If aluminum is added toward the end of the process, or if the slag happens to go carbide at this stage, there is a noticeable effect on the steel as it is teeming. The metal appears to be reasonably fluid in the molds but skulls badly in the nozzle, necessitating the frequent use of oxygen. If there is no excessive aluminum addition toward the end and the slag does not go carbide, the metal will teem well throughout. In some cases, when a cold cast has been tapped, there will be a heavy skull in the ladle and the steel will be sluggish and heavy in the molds but there is no appreciable skulling in the nozzle.

Temperatures taken with the quick-immersion thermocouple have shown that this is not a temperature effect, so it was naturally put down to overdeoxidation, as silicon was then assumed to be much less powerful than aluminum, and if this latter element was not used and the deoxidizing carbide slag was absent the higher residual oxygen in the steel had an effect on the surface tension and fluidity. Since it is almost conclusively proved in the paper by Zapffe and Sims that silicon is somewhere about as powerful a deoxidizer as aluminum, this hypothesis is rendered invalid.

The only alternative is that the monoxides in the steel have the power of conferring fluidity on the steel but that these are reacted on by aluminum and calcium carbide present in the slag. Have the authors any experimental or theoretical data either to confirm or deny this opinion? Their personal views on the question would be appreciated by many practical steel-makers besides the writer.

L. J. T. BROM, Cleveland, Ohio.—In my work in an iron foundry (the Frank J. Brom Machine and Foundry Co., Winona, Minn.) I have seen a reaction that could not be explained. In running a cupola-melted metal of about 3.5 per cent C and 1.1 per cent Si, we encountered at times a boiling or rimming action in the receiver ladle soon after the metal was tapped from the furnace. This reaction would persist for upward of 30 sec. (½-ton ladle) and often would be resumed after the metal was poured into smaller ladles.

It appeared that there was some liberation of oxygen from the metal as it cooled off. This could not be satisfactorily explained by the equilibrium $(C)(FeO) = K''_c$ because at this high carbon concentration there should not be enough oxygen to cause such a reaction.

Could these observed phenomena be explained by the formation of silicon monoxide and its changing equilibrium constant with the drop in temperature?

N. A. ZIEGLER,* Chicago, Ill.—I am very much interested in this paper, particularly in Figs. 14 and 15 as well as in conclusions 10 and 11, indicating that total oxygen content of a steel or cast iron may increase in a certain proportion with the increase of a third element, such as carbon.

In the iron and steel volume of the A.I.M.E. TRANSACTIONS for 1929 (vol. 84), page 444, appears my paper in which some of my early experiments on "gases in metals" are presented.

Briefly, a series of iron-carbon alloys was prepared in a magnesia-lined graphite crucible placed in a high-frequency laboratory furnace open to the atmosphere. The materials used were electrolytic iron and Acheson graphite. Each alloy, after it was completely molten, was kept in the liquid state for 10 min., cast into a small iron mold, and cooled in air to room temperature. In this way, a series of castings weighing about 1 kg. each, and ranging in carbon from 0.0038 to 4.45 per cent, was obtained. I still can remember that the alloy containing 4.45 per cent C, after it was cast in the iron mold and before it was completely frozen, effervesced like a glass of soda water.

Each of these alloys was remelted in the bell-jar vacuum furnace, the gases given off were collected and analyzed in the way previously described. High refractory porcelain crucibles were used for remelting the alloys.

---

* Research Metallurgist, Crane Company.

The surprising thing was that in low-carbon alloys, containing up to 0.0291 per cent C, a moderate amount of gases was obtained, while for the high-carbon samples the amount of gases that could be extracted was so great that it took sometimes two days to degasify them completely. From the sample originally containing 4.45 per cent C, as much as about 1 per cent of CO by weight was extracted.

The discussion of that paper was rather severe. The general opinion was that most of the gases collected and reported as coming from the metal were products of reaction of carbon of the molten sample and oxygen of the porcelain refractory crucible. Should this be true, why was it that in all cases, for low-carbon as well as high-carbon samples, a very definite end point in the degasification by vacuum melting was observed? Dr. H. W. Gillett, in discussing that paper, said: "I do not believe that Mr. Ziegler can wave a magic hand over his melt and prevent the reduction of refractory oxides by the carbon of the melt in Pittsburgh. Reduction takes place in Long Island City, in Washington and in Aachen . . . "

From reading Zapffe and Sims' paper, I begin to suspect that the magic that 14 years ago was practiced in Pittsburgh has now found at least partial explanation in Columbus, among Dr. Gillett's associates.

C. A. ZAPFFE AND C. E. SIMS (authors reply).—Post and Schoffstall add some interesting material. In regard to their and Flanders' use of the aluminum method for oxygen analysis, it should be recognized that the oxygen pressure of a steel containing appreciable SiO approaches that of Al_2O_3 itself. Consequently, one must not expect Al to take the oxygen away from SiO as easily as it does from FeO, or even from SiO_2. For total oxygen, the aluminum method must become less and less efficient as the silicon, or carbon, content increases, since either C or Si alone will actually reduce Al_2O_3. The popular tendency to divorce Al from all the principles that govern chemical reactions and to consider it an infallible deoxidizer is a misapprehension.

For the effect of Al upon dissolved SiO, the actual quantities and the equilibrium of the presumed reaction:

$$2Al + 3SiO = Al_2O_3 + 3Si$$

are not known. But we *do* know that Al can reduce SiO only down to its equilibrium concentration, whatever it is, and that a given quantity of Al added as an "excess" in the Al method must fail to deoxidize more and more SiO as the steels have higher Si contents. That conclusion follows simply from the equilibrium constant for this presumed reaction:

$$K = \frac{(Al_2O_3)[Si]^3}{[Al]^2[SiO]^3}$$

which, with Al_2O_3 as a precipitated phase, becomes:

$$K' = \frac{[Si]}{[SiO][Al]^{2/3}}$$

or simply $K'' = [Si]/[SiO]_{Al}$

if the "excess" Al added in each test is kept constant.

Who, then, can say how efficiently the aluminum method reports total oxygen in silicon steels? As a matter of fact, Flanders has just confirmed our suspicions by reporting for his aluminum-treated specimens as much O as SiO_2—which could be a dissociated precipitate representing SiO—as the total O obtained by the Al method. The literature is so crammed with the same type of observation that it is difficult to understand the complacency with which this and the vacuum-fusion method, employing carbon instead of aluminum, are used on steels containing unlimited amounts of carbon, manganese, etc., to supply values for "total oxygen." It should not be forgotten that the birth of physical chemistry for steel-making 30 years ago was enabled only by making certain assumptions, principal among which was that its application was only to dilute solutions where Henry's law could hold. The iron-oxygen system is a gas-metal system obeying strictly the laws for the absorption of gas by a liquid. When a strongly associating third element, such as all the "deoxidizers" are with respect to oxygen, is placed in that liquid as a residual, alloying entity, the total absorption *must increase* for any given gas pressure less than saturation for both systems. Such a system is no longer liable to Henry's law.

This third element, as its quantity increases, soon imposes its own solubility for oxygen upon the system. One has no right to di cuss ferro-silicon alloys upon the basis of the behavior of

oxygen in iron. Similarly, one must remember that cast iron contains from 8 *to* 20 *per cent* C (mol per cent)—not 2 to 5—if chemistry is to be applied to its reactions. Although the opinion among metallurgists seems to be that the solubility of oxygen is low in these two particular elements, chemists recognize carbon as having a phenomenal ability to occlude oxygen, and Stadeler[21] shows by extremely careful research that ferrosilicon may contain four times as much oxygen as iron will hold at saturation at 1550°C.

The chemical principles underlying the solution of oxygen in iron alloys and methods for its extraction—particularly the vacuum-fusion method—are so misunderstood and so misapplied, in our opinion, that the questions of Post, Schoffstall, and Derge will be waived for answer in a projected publication devoted to that problem. If Fig. 15, which represents the best vacuum-fusion technique at Battelle and at Dr. Chipman's laboratory for analyzing oxygen in iron-silicon alloys, should not be "used . . . to support the reversed oxygen-curve argument," then Dr. Derge is presumably with us in urging that the vacuum-fusion technique should not be used on such material to support any argument. Fig. 15 was used simply to show that even vacuum fusion responds, though feebly, to the thoroughly sound principle of the reversed curve, in rough agreement with another sound principle, which instructs us that melting iron-carbon and iron-silicon alloys in a graphite crucible under vacuum need not result in the gaseous reaction necessary for an efficient removal of dissolved CO and SiO.

For essentially the same reasons, the data of Post and Schoffstall stand as qualitative corroboration of our work only. With the aluminum method, there is the further complication of a possible aluminum monoxide,

AlO, representing oxygen dissolved in the resulting Fe-Al alloy by virtue of its aluminum content.

Dufty raises a most interesting question, but one to which there seems to be no ready answer. The varying fluidity of killed steels of the same nominal composition and temperature has been a major mystery in steelmaking. What we speak of as fluidity, of course, is an integration of several factors such as fluidity, surface tension, film formation, and freezing characteristics.

A number of explanations have been advanced to explain poor fluidity, such as tough surface films produced by the oxidation of aluminum, the presence of colloidal precipitates of silica or alumina, and dissolved gases (H and N). None of these seems to fit all cases, as noted by Mr. Dufty. One thing appears certain, however, that the fluidity is greatly influenced by the oxidation and deoxidation practice. For example, a thorough oxidation of steel preceding the deoxidation is almost assurance of good fluidity. A dead, sluggish steel can be livened up by the addition of a little iron oxide. Steel made with a prolonged treatment under a carbide slag is notorious for poor fluidity.

All these observations seem to affirm the suggestion of Dufty that the presence or absence of monoxides may be a prime factor controlling fluidity. In fact, this theory appears as plausible as any yet postulated, but confirmatory evidence is lacking.

Brom's surmise regarding the boiling in his alloy is agreeable to us, though the evolved gas was probably CO rather than oxygen. As for Ziegler, it is apparent that he truly rediscovered a fact pointed out by no less than a hundred previous authors, but still unaccepted today—that these alloys of iron with the deoxidizing elements may contain extraordinary amounts of oxygen. Unfortunately, the rebuttal to Ziegler's argument was based on a rather unanswerable point, since carbon does reduce refractories to some extent.

---

[21] A. Stadeler: The Determination of Silica Associated with the Silicon in Ferrosilicon. *Archiv Eisenhüttenwesen* (July 1930) **4**, 1–6.

Equilibria of Liquid Iron and Simple Basic and Acid Slags in a Rotating Induction Furnace

By C. R. Taylor* and John Chipman,† Members A.I.M.E.

(Cleveland Meeting, October 1942)

The study of chemical reactions of liquid steel and basic open-hearth slag involves a complex slag system of at least eight important components, and often a number of others. In initiating an experimental program on the equilibrium relationship of slag and metal, it became evident that but little progress could be expected in the interpretation of the complex slags until an understanding had been gained of the simpler liquid systems composed of a limited number of slag constituents. The simplest system that in any way resembles open-hearth slag must contain lime, silica and iron oxide.

Attempts to produce in an induction furnace slags containing only these constituents have met with serious limitations because of the solubility of refractories in the slag. Thus in acid-lined furnaces the slag is always saturated with silica and consequently contains between 48 and 63 per cent of this component. In basic-lined furnaces an undesired additional component, magnesia, is introduced to the extent of some 3 to 15 per cent, depending upon the acidity, sometimes with disastrous results to the furnace. Thus in a magnesia-lined furnace, Fetters and Chipman[1] found it impossible to prepare slags in which the ratio $(CaO + MgO)/SiO_2$ was less than that corresponding to the metasilicate (approximately 0.8:1). Between this composition and that of the true acid slags lies a field of composition about which very little is known and which cannot be explored by any ordinary means.

This circumstance, as well as the desire to study the more basic slags in the absence of magnesia, calls for the development of a method by which slags may be brought into equilibrium with molten metal without coming in contact with refractory. Such a technic has been provided by the rotating induction furnace developed by Barrett, Holbrook and Wood.[2] Three modifications of the rotating furnace were described by these authors. The first was essentially a rotating refractory cylinder containing the magnesia crucible, which was itself heated by a graphite crucible. In the second, only the magnesia crucible rotated, the cylindrical graphite heater being stationary. In the third, the coil and crucible revolved, and the metal was heated directly by induction.

Experimental Method

Furnace

The furnace used in this investigation differed from previous designs and may be considered a fourth modification of the original rotating furnace. Its essential features are shown in Fig. 1. The outer case A is a fire-clay flue liner for control of the atmosphere. The top B and base C are alberene stone. The coil supports D are of "Formica," a material formed from phe-

nolic resin and pressed paper. The driving mechanism E rotates the steel shaft F, the alberene base of the furnace G, the transite ring H, the silica tube I, and the Babcock

acts as a powerful oxidizing agent on molten iron.

The fire-clay flue liner A was cemented to the alberene base C, by means of an
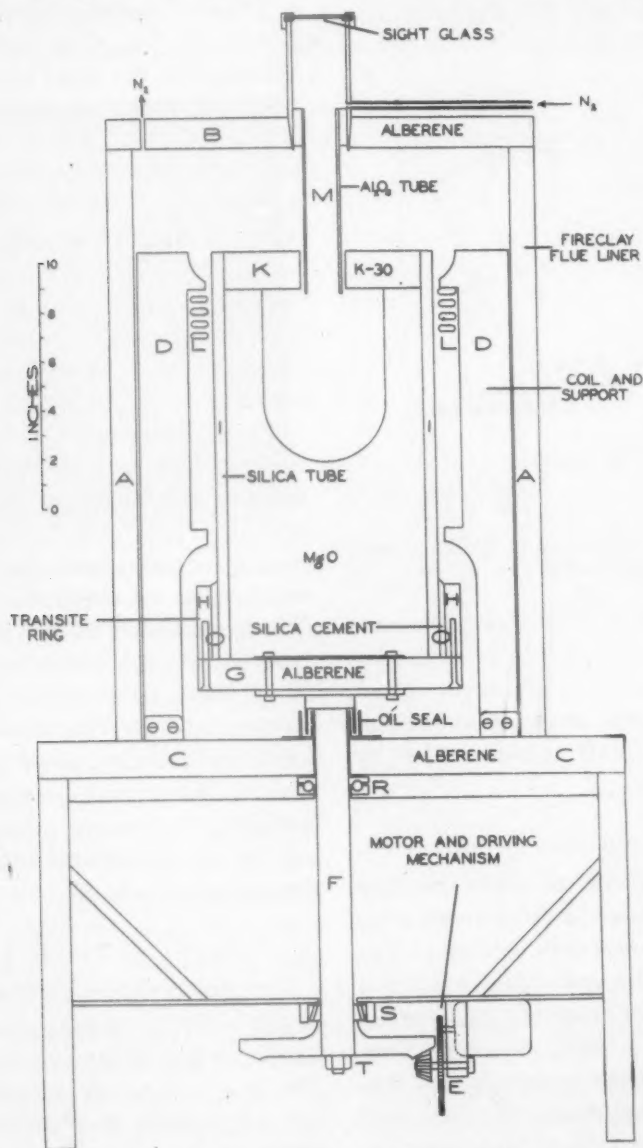
FIG. 1.—ROTATING CRUCIBLE FURNACE.

and Wilcox K-30 brick cover K. All other parts of the unit are stationary, including the coil L and the alumina entry tube M.

It was found desirable to keep the amount of transite used to a minimum, since it gives off large volumes of water vapor when the temperature is raised, and water vapor

asphalt-base cement applied with a torch. All water and power leads were brought in through the alberene base C and similarly cemented so that they were gastight. The oil-seal cup was also cemented to the alberene in this manner. The alberene top B was made gastight with the

fire-clay flue liner by means of ordinary impervious medical adhesive tape. This made a surprisingly good seal, even when the top of the furnace became fairly hot.
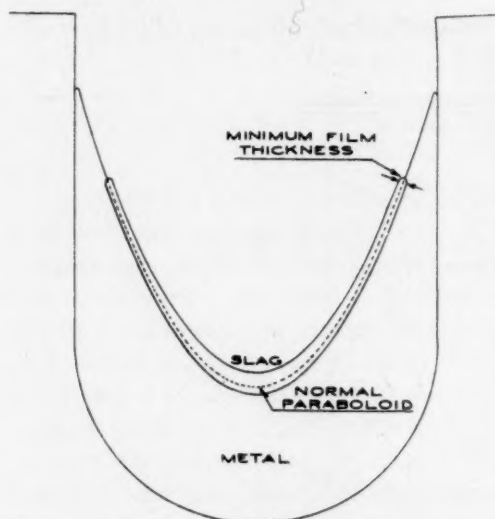
FIG. 2.—POSITION OF SLAG AND METAL DURING ROTATION.

The alignment of the silica tube is of great importance, and should be done carefully. Since these tubes are never round, they must be aligned as nearly as possible about an axis of rotation, more or less by trial and error.

CRUCIBLE

The crucible was formed inside the silica tube by packing electrically sintered magnesia around a sheet-iron cylinder. The cylinder, which was spun from ingot-iron sheet, was carefully centered, its spherical bottom resting on a bed of magnesia. Then the 60-mesh and finer magnesia sand was carefully poured around the shell and settled by tamping with a $\frac{1}{4}$-in. wire, so as not to disturb the alignment.

ATMOSPHERE

Commercial tank nitrogen was passed through a furnace containing copper wire, at about 450°C., to remove oxygen; then through ascarite and P_2O_5 to remove carbon dioxide and water. A slight positive pressure of nitrogen was maintained in the furnace.

ROTATION

The final design utilized a tapered roller bearing S (Fig. 1) at the base, and a ball bearing R at the point where the shaft goes through the alberene base C. The top race of the bearing R was welded to the shaft and the lower race was welded to two angle-iron supports, which were bolted to the frame. These supports were insulated electrically from the rest of the frame, to avoid making a completed circuit in the neighborhood of the coil. The bolt T was then tightened to take all play out of the assembly.

The motor used at first was a direct-current series-wound motor, so that the speed could be varied by means of a rheostat. This was later changed to a constant-speed alternating-current motor, which operated the furnace at 220 r.p.m. This is somewhat faster than a theoretical analysis calls for, which may be accounted for on the basis of the strong counter currents caused by the high-frequency field tending to push the metal up in the center. Considerable turbulence was present on the surface of the rotating metal, while the field was on, but it completely disappeared when the power was cut off.

ROTATING METAL SURFACE

The shape of the surface of the metal during rotation is a paraboloid, whose slope is independent of the density of the liquid.[9] The slag and metal surfaces should form two paraboloids of revolution, which are displaced along the axis of rotation of the crucible. If an infinitely thin film of slag could form, a slag layer could not be kept on the metal, since it would gradually creep up the metal walls and be absorbed by the crucible. The interfacial tension existing between the slag and the metal prevents this by establishing a minimum film thickness. This effect is shown in Fig. 2. The

slag also displaces its weight of iron, the displacement taking place normal to the paraboloid. Fig. 2 is drawn assuming that the slag has one fourth the density of the metal and that the speed of rotation is 220 r.p.m. This curve checks exactly the

FIG. 3.—SHAPE OF METAL ALLOWED TO SOLIDIFY DURING ROTATION.

actual shape of the metal, which was allowed to solidify with the power off, as is shown in Fig. 3. When the power is on, however, the induced convection currents in the metal will tend to make the parabola slightly shallower.

SLAG SAMPLING

The slags were sampled from the furnace by means of small 16-gauge ingot-iron spoons. Blanks $1\frac{3}{8}$ in. in diameter were forced through a 1-in. die to make a cup 1 in. in diameter and $\frac{1}{2}$ in. deep. These were welded to a rod and pickled before use. Some care must be taken in sampling the slag, since the layer is usually very thin. The slag and spoon were then quenched in distilled water. With care and practice, sufficient slag could be obtained with one spoon for complete analysis. These slags were analyzed for SiO_2, CaO, MgO, Al_2O_3, FeO, Fe_2O_3. Other constituents such as P_2O_5 and sulphur, being very low, were not considered in this study. Consecutive samples showed that duplicate results could be

obtained by this sampling method, and that the slags were homogeneous.

METAL SAMPLING

A drawing of the metal sampler is shown in Fig. 4. A 1-in. piece of copper rod was
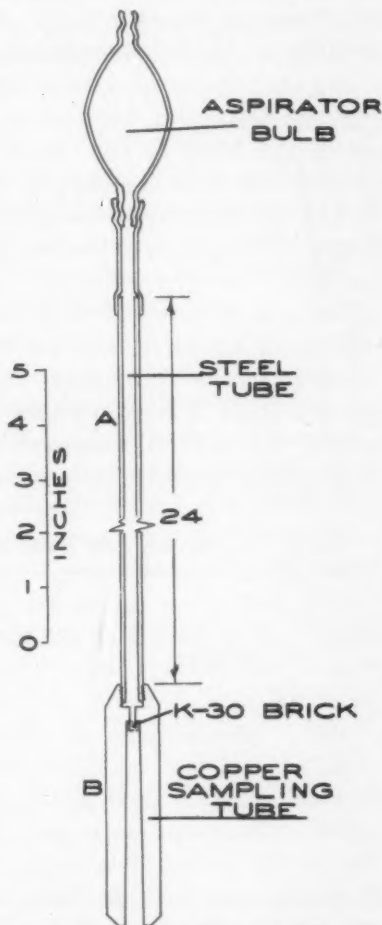
FIG. 4.—COPPER SAMPLER.

drilled axially and then reamed with a standard No. 6 tapered pin reamer. The whole length of the reamer, about $3\frac{1}{2}$ in., was used to get as long a sample as possible. The pipe A served as a handle and as a tube through which air from the sampler could be withdrawn. A plug cut from K-30 brick prevented the metal from getting up into the pipe. This plug was cut almost to size and forced into the sampler, the dust and fragments being carefully

blown out. The outside of the copper was wiped with a cloth that had a small amount of vaseline on it. This put a film of oil on the sampler, not enough to increase the carbon content of the bath, but enough to blow the slag away by gas evolution and inhibit the solidification of the metal on the outside of the sampler. The bevel at the bottom of the copper tube *B* excludes some of the slag that would have been carried down into the metal on a flat bottom. The purpose of the bevel at the top of the copper tube is to allow the sampler to be withdrawn quickly from the furnace chamber without catching on the bottom of the alumina tube.

In taking a sample, the bulb is depressed and the sampler is lowered rapidly into the melt until it strikes the bottom of the crucible; the bulb is then released and the sampler immediately withdrawn and quenched into water. After it is cool, the

of the sampler from the furnace, the outside diameter of the copper was reduced to ¾ in. for cold heats. No difficulty was experienced in sampling heats above 1590°C. The hottest heat sampled was at 1690°C.

Several samplers were tried, using holes of different diameters. The No. 7 tapered pin reamer gave a sample that had holes in it, since the metal tended to run out before it solidified. If the sampler was left in the furnace long enough to solidify, the copper usually melted in some place. The No. 6 tapered pin reamer was the most successful. A No. 4 tapered pin reamer was also tried, but the sample obtained from this proved to be inhomogeneous from end to end, so the No. 6 was used exclusively.

Table 1 shows some homogeneity results on several samples. The numbers refer to consecutive sections of the sample. In each case all the sample numbering from the top or small end was analyzed.

TABLE 1.—*Oxygen and Nitrogen Analyses to Test Uniformity of Samples*

Tapered Pin Reamer	Analysis, Per Cent						
	Constituent	1	2	3	4	5	6
No. 6.........	Oxygen	0.152	0.152	0.153	0.152	0.154	0.153
	Nitrogen	0.054	0.028	0.027	0.029	0.029	0.033
No. 4.........	Oxygen	0.297		0.274			0.265
	Nitrogen	0.032		0.027			0.040
No. 4.........	Oxygen	0.192		0.187			0.184
	Nitrogen	0.015		0.013			0.031

sample usually can be easily withdrawn from the sampler. The metal that adheres to the outside does not interfere. If the sample sticks, it can always be driven out by inserting a piece of drill rod (preferably heat-treated) through the hole in the upper end of the copper tube and hitting it a few blows with a hammer. The cold heats are much more difficult to sample, using this device, than the hot heats. With a cold heat, a ball of metal freezes immediately on the outside of the sampler, and often melts the sampler before it can be withdrawn and quenched. To facilitate removal

The erratic nitrogen values can be partly explained on the basis of the small samples taken, usually 2.5 to 3 grams. It was also found that the metal on the outside of the sampler checked that on the inside; i.e.,

	OXYGEN	NITROGEN
Inside..................	0.171	0.028
Outside................	0.173	0.020

Table 2 gives a comparison of three different sampling methods. The dipped samples were taken in the rotating furnace, and so were solidified in nitrogen. The poured samples were poured over the lip of a 12-lb.

magnesia-lined induction furnace into a cylindrical copper mold 1 cm. in diameter and about 9 cm. long.

The dipped samples show that they are all right if they do not solidify in the presence of an appreciable amount of slag. If this occurs, the sample is invariably lower than the true value for high oxygen contents.

All the poured samples were taken from iron saturated with FeO. The error apparently is a function of temperature. The postulation of two effects will explain these results. First, the liquid iron, even though saturated with FeO, will form a film of iron oxide on the surface, which will be trapped by the metal as it solidifies. This will result in an apparent increase in oxygen content. On the other hand, the metal must flow over the cold lip of the crucible, and in doing so FeO may be precipitated out on cooling. A canceling of these two factors at any temperature might agree fortuitously with the true result. At any rate, pouring the sample leads to erratic results, as does dipping, unless the metal solidifies out of contact with slag. The lower oxygen results on metal solidified in contact with slag indicate that equilibrium is attained very rapidly.

TABLE 2.—*Comparison of Sampling Methods*

Oxygen, Per Cent			Remarks
Copper Sampler	Dipped Sample	Poured Sample	
0.164	0.149		⅔ metal, ⅓ slag in spoon
0.168	0.130		¼ metal, ¾ slag in spoon
0.137	0.139		Very small amount of slag
0.143	0.125		Small amount of slag
0.150	0.142		⅟₁₀ slag, ⁹⁄₁₀ metal
0.182		0.184	1532°C.
0.192		0.212	1548°C.
0.188		0.215	1554°C.
0.234		0.237	1604°C.
0.300		0.290	1673°C.
0.327		0.299	1686°C.
0.216		0.235	No temperature

Consecutive samples were taken about two minutes apart, with the following oxygen analyses, indicating excellent reproducibility:

Heat R-26   Sample 1   0.242 ⎱ Two minute
             2   0.240 ⎰ interval

Heat R-24   Sample 1   0.170 ⎱ Three minute
             2   0.169 ⎰ interval

The sampler has since been used on larger induction furnace heats to study the oxygen content, and has proved more convenient and more accurate than other methods of sampling.

TEMPERATURES

Of the several methods that have been used in measuring temperatures of molten steel, the thermoelectric stands out as much superior to various optical methods. The use of a thermocouple at these high temperatures and in the presence of metal and slag involves numerous difficulties. In the first place, the resistivity of the refractories normally used drops to a low value, and that of the thermoelements goes up. There is considerable danger that, unless they are chosen with some care, the refractories used will exert an appreciable shunting effect on the thermocouple. In the measurement of temperatures in the presence of both slag and metal, several effects must be guarded against. Of primary importance is the possibility of contamination of the couple by iron vapor or carbon monoxide and dioxide in the furnace gases. Also, a choice must be made as to protection tubes. This may be governed by two basic factors: the rate at which the slag and metal erode the tube, and the rate at which thermal equilibrium is established.

If the temperature equilibrium is reached rapidly, the rate of erosion by slag need not become important. The problem has been attacked from both directions, but in the case of this experiment the resistance to slag and metal erosion was sacrificed to the end of obtaining rapid readings. Silica protection tubes and Norton "alundum" insulators were used throughout.

Two types of thermoelements were used, tungsten-molybdenum and platinum-10 per

cent rhodium platinum. Since the techniques of handling these differ, they will be discussed separately.

The platinum couple was first annealed by passing sufficient current through it to

FIG. 5.—METHOD OF ANNEALING TUNGSTEN-MOLYBDENUM THERMOCOUPLES.

heat it to a cherry red for about 10 min. It was sometimes possible to locate points of contamination by the difference in color while hot. The wires were then threaded through the insulators and the couple was calibrated at the melting point of pure palladium wire (1554°C.) by the method described by Foote.[3]

The usual method of calibration of the tungsten-molybdenum couple was to determine the melting point of copper, nickel, and iron, using these three points to determine constants in the equation of the parabola $mv = aT^2 + bT + C$. This calculated curve was then taken as the calibration.

The molybdenum wire (both wires were 0.020-in. diameter) was much the more ductile of the two, so in making up a thermocouple all the bending was confined to the molybdenum. The two wires of suitable length (9 in.) were placed parallel in a vise about ⅛ in. apart, and protruding about ⅝ in. The molybdenum wire was then wrapped three or four times around the tungsten wire, leaving the latter protruding ⅛ in. from the coil of molybdenum wire. The wires were then welded together with an arc welder, by momentarily striking an arc from the wires to a carbon electrode. This melted the protruding tungsten wire down over part of the molybdenum, making a good solid bead.

At first these wires were used in the same condition as received from the suppliers, but it was found that apparently they recrystallized during the measurement of the high temperatures, changing the calibration by producing an inhomogeneity in the wire at some point. This was completely remedied by annealing the wires in hydrogen for about 5 min. at a temperature close to the melting point of molybdenum (2625°C.). The annealing was accomplished as shown in Fig. 5, by suspending the couple A in a silica tube B. The weight C held the couple in position, and was attached to the thermocouple by the tungsten wire hook D. The current was gradually raised until the molybdenum wire melted. A setting somewhat below this was used for subsequent thermocouples. This treatment made the tungsten wire very fragile, so that it had to be handled with care. It was found that this annealing treatment did not affect the characteristics of the electromotive force in the zone of 0 to 100°C., so the green wire could be used as compensating lead wire.

A separate calibration had to be supplied for the annealed wire, however.

Both types of thermocouples were used in a water-cooled tube shown in Fig. 6. The tube was constructed of copper-tubing water leads A leading to the central cooling chamber B. As the silica protection tube C eroded away or failed, the end was cut off and resealed by means of an oxyacetylene torch. The silica tube was moved down, as the end had to be repaired, until it became too short to clamp when another tube was fused on.

In this way all the silica tube could be utilized. A small coupling block was used to make the connection between the couple and the lead wire. It was made of a Formica cylinder about ¾ in. long, small enough to fit into the silica tube, the electrical contact being made by a "jam" fit into two small brass tubes embedded in the Formica. The electrical contact so obtained was sufficiently good.

SOLUBILITY OF IRON OXIDE IN LIQUID IRON

The most complete work along this line was done by Herty[4] and by Körber and Oelsen,[5] whose results agree fairly closely, and by Fetters and Chipman,[6] whose solubility values are significantly lower. The results obtained in this investigation are shown in Fig. 7; they differ only slightly from those obtained by Fetters and Chipman, whose data are represented by the dotted line. The solubility of FeO in liquid iron may be expressed by the equation:

$$\log \% \text{ oxygen} = \frac{-6320}{T} + 2.734$$

as calculated by the method of least squares, T being the absolute temperature.

An effort was made to determine the reason for the discrepancy between this work and that reported by Herty, Körber and Oelsen. To check on the effect of the different sampling methods, a small 10-lb. heat was melted in air in an open magnesia

crucible. The metal was saturated with FeO, and samples were taken by the copper sampler and also by pouring a small amount of the metal into a similar sampler. Tem-
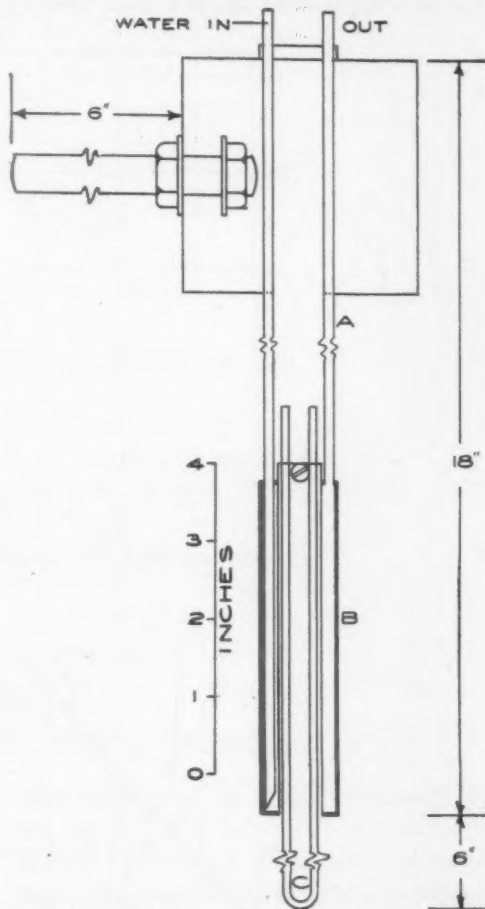
FIG. 6.—WATER-COOLED TUBE FOR TEMPERATURE MEASUREMENT.

peratures were taken with the tungsten-molybdenum thermocouple. The results are shown in Table 2. When these results were corrected for dissolved MgO, those taken with the sampler fell on the calculated line within the apparent experimental error, while those poured through the air were quite erratic. The tendency of the poured samples seemed to be for those poured at low temperatures to run high in oxygen, and for those poured at high temperatures to run low. It has been shown previously that a dipped sample will check the copper

sampler, provided the amount of slag trapped in the dipped sample is kept very low. Herty used dipped and poured samples, as did Körber and Oelsen, the latter stating that poured samples were used for high temperatures only.

taken in nitrogen could be determined. Several samples were taken from the rotating crucible furnace, while a stream of air flowed over the melt, without altering the results.
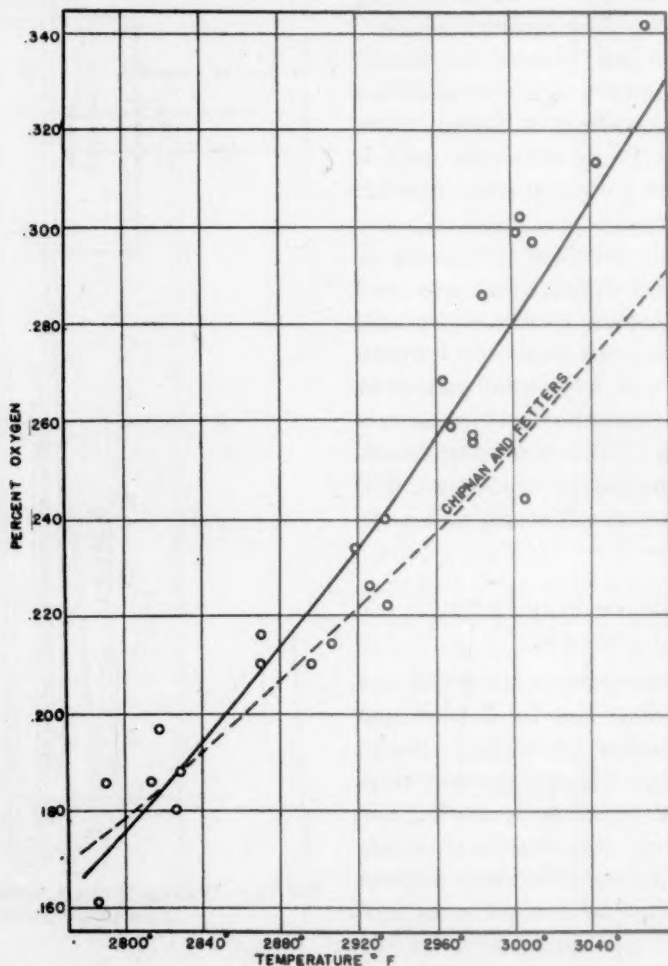
FIG. 7.—SOLUBILITY OF OXYGEN IN LIQUID IRON AS A FUNCTION OF TEMPERATURE.

high temperatures only. On the basis of this experiment, neither of the two techniques of sampling used by Herty and Körber, if properly handled, could lead to the excessively high oxygen contents reported.

The effect of atmosphere was considered next. Both Herty and Körber and Oelsen melted their heats in air. The small heat described above was also melted in air, and no significant difference from the samples

The most important variable remaining is the temperature. Six of the points on the graph in Fig. 7 were taken with a platinum thermocouple; the others with the tungsten-molybdenum thermocouples. There is no significant difference between these two types of temperature measurement as shown by solubility values. Herty says that occasionally he checked the temperature of his melts with a platinum couple. The remainder of the readings, as were all of

those of Körber and Oelsen, were taken with an optical pyrometer, which, as has been shown elsewhere, is not reliable.

Up to the present time, this difference in

system $(CaO + MgO)$-SiO_2-FeO and liquid iron. The portion of the diagram investigated is shown in Fig. 8. The lines A and B represent the approximate location of the
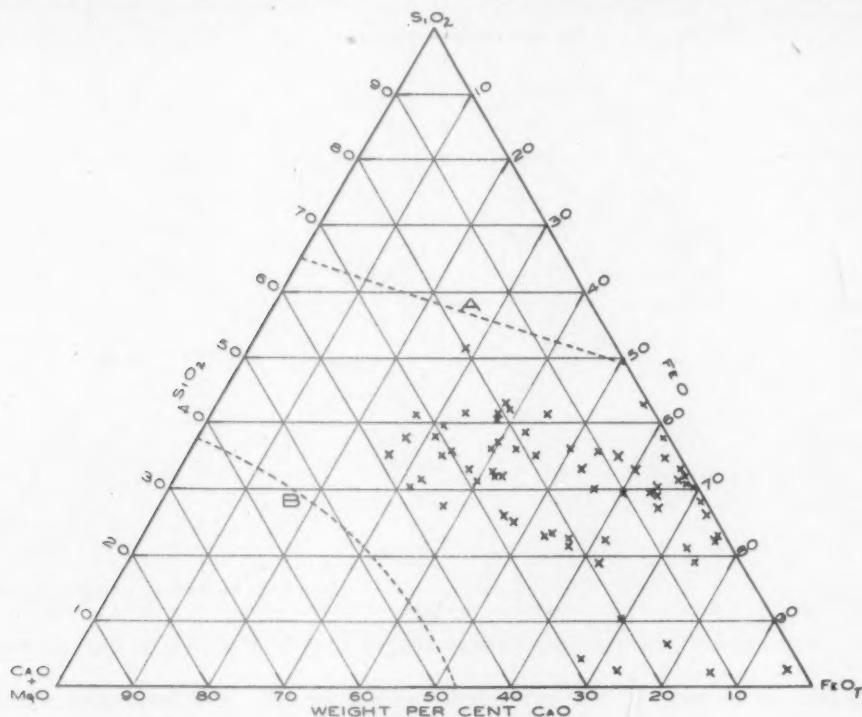
FIG. 8.—SECTION OF TERNARY SYSTEM INVESTIGATED.

the oxygen solubility in liquid iron has not been reconciled. Every attempt to reproduce the curve of Herty, Körber, and Oelsen has only strengthened the evidence in favor of the solubility line reported in this work. It seems necessary, therefore, to conclude that for some reason their results are in error, the most probable error being in their measurement of temperatures. The relationship between oxygen solubility and temperature given in Fig. 7 will be used as a basis for the calculation of fractional saturation values.

DISTRIBUTION OF IRON OXIDE BETWEEN SLAGS OF THE SYSTEM $(CaO + MgO)$-SiO_2-FeO AND PURE LIQUID IRON

The primary aim of this investigation was to determine the distribution of iron oxide or oxygen between the slags of the

solid boundaries at 1600°, estimated from the work of Bowen and Schairer[7] for the system CaO-SiO_2-FeO at lower temperatures. The location of the lines is undoubtedly altered by the presence of MgO in the slags and by changes in temperature.

Effect of Temperature

In order to plot the results on a comparable basis, it was necessary to correct for the temperature effect. Fetters and Chipman[1] have shown that the temperature dependence of the oxygen distribution for these slags is the same as for the pure iron oxide slags. The temperature correction was made graphically, since this was sufficiently accurate, and since the actual calculation was somewhat tedious. An example follows:

Sample R-36-5   Oxygen —0.136
Temperature 1575°C.

The saturation value was taken from a graph as 0.206 per cent oxygen; 0.136/0.206 = 0.660, the fractional saturation. The saturation value at 1600°C. is 0.229 per

diagram is that it enables us to measure immediately the oxygen potential between the slag and metal. If a furnace is being operated at a basicity of 2.0 and an FeO,
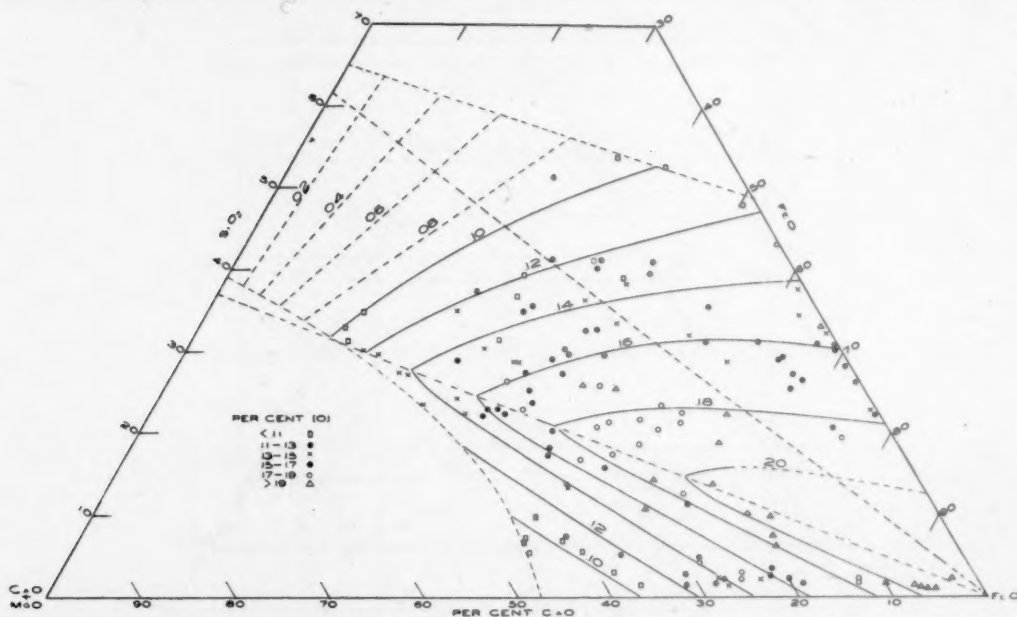
FIG. 9.—ISO-OXYGEN CONTOURS IN TERNARY SYSTEM $CaO + MgO$, FeO_T, SiO_2 AT 1600°C.

cent oxygen, so at 1600°C. the corrected oxygen content is

$$0.660 \times 0.229 \text{ per cent} = 0.151 \text{ per cent oxygen.}$$

The distribution coefficient L_o can be corrected very simply by merely using the corrected oxygen content in its calculation. All the data, including that obtained by Fetters and Chipman, were calculated in this manner.

Effect of Composition

The results of correcting the oxygen values to 1600°C. are plotted in Fig. 9. Since a ternary diagram is somewhat awkward for an operating man to use, the results are replotted in a somewhat different manner in Fig. 10. Here all data are kept on a percentage basis, and basicity, defined as $(\% CaO + \% MgO)/\% SiO_2$, is used to combine two of the variables, $(CaO + MgO)$ and SiO_2. The utility of this

of 30 per cent, the saturation value to be expected would be about 0.130 per cent oxygen. However, the actual oxygen content of the metal as calculated from its carbon content may be only 0.050 per cent. An oxygen potential difference of 0.080 per cent may be said to exist between the slag and the metal. The magnitude of this potential may materially alter the rate of the various refining reactions in the furnace.

In Fig. 11 the oxidizing activity, or the activity of FeO in the slag, is plotted against the composition on a mol fraction basis. The activity of pure liquid iron oxide in equilibrium with liquid metal is taken as one and that of the iron oxide in any other slag is accordingly less than unity. It is equal to the fractional saturation of the metal in equilibrium with the slag and is determined by dividing the oxygen content of the metal by the saturation value at that temperature. The lines of Fig. 11 are drawn so as to connect points of equal FeO ac-
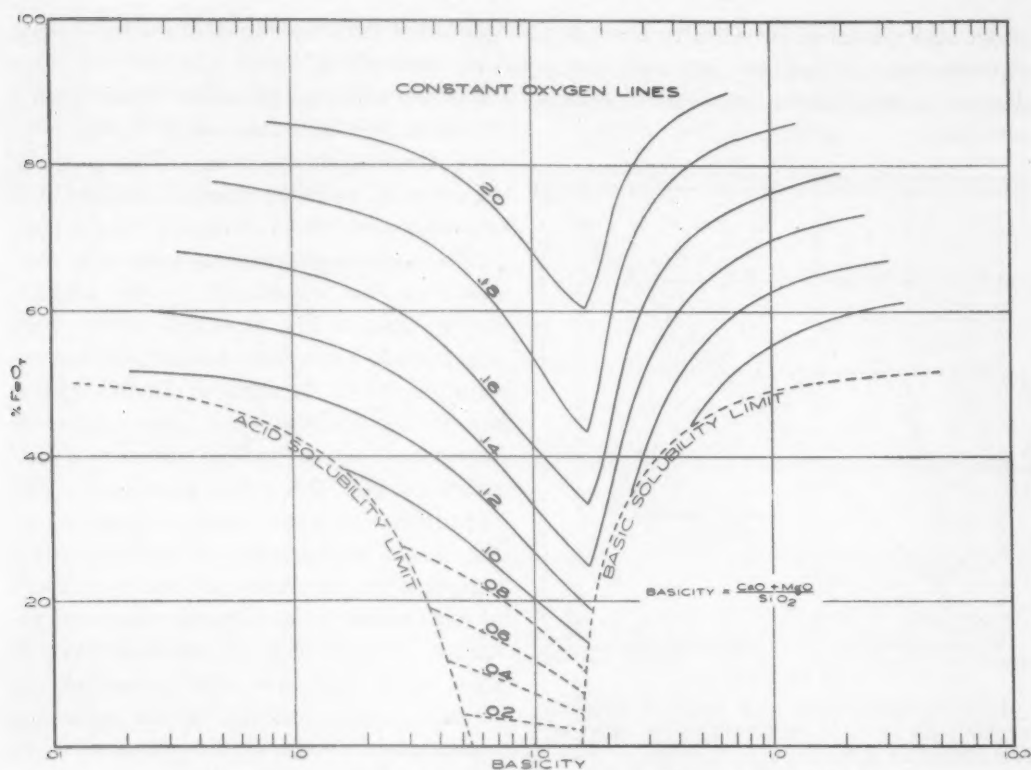
FIG. 10.—ISO-OXYGEN LINES FOR VARYING BASICITIES AND FeO$_T$.
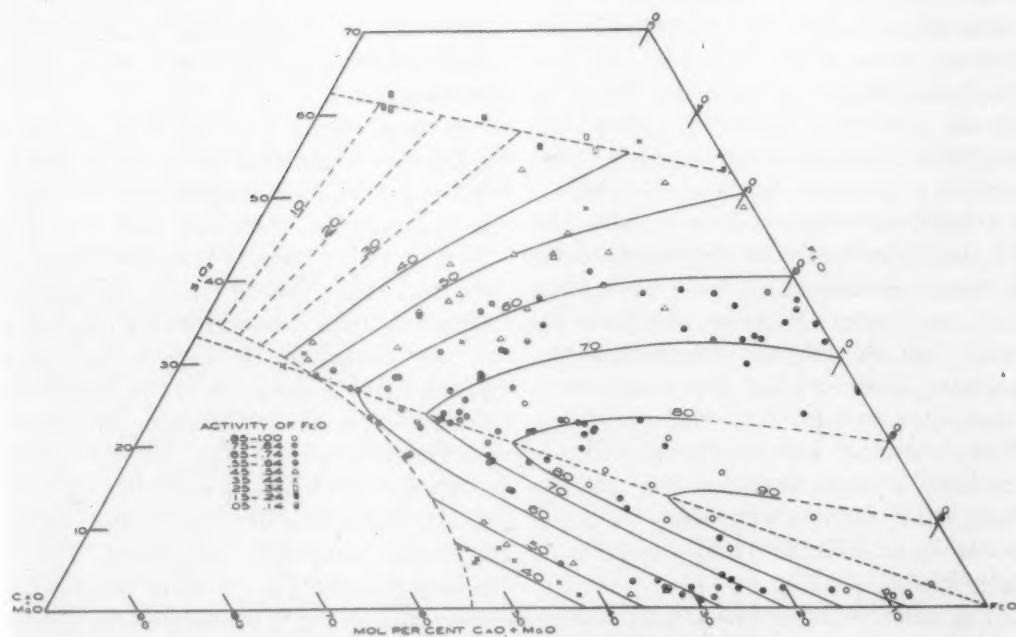
FIG. 11.—ISO-ACTIVITY LINES IN TERNARY SYSTEM.

tivity and are called iso-activity lines. It is obvious that the data are not sufficient to determine all of these lines with complete certainty.
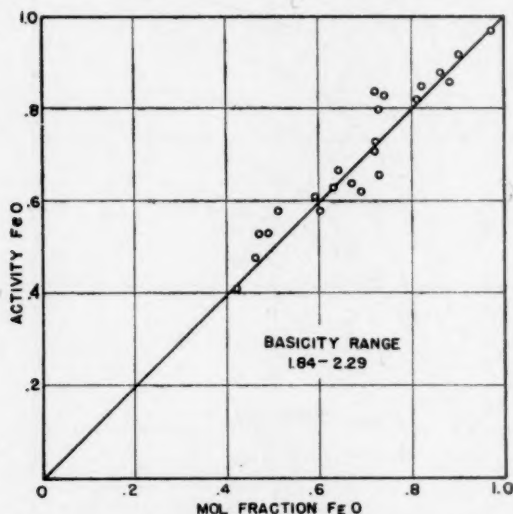
FIG. 12.—RAOULT'S LAW PLOT IN BASICITY RANGE 1.84 TO 2.29, ASSUMING ONLY MOLECULAR SPECIES $(2CaO \cdot SiO_2)_2$ AND FeO_x.

MOLECULAR CONSTITUTION
OF THE LIQUID SLAGS

We may define the system under consideration as composed of liquid iron as one solvent and a solution composed of lime, magnesia and silica as the other. These two liquids will be considered as being substantially immiscible in each other. Their mutual insolubility indicates that there is an enormous deviation from Raoult's law; i.e., that the liquids are sufficiently unlike so that their molecules will not interchange with each other. However, the FeO, the solute that is distributed between these two solvents, itself is only partly soluble in liquid iron. In spite of its conformity with Henry's law at low concentrations,[8] this indicates a wide deviation from ideality since, if the solution were ideal, the solute would be miscible with the solvent in all proportions.

The actual wide deviation from ideality of the metallic phase might justify the ex-

pectation that the two nonmetallic liquids, one insoluble in liquid iron and the other only slightly so, may themselves form a solution that is nearly ideal. If that were true, the iso-activity lines in Fig. 11 would be expected to follow lines of constant FeO concentration which obviously they do not.

The usual explanation of such wide deviation as that evidenced by the strongly curved lines of Fig. 11 is that one or more compounds have been formed among the components of the solution. In this system many compounds have been definitely recognized as crystalline phases of the solidified slags. One might assume, as a first approximation, that these compounds persist in the liquid state. In the past such assumptions have been justified by the lack of experimental data on the chemical behavior of liquid slags. It now becomes possible, with the data here presented, to reexamine the question of the molecular constitution of the liquid phase without direct recourse to hypotheses based upon the crystalline species formed on solidification. This examination will be based solely upon the experimental data and Raoult's law, which may be stated as follows: "In an ideal solution the activity of each molecular species is proportional to its mol fraction."

It is generally accepted that at these temperatures the silica takes on the characteristics of an acid, and lime that of a base. It is significant, therefore, that at a mol ratio of 2 to 1 there is a marked break in the iso-activity lines in Fig. 11. Fetters and Chipman[1] have investigated the possibility of the compound $2CaO \cdot SiO_2$ and have shown that the existence of this compound in the liquid is not sufficient to account for the observed deviation. However, if the compound is chosen as a double molecule $(2CaO \cdot SiO_2)_2$, the deviation from ideality is almost completely eliminated. This is demonstrated in Fig. 12, which includes the same data as Fig. 9 of the previous paper,[1] i.e., all of the points that lie at a mol ratio

of approximately 2:1. In contrast to the rather curved result previously found, the points of Fig. 12 lie fairly close to the straight line. It may be concluded therefore

lines in Fig. 11 are drawn on the assumption then that $(2CaO \cdot SiO_2)_2$ is undissociated and that there are no stable compounds between FeO and SiO_2.
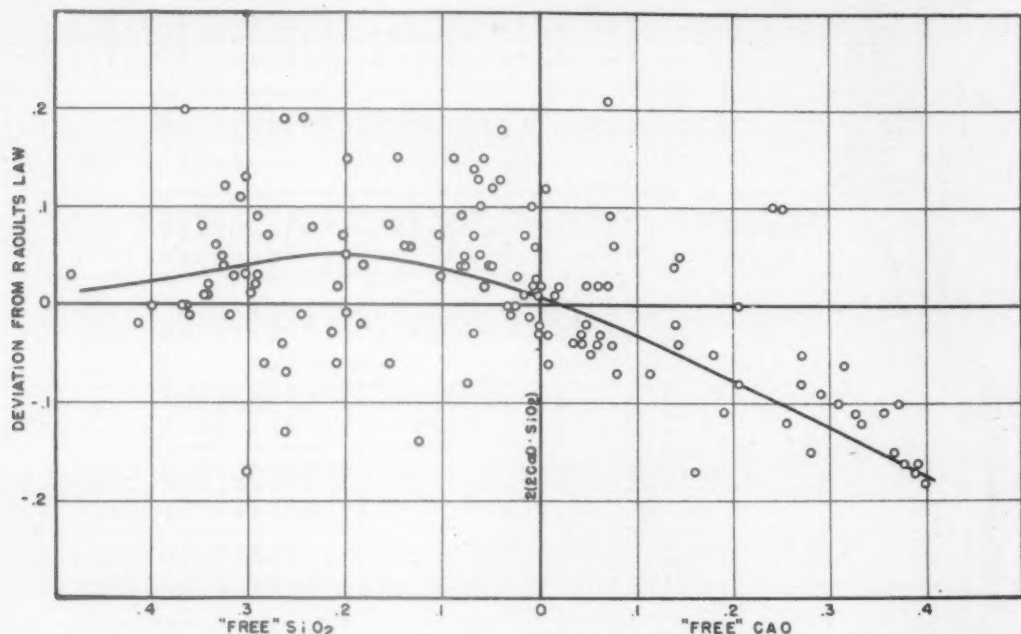
FIG. 13.—DEVIATION FROM RAOULT'S LAW AS FUNCTION OF BASICITY, ASSUMING ONLY $(2CaO \cdot SiO_2)_2$.

that for slags of approximately ortho-silicate composition the activity of FeO in the slag is proportional to its mol fraction provided the other component is assigned the formula $(Ca, Mg)_4Si_2O_8$. In these computations the mol fraction of FeO was based upon the total iron of the slag; i.e., its molecular formula was arbitrarily written FeO_x.

A further inspection of Fig. 11 shows that along the silica-FeO side of the diagram, the iso-activity lines may reasonably be drawn so as to terminate at the points where the activity is equal to the mol per cent. This would mean that any compound between FeO and SiO_2 is completely dissociated at 1600°C. Although it cannot be considered proved that this dissociation is complete, the data certainly indicate that the molten ferrous silicates are far from stable substances, a conclusion that agrees with observations on acid slags. The dotted

In order to investigate the rest of the ternary diagram more easily, the graph in Fig. 13 was constructed. Ideality and the compound $(2CaO \cdot SiO_2)_2$ were assumed. The deviations plotted are the deviations in activity of each experimental point from the calculated value. The average deviation is small at the "acid" side and at the point at which the compound exists. There is an intermediate range between the pure silica and the pure dicalcium silicate slags where there appears to be on the average a slight deviation from ideality. On the "basic" side, however, there is a decided and strong negative deviation from the calculated values with increasing basicity, and the picture becomes more complicated.

It has been shown[1] that in the nearly silica-free slags, the data indicate the probable existence of $CaO \cdot Fe_2O_3$. If, however, the small amount of silica in these slags actually ties up a considerable quan-

TABLE 3.—*Summary of Experimental Data*

Heat No.	Metal Test	Total Fe	FeO	Fe_2O_3	CaO	SiO_2	MgO	Al_2O_3	Total	O	N_2	Temperature	L_0	Per Cent O Corrected to 1600°C	L_0 Corrected to 1600°C	$R_1 = \dfrac{CaO + MgO}{SiO_2}$
R-20	1	52.18	66.30	0.92		30.20	0.32	0.28	98.02	0.144	0.044	1588	0.209	0.151	0.220	0.0107
	4	45.75	58.25	0.69		36.12	0.76	1.96	97.83	0.144	*	1623	0.234	0.119	0.213	0.0212
R-21	1-B	42.70	53.29	1.84		42.20	0.31	0.31	99.00	0.148	0.037	1640	0.263	0.126	0.223	0.0074
	2	52.50	66.51	1.15		29.96	0.18	1.21	99.31	0.181	0.043	1642	0.262	0.153	0.221	0.0059
	3	52.02	65.27	1.84		26.72	0.41	4.67	98.91	0.181	0.039	1641	0.259	0.154	0.215	0.0155
	4	49.93	62.79	1.61		29.88	2.11	0.71	97.85	0.182	0.047	1632	0.277	0.162	0.243	0.0705
	5	47.68	60.72	0.69		33.70	2.21	0.26	98.03	0.185	0.040	1627	0.247	0.140	0.222	0.0655
R-24	1		61.61	10.42	24.06	2.08	0.24	0.36	98.67	0.156	0.026	1581	0.233	0.184	0.252	11.66
	2		64.37	9.40	18.15	6.26	0.54	0.87	99.08	0.170	0.026	1581	0.258	0.208	0.279	2.986
	3		53.70	11.85	27.65	4.12	0.10	1.80	98.29	0.192	0.020	1584	0.273	0.182	0.270	6.732
	4		77.24	6.54	0.09	2.02	12.23	0.95	99.92	0.170	0.020	1584	0.198	0.181	0.212	6.106
	6		51.13	2.04	9.62	34.96	0.77	1.17	99.47	0.169	0.022	1581	0.277	0.159	0.273	0.275
	7		56.09	3.27	8.70	28.98	1.21	0.66	99.42	0.149	0.022	1573	0.290	0.190	0.295	0.341
	8		60.69	2.04	3.73		2.82	0.66	98.92	0.175	0.028	1567	0.232	0.156	0.315	0.226
	9		36.78	1.43	14.30	40.58	5.42	0.46	99.76	0.148	0.028	1559	0.258	0.114	0.245	0.486
	10		29.06	2.25	7.71	39.11	21.17	0.23	99.76	0.100	0.029	1556	0.271	0.101	0.295	0.739
R-25	6		87.91	7.15		2.25	2.59	0.29	100.13	0.085	0.031	1635	0.202	0.230	0.322	1.150
R-26	3		64.00	2.25		33.14	0.67	0.41	100.35	0.192	0.021	1650	0.334	0.192	0.242	0.0202
	4		60.69	0.41		22.20	16.33	0.49	100.04	0.221	0.021	1662	0.385	0.193	0.290	0.735
	5		50.94	4.91		22.16	20.72	1.43	99.22	0.236	0.021	1665	0.438	0.192	0.315	0.935
	6		47.82	5.22		23.00	22.54	1.51	100.31	0.247	0.022	1660	0.449	0.186	0.342	0.980
	8		50.21	5.93		20.74	21.12	0.93	99.51	0.242	0.023	1634	0.424	0.189	0.345	1.018
	10		62.71	5.11		9.28	12.10	0.82	98.13	0.242	0.020	1608	0.351	0.211	0.331	2.005
R-28	1		55.73	5.52	7.50	18.42	2.41	0.40	99.00	0.244	0.021	1612	0.359	0.214	0.303	1.005
	2		37.70	5.11	16.10	36.10	4.29	0.39	99.17	0.223	0.023	1629	0.369	0.139	0.344	0.649
	3		42.85	1.43	19.25	40.62	3.84	0.40	99.23	0.140	0.025	1615	0.307	0.120	0.351	0.353
	4		30.52	2.66	10.51	34.46	1.24	0.79	99.10	0.136	0.025	1668	0.401	0.126	0.271	0.901
	6		31.26	1.02	29.81	31.12	15.84	0.53	99.51	0.134	0.027	1604	0.392	0.0975	0.377	1.135
	7		33.47	3.07	19.48	26.52	0.17	0.38	97.67	0.128	0.028	1608	0.425	0.298	0.298	1.286
	8		23.91	1.84	34.00	34.00	13.41	0.42	97.52	0.159	0.026	1608	0.554	0.156	0.417	1.100
	9		25.38	1.64	37.22	36.80	0.08	0.48	98.47	0.146	0.032	1595	0.470	0.141	0.534	0.930
R-29	5		40.56	1.42	20.82	37.60	0.13	0.61	98.30	0.129	0.023	1590	0.339	0.124	0.452	0.485
	6		38.19	2.02	18.16	31.76	0.08	0.50	97.86	0.145	0.025	1597	0.381	0.148	0.346	0.796
R-30	7		27.46	0.81	19.72	50.66	0.08	0.48	99.23	0.157	0.023	1606	0.402	0.164	0.498	0.391
	8		31.83	1.21	24.64	40.80	0.08	0.90	99.23	0.115	0.028	1641	0.380	0.117	0.409	0.606
	9		27.10	3.75	36.70	29.30	0.20	0.17	99.41	0.127	0.028	1657	0.520	0.123	0.368	1.255
	10		31.64	1.62	29.10	34.60	0.12	0.14	97.94	0.164	0.031	1615	0.492	0.139	0.440	0.843
R-36	1	55.9	62.3	10.8	5.62	20.30	0.14	0.20	99.39	0.168	0.029	1612	0.233	0.126	0.369	0.287
	2	44.0	46.3	11.7	7.72	34.30	0.20	0.20	100.28	0.171	0.026	1604	0.276	0.161	0.219	0.229
	3	49.6	54.9	9.9	5.50	28.84	0.18	0.14	99.48	0.158	0.034	1574	0.247	0.150	0.262	0.200
	4	49.0	54.1	9.9	6.20	29.16	0.08	0.17	99.67	0.160	0.033	1575	0.219	0.157	0.242	0.217
	5	46.3	53.6	6.4	6.51	32.81	0.12	0.15	99.55	0.140	0.039	1576	0.225	0.156	0.244	0.204
	6	50.2	57.1	8.4	5.09	26.45	2.48	0.12	99.64	0.136	0.039	1584	0.214	0.151	0.250	0.286
	7	56.4	62.6	11.1	4.45	18.6	0.99	2.40	100.14	0.140	0.036	1590	0.224	0.179	0.238	0.292
	8	40.93	42.0	11.85	4.8	22.62	18.40	0.17	99.84	0.187	0.030		0.350	0.195	0.365	1.025

Heat No.	Metal Test	Slag Analysis, Per Cent								Metal Analysis, Per Cent						$\frac{R_1}{CaO + MgO}$ SiO_2
		Total Fe	FeO	Fe$_2$O$_3$	CaO	SiO$_2$	MgO	Al$_2$O$_3$	Total	O	N$_2$	Temperature	L_o	Per Cent O Corrected to 1600°C.	L_o Corrected to 1600°C.	
	9	37.2	40.8	7.8	5.70	25.40	20.75	0.24	100.69	0.182	0.039	1582	0.370	0.196	0.409	1.042
	10	36.1	40.0	7.1	6.00	26.14	21.92	0.24	101.40	0.180	0.035	1588	0.390	0.186	0.403	1.068
	11	36.2	40.3	7.0	13.22	34.96	5.91	0.14	101.53	0.155	0.037	1572	0.335	0.174	0.376	0.547
	12	30.8	20.2	21.6	10.06	35.88	12.58	0.24	100.56	0.109	0.046	1586	0.299	0.116	0.287	0.631
	13	29.8	27.9	11.7	17.49	43.64	1.07	0.14	101.94	0.114	0.038	1585	0.225	0.122	0.320	0.425
	14	40.7	43.1	10.3	12.99	32.84	0.08	0.19	99.50	0.120	0.040	1592	0.272	0.124	0.233	0.398
	15	38.6	40.8	9.9	13.66	35.22	0.65	0.31	100.23	0.136	0.039	1607	0.253	0.132	0.264	0.406
	16	43.2	46.7	9.9	11.50	30.49	0.61	0.22	99.42	0.143	0.041	1614	0.325	0.135	0.238	0.397
	17	29.4	34.8	3.3	20.25	41.07	0.08	0.22	99.72	0.124	0.038	1618	0.196	0.115	0.301	0.495
R-37	1	59.0	69.1	7.5		22.48	0.08	0.5	99.66	0.151	0.032	1597	0.155	0.152	0.197	0.0036
	2	56.8	67.7	5.9		26.46	0.04	0.3	100.36	0.114	0.036	1586	0.178	0.121	0.165	0.0030
	3	59.1	69.9	6.7		22.68	0.08	0.3	99.62	0.137	0.039	1595	0.212	0.139	0.181	0.0018
	4	51.9	63.3	3.8		32.30	0.08	0.3	99.78	0.143	0.037	1601	0.340	0.142	0.211	0.0025
	5-R	33.1	39.5	3.8	20.37	32.46	21.43	0.51	97.70	0.150	0.041	1615	0.381	0.141	0.319	0.135
	6-R	37.5	39.3	2.8	19.01	32.36	24.22	0.41	99.09	0.162	0.040	1617	0.355	0.151	0.355	0.660
	7-R	21.0	26.2	0.8	19.45	41.56	9.02	0.44	98.39	0.098	0.044	1579	0.299	0.107	0.388	0.707
	8	23.9	26.1	5.2	17.85	38.38	10.76	0.55	100.00	0.093	0.044	1572	0.263	0.104	0.334	0.776
	9	28.0	29.8	6.9	18.20	43.16	0.08	0.48	99.87	0.090	0.041	1589	0.264	0.100	0.274	0.453
	10	30.9	32.8	7.7	17.03	42.18	0.04	0.41	101.08	0.105	0.042	1595	0.323	0.107	0.269	0.424
	11	29.9	32.1	7.1		32.56	10.07	0.31	100.34	0.125	0.038	1614	0.396	0.117	0.302	0.868
	12	30.8	35.7	4.4		31.15	11.24	0.48	100.00	0.158	0.040	1609		0.152	0.381	0.897
R-22	1									0.297		1655				
	2									0.286		1640				
R-23	5									0.222		1613				
	6									0.210		1577				
	7									0.216		1637				
	8									0.256		1637				
	9									0.257		1597				
R-25	1									0.214		1591				
	2									0.210		1608				
	4									0.226		1629				
R-26	1									0.268		1631				
	2									0.259		1652				
	9									0.244		1530				
	11									0.161		1552				
R-29	1									0.181		1545				
	2									0.186		1612				
R-30	1									0.240		1651				
	2									0.302		1650				
	3									0.208		1554				
R-38	1									0.188		1604				
	3									0.234		1673				
	4									0.313		1687				
	6									0.342		1548				
	7									0.197		1532				

* Data missing or questionable.

tity of lime in double molecules of dicalcium silicate, the deviations from ideality appear to be more adequately explained if the ferrite formula be taken as $CaO \cdot Fe_3O_4$. The
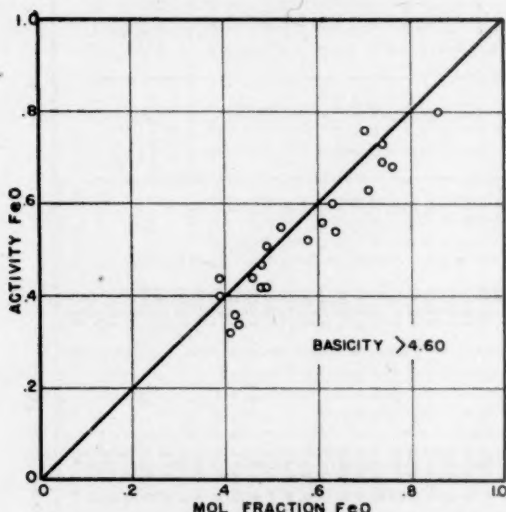
FIG. 14.—RAOULT'S LAW PLOT FOR BASICITIES > 4.60, ASSUMING EXISTENCE OF UNDISSOCIATED $(2CaO \cdot SiO_2)_2$ AND $CaO \cdot Fe_3O_4$.

comparison with Raoult's law is shown in Fig. 14 which includes only the most basic slags of Fig. 13. This plot shows that, assuming the molecular species $4CaO \cdot 2SiO_2$, $CaO \cdot Fe_3O_4$, and FeO, the activity of FeO is proportional to its mol fraction. Similar calculations assuming the ferrites $CaO \cdot Fe_2O_3$ and $2CaO \cdot Fe_2O_3$ showed definitely poorer agreement with the theory.

One of the objects of this investigation was to determine the effect of magnesia on the simple slag system. This can be answered only qualitatively since there was insufficient time for an investigation into the MgO-SiO_2-FeO system. In general, high-magnesia slags tend to be very crystalline, the surface presenting the appearance of a mesh of interlacing crystals. Excess MgO above that which is actually in solution makes the results erratic, but at the MgO contents encountered in normal openhearth practice, up to 10 per cent, no error within the experimental limits is introduced by substituting magnesia for lime in the

various calculations. Slags entirely free from magnesia and others containing up to 10 per cent of this oxide can be represented on the same ternary diagram within the limits of our experimental uncertainties.

Incidental to the slag studies, it was found that the rim of bare metal allowed a slow absorption of nitrogen. This element was determined along with oxygen in the vacuum-fusion analysis, and it was observed that the end point toward which all these heats tended was 0.040 per cent nitrogen. This is in agreement with the work reported by Chipman and Murphy.[10]

SUMMARY

The results of an experimental study, in a rotating induction furnace, of the equilibrium between liquid iron and slags of the system $(CaO + MgO)$—SiO_2—FeO at the temperatures encountered in steelmaking practice have been presented.

The solubility of iron oxide in liquid iron under pure iron oxide slags was redetermined and the results differ only slightly from those recently reported.

The equilibrium oxygen content of the metal at $1600°C$. is taken as a measure of the activity of iron oxide in the slag. The results are shown graphically as a function of composition of the slag.

The variation of the activity of iron oxide in slag is explained by the assumption of certain molecular species in the liquid slag and application of the laws of the ideal solution. The indications are that no compound is formed between silica and ferrous oxide at $1600°C$. Dicalcium silicate exists as a double molecule $(2CaO \cdot SiO_2)_2$ and is substantially undissociated at $1600°C$. On the basic side of the orthosilicate, the excess lime combines with the iron oxide to form $CaO \cdot Fe_3O_4$ in amounts depending on the CaO available after the formation of the $(2CaO \cdot SiO_2)_2$.

The effect of magnesia has been qualitatively found to be almost the same as lime in concentrations at least up to 10 per cent.

The solubility of nitrogen in pure iron has been checked at 0.040 per cent.

ACKNOWLEDGMENT

REFERENCES

1. Fetters and Chipman: *Trans.* A.I.M.E. (1941) **145**, 95–107.
2. Barrett, Holbrook and Wood: *Trans.* A.I.M.E. (1939) **135**, 73–84.
3. Foote: Nat. Bur. Stds. *Tech. Paper* 170, p. 209.
4. Herty and Gaines: *Trans.* A.I.M.E. (1928) **80**, 142–156. Iron and Steel Technology in 1928.
5. Körber and Oelsen: *Mitt.* Kaiser Wilhelm Inst. Eisenforsch. (1932) **14**, 181–204.
6. Fetters and Chipman: Amer. Soc. Metals Preprint 54 (1941).
7. Bowen, Schairer and Posnjak: *Amer. Jnl. Sci.* (1933) **226**, 193–204.
8. Fontana and Chipman: *Trans.* Amer. Soc. Metals (1936) **24**, 313–336.
9. Osgood: Mechanics, 105.
10. Chipman and Murphy: *Trans.* A.I.M.E. (1935) **116**, 179.

DISCUSSION

(W. O. Philbrook presiding)

C. E. SIMS,* Columbus, Ohio.—This paper seems particularly commendable for its rational approach to the phenomena of slag-metal equilibria, particularly in regard to the relation between iron oxide content and oxygen activity. Although many of the deductions are from circumstantial evidence, they appear so logical they are readily acceptable. Metallurgists have long realized that there is no direct relation

---

* Battelle Memorial Institute.

between the iron oxide content of a slag and its oxidizing power or activity, and the present paper gives a reasonable mechanism to account for the variations.

We are indebted to these authors for some valuable improvements in experimental technique, particularly the method of sampling and annealing thermocouples.

K. L. FETTERS,* Pittsburgh, Pa.—I feel that the experiments by Taylor and Chipman have contributed much toward a better understanding of slag-metal relations. Their data on the solubility of oxygen in iron changes slightly and adds confirmation to the earlier oxygen-solubility work of Chipman and Fetters. It is gratifying to have a check on this oxygen-solubility data, since the findings are rather far from agreement with the earlier work by Herty and Körber.

I also view their Figs. 9 and 11 with considerable selfish satisfaction, since the complete data for oxygen activity of lime silica, iron oxide slags justifies positioning of the iso-oxygen and iso-activity lines very nearly at the same point at which we had to guess their location in the earlier Fetters-Chipman work.

The authors' Fig. 10, which shows iso-oxygen lines for varying basicities and slag-oxygen content, offers a very useful means of representing the oxygen activity in a manner that can be used and easily understood in open-hearth plants.

J. W. SPRETNAK,† Cleveland, Ohio.—Of particular interest to those concerned with the mineralogy of slags is the direct information on the constitution of liquid slags obtained in this investigation. As more such direct evidence is available, it will be possible to determine to what extent the structure of solidified slag is indicative of the molecular constitution of the corresponding liquid slag. Qualitatively at least, the change in oxygen in the metal with constant FeO_T in slag with varying basicities shown in Fig. 10 is in accord with what might be expected from the study of solidified slags.

An indication of the role of magnesia in basic slags is the fact that magnesia up to 10 per cent

---

* Assistant Professor of Metallurgy, Carnegie Institute of Technology.
† Research Department, National Malleable and Steel Castings Company.

could be substituted for lime in the calculations. As no free periclase was found in the solidified slags, it appears that magnesia can substitute for lime in the orthosilicate compound.

In basic open-hearth slags, the change in composition of the "oxide phase" can be followed by measuring its lattice parameter by X-ray diffraction methods. This "oxide phase" is a very fine opaque phase, black in color, consisting principally of the oxides FeO, MnO, MgO. These oxides are the RO oxides, which can substitute for lime in the orthosilicate and are precipitated by the reaction

$$CaO(RO)SiO_2 + CaO \rightarrow 2CaO \cdot SiO_2 + RO$$
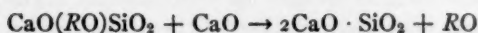
When one attempts to calculate the lattice parameter from the chemical composition and the known parameters for the three oxides, the determined parameter can be accounted for in practically every case without including the MgO in the calculations. The magnesia apparently is not replaced to any appreciable extent by additional lime. Darken and Larsen[11] showed also that FeO has less tendency to be neutralized in the $CaO(RO)SiO_2$ compound than have MnO and MgO. Thus it appears that the order of stability of the oxides in the $CaO(RO)SiO_2$ phase is MgO, MnO, FeO, decreasing in that order.

TABLE 4.—*Slag Compositions*

Heat 1			Heat 2		
Con-stituent	Tap-ping	Ladle	Con-stituent	Tap-ping	Ladle
SiO_2	17.64	27.42	SiO_2	11.68	20.62
CaO	43.25	36.05	CaO	42.40	36.90
Al_2O_3	5.50	6.88	Al_2O_3	5.36	6.14
FeO	6.44	5.37	FeO	13.24	7.70
Fe_2O_3	7.45	0.30	Fe_2O_3	7.72	0.91
MnO	10.72	11.62	MnO	11.39	14.20
P_2O_5	1.554	0.804	P_2O_5	1.485	1.110
S	0.100	0.122	S	0.168	0.144
Total.....	92.654	88.566	Total.....	93.443	87.724

The data presented in Fig. 13 indicate that on the basic side of the orthosilicate the amount of calcium ferrites increases with increasing lime available after formation of the orthosilicate, and that these ferrites are not particularly active as oxidizers.

[11] L. S. Darken and B. M. Larsen: *Trans. A.I.M.E.* (1942) **150**, 87.

Interesting corroborative evidence of this principle (Table 4) was found in an investigation of slag compositions in relation to phosphorus reversion in the ladle. The ladles were on the floor from $1\frac{1}{2}$ to 2 hr. and analyses are given for the tapping slags and the ladle slags at the end of pouring.

A considerable increase in silica content was caused by oxidation of the silicon additions, refractories, etc. The uncorrected lime-silica ratio changed in heat 1 from 2.45 to 1.31 and in heat 2 from 3.63 to 1.79. Under the microscope the slags changed from the multiphased, well-matured type to the typical monomineralic "acid" slag of the $CaO(RO)SiO_2$ structure. The Fe_2O_3 content, which is an indication of the amount of calcium ferrites, dropped from 7.45 per cent and 7.72 per cent to 0.30 per cent and 0.91 per cent, respectively. This decrease is far in excess of that which can be accounted for by dilution.

In order to satisfy the additional silica entering the slag with lime in the orthosilicate ratio, the iron oxides combined with lime in the calcium ferrites were displaced by silica, since the lime-silica linkages are the most stable in liquid basic slags. The ferric oxide thus freed was able to diffuse to the slag-metal interface and be reduced by the metal. The monomineralic structure indicated that the amount of silica was such that some RO oxides had to substitute for lime to maintain the orthosilicate ratio.

W. O. PHILBROOK,* Chicago, Ill.—Perhaps the authors have been too modest in pointing out the implications of their work in the field of basic open-hearth operation. The poor fellow who is accused of having his head in the clouds all the time—to borrow Dr. Chipman's Campbell Lecture metaphor—but is trying to keep his feet on the charging floor, the open-hearth metallurgist has been forced to deal with approximations or guesses as to slag constitution for want of exact information. It has been assumed that because certain compounds have been identified in cooled slags, they might be present in liquid slags in the furnace; or certain chemical constituents have been assumed because they seemed reasonable and logical in the light of conventional ideas of

* Research Metallurgist, Wisconsin Steel Works.

chemistry at lower temperatures. We have been groping in the dark to a great extent in attempting to find useful relationships for control.

Now Dr. Chipman and his collaborators are really getting down to fundamentals. They are obtaining direct information of the behavior of liquid slags at actual steelmaking temperatures, which allows definite conclusions to be drawn about the effective composition of the slags. This paper, following the one by Fetters and Chipman, clarifies the problem of the activity of iron oxides in slags, and gives some valuable clues as to the compounds of lime with silica and with Fe_2O_3. In his Campbell Memorial Lecture, Dr. Chipman gave a preview of further work covering the more complicated systems approaching those of steelmaking slags. Within a few years, we may expect a fairly complete picture of the manner of combination of the various constituents of open-hearth slags in the furnace. This will be of tremendous importance in the practical problems of making better steel faster and cheaper. In addition to its purely theoretical importance, this paper is therefore a definite contribution to the art of steelmaking for which the authors should receive the credit they deserve from the industry.

Regarding the method of sampling metal from the molten bath developed by Dr. Taylor, I have had no personal experience, but I have heard of the use of a very similar method of obtaining metal samples from laboratory furnace melts, to be used as electrodes for spectrographic analysis. This may be helpful to any who are interested in spectrographic techniques.

J. CHIPMAN (author's reply).—In this paper we have published for the first time descriptions of two quite useful experimental techniques that have been employed in several other researches. I refer to the sampling method and the method of annealing and calibrating the tungsten-molybdenum thermocouples, both of which were perfected largely through the efforts of Dr. Taylor. I foresee many useful applications of the Taylor sampler.

Rapid Analysis of Oxygen in Molten Iron and Steel

BY GERHARD DERGE,* MEMBER A.I.M.E.

(New York Meeting, February 1943)

THE extension of metallurgical control of steelmaking processes has always made it desirable to have some quick method for determining the oxygen content of molten steel. To meet the practical demands of the steel industry, this method must also be simple enough so that the sampling can be done by the regular furnace crew. This requirement was kept in mind continually in the work to be described. An oxygen value is required for proper control, whether it be of a rimming steel or of a fully killed steel. However, two factors have discouraged the development of such direct methods:

1. The reaction $C + FeO \rightarrow Fe + CO$ is rapid enough to make the correct sampling of the bath a difficult problem. The most generally accepted means of circumventing this difficulty have been the aluminum-killed bomb test of McCutcheon and Rautio[1] and the aluminum-killed spoon test of Herty.[2] The theory of these tests is that all of the oxygen in the iron is converted to Al_2O_3, which can then be determined by chemical methods. Even when simplified so that the analysis is made by a measurement of turbidity, this method is too slow to be used in routine control. Furthermore, the results obtained have never been entirely satisfactory, and some of the reasons for this will be discussed later in this paper.

2. The ordinary chemical methods of analysis for oxygen in steel are not reliable. The only analysis that seems to possess

sufficient dependability to be of value is vacuum fusion,[3] and the apparatus and technique developed for this have been too complex and slow for routine work.

INDIRECT METHODS

Indirect methods of estimating the oxygen have been resorted to in mill practice. Generally these depend upon the chemical equilibria involved. The oxygen in the bath is related to other components in the slag or metal that can be analyzed more readily. These methods have many difficulties in common. Steelmaking processes involve a complicated set of interrelated reactions, all of which tend to approach equilibrium at varying rates. The degree to which any particular equilibrium is approached is not well established. Moreover, a proper use of theoretical equilibrium constants requires a more extensive knowledge of the activities of the reactants than we now have. This is well illustrated by the irregularities observed when trying to determine the oxygen in the metal by its ratio to the iron oxide in the slag.

Equilibrium relations may be used more readily if they are evaluated by plant experience, but the extent of approach to equilibrium remains an undetermined variable and lack of an entirely satisfactory means of determining oxygen for the calibration is felt keenly. For example, the statistical analysis of the relation between carbon and oxygen[4,5] illustrates that even in a single plant wide variations exist under normal conditions of operation. Nevertheless, this is one of the best methods now

_Manuscript received at the office of the Institute Dec. 1, 1941; revised Dec. 1, 1942. Issued in METALS TECHNOLOGY, January 1943.
* Metals Research Laboratory, Carnegie Institute of Technology, Pittsburgh, Pa.
[1] References are at the end of the paper._

available for the estimation of oxygen and this relation will be used as one means of evaluation of the new method. The difficulties encountered in the use of this carbon-oxygen curve are that it must be determined by extensive tests for each steelmaking practice, that deviations from the curve cannot be predicted because they represent departures from equilibrium, and that the steepness of the curve in the low-carbon range makes it least accurate where it is most needed. The last difficulty is emphasized by the fact that in this range accurate carbon analyses cannot be made rapidly enough for control work.

New Techniques Required

The foregoing discussion shows that either or both of two new techniques are required to make possible the proper determination and control of oxygen in steelmaking:

1. A good method of sampling the molten bath. This would allow an absolute determination of the oxygen present and make it possible to calibrate some of the indirect methods more accurately.

2. A rapid method of analysis of the sample that will give a result soon enough after the sample is taken so that it can be used in the control and finishing of the heat.

The experiments to be described led to the development of a new method of sampling, which gives a satisfactory measure of the oxygen present in the steel bath. The vacuum-fusion analyses of these samples also demonstrate that the conventional technique can be simplified and abbreviated so as to make it rapid enough for routine control work. The entire process of sampling and analysis that finally evolved will be outlined briefly and the individual points of interest will be described in detail.

Survey of New Method

In fractional vacuum-fusion analysis, it is observed that the rates of decomposition of the oxides of iron, manganese, and silicon are much more rapid than the decomposition of alumina. A sample that is free from alumina, therefore, is desirable for rapid analysis. Furthermore, even after the gases have been removed from the sample by vacuum fusion, they must still be analyzed for the three principal components: oxygen, which is measured as carbon dioxide; hydrogen, which is measured as water vapor, and nitrogen. This analysis may be performed in a number of ways. All reported methods[6,7] require upward of half an hour for their completion. The analyses to be reported show that with the method of sampling used the hydrogen and nitrogen are nearly constant and that normally they constitute only a small fraction of the total gases present. Thus, it was found that the time-consuming gas analysis can be avoided by applying a correction factor for the hydrogen and nitrogen. In general, a reliable estimate of the hydrogen and nitrogen can be based upon experience with the practice used, and even a large error in this estimate will have a small effect on the oxygen value obtained.

A variety of experiments led to the adoption of a wedge-shaped copper mold, which could be filled from a small, well-slagged spoon such as is commonly used in taking carbometer samples. This device chills the sample so effectually that it can be removed at once with bare hands, and it remains bright and shiny. Five to 10 grams of sample are cut off the bottom of the wedge for analysis and placed in the previously heated and evacuated vacuum-fusion apparatus, and the evolved gas is collected. The volume of this gas enables the operator to read the amount of oxygen from a chart, which incorporates all necessary corrections. It is estimated that under favorable conditions the percentage of oxygen can be determined within 5 min. of the pouring of the sample; 10 min. is certainly a liberal allowance for the time

required from the dipping of the sample to report of analysis.

SAMPLING METHOD

The considerations and tests that led to the sampling method finally adopted may be reviewed. A rapid method of testing the bath by sucking metal into a previously evacuated tube and analyzing the gases evolved during freezing has been described.[8] However, it has never been widely adopted and apparently is a little too complicated and uncertain to be of general use.

At the Kaiser Wilhelm Institut für Eisenforschung,[9-11] a mold with a cylindrical hole 9 mm. in diameter was used for casting samples. The results were erratic when applied to basic open-hearth and Bessemer steels in which the oxygen in the metal was high. This was demonstrated by using a sealed copper mold.[12]

An attempt was made to adapt the bomb test to this purpose by deoxidizing with electrolytic manganese, but this was soon abandoned because it was clumsy and erratic. A simpler method obviously is required.

It is recognized that a well-slagged spoon can be used to dip samples from a bath without disturbing the carbon-oxygen equilibrium in the metal. Observations on this point have been published by Larsen.[13] Therefore, efforts were made to design a mold so that a test could be poured from a slagged spoon and frozen rapidly enough to produce a satisfactory sample for determination of oxygen in the metal bath of a basic open-hearth furnace.

A large, split copper mold was designed to give a wedge-shaped specimen 9 in. long and 1 in. square at the large end. These samples were analyzed in 1-in. sections in a conventional vacuum-fusion apparatus, and the results were compared with those obtained from aluminum-killed bomb tests taken simultaneously with the wedge, and also with the oxygen estimated from the carbon vs. oxygen curve of Fetters and Chipman.[4] This preliminary exploration indicated that reasonable results could be obtained from the parts of the wedge that were less than $\frac{1}{4}$ in. thick.

Various smaller molds were then designed and a second series of tests led to the adoption of the mold shown in Fig. 1. In practice, this mold should be filled to the top of the wedge, and no additional metal should be added. A large pipe will appear at once, and the helper will want to fill this with extra metal, but no addition should be made because it will not be cooled sufficiently rapidly and will give low results. When properly taken, at least the lower 2 in. will be bright and shiny; above this a graded series of temper colors will appear. A section of the sample shows that the pipe extends nearly to the bottom of the wedge, but the surface of this pipe is also bright and clean. This pipe indicates that some gas, presumably CO, must have escaped during freezing, but the results that follow demonstrate that the amount of this gas must be small. The heat capacity of the mold shown is large enough so that it is again ready for use immediately after the sample has been removed.

ANALYSIS OF RESULTS

The proper evaluation of a new test of this type presents a difficult problem because no absolute standard is available as a basis for comparison. The best procedure would appear to be to compare the results obtained by the new method with those obtained by older methods that are better understood because experience with them has been wider. However, in making the comparison, considerable judgment must be exercised and the older methods must be re-evaluated in the light of the new information obtained. The aluminum-killed bomb test has been selected as a basis of comparison because it has been widely used and has been generally regarded as the best method available for determining oxygen in the bath.[1,4] The carbon vs. oxygen curve

of Fetters and Chipman[4] has been selected as the other basis of comparison. The objection may be raised that this is not an independent method because it is based

ing the wire placed in the bomb before the test. The oxygen is then determined by chemical analysis of the bomb for Al_2O_3. The data in Table 1 show that all of the
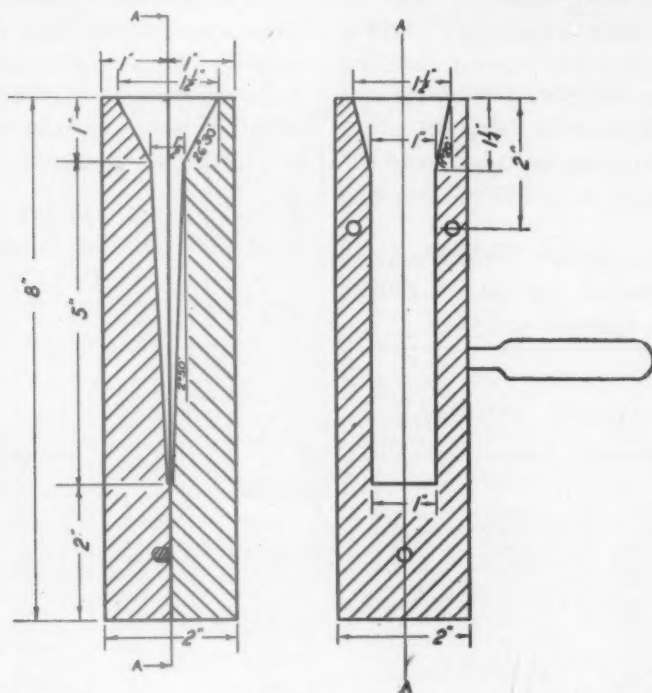
FIG. 1.—DESIGN OF WEDGE MOLD. CONSTRUCTED FROM A COPPER BAR.

upon bomb tests. However, the analysis of the curve made by the authors indicates that this is the best of the indirect methods for estimating oxygen; the results, while in accord with theoretical expectations, are based upon operating data and represent the average experience of a number of different plants and metallurgical practices. In the absence of an absolute test, such a summary of wide experience would appear to be more valuable than any single test or analysis.

Numerous bomb samples were analyzed by fractional vacuum fusion, and some enlightening information on the operation of this method of sampling was obtained. The test is based upon the assumption that all of the oxygen in the metal entering the bomb will be converted to alumina (Al_2O_3) by the excess aluminum supplied by melt-

oxygen is not converted to alumina; however, the oxygen obtained from Al_2O_3 by vacuum fusion agrees well with that obtained by chemical analysis. If individual samples are considered, the same general features are evident, though large differences in the degree of variation occur from sample to sample. This is to be expected, for the amount of oxygen converted to alumina will depend upon a number of factors that cannot be entirely controlled, primarily upon the time during which the sample remains molten in the bomb. Data presented later in the paper will show that the bomb test is not always in error to this extent, but it is certain that under many circumstances all of the oxygen is not converted to Al_2O_3 and is thus missed in chemical analysis.

The correct sampling of the bomb test is difficult, for deep pipes are common, and wide variations in aluminum content from point to point can be observed. Data based upon the bomb test, therefore, may be expected to be erratic to the extent of these variations. It would also appear that the usefulness of the bomb test could be improved further by standardizing the entire technique in such a way as to promote the formation of Al_2O_3 as much as possible.

TABLE 1.—*A Comparison of the Vacuum-fusion and Chemical Analyses of Bomb Samples*

| Sample No. | Total FeO, Per Cent | | FeO as Al_2O_3 (Vacuum Fusion), Per Cent |
	Chemical Analysis	Vacuum Fusion	
1	0.084	0.066	0.055
2	0.106	0.115	0.109
3	0.100	0.130	0.125
4	0.030	0.071	0.034
5	0.024	0.095	0.057
6	0.040	0.052	0.047
7	0.063	0.126	0.075
8	0.090	0.154	0.084
Total[a].......	0.537	0.809	0.586

[a] These totals have no particular mathematical significance and are used merely as a simple means of comparing the entire group of results.

Even if perfected so as to give more reliable and consistent results, the bomb test will remain an awkward and inconvenient method of sampling a steel bath, and it is not readily adaptable to control purposes. Nevertheless it is the one method for the analysis of oxygen that has had general acceptance among open-hearth operators.

With these considerations of the merits and limitations of the bomb test and of the carbon-oxygen curve in mind, we are in a position to evaluate the chilled wedge sample. The data shown in Table 2 were taken during the development of this method and probably do not represent the optimum results that could be obtained with continued use of the method under well standardized conditions. All tests for which complete data are available are included in the table. Many additional samples were taken at different stages of the heat, particularly with carbons below 0.10 per cent, and with slight variations in mold design. Bomb tests were not taken simultaneously and these data are not submitted in support of the method. However, it should be stated that in all cases (totaling about 50) where satisfactory samples were obtained, the vacuum-fusion analysis for

TABLE 2.—*A Comparison of the Wedge Test for* FeO *with the Bomb Test and the* C-FeO *Chart*

| Heat No. | FeO, Per Cent | | Fetters and Chipman (Chart) | |
	Wedge Sample (Vacuum Fusion)	Bomb (Chemical Analysis)	Per Cent FeO	Per Cent C
56347	0.266	0.192	0.230	0.07
64363	0.349		0.300	0.05
63344	0.136	0.126	0.135	0.14
60358	0.195	0.091	0.130	0.15
64016	0.193	0.188	0.200	0.076
58140	0.090	0.042	0.085	0.38
58145	0.197	0.106	0.190	0.11-0.09
62140	0.068	0.089	0.080	0.45
62197	0.151	0.115	0.145	0.13
64194	0.187	0.188	0.180	0.104
62412 {	0.138	0.076	0.125	0.16
	0.112	0.076	0.125	0.16
61401 {	0.260	0.296	0.205	0.08
	0.244	0.296	0.205	0.08
62412 {	0.123	0.114	0.148	0.13
	0.144	0.114	0.148	0.13
58407	0.029	0.032	0.070	0.71
58407	0.054	0.060	0.070	0.91
64402	0.311	0.306	0.250	0.06
Total......	3.247	2.507	3.021	

oxygen was a reasonable value on the basis of the other information available on the heat.

The vacuum-fusion results were obtained by a conventional design of apparatus whose operation was checked periodically with steels from the cooperative project sponsored by the Bureau of Standards.[3] The only novel feature of the apparatus is that the gases are analyzed within the system by fractional freezing. After passing over a copper oxide catalyst, the hydrogen, now converted to water vapor, is removed in a freezing trap surrounded by a mixture of dry ice and acetone. The CO, converted

to CO_2 by the catalyst, is then removed by placing a liquid nitrogen bath over the trap. Also, a new crucible assembly has been used, which possesses desirable fea-

checked gravimetrically. The carbon was also determined on the bomb sample. The hydrogen and nitrogen were determined on the wedge samples only and will be con-
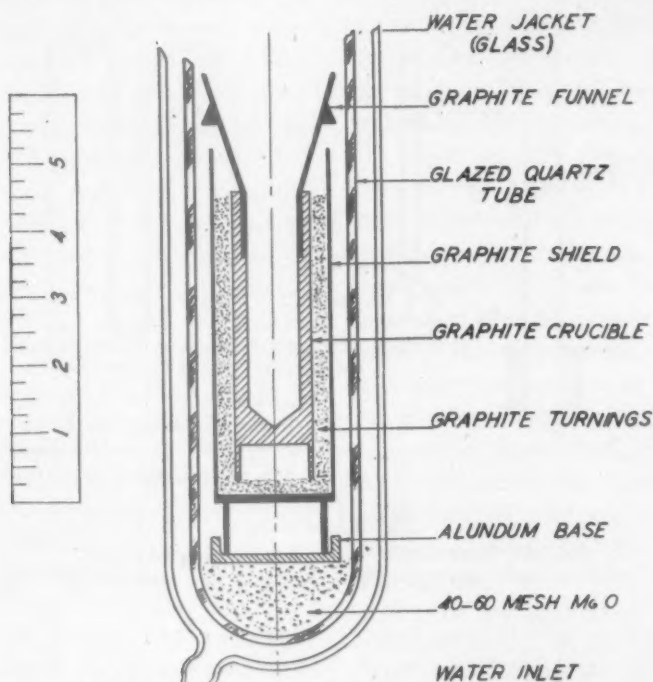
FIG. 2.—SECTION THROUGH FURNACE ASSEMBLY.
Arrangement of the crucible, insulation, shielding, refractories and funnel are shown.

Labels in figure:
WATER JACKET (GLASS)
GRAPHITE FUNNEL
GLAZED QUARTZ TUBE
GRAPHITE SHIELD
GRAPHITE CRUCIBLE
GRAPHITE TURNINGS
ALUNDUM BASE
40-60 MESH MgO
WATER INLET

tures because it simplifies the operation of the equipment. A cross section of the assembly is sketched in Fig. 2. With this arrangement the only oxide refractory material is the alundum base, which is well removed from the hot zone of the furnace. The graphite shield that contains the insulated crucible is substituted for the refractory shield ordinarily used in this position. It can be made easily on a lathe and it is finally slotted with a jeweler's saw to reduce current pickup. This is essentially an all-graphite assembly which can be baked out at high temperature (2200°C.) without any danger of developing hot spots where reaction between the graphite and oxide refractory can be initiated.

The analyses of the bombs for alumina were made in the steelworks laboratory by the turbidity method and frequently

sidered separately in a later section of the paper. Table 2 shows that in most cases the FeO (calculated from the percentage of oxygen found by analysis to conform with the customary method of presenting such data) determined from the wedge sample is within 0.02 per cent of the FeO determined, either by chemical analysis of the bomb test or from the carbon-FeO curve. In most cases where considerable discrepancy is found, the agreement is best between the wedge test and the C-FeO curve. The totals* in each column show that the wedge test is higher than both the bomb test and the C-FeO curve, which is to be expected from our earlier discussion of the bomb method, but the difference between the wedge results and the C-FeO

* See footnote to Table 1.

curve is small and indicates that in some plants the wedge test and the bomb test would give essentially the same results

The correlation coefficients for the re-

operations so that results can be obtained more rapidly. The only proper test of this equipment would be to set it up in the open-hearth analytical laboratory of a

A FURNACE   E H₂ PUMP
B SPECIMAN ARM   F RESERVOIR
C PRISM   G MANOMETER
D RADIATION SHIELD   H OIL PUMP

FIG. 3.—SIMPLIFIED VACUUM-FUSION APPARATUS.
This can be used to give rapid analyses when the hydrogen and nitrogen can be estimated.

lation between carbon and FeO as determined by the wedge tests and by the bomb tests taken simultaneously can be calculated from Table 2.[5] The coefficient for the wedge test is 0.968 while that for the bomb test is 0.889, and the methods described by Fisher[14] can be used to show that the significance of the difference between these two observed correlations is 0.85. These results mean that an investigator can expect considerably less spread from data collected by the wedge test than from similar data collected by the bomb test.

SIMPLIFIED VACUUM-FUSION APPARATUS

The foregoing discussion of the wedge sample shows that this method of sampling satisfies the requirements that were set up as prerequisites for a method of analysis that would be sufficiently rapid to be useful in industrial control. The data collected in the development of the wedge test were all obtained from a conventional apparatus. This apparatus can be simplified for routine

steel plant and operate it over a period of time long enough to demonstrate whether or not the data obtained with it can improve steelmaking practice. This description, therefore, is schematic and subject to the minor variations that occur in adapting any piece of apparatus to a particular laboratory. Numerous detailed descriptions of vacuum-fusion apparatus and its operation are available in the literature,[3,6,7] and it is only necessary to describe here the simplifications that can be made to give rapid analyses.

A suggested arrangement is shown in Fig. 3. The graphite crucible for the fusion is contained in the quartz tube A, which is surrounded by a water jacket for cooling. Heat is derived from the high-frequency induction coil placed around the entire crucible assembly. Portable models of such melting equipment with a power rating of about 6 kw. are available and can be plugged into the regular alternating current supply. This quartz tube is at-

tached to the Pyrex system by a ground joint sealed with Picein or a similar high-melting wax. The specimen arm B is equipped with a large-bore stopcock, so that the specimen will pass through the bore. The specimen can be moved magnetically. This cock is closed when the sample is introduced into the outer arm, which is provided with a ground cap. If the cock is then opened gradually, the vacuum in the system will not be interrupted seriously. The radiation shield at D keeps the prism window at C clean and can be opened magnetically to allow temperature observations with an optical pyrometer.

TABLE 3.—*Manometer Readings Made in Vacuum-fusion Analyses of Wedge Tests*

Sample No.	Inches on Manometer		
	Total Gas	N_2	H_2
1	1.15	0.01	0.01
2	2.08	0.02	0.01
3	1.77	0.03	0.02
4	2.02	0.01	0.03
5	0.51	0.01	0.02
6	0.82	0.02	0.10
7	1.12	0.02	0.01
8	1.27	0.01	0.02
Average........	1.34	0.016	0.028

The three-stage mercury diffusion pump E is designed for high speed against a high back pressure, as it must transfer all of the gas from the fusion chamber A into the calibrated reservoir F. The pressure in the reservoir is read on the butylphthalate manometer G. The mechanical oil pump H is used to evacuate the system but is closed off by a stopcock during the analysis. The amount of gas collected can be calculated directly from the manometer reading.

To convert the determination of the total amount of gas extracted into the percentage of oxygen present in the sample, it is most convenient to make the calculation in millimols of gas. The correction for the amount of hydrogen and nitrogen is based upon previous experience with the particular steelmaking practice under test. The data in Table 3 show that this correction is small and nearly constant. These refer to the last eight samples from Table 2, and were taken on a single day. The table shows the manometer readings made during the analyses of these wedges. The average total gas pressure was 1.34 in. of butyl phthalate. The average nitrogen pressure was 0.016 in. and the average hydrogen pressure was 0.028 in. This would make a total correction for hydrogen plus nitrogen of only 3.5 per cent of the total reading. It seems quite likely that the high hydrogen shown for sample 6 represents an error in reading the manometer, as variations of this degree are extremely rare. An error of 100 per cent in this correction will still give an oxygen value that probably is better than that which can be estimated by any other method, and the result is available within 10 minutes of the time the sample was taken.

If such an apparatus were to be used industrially, its dimensions would be determined to a large extent by the number of heats made per day in the shop. It would probably not be necessary to make more than one or two tests on each heat in the finishing period. A convenient sample weighs about 10 grams. The graphite crucible could be made to accommodate almost any number of samples, but 10 to 15 will probably be found most workable. By using standard taper ground joints, a new crucible assembly can be attached in a few minutes and baked out sufficiently within about ½ hr. In the absence of Al_2O_3, the analysis can be performed below 1500°C., and this low temperature reduces appreciably the difficulty of obtaining satisfactory blanks. Another alternative would be to run two such outfits in tandem. The induction heating equipment is the expensive item in the construction, and a single unit would service two crucible assemblies adequately.

General Significance of the Wedge Sample

The rapid oxygen determination proposed has innumerable applications in steelmaking practice, only a few of which can be suggested here as illustrations. Probably the most important use would be in determining an oxygen value at the end of a heat, which would establish the deoxidation required for that heat. This should result in improved quality and also in greater ingot yields, especially in semi-killed types. In special cases where extreme cleanliness is important or when the rate of refining must be controlled, the test should have great value. The test should prove useful also in Bessemer, acid open-hearth, and electric steelmaking work.

If the rapid features of the test are dispensed with and interest is centered upon the correct sampling of the steel bath to establish a certain plant practice or as a research tool in investigating other steelmaking problems, the wedge test offers many advantages over the bomb test. It is an easier test to make, therefore can be made more frequently and rapidly. It appears to have many advantages over the bomb test in ease of standardization and reliability. It preserves the steel as it is in the bath without superimposing any additional chemical reactions, and it is thus a new tool for studying many steelmaking problems.

Summary

1. A new method of sampling a molten steel bath for oxygen has been described. It consists of a small split copper mold, which gives a wedge-shaped sample. Vacuum-fusion analysis of this sample gives results that indicate that it is as reliable as either the aluminum-killed bomb test or the carbon-oxygen equilibrium for estimating the oxygen in the bath.

2. By simplifying the conventional vacuum-fusion apparatus, this wedge sample can be used to give a determination of the oxygen in the bath within 10 minutes of the taking of the test.

3. The aluminum-killed bomb test has been reexamined in the light of results obtained by vacuum-fusion analysis. Under many conditions of testing all the oxygen in the bath is not converted to alumina, and the results consequently are in error.

Acknowledgments

References

1. K. C. McCutcheon and L. Rautio: Trans. A.I.M.E. (1940) 140, 133.
2. C. H. Herty, Jr., H. Freeman and M. W. Lightner: U.S. Bur. Mines R.I. 3166 (1932).
3. J. G. Thompson, H. C. Vacher and H. A. Bright: Trans. A.I.M.E. (1937) 125, 246.
4. K. L. Fetters and J. Chipman: Trans. A.I.M.E. (1940) 140, 170.
5. K. L. Fetters: Trans. A.I.M.E. (1940) 140, 166.
6. Metals Handbook, good bibliography (1939) 712. Amer. Soc. Metals.
7. Third Report of the Oxygen Subcommittee of the Committee on the Heterogeneity of Steel Ingots. Iron and Steel Inst. Advance Copy, May 1941.
8. W. Hare, L. Peterson and G. Soler: Trans. Amer. Soc. Metals (1937) 25, 889.
9. P. Bardenheuer and W. Bottenberg: Mitt. K. W. I. Eisenfch. (1931) 13, 151.
10. P. Bardenheuer and G. Thanheiser: Mitt. K. W. I. Eisenfch. (1930) 27, 133–147.
11. P. Bardenheuer and G. Thanheiser: Mitt. K. W. I. Eisenfch. (1934) 16, 189.
12. G. Leiber: Mitt. K. W. I. Eisenfch. (1936) 18, 135–147.
13. B. M. Larsen: Trans. A.I.M.E. (1941) 145, 67.
14. R. A. Fisher: Statistical Methods for Research Workers. Edinburgh, 1938. Oliver and Boyd.

DISCUSSION

(*B. M. Larsen presiding*)

B. M. LARSEN,* Kearny, N. J.—The progress
in this field is indicated by the fact that such a
"speed method," involving high vacuum tech-
nique plus high temperatures, would hardly
have been imaginable a few years ago. The
sampling operation is the difficult part of such
an analysis and the author's method is certainly
ingenious. The present writer has made FeO
analyses by spoon sampling, pouring into a
steel mold filled with a loose wad of very fine
aluminum wire, determining precipitated Al_2O_3
by a refined turbidity method. Results in a few
cases have checked with oxygen values by
hydrogen reduction. Fine-grained steel gave
very nearly zero values, good checks on dupli-
cates are obtained, and samples drilled from
various portions of the tiny ingots showed
negligible segregation; in general the values
by this method appeared very reasonable.
This spoon sampling technique did give higher
results (by about 0.03 to 0.05 per cent FeO)
than the bomb sampling technique, which
agrees somewhat with the comparisons in this
paper.

I am still not convinced that the author can
be sure that some loss of oxygen as CO does
not occur, particularly in higher carbon
samples. It would be interesting to compare
this method on higher carbon samples with
the technique mentioned above, in which the
sampling technique is identical, up to the pour-
ing into the mold. Also, I wonder if we can
assume that even the thin wedge end of the
sample has only a relatively negligible amount
of surface oxygen, even though this surface
appears bright? The writer made hydrogen
reduction tests for surface oxygen on cylindrical
pieces as used for vacuum-fusion analyses and
found an amount that would be as much as
10 per cent or more of the actual oxygen con-
tained in the metal, even with bright, ground
or polished surfaces. Such thin oxide films are
transparent to light.

T. D. YENSEN,† East Pittsburgh, Pa.—My
discussion is concerned only with the second

---

* Research Laboratory, U. S. Steel Cor-
poration.
† Research Engineer, Westinghouse Re-
search Laboratories.

part of Dr. Derge's paper; namely, that per-
taining to the actual analysis, which I consider
a distinct advance in the art.

In 1927 N. A. Ziegler built a vacuum-fusion
apparatus for oxygen analysis at our laboratory
and used it successfully until he left in 1934.
It was also used by Wilson Scott for the
cooperative oxygen analysis conducted by the
Bureau of Standards in 1934–1936. After that
time it was never used again, partly because of
lack of personnel and partly because of the
laborious and time-consuming technique. It
required 2 hr. for making a single analysis.

In 1938 we began to look for simpler and
quicker methods, and for analyzing oxygen in
the absence of silica and alumina we developed
the hydrogen reduction apparatus shown in
Fig. 4, in which the H_2O is frozen out in a
liquid-air trap immediately adjacent to the
heating tube. All of the parts were enclosed
in an inverted Dewar flask inside of which the
temperature was maintained at 100°C., so as
to enable us to measure the H_2O with the
McLeod gauge.

Because of a tendency for the H_2O to react
with the cold sample on removal of the liquid
air the apparatus was modified as shown in
Fig. 5. While this is not nearly as compact as
the original one, it worked very well, and
analyses were made in 60 min. with an accuracy
of ±0.001 per cent.

However, as we needed to analyze samples
containing SiO_2 and Al_2O_3 we continued our
search for a method that would do this without
involving actual melting of the samples. In
this we were not successful. We first tried the
method developed and described by L. Singer
in 1940, using a graphite crucible heated to
1250°C., but with the modification of using
vacuum exclusively instead of N after the
initial evacuation and the analyzing scheme
shown in Fig. 6. While it is possible, and indeed
probable, that Mr. Singer's scheme as he has
it arranged—using tin in the crucible—operates
satisfactorily, we usually obtained low results.
This may have been partly because we did not
use tin and partly because the Ni catalyst
failed to convert the CO to CO_2 quantitatively
at 450°C. in the time allotted for the reaction

$$2CO + catalyst \rightarrow C + CO_2$$
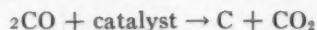
to go to completion. Substituting 2 oz. of
platinized asbestos as catalyst did not remedy
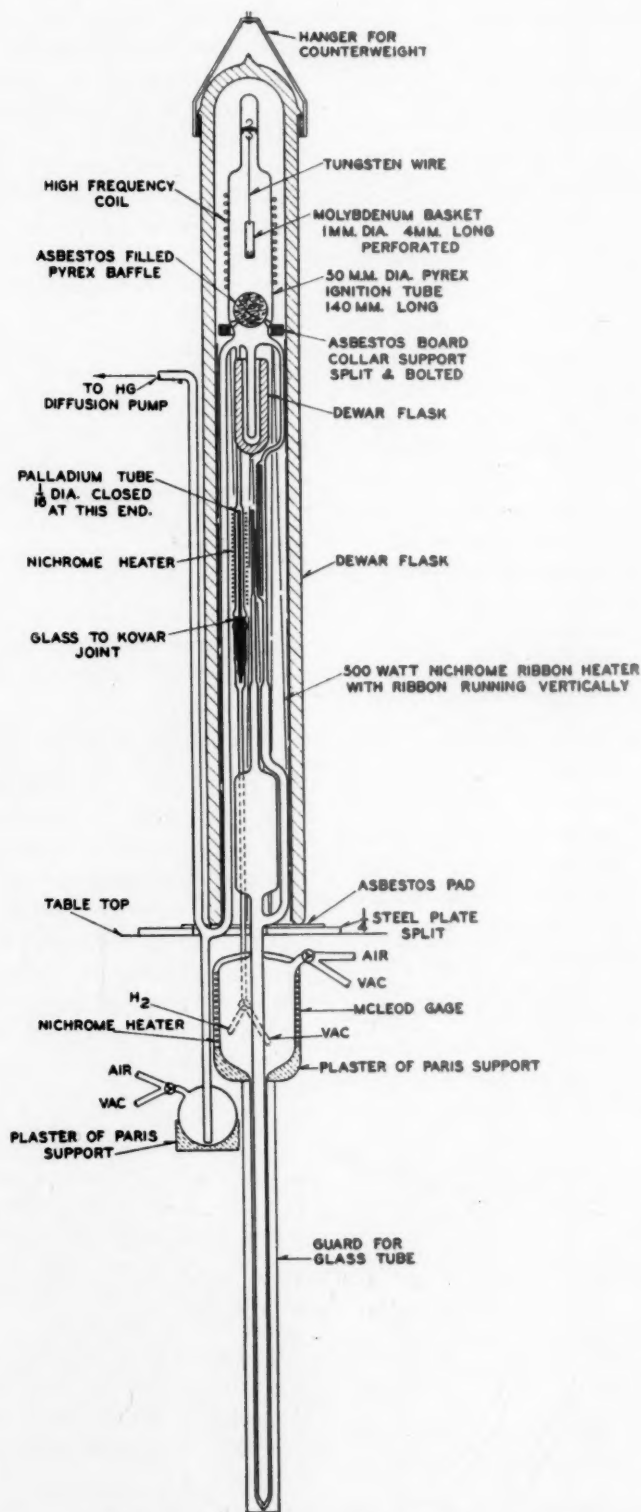
FIG. 4.—APPARATUS FOR HYDROGEN REDUCTION.

this situation. Whatever the cause of our low results, we were not sold on the idea of being able to reduce SiO_2 and Al_2O_3 at $1250°C.$, and became convinced that we had to use higher

substituting CuO, depending on the reaction

$$CO + CuO \rightarrow CO_2 + Cu$$
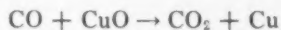
at a temperature of about $300°C.$ With this
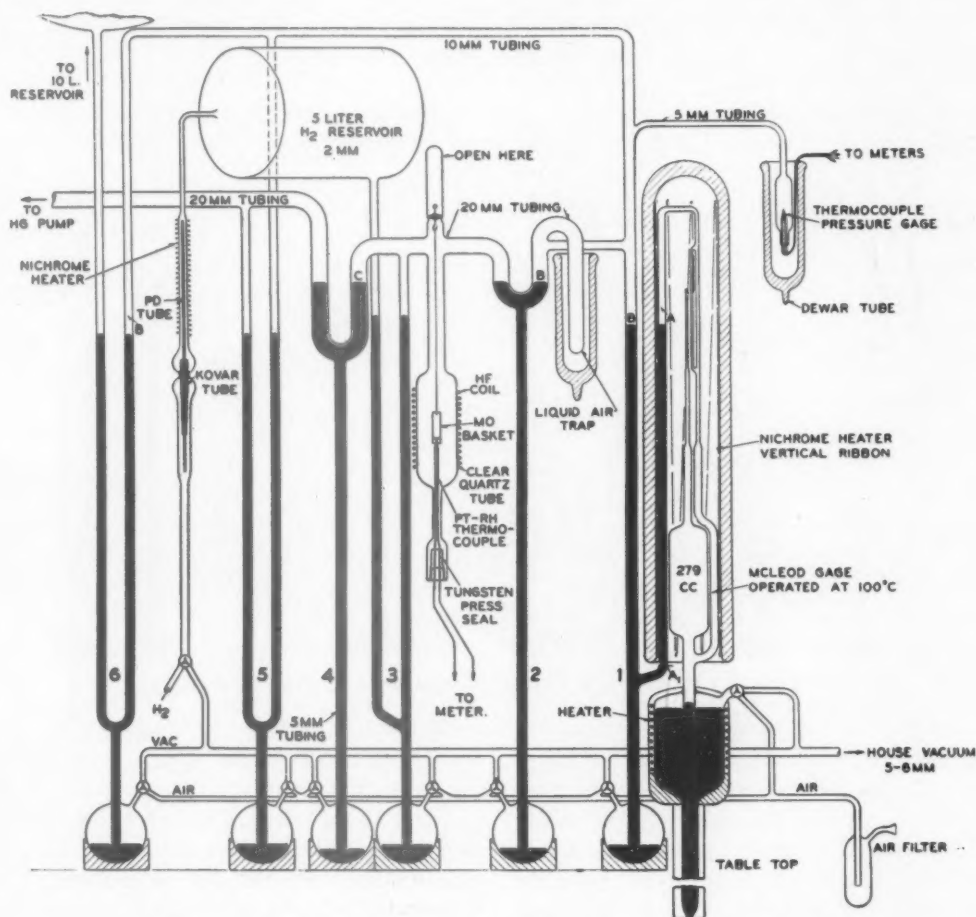
FIG. 5.—IMPROVED APPARATUS FOR DETERMINING OXYGEN IN IRON.

temperatures than could be obtained by this scheme.

We next tried the arrangement advocated by Lewis Reeve in 1933, using a long graphite crucible suspended inside a porcelain tube, but so arranged as not to touch except at the top, which is well out of the heating zone. With this arrangement we were able to get up to $1700°C.$, but still our O_2 values were too low. To remedy this we put in a mercury-circulating pump around the catalyst, so as to give more time for the conversion of CO to CO_2. This worked all right, but our blanks were too high, which was traced to H_2O being given off slowly by the platinized asbestos. This was remedied by

arrangement we found that the reaction goes fast enough so that we could dispense with the circulating pump, but still the blank was too high (0.2 mg. O_2), which we now concluded was due to the porcelain tube, and we decided to go over to the crucible arrangement used by Dr. Derge as described in his present paper. After having used this scheme for analyzing some 100 samples during the past two months, I am ready to testify to the merits of the scheme. Aside from the crucible assembly, our setup is somewhat different from Dr. Derge's: (1) We are using a completely sealed system with a graded seal between the clear quartz bulb and the Pyrex; and (2) we pass the gases

(CO, H_2 and N_2) through the heated CuO catalyst and freeze out the resulting CO_2 (and H_2O) with liquid air, then transfer the CO_2 to a very small volume for analysis. We

bring to perfection a technique that has required attention to several seemingly minor details for its success.

We have had some experience with a wedge
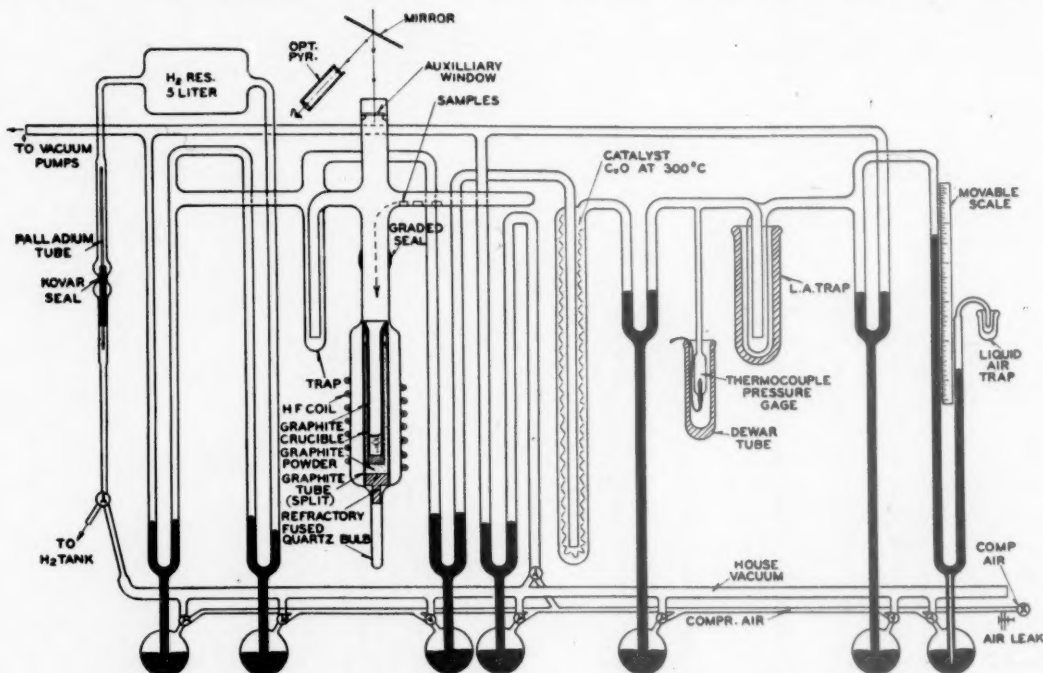
FIG. 6.—IMPROVED VACUUM-FUSION APPARATUS FOR OXYGEN ANALYSIS.

are able to make a complete O_2 analysis in 15 to 20 min. per sample. As we use very small samples (0.5 to 1 gram), we can put 24 samples into the sample tube at one time, moving the samples along the tube by means of a magnet. The blank is only 0.01 mg. ± 0.005, and we have analyzed the Bureau of Standards cooperative samples with consistent accuracy. We have not yet had time to see whether we can determine the H_2 content, but I can see no reason why we should not. On the other hand, we cannot determine the N_2 content, unless we put in another pump for pumping the gases from the furnace through the catalyst into a closed evacuated volume, from which we can freeze out the CO_2 and H_2O, leaving the N_2 to be calculated from the pressure. Ordinarily, however, as Dr. Derge has pointed out, oxygen is the gas we are chiefly concerned with.

F. G. NORRIS,* Steubenville, Ohio.—The author is to be congratulated on persevering to

* Assistant Metallurgical Engineer, Wheeling Steel Corporation.

mold but we used steel instead of copper and we did not have any vent holes in the mold. We can confirm the author's observation that the end of the sample is bright and free from oxidation temper colors. The use of a sample with a clean shiny pipe seems justified and would not be expected to be the source of any discrepancy.

It should be pointed out that the following statement: "The bomb test will remain an awkward and inconvenient method of sampling a steel bath," is merely a matter of opinion, evidently based on some grief in using the bomb test.

With the exception of the early stages of the heat when the bath is cold, the bomb test can be taken without undue difficulty after a moderate amount of practice.

The wedge sampling method has sufficient advantages that the additional equipment required should be considered for use in routine laboratories.

There is a chance that the wedge sampling technique will be useful in sampling the bath for other elements when the time of drilling

represents an appreciable fraction of the total time required for the determination.

G. DERGE (author's reply).—Mr. Larsen's method, pouring a spoon sample on to a wad of finely divided aluminum, seems to have distinct advantages over the bomb test because of its simplicity and because it can be more readily standardized. I agree that it would be of interest to compare this sample with the chilled wedge on the same heat and I hope we can arrange to do this.

His discussion also allows me a chance to emphasize that no claim is made for the absolute accuracy of the chilled-wedge test. However, experiences with this test all indicate that it is at least as correct as any other available method for sampling for oxygen and that it is far simpler than the bomb or any other known method of sampling, and has the additional advantage that no side reactions are introduced. The difficulty is that we have no absolute standard for comparison and can only say that the results obtained by this method of sampling can be correlated with the known facts about an individual heat, and that useful data can be obtained by the use of this test.

Mr. Larsen is also correct in pointing out that there may be some oxygen on the bright surface of the sample. We know of no simple way to prevent the oxidation of a clean iron surface exposed to the air, and it is probable that any practical method of oxygen analysis will include this error. Corrections can be made if desirable. In the present state of the art, I do not believe a 10 per cent error in the oxygen value is alarming, especially when it is nearly constant from sample to sample.

Dr. Yensen's description of the techniques used at Westinghouse will be very much appreciated by all people doing vacuum-fusion work. The refinements he has introduced will no doubt be of value in many applications where accuracy is important. The use of mercury cutoffs instead of stopcocks, the elimination of a circulating pump, and the use of a completely sealed glass and quartz system are all features of special interest. I hope that some of his results on hydrogen will soon be available, for the use of a small volume should make them more reliable than those obtained in the conventional apparatus.

Mr. Norris' experience in obtaining bright samples from steel molds is interesting because we were never successful in this endeavor. I am also glad that he is not concerned about a small pipe in the sample. Actually, when a sample is frozen quickly from all sides, no reservoir of molten metal is available to fill up the pipe, which must result from thermal shrinkage. Such a pipe need not represent gas evolution during freezing.

TABLE 4.—*Comparison of Carbon Analyses of the Chilled Wedge with Those of the Carbometer and Killed Test*

Heat No.	Carbon, Per Cent		
	Carbo-meter	Killed Sample	Wedge Sample
51140	0.24, 0.25	0.226	0.236
58138	0.185, 0.20	0.180	0.182
63141	0.15, 0.13	0.126	0.120
60141	0.16, 0.16	0.140	0.156
60143	0.24, 0.22	0.212	0.186
57149	0.10, 0.15	0.126	0.128
58158	0.15	0.148	0.132
56161	0.10	0.046	0.040
53159	0.09, 0.10	0.058	0.054

Data are now available (Table 4) to substantiate his belief that the wedge sample should be a rapid and convenient method of sampling the bath for other elements. These data show that the carbon analysis of the wedge sample is in excellent agreement with the conventional killed sample and carbometer samples taken at the same time. The general agreement of data is good enough to indicate that the error of heat No. 60143 is not characteristic of the wedge test. It is realized, of course, that the carbometer tests of heats 56161 and 53159 are not reliable. One might expect that a sample that gives satisfactory carbon and oxygen results will be useful for other elements.

Silver Chloride as a Medium for Study of Ingot Structures

By Karl L. Fetters,* Junior Member A.I.M.E., and Margaret Dienes†

It is recognized that ingot structure is important in determining the quality of finished steel. Such elements of ingot structure as the size, shape and distribution of primary crystals; the size, shape and distribution of shrinkage cavities; the degree and kind of segregation (both macro and micro); the distribution of nonmetallic impurities and gas cavities are each the result of solidification phenomena. These structural features vary with variations in ingot practice. Their control requires a knowledge of their correlation with the variables of ingot practice.

The structures of full-sized commercial steel ingots have been studied extensively by the Steel Ingots Committee of the Iron and Steel Institute.[1] This work has contributed much to our knowledge of ingot structure and the factors that control it. These investigations of necessity have been limited in scope because of their costliness and the great amount of time required.

Studies of the structure of small steel ingots have not been very satisfactory because of the rapid rate of freezing of the ingots. Their structures are thus difficult to resolve and to interpret. Medium sizes of steel ingots in the ranges of 150 to 500 lb. do offer opportunity for study, but their cost also becomes greater and their use less expeditious.

Experimental models for the study of steel-ingot structure have been made of nonferrous metals. Gathmann[2] used lead-tin alloys and reported that they were satisfactory for determination of the location of the major shrinkage cavities and the "planes of weakness" resulting from the pattern of crystallization. Certain features of mold design have been illustrated by these results. Bezdenezhnihk[3] has used copper and aluminum ingots similarly and has shown the effect of mold-wall thickness on the depth of columnar grains. These studies of nonferrous models have been useful, but their results have been limited because the analogy with steel ingots obviously is not a close one.

Model wax ingots have also been useful in pointing out important features of mold design. Gathmann[4] watched the solidification of wax ingots, through a glass-walled mold, and has reported the effects of mold type on the location of the shrinkage cavities. Segregation was simulated by using a mixture of paraffin and stearine and adding a red dye that on freezing segregated preferentially to the stearine. Brearley[5] also used wax models to determine the effects of some of the principal features of mold design. Carlsson and Hultgren[6] used stearic acid to show that the columnar crystals of ingots tend to slope upward progressively from the mold wall toward the center of the ingot. As with the nonferrous ingots, the wax ingots have

been useful for certain specific studies, but in general are not particularly satisfactory in analogy with steel. Furthermore, wax is but weakly crystalline and thus their structure is only qualitatively comparable with metals.

It has been found that silver chloride, AgCl, offers several advantages as a material for model ingots. This paper gives the properties of this material, describes the techniques by which it may be applied to the study of several features of ingot structure, and gives a few preliminary results.

PROPERTIES OF SILVER CHLORIDE

AgCl has a molecular weight of 143.34. Its melting point is 455°C., thus presenting no difficulty in melting. Its density at room temperature is 5.45,[7] while its molten density has been reported over the range 4.92 to 5.4.[7]

Since these data do not permit an accurate estimate of the shrinkage to be expected when molten AgCl solidifies, a rough determination of this shrinkage has been made. A small graphite mold was filled with mercury and the top was leveled. Weighing this mercury gave the volume of the mold. The mold was placed in the center of the furnace, to be described later, and heated. Solid AgCl was added until the molten salt filled the mold to the same level reached by the mercury. This ingot was frozen by slowly raising the furnace, thus allowing solidification to proceed from bottom to top. After the ingot cooled, mercury was used to fill the shrinkage cavity and its volume was determined. A contraction of 11.7 per cent was calculated from these data, as compared with 11.8 per cent[8] solidification plus contraction shrinkage for steel. Although more precise determinations might show a somewhat greater difference, the shrinkage of AgCl is certainly comparable to that of steel. The density of AgCl is great enough so that several lighter materials, such as graphite, silica, or possibly a fluorescent material

such as willemite, could be stirred into the melt, affording an opportunity to study the distribution of "inclusions" lighter than the ingot material, analogous to non-metallic inclusions in steel.
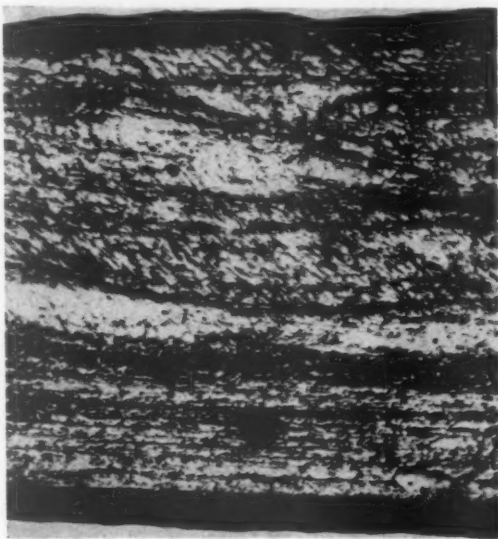
FIG. 1.—SILVER CHLORIDE COLD-ROLLED. × 100.

AgCl crystallizes in the simple cubic system, forming translucent to transparent cubic crystals. When the molten salt freezes, it forms polyhedral crystals very similar to those exhibited by metals. (See Figs. 8 and 9.) The advantages of having a crystalline material as a model for steel ingots are obvious. The grain size is satisfactory for such comparative studies. As cast AgCl has a grain size of the order of A.S.T.M. No. 1.

The freshly cast AgCl is white and almost transparent, but becomes translucent and darkens upon exposure to light. A precipitation of colloidal or atomic silver occurs, giving the material a purplish cast. Because of internal reflections of light, its transparency gives the structure of cast material an apparent relief effect not possible with opaque materials, and permits a ready location of regions of porosity, segregation or concentration of impurities. In thin sections AgCl may be examined by

transmitted light. This transparency might be utilized in observing the material during recrystallization on a heated microscope stage, a feat impossible with metals.
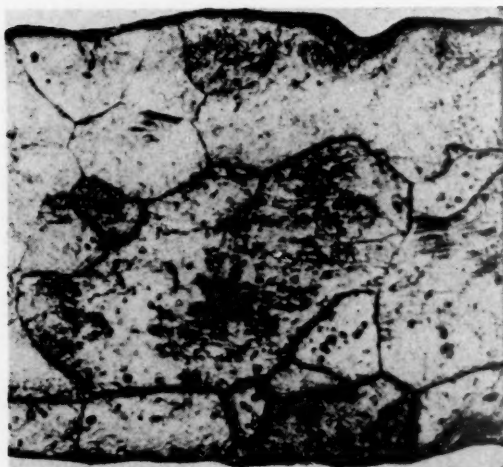
FIG. 2.—SILVER CHLORIDE COLD-ROLLED AND THEN RECRYSTALLIZED FOR 15 MINUTES AT 325°C. × 75.

AgCl may be extensively cold-worked and hot-worked. Tammann[9] made studies of its work-hardening and its recrystalliza-

tures are similar to those for metals. Fugassi and McKinney[10] have cold-rolled thin films of AgCl for use as infrared filters, and have extruded thin tubes. They found it very important that the AgCl be quite pure if extensive working is to be done.

Several samples of AgCl have now been cold-rolled more than 50 per cent and have been examined. A typical photomicrograph of the cold-rolled structure is shown in Fig. 1. A series of these samples was then annealed for 15 min. each at 200°C., 325°C., and 435°C. Recrystallization occurred with successively larger grains as the annealing temperature increased. Fig. 2 shows a typical recrystallized structure.

A stress-free crystal of AgCl is isotropic in polarized light; as stresses are imposed on such a crystal it becomes anisotropic. Thus it will be possible to study stresses in a polycrystalline material by the methods of photoelasticity. This would seem to offer several advantages over the amorphous Bakelite now used for that purpose.

FIG. 3.—MICROSTRUCTURE OF SILVER CHLORIDE CONTAINING 10 MOL PER CENT OF SILVER BROMIDE. × 50.

FIG. 4.—MICROSTRUCTURE OF SILVER CHLORIDE CONTAINING 10 MOL PER CENT OF SILVER IODIDE. × 50.

tion on heating following cold-work. The change of hardness and the change of density on annealing at increasing tempera-

AgCl may also be hot-worked, and it should be possible to study the effect of various forging practices as well as the

effect of various ingot structures on both the longitudinal and transverse mechanical properties of forgings using AgCl as a model substance.

Stepanow[11] has studied the mechanical properties of single crystals of AgCl. He remarks on the ductile properties of the material and shows a stress-strain curve for a tensile sample.

Silver bromide may be added to AgCl to form a continuous series of solid solutions. The composition-temperature diagram[12] has a minimum melting point at 412°C. and at 65 mol per cent AgBr. (The melting point of AgBr is 422°C.) The maximum spread between the solidus and liquidus lines for this system is only 5°. Sufficient segregation occurs in these alloys during solidification so that a dendritic-like pattern may be observed (Fig. 3). The somewhat greater photosensitivity of AgBr as compared with that of AgCl might be used to advantage in studying segregation.

The AgI-AgCl system[12] is of the eutectic type, with very limited solid solubility of AgI in AgCl and somewhat greater solid solubility of AgCl in AgI. The eutectic temperature is 377°C. and the composition is 73 mol per cent AgI. Fig. 4 shows the appearance of this eutectic. Additions of either AgBr or AgI cause appreciably finer grain in the ingots. Fig. 5 shows a typical AgCl-AgBr ingot.

Solid particles of insoluble materials may be introduced into molten AgCl and their separation and distribution during freezing may be noted. Simulation of inclusions in steel is thus possible. Graphite, quartz and other materials may be used for this purpose.

Various miscellaneous additions offer the opportunity to study the effect of segregation of solid solution elements and of insoluble substances upon ingot structures and upon the properties of forgings.

EXPERIMENTAL TECHNIQUES

AgCl may readily be melted in a porcelain or graphite crucible heated by a gas
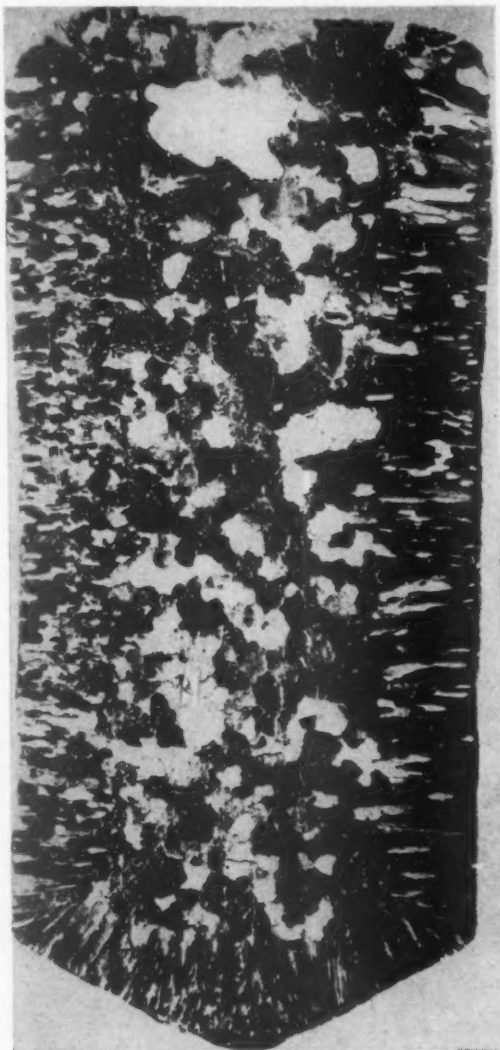
FIG. 5.—INGOT OF SILVER CHLORIDE PLUS 2.5 MOL PER CENT SILVER BROMIDE. $\times 4\frac{1}{2}$.

burner. A series of melts was made in this manner and poured into $\frac{1}{2}$-in. diameter ingot molds, in an effort to establish an optimum ingot size for experimental studies. Graphite, plaster of Paris, and a dental investment mix (White's No. 30 Investment Mixture) having a silica base were used for mold materials. Molds made of plaster or investment must be

thoroughly dried at 500°C. before use,* in order to prevent water vapor from the mold from forming blowholes in the AgCl ingot. In the handling of molten

similar reaction between solid AgCl and metals in a moist atmosphere. This is not serious in ordinary sawing and machining operations. The structure of one of the
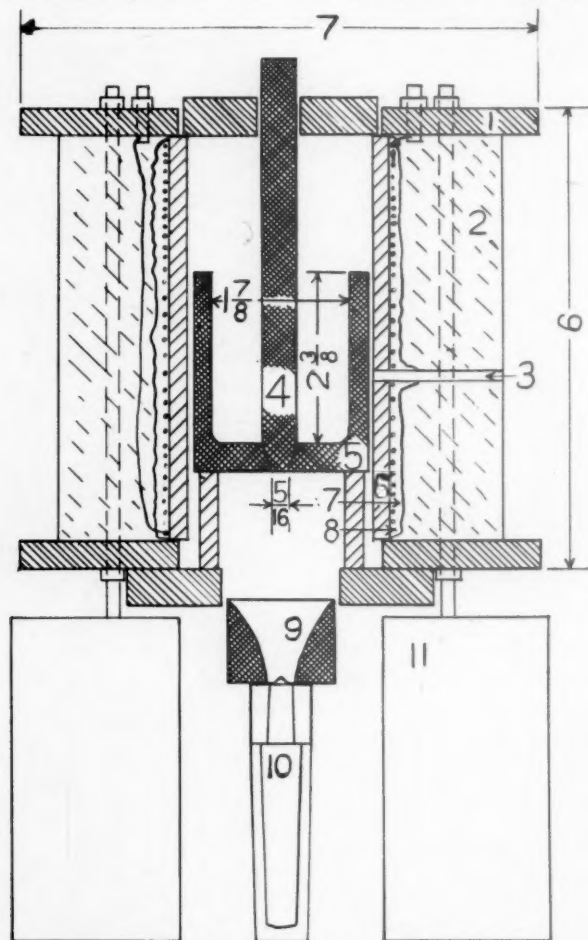
FIG. 6.—SECTION OF FURNACE USED FOR MELTING SILVER CHLORIDE.

1. Transite board.
2. Sil-O-Cel.
3. Silica tube for thermocouple (Chromel-alumel).
4. Graphite stopper.
5. Graphite crucible.
6. McDanel high-temperature tube.
7. Alundum cement.
8. Nichrome wire, Gauge 18, 50 ft.
9. Graphite funnel.
10. Ingot mold with hot top.
11. Brick.

All dimensions in inches.

AgCl, it is necessary to prevent contact with metals less noble than silver, since they will react with it and deposit silver. Some care is also needed to prevent a

* The molds were dried for ½ hr. at 500°C. Although the full strength of the plaster probably did not remain, the molds were satisfactory for the use intended. Most of the molds used in the experiment described were made with a dental investment mixture, which was found to be preferable to the other materials for this use.

small ingots to which AgBr was added is shown in Fig. 5. A grain structure similar to that of a metallic ingot is evident. The structures of ingots of AgCl with additions of AgBr or AgI were studied in these small ingots; as stated before, the additions produce an appreciable decrease in primary grain size, with a greater refining effect in the case of AgI than in AgBr. Several

different designs of molds were used for small, pure AgCl ingots in an effort to determine their effect on the ingot structure, but the differences were so small that

from the bottom of the crucible through a pouring funnel into a mold. An arc-lamp electrode is used as the stopper rod. There is ample clearance between the stopper
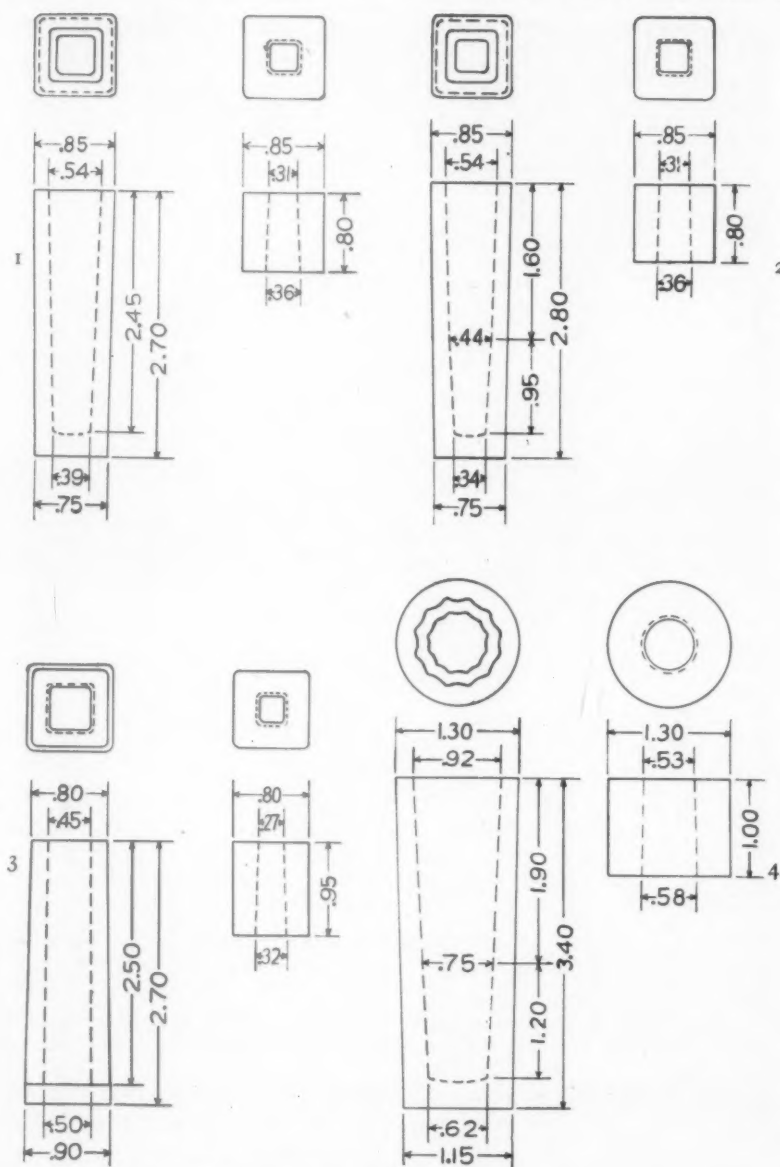
FIG. 7.—INGOT MOLDS. ALL DIMENSIONS IN INCHES.

comparison was difficult, and the need for somewhat larger ingots seemed clear.

An electric resistance furnace was constructed to produce melts under closely controlled conditions. Fig. 6 shows a section of this furnace. A graphite crucible is so constructed as to permit pouring directly

rod and the crucible wall for the insertion of an electrically driven Pyrex stirrer, which was used in several of the melts. In practice, solid AgCl is charged into the furnace in weighed amounts and the furnace is heated above the melting point of AgCl. After melting is completed, the furnace

voltage is adjusted to maintain the desired pouring temperature, and after allowing time to secure a uniform temperature the melt is poured by removing the stopper rod.

dron. The proportions of these molds are similar to a series of iron molds available in this laboratory for pouring 170-lb. steel ingots, and the results on the AgCl
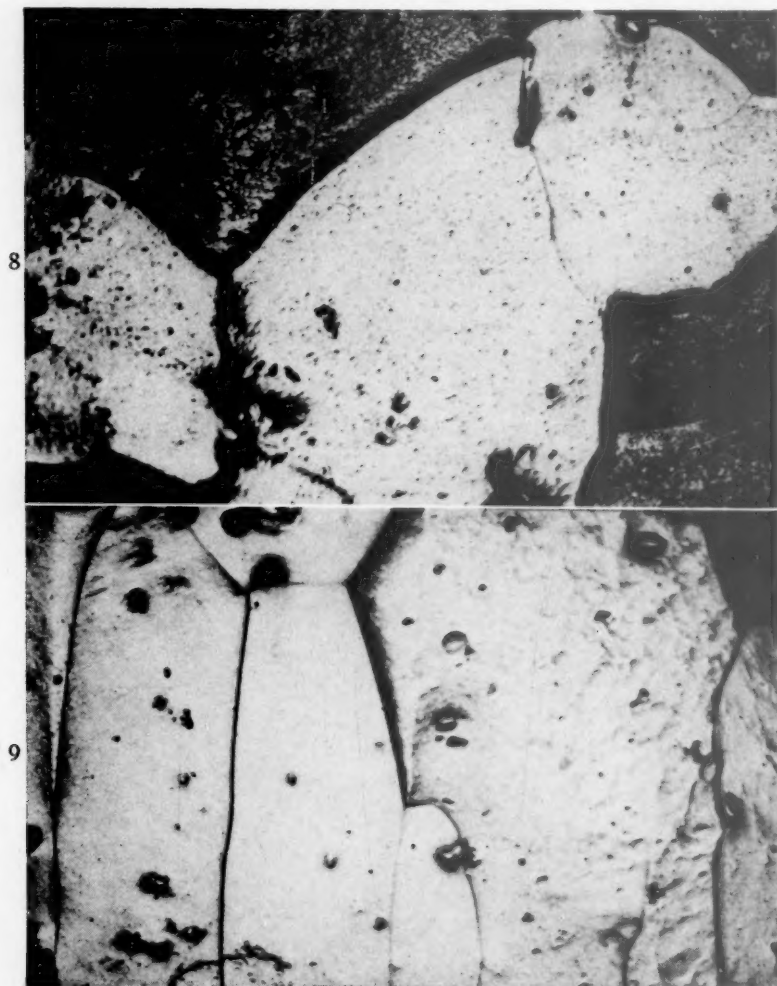
FIG. 8.—MICROSTRUCTURE OF CENTRAL EQUIAXED ZONE OF SILVER CHLORIDE, INGOT No. 4a. × 50.
FIG. 9.—MICROSTRUCTURE OF COLUMNAR ZONE OF SILVER CHLORIDE INGOT No. 4a. × 50.

A series of investment-mix molds were made in shells of copper sheet. The hot tops were made from equal volumes of investment mix and Sil-O-cel. Such a hot top has satisfactory insulating properties. The sections of the molds used are shown in Fig. 7, identified as types 1 to 4. No. 1 is a single-taper big-end-up mold, No. 2 is a double-taper big-end-up mold, No. 3 is a big-end-down mold and No. 4 is a big-end-up, multitaper, fluted dodecahe-

ingots will be compared later to these steel ingots. It will be noted that these molds have a somewhat steeper taper and a greater ratio of length to cross section than many molds used for larger commercial ingots.

After cooling, the cast ingots were removed from the molds and split longitudinally. A hacksaw or jeweler's saw was used. It was noted that immediately after casting sectioning was more difficult

than the following day. The difficulty presumably was caused by the softness of the AgCl prior to precipitation of the colloidal silver by light. The sectioned sulphate may be used as etchants, but the best results were obtained with ordinary Kodak acid fixing solution. Repeated polishing on the final wheel and etching

1a   1b   2a   2b
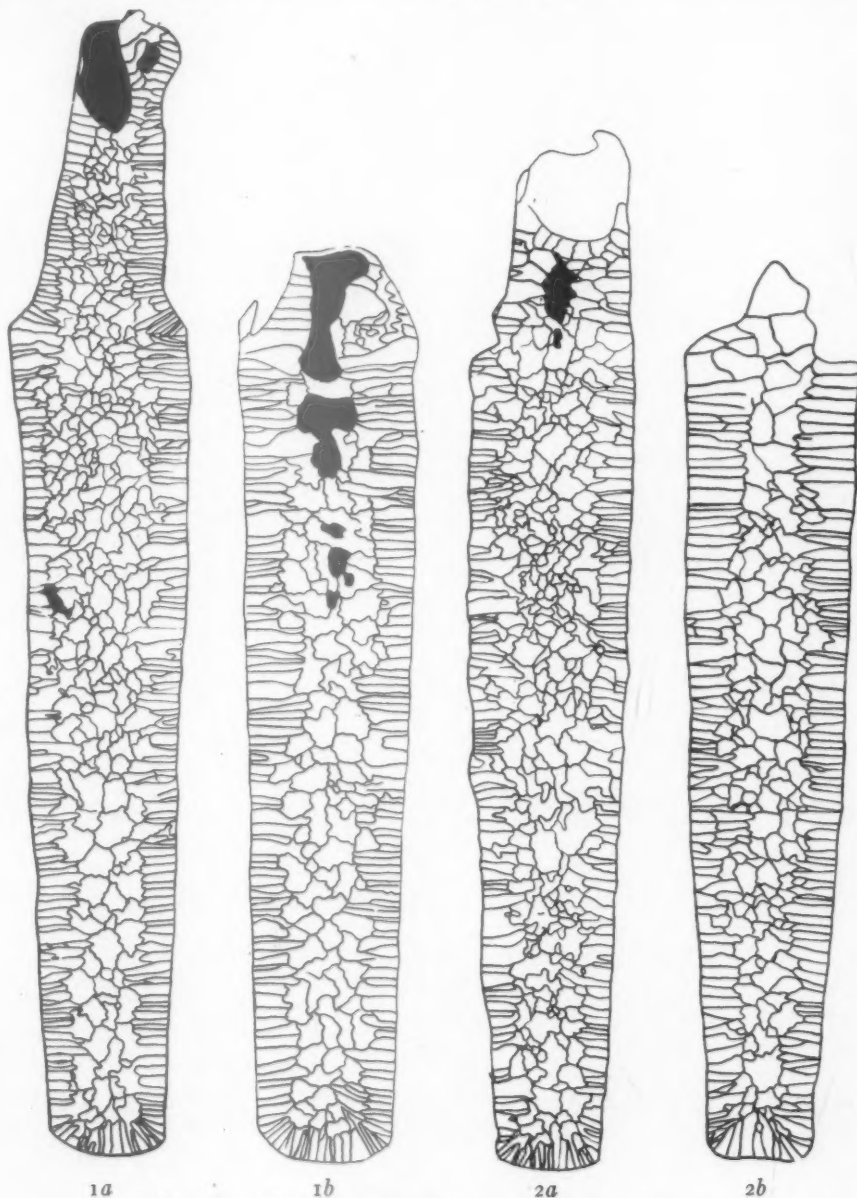
FIG. 10.—INGOT STRUCTURES, MOLDS 1 AND 2. × 1.5.

ingots were flattened with a file, then rough-polished on a moderate-grit polishing belt. A cloth wheel with Norton 600 abrasive was next used, followed by a final polish with green rouge on a Selvyt wheel. Ammonium hydroxide or sodium thio- after each polishing operation is advantageous. Fig. 5 shows the macrostructure observed by these methods and Figs. 8 and 9 show typical microstructures. The latter show, respectively, the equiaxed grains occurring at the center of an ingot and the

columnar grains at the edge. A very thin layer of chill grains usually may be noted

in obtaining good macrophotographs at the magnifications desired.

3a   3b   4a   4b
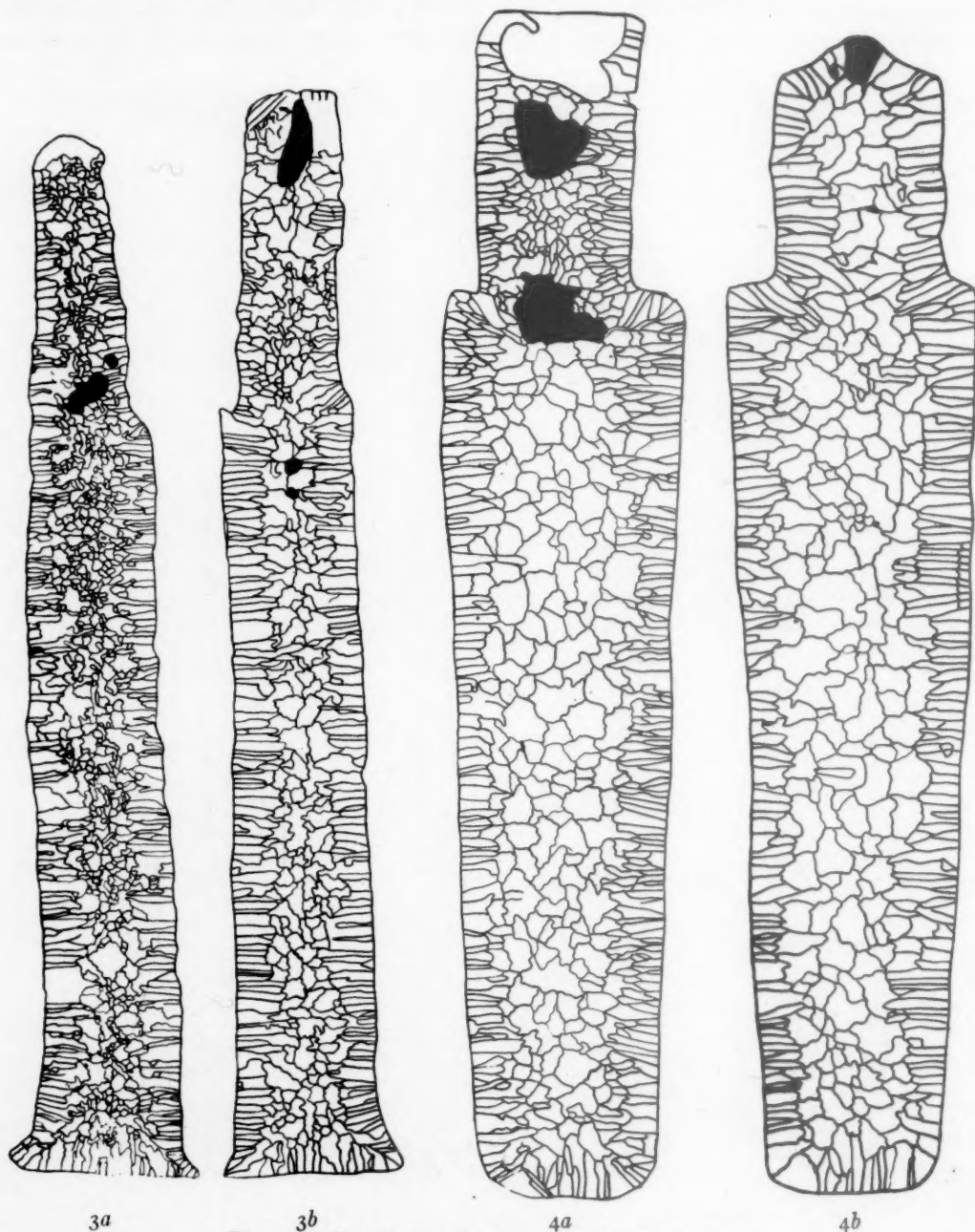
FIG. 11.—INGOT STRUCTURES, MOLDS 3 AND 4. × 1.5.

at the extreme surface of the ingot though these do not show in Fig. 9. The structures of the ingots to be described below have been reproduced by sketches rather than by photographs because of difficulty

STUDIES OF INGOT STRUCTURE

Three series of ingots were poured into the four molds of Fig. 7. Series *a* was poured at about 460°C.; series *b* was poured

at about 520°C., and series *c* was poured at about 510°C. and had 200-mesh graphite stirred into the silver chloride prior to casting. Each of these ingots was sectioned

average depth of the columnar crystals in the low-temperature series is about 0.12 in., whereas the columnar crystals of the higher-temperature series are about 0.17 in.
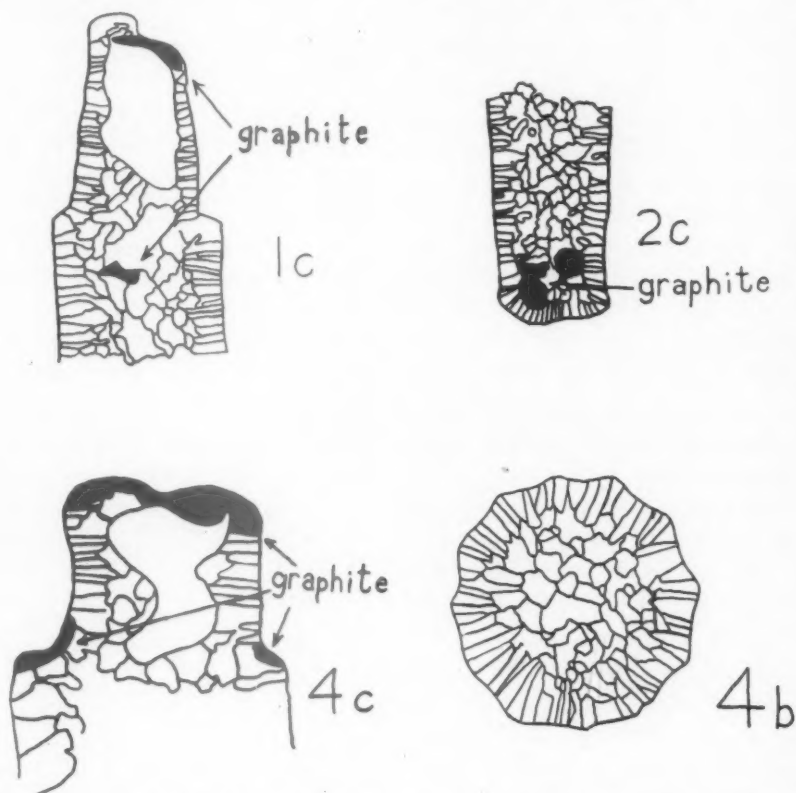
FIG. 12.—INGOTS TO WHICH GRAPHITE WAS ADDED. CROSS SECTION OF INGOT 4*b* ABOUT MID-SECTION. × 1½.

longitudinally, polished and etched. The grain structure of each ingot was carefully outlined at 6 diameters on tracing paper on the ground-glass screen of a macro-camera. The tracing was then reduced photographically (all ingots by the same amount) to give the structures shown in Figs. 10 to 12. In Fig. 12, 4*b* shows the typical grain structure of a transverse ingot section.

Several observations may be made by comparing the ingots of series *a* and *b*:

1. The depth of the columnar crystal is always greater in the ingots poured at the higher temperature. Comparing ingots of series *a* with those of series *b* shows that the
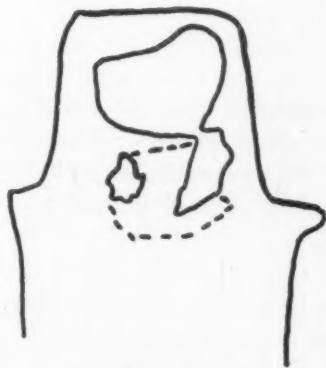
FIG. 13.—LOCATION OF PIPE CAVITY IN INGOT OF SILVER CHLORIDE SIX INCHES HIGH. CROSS SECTION. × 1/10.

long. The higher rate of heat transfer at the start of solidification, as well as the lower

rate of nucleation, would account for these deeper zones of columnar crystals. Similar effects have been noted in steel ingots by Leitner[13] and by Hohage and Schafer.[14]

It may also be noted that there is a slightly finer grain in both the columnar and the equiaxed grain regions of the ingots poured at the lower temperatures. The columnar crystals slope slightly upward from the edge toward the center of the ingots. Northcott[15] found a similar slope to the columnar crystals in steel ingots and described it as an inclination of the crystals toward the direction from which the liquid steel flowed along the mold face. Zhegalov and Tageev[16] explained the slope of the columnar crystals as following the line of heat flow from the thermal center of the ingot through the mold wall.

2. A much greater lack of uniformity of the equiaxed grain size prevails in the big-end-down ingot than was noted in any of the big-end-up ingots. Note particularly ingot 3a, Fig. 11.

The third series of ingots, series c, was made with graphite added to the melt and thoroughly mixed by the electric stirrer. This mixing was allowed to continue up to the time of pouring. The problem of distribution of insoluble nonmetallic particles such as alumina and other refractory oxides is of considerable importance in steel ingots. This problem has not been considered in work on wax or nonferrous models. Fig. 12 shows the location of the graphite in certain of the ingots. Most of the nonmetallics were eliminated in 1c, 3c (not shown), and 4c, having floated to the top. Evidently the particle size used was too large, and the experiment must be repeated with finer material. Some of the graphite, however, was entrapped near the bottom of ingot 2c (Fig. 12). Dickinson[17] and Hare and Soler[18] report predominance of refractory types of nonmetallics in the bottom central portions of steel ingots.

Several ingots of pure AgCl were cast in a larger investment mold similar to mold 4, but 6 in. high and $1\frac{11}{16}$ in. in diameter. These all showed shrinkage cavities very similar to those found in steel ingots (Fig. 13).

SUMMARY

1. The manner in which AgCl freezes, its semitransparency, and the plasticity of solid AgCl recommend it for use in the study of model ingots.

2. The segregation of solid solutions and of nonmetallics may be studied by the addition of suitable materials.

3. Preliminary results give reason to believe that the grain structure, pipe, segregation, and the distribution of nonmetallics in larger ingots may be studied by these models.

REFERENCES

1. Ninth Report on the Heterogeneity of Steel Ingots, Special Report No. 27, Iron and Steel Inst. (1939).
2. E. Gathmann: *Blast Furnace and Steel Plant* (Feb. 1937) **25**, 204.
3. A. Bezdenezhnihk: *Metallurg* (1937) **12** (6), 66–78.
4. E. Gathmann: The Ingot Phase of Steel Production, Ed. 2. Baltimore, 1942.
5. A. W. Brearley and H. Brearley: Ingots and Ingot Molds. London, 1918. Longmans, Green and Co.
6. C. G. Carlsson and A. Hultgren: *Jernkontorets Ann.* (1936) **120**, 577–587.
7. J. W. Mellor: A Comprehensive Treatise on Inorganic and Theoretical Chemistry, **3**, 428. New York, 1937. Longmans, Green and Co.
8. Steel Castings Handbook, 1941. Steel Founders Society of America, Cleveland, Ohio.
9. G. Tammann: *Naturgewissenshaften* (1932) **20**, 958–960.
10. P. Fugassi and D. S. McKinney: *Rev. Sci. Instruments* (1942) **13** (8), 335–337.
11. A. W. Stepanow: *Physik. Ztsch. Sowjetunion* (1935) **8**, 25.
12. International Critical Tables, **4**, 58.
13. F. Leitner: *Stahl und Eisen*, **50**, 1081–1086.
14. R. Hohage and R. Schafer: *Archiv Eisenhuttenwesen*, **13**, 123–125.
15. L. Northcott: *Jnl.* Iron and Steel Inst. (1941) 49–92.
16. A. K. Zhegalov and V. M. Tageev: *Metallurg.* **13**, 35–49.
17. J. H. S. Dickinson: *Jnl.* Iron and Steel Inst. (1926) **113**, 177–271.
18. W. A. Hare and G. Soler: *Trans.* Amer. Soc. Metals, **26**, 903–928.

DISCUSSION

(Gilbert Soler presiding)

C. R. TAYLOR,* Middletown, Ohio.—As the authors have stated, the value of the paper would have been increased many times had they used large molds. They say that the differences in structure were small between the various types of molds. This is certainly not true in large steel ingots. If they had used molds of such a size that the relative size of the crystals developed on etching were in the same ratio as those on large ingots, I believe the results would have been more conclusive.

J. W. HALLEY,† East Chicago, Ind.—A new technique in the study of ingot solidification and structure is always welcome, and the use of silver chloride described in this paper appears promising. However, all attempts to study phenomena on a greatly reduced scale must be viewed critically if we are not to be misled.

In laboratory-scale studies of ingot solidification bath dimensions and temperature are reduced. The authors give the over-all shrinkage of silver chloride from the liquid to room temperature as 11.7 per cent and compare this to an over-all contraction of steel of 11.8 per cent. However, piping is the result of liquid to solid contraction only, which is about 3 per cent for steel and probably much higher for silver chloride. Silver chloride freezes at a constant temperature, while medium carbon steel freezes over a temperature range of 40° to 60°C. The crystals, as shown in Figs. 10 and 11, are much coarser in relation to the size of the ingot than are the crystals in an average sized steel ingot. The proper dimensions of small ingots are difficult to determine. The structure is a function of vertical shrinkage and movement of the liquid, and the rate of horizontal solidification. Since solidification time varies as the square of the cross section, it is evident that the height should be decreased much more rapidly than the cross section.

As far as contraction from liquid to solid and crystal structure are concerned, lead appears more desirable than silver chloride. It has a

contraction of about 3 per cent and a face-centered cubic structure. A small amount of tin, up to 3.6 per cent, can be added to give a gap between the liquidus and solidus without altering the crystal structure.

A. L. FEILD,* Baltimore, Md.—From the standpoint of laboratory technique, this is one of the most interesting and stimulating papers that have been presented before the Institute in a number of years, at least so far as steel-making phenomena are concerned.

The fact that freshly cast silver chloride is almost transparent is indeed a fortunate circumstance, although I must admit that this particular property of transparency comes as a surprise to me. The work of the authors demonstrates conclusively the general value of this medium in the study of solidification phenomena. However, it remains a question in my mind as to what extent the great difference in thermal conductivity between silver chloride and steel affects the validity of at least some of the conclusions that may be drawn from the authors' analogy.

C. E. SIMS,† Columbus, Ohio.—When considering the use of materials such as silver chloride to study miniature ingots, a natural question might be, "Why not use steel, inasmuch as most laboratories have such convenient means of making small batches of steel?" In fact, steel is easier to handle in some respects than silver chloride. The answer seems to be that in small steel ingots all factors are not reduced in the same proportion. The chilling effect of the mold becomes too prominent while in very large ingots the conductivity of the steel itself sets the pace of freezing. Thus a miniature ingot of silver chloride or wax might behave more like a large steel ingot than would a small steel ingot.

I cannot agree with the authors that the behavior of inclusions can be studied by mechanically mixing graphite, silica or other materials with the silver chloride. The evidence is overwhelming that the principal inclusions

of steel ingots do not occur as mechanical entities before the steel is teemed but are precipitated during solidification of the steel.

Since the present work has been available, tests on silver chloride ingots have been made at Battelle Memorial Institute. One disturbing feature of its behavior was the failure to obtain any pipe or shrinkage cavity when poured without a hot top. Fig. 14 shows vertical sections of two ingots, each 3 in. square, one cast in a cast-iron mold preheated to 160°F. and the other in a silica-sand mold bonded with portland cement. The surface was dished but there is no sign of pipe or cavity. The material does shrink, but apparently the linear solid shrinkage is great enough to offset the solidification shrinkage. It appears that this will be a handicap in studying ingot structures.
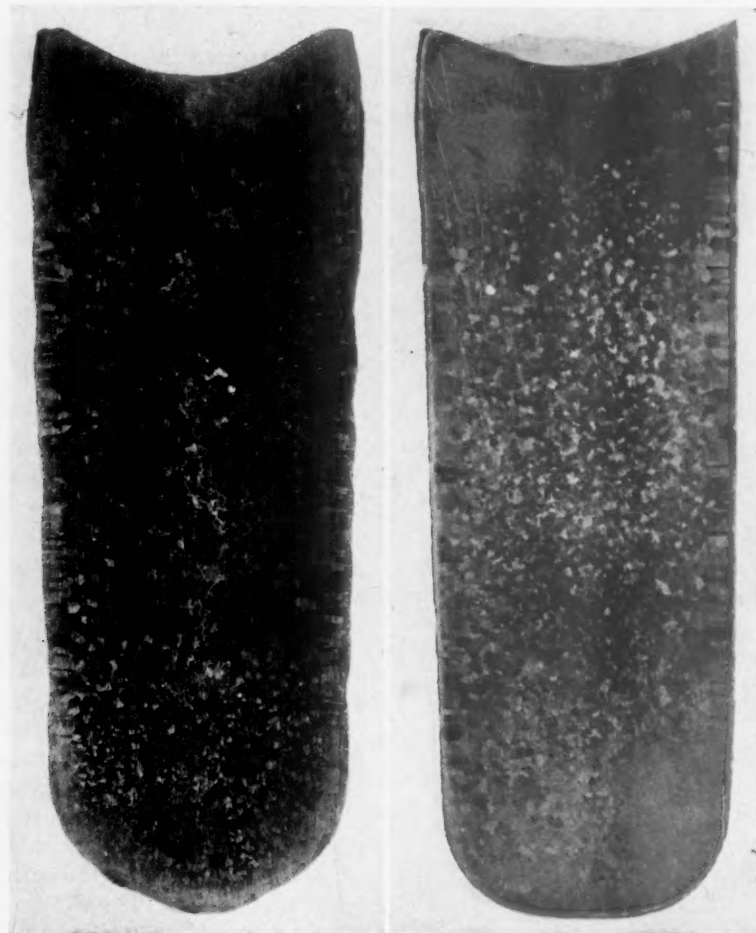
FIG. 14.—VERTICAL SECTIONS OF SILVER CHLORIDE INGOTS CAST WITHOUT HOT TOPS. POLISHED AND ETCHED.

Ingots were 3 inches square. The one on the left was cast into a gray-iron mold while that on the right was cast into a sand-cement mold, for contrast in cooling rate. Neither shows pipe or shrinkage cavity, yet the over-all shrinkage was more than 11 per cent.

The Origin, Definition and Prevention of Scabs

By T. J. Woods*
(Cleveland Meeting, April 1943)

THIS paper deals with the origin, definition and prevention of scabs on semifinished rolled-steel product.

Mold coatings, which are considered essential in scab prevention, were found to be effective only in relation to the ingot surface of semikilled and killed steels and not necessary for the rolled product. That is to say, the scabs on ingots caused by having been cast in uncoated molds are eliminated in the soaking and rolling operations, therefore are not present on the rolled product. This fact, which is contrary to the average opinion, was established after extensive and thorough experiments had proved the ordinary conception of the origin of scabs to be incorrect.

This subject may be of little or no concern to steel plants producing small ingots for the manufacture of small billets and bars, except as it may be of interest in showing why their surface troubles with scabs do not exist on the product of heats with normal pouring practice. But to the producer of large ingots to be rolled into slabs for large plates used in shipbuilding, it is a very important subject.

DEFINITION OF A SCAB

The generally accepted opinion is that the individual scabs present on rolled products (as shown by Fig. 1) are considered to have been individual splashes on the ingot surface. This opinion was found to be incorrect. Experiments showed that there were no individual scabs on the product that had appeared as individuals on the ingot surface. The single scabs seen are either pieces of a shell that is present near the bottom of all top-cast ingots, or a veneer that may be present on any part of an ingot improperly poured, as when the stream strikes the mold wall. This definition is based on a detailed study of scabs and their characteristics in which the following have been found true:

Location.—On the product of heats poured without trouble, scabs, if present, are always on the product that corresponds to the bottom end of the ingot, and usually occur in clusters. This is true whether molds are coated or not.

Shape.—There is no regularity as to shape, size or thickness. It is sometimes possible to separate a few pieces and place them together, like pieces of a jigsaw puzzle, indicating that at one time they had been united as one piece.

If individual splashes were the origin of scabs, the foregoing would not be true. Instead, the splashes, which occur throughout the pouring of the ingots, would be present uniformly over the entire product and there would be considerable similarity in the shape and thickness of the scabs.

EXPERIMENTAL WORK

Our experimental work was conducted on 200-ton heats of semikilled plate steel tapped into an oval ladle 15 ft. high. All ingots were top-cast direct into 24 by 54 by 82-in. molds, straight-sided, set on flat stools. Two separate studies were made about one year apart, each study extending
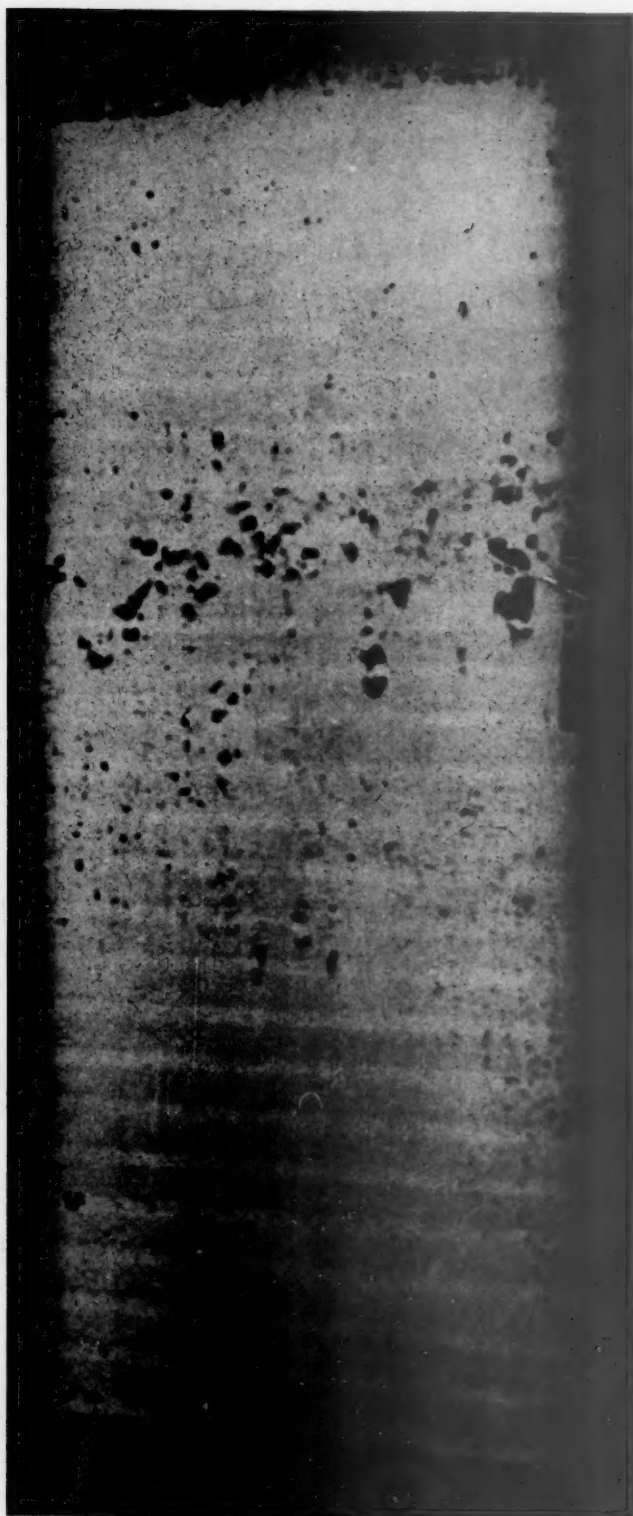
Fig. 1.—Hot slab from extreme bottom end of a 24 by 54-inch ingot. Bottom end at left.

This shows a broken band of black scabs about one-third from the right end. The extreme bottom left end, except the near edge, is free of scabs. This is because the shell at that place is a definite part of the ingot. Between the band of black scabs and the bottom that is free of scabs, there is a band of lighter scabs, which dip toward the left end and run along the edge. The lighter color indicates higher temperature and closer contact with the slab. The degree of adherence of the shell to the ingot varies from top to bottom of the shell. The farther from the bottom, the less the adherence.

If this ingot had been rolled at a temperature high enough to prevent separation of the shell from the ingot, the band of dark colored scabs would be present but not the light colored band.

over a continuous period of approximately two months. The same procedure was followed in each instance, except in the method used to determine the scabby area.

virtually the same, except that in the one in which the linear feet of scabby area was measured the product from the coated molds contained about one square foot of

FIG. 2.—SHELL FORMED AT BOTTOM OF 24 BY 54-INCH INGOT.

In one study the area was estimated, and in the other the linear feet of area covered with scabs was obtained. Four new molds were used for each study and they were kept together throughout their entire life; that is, 126 and 180 pours, respectively. In the first study two molds were dip-coated with tar and in the second two molds were coated with dry pitch; the remaining two in each study were uncoated. In order to keep all variables as constant as possible for each heat, the four molds and the ingots cast in them were treated in the same way in pouring, heating and rolling. The product of each ingot was identified and carefully inspected.

The results of the experiments were

area fewer scabs per slab (three slabs to each ingot) than the product from the uncoated molds. This difference was so slight that in the experiment in which visual examination alone was made it was not noticeable. Such a slight difference is not very convincing evidence that the coating was responsible. Repeated tests along the same lines might reverse the decision. If coatings are the main factor in the prevention of scabs, the difference should have been greater. In fact, no scabs should have been present on the product from the coated mold.

In both experiments, the coated molds failed first; that is, they fire-checked earlier in life and, as a consequence, spalled and

gouged out earlier than the uncoated molds. This also is contrary to the general opinion on this subject.

These experiments proved that, except
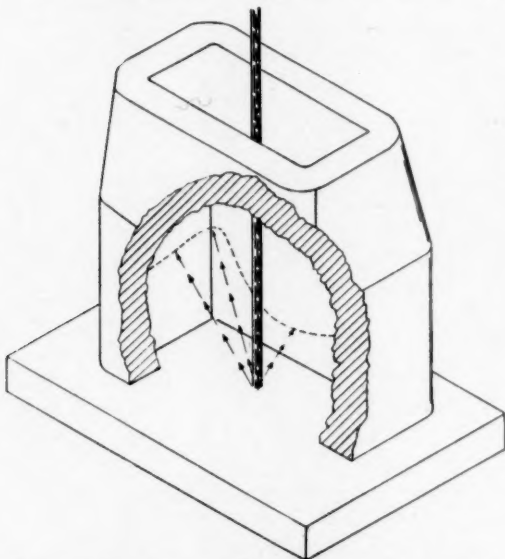
FIG. 3.—ISOMETRIC VIEW OF MOLD, 24 BY 54 BY 82 INCHES.

to a minor degree, coatings are not essential to the prevention of scabs and that such scabs must originate from a source other than single splashes of metal on the mold wall. Even though the coatings did prevent splashes from adhering to the mold wall and the ingots, the rolled product was scabby.

SHELLS

Fig. 2 shows a "shell," which the author believes to be the one and only source of scabs on all top-cast ingots that have had good pouring practice. Such shells can be seen on almost any scrap pile of ingots that are too short to roll. If the rate of metal rise in the mold is fast enough to overtake this shell before it becomes too cold and oxidized, scabs will not form. The rate of rise is estimated to be about 2.7 in. per second for a mold of the size used in these experiments. This rate was established by using various nozzle sizes, ranging from 1½ to 4 in. in diameter. We found, by studying the product of ingots poured with the nozzle sizes mentioned, that a nozzle of about 3½ in.

was necessary. The metal requires approximately 36 sec. to reach the top of the shell when a 1½-in. nozzle is used, and about 15 sec. with a 3½-in. nozzle.

Shells are formed (Figs. 3, 4 and 5) by numerous single splashes of metal rebounding from the stool as the metal first strikes during the pooling operation. After a sufficient depth of metal is reached to withstand the impact, the broken stream of continuous splashes gradually decreases. From that point to the top of the mold, only scattered single splashes reach and adhere to the mold wall and the ingots if molds are uncoated, but are repelled if molds are coated. It is these single splashes, formed in this manner, that appear on the surfaces of ingots cast in uncoated molds. These splashes, loosely adhering to the ingot, cannot, therefore, survive the heating and rolling operations, and for that reason they are not present on the rolled product.

The height of the average shell on a 24 by 54 by 82-in. ingot is approximately 8 to 12 in. on the 54-in. sides, 14 to 16 in. on the 24-in. ends, and 18 to 20 in. on the corners. These heights are reached in about the time it takes to pool 2 to 3 in. of metal on the stool. The ends and corners are higher because of their greater distance from the point of stream contact with the stool and the wave of pooled metal along the ingot bottom, which surges up the ends and corners. The wave is caused by the rushing of the pooled metal along the bottom, when opening to a full stream. On the average ingot, scabs are formed by the tops of the corner and end shells. The remainder does not ordinarily produce scabs. The reason for this is that as long as there is not a sufficient depth of pooled metal to withstand the impact of the stream against the stool, there is a continued splashing of the inside of the shell at these points with molten metal. This prevents cooling and oxidation, so that when the liquid metal arrives a solid union is formed between the shell and the ingot. This is the reason why
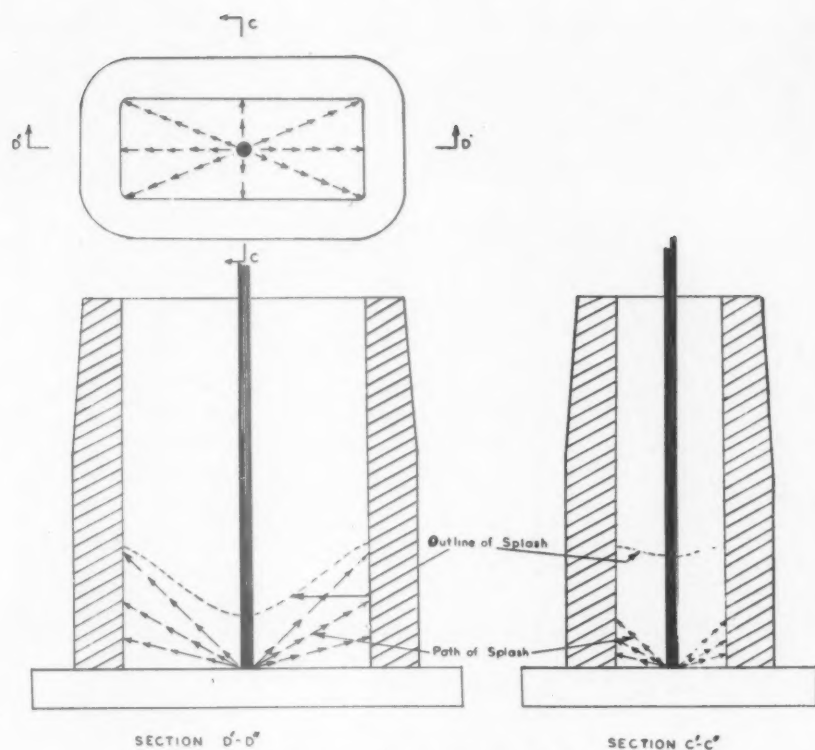
FIG. 4.—INGOT MOLD, 24 BY 54 BY 82 INCHES.
This illustrates why scabs usually are more prevalent on the slab edges near the bottom than at any other place.
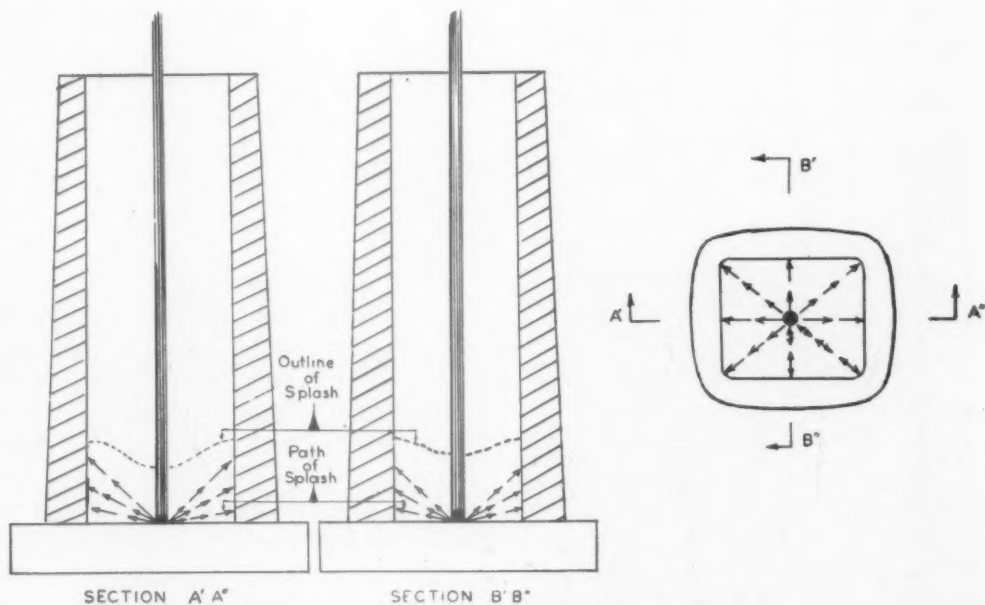
FIG. 5.—INGOT MOLD, 21 BY 24 BY 74 INCHES.
This illustrates the formation of a shell in a small mold.

the extreme bottom of the bottom cut is free from scabs.

Figs. 6 and 7 illustrate the author's opinion of the slight benefit, if any, of coat-

Fig. 8 illustrates the relation of nozzle size to rate of rise in the mold with respect to the shell.

There are three other ingot characteristics
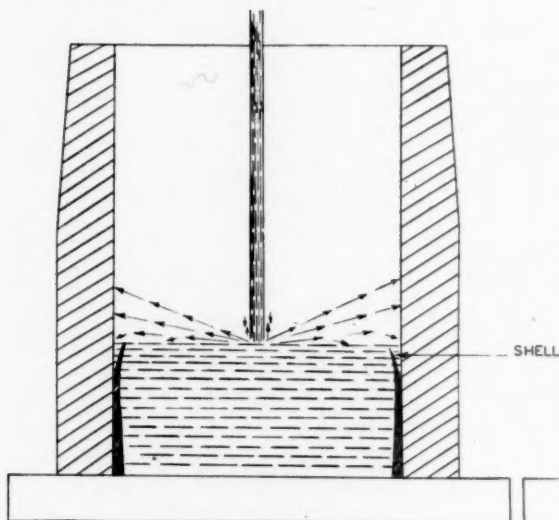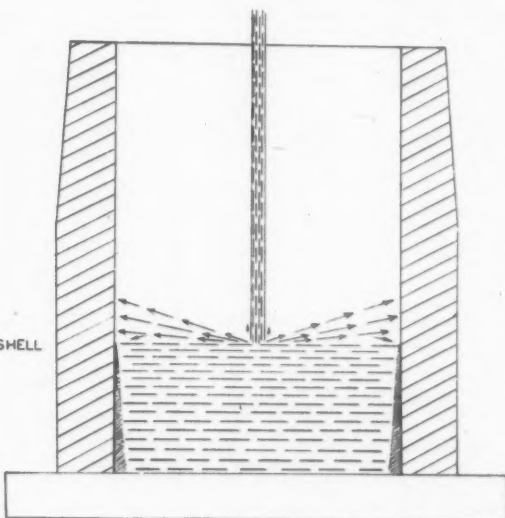
Fig. 6, coated.   Fig. 7, uncoated.

FIGS. 6 AND 7.—INGOT MOLDS, 24 BY 54 BY 82 INCHES.

These show the author's idea as to what probably happens to the extreme top of the shell when molds are coated or not coated. The extreme top of the shell in a coated mold would tend to pull away from the mold wall more quickly than one in an uncoated mold. If there is a benefit from coatings, this is probably the reason.

ings. The extreme top of tne shell in a coated mold would tend to pull away from

that are attributable to the shell and the manner in which it is formed:

1. The ingot surface of the extreme bottom is smooth in comparison with the remainder, because the skin at this point is formed by the impact of the metal against the mold wall, rather than by a slow creeping motion, as occurs after sufficient depth of pooled metal is poured.

2. The curtain effect (Fig. 9) around the ingot bottom at about the top of the shell is the result of the cooling of the top of the shell; the top contracts away from the mold wall, so that when the liquid metal reaches this point it flows down between the contracted shell and the mold. The newer the molds, the more pronounced this condition seems to be.

3. The light colored edge that is present in macro etch tests from the bottom end of bottom-cut billets of killed steel, all grades, top-cast in big-end-up hot-topped molds is
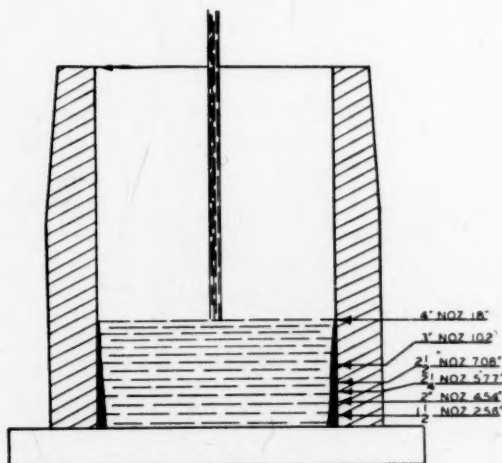
FIG. 8.—METAL RISE IN SIX SECONDS FOR 24 BY 54-INCH MOLDS USING VARIOUS INDICATED NOZZLE DIAMETERS.

the mold wall sooner than from an uncoated wall.

evidence of a shell. Fig. 10 represents this condition. In this case, the shell was a solid part of the ingot, since the rate of rise in the mold was rapid enough to fill the shell before cooling and oxidation took place.

SUMMARY

Scabs either are portions of a shell that is present on normally poured heats, or are parts of a veneer, the result of improper pouring practice.
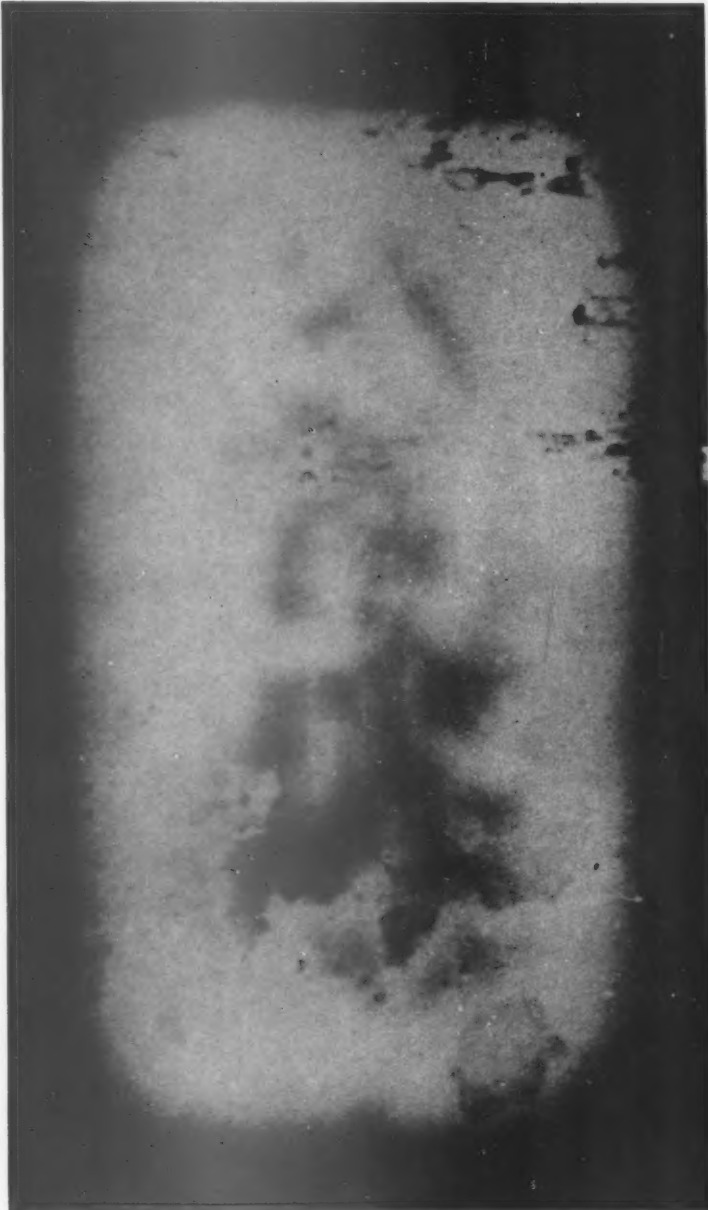
FIG. 9.—A HOT INGOT PHOTOGRAPHED IMMEDIATELY AFTER STRIPPING.
Shows a wavy curtain effect across the ingot about one third from the bottom.

Similar tests of billets rolled from ingots, bottom-cast, should not contain this light colored edge. as no shells are formed when this method of casting is used.

For preventing scabs: (1) use a nozzle size that will permit a filling rate rapid enough to enable the metal to overtake the shells before they become too cold and oxidized;

(2) avoid stop pours, especially near bottoms of ingots. Stool leakers, which necessitate stop pours, are frequent sources of trouble.

manner, for if rimming steel is disturbed by the addition of aluminum, it will recede in the mold and cause a shell to form, causing the formation of scabs.
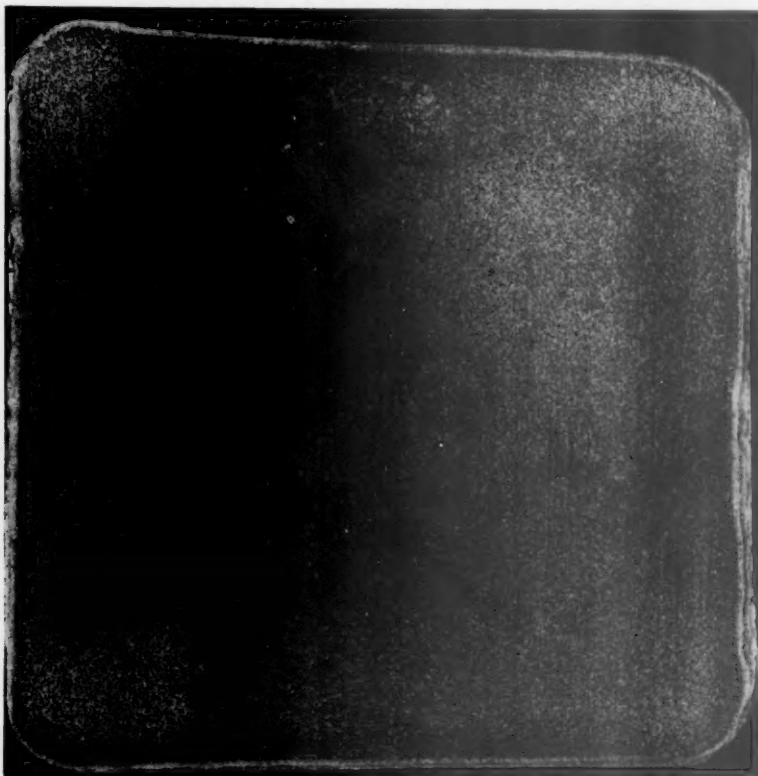
FIG. 10.—MACROGRAPH OF BOTTOM END OF 6 BY 6-INCH BILLET ROLLED FROM A 23 BY 25-INCH BIG-END-UP HOT-TOPPED INGOT OF C-1045 KILLED STEEL. LIGHT EDGE IS EVIDENCE OF A SHELL. The surface condition at this point, which usually is covered with fine seams, may be related to the presence of a shell.

This paper dealt primarily with semi-killed and killed steels, because a sufficient number of rimmed heats were not made during the experiments. However, rimmed steel could be considered in much the same

ACKNOWLEDGMENT

The Cause of Bleeding in Ferrous Castings

By C. A. Zapffe,* Junior Member A.I.M.E.

(Cleveland Meeting, October 1942)

Both the foundryman and the theoretical metallurgist are now generally agreed that the anomalous "rising" or "bleeding" of certain ferrous castings of killed metal is primarily attributable to hydrogen. How and why the phenomenon occurs, however, have not been made clear. The following discussion is intended to harmonize foundry experience with metallurgical theory so that the foundryman may possibly improve his ability to prognosticate whether a certain casting may bleed or not.

Bleeding, Rising, and Piping

The "rising" to be discussed here is not to be confused with the action in rimming ingots as a result of the carbon-oxygen reaction, although a conclusion will be drawn that may apply to the art of controlling the rimming action. Only killed metal is considered, which includes both steels and irons.

In Fig. 1, three killed, chill-cast ingots are shown: a porous ingot whose evolution of gas during late stages of solidification has ejected metal through the top; an ingot in which moderate gas evolution during solidification has lifted the mushy central metal, i.e., it has "risen"; and, third, a sound ingot with good piping characteristics. The first type is referred to as "bleeding," and generally infers that a solid skin had first formed through which the liquid metal later erupted. There is no fundamental distinc-

tion between bleeding and rising in reference to killed metal.*

Porosity

Hydrogen appears as a cause of bleeding because the gas evolution simultaneously leaves a porosity of a type traceable to hydrogen. Twenty years ago, Melmoth[1] noted that killed steel that rose unexpectedly in the mold, if returned while liquid to the furnace and heated further under a reducing lime slag, would again rise in the mold; but that if the ingot were allowed to solidify and was then remelted no rising occurred. A critical quantity of the responsible gas is therefore removed by the rising action. Melmoth associated rising with high silicon (0.7 to 0.9 per cent) and concluded that silicon increased gas absorption. Because silicon is a strong deoxidizer, oxygen must, therefore, be eliminated from consideration of the three common gases in steel—oxygen, nitrogen, and hydrogen.

Butterworth[2] later decided that pinhole porosity was caused by gases dissolved in the metal and that hydrogen was obtained from steam in the mold. Allen's classical work on copper castings,[3] soon followed by

* "Bleeding" and "rising" are colloquialisms whose definitions accordingly vary somewhat from shop to shop. Here, the phenomenon under discussion is simply a late exudation of liquid metal *not* caused by the carbon-oxygen reaction; and minor arbitrary distinctions should not be allowed to confuse the picture. For example, in sand castings the metal often extrudes through the sides, whereas in chill castings extrusion can occur only through the top.

[1] References are at the end of the paper.

Swinden and Stevenson,[4,5] Good,[6] and others, on ferrous castings, then demonstrated that hydrogen was the fundamental cause of unsoundness in castings in the absence of the carbon-oxygen rimming action. Hydrogen-free gases were used for cleansing the melt of hydrogen to promote soundness; and carbon dioxide, which is oxidizing to steel, was adopted by the British Cast Iron Research Association as a gas-removing flush for cast iron.[7] By using argon as a substitute for nitrogen, Swinden and Stevenson[5] showed that the beneficial effect of nitrogen is purely mechanical in that hydrogen is removed thereby.

EMPIRICAL INDICTMENT OF HYDROGEN

As the common cause of porosity in killed ferrous metals, then, hydrogen stands quite alone; although gaseous products from a hydrogen reaction must be included.[8] But the strongest indictment of hydrogen comes from the acknowledged factors causing porosity, rising, and bleeding, for each of these factors plainly affects the hydrogen content of the metal. For example, moisture is the most notorious source of hydrogen throughout metallurgy; and, discussing porosity, Buchanan[8] states: "Moisture is the cause of most gas formation in cast iron." Sources of moisture may be in the furnace atmosphere, humid weather, damp charge, slaked lime, rusty scrap, mold wash, and mold sand; Klopf,[10] Womochel and Sigerfoos,[11] and Sokolov,[12] to mention but a few, express a popular belief that moisture in the mold often accounts for porosity and bleeding.

Experience at Battelle Memorial Institute during the past decade* has shown that bleeding is aggravated by such things as high pouring temperature, closed furnace, absence of slag, and a lime wash on the mold. Each item argues for hydrogen, since hotter metal dissolves more of that gas, a closed furnace tends to maintain a higher

---

* I am indebted to Dr. C. H. Lorig and Mr. H. B. Kinnear for this information.

partial pressure of hydrogen, a slag tends to protect the bath from the atmospheric gases that contain hydrogen, and a lime wash is an obvious source of moisture.

Similarly, a boil is a well-known preventative of bleeding; and in certain marginal cases bleeding of castings may be avoided by using dry molds. The boil may be attained by the customary carbon-oxygen reaction, by piping CO_2 or N_2 through the melt, by adding limestone to get a lime boil, or by adding iron oxide, perhaps as iron ore. The addition of iron oxide is especially effective, whether added to the charge or late to the melt, even though a visible boil is not effected. These things again all conform to the hydrogen argument, for the action of a boil in removing that gas is well recognized, the moisture in the mold is a confirmed source of the gas, and iron oxide by itself would be expected to lower the hydrogen content of the metal as a result of the chemical reaction:

$$FeO + 2H = H_2O + Fe$$

wherein high oxygen values infer that hydrogen is correspondingly low, and vice versa.

As a matter of fact, the "vice versa" is one of its most interesting aspects, for an outstanding fact about bleeding is that the addition of deoxidizers, as they are commonly used, has but little effect on bleeding. At the time of the early work at Battelle, the suggestion then current was to prevent all forms of gas evolution by removing oxygen; but steel killed with excesses of aluminum and silicon continued to bleed. From the equation just given, one may observe that lowering the oxygen activity simply removes the principal obstacle to hydrogen absorption.

To demonstrate the effect of hydrogen in causing bleeding, a group of experiments was performed using a high-silicon cast iron in which the activity of oxygen must be negligibly low. Ten-pound melts were made

FIG. 1.—KILLED, CHILL-CAST INGOTS.
Left, unsound ingot illustrating "bleeding."
Center, unsound ingot illustrating "rising."
Right, sound ingot with good piping characteristics.
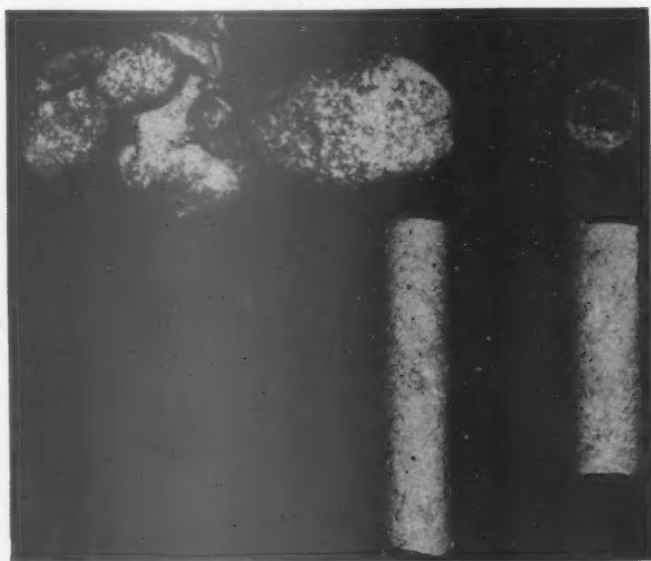
FIG. 2.—TOP AND SIDE VIEWS OF TWO CASTINGS FROM DRY SAND MOLDS.
Left, hydrogen bubbled for five minutes through melt.
Right, nitrogen bubbled for five minutes through melt.

from identical charges of steel punchings, graphite, ferromanganese, and 77 per cent ferrosilicon, the ferrosilicon being added last. A magnesia-lined crucible in an induc-

dried in a dehydration train. The gas flow in most cases was controlled by a bubbler containing a light mineral oil.

The metal was variously cast in chill

N₂ 10 minutes   H₂ 2 minutes   H₂ 5 minutes

FIG. 3.—TOPS OF CASTINGS FROM ONE MELT TREATED PROGRESSIVELY AS INDICATED.
Above, from green-sand molds; below, from dry-sand molds.
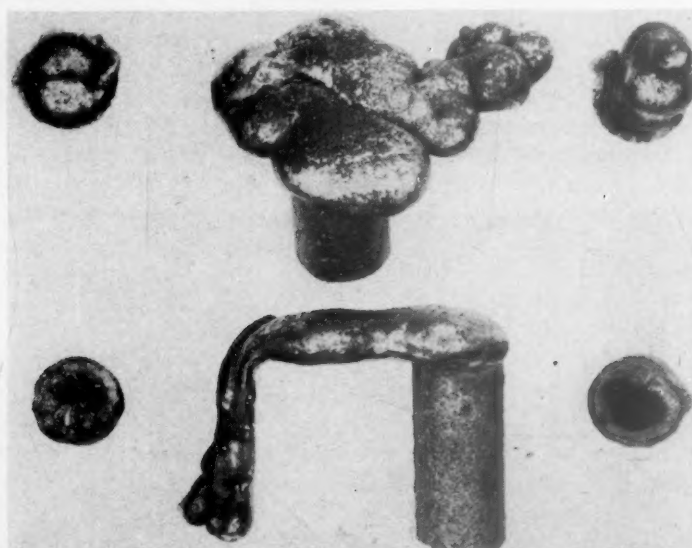
N₂ 10 minutes   H₂ 2 minutes   N₂ 10 minutes

FIG. 4.—TOPS OF CASTINGS FROM ONE MELT PROGRESSIVELY TREATED AS INDICATED.
Above, from green-sand molds; below, from dry-sand molds.

tion furnace was used. The temperature was maintained at approximately 2600°F.

H₂, N₂, NH₃, and H₂O (steam) were variously introduced into the melt through a graphite tube immersed one inch in the metal. The nitrogen was first carefully

(iron) and sand molds, the latter comprising a green-sand group and a group dried by heating to a bright red. They will be referred to as chill, green-sand, and dry molds. Castings were transverse specimens of ¾-in. diameter and 8-in. length.

Fig. 2 illustrates the marked difference in bleeding propensities between hydrogen-treated and nitrogen-treated metal. A 5-min. treatment with nitrogen resulted in

Untreated   N₂ 5 minutes

FIG. 5.—TOPS OF CASTINGS SHOWING EFFECT OF FIVE-MINUTE NITROGEN TREATMENT.
Above, green-sand molds; below, dry-sand molds.

a deeply piped and sound casting, whereas a 5-min. treatment with hydrogen caused nearly half the metal to exude from the top.

Similarly, hydrogen admitted after a nitrogen cleansing will be just as harmful. Fig. 3 shows a series of three casts from one melt: the first, after a 10-min. nitrogen flush, piped deeply in a dry mold; a subsequent treatment of the remaining metal for 2 min. with hydrogen caused some rising in the second casting; and the third, having had 5 min. treatment with hydrogen, bled badly. This figure also shows evidence of the difference between green-sand and dry-sand molds. In spite of the nitrogen treatment, the casting in green sand bled, though not as badly as those treated with hydrogen. Moisture in the sand must be held responsible.

If, however, a nitrogen flush *follows* a hydrogen flush, hydrogen will be removed so that no bleeding will occur in dry molds. Fig. 4 illustrates the powerful effect of both gas treatments. A melt was treated for 10 min. with nitrogen, whereupon a sound

casting in a dry mold was obtained. Hydrogen was then bubbled for 2 min. through the remaining metal, and severe bleeding resulted in the casting. Then a 10-min.

N₂ 5 minutes   N₂ 10 minutes

FIG. 6.—TOPS OF CASTINGS SHOWING EFFECT OF FIVE-MINUTE AND TEN-MINUTE NITROGEN TREATMENTS.
Above, dry sand; center, green sand; below, iron chill molds.

treatment with nitrogen in the same melt removed every trace of the hydrogen treatment. Here again, tests in both green and dry sand show the inevitable hydrogen pickup afforded by green sand.

The difficulty of producing castings free from hydrogen troubles when a green-sand mold is used is further illustrated in Figs. 5 and 6. Fig. 5 shows the tops of castings both untreated and treated for 5 min. with nitrogen for both green and dry molds. No hydrogen has been added. The nitrogen treatment has only ameliorated the bleeding in the green-sand molds, and has stopped a slight tendency to rise in the dry

mold, which must have been prompted by hydrogen inherent in the charge. Further tests in Fig. 6 show a similar effect for 5-min. and 10-min. nitrogen treatments.

chemical action of hydrogen and the mechanical action of nitrogen in removing hydrogen was that for about 30 sec. after immersing the graphite tube in the melt no

Untreated   H₂O 2 minutes   H₂O 5 minutes
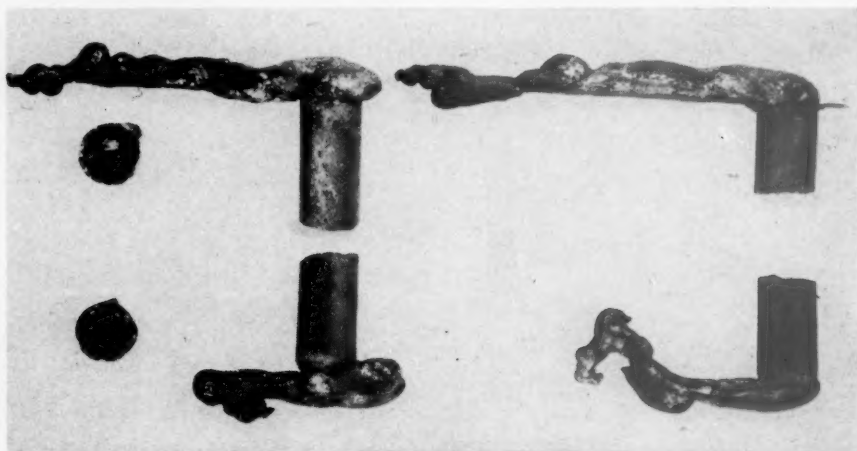
FIG. 7.—TOPS OF CASTINGS FROM ONE MELT PROGRESSIVELY TREATED WITH STEAM AS INDICATED. Above, green-sand molds; below, dry-sand molds.

Untreated   NH₃ 2 minutes   NH₃ 5 minutes   NH₃ 10 minutes

FIG. 8.—SAME AS FIGURE 7, BUT TREATED WITH AMMONIA GAS.

Chill castings are also shown. Even 10 min. of bubbling, which for dry molds completely eliminated bleeding whatever the source or previous content of hydrogen, fails to do more than mitigate bleeding in the green-sand molds.

An incidental observation verifying the

bubbles appeared when hydrogen was used, but bubbles immediately appeared when nitrogen was used. Nitrogen apparently dissolves but little, hydrogen much.

To show whether moisture is as prolific a source for hydrogen as has been claimed on the basis of incidental observations, steam

was bubbled through the molten metal. The results, shown in Fig. 7, leave little choice to be made between steam and hydrogen, the latter undiluted and at full atmospheric pressure, as a source for hydrogen in iron. Because hydrogen rarely attains more than several per cent of that pressure in ordinary furnaces, and because the solubility is a direct function of that pressure, one is safe in placing water vapor at the head of the list as a source of gas-caused evils.

Among such compounds, many carriers of hydrogen exist. Ammonia, NH_3, is one; and the potency of ammonia in causing bleeding is illustrated in Fig. 8. Because ammonia is not an important component of most furnace atmospheres, Fig. 8 is principally of academic interest. Other hydrogen carriers, such as hydrocarbon gases, were not investigated in this particular research; but ample evidence exists to show that they are similarly important.

THEORETICAL PRINCIPLES

Role of Delta Iron

Of all the obvious factors affecting bleeding, none is more outstanding than the composition of the steel; and, from among the fluctuating mass of opinion, the best agreement is on the effects of nickel and chromium. Irons and steels containing chromium are notorious "hemophiliacs," whereas nickel generally exerts a strong opposite effect. Why?

The fundamental nature of bleeding plainly lies in the difference between liquid and solid steel as solvents for hydrogen. A glance at the Fe-H curve[13] in Fig. 9 suffices to show that the greater portion of that gas held by the liquid metal is discharged during solidification. Roughly, each volume of metal will tend to expel *three times* that volume of hydrogen, measured at the temperature under consideration. Because most of the gas from the entire casting leaves principally through the core to which it

diffuses, and from which it must escape in the short period of freezing, little wonder it is that some metal is occasionally extruded.*

The Ni-H curve in the same figure shows that, for a given temperature and pressure, nickel absorbs considerably more hydrogen than does iron;† and the Cr-H curve, though incomplete, indicates that chromium is a poorer solvent than is iron. As a matter of fact, although the data of Luckemeyer-Hasse and Schenck[14] and Martin[15] agree in designating that curve for chromium, Russian research[16] shows that hydrogen is completely insoluble in chromium, and that addition of chromium to steel lowers the solubility of the steel for the gas.

Qualitatively, at least, the data dovetail significantly, for iron alone shows a marked preference for hydrogen when the structure is face-centered cubic (gamma) rather than body-centered cubic (alpha). Nickel has a face-centered lattice, whereas chromium is body-centered. The generalization is, in fact, well made that hydrogen dissolves much more readily in metals that have the face-centered cubic structure.

Bleeding, therefore, whose degree is a rough measure of the change in hydrogen solubility from liquid steel to solid, might tend to be suppressed by alloying with nickel because the solid nickel steel so freely dissolves the gas; whereas chromium

---

* The fact must always be borne in mind that there is no solubility limit for hydrogen in iron such as exists for other alloying elements, including oxygen; but that pressure is also a variable. The Fe-H curve in Fig. 9 is really a binary section taken at $P = 1$ atmosphere through a solid diagram whose third dimension is pressure. Consequently, that curve, which refers only to a solution under one atmosphere of molecular hydrogen, must be used cautiously and only qualitatively when discussing hydrogen in steel; for in steel the partial pressure of atmospheric hydrogen (perhaps under the slag) is not only unknown, but H_2 is one of the least likely sources of the hydrogen that the steel absorbs.

† As might be expected, alloys of iron with these elements usually show hydrogen solubilities that are proportionately placed between the two curves of the pure metals.[14]

might exert an opposite effect for the opposite reason.

Furthermore, there is an even better basis for strengthening the same argument.
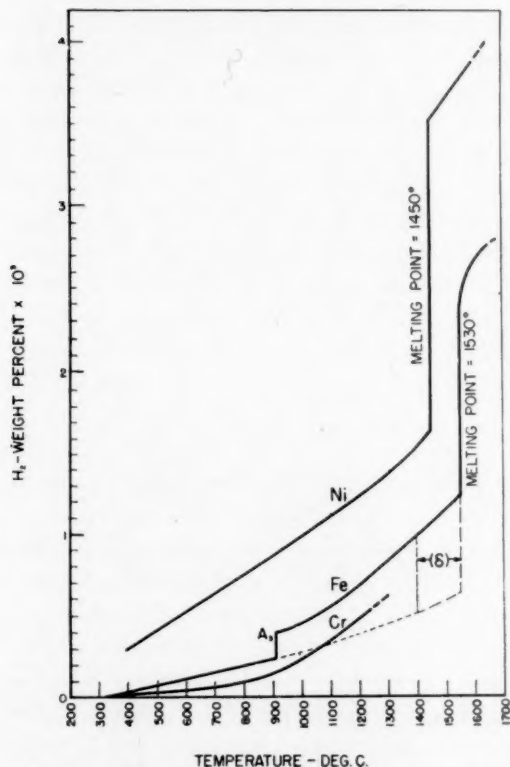
FIG. 9.—SOLUBILITY FOR HYDROGEN IN IRON AND IN NICKEL (SIEVERTS) AND IN CHROMIUM (LUCKEMEYER-HASSE AND SCHENCK, ALSO MARTIN). P = ONE ATMOSPHERE.

A variation in the shape of the conventional Fe-H curve is indicated in Fig. 9. This variation has been fairly well established by Schenck[17] and is consistent with the expectation that the return of iron, during heating, to the body-centered cubic form should similarly bring a reversion of the hydrogen solubility to conform with the trend of the solubility in alpha.

If this is so, an iron freezing into delta will tend to evolve more hydrogen than one freezing into gamma. Nickel and chromium not only have high and low solubilities, respectively, for hydrogen; but, as alloying additions, each favors the corresponding

form of iron. Nickel opens, and chromium closes, the gamma loop. Conversely, nickel *narrows* the temperature range of delta iron; chromium *broadens* it.

On cooling a nickel steel, then, the evolution of hydrogen, which requires a finite period of time, will tend to follow curve I in Fig. 10, bridging the delta dip because its narrowed, or erased, temperature range is traversed too quickly by the cooling casting to permit the complete evolution that would occur if cooled slowly enough to attain equilibrium. On the other hand, a chromium steel, having an enlarged delta temperature range, would tend to expel gas along curve II to the bottom of the recess. Furthermore, the chromium undoubtedly deepens that recess considerably, to aggravate evolution even more; just as nickel increases the solubility of gamma to minimize the evolution even beyond the effect of the bridging.

Speculation on the actual mechanism of the evolution suggests that, in the case of steel containing nickel, but insufficient nickel to erase the delta range completely, much of the gas exuding from the dendrites of solidifying metal may be reabsorbed in those same dendrites when their temperature reaches the gamma range. If that occurs before solidification is complete, the tendency to bleed is again diminished. Chromium steels would retain ferritic dendrites to temperatures lower than could reasonably comprise a cooling gradient through solidifying metal.

As a generalization, then, we may conclude that ferritic steels are more likely to bleed than austenitic steels.

The exceptions to this rule in commercial steelmaking are fairly numerous, however, for each steel has its own set of other conditions that cause variations in the hydrogen content of the liquid metal at the time of casting. The foregoing argument presupposes equal, or at least similar, hydrogen contents.

Other Factors

In the experience at Battelle,* steels containing 5 and 12 per cent chromium were the worst bleeders, and nickel seemed to suppress bleeding, which is in agreement with this discussion. The high hydrogen content of some electrolytic nickel may obscure the favorable action of that metal.

Manganese, which favors gamma iron, seemed harmful in cast iron, however—a content of 1.50 per cent causing a curious type of pinhole, which copper, a face-centered cubic metal, seemed to alleviate. Similarly, silicon as a ladle addition greater than one per cent often led to bleeding. Also, ferrosilicon itself tends to bleed, as does silicon steel for electrical sheet. Other elements could not be classified because a measurement of bleeding is as yet only qualitative and other variables are too numerous.

The effect of manganese can be understood from several viewpoints. First, researches such as that of Herasymenko and Dombrowski[18] agree in showing that the contents of hydrogen and manganese in the steel bath fluctuate together, and closely. Secondly, solubility measurements of hydrogen in manganese by Luckemeyer-Hasse and Schenck[14] (Fig. 11) show values several fold higher than for iron; so that manganese might be expected to increase the solubility of steel for that gas. Lastly, hydrogen, though seldom mentioned seriously as a deoxidizer, is legitimately one, and a powerful one; whereupon hydrogen, if available, should increase with increasing manganese just as does silicon, carbon, and the other deoxidizers. A manganese change does not necessarily *cause* a change in hydrogen—they simply change coincidentally. As a matter of fact, throwing a "reducing" flame (which connotes hydrogen) across a steel bath can *cause* a manganese increase if MnO is present in the slag.

* See footnote on page 284.

Silicon holds a good analogy, for silicon oxide in the slag and refractories constitutes a reserve for that metal just as water vapor in the slag and furnace atmosphere does for
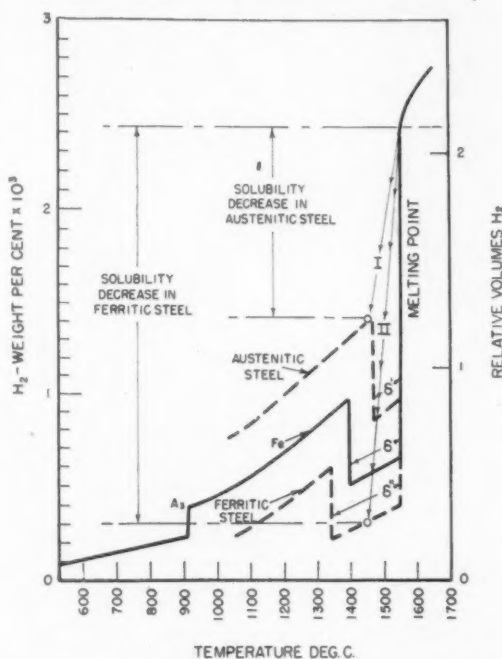
FIG. 10.—SCHEMATIC REPRESENTATION OF ROLE OF DELTA RANGE IN FERROUS ALLOYS REGARDING HYDROGEN EVOLUTION DURING SOLIDIFICATION.

Curves I and II depict a generalized path of evolution for austenitic and ferritic alloys, respectively, wherein narrowing or elimination of delta in austenitic alloys avoids sharp solubility drop in delta; which, conversely, is aggravated and unavoidable in ferritic alloys. (Equal contents of hydrogen in liquid are assumed, and changes in melting point are not considered.)

hydrogen. A drop in oxygen pressure, whether caused by an increase in manganese or in carbon, will simultaneously reduce silicon and hydrogen from their respective oxides. Many have expressed the opinion in the literature that silicon, and other metals notable as deoxidizers, markedly increase the solubility of steel for hydrogen, possibly by forming hydrides; and several investigators have unsuccessfully sought supernormal solubilities in

these metals. The answer is obvious when hydrogen is regarded in its true role as a deoxidizer. An increase in silicon, for example, simply shifts the hydrogen-oxygen

factor in bleeding and rising, there must be one more factor of great importance, *for hydrogen in itself cannot cause a bubble to form inside liquid steel.*
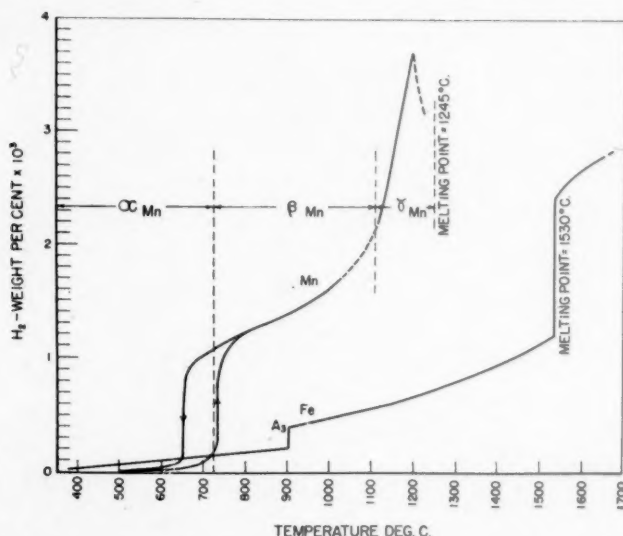
FIG. II.—SOLUBILITY CURVES FOR HYDROGEN IN MANGANESE (LUCKEMEYER-HASSE AND SCHENCK) AND IN IRON (MODIFIED SIEVERTS). P = ONE ATMOSPHERE.

equilibrium toward higher values for hydrogen.

The action of other elements whose effect is minor can possibly be explained along the same general lines. Some added as ferro-alloys or as electrolytic metal may simply bring their own high hydrogen content into the steel. For example, 50 to 100 volumes of hydrogen in one volume of electrolytic metal is not uncommon; whereupon steel made with 1 or 2 per cent of such metal could obtain a volume of hydrogen equal to the volume of the steel, which is sufficient to embrittle most steel throughout and to cause many troubles, such as bleeding. Again, an alloying addition may simply prevent a proper boil from taking place.

WHAT INITIATES THE GAS EVOLUTION?

So far we have considered only factors influencing the rise and fall of hydrogen contents and changes in solubility. Although supersaturation, or precipitation pressure, is obviously the fundamental

In the footnote on page 289, the fact is pointed out that hydrogen has no "solubility limit" in iron as we ordinarily conceive such a limit. That fact underlies most of the misunderstanding regarding hydrogen in steel. *There is no such thing as supersaturation of hydrogen in iron or steel, except at some surface* where temperature or pressure or concentration departs from the equilibrium that is maintaining that particular quantity of the gas in solution.

In liquid steel, regardless of the hydrogen content, that gas has no tendency to precipitate except at boundaries of the metal, and those boundaries may be the natural surface of the melt, or the surfaces of inclusions or bubbles of other gases within the melt. There is no effect whatsoever upon bubble formation when the hydrogen concentration above the bath is reduced, the only reaction being diffusion of the gas to, and effusion from, that surface. Consequently, the supersaturation

that has been discussed can apply only to some surface already created by other means within the liquid metal.*

What agent is it, then, that supplies the trigger action for causing supersaturation and the subsequent release of hydrogen from liquid iron and steel?

When a hydrogen-free gas such as nitrogen is pumped through the liquid, the agent is obvious. A surface suddenly presents itself to dissolved hydrogen; and, because no hydrogen at all exists on that surface, supersaturation becomes a reality. Hydrogen immediately effuses until equilibrium is produced between the remaining dissolved gas and the resulting gaseous phase.

Plainly, a large internal surface is not necessary to initiate that action; and the bubble may grow greatly and rapidly because the creation of a gaseous phase from a solid one is involved—the product requiring many thousands of times greater volume than the reactant.

But mechanical introduction of a foreign body such as nitrogen gas is neither necessary nor present in run-of-mill bleeding. Products formed within the melt, whether gases, liquids or solids, may serve as well; and the most logical of these is the product of the hydrogen-oxygen reaction. In copper, we will remember, porosity is rigidly controlled by the hydrogen-oxygen reaction; and, as in iron, hydrogen alone is unable to form a single blowhole.†

* An analogy is the decapping of a bottle of carbonated water. A popular misconception is that release of the compressed gas above the liquid causes loss of the dissolved gas by effervescence. This is not so. By releasing the pressure, the dissolved gas can only be lost by diffusion to the surface and by silent, invisible evaporation. Any bubbles observed forming throughout the liquid are caused by another agent, such as mechanical agitation, or impurities.

† This conclusion, that the release of hydrogen to cause bleeding depends upon a foreign body, or reaction product such as water vapor, is in agreement with the conclusion reached by Sims and Zapffe[8] regarding the role of the hydrogen-oxygen reaction in the development of pinhole porosity. Porosity, of course, is the counterpart of bleeding.

The viewpoint that bleeding, or rising, is initiated by formation of an insoluble reaction product, probably often H_2O, is strengthened by the peculiar "timing"
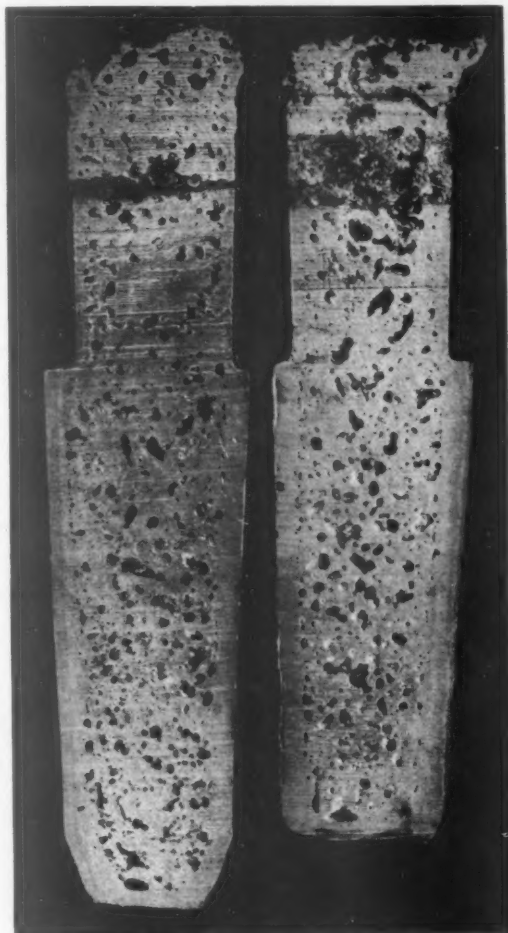
FIG. 12.—CROSS SECTIONS OF TWO BLEEDING INGOTS OF 5 PER CENT CHROMIUM STEEL.
Note fairly solid rim and homogeneously bloated core. Exudation from top has been removed.

of the phenomenon. Thus, the melt lies quiet while the rim freezes and the core collects impurities. Suddenly, after the reactant impurities have concentrated, their solubilities have decreased, and the temperature coefficients for their reactions have changed favorably so that a reaction commences, hydrogen exhales at all surfaces of the reaction product, the core of

mushy metal is bloated, and it exudes from the mold.

Two bleeding ingots, shown in cross section in Fig. 12, support this viewpoint, for the rim is fairly solid, and the whole core is uniformly bloated, suggesting that a homogeneous climatic reaction, much as in rimming, resulted only after conditions of temperature and concentration of the reactants had become favorable.

The question may then arise: Why do deoxidizers, even when added to some excess, not stop bleeding by depriving the melt of oxygen? As a matter of fact, they may conceivably do so, if sufficiently powerful and sufficiently abundant. A melt washed amply with dry hydrogen, for example, will solidify quietly, for no impurities remain to react with the dissolved hydrogen. The answer probably lies in the fact that the optimum combining ratio, or stoichiometric ratio, of $2H:O$ lies at lower oxygen contents than are usually realized in ordinary steel making. Thus, for a hydrogen content of 0.001 weight per cent, which is high in practice, only 0.008 per cent of O is necessary to form even the maximum amount of steam. Steam will still form with but a fraction of that amount. Consequently, the ordinary additions of deoxidizers permit H to increase without seriously threatening a shortage of oxygen.

REMARK ON CONTROL OF RIMMING IN STEEL INGOTS

Recently there was compiled by the Committee on the Physical Chemistry of Steelmaking of A.I.M.E. a list of proposed research problems related to steelmaking processes.[19] One of those problems was entitled: "Study of the Mechanism whereby Sodium Fluoride Affects the Rimming Action."

The rimming action is fundamentally a carbon "boil" taking place in the mold instead of in the furnace. The gaseous phase, to which other gases contribute for the most part only because such a gas phase is already established, is created by the carbon-oxygen reaction; and boiling and rimming differ only in the manner by which the carbon-oxygen equilibrium is upset. In boiling, the solubility product remains fixed for the temperature of the furnace, and excess oxygen is added as iron oxide. In rimming, no oxygen is added, but the solubility product decreases with decreasing temperature and with the liquid → solid phase change so that excesses of both carbon and oxygen are effected.

In both cases, control of the carbon-oxygen reaction is important. Carbon elimination in the boil must neither be too slow nor too rapid if good steel is desired; likewise, the violence of the rimming reaction in the mold measures the worth of the ingot. Sudden escape of the gas may cause a sharp sinking of the metal so that further filling of the mold is necessary. Such an ingot may sink again before solidifying to form "pipe," or it may rise.

Pipe may lead to the defect known as "lamination" and is generally undesirable in rimming ingots. Rising, on the other hand, is usually associated with long, narrow gas holes forming near the surface and perpendicular to it in the butt portion of the ingot. During rolling, these blowholes confer poor surface qualities.

The goal in making rimming ingots, then, is to eliminate both pipe and undue sponginess and to get a thick, solid-skinned butt that will not crack or tear during rolling.

Epstein and Larson[20] found that adding a highly oxidizing agent of the group comprising $KClO_3$, $NaNO_3$, $KMnO_4$, and $K_2Cr_2O_7$ to the metal after tapping prevented the late "rising" that is associated with porosity in the butt. Likewise the use of NaF achieves similar results and has received much discussion.[21] In neither case, however, has an explanation been agreed upon, although suggestions have gone so far afield as to regard viscosity changes in

postulated oxide films, undercooling, and chain reactions with iron, then carbon, to form fluorides.[19]

Such effects, if they do occur, may be only unimportant coincidences, for the preceding discussion of rising, although the rimming action was at first specifically excepted, affords another explanation that may bear considering. Rimming steel, it is true, tends to be low in hydrogen because of its boil in the open hearth. Nevertheless, there is some hydrogen, which is evidenced both by direct analysis of the gases evolved during rimming and by occasional rising of the same steel if killed. Because a mold wash is generally used, some hydrogen absorption during pouring must also be expected.

The gas evolution during the rimming action has a sweeping, or cleansing, effect for this hydrogen, just as does the carbon boil in the furnace. However, in the furnace the hydrogen elimination affects the whole heat uniformly because the metal is entirely liquid, whereas in the mold the gas evolution, or "boil" is, of course, confined to metal away from the skin and away from the ingot base. Thus, the sweeping action is strongest in the upper portions toward which all the gas proceeds, and is weakest toward the butt of the ingot. Consequently, one might expect the butt portion in a certain number of cases to exhibit a tendency to "bleed," which would tend to lift the mushy core to give the effect of "rising." That the skin of rimming steel generally contains disproportionately more hydrogen than the core has been indicated in experiments at Battelle Memorial Institute on defects in vitreous enamel fired on rimmed-steel sheet.

Osborg[22] reported that lithium added to castings promotes soundness. All these additions so far mentioned are gaseous at the temperature of liquid steel,* and all are

hydrogen-free; consequently, all must have the well-known action of nitrogen or carbon oxides in cleansing steel of hydrogen, regardless of other effects upon viscosity, and so forth. Epstein and Larson's oxidizing additions fall in the category with carbon dioxide, wherein hydrogen is removed both mechanically and chemically, by oxidation. Tietig[21] thinks sodium fluoride has an action opposite to that of aluminum. Dehydrogenizing is opposite to deoxidizing.

Of course, the argument for rising and bleeding, when extended to rimming behavior, includes the possibility that these scavenging gases may also be important in removing the products of the carbon-oxygen reaction, which frequently show a tendency to supersaturate and repress the reaction. On the other hand, the butt of an ingot may have a fairly high hydrogen content without contributing much to a total gas analysis for the entire ingot, thereby escaping observation. The discussion of rimming here is only speculative, of course, and the argument for hydrogen is advanced only because it has not received atten-

---

* The boiling point of NaF is reported to be in the neighborhood of 1700°C.[23] Consequently,

some question arises whether that compound in itself could be sufficiently gaseous at rimming temperatures to account for the obvious gas evolution it causes. However, that NaF is amply gaseous is indicated in sundry observations reported by Mellor.[24] NaF in a bunsen flame, Mellor states, volatilizes about eight times as fast as NaCl, its heat of formation being highly exothermic, indicating decomposition at elevated temperatures:

$$Na \text{ (solid)} + F \text{ (gas)} = NaF \text{ (solid)} + 109.3 \text{ cal.}$$
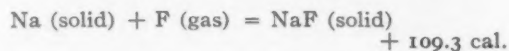
On the other hand, perhaps the action of NaF on dissolved H is a chemical one, for Mellor goes on to state that iron burns with incandescence in fluorine at 500°C. and reacts with NaF to form FeF_2:

$$Fe + 2NaF = FeF_2 + 2Na$$
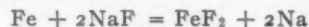
which volatilizes completely at 1100°C. and is also reduced completely at high temperatures by hydrogen:

$$FeF_2 + H_2 = 2HF + Fe \text{ (highly endothermic)}$$
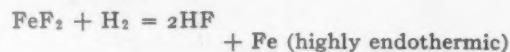
HF is presumably quite insoluble in liquid steel, so that the hydrogen would be removed much as it is by oxidation.

tion before and therefore remains to be disproved.

The important point is that sodium fluoride and such additions can be regarded as mechanical or chemical scavengers for the portion of hydrogen in the bottom of the ingot where the carbon oxides are inefficacious, as well as for the carbon oxides themselves, should they supersaturate. The same beneficial effect should result from piping dry nitrogen to the bottom of the mold. As a matter of fact, in the research at Battelle on hydrogen in steel, the use of gasifying solids has long been considered for scavenging hydrogen; and no more practical method so far can be suggested for removing critical quantities of that gas than placing toward the bottom of the melt some solid element or compound whose state is gaseous at steelmaking temperatures. The quantity of gas that is necessary to purge a melt of hydrogen can be added at ordinary temperatures in the form of a solid having roughly only 1/10,000 of that volume.

It is not unlikely that the beneficial effect of calcium with respect to ductility is a similar one, rather than an ability to deoxidize.

NITROGEN AS A CAUSE OF BLEEDING

In the preceding paragraphs a clear-cut case has been made against hydrogen as the principal cause of bleeding, which is permissible because it is true for ordinary steelmaking. Nevertheless, even though nitrogen has been demonstrated to prevent bleeding when bubbled through the liquid steel, in certain special cases of alloy steelmaking nitrogen itself can cause porosity and bleeding.

In making high-alloy castings, ferrochrome having a high nitrogen content is often used for grain refinement. The nitrogen in the ferrochrome is there undoubtedly as a solid phase, probably chromium nitride. During melting, the nitrogen is carried into the steel through solution of a non-

gaseous phase, whereupon the dissolving is not dependent upon pressure—at least temporarily.

Consequently, nitrogen contents several times greater than those of air-blown steel may occur in a 5 per cent chromium steel made from that ferroalloy. Problems of porosity are then almost insurmountable, so that only a fraction of the total chromium content can be added as the high-nitrogen alloy. Steel blown with air (0.78 atmospheres of N_2) rarely obtains more than 0.01 to 0.02 per cent of that gas, which never causes porosity; and in the present research slightly greater than one atmosphere pressure of N_2 bubbled through the liquid actually prevented porosity.

Chipman and Murphy[25] studied iron under approximately one atmosphere of N_2 and found a solubility for equilibrium conditions of 0.039 per cent at the melting point, which would then be a maximum value always lying above the absorption from air or from flushing with nitrogen. Porosity was noted in some of their ingots, presumably those highest in nitrogen; and that porosity must have been caused by nitrogen, for they did not make the mistake of numerous earlier investigators who used ammonia for studying the iron-nitrogen system and overlooked the fact that NH_3 produces three times as much hydrogen as nitrogen. There must then be something like a "critical" nitrogen content for any given steel, below which nitrogen cannot cause porosity and above which it can.

In the present research, bleeding and porosity attributable to nitrogen was demonstrated quite positively. A 200-lb. melt of 5 per cent chromium steel was made in an induction furnace, using the high-nitrogen ferroalloy. Analysis of other elements showed 0.34 per cent Si, 0.73 per cent Mn, and 0.11 per cent C. Oxygen was eliminated from any future reaction with the small amount of carbon present by adding 0.2 lb. of aluminum just before casting. Hydrogen was excluded from the melt by

every possible precaution; and, as a further insurance, carefully dried nitrogen was flushed through the bath before casting. If a gaseous reaction developed in the mold, only nitrogen could reasonably be held responsible.

Chill-cast 60-lb. ingots were poured in quick succession. The first was untreated; then two portions of titanium were added consecutively to the remaining melt, and a casting was made after each addition. The first and third ingots are shown in cross section in Fig. 13, for comparison.

The porosity in the untreated ingot, which was extreme, must be attributed to the high nitrogen content, which was shown by analysis to be 0.056 per cent. Other tests with the same steel have shown 0.07 per cent, and even that figure must represent only the portion that remains after the effervescence is complete. The two other ingots analyzed 0.81 and 1.39 per cent Ti, respectively. Both were perfectly solid, showing good pipe.

From this it must be inferred that the stability of titanium nitride has prevented evolution of the nitrogen brought into the steel by the ferrochrome. Titanium has behaved with iron nitride much as aluminum does with iron oxide, "killing" the steel with respect to nitrogen. Iron itself, or iron with only 5 per cent chromium, cannot hold that quantity of nitrogen through the decrease in solubility that occurs during solidification, and effervescence and porosity result.

CONCLUSIONS

The following factors regarding the phenomenon of bleeding in ferrous ingots and castings seem fairly well established:

1. In ordinary practice, where the nitrogen content of the steel or iron does not exceed 0.03 to 0.035 per cent, bleeding is primarily a function of the decrease in hydrogen solubility occurring during solidification. Other gases, if present in the
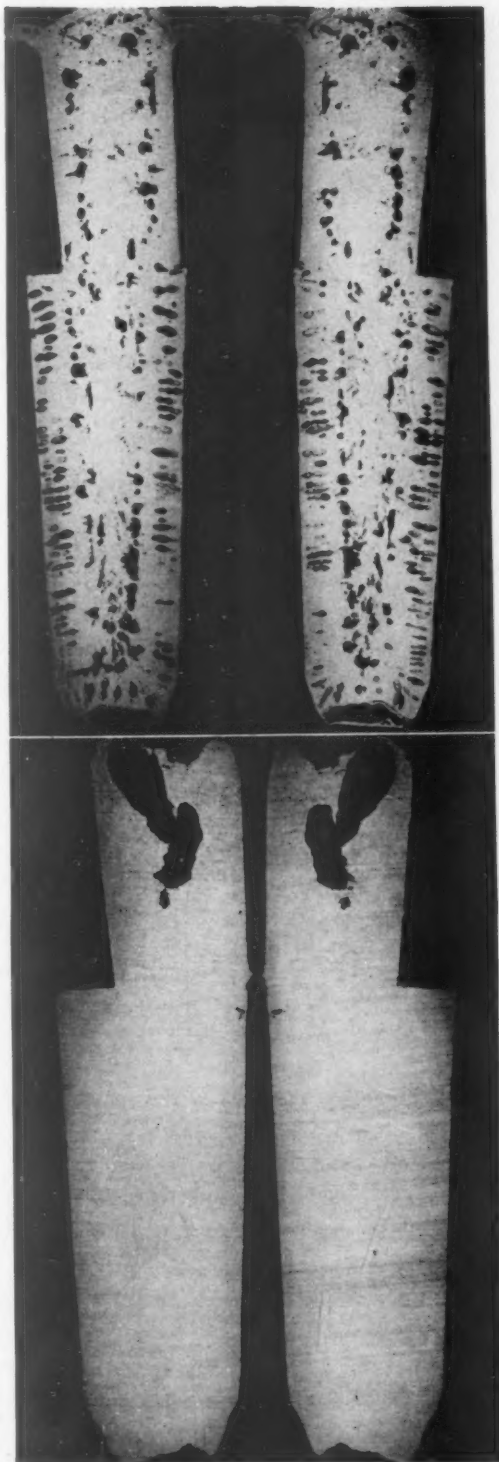
FIG. 13.—CROSS SECTIONS OF 60-POUND INGOTS OF 5 PER CENT CHROMIUM STEEL MADE FROM HIGH-NITROGEN FERROCHROME.
Above, untreated; below, titanium added.

evolution, are usually compounds of hydrogen or are incidental components.

2. Hydrogen alone cannot form a bubble, however; consequently, another agent is necessary. That agent is probably the product of a hydrogen-oxygen reaction in most cases, but also may be other reaction products, or foreign materials within the melt.

3. Hydrogen may be introduced into the liquid metal by numerous well-recognized means, the commonest carrier being moisture; one of the usual sources of that moisture being the mold.

4. Austenitic steels, such as nickel steels, are not as liable to bleeding because the solid metal is a good solvent for hydrogen; in ferritic steels bleeding is aggravated because the solid metal is a poor solvent.

5. Austenitic steels also tend to evolve less gas because the range of gamma structure, a good solvent for hydrogen, approaches the solidus, either erasing the poorly solvent delta range or aiding the evolution to "bridge over" delta's narrowed position. Ferritic steels, conversely, so stabilize delta iron that the solubility decrease upon solidifying is a maximum.

6. The addition of deoxidizers tends to enhance hydrogen absorption because hydrogen is itself a deoxidizer. Consequently, minor deleterious effects from additions of manganese, silicon, and so forth, may be observed because by decreasing the oxygen activity of the steel they increase its capacity for absorbing hydrogen in accordance with the simple equation for hydrogen-oxygen equilibrium. Minor effects from other elements conform to similar reasoning, or to the fact that some are themselves prolific carriers of moisture or hydrogen.

7. The much discussed action of sodium fluoride and similar agents on preventing butt porosity and final rising in rimming-steel ingots may be one of dehydrogenization in butt portions of the ingot where the evolution of carbon oxides is inconsequen-tial. The upper portions of the ingot are properly cleansed of hydrogen by the rimming action, but the bottom is not; whereupon the gas may remove itself at a critical late period by the bleeding action, which would show itself as "rising." The mechanical action of the scavenger also may release carbon oxides if they are in supersaturation.

8. In certain exceptional cases, principally confined to alloy steelmaking, nitrogen itself may cause porosity and bleeding when present in excessive amount. The necessary concentrations—probably >0.035 per cent—are obtained only with difficulty from the gas phase, and usually result from additions of solid nitrides, as in the use of high-nitrogen ferrochrome for grain refinement.

9. Under those conditions, the nitrogen can be stabilized by adding a nitride-forming element such as titanium, and porosity and bleeding from that gas will then not occur.

ACKNOWLEDGMENT

REFERENCES

1. F. A. Melmoth: Some Metallurgical Points in Electric Steel Castings and Notes on Defects. *Foundry Trade Jnl.* (1925) 32, 549–552; discussion, *ibid.* (1926) 33, 13–15.
2. J. Butterworth: Sponginess in Cast Iron. *Ibid.* (1929) 40, 362; discussion, *ibid.*, 362–363.
3. N. P. Allen: Experiments on the Influence of Gases on the Soundness of Copper Ingots. *Jnl.* Inst. Metals (1930) 43, 81–124; also *Engineering* (1930) 129, 457–461.
4. T. Swinden and W. W. Stevenson: Some Experiments on Gases in Iron and Steel and Their Effect on the Solidification of Ingots. Sixth Rept. Heterog. Steel Ingots, Iron and Steel Inst. Spec. Rept. No. 9 (1935) 137–150.

5. T. Swinden and W. W. Stevenson: Some Further Experiments on Gases in Iron and Steel and Their Effect on the Solidification of Ingots. Seventh Rept. Heterog. Steel Ingots, Spec. Rept. No. 16 (1937) 139–142.

6. R. C. Good: Some Recent Developments in Iron and Steel Castings. *Foundry* (1940) **68** (11), 42–44, 103–105.

7. W. West and C. C. Hodgson: Porosity and Sinking in Cast Iron. Paper 699, *Proc.* Inst. Brit. Foundrymen (1938–1939) **32**, 421–441; discussion, *ibid.*, 442–448.

8. C. E. Sims and C. A. Zapffe: The Mechanism of Pinhole Formation. *Trans.* Amer. Foundrymen's Assn. (1941) **49**, 255–270; discussion, *ibid.*, 270–281.

9. W. Y. Buchanan: A Preliminary Study of Gases in Iron. Paper 726, *Proc.* Inst. Brit. Foundrymen (1939–1940) **33**, 223–232.

10. A. S. Klopf: One Cause of Casting Defects. *Amer. Foundryman* (1941) **3** (3), 9; also, *Foundry Trade Jnl.* (1941) **64**, 389.

11. H. L. Womochel and C. C. Sigerfoos: Influence of the Mold on Shrinkage in Ferrous Castings. *Trans.* Amer. Foundrymen's Assn. (1941) **48**, 591–618; discussion, *ibid.*, 619–622.

12. N. N. Sokolov: The Effect of Dry and Wet Molds on the Cooling Process, the Structure, and the Reduction in Volume of Steel Castings. *Liteioe Delo* (1938) **9** (11), 15–20; Abs., *Chem. Zentr.* (1939) **2**, 511–512; also, *Chem. Abs.* (1941) **35**, 3208.

13. A. Sieverts: The Absorption of Gases by Metals. *Ztsch. Metallkunde* (1929) **21**, 37–46; Abs., *Metallurgist* (1930) **5**, 168–172.

14. L. Luckemeyer-Hasse and H. Schenck: Solubility of Hydrogen in Several Metals and Alloys. *Archiv Eisenhüttenwesen* (1932) **6**, 209–214.

15. E. Martin: Consideration of the Question of the Absorption of Pure Iron and Several of Its Alloying Elements for Hydrogen and Nitrogen. *Ibid.* (1929) **3**, 407–416.

16. I. E. Adadurov, N. I. Pevnyi, I. I. Rivlin and G. P. Kushta: Absorption of Hydrogen by Chromium. *Trudy Kharkov Khim.-Teknol.*, Inst. S. M. Kirova (1939) **1**, 12–18.

17. H. Schenck: Physical Chemistry of Steelmaking, **I**, 1932, 306 pages; **II**, 1934, 274 pages. Berlin, J. Springer.

18. P. Herasymenko and P. Dombrowski: Hydrogen Equilibria in the Production of Steel: *Archiv Eisenhüttenwesen* (1940) **14**, 109–115.

19. J. J. Egan: Research Problems Relating to Steelmaking Processes. *Trans.* A.I.M.E. (1941) **145**, 59–66.

20. S. Epstein and H. C. Larson: Steel Treatment. U. S. Pat. No. 2181693 (1939) 3 pages, 12 claims.

21. Use of Sodium Fluoride in Molds. Discussion, *Proc.* 20th Open Hearth Conf. (1937) 83–85. A.I.M.E.

22. H. Osborg: Process of Treating Molten Metals and Alloys with Compositions Containing Lithium and Products Resulting from such Treatments. U. S. Pat. No. 1869495 (Aug. 2, 1932). 4 pages, 14 claims. See also U. S. Pat. No. 1869496, No. 1869497, and No. 1869980.

23. Handbook of Chemistry and Physics, Ed. 21. Cleveland, Ohio, 1936. 2023 pages. Chem. Rubber Pub. Co.

24. S. W. Mellor: A Comprehensive Treatise on Inorganic and Theoretical Chemistry, **2**, 512–514. 894 pages. London, 1937. Longsmans and Co. Also, *Ibid.*, (1934) **13**, 314. (948 pp.) Also (1935) **14**, 1–5. (892 pp.)

25. J. Chipman and D. W. Murphy: Solubility of Nitrogen in Liquid Iron. *Trans.* A.I.M.E. (1935) **116**, 179–90; discussion, 190–196.

DISCUSSION

(Gilbert Soler presiding)

S. F. URBAN,[*] Chicago, Ill.—As Dr. Zapffe pointed out, the austenitic steels are much less susceptible to back-up than the ferritic type of stainless steels. However, his analogy is not rigorous, for the simple reason that steels of the 12 to 6 per cent Cr range are more likely to back up than 17, 21 or 26 per cent Cr. In other words, as the steels that are considered to have a closed gamma loop are approached the worst effect occurs. Those cases, when they do occur, are associated with hydrogen, by such things as improperly dried molds. If water enters a furnace shortly before tap, it will always give a beautiful back-up; that is the hydrogen type.

There is all the nitrogen type of back-up. We made about 100 small heats, split up in three groups, 0.10, 0.40 and 0.60 per cent carbon, and in each carbon range we made three nitrogen ranges by using nitrited silicomanganese as an agent, and for each of those ranges we used about 15 different elements to study their effect in combination with carbon and nitrogen. There was bleeding with almost all the elements except zirconium, titanium and aluminum.

G. SOLER,[†] Canton, Ohio.—We have noticed the same condition in our plant—that a greater percentage of 12 per cent Cr heats are susceptible to hydrogen gassiness as compared with 17 per cent Cr steel. When we have 17 per cent Cr in the bath, the metal is fairly well de-

[*] Assistant to Chief Metallurgist, Carnegie-Illinois Steel Corporation.

[†] Manager, Research and Mill Metallurgy Departments, Timken Roller Bearing Company.

oxidized by chromium, the oxygen content is rather low, thus the 17 per cent Cr steels are more highly deoxidized by the chromium than the 12 per cent. The author stated that a high degree of deoxidation increased the susceptibility to hydrogen gassiness. This theory therefore does not fit in with the differences reported in practice.

S. F. URBAN.—We have made 12 per cent Cr with aluminum and it did bleed.

G. SOLER.—That is right, but it is my belief that hydrogen is picked up in the furnace, on 12 per cent Cr heats. Our experience has indicated that more of the hydrogen pickup could be traced to the furnace than to mold practice, although these factors may vary between different plants.

C. H. JUNGE,* Cleveland, Ohio.—I am a little confused about the sequence of events in explaining this phenomenon. As I understand it, when a molten metal is cast into a wet mold, the hot metal decomposes the water present, to form hydrogen and iron oxide. This hydrogen is in an atomic condition, and it can diffuse into the metal readily. The water vapor is unstable in contact with molten iron. Later on, as I understand it, the hydrogen in the molten metal can react with the oxygen that is in solution in the metal and form steam bubbles.

How can both things occur? First, water vapor is decomposed by molten iron and then the steam bubble is stable at the same temperature. Also, what acts as a nucleus for the steam bubble? We are worrying about what acts as a nucleus for the hydrogen bubble and we say it is a steam bubble, but what makes the nucleus for the steam bubble?

G. SOLER.—Dr. Chipman has done a great deal of work with gases not only in reference to the equilibrium of hydrogen and water vapor but in collecting gases from ingots, and so forth. Would you care to make any comments, Dr. Chipman?

J. CHIPMAN,† Cambridge, Mass.—I do not know anything about hydrogen. I think that

the chromium nitride is sufficiently stable so that when the high-chromium regions are reached the nitride itself is adequately stabilized.

Dr. Zapffe's experiments regarding bleeding and porosity confirm others that have shown previously very similar results; particularly I should like to confirm his statement with regard to nitrogen, that when the maximum amount of nitrogen has been dissolved in the liquid metal, no common elements other than zirconium and titanium can be used to produce a sound ingot. If aluminum does it, it is a pretty good indication that the material had not yet been completely saturated with nitrogen. From experimental evidence, aluminum appears to be a rather poor denitrifier. Vanadium apparently is a little better than aluminum.

K. L. FETTERS,* Pittsburgh, Pa.—In regard to the mechanism of transfer of hydrogen from the furnace atmosphere through slag and into the metal, I wonder if Dr. Zapffe has come across any evidence of the mechanism by means of which that hydrogen is transferred through the slag? Also, has he found any alloy additions that tend to diminish the tendency to bleeding which is attributed to hydrogen?

C. E. SIMS,† Columbus, Ohio.—In reference to Dr. Fetter's question about the transfer of hydrogen through a slag, I find nothing incongruous in the concept of hydrogen or water as a constituent of a ceramic material such as a slag. Many of the minerals, notably the magnesium silicates, contain water that is not present as a hydrate, and under conditions of high pressure and moisture different mineral forms are sometimes obtained from those formed in the absence of moisture.

Herasymenko and Dumbrowski, two Czechs, report from their work at the Skoda plant[18] that analyses disclosed appreciable quantities of hydrogen in both acid and basic slags. Contrary to what might be expected, the acid slags were reported to contain more hydrogen than the basic slags; thus I think we can logically suspect slags of being hydrogen carriers rather than hydrogen barriers.

* Research Metallurgist, National Malleable and Steel Castings Company.
† Professor of Metallurgy, Massachusetts Institute of Technology.

* Assistant Professor of Metallurgy, Carnegie Institute of Technology.
† Supervising Metallurgist, Battelle Memorial Institute.

In regard to addition elements that will prevent bleeding, it may be said that all deoxidizers will, within limits, prevent bleeding.

As an example, for a given content of hydrogen there will be a certain content of iron oxide that will exceed the equilibrium quantity and will react to form H_2O. If the iron oxide is reduced below this content by a deoxidizer there can be no reaction to start the gas evolution. The relative quantities of FeO and H_2 are, therefore, important.

If a steel contains x content of H_2, silicon deoxidation will lower the FeO to the point where there will be no reaction and no bleeding. If, however, $2x$ of H_2 is present in a silicon-killed steel, reaction will take place to cause bleeding. A steel containing $2xH_2$ and deoxidized with some stronger deoxidizer such as aluminum will not bleed. But even aluminum deoxidation may not take the FeO low enough to prevent bleeding in a steel containing $3xH_2$.

J. S. Marsh,* Bethlehem, Pa.—How is it that in World War I the acid steels had notoriously fewer flakes than the basic?

T. S. Washburn,† East Chicago, Ind.— Considering the problem of shatter cracks in rails and billets, and assuming that the hydrogen content of the steel effects the formation of these shatter cracks, I would like to have the author's opinion of the relation between the hydrogen content of steel and the open-hearth bath and slag characteristics. It is our observation that heats in which the slags are low in iron oxide and with a high residual manganese content of the bath are more likely to develop shatter cracks than heats with high iron oxide and low residual manganese. If the former conditions are associated with a higher hydrogen content of the bath, should this be attributed to the oxidizing characteristics of the slag, or to increase in hydrogen solubility due to the manganese content of the bath?

R. E. Cramer,‡ Urbana, Ill.—We are considerably indebted to Dr. Zapffe for this very complete report regarding the development of

* Research Engineer, Bethlehem Steel Company.
† Assistant Chief Metallurgist, Inland Steel Company.
‡ Assistant Professor of Engineering Materials, University of Illinois.

porosity in castings and ingots. My interest in the subject is in regard to defects found in steel bars produced from porous ingots.

I first observed this condition in 1924, in 1 per cent Cr ball-bearing steel. The bars were about 4 in. in diameter, and were to be forged into large bearing races. The pieces for forging were sawed off, and on several of the cross-section cuts holes were observed near the centers of the bars, about $\frac{1}{4}$ in. in diameter and from $\frac{1}{2}$ to $\frac{3}{4}$ in. in length longitudinally in the bars. These holes were bright inside.

This same condition has also been found in plain high-carbon steel bars, the porosity extending to within $\frac{1}{2}$ in. of the surface. Such a condition is shown in Fig. 14. These blowholes had bright crystalline interior surfaces but because of oblique lighting appear dark in the picture. Fig. 15 shows a similar slice from the same bar deep-etched in hot 50 per cent hydrochloric acid. This shows that the bar is very porous except in the outside $\frac{1}{2}$ in. of metal.

It has been found that this porous condition does not often exist throughout all the bars from one ingot. In fact, often it is present in only 3 or 4 ft. of the length of a bar taken from near the middle or the lower half of the ingot. This short length of the porous area makes it difficult to locate such areas during routine inspection. I would be very much interested in a chemical or physical explanation of how or why this porosity develops in only a short length of the original ingot.

Dr. Zapffe apparently has considered electric-furnace steel in his explanations of the source of hydrogen in steel. In considering open-hearth steel the source of the largest quantity of hydrogen is the fuel of the open-hearth furnace, which often is 15 to 25 per cent hydrogen. This, of course, mostly burns to water vapor but it is still available to be disintegrated by the slag and the hydrogen absorbed by the liquid steel.

G. F. Comstock,* Niagara Falls, N. Y.— This paper is not only interesting but seems to be a valuable and logical explanation of gas absorption and evolution in steel. One apparent discrepancy in the argument regarding

* Metallurgist, The Titanium Alloy Manufacturing Company.

FIG. 14.—LONGITUDINAL SECTION OF POROUS BAR.
Rough saw cut, approximately natural size.
FIG. 15.—LONGITUDINAL SECTION OF POROUS BAR.
Etched in hot 50 per cent HCl. Approximately natural size.

hydrogen, however, seems to demand some further clarification.

In the footnote on page 289 and again on page 292 it is emphasized that there is no solubility limit for hydrogen in iron, yet it seems somewhat doubtful whether the author really means that literally. Presumably this refers only to *liquid* iron, though it is not stated in that way. And the discussion of deoxidizers in conclusion 6 mentions the possibility of increasing the steel's capacity for absorbing hydrogen; if there is no limit to the solubility anyway, how can something that is infinite be increased? Also, if there really is unlimited solubility in liquid steel, why do not the right-hand ends of the curves in Figs. 9 and 10 extend straight upward, instead of curving off to the right? It seems that something is missing here, at least in order to make the paper completely understandable by one of no higher mental capacity than the writer.

The illustration of the effect of titanium in eliminating unsoundness due to nitrogen is naturally of great interest to the writer, who has been working with titanium for a long time. This subject was also discussed in an interesting manner by Dr. G. R. Fitterer at the Open Hearth Conference held by the A. I. M. E. at Cincinnati, Ohio, in April 1942, as reported on pages 245 to 252 of the 1942 PROCEEDINGS of the conference. He explained how even plain carbon steel in the acid openhearth furnace, when its silicon content is high, may absorb nitrogen, which later may be evolved when the steel solidifies, causing unsoundness of the ingot or casting. Titanium or zirconium was stated to be a cure for this trouble, since they lock up the nitrogen in an inactive form so that it is not evolved in the freezing steel. This occurrence of nitrogen is somewhat similar to that which is illustrated to a much greater degree by Dr. Zapffe in Fig. 13, except that silicon instead of chromium was the element tending to increase the nitrogen absorption.

The same condition probably is more commonly encountered in acid electric practice. The late George Batty, when he was Research Director of the Steel Castings Development Bureau, was one of the first to call attention to the fact that silicon nitride might be the cause of porosity in electric steel, where nitrogen is well known to be absorbed under the arc; and

titanium has been often used in electric-steel foundries to overcome that trouble.

Thermodynamic data on various nitrides, published by Dr. K. K. Kelly, of the Bureau of Mines, are of interest in this connection. In Table 1 the stability of the compounds increases as the free energy value becomes more negative, the positive value for the iron compound indicating that it is unstable.

TABLE 1.—*Thermodynamic Data*

Compound	Standard Free Energy of Formation at Ordinary Temperature, Cal. per Gram-atom of Metal
Fe₄N	+223
CrN	−22,520
AlN	−50,050
Si₃N₄	−51,580
TiN	−74,040
ZrN	−75,640

This shows that titanium and zirconium are practically equal in nitride-stabilizing power, both holding nitrogen much more effectively than the other elements. That their nitrides are not decomposed when the steel solidifies is indicated by the presence of the characteristic angular pink or yellow crystals in titanium or zirconium steels, as well as by the effectiveness of these elements in preventing nitride porosity in hot steel.

TABLE 2.—*Effect of Titanium on Nitrogen in Steel*

Number of Heats	Titanium, Per Cent		Average Nitrogen, Per Cent	
	Added	Content	Soluble	Total
3	None	None	0.0143	0.0146
7	0.1–0.23	0.045–0.180	0.0039	0.0128
8	0.3–0.48	0.202–0.345	0.0017	0.0102

Nitrogen before Addition of Titanium, Per Cent		Titanium, Per Cent		Final Nitrogen, Per Cent	
Soluble	Total	Added	Content	Soluble	Total
0.0250	0.0267	0.31	0.202	0.0021	0.0176
0.0103	0.0103	0.45	0.330	0.0009	0.0060

Some recent experience with nitrogen in 18 heats of killed low-carbon steel made in our metallurgical research laboratory, most of them with titanium additions, shows how nitrogen in steel is affected by titanium. Each of this series of heats had about 0.2 per cent nitrogen added to it after deoxidation, in the form of sodium cyanide. When titanium was used, it was added 5 or 6 min. later in the form of TAM 40 per cent low-carbon ferrotitanium, and 2 min. after that the steel was poured. Table 2 gives the average nitrogen contents of the steels, classified according to the size of the titanium addition.

In a few heats the nitrogen was determined on a small sample poured before the titanium addition, as well as on the final ingot. These results are given in the second half of Table 2.

These results show clearly how titanium added to high-nitrogen steel, even only a few minutes before pouring, converts nearly all the nitrogen to an insoluble form, which is probably harmless, and also decreases appreciably the total nitrogen content of the steel.

C. A. Zapffe (author's reply).—Both Urban and Soler mention the fairly well-established fact that 17 per cent Cr steels show less tendency to bleed than do those with less chromium. The explanation probably lies in the caption of Fig. 10, where it is pointed out that "equal contents of hydrogen in the liquid are assumed and changes in the melting point are not considered." In other words, *other things being equal*, the conclusions of the paper are probably sound and applicable to steels that are still essentially iron and respond to hydrogen absorption in the melt roughly as does iron itself. When chromium attains 17 per cent, the low solubility of that element for hydrogen must begin to influence markedly the total hydrogen content of the liquid. With lower initial hydrogen content, the steel is obviously less liable to bleeding.

Junge's denouncement of the steam-iron equilibrium as a Janus is a criticism often heard, but its answer is elementary. Any chemical system,

$$A + B = C + D$$

is in reality a composite of two reactions proceeding in opposite directions:

$$A + B \rightarrow C + D$$
$$A + B \leftarrow C + D$$
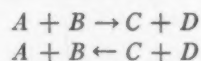
At equilibrium, A and B react to form C and D at the same rate that C and D react to reproduce A and B. Either reaction may domi-

nate when the system is not at equilibrium, the direction simply depending upon the concentrations of the various constituents with respect to their concentrations when the system is at equilibrium.

It seems clear that the steam-iron equilibrium

$$x \text{ Fe} + y \text{ H}_2\text{O} = \text{Fe}_x\text{O}_y + y \text{ H}_2\text{O}$$

comprises two reactions proceeding in opposite directions:

steam + iron → hydrogen + iron oxide
hydrogen + iron oxide → steam + iron
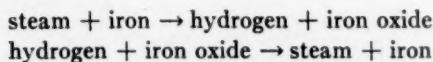
The equilibria for this system have been carefully studied from the temperatures of liquid steel down to the rusting reaction in cold water, and the equilibrium concentrations for each entity have been published.[26]

Thus, steam alone is *not* stable in contact with iron at any temperature, whether within as a bubble or without as moisture in mold. But steam *plus an equilibrium concentration of* H_2 is perfectly stable. In the mold, the H_2 is absent; whereupon H_2O reacts with the iron to form some H_2. In the metal, H_2O is absent; so dissolved H reacts with dissolved FeO to form some H_2O. The resulting steam is insoluble, since it represents the quantities of H and FeO that have exceeded the solubility product

$$K = [\text{H}]^2[\text{FeO}]$$

for the reaction

$$2 [\text{H}] + [\text{FeO}] = \text{H}_2\text{O} + \text{Fe}$$
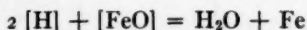
Referring for a moment back to pages 292 and 293, one will recognize that a very definite solubility limit exists for H in *iron-oxygen alloys*, in contrast to the absence of an observable limit in pure Fe. We may speak quite safely of the "solubility product" in the Fe-O-H system, though no corresponding function is yet known in the Fe-H system.

Consequently, H_2O needs no nucleation. It possesses sufficient chemical attributes to separate the Fe matrix and form its own phase wherever and whenever $[\text{H}]^2 \times [\text{FeO}]$ exceeds K. H alone cannot do that within the observable pressure range.

But H_2O cannot—and does not—exist alone

in the bubble, because of the equilibrium just discussed. H must promptly "evaporate" into this newly established gas phase until equilibrium is attained, or the H_2O in the bubble will provide that required proportion of H_2 by losing some of its oxygen back to the metal. In a paper entitled "Boiler Embrittlement," recently presented by the writer before the American Society of Mechanical Engineers, these reactions of hydrogen with oxygen and other nonmetallics within steel are discussed at length. If further question remains on the subject, that reference might be consulted.

It is always reassuring to an author to find Chipman in substantial agreement with him. On the other hand, Chipman's opening remark is without doubt erroneous and indefensible: "I do not know anything about hydrogen!"

In regard to Fetters' first question, only our opinion can be offered—that hydrogen resides in the slag as an oxide phase, just as do all the other deoxidizers. Perhaps it is present as hydrate of other oxides, as bubbles of $H_2 - H_2O$ mixture, or as H^+ and OH^- ions. Perhaps the conductivity of slags is influenced by, or depends upon, these ions from moisture. Transfer of H from the furnace atmosphere then would involve approximately the same mechanism that metallic Mn, or Si, would use if thrown on top of the slag and allowed to adjust itself throughout the depth of slag until it reached the surface of the metal. There can be no question that H from the furnace atmosphere reduces the oxides in the slag to some extent, forming a proportion of H_2O. If that H_2O all escapes, H obviously cannot penetrate the slag. If it does not entirely escape, *ipso facto*, H_2O, and therefore H, will reach the steel. The mechanism can be little other than chemical diffusion; and for other chemical reasons, hydrogen oxide must be involved in the diffusing phase.

As for Fetters' second question, his term "alloy additions" needs breaking down. The paper discusses the inhibition of bleeding one might expect from substantial additions of nickel, and possibly manganese—additions that open the gamma loop and shrink the delta dip of the absorption curve. Elements added in small amounts with deliberate attempt to "kill" H, as one kills O with Al, are not known to us. But additions of elements or substances that gasify at the temperature of liquid steel,

[26] M. G. Fontana and J. Chipman: Equilibrium in the Reaction of Hydrogen with Ferrous Oxide in Liquid Iron at 1600 Degrees Centigrade. *Trans.* Amer. Soc. Metals (1936) 24, 313–336; also ref. 17.

such as sulphur, calcium, lithium, sodium fluoride, counteract the tendency to bleed by outright removal of H in a manner identical with the nitrogen flush.

In World War I, to answer Marsh's question, basic steels undoubtedly contained more hydrogen than did acid steels, as some rough analyses at that time purport to show. The reason very likely lies in the fact that H carried into the steel as moisture in the lime was not recognized then as something to guard against in basic practice. Today there should be little to choose between the two processes with respect to the H menace.

Washburn's observations seem consistent with the argument in the paper, in spite of the fact that the presumed difference in oxygen pressure of the slag and metal throws the problem from equilibrium into kinetics. When the residual Mn is high, giving a high absorbing power for H to the bath, and the iron oxide in the slag is low, undoubtedly favoring the presence of a deoxidizer like H, absorption of H is certainly favored. Again, when the slag allows H to pass through it toward the metal, the metal must be enabled to receive it; conversely, a low absorbing power of the metal for H renders a "hydrogen slag" ineffective. Washburn's steel, in which he observes shatter cracks, apparently absorbs an extraordinary quantity of H under the favorable conditions of high Mn and low (FeO) and does not later lose it.

Cramer's specimen is suggestive of the chromium steel with the solid rim in Fig. 12 of the paper, except for his statement that the porosity is limited to the lower half of the ingot. Perhaps his is secondary piping, possibly aggravated by gas evolution. Ordinary porosity is not involved, since the holes are not rounded.

Comstock's confusion about H solubility in iron-oxygen alloys and in pure iron is presumably already cleared up by the reply to Junge. The solubility of H in pure Fe is not necessarily unlimited; it is simply sufficiently high so that no one has ever yet observed it. Stated more conveniently, the quantities of H with which we have to worry ourselves in ferrous studies are so small in proportion to the iron that a solubility limit is never within the horizon. Who has ever heard of an iron-hydrogen alloy containing even half a per cent of H? Cathodic specimens supercharged with 200 relative

volumes of hydrogen still represent an alloy containing only 0.2 per cent H by weight—a figure far exceeding any obtained by absorption in equilibrium with a gas phase of molecular H_2 at any pressure or temperature whatever. If that H were in solution, which it definitely is not, the alloy would be about 10 atomic per cent hydrogen. The curves in Figs. 9 and 10 have a *shape* that is significant, since undoubtedly it is also the shape of the true solubility curve at the critical pressure; but quantitatively they are significant only as the absorption limit for hydrogen in iron at that particular temperature and that particular pressure.

In closing, a remark might be made on the intriguing loss of nitrogen shown both by Comstock's analyses and by our own when titanium is added to steels. How does the nitrogen leave the steel? Does titanium nitride float out? Is it gaseous? Under the microscope the evidence of the nitride crystals is that they are primary in solidification, which argues against their vapor pressure being important; and the abundance of the crystals and their good dispersion argues against levitation, as does the fact that our steels were poured quickly after the titanium addition.

R. M. MacIntosh, in charge of the analytical laboratory at Battelle, had the following to say when the unexpected results on our ingots were returned for his attention: "In this case I know that every precaution was taken to decompose the samples completely by acid digestion of the insoluble. Furthermore, two analysts working independently and by different methods reported results within 0.003 per cent N. The analysis of these heats was as follows:

Sample	Ti, Per Cent	Total N, Per Cent
T-1	Nil	0.056
T-2	0.8	0.044
T-3	1.4	0.014

These results indicate, as do Comstock's, that a loss of nitrogen occurs with the addition of titanium. If the analysis of T-3 is low, the nitrogen must either be lost in the decomposition or a colorless compound is formed, which does not liberate ammonia from a basic solution, because no residue remains to hold the nitrogen."

Quantitative Determination of Retained Austenite by X-rays

By Frank S. Gardner,* Junior Member, Morris Cohen,† Member A.I.M.E., and Dara P. Antia†

There is a conspicuous lack of information in the literature on the precise role played by residual quantities of austenite in heat-treated steels. While retained austenite may be expected to have significant effects on such important properties as the impact resistance of tools and carburized parts and the dimensional stability of dies and gauges, attempts to study these problems systematically have suffered from the absence of a reliable technique for ascertaining absolute amounts of austenite. With such a technique, not only could the relation between residual austenite and service behavior be investigated, but the chemical and heat-treatment factors that control the quantity of the austenite could also be established. Thus, the retained austenite content could then be regulated in accordance with the results desired.

The presence of retained austenite may be inferred by observing the changes in properties (hardness, specific volume, electrical resistance, etc.) due to its decomposition on subatmospheric cooling[1] or on tempering,[2] but these indirect measurements are not readily translated into percentages of austenite. Quantitative determinations have been achieved in special cases by means of dilatometric[3] and magnetic[4,5] measurements; but the former procedure requires that observations be conducted *during* the hardening and involves difficult calibrations that limit its applicability, while the magnetic procedure is very sensitive to extraneous influences and depends upon assumptions that can only be considered as approximate in an absolute sense. Furthermore, both the dilatometric and magnetic effects are volume properties, and cannot be conveniently utilized to explore variations in retained austenite from point to point in a specimen. Some microstructures lend themselves to accurate evaluation of retained austenite contents by metallographic methods,[3] but such instances are not too common, and at best, the procedure is tedious.

The characteristic X-ray diffraction lines of austenite permit positive identification of its presence; and in the present paper the intensities of these lines, or the corresponding densities* on photographic film, are employed to measure the amount of the retained austenite. In order to cancel the effect of uncontrollable variations in the X-ray exposure and film-development conditions, a standard reference line is superimposed on each film by maintaining a foil of aluminum in the path of the incident X-ray beam during the entire exposure. With different samples of steel and the same foil, the ratio of the density of some one austenite line to the density of

* Calculated from microphotometer traces.

the reference line becomes a direct function of the retained austenite content. This functional relationship is established experimentally by making a series of X-ray films with specimens of known austenite content, these specimens having about the same chemistry as the unknowns to which the method is to be applied. In developing this technique, 5 per cent nickel steels were used, and typical results relating to these steels are given as illustrations of the method.

An analogous X-ray procedure has been reported by Tamaru and Sekito,[6] who constructed a modified Debye-Scherrer camera, arranged so that a strip of gold could be exposed alternately with the steel sample. This arrangement was limited to small cylindrical specimens, and the results obtained are open to question because austenitic manganese steel was employed to calibrate the method for the plain carbon steels under investigation. Furthermore, the physical heights of the microphotometer peaks, rather than the actual densities of the diffraction lines, were used for calculating the amounts of retained austenite. To the authors' knowledge, this seems to be the only reference to any technique at all similar to the one described in the present paper, although diffraction-line densities have been employed in a qualitative way for rough estimations.

PRINCIPLE OF METHOD

By locating the steel specimen, photographic film and primary slit on the periphery of the same circle, as in a Phragmén-type camera, all of the X-ray diffraction lines emanating from the steel converge on the film, even though the incident beam is divergent.[7] The intensity of some conveniently observable austenite line is dependent upon the amount of retained austenite in the sample as well as upon the intensity of the incident beam (I_o). In order to compensate for the effect of variations in the latter factor, an aluminum foil is used for reference purposes. As shown in Fig. 1, the foil intercepts the entire incident beam, and is so positioned that its characteristic $(200)\alpha$ line is
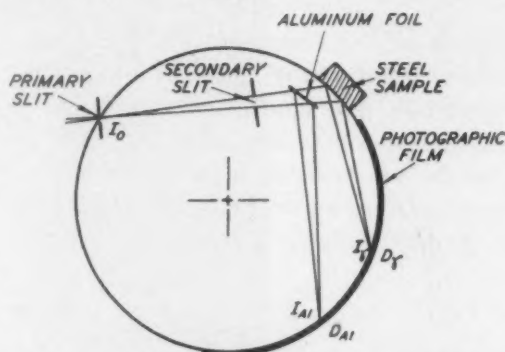
FIG. 1.—SCHEMATIC ARRANGEMENT OF ALUMINUM REFERENCE FOIL IN PHRAGMÉN X-RAY CAMERA.

"focused" on the film in a region not occupied by ferrite, martensite, austenite or carbide lines. However, the foil is relatively transparent to X-rays, and the diffraction lines from the steel specimen are obtained simultaneously in the same film. Variations in I_o caused by fluctuations in X-ray tube operation change the intensity of the selected austenite line (I_γ) in the same proportion as the intensity of the reference aluminum line I_{Al}. During the exposure of a given sample, therefore, the ratio $\frac{I_\gamma}{I_{Al}}$ at any instant is independent of I_o, and remains constant throughout the exposure. Hence,

$$\frac{I_\gamma}{I_{Al}} = c = \text{a function of the percentage of austenite} \quad [1]$$

Now the exposure E, which the film receives from a beam whose intensity may vary during the exposure, is the cumulative product of intensity and time, or

$$E = \int_o^t I dt *$$

---

* If I is constant throughout the exposure time, then $E = It$, which is a statement of the Bunsen reciprocity law.[8,9]

FIG. 2.—TYPICAL MICROPHOTOMETER TRACE, ILLUSTRATING VARIOUS MEASUREMENTS UPON WHICH DENSITY CALCULATIONS ARE BASED.
Determination of the total density (including background) of the aluminum standard line is shown separately at the left, and is generally included to, ensure that the maximum density does not, exceed the linear range of the film (see Fig. 4). No. 2 camera and aluminum foil used.

Thus, with the aid of Eq. 1:

$$\frac{E_\gamma}{E_{Al}} = \frac{\int_o^t I_\gamma dt}{\int_o^t I_{Al}dt} = \frac{c\int_o^t I_{Al}dt}{\int_o^t I_{Al}dt} = c = \frac{I_\gamma}{I_{Al}} \quad [2]$$

or

$$\frac{E_\gamma}{E_{Al}} = \text{a function of the}$$

percentage of austenite [3]

It will be demonstrated here that there is a direct proportionality between the expo-

cordingly, to obtain D_γ or D_{Al}, the background density must be subtracted,

$$D_M - D_B = \log\frac{G_o}{G_M} - \log\frac{G_o}{G_B} = \log\frac{G_B}{G_M} \quad [4]$$

and henceforth references to line density will mean "density above background." A microphotometer trace and illustrative density calculations are shown in Fig. 2.

The relationship between line density and the corresponding exposure is indicated by Fig. 3. Using a single specimen of
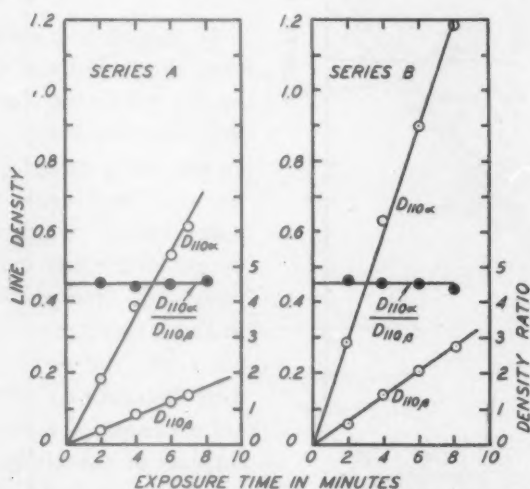
FIG. 3.—RELATION BETWEEN LINE DENSITY AND EXPOSURE TIME.
Sample was annealed iron. I_o maintained constant at higher level in series B than in series A. Developing time, $4\frac{1}{2}$ min. at 70°F. for series A and $5\frac{3}{8}$ min. at 70°F. for series B.

sure quantities E_γ and E_{Al} and the resulting line densities D_γ and D_{Al}. This relationship is particularly fortunate because the latter values are much easier to measure than the former. Photographic density is defined as $D = \log\frac{J_o}{J}$ where J_o is the intensity of a light beam falling on the processed film and J is the intensity of the transmitted beam. With the recording microphotometer used in this work, the displacement G on the trace is proportional to the light intensity. Hence, $D = \log\frac{G_o}{G}$. However, the density of a diffraction line as measured (D_M) includes the background density (D_B) as well as the line densities $(D_\gamma$ or $D_{Al})$. Ac-

annealed iron, a set of diffraction patterns was made with different times of exposure. Particular care was taken to maintain constant tube operation so that I_o could be considered constant. All the films were developed simultaneously, and the resulting line densities are plotted in Fig. 3a. Months later, a similar series of films was prepared from the same specimen, but I_o was held constant at a higher level, and the developing time was also deliberately increased over that of the first series. The data for the second series are given in Fig. 3b. In both cases, the line densities turn out to be directly proportional to the exposure time. Because of the interchangeability of intensity and time (reciprocity law),

these results demonstrate not only that $D = kt$ when I is constant, but also that $D = kI$ if t is constant, and that

$$D = kE \qquad [5]$$

if neither I nor t is constant. As shown in Fig. 4, similar linearity was observed using
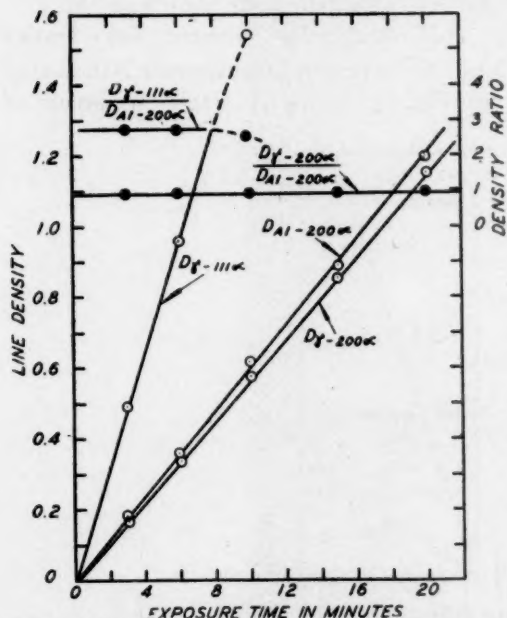
FIG. 4.—RELATION BETWEEN LINE DENSITY AND EXPOSURE TIME, I_0 BEING HELD CONSTANT. Sample austenitic stainless steel (18 per cent chromium, 8 per cent nickel) exposed through aluminum reference foil in No. 2A camera.

exposure-time variations with a sample of austenite (18 per cent Cr, 8 per cent Ni) and the aluminum reference foil. Glocker has also reported this straight-line relationship.[8]

It is further evident from the horizontal lines in both Figs. 3 and 4 that the ratio of line densities on the same film is independent of the exposure time. Moreover, the proportionality constant that depends upon the photographic film and its development drops out when such ratios are evaluated, since, from Eq. 5:

$$\frac{D_\gamma}{D_{Al}} = \frac{kE_\gamma}{kE_{Al}} = \frac{E_\gamma}{E_{Al}} \qquad [6]$$

The insensitivity of these density ratios to variations in film development as well as in tube operation is clearly demonstrated by the virtual coincidence of the $\frac{D_{110\alpha}}{D_{110\beta}}$ ratios in Fig. 3. Hence, the largest errors commonly associated with quantitative X-ray densitometry are effectively eliminated, and by combining Eqs. 3 and 6,

$$\frac{D_\gamma}{D_{Al}} = \text{a function of the}$$

percentage of austenite   [7]

It should not be assumed prematurely that the functional relationship expressed by Eq. 7 is linear. To establish the relationship experimentally, a series of 5 per cent nickel steels ranging in carbon from 0.38 to 1.50 per cent was quenched from austenitizing temperatures at which all excess ferrite and carbide were completely dissolved. After darkening the martensite in these specimens by tempering at 300°F. for 1 hr., the retained austenite contents were determined metallographically by a point-counting method.[3] This procedure consists of superimposing fine-ruled paper over high-contrast prints of the microstructures, and counting the number of line intersections on the graph paper falling over the white austenite and the number falling over the black martensite. By making such counts on sets of prints representing systematically chosen positions in each steel sample, measurements of the retained austenite are usually reproducible to within ±0.5 per cent by volume.*

An entirely independent check on this point-counting technique was obtained by measuring the surface reflectivity of the prints.† The reflectance of the mixture of white and black areas depends upon the

---

* Percentage by volume is equivalent to percentage by area on the prints.
† Saunders and Kahles[10] have reported a photometric method based on the reflectance of the etched microstructure, but it is difficult to secure consistently the necessary contrast between the light and dark constituents without the aid of photography.

relative areas as follows:

$$R_M = \frac{\alpha R_\alpha + \gamma R_\gamma}{100} \qquad [8]$$

or

$$\gamma = \frac{R_M - R_\alpha}{R_\gamma - R_\alpha} \times 100 \qquad [9]$$

where R_M = reflectance of the mixture, R_γ = reflectance of the white areas,

tively. Fig. 5 shows the reflectance values for a single print, plotted against the wave length of the light used for the measurements. While the reflectances vary with the wave length because of the inherent color of the printing paper, the percentage of austenite as calculated from Eq. 9 is nearly independent of the wave length; and for routine runs, a wave length of 580 milli-
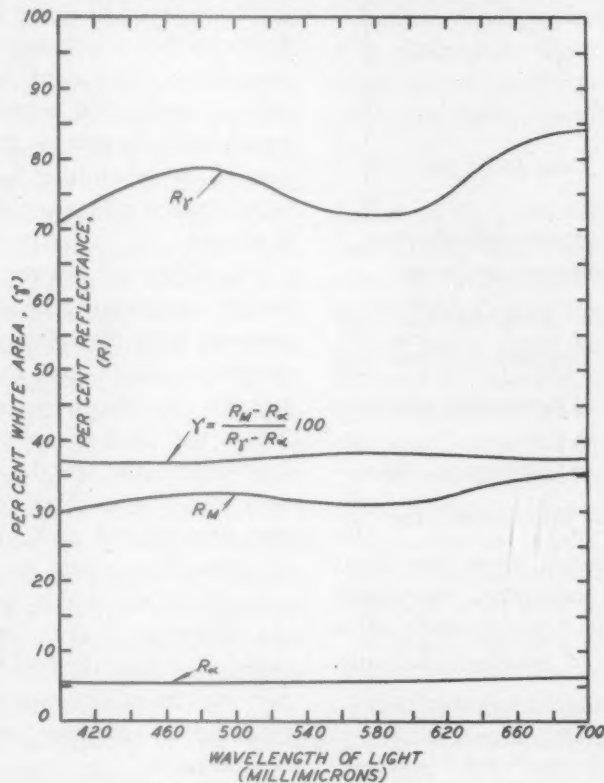
FIG. 5.—REFLECTIVITY CURVES FOR PRINT OF 1 PER CENT CARBON, 5 PER CENT NICKEL STEEL CONTAINING 38 PER CENT AUSTENITE.

R_α = reflectance of the black areas, γ = percentage of retained austenite, α = percentage of tempered martensite, and $\alpha + \gamma$ = 100. The reflectances were determined with a high-precision spectrophotometer, completely described elsewhere.[11] In view of the extreme contrast, the white areas corresponded to the unexposed print surface, while the black areas approached saturation blackening. Hence, R_γ and R_α could be measured separately from blank prints, which were processed after receiving no exposure and complete exposure, respec-

microns was adopted. The validity of this photometric method was confirmed by constructing a series of accurate rectilinear white and black patterns whose relative areas could be measured by reflectivity as well as calculated directly from the geometry. Agreement within ±0.5 per cent was found.

Table 1 shows typical correlations between the point-counting and reflectance techniques. In the worst case (specimen 2), there was a difference of ±1 per cent austenite between the two methods, but

usually the agreement was within about ±0.5 per cent and justified the use of point counting for ascertaining the austenite contents of the calibration specimens.
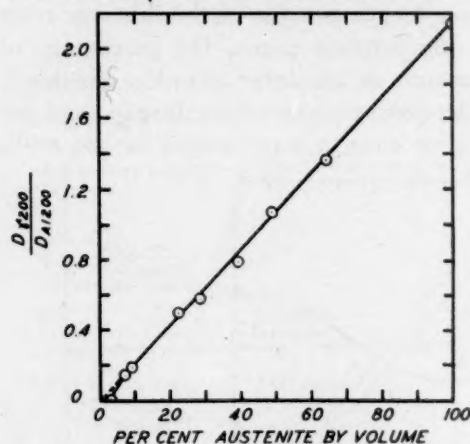
FIG. 6.—RELATION BETWEEN $\dfrac{D_\gamma}{D_{Al}}$ AND RETAINED AUSTENITE CONTENT IN 5 PER CENT NICKEL STEELS.
Calibration for No. 2 camera and aluminum foil.

Using the (200) α diffraction lines of the austenite and aluminum, the $\dfrac{D_\gamma}{D_{Al}}$ ratios were determined from the X-ray photograms of the calibration specimens, and are shown in Fig. 6 as a function of the volume percentage of retained austenite.

TABLE I.—*Correlation between Point Counting and Reflectance Method*

Speci-men No.	Austenite, Per Cent			
	Point Counting			Reflec-tance Method
	Observer A	Observer B	Average	
1	27.5	26.8	27.2	26.5
2	37.9	38.7	38.4	36.5
3	47.9	49.2	48.6	48.9

In general, the X-ray determinations were reproducible to ±1 per cent austenite. The relationship is quite linear except at very low austenite contents, where the very small size of the austenite particles or the absorption effect of the surrounding matrix

causes disproportionately low intensities of the austenite lines. In fact, the $\dfrac{D_\gamma}{D_{Al}}$ ratio becomes substantially zero for austenite contents below 3 per cent. If the linear portion of the curve is extended, it passes through the origin, thus suggesting that a single specimen .may serve as a basis for establishing a valid calibration for most of the range. The curve in Fig. 6 not only holds for the 5 per cent nickel steels, but also for 3.5 per cent nickel[12] and plain carbon steels.[13] Of course, the calibration varies with the nature, thickness, and position of the aluminum foil, and should be redetermined whenever one of these factors is altered.

The difference between the volume and weight percentages of retained austenite depends upon the relative specific volumes of the austenite and the coexisting constituent. In the most extreme case—i.e., when the second phase is tetragonal martensite—the specific volumes differ by only 4 per cent. From this, it turns out that the volume and weight percentages of retained austenite are never more than 1 per cent apart, and in tempered structures the difference is even less. For most purposes, therefore, the two ways of expressing the amount of retained austenite may be regarded as equivalent within the experimental error.

EXPERIMENTAL DETAILS

Preparation of Sample.—Before heat-treatment, one surface of the specimen is hollow-ground to fit the curvature of the X-ray camera. After heat-treatment, at least 0.040 in. of this surface is removed, to avoid extraneous surface effects. Most of this removal is accomplished with emery cloth, and the rest by electrolytic dissolution at a current density of 3 to 6 amp. per sq. in. in a solution of 5 per cent HCl + 5 per cent H_2SO_4. It is only necessary to remove about 0.003 in. by electrolysis in order to eliminate the cold-working effects

of the emery polishing. Care is taken to avoid undue heating at all times.

In order to produce uniformly intense diffraction lines, the grains should be random in orientation and small in size. A grain size of A.S.T.M. No. 6 or finer is usually quite satisfactory, but sizes as coarse as No. 3 may be handled by moving the specimen during the exposure or by preparing new surfaces from time to time during the exposure.

Preparation of Reference Foil.—Aluminum seems to be the most suitable material for the reference foil because of its relative transparency to X-rays and its distribution of diffraction lines. However, the proper combination of foil thickness, grain size, and freedom from preferred orientation is difficult to secure in sheet form. Accordingly, the foil in question is prepared by applying several uniform layers of aluminum paint on hard filter paper, and is covered finally with a protective coating of shellac. The foil is mounted on a small brass frame, which is accurately fitted into the camera so as to locate the foil in the exact position for fulfilling requirements described on page 2. This positioning is first attained by cut-and-try, but after the frame has been adjusted it slips into the same place each time.

Exposure and Development.—The source of X-rays is a modified Hägg tube[14] with a chromium target, operating at 45 to 50 kilovolts and approximately 10 milliamperes. Exposure times vary from 10 to 20 min., and though not critical, are generally selected to yield a maximum density of 0.6 to 1.2 in the aluminum standard line $(200)\alpha$. Kodak Duplitized No-Screen film is used, and the developing time is approximately twice that recommended for the film, since both double-coated film and long development favor the straight-line relationship between line density and exposure.[8] Under these conditions, the linearity holds at least up to densities of 1.3.

A Phragmén camera of intermediate range is used with the primary slit width adjusted to 0.005 in. The exposed surface of the specimen is limited to about ⅛ in. square.

Microphotometer Traces.—The film densities are measured with a type A, Moll recording microphotometer with a slightly defocused scanning beam to smooth out irregular density fluctuations caused by film graininess. Fig. 2 shows a typical trace, as well as the method for converting the trace measurements into line densities.

For the most part, the $\dfrac{D_\gamma}{D_{Al}}$ values are based on the $(200)\alpha$ lines, since these lines provide sharp, easily measured peaks, and also are unobscured by other lines. Actually, the $(111)\alpha$ line of the austenite is about three times more sensitive to the amount of austenite than the $(200)\alpha$ line (see Fig. 4), but the density of the former is frequently a questionable quantity because of interference by the $(101)\alpha$ martensite line. However, in a qualitative way, the $(111)\alpha$ line is helpful when dealing with very small amounts of austenite, since as little as 1 per cent austenite may be detected by observing the $(111)\alpha$ line on the trace, whereas the $(200)\alpha$ line is not measurable with less than about 3 per cent of austenite (see Fig. 6). Of course, all the diffraction lines may be used for lattice-parameter measurements.

Careful consideration was given to the possible utilization of integrated densities (corresponding to the area under the peak above background) instead of the peak densities (corresponding to the height of the peak above background). It has been observed, for example, that the integrated densities of ferrite lines are relatively insensitive to cold-working, whereas the peak densities may be affected appreciably. However, in the problem at hand the density distribution of the austenite lines is almost constant, even in the comparison of quenched specimens with tempered speci-

mens, and the peak density becomes a good criterion of the integrated density. Moreover, the measurement of areas on the traces is less precise and more tedious than
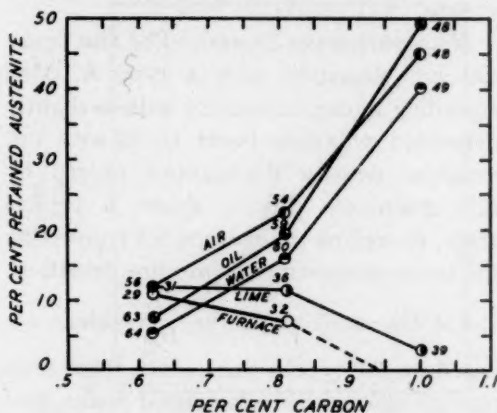
FIG. 7.—EFFECT OF CARBON CONTENT AND COOLING RATE ON AMOUNT OF RETAINED AUSTENITE IN 5 PER CENT NICKEL STEELS.
Austenitizing temperature, 1700°F. Superimposed numbers are Rockwell C hardness values.

the measurement of linear distances. Accordingly, all the line densities reported here are in terms of the peak densities.

SOME RESULTS ON 5 PER CENT NICKEL STEELS

Effect of Carbon and Quenching Rate on Retained Austenite Content.—Specimens of three induction-furnace steels (Table 2),

TABLE 2.—*Compositions of Nickel Steels Per Cent*

C	Mn	Si	Ni
0.62	0.52	0.54	4.76
0.81	0.52	0.54	4.76
1.00	0.43	0.01	4.82

½ by ½ by ⅝ in., were completely austenitized at 1700°F. and cooled in water, oil, air, lime and furnace, respectively. The resultant amounts of retained austenite as measured by the X-ray technique are shown in Fig. 7. Among the samples cooled in water, oil and air, the austenite increases in the order named, and also increases with the carbon content. There is only

one exception to this statement: in the 1 per cent carbon steel the amount of retained austenite is slightly greater after oil quenching than after air cooling.

In the lime-cooled and furnace-cooled specimens, the trends are just the opposite. Here, the anomalous decrease in retained austenite with increasing carbon is due to the separation of acicular ferrite from the 0.62 and 0.81 per cent carbon steels during the slow cooling, while proeutectoid carbide precipitates in the 1.00 per cent carbon steel. The formation of free ferrite concentrates the carbon in the remaining austenite, which thereby becomes more stable, while the formation of free carbide acts in the reverse direction. These changes in the composition of the austenite during slow cooling were confirmed by lattice-parameter measurements, which showed that in the lime-cooled samples the carbon content of the retained austenite had risen to 1.2 per cent in the 0.62 per cent carbon steel and to 1.1 per cent in the 0.81 per cent carbon steel, but had dropped to 0.8 per cent in the 1.00 per cent carbon steel. The various hardness values shown in Fig. 7 also substantiate the X-ray findings.

Austenite Decomposition during Tempering.—Duplicate specimens of the 1 per cent carbon, 5 per cent nickel steel were oil-quenched from 1700°F. and then tempered intermittently at 500°F. Each time the specimens were cooled to room temperature, the percentage of retained austenite, specific volume, and Rockwell C hardness were measured. As is evident from Fig. 8, the tetragonal martensite decomposes very quickly with a marked contraction and decrease in hardness, but with no change in the austenite content. On further tempering, however, the volume and hardness begin to increase simultaneously with a decrease in the amount of austenite. The excellent conformity of the specific volume, hardness and austenite changes during this stage of tempering speaks well for the X-ray method.

Measurement of Retained Austenite versus Depth.—To demonstrate the application of the X-ray method to an "exploration" problem, the retained austenite was deter-

the steel specimen, a reference line is superimposed on the X-ray film along with the diffraction lines emanating from the steel. The ratio of the density of the austen-
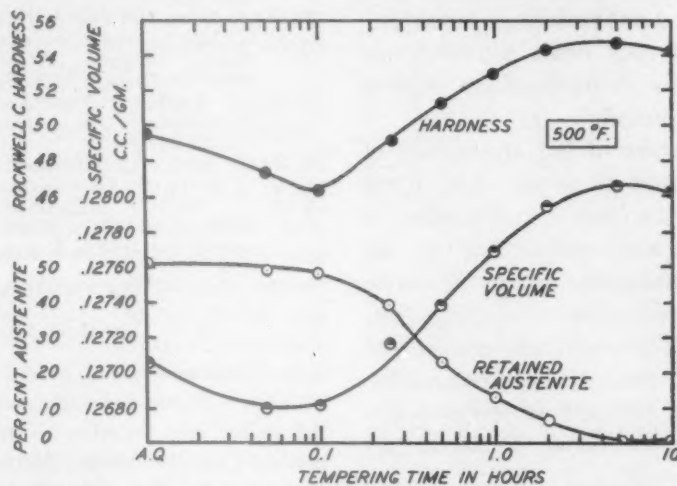
FIG. 8.—TEMPERING CURVES FOR 1 PER CENT CARBON, 5 PER CENT NICKEL STEEL, OIL-QUENCHED FROM 1700°F.
Tempering temperature, 500°F.

mined as a function of depth in the three 5 per cent nickel steels after oil quenching from 1700°F. For these experiments, the usual 0.040 in. was not removed; the X-ray measurements were made first on the heat-treated surfaces and then progressively at various depths. The curves in Fig. 9 clearly demonstrate a depletion of retained austenite near the surface with a general increase to a depth of 0.012 to 0.016 in. where the normal austenite content of the sample as a whole is reached. Parameter measurements on the retained austenite in this range indicate that decarburization was mainly responsible for these gradients. The method is now being applied in a similar way to the carburizing of 5 per cent nickel steels.

SUMMARY

An X-ray diffraction method has been described for the quantitative measurement of retained austentite in heat-treated steels. By means of an aluminum foil, which is exposed simultaneously with

ite $(200)\alpha$ line to the density of the aluminum $(200)\alpha$ line then becomes a direct function of the austenite content, substantially independent of tube fluctua-
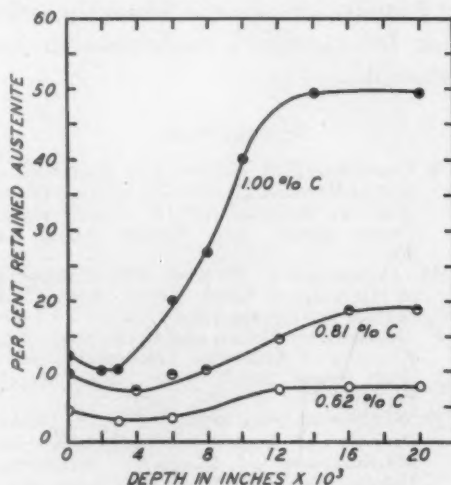
FIG. 9.—AUSTENITE GRADIENT IN 5 PER CENT NICKEL STEELS, OIL-QUENCHED FROM 1700°F.

tions, exposure time, and film-development conditions. The functional relationship between this density ratio and the per-

centage of retained austenite was established experimentally with the aid of 5 per cent nickel steels heat-treated to obtain various austenite contents, which, in turn, were determined independently by a metallographic point-counting procedure. The validity of such point counting was demonstrated by cross-checking with a photometric technique.

Typical examples of the application of the X-ray method to 5 per cent nickel steels are given to show: (1) the effect of carbon content and cooling rate on the amount of retained austenite, (2) the course of austenite decomposition during tempering, and (3) the austenite gradient in quenched steel due to decarburization. In general, the retained austenite determinations are reproducible to about ± 1 per cent of austenite.

ACKNOWLEDGMENTS

The authors wish to acknowledge their indebtedness to Dr. John T. Norton, whose advice was frequently sought throughout the development of this X-ray method, and to the American Brake Shoe and Foundry Co., for the fellowship under which Dr. Gardner's thesis research was conducted.

REFERENCES

1. P. Gordon and M. Cohen: The Transformation of Retained Austenite in High Speed Steel at Subatmospheric Temperature. *Trans*. Amer. Soc. Metals (1942) **33**, 569.
2. M. Cohen and P. K. Koh: The Tempering of High Speed Steel. *Trans*. Amer. Soc. Metals (1939) **27**, 1015.
3. P. Gordon, M. Cohen and R. S. Rose: The Kinetics of Austenite Decomposition in High Speed Steel. Amer. Soc. Metals Preprint No. 30 (Oct. 1942).
4. E. Maurer and K. Schroeter: The Determination of Austenite Contents by the Measurement of Magnetic Saturation Values. *Stahl und Eisen* (1929) **49**, 929.
5. A. Gulyaev: Mechanism of Structural Transformations in Tempering High Speed Steel. *Metallurg* (1936) **11** (12), 73.
6. K. Tamaru and S. Sekito: On the Quantitative Determination of Retained Austenite in Quenched Steels. *Sci. Repts.*, Tohoku Imp. Univ. (1931) [1] **20**.
7. A. F. Westgren: X-ray Determination of Alloy Equilibrium Diagrams. *Trans*. A.I.M.E. (1931) **93**, 13.
8. R. Glocker: Materialprüfung mit Röntgenstrahlen, Ed. 2, 59–62. Berlin, 1936. J. Springer.
9. G. L. Clark: Applied X-rays, Ed. 3, 76. New York, 1940. McGraw-Hill Book Company.
10. E. R. Saunders and J. F. Kahles: A Study of Martensite Formation by a Photometric Method. Amer. Soc. Metals Preprint No. 43 (Oct. 1941).
11. A. C. Hardy: A New Recording Spectrophotometer. *Jnl*. Optical Soc. Amer. (1935) **25**, 305.
12. D. P. Antia: Unpublished research.
13. S. G. Fletcher: Unpublished research.
14. J. T. Norton: Simplified Technique for Lattice-parameter Measurements. *Metals and Alloys* (1935) **6**, 342.

DISCUSSION

(*E. S. Davenport presiding*)

G. FREEDMAN,* Newton, Mass.—In a bachelor's thesis investigation at M. I. T., the writer had occasion to apply this X-ray method to the determination of retained austenite at different depths in the carburized case of 5 per cent nickel steel. The method was found to lend itself readily to this type of quantitative analysis since each new level in a carburized specimen exposed by grinding and etching presents, in effect, a new sample to the X-ray beam. Figs. 10 and 11 show the data obtained after pack-carburizing for 8 hr. at 1550° and 1650°F., respectively. A commercial carburizing compound (charcoal-coke base) was used, and the specimens were quenched in oil directly from the carburizing temperature.

The austenite contents given in Figs. 10 and 11 were determined with the same aluminum reference foil and density calibration developed by the authors. Rockwell C hardness values were also measured at various depths in the carburized case, and are plotted in Figs. 10 and 11. The corresponding carbon content at each level was ascertained from the known relationship between the lattice parameter of the austenite and its carbon content in 5 per cent nickel steels.

It is interesting to note that: (1) there is considerably more retained austenite after carburizing at 1650°F. than at 1550°F., owing to the higher carbon content in the former; (2) the surface hardness is materially reduced because of the presence of the retained austenite, but Rockwell C values of 62 to 63 may

---

* Raytheon Production Corporation.

be obtained even in the presence of 15 to 25 per cent of austenite; (3) the hardness increases below the surface because of the decreasing amounts of retained austenite; and (4) with increasing depth, the hardness reaches a maximum and then falls off as the softening effect of the lower carbon in the martensite offsets the diminishing amounts of austenite.

The specimens upon which Figs. 10 and 11 are based were not given any subsequent heat-treatment to decompose the retained austenite, but it is evident that the authors' X-ray technique would be ideal for following such variations. In the same way, one could evaluate directly the comparative efficacy of various carburizing compounds, thermal cycles and modified steel analyses aimed at inhibiting excessive amounts of retained austenite in these high-nickel carburizing steels.

F. S. GARDNER, M. COHEN AND D. P. ANTIA (authors' reply).—It is most gratifying to see Mr. Freedman's practical and independent application of our new technique to a carburizing problem. The way is now open for a comprehensive study of the dependence of austenite

retained austenite contents, it should be possible to adjust the variables for obtaining the desired amounts of austenite.
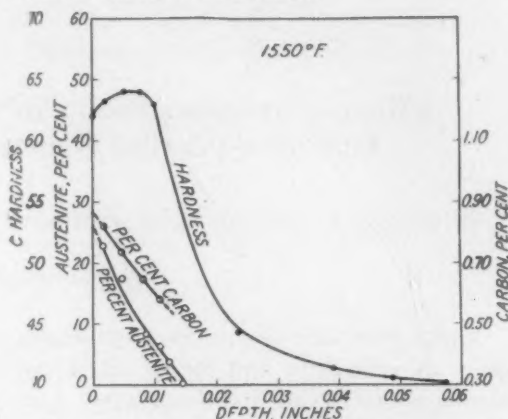
FIG. 10.—CASE CHARACTERISTICS OF 5 PER CENT NICKEL STEEL, CARBURIZED FOR EIGHT HOURS AT 1550°F. AND QUENCHED DIRECTLY IN OIL.

The principle utilized in this X-ray method is undoubtedly applicable to the quantitative measurement of phases other than austenite For example, one could determine the relative amounts of alpha and beta solid solutions in
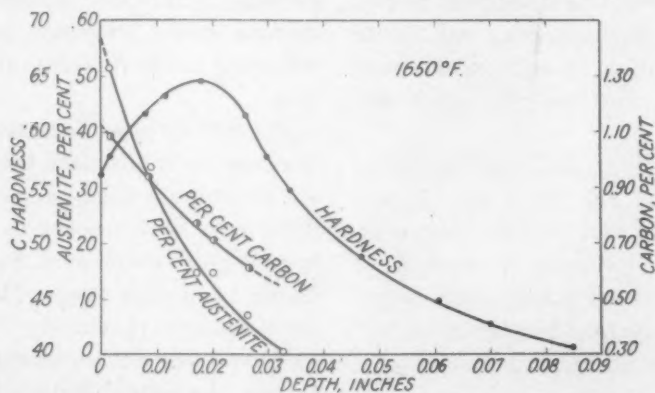
FIG. 11.—CASE CHARACTERISTICS OF 5 PER CENT NICKEL STEEL, CARBURIZED FOR EIGHT HOURS AT 1650°F. AND QUENCHED DIRECTLY IN OIL.

retention on steel composition, carburizing conditions and subsequent heat-treatment. With this straightforward determination of the

60-40 brass, as well as the amount of ferrite in austenitic steel, provided the particles were not too finely dispersed.

Effect of Inhomogeneity in Austenite on the Rate of the Austenite-pearlite Reaction in Plain Carbon Steels

By George A. Roberts,* Junior Member, and Robert F. Mehl,† Member A.I.M.E.

When austenite first forms from aggregates of cementite and ferrite, it is not homogeneous.[1] This inhomogeneity, consisting of both undissolved carbide and carbon concentration gradients, has a profound effect upon the characteristics of the austenite-pearlite reaction. The rate of formation of pearlite is increased by the presence of inhomogeneities[2,3] and because of this (when the inhomogeneity is sufficiently pronounced) the hardenability of the steel is reduced.[4,5] In addition to this kinetic effect, inhomogeneities will cause the direct formation of spheroidite from austenite at temperatures just below the Ae_1.[6-11]

The present report attempts quantitatively to evaluate the effect of inhomogeneity upon the rate of the austenite-pearlite reaction, presents a method of determining the austenitizing cycle necessary to obtain "practical homogenization," and considers the effect of inhomogeneity on hardenability.

Effect of Inhomogeneities on Reactions Near Ae_1

Few quantitative data are available representing the effect of undissolved carbide or of carbon concentration gradients upon the rate of the austenite-pearlite reaction. In procuring such data it is necessary to separate the effect of undissolved carbide from that of grain size, and this is not an easy task. The solution of carbide is always accompanied by an increase in the grain size, both effects contributing to the retardation of the reaction rate.

It has been possible to make this separation and to obtain data that are independent of the grain size by the use of steels that differ only with respect to their tendency toward grain-coarsening. Steels C and D in Table 1 are such steels. These steels have been studied previously;[1,2,12] they differ only with respect to deoxidation practice; C was deoxidized with silicon while D, teemed from a portion of the same heat, was deoxidized with additional quantities of aluminum in the mold. C therefore is what is normally termed a "coarse-grained steel" and D is a "fine-grained steel." These steels can be compared at the same grain size by heating C to a low temperature and heating D to an elevated temperature, producing a structure of austenite plus residual carbide in the former while forming homogeneous austenite in the latter; in such

a case, grain-size differences are eliminated and differences in homogeneity alone remain.

Accordingly, C was austenitized in lead for 10 min. at 730°C. (1345°F.), furnishing

isothermal and metallographic techniques. Fig. 1 shows the resulting curves.*

The two curves to the left represent the conditions for an austenite containing undissolved carbide, and those to the right

TABLE 1.—*Analyses of Steels*

Designation	Composition, Per Cent								
	C	Mn	Si	S	P	Cr	Ni	Al	Cu
A	0.78	0.63	0.18	0.030	0.014				..
B	0.80	0.74	0.24	0.029	0.019	0.01	0.11		0.09
C	0.78	0.63	0.23					0.008	
D	0.79	0.62	0.21					0.058	
I	1.04	0.21	0.20	0.013	0.014	0.03	0.02		
K	1.06	0.26	0.13	0.019	0.011	0.02	0.02		
E	0.88	0.27	0.23	0.017	0.017	0.03	0.02	0.19	

austenite of a fracture grain size of 6½ with residual carbide. Steel D was austenitized for 30 min. at 875°C. (1610°F.), furnishing austenite of a grain size of 6 to 6½ with no residual carbide. Examination for residual carbide and fracture grain size was made on

represent homogeneous austenite. It can be shown that this increase in the reaction rate is caused solely by an increase in the rate of nucleation, for the rate of growth of the pearlite is unchanged. At 690°C. (1275°F.) the rate of growth for the steel
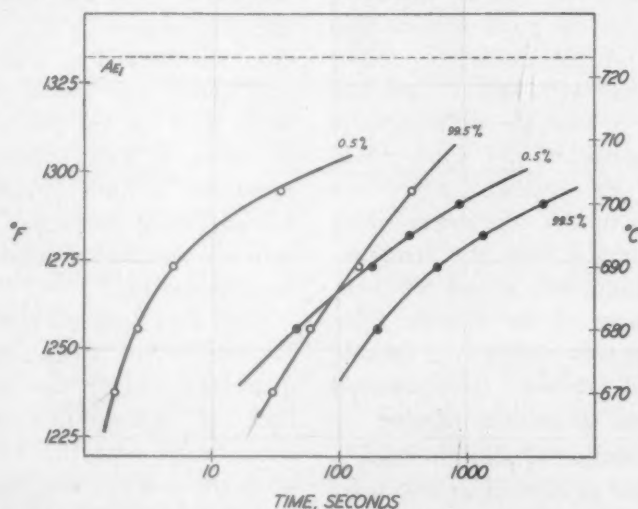
FIG. 1.—EFFECT OF UNDISSOLVED CARBIDE ON POSITION OF THE S-CURVE.
Eutectoid steel. Pair of curves to left represents inhomogeneous austenite (steel C). Pair of curves to right represents austenite free from carbide (steel D). Fracture grain size 6 to 6½.

samples that were water-quenched after the austenitizing treatment. After austenitizing, the steels were immediately transferred to another lead bath held at a subcritical temperature, and the upper portion of the S-curve was determined by the usual

with undissolved carbide was found on measurement† to be 4.3 × 10⁻⁴ mm. per

* A few of the results presented here were included in a general way in a previous publication.[3]
† For a discussion of the methods employed to measure the rate of nucleation and the rate of growth see reference 2.

sec., and for the steel with homogeneous austenite 5×10^{-4} mm. per sec., which are virtually identical, so that differences in reaction rate originate in differences in the rate of nucleation alone. It is interesting to note that the slow-reacting steel has been deoxidized with aluminum and thus contains alumina inclusions; in this case, however, the effect of the residual carbide on the rate of nucleation (or on the over-all rate of formation of pearlite) is greater than any effect of the deoxidation products. This has been discussed by Hull, Colton and Mehl.[2]

It is also clear that the difference between these two S-curves is smaller, the lower the temperature of reaction. Davenport, Grange and Hafsten[13] reported a somewhat similar phenomenon with respect to the effect of change of grain size on the reaction rate, when comparing samples reacted near Ae_1 with those reacted near the knee of the S-curve. It will be seen later that the true effect of grain size at high reaction temperatures does not follow this pattern. Mehl[3] and Hull, Colton and Mehl[2] have shown that the differences in the rate of nucleation per unit grain-boundary area of pearlite caused by increased holding times at the austenitizing temperature are much greater at temperatures near Ae_1 than they are at temperatures near the knee of the S-curve. This behavior suggests that undissolved carbide and undissolved carbon concentration gradients provide a certain number of nuclei for the formation of pearlite which is nearly as effective at high as at low temperatures, and that this number is very large compared with the small number of normal nuclei formed in unit time near Ae_1, but is relatively small compared with the very large number of normal nuclei formed in unit time near the knee.

In passing, it may be noted that the ratios of the amount of spheroidite to pearlite obtained confirm the findings of previous investigators regarding the direct production of spheroidite from austenite.[9,10]

Testing for Homogeneity

Most of the information now available on the rates of solution of carbide particles in austenite has been obtained by microscopic methods. These include studies by Lauderdale and Harder,[14] Walldow,[15] Tran and Osborn,[16] and Bain.[4] Recently the use of electrical resistance methods has received attention from Mirkin and collaborators.[17,19] In general, it is agreed that surprisingly long times are required to eliminate inhomogeneities in the austenite even at temperatures considerably above the Ae_1.

Hull, Colton and Mehl[2] have shown that the rate of nucleation of pearlite per unit austenite grain boundary varies with the degree of carbide solution attained. The rate of nucleation in all cases was calculated from the time of half-reaction, the rate of growth and the fracture grain size. No method of analyzing these data was found that would permit a selection of a limit to the homogenizing process in terms of austenitizing times or temperatures, a limit beyond which further homogenizing would give no change in the rate of formation of pearlite resulting from homogenization.

Such a method has now been developed. It requires the measurement of but two quantities, the fracture grain size and the time of half-reaction at a subcritical temperature near the Ae_1, in dependence upon the austenitizing time. A calculation is first made of the theoretical change in the time of half-reaction with a change in the austenite grain size when the austenite is homogeneous; deviations from the calculated relationship show the presence of inhomogeneity. The conditions to be met in deriving and applying this relationship are the following:

1. The subcritical reaction from which the time of half-reaction is determined

must take place at a temperature near the Ae_1 where "group nodule transformation" occurs.

2. The general nucleation equations of Johnson and Mehl[20] apply.

volume. Knowing the amount of this decrease in the rate of nucleation, the increase in the time of half-reaction can be calculated. By assuming different base values of t_{50}, austenites of different char-

FIG. 2.

FIG. 3.

FIGS. 2 AND 3.—CALCULATED RELATIONSHIP BETWEEN AUSTENITE GRAIN SIZE AND TIME OF HALF-REACTION FROM HOMOGENEOUS AUSTENITE TO PEARLITE AT TEMPERATURES NEAR Ae_1.
Fig. 2, linear time scale.
Fig. 3, logarithmic time scale.

3. The pearlite nuclei form entirely at the austenite grain boundaries if the austenite is homogeneous, and a specified change in the grain-boundary area of the austenite will cause the same fractional change in the rate of nucleation.

The details of the calculation are given in Appendix I.* These yield a series of curves of fracture grain size versus the time of half-reaction, t_{50}, for a series of homogeneous austenites of different characteristic reaction rates, as obtained by variation in alloy content. A base value for the time of half-reaction is assumed—i.e., 10 sec.—at a base value of the fracture grain size—i.e., FGS 10. An increase in the grain size will cause a decrease in the grain-boundary area, and in turn a proportionate decrease in the rate of nucleation per unit

acteristic reaction rates can be considered. Figs. 2 and 3 show the derived relationships on a linear and a logarithmic time scale, respectively. The latter yields a *linear relationship* which has a *constant slope independent of the true reaction rate of the austenite* (i.e., independent of the base value of t_{50} selected). The proof of this constancy of slope and linearity is given in Appendix II.*

Experimental Determinations

In order to determine experimentally the change of the time of half-reaction with a change of the austenite grain size, samples of various steels, after austenitizing for different times at one temperature, were reacted at a subcritical temperature. To obtain the necessary data in the most rapid manner, the extent of the reaction was measured dilatometrically; on one occasion the data obtained in this way were checked against metallographic samples and the respective times of half-reaction were found to coincide within 2 per cent. The fracture

* Appendix I and Appendix II have been deposited with the American Documentation Institute. To obtain them, write to the American Documentation Institute, Bibliofilm Service, 1719 N St., NW., Washington, D. C., asking for Document No. 1656 and enclosing 30¢ for microfilm (images 1 in. high on standard 35-mm. motion-picture film) or 80¢ for photostat (6 by 8 in.).

sec., and for the steel with homogeneous austenite 5×10^{-4} mm. per sec., which are virtually identical, so that differences in reaction rate originate in differences in the rate of nucleation alone. It is interesting to note that the slow-reacting steel has been deoxidized with aluminum and thus contains alumina inclusions; in this case, however, the effect of the residual carbide on the rate of nucleation (or on the over-all rate of formation of pearlite) is greater than any effect of the deoxidation products. This has been discussed by Hull, Colton and Mehl.[2]

It is also clear that the difference between these two S-curves is smaller, the lower the temperature of reaction. Davenport, Grange and Hafsten[13] reported a somewhat similar phenomenon with respect to the effect of change of grain size on the reaction rate, when comparing samples reacted near Ae_1 with those reacted near the knee of the S-curve. It will be seen later that the true effect of grain size at high reaction temperatures does not follow this pattern. Mehl[3] and Hull, Colton and Mehl[2] have shown that the differences in the rate of nucleation per unit grain-boundary area of pearlite caused by increased holding times at the austenitizing temperature are much greater at temperatures near Ae_1 than they are at temperatures near the knee of the S-curve. This behavior suggests that undissolved carbide and undissolved carbon concentration gradients provide a certain number of nuclei for the formation of pearlite which is nearly as effective at high as at low temperatures, and that this number is very large compared with the small number of normal nuclei formed in unit time near Ae_1, but is relatively small compared with the very large number of normal nuclei formed in unit time near the knee.

In passing, it may be noted that the ratios of the amount of spheroidite to pearlite obtained confirm the findings of previous investigators regarding the direct production of spheroidite from austenite.[9,10]

Testing for Homogeneity

Most of the information now available on the rates of solution of carbide particles in austenite has been obtained by microscopic methods. These include studies by Lauderdale and Harder,[14] Walldow,[15] Tran and Osborn,[16] and Bain.[4] Recently the use of electrical resistance methods has received attention from Mirkin and collaborators.[17,19] In general, it is agreed that surprisingly long times are required to eliminate inhomogeneities in the austenite even at temperatures considerably above the Ae_1.

Hull, Colton and Mehl[2] have shown that the rate of nucleation of pearlite per unit austenite grain boundary varies with the degree of carbide solution attained. The rate of nucleation in all cases was calculated from the time of half-reaction, the rate of growth and the fracture grain size. No method of analyzing these data was found that would permit a selection of a limit to the homogenizing process in terms of austenitizing times or temperatures, a limit beyond which further homogenizing would give no change in the rate of formation of pearlite resulting from homogenization.

Such a method has now been developed. It requires the measurement of but two quantities, the fracture grain size and the time of half-reaction at a subcritical temperature near the Ae_1, in dependence upon the austenitizing time. A calculation is first made of the theoretical change in the time of half-reaction with a change in the austenite grain size when the austenite is homogeneous; deviations from the calculated relationship show the presence of inhomogeneity. The conditions to be met in deriving and applying this relationship are the following:

1. The subcritical reaction from which the time of half-reaction is determined

must take place at a temperature near the Ae₁ where "group nodule transformation" occurs.

2. The general nucleation equations of Johnson and Mehl[20] apply.

FIG. 2.

FIG. 3.

FIGS. 2 AND 3.—CALCULATED RELATIONSHIP BETWEEN AUSTENITE GRAIN SIZE AND TIME OF HALF-REACTION FROM HOMOGENEOUS AUSTENITE TO PEARLITE AT TEMPERATURES NEAR Ae₁.
Fig. 2, linear time scale.
Fig. 3, logarithmic time scale.

3. The pearlite nuclei form entirely at the austenite grain boundaries if the austenite is homogeneous, and a specified change in the grain-boundary area of the austenite will cause the same fractional change in the rate of nucleation.

The details of the calculation are given in Appendix I.* These yield a series of curves of fracture grain size versus the time of half-reaction, t_{50}, for a series of homogeneous austenites of different characteristic reaction rates, as obtained by variation in alloy content. A base value for the time of half-reaction is assumed—i.e., 10 sec.—at a base value of the fracture grain size—i.e., FGS 10. An increase in the grain size will cause a decrease in the grain-boundary area, and in turn a proportionate decrease in the rate of nucleation per unit

volume. Knowing the amount of this decrease in the rate of nucleation, the increase in the time of half-reaction can be calculated. By assuming different base values of t_{50}, austenites of different characteristic reaction rates can be considered. Figs. 2 and 3 show the derived relationships on a linear and a logarithmic time scale, respectively. The latter yields a *linear relationship* which has a *constant slope independent of the true reaction rate of the austenite* (i.e., independent of the base value of t_{50} selected). The proof of this constancy of slope and linearity is given in Appendix II.*

Experimental Determinations

In order to determine experimentally the change of the time of half-reaction with a change of the austenite grain size, samples of various steels, after austenitizing for different times at one temperature, were reacted at a subcritical temperature. To obtain the necessary data in the most rapid manner, the extent of the reaction was measured dilatometrically; on one occasion the data obtained in this way were checked against metallographic samples and the respective times of half-reaction were found to coincide within 2 per cent. The fracture

* Appendix I and Appendix II have been deposited with the American Documentation Institute. To obtain them, write to the American Documentation Institute, Bibliofilm Service, 1719 N St., NW., Washington, D. C., asking for Document No. 1656 and enclosing 30¢ for microfilm (images 1 in. high on standard 35-mm. motion-picture film) or 80¢ for photostat (6 by 8 in.).

grain size was determined on separate specimens given identical austenitizing treatments.

Dilatometer specimens, $3/32$ by $1/4$ by

- It should be pointed out that the actual value of the subcritical reaction temperature is immaterial as long as it is maintained constant for each run at one austenitizing
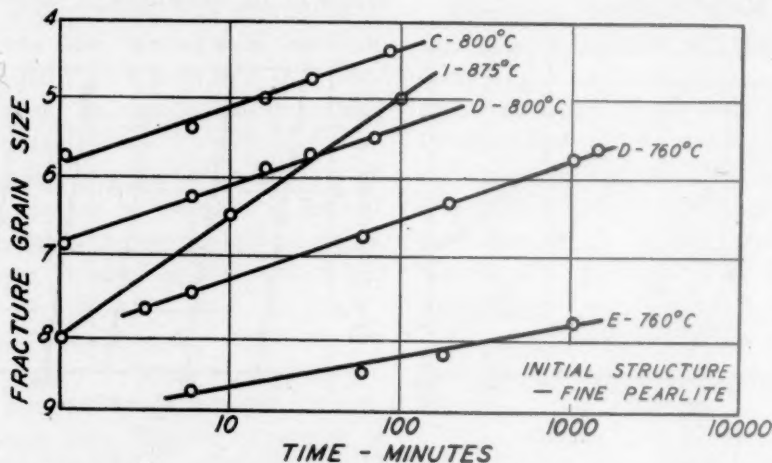
FIG. 4.—RELATIONSHIP BETWEEN FRACTURE GRAIN SIZE AND AUSTENITIZING TIME FOR STEELS C, D, E AND I AT THREE TEMPERATURES.

3 in., were cut from bars previously homogenized 24 hr. at 1100°C. (2010°F.). These were austenitized in a lead bath held at constant temperature above the critical temperature for periods of time ranging from 1 min. to 300 min. At least six different austenitizing times were studied for each steel at each austenitizing temperature. The lead bath was at all times covered with carburizing compound to prevent decarburization. After austenitizing, the specimens were quickly transferred to a quenching dilatometer mounted over another lead bath. The quenching bath was maintained at a temperature of either 686° or 690°C. (1255 or 1275°F.) for the majority of the runs. The control of this temperature in the well-stirred lead bath used is to within plus or minus one degree centigrade. The dilatometer and specimen were plunged into this bath, and the dial readings were taken every 2.5 sec. Duplicate runs, conducted for each austenitizing cycle, revealed a difference of less than 3 sec. in the time of half-reaction in a majority of the cases, and at no time was the discrepancy greater than 5 seconds.

temperature, and as long as it lies above 650°C. (1200°F.), so that "grain-boundary transformation"[20] will not occur. In selecting this temperature for these experiments, a mean was chosen so that the reaction would not occur too fast to allow an accurate determination of the reaction curve (at low temperatures), and so that it would not take an excessive amount of time (at high temperatures). For most of the steels tested this was chosen to be 680°C. (1255°F.), although runs on the high-carbon steels (hypereutectoid) were conducted at temperatures near 700°C. (1290°F.) in order to slow the progress of the reaction.

The ratings of fracture grain size were made by comparison with the fracture standards. It was found that the fracture grain size varied linearly with the logarithm of the austenitizing time at any one austenitizing temperature, as shown earlier for eutectoid steels by Tobin and Kenyon.[21] Employing this relationship, but four determinations of the fracture grain size at different austenitizing times were made for each austenitizing temperature, and the

actual value in question was determined by interpolation from the charts, such as Fig. 4, which represents the relationships ship between the fracture grain size and the time of half-reaction (F-t curve) is shown in Fig. 7 for A and B austenitized at 875°C.
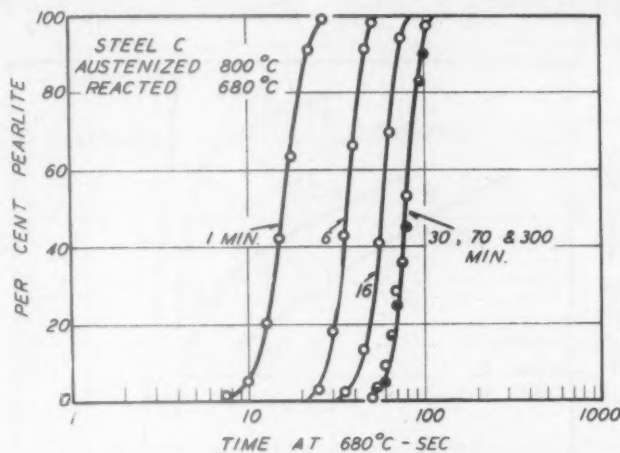
FIG. 5.—ISOTHERMAL REACTION CURVES AT 680°C. FOR STEEL C AUSTENITIZED AT 800°C. FOR 1,6, 16, 30, 70 AND 300 MINUTES.

between fracture grain size and time for several steels at several temperatures.

Steels A B, C, and D were studied. Fig. 5 shows typical reaction curves at 680°C. (1610°F.) and for B austenitized at 800°C. (1470°F.). The numbers near the experimental points correspond to the austenitizing time in minutes. Fig. 8 shows the F-t
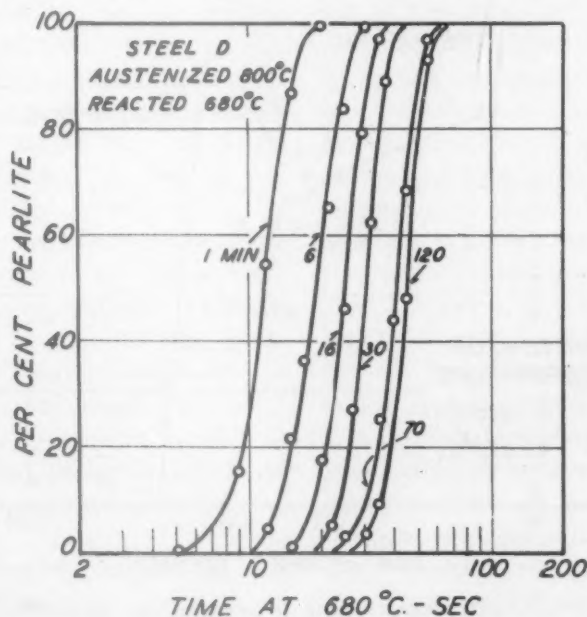
FIG. 6.—ISOTHERMAL REACTION CURVES AT 680°C. FOR STEEL D AUSTENITIZED AT 800°C. FOR 1, 6, 16, 30, 70 AND 120 MINUTES.

(1255°F.) for austenitizing C for different times at 800°C. (1470°F.) and Fig. 6 shows the same relationship for D. The relation- curves for C austenitized at 875° and 800°C. and Fig. 9 represents the behavior of D austenitized at 800° and 875°C. The

straight lines in each figure represent the slope of the theoretical curve calculated in accordance with the previous assumption. The experimental curves approach the

genization point, and it will correspond to a definite austenitizing time at each temperature; the times for homogenization of different steels may be compared on this
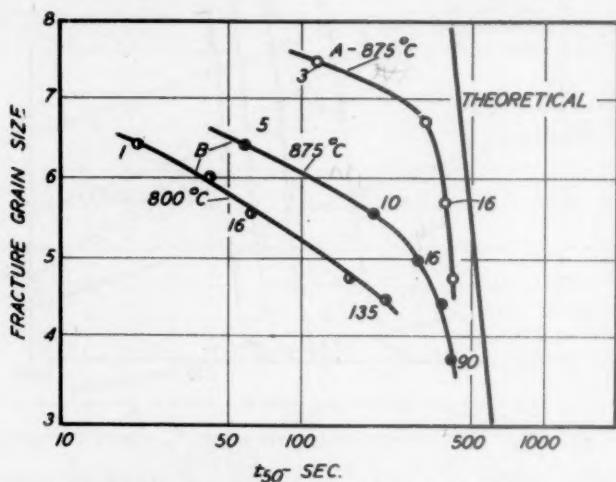
FIG. 7.—*F-t* CURVES FOR STEELS A AND B.
Steel A austenitized at 875°C. and steel B austenitized at 800° and 875°C., compared with theoretical curve. Coincidence of slopes indicates "practical homogeneity." Numbers opposite experimental points refer to austenitizing times in minutes.
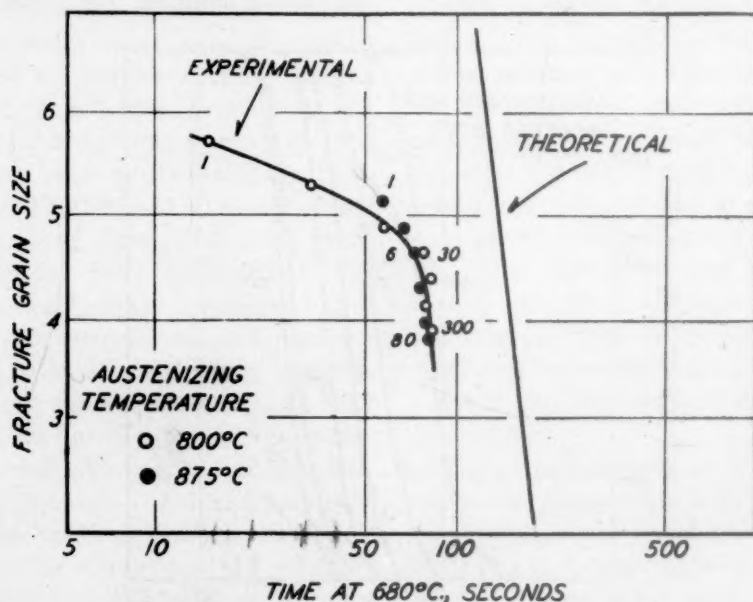
AUSTENIZING TIMES, IN MINUTES, AS INDICATED
FIG. 8.—*F-t* CURVES FOR STEEL C. AUSTENITIZED AT 800°C. AND AT 875°C.

slope of this theoretical line as the time of austenitizing increases.

The point at which the coincidence in slope is made can be termed the homo-

basis. For example, Fig. 8 shows that 30 min. at 800°C. is sufficient to reach this point in C, while at 875°C. only 6 min. is required. Similar points can be selected

from each of the other *F-t* curves. The meaning of these data is clear: At short times of austenitizing, carbide is undissolved, and both the lowered concentration

curve should not be interpreted as the point at which the austenite is perfectly homogeneous. (Solid solutions always approach perfect homogeneity asymptotically, and
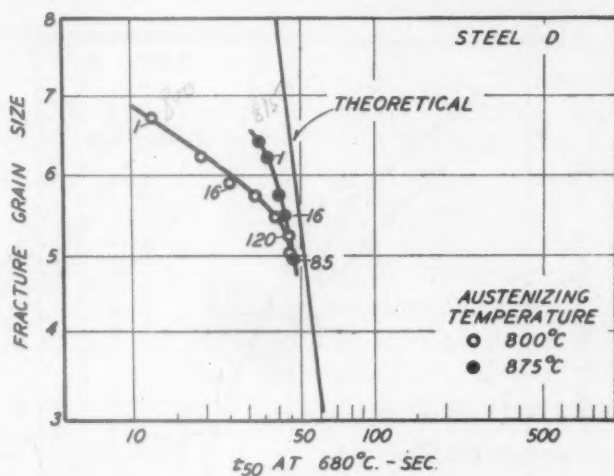
FIG. 9.—*F-t* CURVES FOR STEEL D. AUSTENITIZED AT 800°C. AND AT 875°C.

of carbon in the austenite and the nucleating effect of the carbide particles decrease the time of half-reaction well below that for homogeneous austenite. As the carbide particles dissolve there is a rapid increase in the half-reaction time, and this increase will continue even after visible carbide has been eliminated, owing to the effect of carbon concentration gradients.[3,2] For B, no carbide was visible at 16 min. at 875°C. (1610°F.), yet there is a change in the time of half-reaction between the 16-min. and 30-min. austenitizing periods, which is larger than would be expected from grain-size change alone (Fig. 7). Similarly, the carbide in C austenitized at 800°C. (1470°F.) appears to dissolve in advance of the 30-min. time period at which the experimental curve approaches the calculated curve.

Thus both undissolved carbide and carbon concentration gradients cause deviations from the calculated behavior at these high reaction temperatures, although the former is greatly more effective than the latter. The point at which the experimental curve begins to parallel the calculated

thus this ideal state can never be achieved in finite time periods.) There may be scattered carbon concentration gradients left at this time, and there may even be some carbide undissolved, but these will be ineffective in changing the rate of reaction to pearlite even at a reaction temperature where sensitivity is greatest. It will be shown later that the extent of homogenization achieved when this point is reached is greater than that required to assure the maximum hardenability for a given grain size. The extent of homogenization at this point, however, is certainly not excessive for the heat-treatment of large sections, which upon quenching react to pearlite at relatively high temperatures, or for the normalizing of sections of a large size. In these cases, at all austenitizing times or temperatures lower than that indicated on the *F-t* curves to give parallelism, the inhomogeneity will cause an increase in the reaction rate at high temperatures, and accordingly the steel will react at a higher temperature, producing a coarser pearlite of lower strength and ductility. Holding at temperature beyond this point will result

in a retardation of the pearlite reaction only through an increase in grain size.

It is interesting to note that the aluminum-deoxidized steel D requires longer

on the one hand and spheroidite on the other. The spheroidized steel, representing a coarser dispersion of carbide, reacts more slowly than the pearlitic steels when
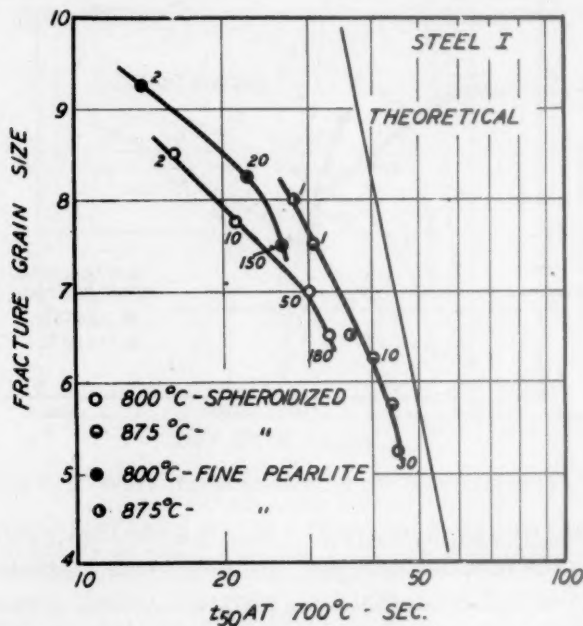
FIG. 10.—*F-t* CURVES FOR STEEL I. AUSTENITIZED AT 800°C. AND AT 875°C.
Comparison of effect of initial structure on hypereutectoid steel.

times for homogenization than C (compare Figs. 8 and 9). This is in conformity with the earlier observation[1] that the rate of austenitizing of D (as shown by the isothermal austenitizing reaction curves) is slower than that of C. It may be possible that a comparison of the homogenization rates of different plain carbon steels can be made by measuring isothermal austenitizing reaction curves. In comparing plain carbon steels with alloy steels, however, and in comparing different alloy steels, where large differences in the critical temperatures may exist, and where slowly dissolving carbides may complicate, it may be necessary to resort to the use of the *F-t* homogenization test as described.

Fig. 10 shows the *F-t* curves for a 1.04 per cent carbon steel austenitized at 800°C. and 875°C. (1470°F. and 1610°F.) from initial structures consisting of fine pearlite

austenitized at the same temperature for the same time.

It follows from the reasoning given above that the more homogeneous the austenite, the more the nucleation, and therefore the initial transformation near the knee of the S-curve is restricted to grain boundaries; or, conversely, the occurrence of initial transformation within the austenite grain can be taken as a sign of and a qualitative measure of austenite heterogeneity. Such a condition should be visible in gradient-quenched samples. This has been studied in steels C and D, austenitized 1, 6, 16, 30, 70, 125, and 180 min. at 800°C. and gradient-quenched in water. The results show that this is a much less sensitive measure of the degree of homogeneity than the *F-t* test. The grain boundary outline is slightly more complete in the samples austenitized for 180 min. than in those

austenitized one minute but the difference is not sufficient to permit determination of equivalent homogenization times.

Williams[22] has presented a test for
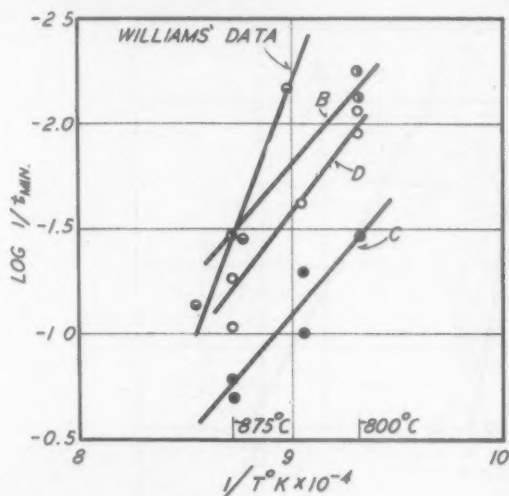
FIG. 11.—EFFECT OF TEMPERATURE ON HOMOGENIZATION TIME FOR STEELS C, B AND D.
Results of Williams on S.A.E. alloy steel included.

homogenization based upon the hardness gradient along the slowly cooled end of an end-quenched bar. By holding samples different lengths of time at the austenitizing temperature before quenching, he has been able to show that this hardness gradient diminishes as the austenitizing time is increased. Obviously this is based upon a phenomenon similar to that of the F-t method, for along this section of the end-quenched bar the cooling rates do not vary considerably; thorough homogenization, therefore, would cause the reaction to pearlite to occur at approximately the same temperature along the length of the bar and thus approximately the same hardness would result at each point.

The temperature dependence of any process that is dependent primarily upon diffusion can be represented by an "activation energy";[25] consequently, in an effort to calculate the "activation energy" for the homogenization process, the approximate

time required to give parallelism between the experimental and the calculated curves in the F-t test was selected for each austenitizing temperature (Table 2), and the logarithm of the reciprocal of this homogenization time was plotted against the reciprocal of the absolute temperature* in Fig. 11, yielding approximate straight lines. The slope Q'/R of the line for steel B is 26,000 to 30,300; that for steel D is 30,200; and that for steel C is 26,500. This would indicate that the Q' value, which represents the activation energy required for homogenization, is between 50,000 and 60,000 calories. As can be seen from Fig. 11, Williams' data give an even higher value of the activation energy.

TABLE 2.—*Homogenization Data Used to Construct Figure 11*

Steel	Temperature	Homogenization Time, Min.
B	875°C. (1610°F.)	30
	800°C. (1470°F.)	135–180
C................	875°C.	5–6
	835°C. (1535°F.)	10–20
	800°C.	30
D................	875°C.	10–20
	835°C.	30
	800°C.	90–120
Williams[a]........	899°C. (1650°F.)	15
	871°C. (1600°F.)	30
	843°C. (1550°F.)	150
	816°C. (1500°F.)	600

[a] These data for some partial degree of homogenization as indicated by coincidence of hardness-penetration curves on end-quenched specimens.[22]

It is not surprising that these values appear much higher than the activation energy for simple diffusion of carbon in austenite (32,000 cal.).[23] The rate of reaction of aggregates of ferrite and carbide to homogeneous austenite will be determined not only by the rate of diffusion of carbon in austenite but also by the rates of reaction at the ferrite-austenite interface and the carbide-austenite interface, and also by the active concentration gradients of carbon in austenite. It can be shown that

---

* The equation representing these data is:
$$\frac{\log 1/t}{0.4343} = \ln A - Q'/RT$$

if the reciprocal of the product of the homogenization time and the carbon concentration gradient (dc/dx) is plotted against the reciprocal of the absolute temperature,*

REACTIONS NEAR THE KNEE OF THE S-CURVE

Undissolved carbide affects the rate of reaction at the knee but it is doubtful
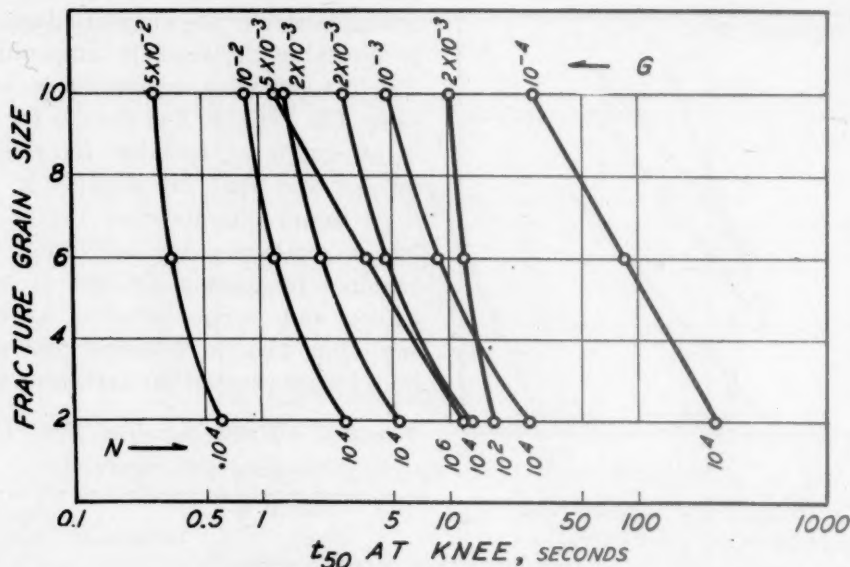
FIG. 12.—CALCULATED RELATIONSHIP BETWEEN AUSTENITE GRAIN SIZE AND TIME OF HALF-REACTION FROM AUSTENITE TO PEARLITE AT KNEE OF S-CURVE.
Calculations based on several values of N and G as indicated.

the resulting activation energy, Q'', is 41,400 cal. for steel C.

Further modification is impossible, for the rates of interface reactions are important data now entirely lacking. In any event the activation energies and the values of A in the equation in the footnote on p. 327, both derived directly from Fig. 11, fully describe the homogenization behavior of any steel, and may be used in a practical sense for this purpose.

---

* This modification results in the following equation:

$$\ln \frac{1}{t \times dc/dx} = \ln A - \frac{Q''}{RT}$$

since it can be shown that when dc/dx varies, D is proportional to $\dfrac{1}{t \times dc/dx}$. The values of dc/dx were selected from the iron-carbon diagram of Mehl and Wells[34] and represent the difference between the carbon contents shown by the GOS and the SE lines at any particular temperature. It is probable that the active concentration gradients are somewhat less than these values.

whether the presence of carbon concentration gradients affects the rate to an appreciable degree. The effect of variations in austenitizing treatments on the rate of reaction at the knee seems primarily to result from changes in the austenite grain size. Grossmann and Stephenson[24] have calculated the change in the time at constant temperature for 50 per cent reaction to pearlite based on Johnson and Mehl's equations for grain-boundary nucleation. They selected a rate of nucleation, N, of 1.0×10^6 and a rate of growth, G, of 1.0×10^{-3}. To show steels of lower and higher hardenability, G was assigned twice this value and half this value, respectively, while N was assumed to be the same.

If such a relationship exists for all combinations of N and G, a test might be devised similar to that described above for the reaction near Ae_1, which would permit a determination of the part played by inhomogeneities in increasing the reaction

rate at the knee. Fig. 12 shows a calculation of t_{50} for reaction at the knee using variations in both N and G. The slopes of the curves are dependent upon the values of

isothermal reaction to pearlite at subcritical temperatures near the knee of the S-curve, for it is necessary completely to suppress the pearlite reaction in order to produce
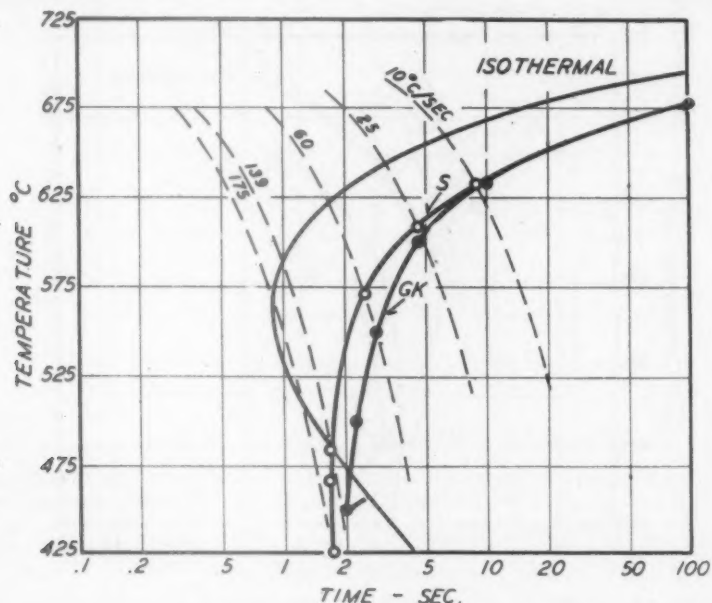
FIG. 13.—COMPARISON OF COOLING RATE S-CURVES OBTAINED BY GRANGE AND KIEFER (GK) AND STEINBERG (S) METHODS FOR HOMOGENEOUS AUSTENITE.
Hypothetical isothermal S-curve for homogeneous austenite shown as indicated.

N and G assumed. Thus even if experimental data were available or easily measured for the time of half-reaction at the knee, unless a knowledge of the actual rates of nucleation and growth were obtained the theoretical slope could not be calculated, and thus the test for homogeneity illustrated in Figs. 7 to 10 could not be applied. With respect to practical cases, the data of Grossmann and Stephenson may be representative of the actual N and G values and the variations of t_{50} with grain size would then be satisfactorily represented by their curves. Grossmann[5] has made practical use of grain size-hardenability curves which agree well with these assumptions.

Relation of Inhomogeneities to Hardenability

Without doubt the hardenability is related to and determined by the rates of

structures of 100 per cent martensite. Recently several attempts have been made to calculate the hardenability of steel from the knowledge of such reaction rates; i.e., from the S-curve. These studies have resulted in the concept of the cooling rate S-curve, a curve of more practical usefulness than the isothermal S-curve, since it bears a direct relation to hardenability.

Scheil,[25] Krainer,[26,27] and Steinberg[28] assume that any cooling time below the critical temperature is effective in producing pearlite nuclei; i.e., that pearlite nuclei form continuously during cooling from the Ae_1 to the temperature of reaction, and thus initiate the austenite-pearlite reaction. Steinberg offers a graphical solution to the problem. In 1940, Grange and Kiefer[29] proposed a somewhat different method, which has less theoretical basis than the others but which is reputed to give satis-

factory results agreeing with the experimental values. In this case the calculations are started at the point at which the cooling curve intersects the zero per cent line of the isothermal S-curve.

Steinberg solution would recognize the importance of the shift at higher temperatures. To illustrate this an extreme case has been taken in which the time of reaction at the knee is not changed from that
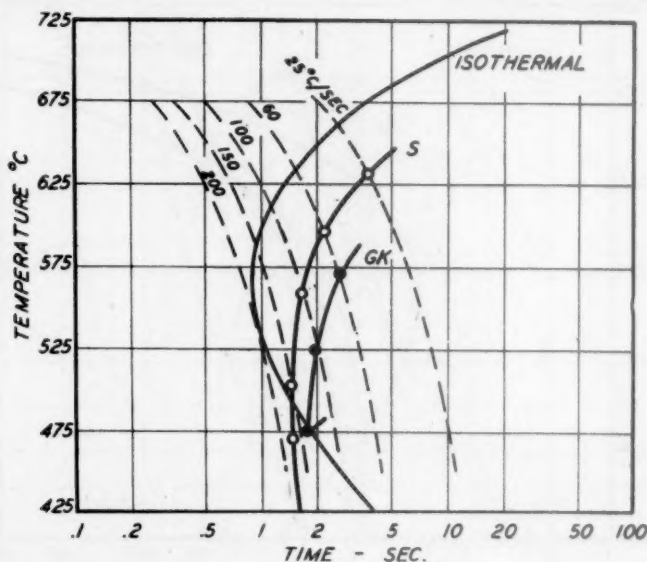
FIG. 14.—SAME AS FIG. 13 BUT FOR INHOMOGENEOUS AUSTENITE.
Reaction rate on isothermal curve has not been altered at the knee, but has been arbitrarily increased at higher temperatures from that shown in Fig. 13.

Fig. 13 represents a comparison of the results obtained with both methods. The base S-curve is the curve at the left showing the knee. The graphical method of Steinberg has been used in determining the cooling S-curve marked S and the Grange and Kiefer method used to determine the curve marked GK. The latter predicts a critical cooling velocity of 139°C. per sec. while the Steinberg analysis gives approximately 175°C. per sec. There is less discrepancy between the two curves at higher temperatures, where the results fall within the ordinary range of experimental error.

It will be remembered that undissolved carbide shifts the isothermal S-curve to the left more at temperatures just below Ae_1 than at the knee (Fig. 1). The Grange and Kiefer method would predict that this effect would shift the critical cooling velocity only inasmuch as it shifts the rate of the reaction near the knee, while the

shown in Fig. 13 but the time of reaction above the knee has been shifted by the amounts usually found when undissolved carbide is present. Fig. 13 thus applies to homogeneous austenite and Fig. 14 applies to inhomogeneous austenite. In the latter case it is seen that the Steinberg method indicates that the critical cooling velocity is approximately 200°C. per sec., while the results obtained using the Grange and Kiefer analysis remain approximately the same (140°C. per sec.). Although this is an extreme case, it demonstrates that employment of only the times of reaction at the knee may lead to appreciable errors in calculating hardenability, and that if the Scheil-Krainer-Steinberg assumptions prove to be correct, the whole character of the isothermal S-curve must be considered.

It was shown earlier that no simple relationship between the fracture grain size and t_{50} at the knee can be established on the

basis of which the progress of the homogenization of austenite may be studied. Accordingly, it seems impossible to derive a simple relationship between the fracture

initial structure in all cases was a fine spheroidite. These were then heated in a semimuffle furnace and held at 927°C. (1700°F.) prior to quenching for 3, 10, 30,
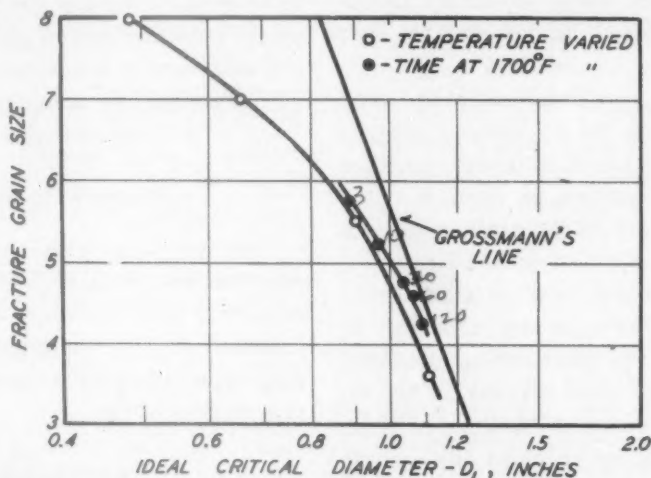
FIG. 15.—EFFECT OF FRACTURE GRAIN SIZE ON IDEAL CRITICAL DIAMETER, STEEL K.
Solid circles represent samples held at 927°C. (17c0°F.) for 3, 10, 30, 60 and 120 min. before brine quenching.
Open circles represent samples held 6 min. at 788°C. (1450°F.), 857°C. (1575°F.), 927°C. (1700°F.), and 1010°C. (1850°F.). Compared with empirical curve of Grossmann.

grain size and hardenability. Any such relationship, in addition to following the pattern of the change of t_{50} at the knee with grain size, would be further complicated by the effect of grain size on the reactions at higher subcritical temperatures. Empirical relations between the austenite grain size and the hardenability have been discovered,[5,30,31] however, which will prove satisfactory for purposes of predicting the change of hardenability with a known change in grain size. The Grossmann chart shows a linear relation between the austenite grain size and the logarithm of the ideal critical diameter. The data from which this has been obtained show slight variations, the diagram thus representing an average effect.

In order to compare the hardenability of steels containing carbon concentration gradients with these charts, the following tests were conducted: Hardenability specimens, 1 in. round by 3 in. long, were cut from a forged 1¼-in. bar of steel K. The

60 and 120 min., respectively. Quenching was performed in a submerged brine-spray fixture. Duplicate specimens were run for each treatment. The penetration-fracture results were obtained and expressed in terms of the ideal critical diameter, assuming an H-value (severity of quench) of 4.

Fig. 15 shows the fracture grain sizes plotted against the logarithm of the ideal critical diameter. The straight line on the figure is a corresponding line taken from Grossmann. It will be seen that the experimental curve, if drawn as a straight line, has less slope than Grossmann's curve, and if drawn exactly through the points would tend to approach the slope of the latter at the larger grain sizes. The accuracy of the data does not warrant a choice between these two possibilities. Carbide was visible in these samples after 3 min. at 927°C. (1700°F.) but was almost completely dissolved after 10 min. at this temperature (the second point from the top).

These results may be interpreted as showing that the effect of carbon concentration gradients upon hardenability is slight, and in view of the possibility that slopes other than those shown by Grossmann may obtain, it is questionable that any effect exists.

Experiments conducted at the same austenitizing time but at different temperatures show the effect of inhomogeneities more clearly. Samples of steel K were heated 6 min. at 788°, 857°, 927° and 1010°C. (1450°, 1575°, 1700° and 1800°F.) and brine-quenched. The fracture grain sizes are shown as open circles in Fig. 15 plotted against the ideal critical diameter calculated in the same manner as before. This curve shows a slight break near a grain size of 5 to 6, at which point the carbide begins to disappear. At larger grain sizes the curve is nearly parallel to Grossmann's curve, though carbon concentration gradients remain. Accordingly, undissolved carbide reduces the hardenability, but carbon concentration gradients have extremely little effect.

Summary

1. Undissolved carbide when present in considerable quantity increases the rate of the austenite-pearlite reaction. The effect is greater, the higher the temperature of reaction, and is much greater than the effect of alumina inclusions in the particular steels studied. Carbon concentration gradients increase the rate of the austenite-pearlite reaction at high temperatures.

2. Undissolved carbide when present in considerable quantity materially reduces the hardenability of steels. Carbon concentration gradients have little effect upon hardenability.

3. By calculating the true effect of austenite grain size upon the rate of reaction at high subcritical temperatures and thus excluding it from consideration, a sensitive test for austenite homogeneity is devised. This will provide schedules of homogenization for equivalent states of homogeneity in steels of different homogenizing characteristics.

4. If steels are austenitized for lengths of time dictated by the F-t test, no effect of minor inhomogeneities should be found in the reactions at temperatures near Ae_1, in the reactions at temperatures near the knee, or in the hardenability.

References

1. G. A. Roberts and R. F. Mehl: The Mechanism and the Rate of Formation of Austenite from Ferrite-Cementite Aggregates. Amer. Soc. Metals Preprint No. 22 (October 1942).
2. F. C. Hull, R. A. Colton and R. F. Mehl: The Rate of Nucleation and the Rate of Growth of Pearlite. Trans. A.I.M.E. (1942) 150, 185.
3. R. F. Mehl: The Structure and Rate of Formation of Pearlite. 16th Campbell Memorial Lecture. Trans. Amer. Soc. Metals (1941) 29, 813.
4. E. C. Bain: The Alloying Elements in Steel. Amer. Soc. Metals (1939). Cleveland, Ohio.
5. M. A. Grossmann: Hardenability Calculated from Chemical Composition. Trans. A.I.M.E. (1942) 150, 227.
6. H. M. Howe and A. G. Levy: Notes on Pearlite. Jnl. Iron and Steel Inst. (1916) 94, 210.
7. K. Honda and S. Saito: On the Formation of Spheroidal Cementite. Jnl. Iron and Steel Inst. (1920) 102, 261.
8. J. H. Whiteley: The Formation of Globular Pearlite. Jnl. Iron and Steel Inst. (1922) 105, 339.
9. F. Korber and W. Koster: On Spheroidized Cementite. Mitt. K. W. I. Eisenforshung (1925) 5.
10. P. Payson, W. L. Hodapp and J. Leeder: The Spheroidizing of Steel by Isothermal Transformation. Trans. Amer. Soc. Metals (1939) 27.
11. R. J. Hafsten: Spheroidize Annealing of S.A.E. 52100 Steel. Metal Progress (1942) 42, 869.
12. G. V. Cash, T. W. Merrill and R. L. Stephenson: Effect of Deoxidation on Hardenability. Trans. Amer. Soc. Metals (1941) 29, 755.
13. E. S. Davenport, R. A. Grange and R. J. Hafsten: Influence of Austenite Grain

Size on Isothermal Transformation. *Trans.* A.I.M.E. (1941) **145**, 301.

14. R. H. Lauderdale and O. E. Harder: Study of Carbide Solution in Hypoeutectoid Plain Carbon and Low Alloy Steels. *Trans.* Amer. Soc. Metals (1939) **27**, 581.

15. E. Walldow: The Mechanism of Solution of Cementite in Carbon Steel and the Influence of Heterogeneity. *Jnl.* Iron and Steel Inst. (1930) **122**, 301.

16. M. A. Tran and H. B. Osborn, Jr.: Inherent Characteristics of Induction Hardening. Amer. Soc. Metals (1940).

17. I. L. Mirkin: Influence of the Conditions of Heating on the Course of Secondary Crystallization in Steel. Trudy Moskov Inst., Stahl im I. V. Stalina (1938, No. 18) 65.

18. I. L. Mirkin and N. D. Diterichs: *Ibid.*, 91.

19. I. L. Mirkin and I. Blanter: The Transformation of Pearlite into Austenite. *Ibid.*, 122.

20. W. A. Johnson and R. F. Mehl: Reaction Kinetics in Processes of Nucleation and Growth. *Trans.* Amer. Soc. Metals (1939) **135**, 416.

21. H. Tobin and R. L. Kenyon: Austenite Grain Size in Eutectoid Steel. *Trans.* Amer. Soc. Metals (1938) **26**, 133.

22. G. T. Williams: Hardenability Variations in Alloy Steels—Some Investigations with the End-quench Test. *Trans.* Amer. Soc. Metals (1940) **28**, 157.

23. C. Wells and R. F. Mehl: The Rate of Diffusion of Carbon in Austenite in Plain Carbon, in Nickel and in Manganese Steels. *Trans.* A.I.M.E. (1940) **140**, 279.

24. M. A. Grossmann and R. L. Stephenson: The Effect of Grain Size on Hardenability. *Trans.* Amer. Soc. Metals (1941) **29**, 1.

25. E. Scheil: Anlaufzeit der Austenitumwandlung. *Archiv Eisenhüttenwesen* (1935) **8**, 565.

26. H. Krainer: Die Bedingungen für die Durchvergutung von Stahl. *Ibid.* (1936) **9**, 619.

27. H. Krainer: The Relationship between the Velocity of Transformation of Austenite and the Deoxidation Practice. *Ztsch. Elektrochem.* (1937) **43**, 503.

28. S. Steinberg: Interrelation between Cooling Velocity, Transformation Velocity, Supercooling Degree of Austenite, and the Critical Velocity of Cooling. *Metallurgie* (1938) **13** (97), 7.

29. R. A. Grange and J. M. Kiefer: Transformation of Austenite on Continuous Cooling and its Relation to Transformation at Constant Temperature. *Trans.* Amer. Soc. Metals (1941) **29**, 85.

30. T. G. Digges and J. H. Jordan: Hardening Characteristics of One Per Cent Carbon Tool Steels. *Trans.* Amer. Soc. Metals (1935) **23**, 839.

31. C. B. Post, O. V. Greene and Fenstermacher: The Hardenability of Shallow Hardening Steels. Amer. Soc. Metals Preprint No. 17 (1941).

32. J. R. Villella and E. C. Bain: *Metal Progress* (1936) **30** (3), 39.

33. J. B. Rutherford, R. H. Aborn and E. C. Bain: The Relation between the Grain Areas on a Plane Section and the Grain Size of a Metal. *Metals and Alloys* (1937) **8**, 345.

34. R. F. Mehl and C. Wells: Constitution of High-purity Iron-carbon Alloys. *Trans.* A.I.M.E. (1937) **125**, 429.

35. R. F. Mehl: Diffusion in Solid Metals. *Trans.* A.I.M.E. (1936) **122**, 11.

DISCUSSION

(*E. S. Davenport presiding*)

G. A. MOORE,[*] Columbus, Ohio.—The information in this paper is very timely, since it aids greatly in explaining some unforeseen effects that are observed when certain steels are treated according to procedures in which they spend a very short time in the austenitic condition. At Battelle Memorial Institute we have observed marked differences in hardness, after rapid heat-treatment, of certain low-carbon steels of identical analysis but different carbide distribution. The spheroidized steels attain appreciably lower hardness values than do those of the fine pearlitic type.

The authors give major consideration to the effect of undissolved carbides on the critical cooling rate and to the hardenability in the sense of depth of hardening or critical diameter. I would like to ask whether they have also observed, in samples cooled at rates in excess of the critical rate, a decrease in the maximum hardness attained? Such a decrease could normally be ascribed to a deficiency of carbon in the austenite when part of the carbides remain undissolved, but also it would be of interest to know whether the same effect would be produced by the concentration gradients that persist for a longer period.

E. S. DAVENPORT,[†] Kearny, N. J.—The authors' reported results deal with steels of approximately eutectoid or slightly hyper-eutectoid carbon content; presumably the authors did not extend their studies to steels of distinctly hypoeutectoid composition. I wonder if they would care to express an opinion as to the possible effect of proeutectoid ferrite, as in hypoeutectoid steels, on the relationships discussed in their paper?

M. A. GROSSMANN,[‡] Chicago, Ill.—This paper by Roberts and Mehl clarifies a number

[*] Research Metallurgist, Battelle Memorial Institute.

[†] Research Laboratory, U. S. Steel Corporation.

[‡] Director of Research, Carnegie-Illinois Steel Corporation.

of features about which many of us have wondered. One of the particularly interesting items is Fig. 12, showing the calculated rates of austenite decomposition when assuming a variety of values for nucleation rate N and growth rate G. As the authors point out, R. L. Stephenson and the present writer (ref. 24) used Johnson and Mehl's equations for grain-boundary nucleation, to derive diagrams similar to Roberts and Mehl's Figs. 2 and 3. However, the assumed values that were employed were $N = 1.0 \times 10^6$ and $G = 1.0 \times 10^{-3}$. With these assumptions a set of parallel lines was obtained similar in parallelism to Roberts and Mehl's Fig. 3, but the slope was different from the actual slope derived empirically, as reproduced in Roberts and Mehl's Fig. 15. Roberts and Mehl properly point out that the slope obtained by us does not by any means necessarily apply to all steels.

The true values of such a slope are of great importance in predicting hardenability. We are in entire agreement with the authors' statement that when carbide is undissolved, "both the lowered concentration of carbon in the austenite and the nucleating effect of the carbide particles decrease the time of half-reaction." This, of course, explains the marked departure of the curves in Fig. 15 from a straight line of definite slope, when the austenitizing time was short or the austenitizing temperature was low. It is to be noted that Fig. 15 refers to a hypereutectoid steel, 1.06 per cent carbon. It may be mentioned that our average slope was derived from various steels having carbon contents from 0.35 to 0.79 per cent, and that these slopes seemed to obtain approximately with steels of higher carbon content as well; and, indeed, in one case with higher alloy content.

G. A. ROBERTS (authors' reply).—Since the majority of our tests were conducted on eutectoid or hypereutectoid steels, we do not have direct experimental evidence upon which to base an answer to the inquiries of Messrs. Moore and Davenport. The quenched hardness in the high-carbon steels with which we worked, however, is not materially affected by the presence of undissolved carbide or carbon concentration gradients. In fact, as was shown in an earlier paper,[1] small quantities of pearlite may exist in a martensitic matrix with no appreciable change in the hardness. In low-carbon steels a small change in the carbon content of the austenite (or martensite) has a more pronounced effect upon the quenched hardness than in high-carbon steels, and the phenomenon of a low hardness resulting from rapid heating of spheroidized low-carbon steels can be attributed therefore to undissolved carbide. We feel that carbon concentration gradients would probably have but little influence on the *hardness* in any steel.

Proeutectoid ferrite in a hypoeutectoid composition should alter the rate of the austenite-pearlite reaction only through its effect in increasing the carbon content of the remaining austenite, since carbide, and not ferrite, is the active nucleus in the formation of pearlite. It is interesting to note in this connection that it is possible to have both ferrite and carbide present as undissolved constituents when heating to a temperature just above Ae_1, a hypoeutectoid steel originally consisting of ferrite and pearlite. If this steel is then cooled to below Ae_1, the austenite decomposition rate should be determined only by: (1) its carbon content and (2) the nucleating effect of the undissolved carbide.

We are pleased to have Dr. Grossmann's comments, for this research was partly inspired by his investigations on the subject of hardenability.

A Micrographic Study of the Cleavage of Hydrogenized Ferrite

By Carl A. Zapffe* and George A. Moore,* Junior Members A.I.M.E.

(New York Meeting, February 1943)

In a previous publication from this laboratory[1] the conclusion was drawn that the embrittling effect of occluded hydrogen on iron and steel must result from the precipitation of the gas within small openings through the crystal structure. A review of the literature then published indicated the real existence of crystal substructures of the mosaic type and gave presumptive evidence that the "rift openings" associated with hydrogen occlusion are the same as the "disjunctions" of the mosaic theory.

Inasmuch as no clear conception of the actual nature of the crystal fragments and openings inherent in these theories has been established, it was considered desirable to obtain direct micrographic evidence of their true configuration. In this direction the standard methods of metallographic attack have proved useless. Recourse was had, therefore, to the direct examination of the surfaces upon which failure by cleavage had resulted from the presence of hydrogen. It was expected that such a surface, unaffected by chemical attack and undistorted by polishing, would reveal the fine openings penetrated by the gas and thus indicate the real nature of the substructures.

Materials Studied

In commercial steels, defects caused by hydrogen take various external forms according to such factors as structure and purity, and to the extent to which hydrogen

either occludes or produces chemical changes. The present work relates only to the well-known transcrystalline hydrogen embrittlement—"pickling brittleness"—in which elemental hydrogen occluded within the grain develops cleavage characteristics. For example, hydrogen embrittlement resulting from hydrogen reaction products is excluded from detailed study. It was also desirable, as far as possible, to have the study uncomplicated by other elements which themselves cause brittleness.

Three types of iron were used. These included ingot iron, decarburized free-machining steel, and a specially prepared, aluminum-killed, electrolytic iron. This choice allowed a comprehensive selection of unavoidable minor impurities and inclusions, which could subsequently be shown to have no specific effects on the structures within the grains. Carbon, and any other impurities free to react with hydrogen, were first removed by a preliminary annealing treatment in hydrogen. Subsequent treatment in vacuo extracted much of this hydrogen and its gaseous reaction products. The resultant ductile iron was then embrittled either by a second anneal in hydrogen, followed by rapid cooling, or by cathodic electrolysis.

Group I: Prepared from Armco Ingot Iron

As shown in Table 1, the principal impurity in this iron was oxygen, which survived the purifying treatment to a large extent. Two series were prepared. The first (Nos. S10–24) was purified only one day in hydrogen and dehydrogenized one day in nitrogen. Containing both hydrogen and its

TABLE I.—*History of Microsamples*
GROUP I.—INGOT IRON

Bar No.	Treatment	Type of Fracture	Impact, F t-lb.	Hardness, Rockwell B

Series I: In moist hydrogen 24 hours at 1000°C., in dry hydrogen 22 hours, in dry nitrogen 22 hours, cooled in nitrogen. Grain size No. 1. Microstructure normal.

Bar No.	Treatment	Type of Fracture	Impact	Hardness
S12[a]	Cathodic charge A[b]	Granular	0.75	48
S13	Cathodic charge A	Granular + facets	14.5	50
S14	Cathodic charge B	Granular + facets	17.5	50
S15	Cathodic charge B	Fibrous + facets	55	43
S16	Cathodic charge B2	Mixed types	18	52
S18	Cathodic charge B2	Mixed types	24.3	50
S19	Cathodic charge B2	Fibrous + facets	50.5	40

Series II: In moist hydrogen 392 hours at 1000° to 1050°C., 4 hours in dry hydrogen, 24 hours in vacuo, cooled in vacuo. Grain size No. 1. Microstructure, oxide veining.

Bar No.	Treatment	Type of Fracture	Impact	Hardness
S25	Residual hydrogen only	Granular + facets	2.8	26
S26	Residual hydrogen only	Granular + facets	2.9	25
S32	Cathodic charge B	Granular + facets	3	19

GROUP II.—DECARBURIZED FREE-MACHINING STEEL, S.A.E. X-1112

Bar No.	Treatment	Type of Fracture	Impact, Ft-lb.	Hardness, Rockwell B

Series I: Decarburized in moist hydrogen 392 hours at 1000° to 1050°C., 4 hours in dry hydrogen, 24 hours in vacuo, cooled in vacuo. Grain Size No. 5. Microstructure: many inclusions, no detectable carbon.

Bar No.	Treatment	Type of Fracture	Impact	Hardness
S52	Residual hydrogen only	(Fibrous skin, faceted core.)	37	58
S59	Cathodic charge B		35.5	59

Series II: Specimens from Series I deoxidized 18 hours in dry hydrogen at 1050°C., degassed 72 hours in vacuo, cooled in vacuo. Microstructure unchanged.

Bar No.	Treatment	Type of Fracture	Impact	Hardness
S61[d]	As annealed	No fracture	130.+	48
S62[d]	As annealed	No fracture	130.+	54
S63[d]	As annealed	Fibrous partial fracture	120.5	53
S66[d]	Cathodic charge A	Facets	35	52
S67	Cathodic charge B	Facets	62	50
S69	Cathodic charge B	Facets	33.5	48
S70	Cathodic charge C	Facets	65	51

Series III: Specimens from Series II soaked in dry hydrogen 64 hours at 850°C. and normalized.

Bar No.	Treatment	Type of Fracture	Impact	Hardness
S75	Residual hydrogen only	Facets	3	48

GROUP III.—SPECIALLY PURIFIED IRON[c]

Bar No.	Treatment	Type of Fracture	Impact, Ft-lb.	Hardness, Rockwell B

Series I: Short deoxidation in hydrogen, degassed in vacuo 16 hours at 850°C., 120 hours at 1050°C., and 24 hours at 700°C., cooled in vacuo. Grain size much larger than No. 1. Microstructure clean except for traces of Al_2O_3.

Bar No.	Treatment	Type of Fracture	Impact	Hardness
S251[d]	As annealed	No fracture	155	−5
S252[d]	As annealed	No fracture	152	−7
S253[d]	As annealed	No fracture	163	0
S257	Cathodic charge C	Large facet	17	3
S260	Quenched from 67-hour anneal at 850°C. in hydrogen	Few facets	4	11

TYPICAL ANALYSES, WEIGHT PER CENT[e]

Material	O[f]	N	P	S	Si	Al (metal)	Mn
Group I	0.082	0.004	0.011	0.044			
Group II	0.034	0.004	0.084	0.25	0.02		0.76
Group III	0.012		<0.005	0.010	<0.01	0.14	

[a] Specimen numbers listed in figure captions throughout paper give first this number, then *A* or *B* to designate the two halves of the fractured specimen, finally a number designating the particular grain among those photographed.

[b] Cathodic electrolysis from platinum anodes in 5 per cent H_2SO_4:
  Charge A: 30 min. at 1 amp. per sq. decimeter.
  Charge B: 2 hr. at 7.5 amp. per sq. decimeter.
  Charge B2: Same, followed by ½ to 10 min. with polarity reversed, designed to remove hydrogen and return ductility, but completely ineffective.
  Charge C: 6 hours at 4.8 amp. per sq. decimeter, believed to be the current density of maximum efficiency.

[c] Prepared by melting electrolytic iron in a magnesia crucible under a calcium aluminate slag and deoxidizing with excess aluminum metal (0.60 per cent added). The ingot was hot-rolled, bars scalped and cut to size, cleaned and stacked in the furnace and given the treatment listed.

[d] Samples not included in photomicrographs shown, but listed for comparison of physical properties.

[e] After "series" treatments and before hydrogen charging.

[f] O by vacuum fusion.

reaction products, this material yielded fractures of all types from intergranular to the most detailed transgranular facets, further hydrogen additions having but little effect. Notched-bar impact values ranging from 50 to 0.75 ft-lb. show the degree of embrittlement produced in each sample, but are not considered to show any direct relation to the hydrogen content.

A second series of bars in this group (S25–49) was treated for 16 days in hydrogen, without, however, completely removing the oxides and similar impurities. Extensive gaseous reaction was evident, especially at the grain boundaries, which appear to have been greatly weakened by the partial removal of the boundary films and by the gases that must have collected there. The fractures passed both through these films and through some of the grains, where the usual facets were formed. All samples were brittle, showing only about 3 ft-lb. notched-bar impact strength.

The oxide-hydrogen reaction causes intergranular embrittlement that is characteristic of this type of material. The transgranular facets formed, however, were always identical with those in the other materials.

Group II: *Prepared by Decarburizing Commercial Free-machining Steel*

The material of group II, having less oxygen, is better suited for studying transcrystalline hydrogen embrittlement. The steel was decarburized 16 days and vacuum-treated to remove hydrogen. In the first series (S50–60), the hydrogen was incompletely removed and the samples remained brittle at the center. Further vacuum treatment of series II (Nos. S61–99) produced a ductile material having a notched-bar impact strength of 120 to 130 ft-lb. Hence it is evident that the large amounts of sulphur and phosphorus still remaining do not themselves lead directly to brittleness. Cathodic hydrogenizing of this

material lowered the impact value to 33 and 65 ft-lb., producing transgranular cleavage only. The residual hydrogen of the first anneal left the material with about equal brittleness. Resaturation at 850°C. in a hydrogen atmosphere gave complete embrittlement, with the notched-bar impact value falling to 3 foot-pounds.

Important to observe is that the impurities remaining in this iron do not react with hydrogen sufficiently to impose any fracture structures not caused by hydrogen alone. The facets in this material are identical with those in the first group where the impurities were of completely different nature.

Group III: *Prepared from Electrolytic Iron, Remelted and Deoxidized with Excess Aluminum*

The only appreciable impurities in the iron of group III were aluminum metal and Al_2O_3. A shorter hydrogen anneal and longer vacuum treatment than ordinary were given. The gas-free material was very ductile, with notched-bar impact values between 152 and 186 ft-lb. As might be expected,[2] diffusion seemed slow in such pure metal and complete embrittlement was difficult to obtain. Many samples showed only a mild drop in impact value, while others were more thoroughly affected. A cathodically charged piece broken with 17 ft-lb., and a gas-saturated piece broken with only 4 ft-lb., were subjected to detailed study when found to give the most complete representation of all observed structures.

The facets of this relatively pure material were similar to those in the other specimens. In Figs. 3c and 5d the detailed structures shown cover the entire range of types found in any other cases. This effectively shows that all structures found within the grain must be due primarily to the ferrite structure as developed, or revealed, by hydrogen, and not by any other impurity.

Comparative Properties of the Three Groups

The response of these materials to hydrogen treatment varied widely, which might be expected, since published studies on the rate of hydrogen diffusion[2-7] show large variations both with the state of purity of the iron and with its structural condition. Thus material II, allowing free diffusion, responds quickly both to charging and to annealing. Material I, because of the films of impurity, is slow to surrender its gas content and does not readily regain ductility. Material III, as is common with pure and well-annealed metals, seems slow to absorb the gas,[8] hence slow to pass from its natural ductile state to that of complete embrittlement.

The gross differences in rate of diffusion between materials, and the smaller differences between samples, cause the various samples to attain varying degrees of embrittlement after similar treatment. Therefore, physical properties, such as the impact resistance, cannot be related directly to the treatment given, but do give some indication of the result obtained. In spite of these differences in rate, once transcrystalline embrittlement is attained, the structure always appears the same.

METHOD OF INVESTIGATION

Although hydrogenizing has been shown to accelerate etching or chemical attack of iron on a macroscopic scale,[1] attempts to reveal a fine system of rifting within the grain by chemical etching have been indecisive. The present work takes advantage of a more specific method.

When hydrogen-embrittled iron is fractured, the fracture surface is brilliant and silvery. In the stereoscopic view* in Fig. 1a, such a surface shows many flat, mirrorlike cleavage surfaces, or "facets," which pass directly through the grains—a single facet often traversing an entire grain. An individual facet, oriented correctly on a microscope, proves quite suitable for examination at high magnification and is free from the effects of the ordinary metallographic preparation.

Facets are found in all simple hydrogen breaks.[1] The structure of a "snowflake," or a "fisheye," is typical. In tensile testing, the longer period for fracturing may allow the surfaces to be distorted by secondary deformation, and the fracture may cause inconvenient orientation of the facets. The choice for this study of fracturing by impact insured undamaged cleavage surfaces lying in positions where they could be conveniently examined by the microscope. The impact values also are useful as a qualitative indication of the degree to which hydrogen embrittlement has developed in each specimen.

By macroscopic examination, the effectiveness of the annealing operations could be followed in preparing the specimens. Fig. 1b shows the result of the incomplete vacuum treatment first given irons of group II. A ductile, degassed surface layer encloses a central core, which remains embrittled. An area of facets is thus seen surrounded by a dark layer of deformed metal.

---

* These stereographs may be examined with any viewer made to fit the standard interpupillary distance. Such viewers are available for about one dollar. Two cheap magnifying lenses of about $3 \times$ power will serve the same purpose. Most people can obtain fusion by holding the stereograph directly before the unaided eyes and staring *through* it at an imaginary distant object.

FIG. 1.—SUPPLEMENTARY CAPTION.

a. Ingot iron (S13A) purified in hydrogen and vacuum and embrittled by cathodic electrolysis.

b. Small facets in hydrogen-treated iron (S53A) after treating 24 hours in vacuo at 1050°C., showing removal of hydrogen from the surface layer only.

c. Intergranular fracture in ingot iron (S12A) probably caused by grain-boundary accumulation of reaction products of hydrogen and nonmetallic impurities.
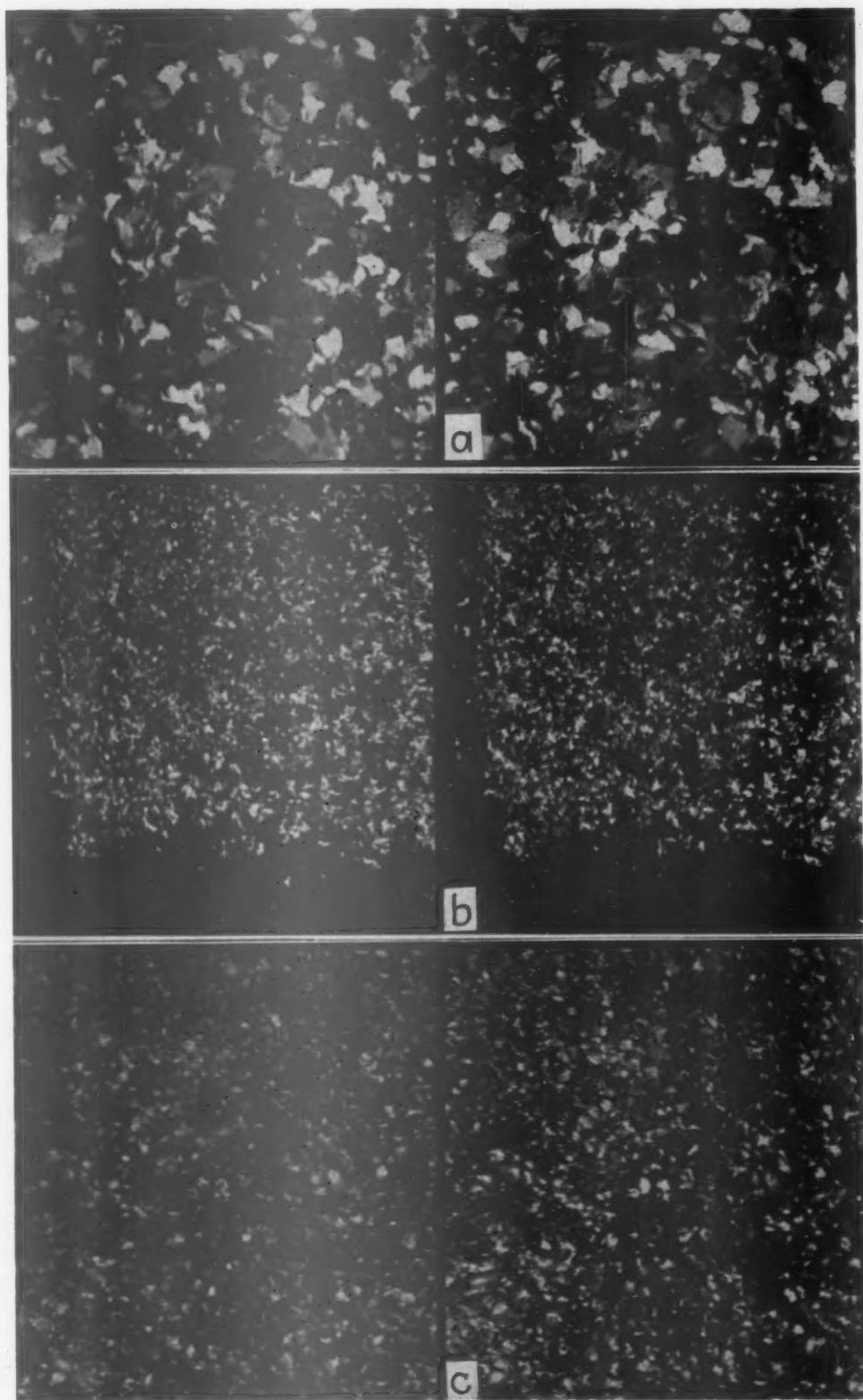
FIG. 1.—STEREOMACROGRAPHS OF CLEAVAGE FRACTURES CAUSED BY HYDROGEN. ×10.
Supplementary captions on opposite page.

Macroscopic examination also shows the nature of the intergranular fracture found in many specimens of the group I irons made from Armco ingot iron. As shown in Fig. 1c, the surfaces of failure are rounded and irregular, to be distinguished from the flat surfaces formed by hydrogen in the absence of oxide-film types of impurities.

The various specimens were cut to standard dimensions for Charpy bars (1 × 1 × 5.5 cm.) and then loaded with hydrogen either by a cathodic treatment or by soaking in the gas (Table 1). Immediately after charging, a 2-mm. V-notch was cut, and the bar was broken. One half of the bar was mounted with the broken end projecting from a 1-in. ring, which could then be mounted in a special orienting mechanism on the microscope. Adjustment of three leveling screws allowed a desired facet to be oriented exactly perpendicular to the axis of the microscope. When the specimen was properly set, examination was possible well into the oil-immersion range, long-nose objectives generally being necessary to prevent contact with promontories on the rough surface.

MICROSCOPIC EXAMINATION AND TYPES OF STRUCTURE

The only tenable explanation for "pickling brittleness" and the occlusion of hydrogen at room temperature requires the accumulation of the gas in fluid form within openings through the metal structure. Brittle failure is held to occur through or along these openings, which lack cohesion when filled with gas. Microscopic examination, therefore, was directed toward finding these openings, describing, and classifying them.

Large openings such as cracks, blowholes and blisters have been discussed in other places.[1,9] It has been shown that these usually do not account for more than a small portion of the hydrogen involved, and that they do not explain general embrittlement. The openings of interest here are expected to be less than the size of the grain. Some small openings may form in the boundary, or along oxide veins. Smaller openings may, in theory, take the form of minute holes or "canals" through the grain,[10] or of "rifts." A "rift" may be defined as a flat opening, within a grain, ranging in size down to any space just large enough to admit a hydrogen molecule. Originally they were proposed as lying along slip planes after deformation.[11,12] More generally, they may be considered intimately associated with the structure of the crystal. The major cleavage forming a flat facet is considered to pass through a rift that has grown until it completely traverses the grain. It has been shown[13] that the thinner an opening of this type, the greater the forces acting to retain the gas molecules, and hence the greater the occlusive effect. Most of the openings in the present samples may be considered as rifts.

Since rifts derive from the structure of the crystal, they should be discussed and classified in terms of this structure. Greninger[14] has simplified the many possible intragranular structures of metals into two main types, lineages and mosaics. According to Buerger,[15] a "lineage" is any structure that is basically continuous, but formed in branches. The branches are separated by discontinuities at which there is a change of orientation. Reconciling Darwin[16] with Webster, one may define a "mosaic" as any structure built up of small units or fragments. No restriction is placed on the dimension, shape, or order of the arrangement. Mosaic fragments are separated by "disjunctions" from which part, or all, of the possible metal atoms are missing. A change of orientation is possible, but not required, at the disjunction. By definition alone, a rift and a mosaic disjunction, therefore, are essentially the same. In general, a lineage pattern is expected to be larger than a mosaic, which may therefore compose one of the branches
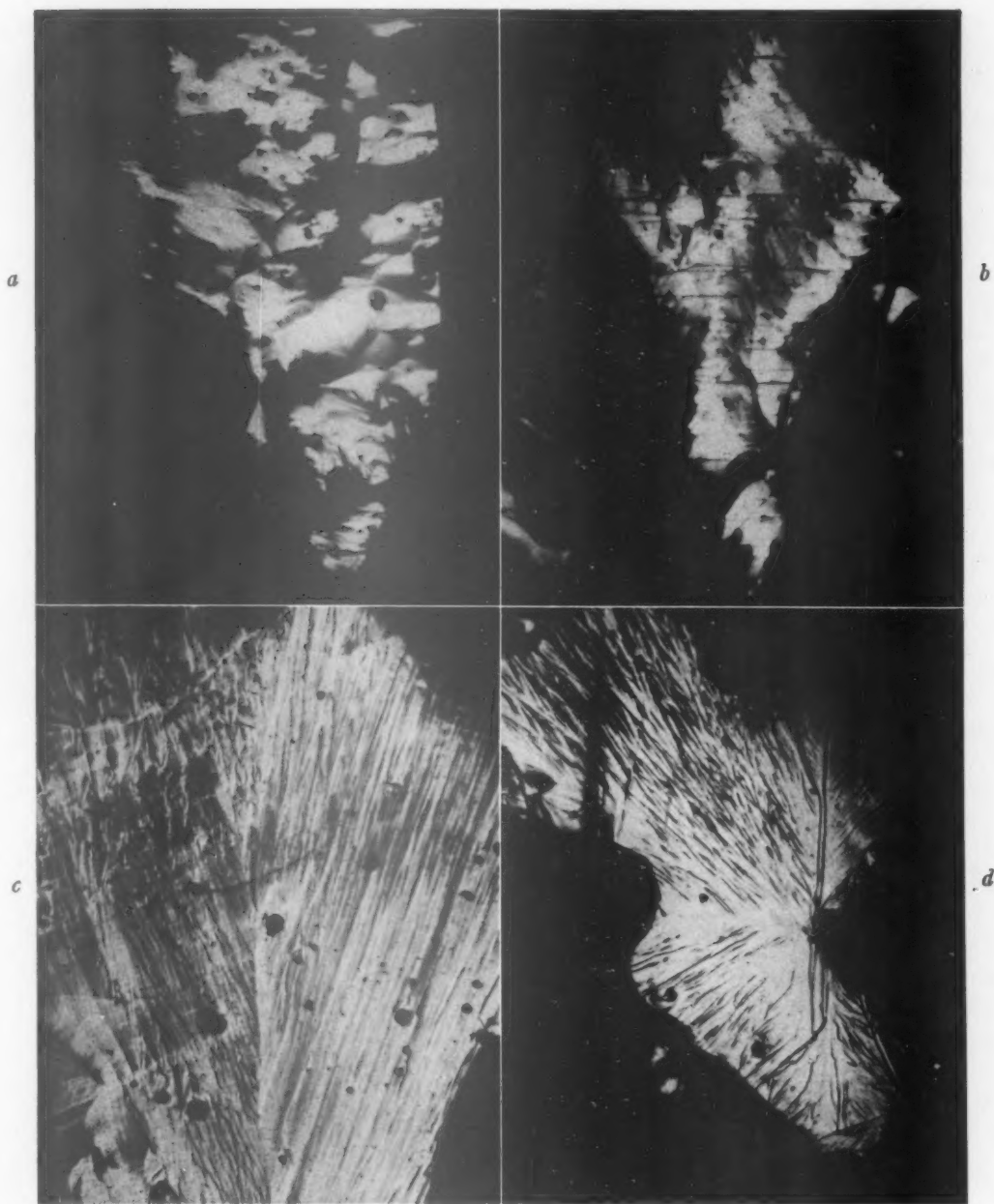
FIG. 2.—FRACTURE TYPES.
Original magnifications given. Reduced ⅓ in reproduction.
a. Grain boundary in high-oxygen iron (S25A2). ×200.
b. Grain boundary, showing one family of planes sprung by hydrogen (S32A1). ×200.
c. Lineage, showing interlineage discontinuity and wavy surface (S26A2). ×200.
d. Sharp lineage centering on impurity (S19B3). ×350.

of the lineage. There is, however, no pro-hibition of the separate existence of the two types in overlapping size scales.

Examination of the detailed structure of a large number of facets of hydrogenized ferrite reveals that all of these structures can be arranged in a progressive series from the grain itself through lineage types and then mosaic types to the limit of optical resolution. The crystallographic perfection

increases with decreasing size of the structural unit and does not depend on the material. As already noted, all of the intragranular structures can be realized on any of the materials studied, regardless of purity. This will be illustrated by interlacing pictures from the different groups of material throughout the progression of types to be shown. Without reference to the identifying numbers and the table, it will be impossible to determine that a picture came from any particular quality of iron. Thus, the embrittling mechanism is fundamentally the same in all types of ferrite, and relates to the same basic structures.

Grain Boundary or Intergranular Embrittlement

This type of embrittlement can be found only in the first group of samples where the presence of films of iron oxide and similar substances allows their reaction with the hydrogen to form gases, such as steam, which create and open voids between the grains. Two unusual views of the rough, outer surfaces of grains are shown. In Fig. 2a there is no sign of fracturing except through the grain boundary, the hydrogen having so far failed to show any effect on the body of the grain. In Fig. 2b, the grain itself shows some response, one set of parallel rifts having been opened, intersecting the surface. Apparently the fracture was on the verge of passing down one of these rifts to form a facet.

Lineage Structures

All pictures to follow are made directly on the untouched, flat cleavage facets without mechanical or chemical modification. Branched, diffuse structures showing poor crystallographic development are found intersecting this facet plane in all types of iron. A typical example in Fig. 2 shows two major branches, which redivide on smaller scales. The facet surface itself

is seen to be somewhat wavy, indicating variations in orientation in this direction as well. Also, it is evident that only a few of the sharper and darker lines may with any certainty be identified as disjunctions, or openings, while most of the discontinuities fail to show evidence that they involved voids large enough to take part in the embrittling process. Thus the rift volume resulting from lineage irregularities appears to be comparatively small.

A sharper lineage pattern appears in Fig. 2d. What appears to be an inclusion occurs at the center of this structure. This raises the possibility that the production of the lineage could be controlled by the action of some impurity. A coarse lineage structure is shown in Figs. 3a and b, first in ordinary and then in polarized light. The major discontinuities are plainly anisotropic, indicating the presence of impurities, or representing severe distortion in the lattice arrangement. These structures are all from the high-oxygen iron, group I. Many similar structures, not reproduced, were found in the free-machining iron. The supposition that impurities cause the lineage is opposed by the presence of this structure in the relatively pure iron of group III. A well-developed structure from this material appears in Fig. 3c. Thus, if an impurity is active, it must operate in very small concentration to be present in all three materials. Inclusions, comprising the usual impurities, are often carefully avoided by the lineage discontinuities (see Fig. 2c).

Transition Structures

The diffuse and noncrystallographic arrangement of the lineage passes gradually into the sharper crystallographic structures associated with the mosaic type of substructure. A puzzling example appears in Fig. 3d. Lines falling close to two different crystallographic directions appear in Fig. 4a.
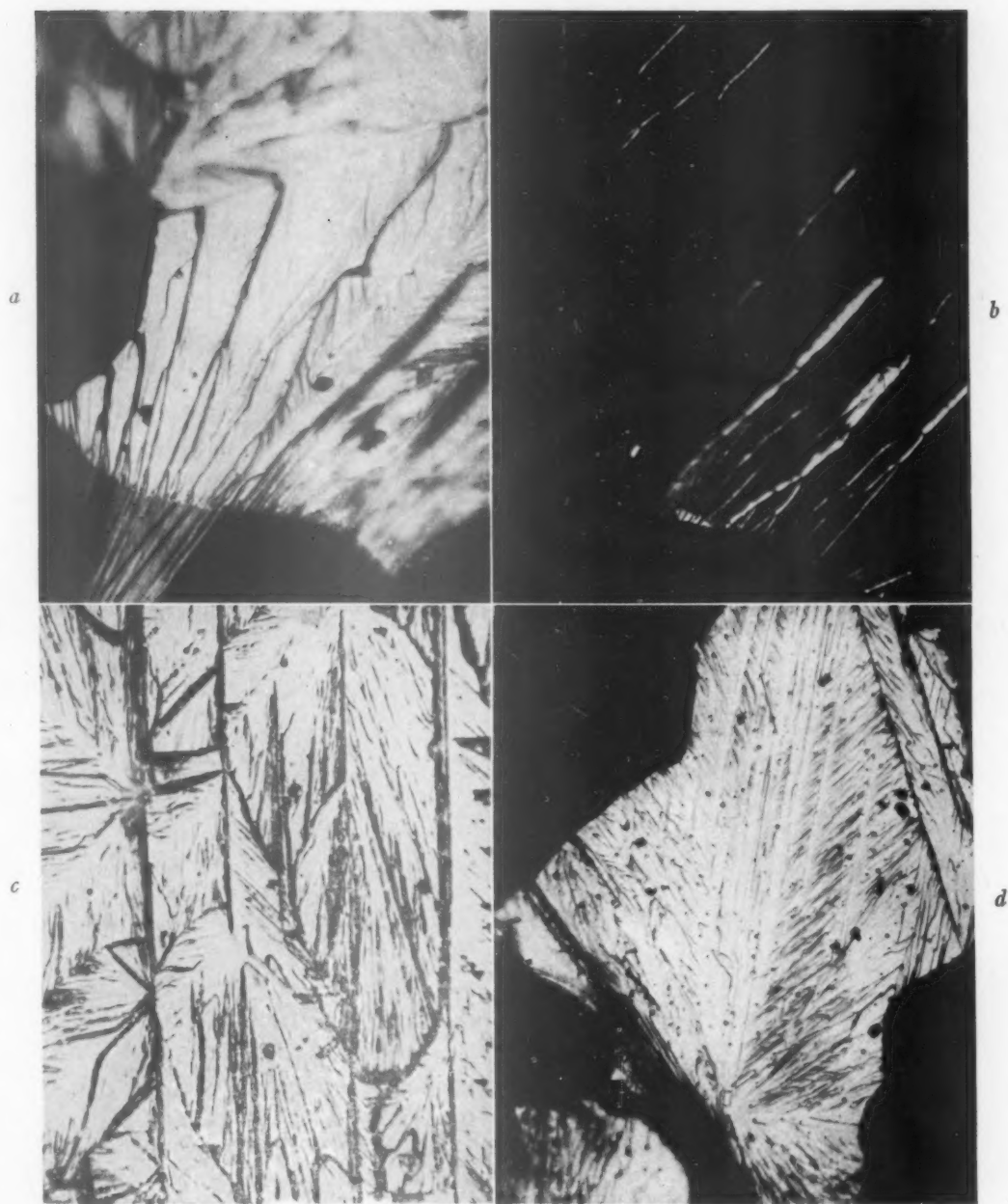
FIG. 3.—LINEAGE AND TRANSITION PATTERNS.
Original magnifications given. Reduced ⅓ in reproduction.
  a. Lineages and facets on three planes (S14A4). ×500.
  b. Same area in polarized light, showing anisotropy of discontinuities.
  c. Lineage patterns in purified iron (S257A1). ×250.
  d. Transition stage between lineage and crystallographic structure (S69B1). ×350.

Mosaic Structures with Line Dislocations

Regular crystallographic arrangements of dislocations associated with mosaic patterns may occur within, or may be associated with, lineage structures, as shown, or may descend directly from the grain without the complication of branching arrangements. The development of a single parallel set of rift openings traversing the whole
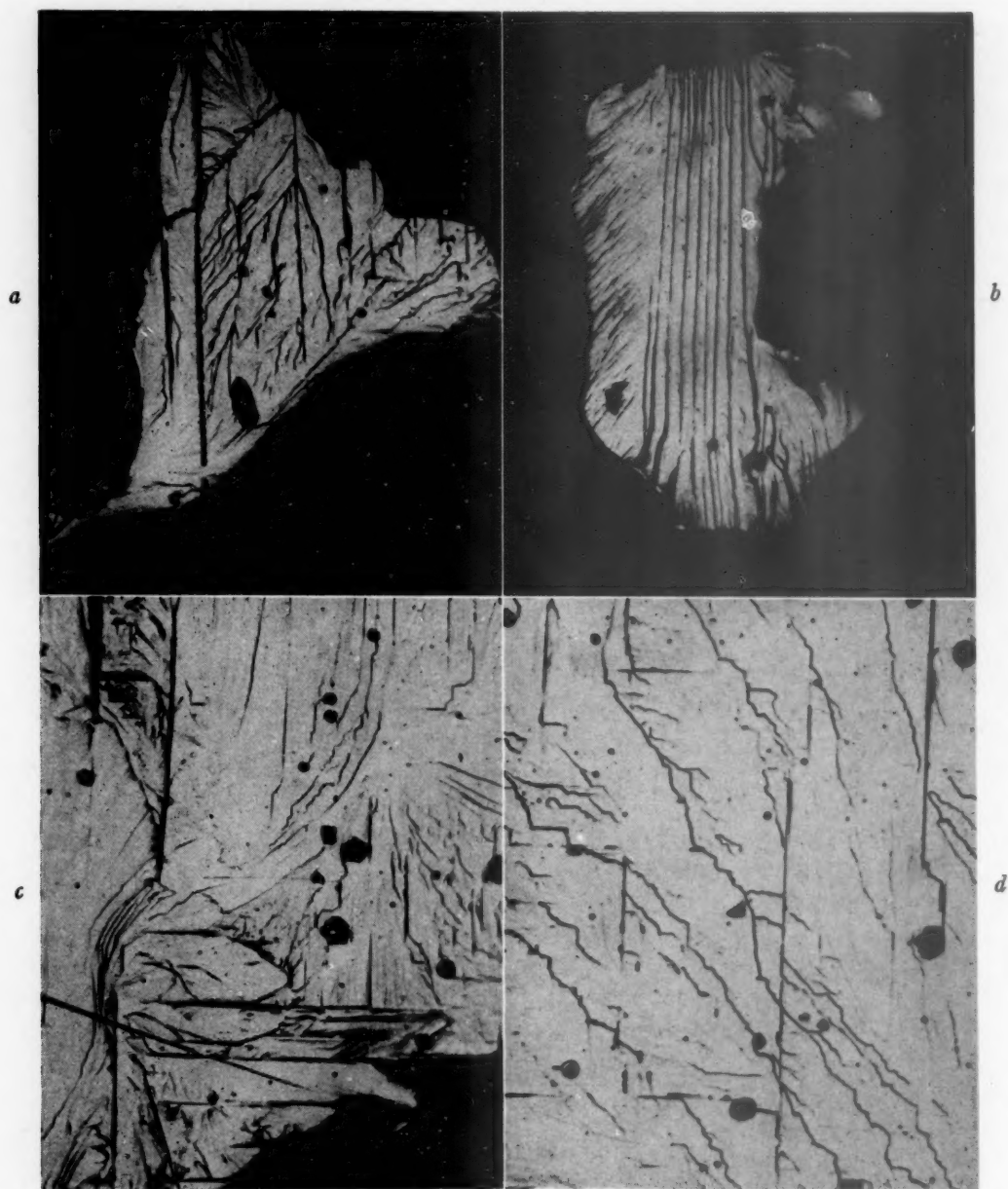
FIG. 4.—MOSAIC LINE PATTERNS.
Original magnifications given. Reduced ⅓ in reproduction.
a. Transition from lineage; lines in two crystal directions (S19B1). ×350.
b. Crystallographic rifts on single set of planes (S18A2). ×350.
c. Mosaic lines lightly developed (S26A1b). ×350.
d. Sharp crystallographic lines with steps around mosaic blocks (S25A1). ×500.

grain is shown in Fig. 4*b*. This is to be compared with Fig. 2*b*, where a similar set of rifts appears on the outer grain surface.

The line dislocations are seldom confined to a single set of planes, but usually run in several directions as the opened plane changes from one crystal position to another (see Fig. 4*c*). Many of the lines of intersection of these rift openings with the facet appear at first to be curved. These
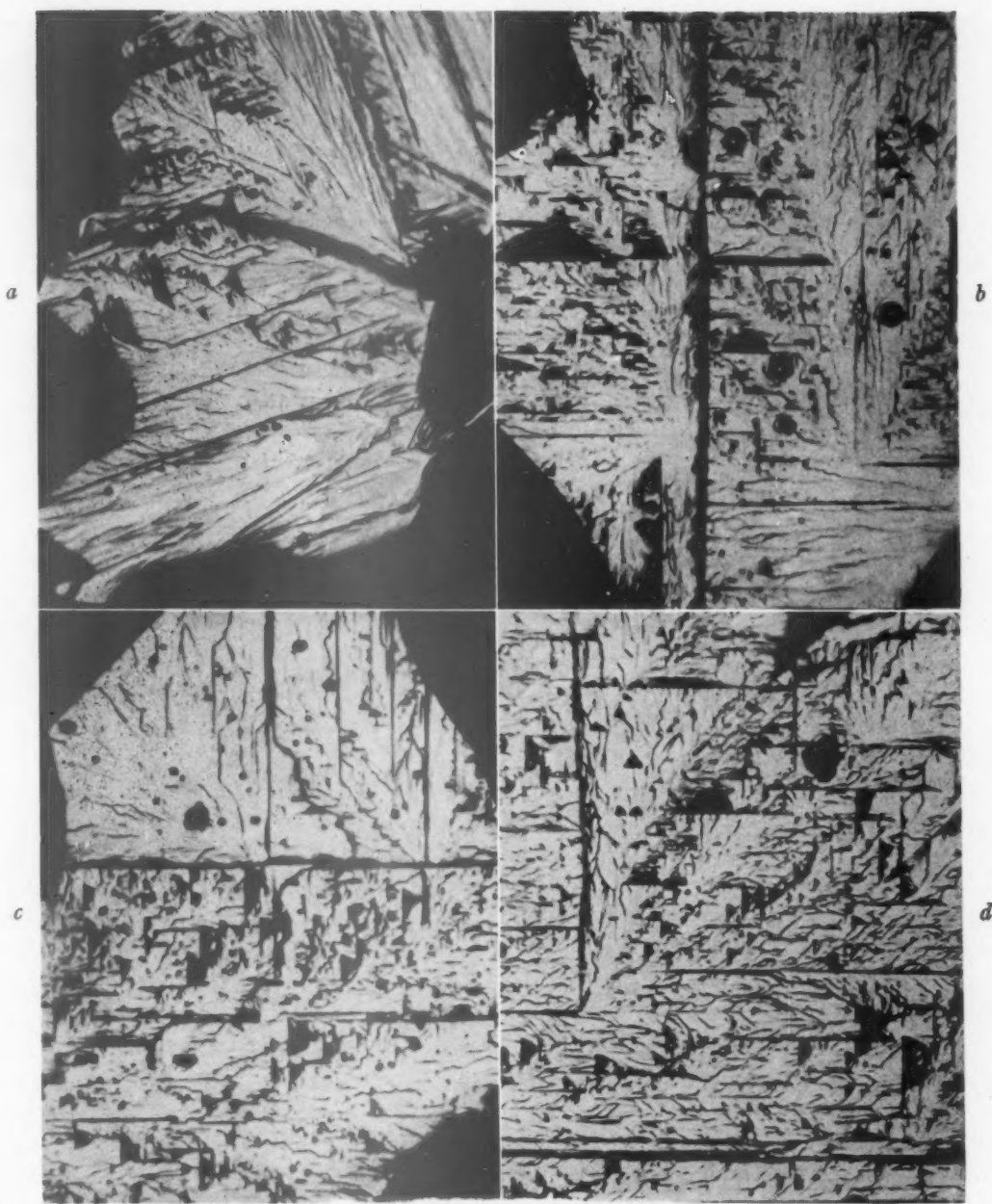
FIG. 5.—MOSAIC BLOCK PATTERNS.
Original magnifications given. Reduced ⅓ in reproduction.
a. Lineage, line, and block structures with hole and crack (S15A2). ×350.
b. Mosaic blocks in high-oxygen iron (S16A1). ×500.
c. Mosaic blocks in impure iron (S69A2). ×500.
d. Mosaic blocks in purified electrolytic iron (S257A1a). ×250.
All samples cathodically charged with hydrogen.

curved traces, however, may usually be resolved at sufficient magnification, showing themselves *to proceed stepwise* around small blocks of regular crystallographic form. These steps may be clearly seen in Fig. 4d, and in other photographs. Some of these lines are found preserved in all patterns of finer detail.

Mosaic Block Structures

The crystallographic blocks bounded by two rift planes in the stepped line patterns may often border instead on three or more well-developed disjunctions. In this case the blocks are loosely held together, and pull away during the cleavage. A complete progression to this stage is seen in Fig. 5a. A small blowhole and a fine crack are included among the openings in this grain.

Three views of grains running largely to the block type of fracture are shown in Fig. 5. The removed fragments vary from single, small particles about 1 micron in true diameter up to large and irregular pieces, probably composed of many of the smaller units. Fig. 5b is from the high-oxygen iron, group I, whereas Fig. 5c is from the group II iron made from free-machining stock. The two structures are for all practical purposes identical. The purified iron of group III, having a larger grain size, also shows a somewhat larger block size, so is shown at lower magnification in Fig. 5d.

Laminated Structures

A reasonable supposition, confirmed by direct observation, is that the fragmentation exposed on the cleavage face of these crystals is in no way unique on that plane. Each of the last three pictures in Fig. 5 shows the edge of another extensive plane, which can be only a little less completely opened than the facet rift itself. Pure chance has thus determined that the facet fell as observed, rather than on a similar plane parallel to this surface. The fine structures that are evident may thus be supposed to extend through the entire body of the grain.

By varying the focus of the microscope during visual observation, it is possible to see that the original cleavage has often traveled on a series of parallel planes of the order of one micron in separation. The exposure of a series of these rift planes leads to a stepped or terraced structure, which is much more common than would appear from the photomicrographs. An identical situation has been observed previously in other hydrogenized metals.[11,12] By special focusing and lighting, the terraces may be photographed as a series of parallel lines. In Fig. 6a the lines marking the edges of these laminations are shown bordering the two largest rifts, and also along the junction of the two dissimilar areas. In Fig. 6b the terraces may be seen along several large rifts. At higher magnification, the holes of the larger block structure may also be seen to take the form of steps, as in Fig. 6c. Finally, in Fig. 6d, the terraces are shown at the outer edges of fractured grains, especially between the two facets.

The exposure of these laminations indicates that the fine structures observed in these metals are essentially the same in all three principal directions.

INTERPRETATION OF RESULTS

Origin of Structures

The evidence of the present experiments appears to show that intragranular structures are inherent in the ferrite crystal and are delineated and made visible on a fracture by the action of hydrogen. The hydrogen may be regarded as playing the part of an etching agent, but an agent which, by being noncorroding and much more fluid than a liquid, is capable of revealing finer detail. Impurities may be discounted as the cause of the internal structures because similar structures are found regardless of the degree of purity. If some secondary element does control the production of these structures, it must act in amounts not shown by chemical analysis.

In the present case, the brittleness, and consequently the exposure of these structures on the fracture, is the direct result of the action of hydrogen. All of the materials when freed of hydrogen are very ductile and tough, in spite of the presence of their various impurities.
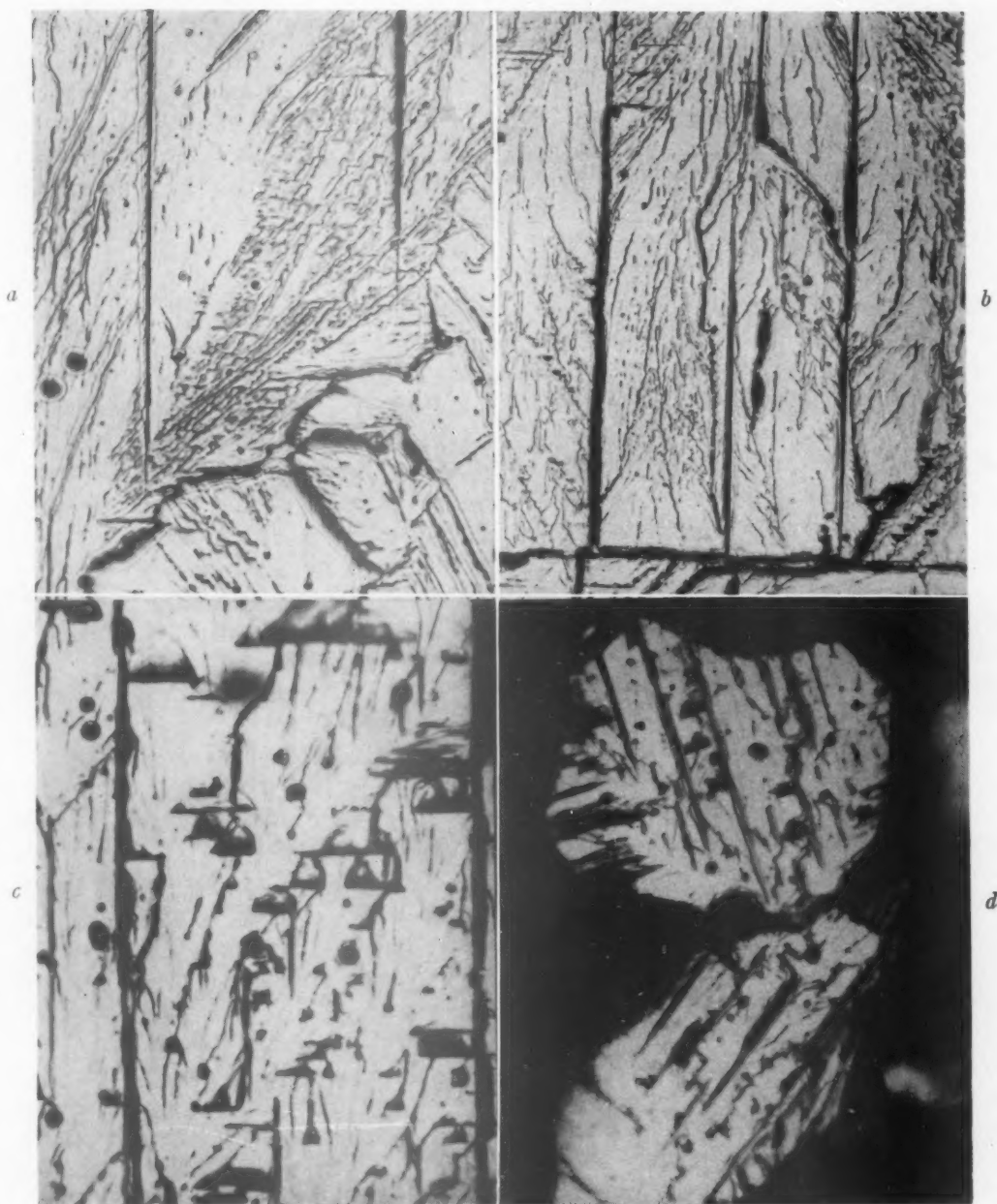
FIG. 6.—TERRACED AND LAMINATED STRUCTURES.
Original magnifications given. Reduced ⅓ in reproduction.
a. Terraces at large cleavages and junction of grains (S260B1). ✕350.
b. General terracing of surface (S260B2). ✕350.
c. Terraced edges of mosaic block vacancies (S67B1). ✕1000.
d. Terraces at blocks and between grains (S59A1). ✕1000.

Possible intergranular structures of the ductile state cannot be detected by the present technique, since any facets that may be formed are too small for observation. The actual amount of hydrogen present, although probably critical in determining the transition from the ductile to the brittle state, does not appear to control closely the type of structure obtained. There is no analytical method

adequate to determine the true concentration at the exact areas studied.

There does, however, appear to be a definite trend toward finer detail as the hydrogen content increases. Facets are observed to be more numerous, hence smaller, in the most thoroughly hydrogenized samples; and in the long run more of the complicated block structures are found in the most completely embrittled pieces. A comparison of the pictures with the brittleness of the bars from which they are taken shows this trend.

Of course, structures of both the mosaic and lineage types may be developed by other methods than hydrogen embrittlement. The specific advantage of this treatment lies in the fact that hydrogen is known in advance to be occluded in openings. Consequently, while the diffuse markings of the lineage structures are of uncertain meaning, the sharp lines in the mosaic line and block structures give every evidence of being the thin, sheetlike voids, or rifts, which were postulated.

Similar brittle facets produced without benefit of hydrogen show similar structures, modified by their different lattice arrangements. Bismuth, zinc, magnetic iron oxide (mill scale), and other materials may be mentioned. The faceted fracture may be induced in ferrite by the addition of silicon—below the supposed solubility limit, incidentally. A similar fracture was even produced by cooling the pure gas-free iron to the temperature of liquid air, under which conditions a notched-bar impact value of 3 ft-lb. was obtained.

These similarities of cold ferrite or silicon ferrite to the hydrogenized structures indicate that the same type of embrittlement may be developed in different ways, thereby lending credence to the belief that the lineage and mosaic patterns are inherently present in at least incipient form in pure ferrite. Hydrogen embrittlement, then, simply utilizes this existing vacuous structure, as will now be explained.

Action of Hydrogen

In other places,[1,9,13] the voluminous literature on the iron-hydrogen system has been considered. Pertinent to present understanding are measurements in the Sieverts' laboratory[17,20] which thoroughly establish the values of true lattice solution of hydrogen at higher temperatures, and the experiments of Smith and others,[8,9,11,12,21] which demonstrate that the gas is occluded in small openings at lower temperature. In experiments on other metals,[11,12] these openings were established as rifts, which lay along slip planes when the metal was studied in the worked condition. No conflict with this is raised by the present study placing the rifts at the faces of mosaic blocks, since one of the accepted modes of formation of such blocks is the fragmentation occurring during cold-working.

Previously, published diagrams of the solubility of hydrogen in iron have used reversed coordinates, thereby obscuring consideration of the system in a metallurgical sense as a series of hydrogen-iron alloys. In Fig. 7, the best available solubility data are replotted[17-20,22,23] to simulate the iron-rich side of a typical binary constitutional diagram. Actually, however, the behavior of hydrogen-iron alloys requires consideration of *both pressure and temperature* as variables. The diagram represents a section taken at $P = 1$ atmosphere through a solid model. The variation of P with the square of the concentration is lost in the third dimension. Thus, there is no true "solubility limit" for hydrogen in iron unless *both* P and T are fixed.

Especially impressive are the precipitation-hardening characteristics of the solubility curve, showing two unusual isothermal precipitations. This system is again unusual because the precipitate is a gas, which fortunately allows the precipitation pressure to be calculated[23] from the solubility law.[18] The three dotted curves superimposed on the diagram show the pressures

in equilibrium with three typical alloys during cooling. Of course, the loss of gas from the lattice to discontinuities modifies these pressures slightly.

Measurements of the density of ideal and real iron crystals[24] show a divergence of 0.01 to 0.1 per cent, which may be partly interpreted as indicating the volume of the
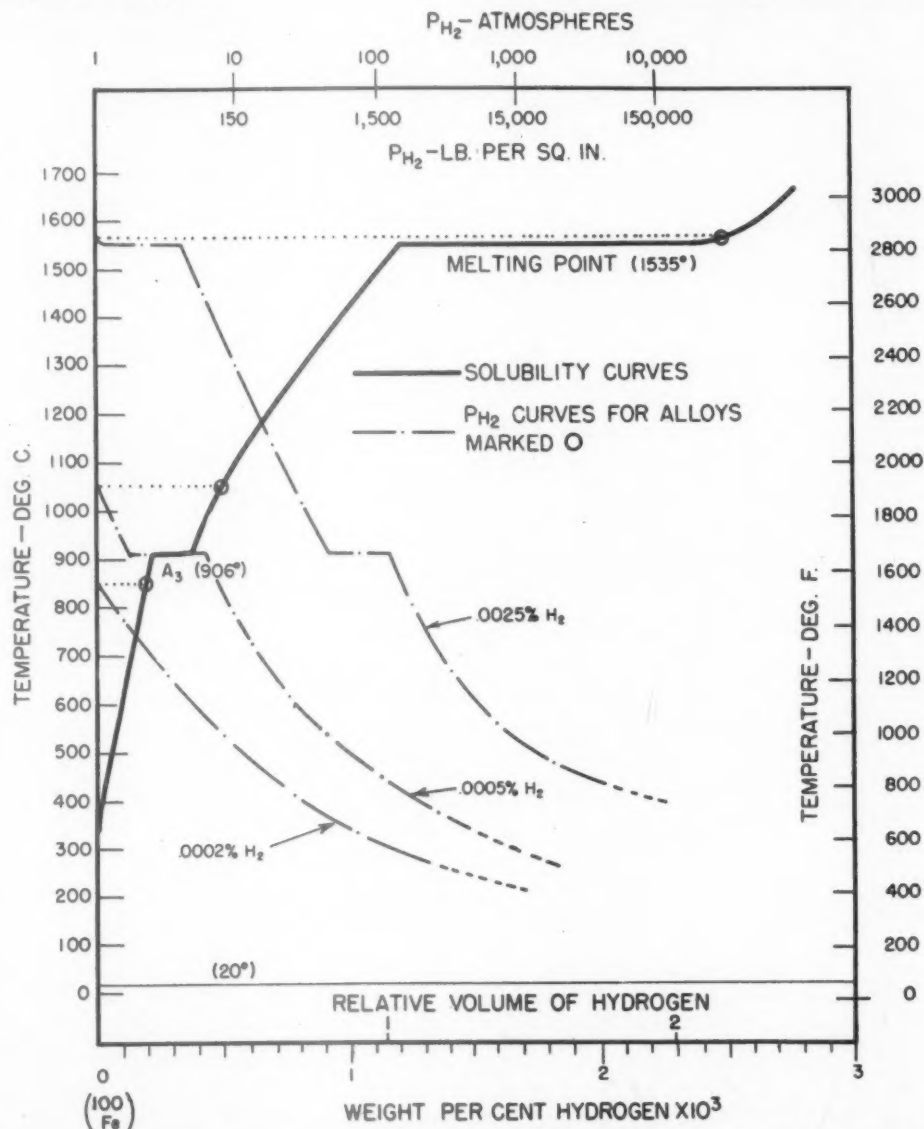
Fig. 7.—Full curve: Solubility of hydrogen in hydrogen-iron alloys at P = one atmosphere, showing strong precipitational characteristics.

Broken curves: Calculated precipitation pressures for the cooling of three alloys designated by circles.

Curves are sections of solid C-P-T model.

For iron to become embrittled in practice, from two tenths to one relative volume of hydrogen is required, a quantity frequently present, but often regarded as negligible.

voids under consideration. If a ratio of the order of 1:10,000 for space-to-solid occurs in ordinary metal, one relative volume of hydrogen forced into that vacuity by a declining solubility relationship would

suffer compression to 10,000 atmospheres, or 150,000 lb. per sq. in. Naturally, residual solution, or reaction, can modify these values, and the introduction of larger openings, such as blowholes, can greatly decrease the pressures realized. It is nevertheless evident that on cooling a solution of hydrogen in iron there is ample opportunity for the gas to precipitate under pressures that may exceed some critical value probably lying near the elastic limit, or the yield point.

The analogy of this precipitation to the crystallographic Widmanstätten precipitation of solid phases is marked, except for two important differences. First, the precipitation of the gas appears to require the pre-existence of openings, or internal surfaces, on which the dissolved atoms can combine to form as molecules. The pressure developed is sufficient to spread or "spring" these surfaces, enlarging existing openings, yet apparently seldom sufficient to create entirely new openings. While such openings could probably be utilized by solid precipitation, there is yet no evidence to indicate that Widmannstätten reactions are unable to force whatever crystallographic adjustments may be necessary.

Secondly, in the Widmanstätten action, the precipitate, being solid, has a strength and ductility of its own and may add to the strength of the base metal. In hydrogen, however, the pools of gas can have no ductility, and, lacking cohesion, can add nothing to the total strength. The gas-filled rifts will then fail very easily in cleavage, whereas this result does not necessarily follow from a solid precipitation.

Absence of Slip

Tensile bars of hydrogenized iron break without elongation or yield point,[1,13] hence without operation of the slip mechanism. The photomicrographs also indicate little evidence of deformation by slip. The presence in the structure of easy planes of cleavage need not in itself preclude slip when the breaking load is above the normal yield point, hence an explanation is necessary. Two lines of reasoning are possible.

The gas pressure existing within the rifts or mosaic disjunctions compresses only the portions of the structure that are not coherent with adjoining metal. This pressure is balanced by a state of tension on all parts that are still coherent and are capable of supporting external stresses. Deriving from a fluid pressure, the tension is triaxial. Varying importance may be attached to such a state, but it is generally agreed that it always results in a preference of cleavage over slip.[25,26] On some proposed models this triaxial tension would make slip more difficult.

An alternate idea has been developed by Bragg,[27] who shows that in order that a small crystal, or mosaic block, may undergo internal slip it is necessary for two opposite faces to be displaced in shear a distance greater than one half an interatomic distance. As the size of such a block falls to a fraction of one micron, the force necessary to establish the initial displacement against the elastic modulus rises rapidly until it passes the ultimate strength of the structure, making slip before failure impossible. Although in the present photomicrographs blocks are not resolved quite as small as those in Bragg's calculations, there is reason to suppose that smaller units are present, but unresolved. In ordinary iron of normal, small grain size, better agreement with the calculated block size might be expected. In the presence of easy cleavage, slip in these structures appears likely to be subjected to Bragg's restriction.

Both the triaxial tension resulting from the gas pressure and the separation into small mosaic blocks probably cooperate to suppress the activity of the slip mechanism in this system.

CONCLUSIONS

Previously published conclusions regarding the occluding and embrittling processes are confirmed and extended, as follows:

1. The occlusion of hydrogen by iron at ordinary temperatures occurs as the retention of fluid, compressed gas within microscopic openings, or rifts, into which the gas precipitates from supercooled or supersaturated solid solutions.

2. The failure of hydrogen-embrittled iron occurs by direct cleavage through these gas-filled rifts, which have no ductility.

3. The action of slip is restricted in this structure either by the action of triaxial tensile forces reacting against the pressure of the occluded gas, or by the fact that the rifts cut the structure into fragments too small to experience internal slip under the forces available, or by the cooperation of both mechanisms.

4. The rifts constitute internal surfaces within the grain and may be broadly classified in two types:

a. The Lineage, a continuous structure composed of branches in angular disarray. Some rifts form on or through this structure. Failure is by major cleavage. Within the structure only a small number of true openings can be observed. The lineage discontinuity thus appears as a change of orientation without visible disjunction, and the total rift volume of this structure appears comparatively small.

b. The Mosaic, a structure obtained by fitting together small particles or blocks of more or less regular crystallographic form. These blocks are separated by disjunctions, which probably compose the largest proportion of the total rift volume.

5. Some mosaic and lineage structures apparently are inherent in the nature of the ferrite crystals themselves, and are present, even though not observable, in all ferrite grains. Hydrogen may be regarded as a tool, or a noncorroding agent, which by mechanical action develops the disjunctions of these structures to the stage where the material may be parted on some disjunctions and the intersections with others made visible.

6. Intercrystalline embrittlement by gas films in openings between the grains appears to be limited to cases where the openings can be created by the reduction of nonmetallic films by hydrogen, and is to be distinguished sharply from the transcrystalline brittleness from elemental hydrogen considered in the present experiments.

SUMMARY

The rift openings within the iron structure in which hydrogen is occluded at ordinary temperatures are studied micrographically. Ferrites of three different origins were first rendered ductile by purification in hydrogen with a subsequent treatment *in vacuo* and were then embrittled by the addition of hydrogen alone. The ferrites were so chosen that their individual impurities did not lead to brittleness, and there was no common impurity to interact with the hydrogen subsequently added.

Micrographic examination is made directly upon the flat cleavage facets formed when the hydrogenized ferrite suffered brittle fracture. Without etching or polishing, these surfaces are unaffected by either chemical attack or physical distortion. On such surfaces the disjunctions utilized and affected by the gas are found to be revealed in great detail. Examples are shown of structures ranging in size from the grain itself down to the limits of resolution of the microscope. These structures are considered in relation to the phenomenon of hydrogen embrittlement and to the theory of metallic crystals. The crystal fragments lying between the rift openings are presented as direct evidence for the reality of "mosaic structure."

ACKNOWLEDGMENT

whose valuable supervision the research was conducted.

REFERENCES

1. C. A. Zapffe and C. E. Sims: Hydrogen Embrittlement, Internal Stress, and Defects in Steel. *Trans.* A.I.M.E. (1941) **145**, 225–261; discussion, 261–271.
2. W. Baukloh and W. Retzlaff: Hydrogen Permeability of Steel in Electrolytic Pickling. *Archiv Eisenhüttenwesen* (1937), **11**, 97–99.
3. T. S. Fuller: The Penetration of Iron by Hydrogen. *Trans.* Amer. Electrochem. Soc. (1919) **36**, 113–129; discussion, 130–138.
   Gen. Elec. Rev. (1920) **23**, 702–711.
4. W. Baukloh and H. Guthmann: Hydrogen Diffusibility and Hydrogen Decarburization of Steel, Armco Iron, Copper, Nickel and Aluminum at High Pressures. *Ztsch. Metallkunde* (1936) **28**, 34–40.
5. T. C. Poulter and L. Uffelman: The Penetration of Hydrogen through Steel at Four Thousand Atmospheres. *Physics* (1932) **3**, 147–148.
6. V. Lombard: Permeability of Iron and Platinum to Hydrogen. *Compt. rend.* (1927) **184**, 1557–1559.
7. W. R. Ham and J. D. Sauter: Diffusion of Hydrogen through Iron and Palladium. *Phys. Rev.* (1935) [2] **47**, 337.
8. D. P. Smith and G. J. Derge: Role of Intragranular Fissures in the Occlusion and Evolution of Hydrogen by Palladium. *Jnl.* Amer. Chem. Soc. (1934) **56**, 2513–2525.
9. G. A. Moore and D. P. Smith: Occlusion and Evolution of Hydrogen by Pure Iron. *Trans.* A.I.M.E. (1939) **135**, 255–292.
10. G. Tammann and H. Bredemeier: Channels in Metal which Communicate with the Surface. *Ztsch. anorg. allge. Chem.* (1925) **142**, 54–60.
11. D. P. Smith and G. J. Derge: The Occlusion and Diffusion of Hydrogen in Metals: A Metallographic Study of Palladium-Hydrogen. *Trans.* Electrochem. Soc. (1934) **66**, 263–270.
12. G. A. Moore and D. P. Smith: Occlusion and Diffusion of Hydrogen in Metals: A Metallographic Study of Nickel-Hydrogen. *Trans.* Electrochem. Soc. (1937) **71**, 545–564.
13. C. A. Zapffe and C. E. Sims: Hydrogen, Flakes and Shatter Cracks. *Metals and Alloys* (1940) **11**(5), 145–151; **11**(6), 177–184; **12**(1), 44–51; **12**(2), 145–151.
14. A. B. Greninger: Crystallographic Uniformity of Lineage Structure in Copper Single Crystals. *Trans.* A.I.M.E. (1935) **117**, 75–88.
15. M. J. Buerger: The Lineage Structure of Crystals. *Ztsch. Krist.* (1934) **89**, 195–220.
16. C. G. Darwin: Theory of X-ray Reflection. *Phil. Mag.* (1914) **27**, 315–333, 675–690.
17. A. Sieverts: On the Knowledge of the Occlusion and Diffusion of Cases by Metals. *Ztsch. physik. Chem.* (1907) **60**, 129–201.
    P. Beckman: Dissertation. Leipzig, 1907.
18. A. Sieverts: The Absorption of Gases by Metals. *Ztsch. Metallkunde* (1929) **21**, 37–46. Abst., *Metallurgist* (1930) **5**, 168–172.
19. A. Sieverts and H. Hagen: Observation on the System Iron-Hydrogen. *Ztsch. physik. Chem.* (1931) **155-A**, 314–317.
20. Sieverts, G. Zapf and H. Moritz: Solubility of Hydrogen, Deuterium and Nitrogen in Iron. *Ztsch. physik. Chem.* (1938) **183-A**, 19–37.
21. G. A. Moore: The Comportment of the Palladium-Hydrogen System toward Alternating Electric Current. *Trans.* Electrochem. Soc. (1939) **75**, 237–269.
22. E. Martin: A Contribution to the Question of the Absorptive Capacity of Pure Iron and Some of Its Alloying Elements for Hydrogen and Nitrogen. *Archiv Eisenhüttenwesen* (1929) **3**, 407–416; *Ztsch. ver. deut. Ing.*, (1930) **74**, 976.
    The Occlusion of Hydrogen and Nitrogen by Pure Iron and Some Other Metals. *Metals and Alloys* (1930) **1**, 831–835; *Stahl und Eisen* (1929) **49**, 1861.
23. L. Luckemeyer-Hasse and H. Schenck: Solubility of Hydrogen in Several Metals and Alloys. *Archiv Eisenhüttenwesen* (1932) **6**, 209–214.
24. C. G. Maier: Theory of Metallic Crystal Aggregates. *Trans.* A.I.M.E. (1936) **122**, 121–170; discussion, 170–175.
25. M. Gensamer: The Strength of Metals under Combined Stresses. Amer. Soc. Metals Lectures, Cleveland, Oct. 21–25, 1940. Pub. Amer. Soc. Met., Cleveland (1941), 100 pp.
26. P. W. Bridgman: Rupture under Triaxial Stresses. *Mech. Eng.* (Feb. 1939) **61**(2), 107–111.
27. Sir Lawrence Bragg: A Theory of the Strength of Metals. *Nature* (May 9, 1942) **148**, 511–513.

DISCUSSION

(B. M. Larsen presiding)

B. M. LARSEN,* Kearny, N. J.—Is not the embrittlement of iron by hydrogen due to formation of a compound of hydrogen with iron?

G. A. MOORE (author's reply).—That is an assumption very commonly made, which on the surface presents a very simple and easy explanation of the effect. However, the amount of hydrogen needed for such action would be even greater than that required to form a brittle solid solution, hence several orders larger than that usually present. It is also to be noted that search for the hydride has been made by X-ray, electrical resistance, and physicochemical methods, and, so far as we are aware, no

evidence of its existence has been obtained by any of these investigations.

Prof. D. P. Smith has just completed a comprehensive survey of the literature on this particular point and might add to this information.

D. P. SMITH,* Princeton, N. J.—In relation to the question whether the hydrogen contained in electrolytically charged iron is present in solid solution, in combination, or in another state, the several investigations of such hydrogen-charged iron made by X-ray methods have indicated, with two apparent exceptions, that there is no expansion or alteration of the iron lattice; and the seeming exceptions were studies in which the metal was charged from arsenical electrolytes, so that the small displacements of the lines of the X-ray spectrum, which were reported, may not improbably have been due to combination between iron and arsenic. The weight of evidence therefore is against the formation either of solid solutions or of hydrides, and appears to show that the absorbed hydrogen is contained outside the regular structure of the iron lattice, in rifts or voids such as those supposed by the present authors. As yet, however, such direct evidence is available only for ordinary temperatures and does not exclude the possibility of formation of solid solution at the higher temperatures where iron exhibits a much greater absorptive capacity for hydrogen.

B. M. LARSEN.—The microscopic technique given in this paper is a very interesting development, and the pictures shown certainly add something to our knowledge about the characteristics of brittle fractures in metallic crystals. When we pass to the question of interpretation in relation to the H-Fe system, however, we should keep in mind the fact that such microscopic observations rarely give definite proof of anything, except when taken together with other evidence. In this case it is first of all very difficult to accept the idea that hydrogen in solution can exert a pressure, even though highly supersaturated. This difficulty leads the authors to postulate the presence of tiny discontinuities in the crystal lattice. But this immediately puts us on uncertain ground,

because we still do not really know why metals slip along certain planes, nor why they have such a weak resistance to separation or fracture, any more than we have any degree of certainty about the presence of discontinuities or "imperfections" in the crystal lattice. Also, the type of data given in this paper has very little value in application to such problems about the nature of the solid state in metals.

The authors infer the presence of cracks from their pictures but these are not proved to be present, and even if they are there in the broken pieces, they may have been formed at the fracture planes at the time of fracture from normally homogeneous crystals.

The indication given in the paper that the structures shown are not peculiar to hydrogen-saturated ferrite but are more or less common to all brittle fractures would seem to make the problem that of the general cause of such fractures rather than some special condition caused by hydrogen in supersaturated solution. The data given do add something to the picture of a condition of *relative* brittleness in ferrite caused by dissolved hydrogen, but such a condition does not necessarily indicate the presence of "disrupted" zones in the lattice. Most normally ductile metals can be made to fracture in a brittle fashion under certain conditions of temperature and application of force, and ferrite is especially prone to such a condition. In some experiments on aging and notch-impact resistance by the writer several years ago, annealed bars of nearly pure iron gave a tough fracture at −30°C. and a very brittle fracture at −50°C. Heindlhofer[28] interprets such an effect as due to a different rate of change with temperature of (1) the resistance to slip, and (2) the resistance to separation in the crystal lattice. Likewise, a supersaturated solution of hydrogen in ferrite may differ from normal ferrite only in an increased resistance to gliding along its slip planes relative to the resistance to separation on these planes.

C. S. BARRETT* AND G. DERGE,* Pittsburgh, Pa.—The authors of this paper have developed a new experimental technique that is capable of providing interesting information on frac-

tured metal surfaces. It is to be hoped that they will pursue their studies further and apply the technique to other problems.

Many of the markings observed on hydro-

polished and etched and the markings thus revealed were also photographed (Fig. 9).

From a stereographic projection of the Laue pattern the poles of (100) cleavage and (112)
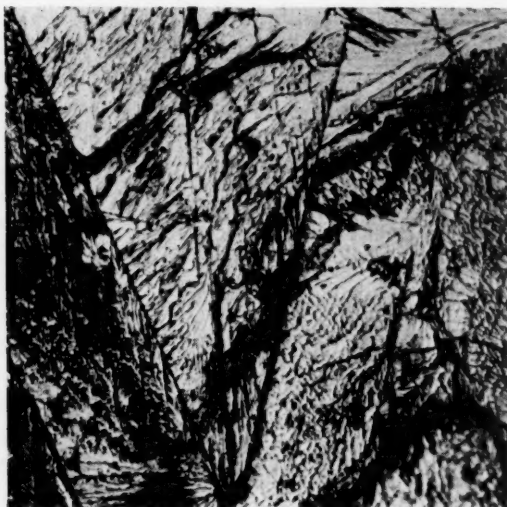
FIG. 8.—CLEAVAGE SURFACE OF IRON SINGLE CRYSTAL. ✕ 100.
Charged with cathodic hydrogen at 4 amperes per square decimeter for 24 hours. Fractured after cooling in liquid nitrogen.
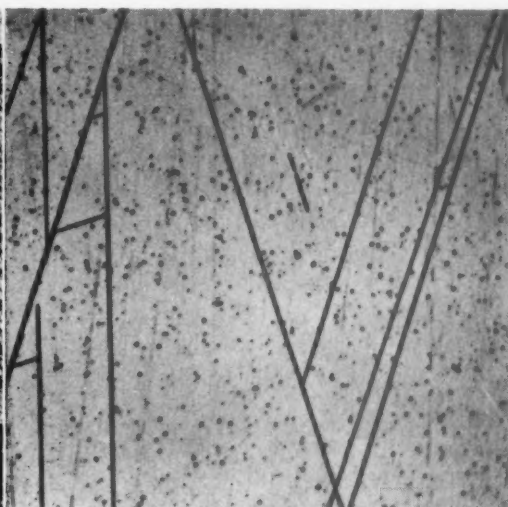
FIG. 9.—NEUMANN BANDS NEAR CLEAVAGE SURFACE OF IRON SINGLE CRYSTAL. ✕ 100.
Same specimen as Fig. 8 after polishing and etching.

genized ferrite are distinctly crystallographic in character. These are well illustrated in Fig. 5. We felt that a study of these markings in single crystals would simplify their identification, and were soon led to the conclusion that the straight-line markings in this figure possess all the characteristics of Neumann bands. The most definite evidence of this rests upon their crystallographic identification.

We have studied a single crystal of iron in the form of a rod about ¼ in. in diameter prepared by decarburization and strain-anneal treatments. The rod had been hydrogenated 24 hr. at 4 amp. per sq. dcm. sawed through about one fourth and then fractured at liquid-air temperature. The cleavage surface was almost a plane and showed numerous markings. A back-reflection Laue photograph was made in order to determine the crystal orientation, and it was found that a cube face was located 2° from the cleavage surface.

Optical photographs were taken of a number of sections on the cleavage surface, giving markings directed at numerous angles to the straight edge in Fig. 8. The surface was then

twinning planes were plotted as filled squares and open circles respectively (Fig. 10). The normals to the average directions of the crystallographic markings on the cleavage surface were then plotted as solid-line diameters. The markings on the polished-etched surface were similarly plotted (dashed lines). It will be seen from Fig. 10 that all these diameters pass through or within 2° of the twinning planes and in no case do they approach the cleavage planes. Therefore, the long, straight lines observed on the surface of this specimen of ferrite may be identified as Neumann bands, not cracks. The markings were not seen on the polished surface before etching, as cracks should be.

Brittle fractures of silicon steels that do not contain hydrogen show similar markings, and it is known that Neumann bands form readily under these conditions. Apparently hydrogen is similar to silicon in that it develops conditions favorable to the formation of Neumann bands when the metal is subjected to cold-work.

It is possible to see additional detail on cleavage surfaces with the electron microscope. A typical micrograph of a 4.96 per cent Si steel

that had not been charged with hydrogen is shown in Fig. 11. This was prepared with the polystyrene-silica technique. The complete interpretation of such a picture will require additional study, but it is probable that the heavy, parallel, diagonal markings are to be associated with either the Neumann bands or the lineage markings seen with the optical microscope. The pattern found between these lines may possibly represent imperfections of some sort existing on a finer scale ($\frac{1}{4}$ micron or less) within the grains.

In connection with the interesting wavy-surface fracture illustrated in Fig. 2a and 2b we wish to report that this type can be obtained on a single crystal. Therefore it is not necessarily associated with a grain boundary. Straight lines such as those seen in Fig. 2b are common on these rounded fractures, and these prove to be Neumann bands.

H. H. UHLIG,* Schenectady, N. Y.—It is gratifying to learn that further fundamental work on this important problem is continuing at Battelle Memorial Institute. The effect of hydrogen in alloys, steels particularly, as the writers—among several investigators—have pointed out, is, first, one of considerable practical importance as yet not fully realized in industry and, second, of value to our understanding of the structure of metals. The latter objective is also practical, but, like most objectives in fundamental investigations, the application is not immediate nor is it necessarily foreseen.

The authors lean rather heavily toward emphasis on the mosaic structure of crystals, and not without cause. Whether or not their experiments constitute proof of such a structure, the evidence contributed by many investigators, to which evidence in this paper adds, shows unequivocally that lattice irregularities exist in otherwise perfect appearing crystals. It is rather the exact nature of these imperfections that is still a subject of opinion.

A satisfactory picture of the mechanism whereby hydrogen embrittles steel must account for several facts. Some of these facts given by the authors raise the legitimate question as to how they fit in with their proposed mechanism of embrittlement.

* Research Laboratory, General Electric Company.

1. Why is pure iron embrittled only slowly? Is the solubility for hydrogen less; is the rate of diffusion less; or are the lattice imperfections of a different kind than exist, for example, in mild steel?
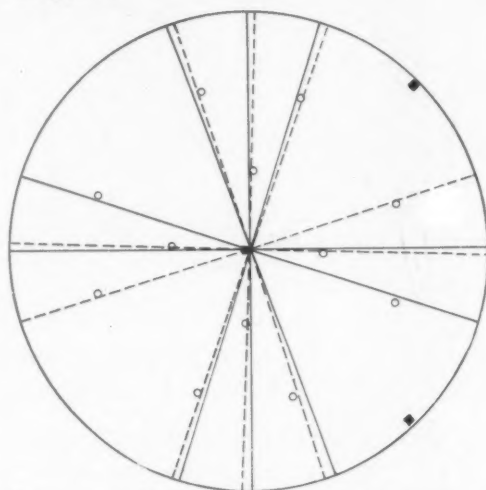
FIG. 10.—STEREOGRAPHIC PROJECTION OF CLEAVAGE SURFACE OF IRON SINGLE CRYSTAL.
■ Poles of cleavage planes, (100).
○ Poles of twinning planes, (112).
——— Normals to crystallographic markings on cleaved surface.
- - - Normals to crystallographic markings on polished and etched surface.

2. If it is the addition of a few tenths per cent carbon to iron that increases the rate of embrittlement, why is the rate of embrittlement of iron decreased upon alloying it with chromium? 18-8, for example, in 0.16-in. diameter rods, we found, is not embrittled after 2 hr. of cathodic polarization. Carr, Schneider and the writer of this discussion[29] showed that H_2 diffusion through chromium-iron alloys containing o to 20 per cent chromium occurs much less rapidly, the greater the chromium content. Do the authors propose that the rifts and vacuous imperfections of the alloy lattice change regularly with addition of chromium to iron, so as markedly to reduce diffusion? Or does the alloy substitution type lattice with irregularities imposed by the alloying atoms themselves, independent of vacuous imperfections, offer greater resistance to diffusion of hydrogen?

3. What is the nature of the rifts and imperfections produced by silicon in iron that ac-

[29] Carr, Schneider and Uhlig: Trans. Electrochem. Soc. (1941) 79, 111–119.

count for a brittle fracture, and how does the mechanism of embrittlement differ from that produced by hydrogen? By what mechanism does fracturing of iron occur at low tempera-

cold-work. Slippage of lattice planes past one another is thereby made much more difficult, the hydrogen atoms serving to lock the slip planes into position. On application of stress,
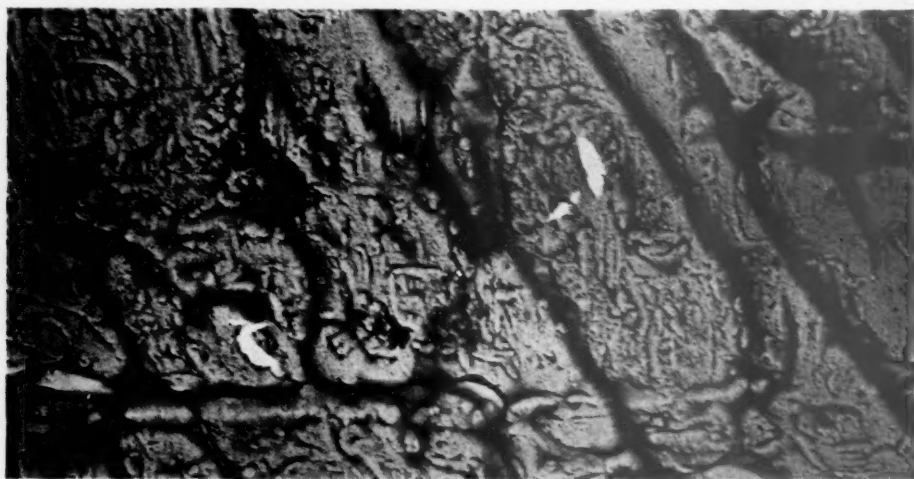
FIG. 11.—ELECTRON PHOTOMICROGRAPH OF CLEAVED SURFACE OF SILICON STEEL. × 8000.
Replica prepared by polystyrene-silica technique. Sample cleaved at liquid nitrogen temperature.
Original magnification given. Reduced ⅓ in reproduction.

tures, and how is this related to similar appearing fractures caused by hydrogen at higher temperatures?

In other words, as the authors themselves indicate, hydrogen is not unique in producing brittle fractures. The facility with which it enters the lattice and the high pressures it can produce at favorable nuclei are most outstanding. This latter property is not characteristic of silicon in iron nor can localllized high pressures reasonably enter into the mechanism of embrittlement of iron at low temperatures.

From the evidence, therefore, the relation between the behavior of hydrogen in macroscopic holes extrapolated to the behavior of hydrogen in submicroscopic channels, and the relative ease of slippage in the iron lattice, is not altogether clear. We can only hope that further evidence will be forthcoming.

One possible mechanism for the embrittlement of iron by hydrogen was not mentioned by the authors but probably deserves consideration. When hydrogen enters the iron lattice, the fields of the interstitial atoms distort and extend the lattice, as X-ray evidence has proved.[30] This distortion is equivalent to strains produced otherwise; for example, by

[30] F. Wever and B. Pfarr: *Mitt*. K. W. I. Eisenforschung (1933) **15**, 147.

this results in a brittle transcrystalline fracture. It is very likely that by a mechanism of this kind carbon renders iron brittle in martensite.

C. A. ZAPFFE AND G. A. MOORE (authors' reply).—Larsen raises the point that photomicrographs in themselves do not prove any structure. There are hundreds of so-called "etch-pit" photomicrographs in existence, which we would like to consider as evidence of mosaic imperfections. It is, however, difficult to overcome the objection that such patterns result from "specific actions of the etching agents." In the case of fractures, if the energy used in breaking is assumed to be distributed over a thin section of the depth of the rough surface, it is found to amount to about 0.02 cal. per mol, as compared with about one million times this value for the energy released at the surface in etching. This would indicate that there is much less chance for the development of false patterns in the fracture method.

In regard to the comments of Uhlig and Larsen on the pre-existence of those structures, there appeared to be very good evidence in advance of this work (refs. 1 and 9); (1) that the hydrogen was present in small openings of some form, and (2) that most metals possess a system of imperfections within the crystal, for

which we find the word "mosaic" most descriptive. Certain similarities in the effects of mechanical and thermal treatments indicated that the two should be associated. Naturally, the exact form of these imperfections was unknown. The present experiment, therefore, is primarily to locate, identify, and describe these openings, rather than to prove their existence.

In further support of this conception, and also in answer to Larsen's last point, note should be taken of the peculiar behavior of the physical properties of iron when hydrogen is added. The ductility and the work necessary to fracture in impact are decreased by the order of 30 times, while the hardness is unaffected, as is the maximum load; but the true tensile strength per unit area at fracture shows some decrease. This situation, true embrittlement, certainly indicates that the continuity of the structure has been disturbed. True embrittlement should be contrasted with the apparent embrittlement on alloying, heat-treating, or cold-working, in which the ductility goes down in inverse proportion as the hardness and strength increase, with the work of fracture changing a smaller amount in either direction. Here it may be fairly said that the difficulty of slip is increased until failure takes place at the higher stress characteristic of an undisturbed cleavage structure.

Final assignment of the various markings to inherent mosaics, hydrogen, deformation, and forced cleavage during fracture obviously must await further study. False markings formed during breaking can soon be eliminated, since the deformation behavior of iron is well known, and it may be assumed that the markings should conform. The pictures by Barrett and Derge are very enlightening. We agree absolutely with their analysis of their pictures, and specifically with the statement that the marks in their Fig. 9 are twin bands. However, we must point out that in each picture they have introduced *two* causes of embrittlement instead of one. Therefore, their findings need not apply to ours. Very few of the structures of Fig. 8 closely resemble our mosaic pictures. Fig. 12a has a very similar crystallographic structure and also contains evidence of twins. This is "hydrogen-free" iron, broken at liquid-air temperature. Thus, the twinning appears to relate to temperature, rather than hydrogen,

both of which influenced the fracture of the Barrett and Derge sample.

A report on the square type of hydrogen patterns will soon be published, in which it will be shown that the markings there are almost entirely on the (001) and (011) planes, rather than on (112) planes, as in these special cases.

We appreciate the electron micrograph of the cold-fractured silicon ferrite and regret that we do not have electron pictures of hydrogen samples. However, Fig. 12b shows silicon ferrite broken at room temperature, and it will be seen that the one picture might almost be an enlargement of the other. This time, Barrett's silicon must have controlled the structure, temperature being ineffective. It should, however, be noted that we have photographed silicon ferrite and have obtained both regular block structures, almost identical with the hydrogen structures, and curved patterns having no crystallographic disposition. The particular irregular structure shown here should, therefore, be tentatively classified as another of the many possible forms of mosaic patterns, and one apparently different in both form and origin from the type common in hydrogen ferrite.

In answer to Barrett and Derge's remarks on the wavy structure of Figs. 2a and 2b, we find them generally associated with the situation known as "veining" in the polished section and apparently with the disorientation referred to here as lineage. We take the two particular cases to be grain boundaries because the areas revealed are of the proper size, but we do not doubt that they may also be formed through the grain when it is large enough to harbor veins and disorientations of similar size. There are not enough crystallographic markings in Fig. 2b to justify any statement of the disposition of the straight lines.

Preliminary examination of cleavages of zinc and bismuth shows a whole new group of markings, with at least five types of irregularities in bismuth. Thus, the study of structures revealed by cleavage, and their interpretation in terms of inherent structure and deformation, is hardly begun. We sincerely hope that Barrett and Derge will continue to collect evidence on these structures and that others will be disposed to join the hunt.

Larsen is bothered by the concept of pressure. We might ask if there is any difference between

internal pressure and the commonly mentioned internal stresses and strains, beyond the fact that pressure here implies that the stresses are equally distributed on the three axes? Even of martensite or silicon? It would appear that the entire field of precipitation reactions involves the generation of pressures of large magnitude.
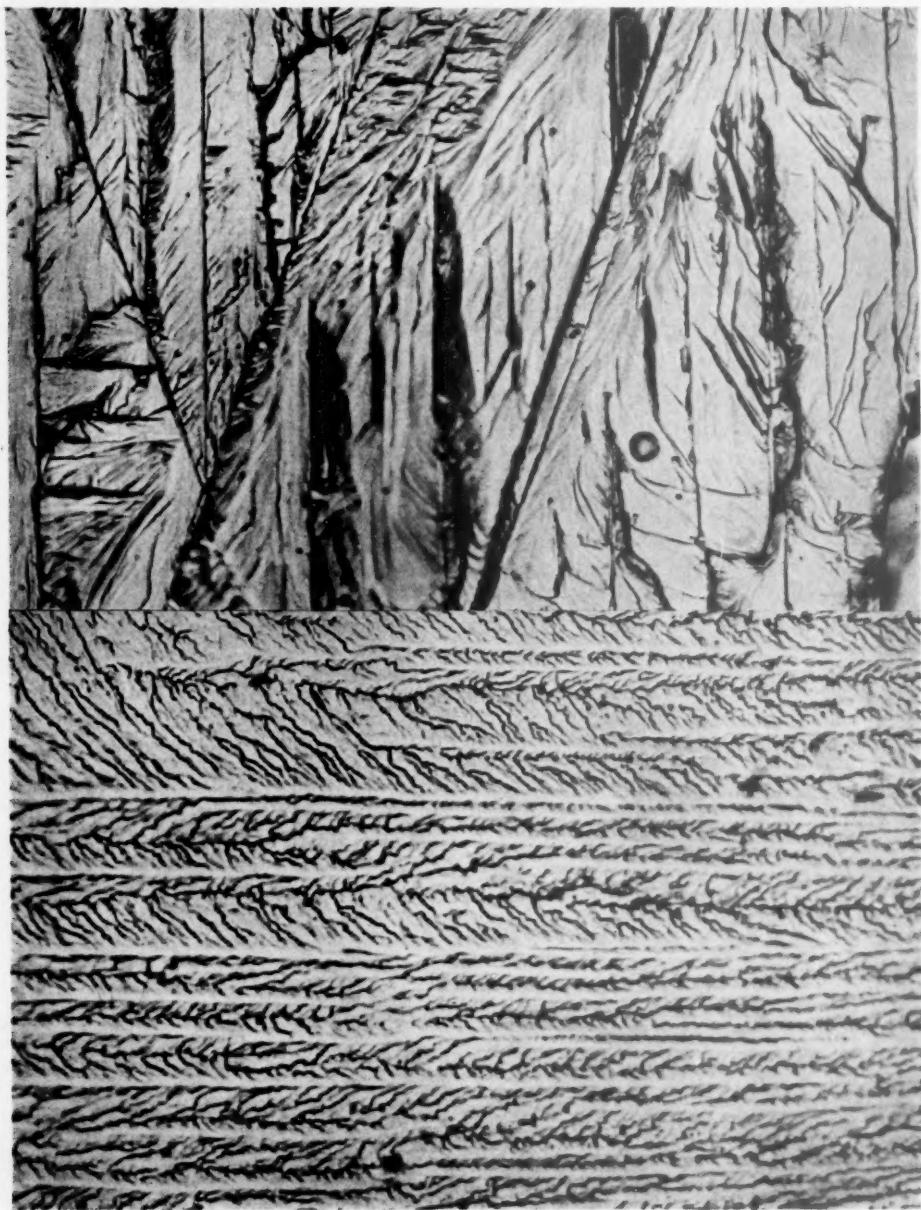
FIG. 12.

a. Pure iron (0.0027 per cent C, no hydrogen) broken at liquid-air temperature. Sample No. S292B1c. × 500.

b. Silicon ferrite broken at room temperature. Sample No. T22B1a. × 1000.

Original magnification given; reduced ⅓ in reproduction.

though we could not measure it on a manometer, would there be anything irrational in discussing pressures caused by the precipitation Uhlig raises additional questions on the mechanism of embrittlement. We have stated in conclusions 1, 2, and 3 a self-consistent

mechanism in the limited terminology of occlusion in mosaic rifts, cleavage through these rifts, the action of triaxial tension resulting from gas pressure, and the effect of fragmentation. Many specific observations do not at once appear to fit this mechanism, yet all that have come to our attention are found to fit when considered in the same terminology and when allowance is made for occlusion and diffusion factors already known from the work of others. Uhlig's questions can be answered in this way:

1. The "passivity" of pure and well-annealed metals to hydrogen has been observed many times. Mathematical diffusion studies tend to indicate that the rates observed at room temperature are more appropriate to diffusion through openings than through the lattice. It need not be presumed that the imperfections are of different kind in the purer metal, but only that they are of more limited extent, so that a condition is reached where no single group of connecting imperfections can extend entirely through the piece. With diffusion to many sections limited by the slower process of passage through the lattice, the time for saturation and embrittlement becomes very long.

2. Very little is yet known of the effect of alloys and impurities. Carbon and sulphur appear to increase the diffusion rates, while chromium probably causes a decrease. Chromium appears to reduce the difference between the high-temperature and low-temperature solubilities, hence to reduce the available dissociation pressure of the solution, and, therefore, the embrittlement. Nickel probably increases the temperature coefficient of solubility, leading to higher pressure and more embrittlement. There is no evidence yet that a difference exists in the irregularities of structure, yet it is logical to presume that when a change in normal microstructure occurs, a change in mosaic structure may also occur. Thus, carbon and sulphur might be expected to affect the structure more than the solubility, while the effect of nickel and chromium is in line with the known solubilities in the pure metals.

The observation on 18-8 is inapplicable to this problem, since hydrogen embrittlement appears to be exclusive with the alpha lattice alloys. In the gamma lattice, the solubility of hydrogen is much higher, hence the available pressure is limited to 100 to 1000 atmospheres for attainable solutions. Consequently, the yield or critical stress is not exceeded and embrittlement cannot take place.

3. The nature of the imperfection structure in silicon ferrite and cold iron is largely unknown, although it has a resemblance to iron-hydrogen. The possibility of precipitation of small residual traces of various impurities on cooling from room temperature to liquid-air temperature should not be too freely discarded as a cause of low-temperature embrittlement. Stress, if not pressure, must remain an important factor in all cases.

4. It does not appear to be possible to make a complete interpretation of the work of Wever and Pfarr by the X-ray method. Their measurements show either stress, distortion, or fragmentation of the lattice. We feel that the observed effect is primarily fragmentation, but that some effect of the pressure may be included. True embrittlement cannot be explained exclusively as strain-interference with slip, because the first effect is that of hardening. Hydrogen does not harden or strengthen the iron. We accounted for a minor contribution from slip interference in the third conclusion of the paper.

Constitution of the Iron-rich Iron-nickel-silicon Alloys at 600°C.

By Earl S. Greiner* and Eric R. Jette,† Members A.I.M.E.

(New York Meeting, February 1943)

Abstract‡

THE constitution of the iron-rich iron-nickel-silicon alloys at 600°C. has been determined by X-ray crystal structure methods. If the results are represented isothermally by a conventional equilateral triangular plot, the single-phase solid solution (body-centered cubic structure) of the iron-rich alloys at 600°C. is bounded by four two-phase areas. Three three-phase areas separate the respective two-phase areas. Three of the phases in the polyphase areas have the same structures as the corresponding phases in the binary iron-nickel or iron-silicon alloys. There are two phases, however, that have not been reported previously and whose structures have been tentatively identified in the present investigation.

The solid solubility limit of the iron-rich solid solution at 600°C. was determined by comparing the lattice constants of this body-centered cubic phase in the single and polyphase areas. It has been shown that the lattice constants of ternary alloys may be represented by surfaces whose distances above the ternary plot (representing atomic composition) are proportional to the lattice constants of the respective alloys. Then the intersections of the surface for the single-phase alloys with those for the corresponding phase in the polyphase alloys, at the respective temperatures, are the solid solubility limits of the single-phase alloys at these temperatures. The data of the present investigation were evaluated by this method, although by a system of orthographic projection it was possible to represent the three-dimensional model in two-dimensional diagrams.

This investigation has shown that the solid solubility of nickel in the body-centered cubic phase of the iron-rich iron-nickel-silicon alloys at 600°C. changes from 3.7 weight per cent (Owen and Sulley) in the binary iron-nickel alloys to 5.0 per cent in the ternary alloys containing 4.8 per cent silicon. Further additions of silicon increase the solid solubility limit of nickel to 16.0 per cent at 12.6 per cent silicon. From this point the limit decreases to 9.5 per cent nickel at 15.5 per cent silicon and is, of course, zero at 15.3 per cent silicon in the binary iron-silicon alloys.

* Graduate Student in Metallurgy, Columbia University, New York, N. Y.

† Professor of Metallurgy, Columbia University, N. Y.

Carbides in Low Chromium-molybdenum Steels[1]

By Walter Crafts,* Member A.I.M.E., and C. M. Offenhauer*

In a previous study[1] of the carbide phase of chromium steels, it was shown that chromium carbide (Cr_7C_3) is a more stable carbide than cementite (Fe_3C) at tempering temperatures above about 500°C. in quenched steels containing from about 1 to 7.5 per cent chromium. Below this temperature the carbide phase was found to consist of cementite in all of the steels examined.

In the present investigation it was found that a similar change in the carbide phase takes place in molybdenum and in chromium-molybdenum steels at approximately the same tempering temperatures. The approximate ranges of occurrence of the alloy carbides Cr_7C_3, Cr_4C, and Mo_2C have been determined in steels containing up to 5 per cent chromium, 1 per cent molybdenum and 0.60 per cent carbon.

The experimental steels were made in small high-frequency furnaces from Armco ingot iron, low-carbon ferrochromium and calcium molybdate and were poured into 2-in. ingots, which were forged to 1-in. round bars. Sections of the bars were heated to the carbide-solution temperature and cooled rapidly to induce austenite transformation at relatively low temperatures. The steels were subject to some segregation, therefore comparatively high temperatures were necessary to dissolve all of the carbides. The microstructure of the quenched specimens was examined to

verify the belief that the carbides had been dissolved, and also to determine the nature of the nonmartensitic structure of incompletely hardened steels. Ferrite and pseudomartensite were present in some of the specimens, but all specimens were quenched at such a rate that pearlite was not formed, in order to ensure the formation of the carbides at temperatures lower than about 500°C. It had been found previously[1] that in chromium steels the chromium carbide could be produced by transformation of austenite in the pearlite range above 500°C., and, in order to start the tempering treatment with the carbide present as cementite, the absence of pearlite was considered to be essential. The specimens were tempered for 64 hr. to permit the formation of the stable carbide.

After tempering, the specimens were submitted to microscopic and X-ray examination. The carbides were separated either electrolytically in a 5 per cent HCl electrolyte or with an acidified copper-potassium chloride solution. The crystal structure of the carbide phases was determined by the Debye-Scherrer type of X-ray patterns. The X-ray patterns obtained from specimens near the boundaries between two types of carbides were generally weak and diffuse as compared with the other patterns. For this reason, and because the more soluble components may be masked, the boundaries between the phases could not be determined precisely. However, the X-ray analysis of electrolytically separated carbides has given consistently reproducible results

and is believed to be reliable in the identification of the principal ranges of the carbide phases.

MOLYBDENUM STEELS

The carbides in plain molybdenum steels were studied in steels containing up to 1.5 per cent Mo and 0.40 per cent C. The results of X-ray examination, together with the chemical compositions and heat-treatment, are given in Table 1 and illustrated graphically in Figs. 1, 2 and 3. A transition was found from cementite (Fe_3C) in steels tempered below about 550°C. to a molybdenum carbide (Mo_2C) in the higher-molybdenum steels tempered at higher temperatures. The effect of composition on the ranges of occurrence of

TABLE 1.—*Molybdenum Steels*

Heat No.	Composition, Per Cent				Quench		Tempering Temperature, Deg. C.	X-ray Structure
	C	Mn^a	Si^a	Mo	Temperature Deg. C.	Medium		
1	0.08	0.50	0.25	0.16	925	Water	550	Fe_3C
							600	Fe_3C
							650	Fe_3C
							700	Fe_3C
2	0.08	0.50	0.25	0.45	925	Water	550	Fe_3C, Mo_2C ?
							600	Fe_3C, Mo_2C
							650	Mo_2C, Fe_3C
							700	Mo_2C, Fe_3C
3	0.11	0.50	0.25	0.78	1100	Water	500	Fe_3C
							550	Fe_3C
							600	Mo_2C
							650	Mo_2C
4	0.11	0.50	0.25	1.40	1100	Water	450	Fe_3C ? (poor pattern)
							500	Blank
							550	Blank
							600	Mo_2C (poor pattern)
5	0.22	0.50	0.25	0.18	925	Water	600	Fe_3C
							650	Fe_3C
6	0.19	0.50	0.25	0.52	925	Water	500	Fe_3C
							550	Blank
							600	Fe_3C
							650	Fe_3C (poor pattern)
7	0.17	0.50	0.25	1.00	925	Water	450	Fe_3C
							500	Fe_3C
							550	Mo_2C, Fe_3C
							600	Mo_2C, Fe_3C
8	0.15	0.50	0.25	1.67	1050	Water	450	Fe_3C ? (poor pattern)
							500	Fe_3C (poor pattern)
							550	Fe_3C (poor pattern)
							600	Mo_2C
9	0.30	0.50	0.25	0.19	925	Water	550	Fe_3C
							600	Fe_3C
							650	Fe_3C
							700	Fe_3C, Mo_2C ?
10	0.28	0.50	0.25	0.47	925	Water	550	Fe_3C
							600	Fe_3C
							650	Fe_3C
							700	Fe_3C (poor pattern)
11	0.20	0.50	0.25	0.83	1100	Water	450	Fe_3C
							500	Fe_3C
							550	Fe_3C, Mo_2C
							600	Mo_2C, Fe_3C
12	0.25	0.50	0.25	0.83	1000	Oil	450	Fe_3C (poor pattern)
							500	Fe_3C
							550	Fe_3C
							600	Mo_2C, Fe_3C
13	0.26	0.50	0.25	1.43	1000	Oil	450	Fe_3C
							550	Fe_3C (poor pattern)
							600	Mo_2C, Fe_3C
14	0.40	0.50	0.32	0.24	925	Water	550	Fe_3C
							600	Fe_3C
							650	Fe_3C
15	0.31	0.50	0.25	1.16	1100	Water	500	Fe_3C
							550	Fe_3C, tr. Mo_2C
							600	Fe_3C, Mo_2C

ᵃ Approximate analysis.

the carbides is illustrated more clearly in Fig. 4, which shows the isothermal section at 600°C. Molybdenum carbide was formed as the molybdenum content

In comparison with the Fe-C-Cr system at 0.10 per cent C, which is shown in Fig. 5, it is apparent that the relative position of Cr_7C_3 to Fe_3C is similar to the relation
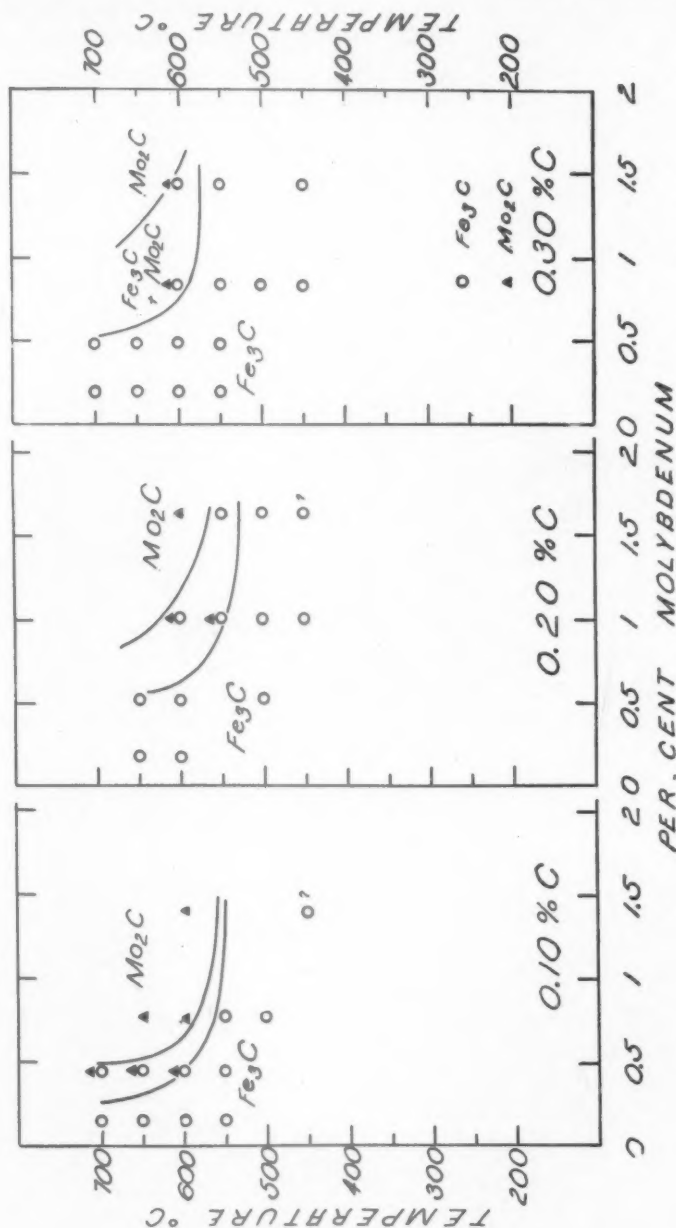
FIGS. 1-3.—CARBIDES IN QUENCHED AND TEMPERED MOLYBDENUM STEELS.

Fig. 1, C, 0.10 per cent.   Fig. 2, C, 0.20 per cent.   Fig. 3, C, 0.30 per cent.

exceeded 0.25 per cent at low carbon contents, and with increasing amounts of molybdenum at higher carbon levels in the ratio of about five parts of molybdenum to one part of carbon.

between Mo_2C and Fe_3C illustrated in Fig. 1. However, molybdenum is almost two times as effective as chromium in terms of weight per cent required to produce the alloy carbides at high tempering

temperatures, and the transition range between cementite and the alloy carbide is slightly greater in the molybdenum system.

The molybdenum carbide (Mo_2C) that was found in the molybdenum steels has a closely packed hexagonal crystal structure. This carbide (Mo_2C) has been reported in very high-molybdenum alloys by Takei[2] and Lester,[3] but has not previously been noted in low-molybdenum steels.[3,4] The double carbide of iron and
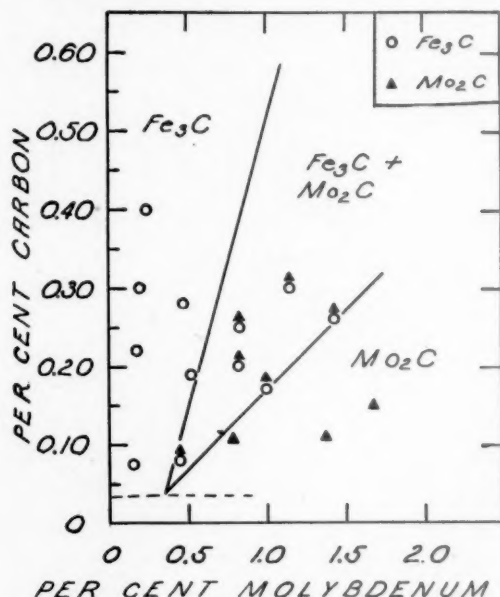
FIG. 4.—CARBIDES IN MOLYBDENUM STEELS QUENCHED AND TEMPERED AT 600°C.
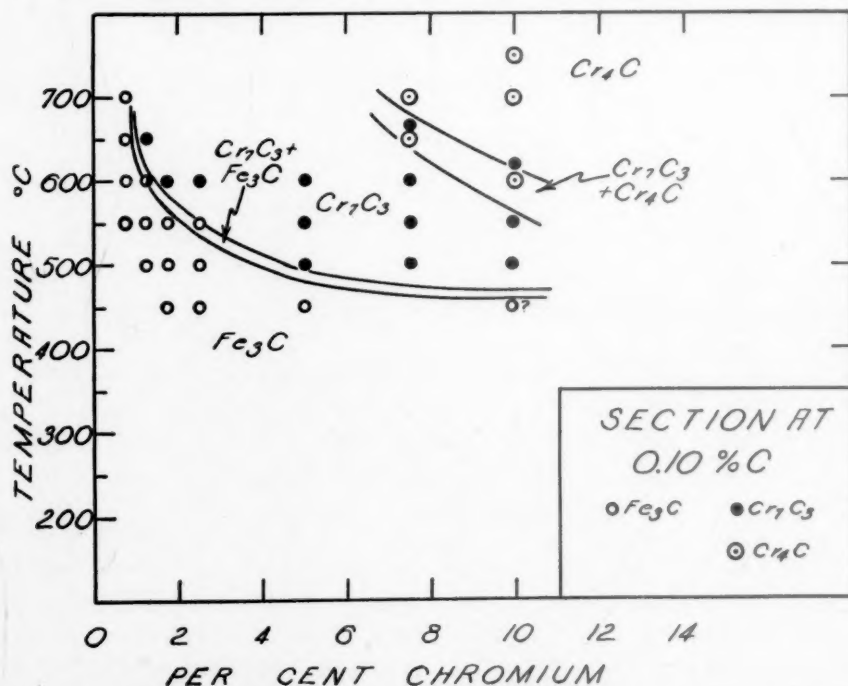
FIG. 5.—CARBIDES IN QUENCHED AND TEMPERED 0.10 PER CENT C CHROMIUM STEELS.

molybdenum, which has been reported to be present in steels of somewhat higher molybdenum content, was not found in these low-molybdenum steels.

Chemical analysis was made on carbides extracted electrolytically from samples tempered at temperatures designed to develop Mo_2C at one temperature and Fe_3C at another temperature. The presence of the desired carbide was confirmed by X-ray analysis. The results of the chemical analysis are given in Table 2.

were found in simple chromium and molybdenum systems. As shown in Fig. 6, the carbides produced in 0.10 per cent C chromium steels were not appreciably altered by the addition of 0.25 per cent Mo. At the 0.50 and 1.0 per cent Mo levels, as shown in Figs. 7 and 8, the molybdenum carbide was present in low-chromium steels after tempering at relatively high temperatures. As the chromium content was increased, the form of the carbide changed progressively from Mo_2C to

TABLE 2.—*Chemical Analysis of Carbides Extracted Electrolytically*

Heat No.	C, Per Cent	Mo, Per Cent	Tempering Temperature, Deg. C.	Crystal Structure	Ratio Mo:Fe	Fe in Mo_2C, Per Cent	Mo in Fe_3C, Per Cent
3	0.11	0.78	600	Mo_2C	1.15:1	43.7	
			650	Mo_2C	3.00:1	23.5	
8	0.15	1.67	650	Mo_2C	3.77:1	19.7	
3	0.11	0.78	500	Fe_3C	0.63:1		39.0

The Mo_2C type carbide contained 19.7 and 23.5 per cent iron in samples tempered at 650°C.; it appears that the solubility of Mo_2C for iron at 650° is in the neighborhood of 20 per cent. In the sample tempered at 600°C., the iron content was much higher. As shown in Fig. 1, this sample was treated at a temperature close to the mixed field of Fe_3C and Mo_2C. A similarly high iron content in Cr_7C_3 was also found near the transition range in chromium steels[1] and is believed to result from a mixture of Fe_3C with Mo_2C as well as from the iron soluble in the molybdenum carbide. It also appeared that Fe_3C was capable of dissolving up to about 39 per cent Mo.

COMBINATION OF ALLOYING ELEMENTS

Chromium-molybdenum steels (Table 3) were studied in order to determine the combined effects of these elements on the carbide phase. Steels containing up to 0.60 per cent C, 5.0 per cent Cr, and 1.0 per cent Mo were investigated by X-ray analysis, and it was found that these alloys contained all of the carbides that

Cr_7C_3 to Cr_4C at 5 per cent Cr. An insufficient number of steels was available to define their ranges of occurrence accurately, but the probable fields and their approximate ranges have been indicated. Molybdenum appeared to increase the tendency toward the formation of the Cr_4C type carbide. In plain chromium steels tempered at 600°C., Cr_4C was not found at less than about 9 per cent Cr, but in 1 per cent Mo steel Cr_4C was found at 5 per cent Cr. The temperature of transition from cementite to the alloy carbides was raised by molybdenum from about 500°C. in plain chromium steels to over 550°C. in the 1 per cent Mo steels. However, the transition temperature did not change significantly with increase in the chromium content.

Sections of the diagram at 0.40 per cent C are shown in Figs. 9, 10 and 11. Larger amounts of alloying agents were required for the formation of the alloy carbides, and the molybdenum carbide was found only in the 1 per cent alloys.

The isothermal sections of the chromium and chromium-molybdenum systems at
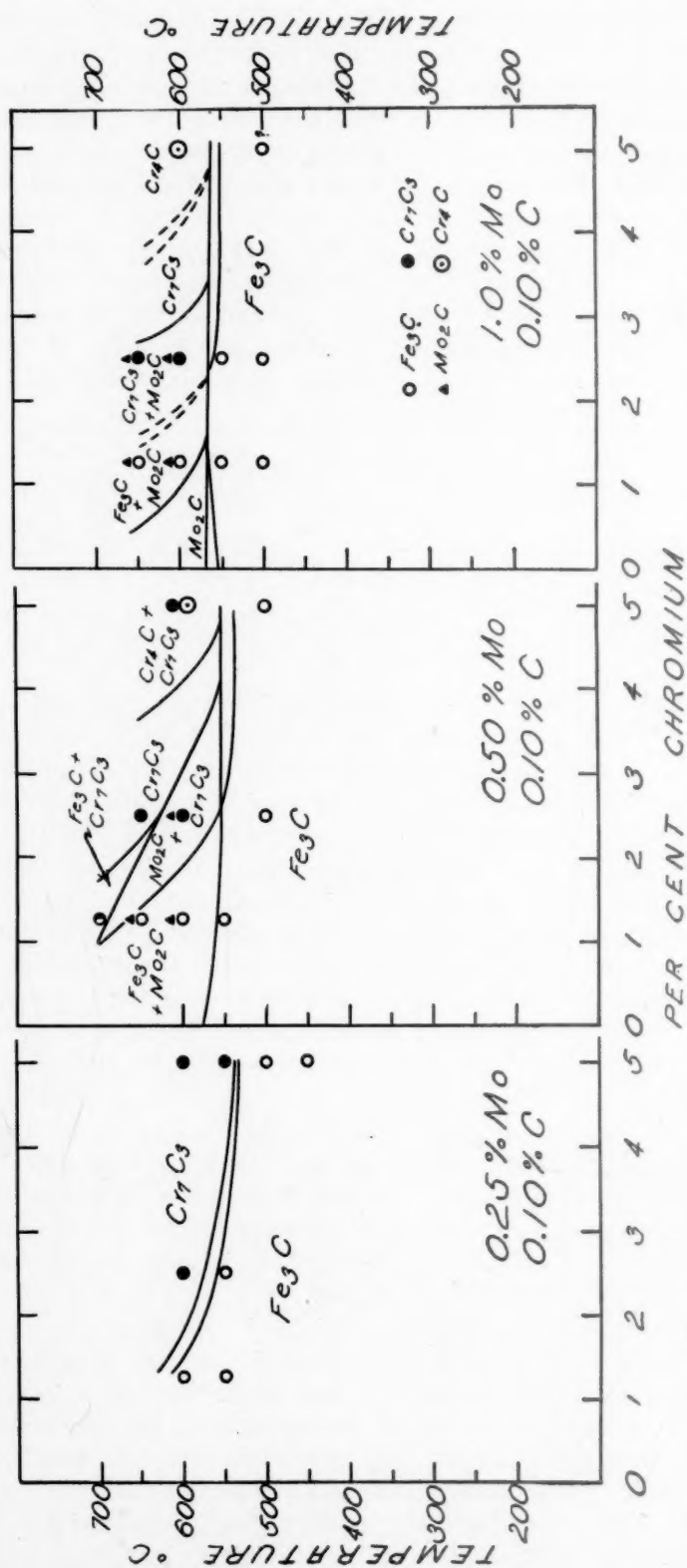
Fig. 6.   Figs. 6–8.—Carbides in quenched and tempered chromium-molybdenum steels.

Fig. 6, C, 0.10 per cent; Mo, 0.25 per cent.
Fig. 7, C, 0.10 per cent; Mo, 0.50 per cent.
Fig. 8, C, 0.10 per cent; Mo, 1.0 per cent.
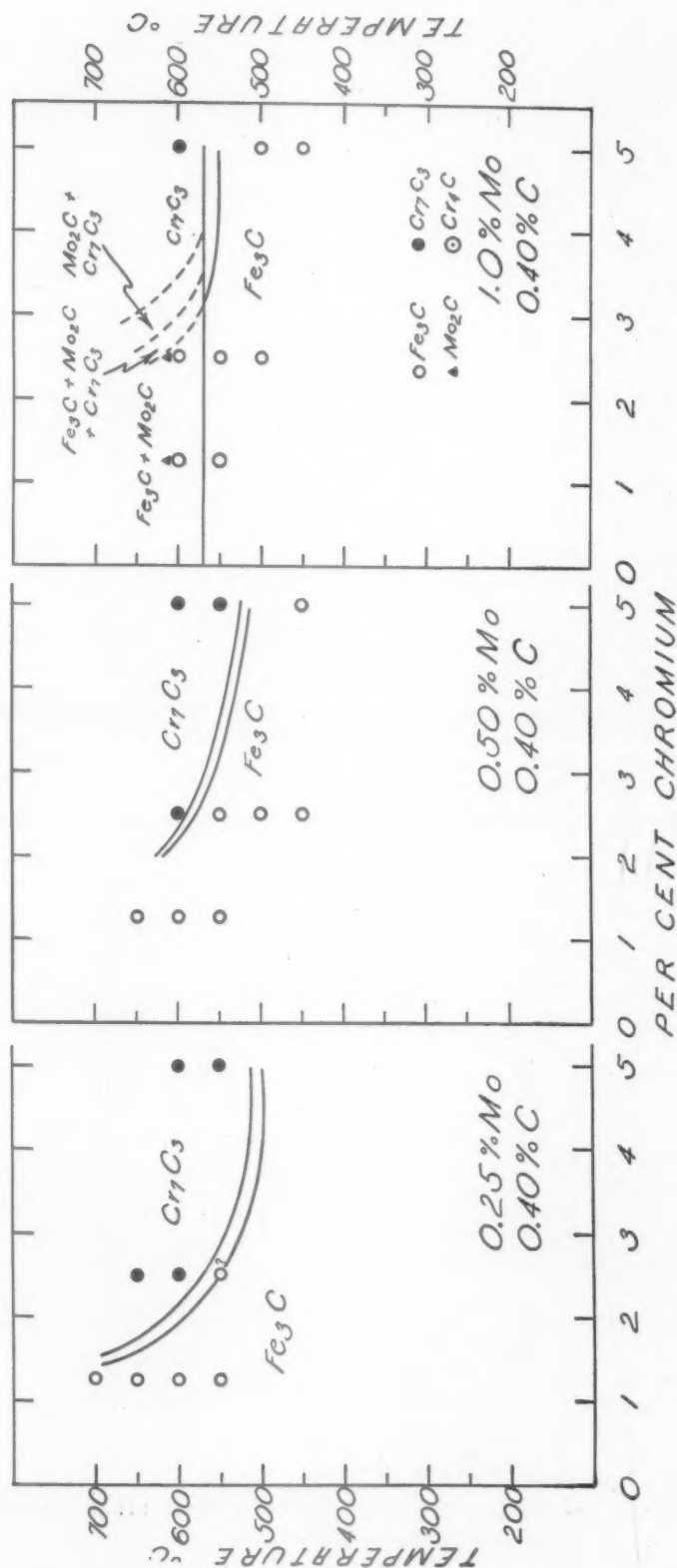
FIG. 9.

FIG. 10.

FIG. 11.

FIGS. 9–11.—CARBIDES IN QUENCHED AND TEMPERED CHROMIUM-MOLYBDENUM STEELS.

Fig. 9, C, 0.40 per cent; Mo, 0.25 per cent.
Fig. 10, C, 0.40 per cent; Mo, 0.50 per cent.
Fig. 11, C, 0.40 per cent; Mo, 1.0 per cent.
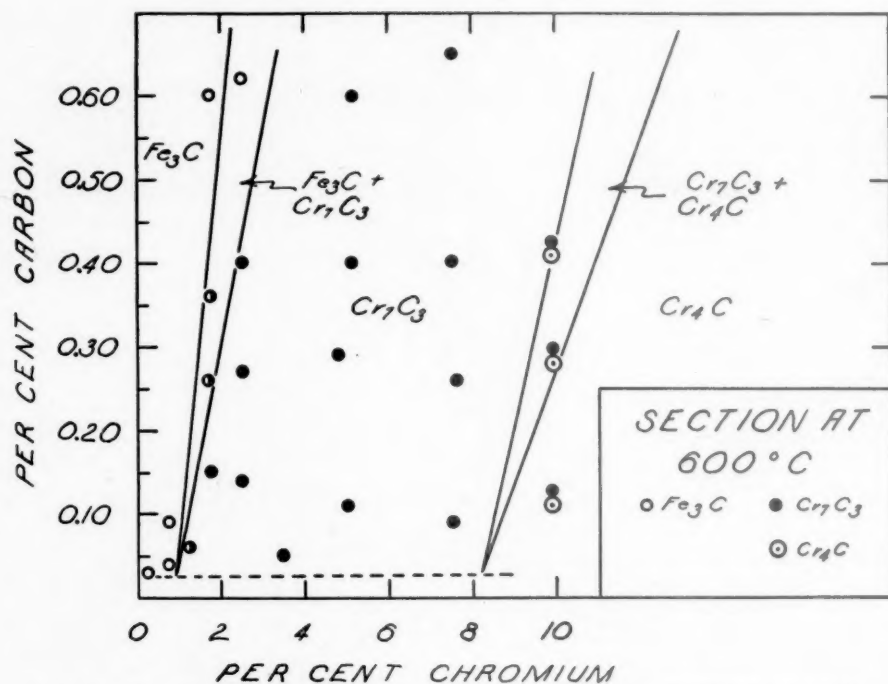
FIG. 12.—CARBIDES IN CHROMIUM STEELS QUENCHED AND TEMPERED AT 600°C.
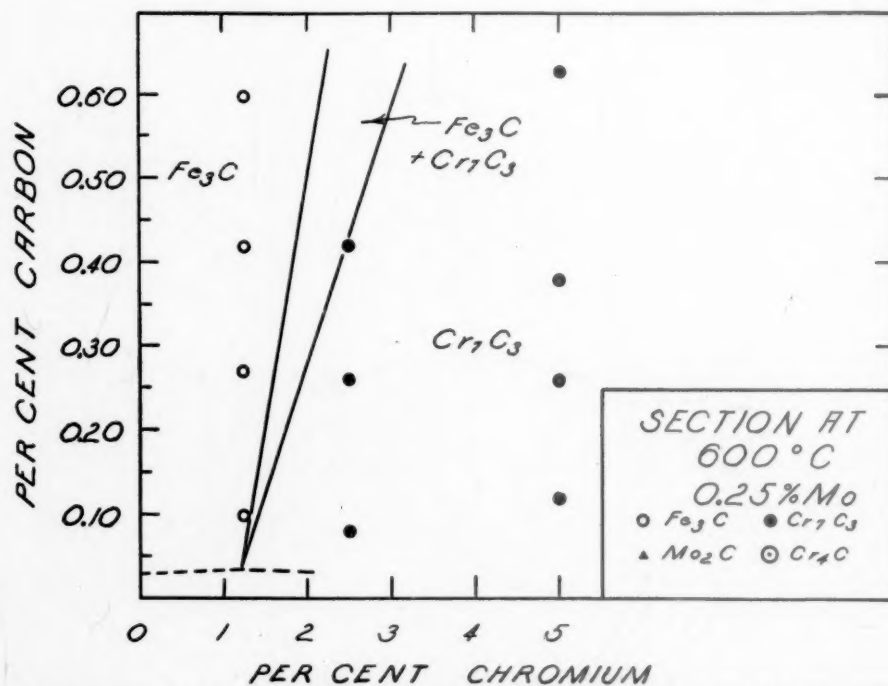
FIG. 13.—CARBIDES IN 0.25 PER CENT MO CHROMIUM-MOLYBDENUM STEELS QUENCHED AND
TEMPERED AT 600°C.
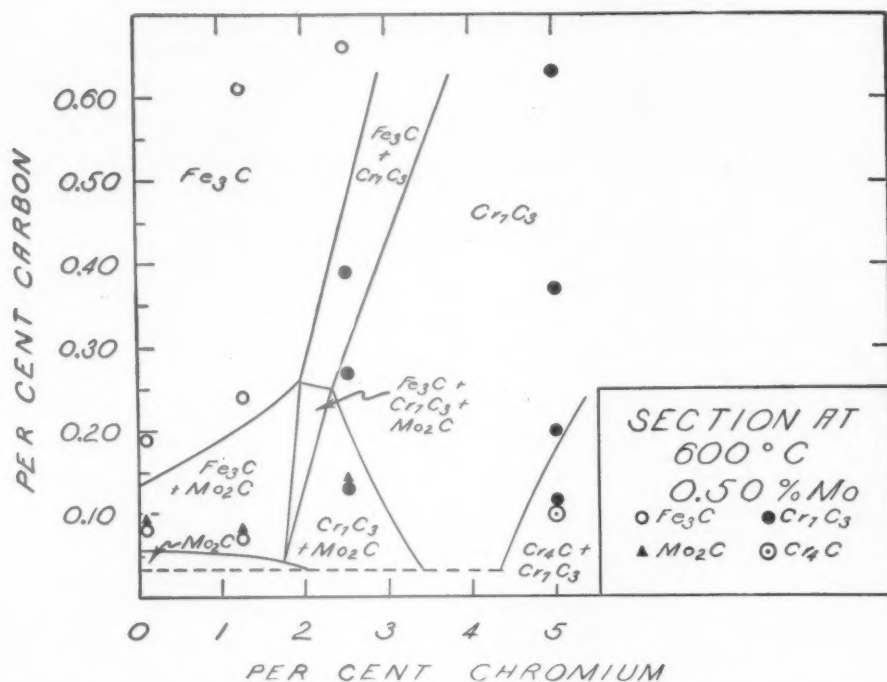
FIG. 14.—CARBIDES IN 0.50 PER CENT MO CHROMIUM-MOLYBDENUM STEELS QUENCHED AND TEMPERED AT 600°C.
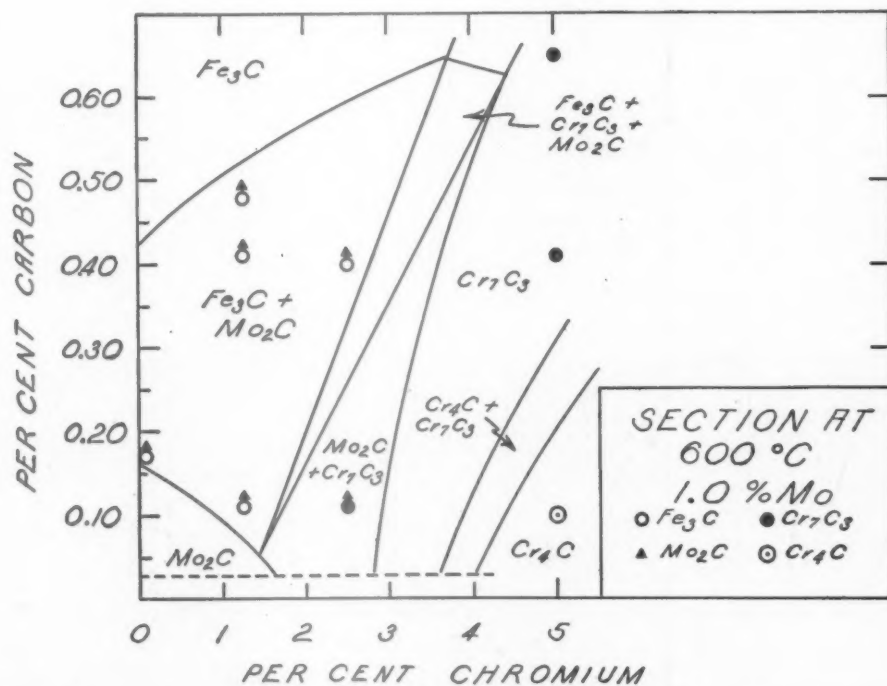
FIG. 15.—CARBIDES IN 1.0 PER CENT MO CHROMIUM-MOLYBDENUM STEELS QUENCHED AND TEMPERED AT 600°C.

TABLE 3.—*Chromium-molybdenum Steels*

Heat No.	Composition, Per Cent					Quench		Tempering Temperature, Deg. C.	X-ray Structure
	C	Mn	Si	Cr	Mo	Temperature, Deg. C.	Medium		
16	0.10	0.50[a]	0.25[a]	1.25[a]	0.28	925	Water	550	Fe_3C
								600	Fe_3C
17	0.08	0.50[a]	0.25[a]	2.5[a]	0.20	925	Water	500	Blank
								550	Fe_3C (broad lines)
								600	Cr_7C_3 (poor pattern)
18	0.12	0.50[a]	0.23	5.0[a]	0.20	925	Air	450	Fe_3C
								500	Fe_3C
								550	Cr_7C_3
								600	Cr_7C_3
19	0.07	0.51	0.25[a]	1.25[a]	0.43	925	Water	550	Fe_3C
								600	Mo_2C, Fe_3C
								650	Mo_2C, Fe_3C
								700	Cr_7C_3, Fe_3C
20	0.13	0.50[a]	0.25[a]	2.53	0.37	925	Water	500	Fe_3C
								600	Mo_2C, Cr_7C_3 (distorted)
								650	Cr_7C_3
21	0.09	0.50[a]	0.25[a]	5.0[a]	0.53	925	Oil	500	Fe_3C
								600	Cr_4C, Cr_7C_3
22	0.11	0.50[a]	0.15	1.25[a]	0.86	1000	Water	500	Fe_3C
								550	Fe_3C (poor pattern)
								600	Mo_2C, Fe_3C
								650	Mo_2C, Fe_3C
23	0.11	0.50[a]	0.07	2.5[a]	1.14	1000	Water	500	Fe_3C (poor pattern)
								550	Fe_3C ? (poor pattern)
								600	Mo_2C, Cr_7C_3
								650	Mo_2C, Cr_7C_3
24	0.10	0.50[a]	0.14	5.0[a]	1.16	1000	Air	500	Fe_3C ?
								600	Cr_4C
25	0.27	0.50[a]	0.25[a]	1.25[a]	0.22	925	Water	550	Fe_3C
								600	Fe_3C
								650	Fe_3C
								700	Fe_3C
26	0.26	0.50[a]	0.25[a]	2.5[a]	0.23	925	Water	500	Fe_3C
								550	Fe_3C
								600	Cr_7C_3
								650	Cr_7C_3
27	0 26	0.50[a]	0.25[a]	5.0[a]	0.23	925	Air	450	Fe_3C
								500	Fe_3C (poor pattern)
								550	Cr_7C_3
								600	Cr_7C_3
28	0.24	0.50[a]	0.25[a]	1.25[a]	0.42	925	Water	500	Fe_3C
								550	Fe_3C
								600	Fe_3C
								650	Fe_3C
29	0.27	0.50[a]	0.25[a]	2.5[a]	0.51	925	Water	450	Fe_3C
								500	Fe_3C
								550	Fe_3C, Cr_7C_3 ?
								600	Cr_7C_3, Fe_3C ?
30	0.20	0.50[a]	0.25[a]	5.0[a]	0.43	925	Air	450	Fe_3C
								500	Blank
								550	Cr_7C_3 ?
								600	Cr_7C_3 (poor pattern)
31	0.18	0.50[a]	0.25[a]	2.5[a]	0.96	1100	Water	450	Fe_3C
								500	Fe_3C (poor pattern)
								550	Fe_3C, Fe_3O_4 type (poor pattern)
32	0.18	0.50[a]	0.25[a]	5.04	0.92	1100	Air	450	Fe_3C (poor pattern)
								500	Cr_4C, Fe_3O_4 type
								600	Cr_4C
33	0.42	0.50[a]	0.25[a]	1.25[a]	0.25[a]	925	Oil	550	Fe_3C
								600	Fe_3C
								650	Fe_3C
								700	Fe_3C
34	0.42	0.50[a]	0.25[a]	2.5[a]	0.25[a]	925	Oil	550	Fe_3C ?
								600	Cr_7C_3
								650	Cr_7C_3
35	0.38	0.50[a]	0.25[a]	5.0[a]	0.25[a]	1000	Air	550	Cr_7C_3
								600	Cr_7C_3
36	0.39	0.50[a]	0.25[a]	2.5[a]	0.50[a]	925	Oil	450	Fe_3C
								500	Fe_3C
								550	Fe_3C, Cr_7C_3 ?
								600	Cr_7C_3

TABLE 3.—(*Continued*)

Heat No.	Composition, Per Cent					Quench		Tempering Temperature, Deg. C.	X-ray Structure
	C	Mn	Si	Cr	Mo	Temperature, Deg. C.	Medium		
37	0.37	0.50ᵃ	0.25ᵃ	5.0ᵃ	0.47	1000	Air	450 500 550 600	Fe_3O_4 type, Fe_3C ? Blank Fe_3C ? Cr_7C_3
38	0.41	0.50ᵃ	0.25ᵃ	1.25ᵃ	1.10	1100	Water	550 600	Fe_3C, Mo_2C Tr. Mo_2C, Fe_3C
39	0.40	0.50ᵃ	0.25ᵃ	2.5ᵃ	1.04	1100	Oil	500 550 600	Fe_3C (poor pattern) Fe_3C, Cr_4C ? (poor pattern) Mo_2C, Fe_3C
40	0.41	0.50ᵃ	0.25ᵃ	5.0ᵃ	1.08	1100	Air	450 500 600	Fe_3C, Fe_3O_4 type Fe_3C Cr_7C_3
41	0.60	0.50ᵃ	0.25ᵃ	1.25ᵃ	0.25ᵃ	850	Water	600 650 700	Fe_3C Fe_3C Fe_3C
42	0.72	0.50ᵃ	0.25ᵃ	2.5ᵃ	0.25ᵃ	900	Oil	600 650	Fe_3C, Cr_7C_3 Fe_3C, Cr_7C_3
43	0.63	0.50ᵃ	0.25ᵃ	5.0ᵃ	0.25ᵃ	1050	Air	550 600	Cr_7C_3, Fe_3C ? Cr_7C_3
44	0.61	0.50ᵃ	0.25ᵃ	1.25ᵃ	0.36	850	Water	600 650 700	Fe_3C Fe_3C Fe_3C
45	0.66	0.50ᵃ	0.22	2.5ᵃ	0.41	900	Oil	600 650	Fe_3C Fe_3C
46	0.63	0.49	0.20	5.0ᵃ	0.50	1100	Air	600	Cr_7C_3
47	0.48	0.50ᵃ	0.06	1.25ᵃ	1.16	1100	Oil	600 650 700	Mo_2C, Fe_3C Mo_2C, Fe_3C Mo_2C, Fe_3C
48	0.75	0.51	0.25	2.5ᵃ	0.85	1100	Oil	550 600	Fe_3C (poor pattern) Fe_3C (poor pattern)
49	0.65	0.50ᵃ	0.24	5.05	0.75	1100	Air	550 600	Fe_3C ? Cr_7C_3

ᵃ Approximate analysis.

600°C. are shown in Figs. 12, 13, 14 and 15. As in the diagrams just described, only approximations of the ranges of the probable carbide fields are indicated. There is a close similarity between the chromium system in Fig. 12 and the molybdenum system shown in Fig. 4. In the chromium-molybdenum series at 0.50 per cent Mo, the molybdenum-carbide Mo_2C was indicated at low carbon and chromium contents. As the carbon was increased, the carbide phase changed to a mixture of Mo_2C and Fe_3C and finally to Fe_3C alone. As the chromium content was increased, a mixture of the molybdenum carbide and the chromium-carbide Cr_7C_3 was formed. At higher chromium contents, Cr_7C_3 and a mixture of Cr_7C_3 and Cr_4C were produced.

In the 1 per cent Mo chromium-molybdenum series the same tendencies may be noted, but with the differences that the fields containing molybdenum carbides were expanded and that the Cr_4C type carbide was produced at much lower chromium contents than in the plain chromium steels.

SUMMARY

Steels containing up to 1.5 per cent Mo without chromium and steels with up to 1 per cent Mo and 5 per cent Cr have been examined to determine the nature of the carbide phases after quenching and tempering. Cementite was found in steels tempered below 500° to 550°C. and alloy carbides were found after tempering at higher temperatures. The types of alloy carbides, which depended on the composition of the steel and the temperature of formation, were: Cr_7C_3 in intermediate chromium steels; Cr_4C in higher chromium steels; and Mo_2C in molybdenum steels.

This molybdenum carbide (Mo_2C), which previously has been observed only in high-molybdenum alloys, was found by chemical analysis to contain about 20 per cent iron. All of these carbides were found in chromium-molybdenum steels, and the approximate ranges of the carbides with respect to tempering temperature and composition have been correlated in phase diagrams.

ACKNOWLEDGMENTS

The authors wish to acknowledge the generous cooperation of the staff of the Union Carbide and Carbon Research Laboratories, Inc., and especially the valuable assistance of W. D. Forgeng, in carrying out this investigation.

REFERENCES

1. W. Crafts and C. M. Offenhauer: *Trans.* A.I.M.E. (1942) **150**, 275–282.
2. T. Takei: *Sci. Repts.* Sendai (1932) [1] **21**, 127–148.
3. J. L. Gregg: The Alloys of Molybdenum and Iron. New York, 1932. McGraw-Hill Book Co.
4. J. R. Blanchard, R. M. Parke and A. J. Herzig: *Trans.* Amer. Soc. Metals (1939) **27**, 697–718.

DISCUSSION

(*A. B. Greninger presiding*)

G. A. MOORE,* Columbus, Ohio.—It is quite apparent that this paper opens a field of investigation that may be expected to be very important to the alloy-steel industry. Going beyond the valuable equilibrium data presented here, it may be presumed that various specimens of the same analysis will differ in their carbide compositions, and hence will show different reactions to subsequent heat-treatments. Analysis of the carbides, therefore, is of immediate and practical importance.

In making such analyses at Battelle Memorial Institute, it has been observed that some of the carbide fraction decomposes to graphite during solution of the metal. Since we do not know whether this effect is preferential among the various carbides, the validity of the analysis is

* Research Metallurgist, Battelle Memorial Institute.

subject to question. I would therefore like to ask the authors to state in some detail the solution procedures they have found most satisfactory, and to give any evidence they may have of the degree to which the separation of the carbides may be considered quantitatively correct.

M. COHEN,* Cambridge, Mass.—Would it be feasible to use the authors' carbide extraction method for determining the percentage of carbide phase in the steel? If so, is the method reliable for the range of particle sizes encountered in tempered steels?

Do the authors have any data on the weight of carbide residue extracted per unit weight of steel dissolved?

F. R. MORRAL,† State College, Pa.—The authors refer several times to the cubic chromium carbide Cr_4C. I believe it would be preferable to use the expression $(Cr,Fe)_{23}C_6$ because:

1. Crystal-structure analysis[6] showed that agreement could be obtained between calculated and measured intensities of X-ray diffraction lines only when the calculations were based on a unit cell containing 116 atoms. Cr_4C corresponds to a unit cell containing 120 atoms.

2. The authors have found that their cubic chromium carbide may have some iron in solid solution.

In a paper of this nature, limited in length, it is not possible to present all the data obtained. Yet I would like to point out that other carbides of the $Cr_{23}C_6$ have been found and I wonder if they may be present in the steels studied by Crafts and Offenhauer. Lattice parameters and chemical analysis would help to identify them.

CARBIDES	LATTICE PARAMETER, Å.[5]
$Cr_{23}C_6$	10.638
$(Cr,Fe)_{23}C_6$	10.565[6]
$(Fe,Mo)_{23}C_6$	10.527[7]
$(Cr,Mo)_{23}C_6$	?

* Assistant Professor of Physical Metallurgy, Massachusetts Institute of Technology.
† School of Mineral Industries, The Pennsylvania State College.

[5] A. Westgren: *Jernkontorets Ann.* (1933) 511.
[6] A. Westgren, G. Phragmén and T. Negresco: *Jnl.* Iron and Steel Inst. (1928) **117**, 390; also *Jernkontorets Ann.* (1927) 513.
[7] F. R. Morral: Discussion to *Preprint* 14. Amer. Soc. Metals (1942).

$(Cr,W)_{23}C_6$ with a lattice parameter of 10.73 Å. has been identified[8] and by identity the existence of the $(Cr,Mo)_{32}C_6$ is possible. These carbides are all similar in crystal structure; they differ only in lattice parameter.

In Fig. 12, the authors indicate the region Cr_4C, yet their data place Cr_7C_3 and Cr_4C there. A correction seems necessary.

W. CRAFTS AND C. M. OFFENHAUER (authors' reply).—The anodic solution of the specimens was accompanied by the formation of some graphite or amorphous carbon. The amount and character of the decomposition were not determined, although the degree to which it occurred did not appear to invalidate the qualitative determination of the types of carbides. As pointed out in the previous paper on the carbides in plain chromium steels,[1] the method is capable of demonstrating positively only the presence, but not the absence, of a constituent. The method used in this investigation is believed to be unsuitable for quantitatively accurate determination of the quantity of carbides in the steel or the composition of the carbides.

The solution procedure was described in the earlier paper and was used for all except the high-alloy, low-carbon steels of this series, which were treated in a copper-potassium chloride solution. In this solution treatment, the specimens were immersed in a solution of 300 grams $2KClCuCl_2.2H_2O$, 70 ml. HCl per liter and allowed to react for 24 hr. The deposited copper shell was then removed and the residue was carefully scraped from the surface,

washed and placed in the X-ray specimen holder. Occasionally copper patterns were found in these residues but the interference could be minimized by careful stripping and by washing with NH_4OH or HCl solutions. With reference to particle size, it has been found that satisfactory X-ray patterns could be obtained from specimens quenched and tempered at temperatures as low as 350°C. No attempts were made in this work to obtain data on the weight of carbide residue, since we were concerned primarily with the crystallographic structures.

We agree that the cubic chromium carbide is more probably $Cr_{23}C_6$ than Cr_4C. Reference was made to the work of Westgren in the previous paper, but the term Cr_4C was used for the sake of simplicity. The chemical composition of the carbides found in these steels was probably variable and so we have preferred to designate the carbides as Fe_3C, Cr_7C_3, Cr_4C, Mo_2C types in order to avoid suggestion of specific chemical composition. The data obtained on the high-chromium steels did not entirely conform to the pattern that has been indicated by the phase-rule studies, which have shown that in isothermal sections of three-component systems the three-phase regions are always bounded by straight lines, whose intersections are defined by the composition limits of the monophase regions.[9] It was presumed that the sample containing mixed carbides in the Cr_4C region of Fig. 12 was in error, as only a minor deviation of composition or tempering temperature would change the carbide constituents.

[8] V. Adelsköld, A. Sundelin and A. Westgren: *Ztsch. anorg. allg. Chem.* (1933) **212**, 404.

[9] J. S. Marsh: Principles of Phase Diagrams. New York, 1935. McGraw-Hill Book Company.

Effects of Tin on the Properties of Plain Carbon Steel

By J. W. Halley,* Member A.I.M.E.

(Cleveland Meeting, October 1942)

The effects of tin on steel have become increasingly important because of the necessity of using poorly detinned scrap, tin cans, and terne plate, in the open hearth. Since a tin can contains about 1.5 per cent tin, it would be possible to have up to 0.75 per cent tin in steel made with a 50 per cent scrap charge. In order to use tin-containing scrap, it is necessary to know the effect of tin on various grades of steel. The following investigation is by no means comprehensive but covers a number of steels in which tin content is important.

Published Work

A number of investigations of the effects of tin on rolling quality and physical properties have been published. It has been found that tin increases strength and hardness and reduces ductility and notched impact resistance. The decrease in ductility and notched impact resistance becomes more marked as the carbon decreases.

McKimm[1] found no change in Olsen ductility, Rockwell hardness, yield strength, tensile strength or elongation in cold-reduced strip containing up to 0.124 per cent tin. A tin content of 0.15 per cent gave difficulties in rolling and increased the hardness but 0.21 per cent tin showed no change in properties from material containing very little tin. No explanation of this contradiction is offered.

Andrew and Peile[2] investigated steels containing 0.10 to 0.25 per cent carbon and up to 0.63 per cent tin. They found an increase in tensile strength of from 100 to 200 lb. per sq. in. for each 0.01 per cent tin on normalized samples. The elongation and reduction of area were decreased and the notched impact resistance was reduced markedly. Quenched and drawn samples did not show embrittling if water-quenched from the draw temperature of 1148°F. (620°C.). They could find no evidence of tin under the microscope.

Whitely and Braithwaite[3] investigated the effect of tin on rail steel containing 0.55 to 0.60 per cent carbon. They found that 0.08 per cent tin caused a marked decrease in elongation, notched impact resistance and the degree of bend. The tensile strength was increased in some tests and not in others.

Bolsover and Barraclough[4] investigated the effect of tin up to 0.50 per cent on a 0.35 per cent carbon steel and on several alloy steels with from 0.30 to 0.40 per cent carbon. They found a comparatively uniform decrease in notched impact resistance with increasing tin on quenched and drawn samples. If the samples were quenched from the drawing temperature or reheated to the drawing temperature and quenched, the embrittling was much less severe. Steels containing molybdenum suffered much less embrittlement than other steels.

Experimental Work

Effect of Tin on Low-carbon Rimmed Steel

Increasing quantities of tin were added to four ingots of a heat of the following ladle analysis: carbon, 0.08 per cent; manganese, 0.39; phosphorus, 0.009; sulphur, 0.025.

The tin additions amounted to 0.01 per cent for the first ingot, 0.02 per cent for the second ingot, 0.04 per cent for the third ingot and 0.06 per cent for the fourth ingot.

segregation. The analyses for tin* and sulphur are shown in Table 1. Tin segregates in the same manner as sulphur but not to as great a degree.

TABLE 1.—*Segregation of Sulphur and Tin in Rimmed Ingots*
PER CENT

Ingot No.	Ingot Position								Degree of Segregation,[a] Per Cent	
	Top				Bottom					
	Edge		Center		Edge		Center			
	S	Sn	S	Sn	S	Sn	S	Sn	S	Sn
1	0.018	0.001	0.077	0.009	0.018	0.001	0.017	0.001	+140 − 47	+200 − 66
2	0.019	0.010	0.046	0.024	0.019	0.010	0.028	0.014	+ 64.3 − 47.5	+ 65.5 − 45.0
3	0.020	0.022	0.085	0.056	0.020	0.022	0.024	0.028	+128 − 46.3	+ 75 − 31.2
4	0.020	0.041	0.077	0.117	0.020	0.041	0.019	0.056	+127 − 73.3	+ 83.2 − 36.7
5	0.019	0.066	0.064	0.157	0.019	0.066	0.022	0.081	+106 − 38.8	+ 70.3 − 28.7

[a] The degree of segregation represents the maximum departure from the average analysis of the ingot as a percentage of the average analysis.

TABLE 2.—*Physical Properties of 0.093-inch Gauge Hot Strip with Increasing Tin Content*

Ingot No.	Position of Test	Tin, Per Cent	Rockwell Hardness	Yield Strength, Lb. per Sq. In.	Tensile Strength, Lb. per Sq. In.	Elongation in 2 In., Per Cent
1	Edge	0.001	B-58	35,180	48,100	28.0
2	Edge	0.010	B-58	32,440	47,240	32.5
3	Edge	0.022	B-59	37,550	47,670	34.5
4	Edge	0.041	B-58	34,310	48,510	33.2
5	Edge	0.066	B-65	44,680	54,240	26.5
1	Top center	0.009	B-52	29,220	45,780	33.0
2	Top center	0.024	B-57	36,670	47,580	33.0
3	Top center	0.056	B-55	28,980	45,600	37.5
4	Top center	0.117	B-60	30,790	48,280	37.5
5	Top center	0.157	B-62	33,510	48,800	34.0
1	Bottom center	0.001	B-48	28,270	44,400	35.5
2	Bottom center	0.014	B-61	29,430	45,420	37.0
3	Bottom center	0.028	B-53	29,380	45,320	42.5
4	Bottom center	0.056	B-64	29,500	47,100	34.0
5	Bottom center	0.081	B-61	36,080	49,230	25.2

Top and bottom slabs from a comparison ingot and the tinned ingots were rolled to 0.093-gauge bands on a continuous hot strip mill. All of the ingots rolled with no evidence of checking.

Edge and center analyses of the slabs were made to determine the extent of tin

The physical properties of the hot bands are shown in Table 2.

* Tin analyses were made by the "Sellars" method with a slight modification. After solution in HCl under a CO_2 atmosphere, the solution is oxidized with potassium iodate and the tin reduced with metallic aluminum. The final titration is with the iodate solution as in the standard method.

The hardness and tensile strength are increased by tin. The effect of 0.01 per cent tin is approximately as follows: Rockwell B

shown in Table 3. The hardening effect of tin is not as marked in the cold-reduced annealed sheets as in the hot bands, and

TABLE 3.—*Physical Properties of 0.040-inch Gauge Cold Strip with Increasing Tin Content*

Ingot No.	Position of Test	Tin, Per Cent	Rockwell Hardness	Olsen Ductility	Yield Strength, Lb. per Sq. In.	Tensile Strength, Lb. per Sq. In.	Elongation in 2 In., Per Cent
1	Edge	0.004	B-35	0.408	26,190	41,190	42.8
2	Edge	0.011	B-35	0.404	25,450	39,760	40.9
3	Edge	0.020	B-35	0.403	27,020	42,090	41.2
4	Edge	0.034	B-36	0.410	26,430	41,400	42.2
5	Edge	0.064	B-37	0.413	27,120	41,970	42.0
1	Top center	0.006	B-43	0.394	29,280	44,600	39.0
2	Top center	0.016	B-43	0.390	30,800	45,400	38.8
3	Top center	0.028	B-40	0.400	26,730	41,420	42.0
4	Top center	0.056	B-45	0.388	30,650	45,950	38.0
5	Top center	0.090	B-46	0.397	39,860	45,760	40.0
1	Bottom center	0.004	B-40	0.393	27,740	43,300	41.0
2	Bottom center	0.012	B-40	0.394	27,270	42,860	38.2
3	Bottom center	0.023	B-38	0.396	27,600	42,280	39.5
4	Bottom center	0.040	B-40	0.402	27,600	42,080	40.0
5	Bottom center	0.058	B-40	0.404	28,560	44,380	42.7
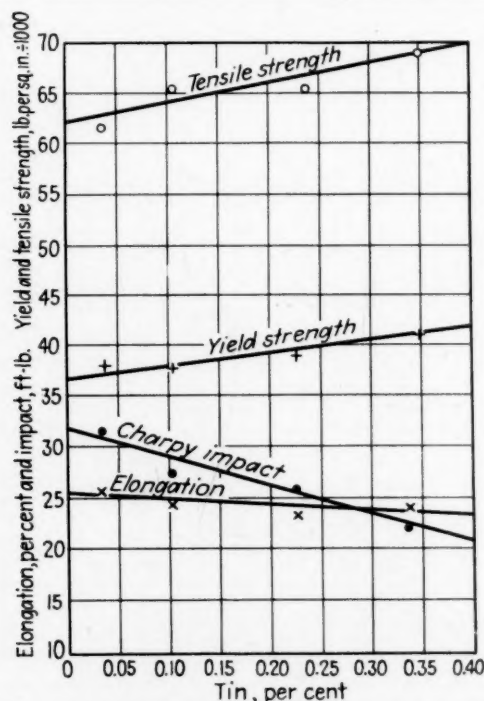
FIG. 1.—EFFECT OF TIN ON PHYSICAL PROPERTIES OF HOT-ROLLED STRUCTURAL STEEL.

FIG. 2.—EFFECT OF TIN ON PHYSICAL PROPERTIES OF ANNEALED STRUCTURAL STEEL.

hardness is increased 0.6 points; tensile strength is increased 300 lb. per sq. inch.

The hot bands were cold-reduced to 0.040-in. gauge cold strip and box-annealed. The properties of the annealed sheets are

there is no apparent effect on ductility. The Rockwell B hardness is increased approximately 0.4 per cent for each 0.01 per cent

tin and the tensile strength is increased 150 lb. per sq. inch.

0.32; phosphorus, 0.010 and sulphur, 0.030. The tin addition amounted to 0.10 per cent

TABLE 4.—*Segregation of Tin in Semikilled Structural Steel*

Ingot No.	Position of Test	Edge		Midway		Center		Degree of Segregation, Per Cent	
		S	Sn	S	Sn	S	Sn	S	Sn
2	Top	0.034	0.028	0.033	0.028	0.032	0.029	+18.3	+12.3
	Middle	0.032	0.028	0.039	0.032	0.040	0.032	−11.2	−12.3
	Bottom	0.034	0.027	0.030	0.025	0.030	0.026		
3	Top	0.032	0.096	0.028	0.100	0.028	0.101	+14.2	+10.4
	Middle	0.035	0.112	0.037	0.124	0.032	0.119	−13.6	−14.5
	Bottom	0.034	0.121	0.033	0.119	0.033	0.119		
4	Top	0.032	0.142	0.029	0.206	0.028	0.190	+37.0	+24.8
	Middle	0.031	0.181	0.031	0.236	0.043	0.270	−10.8	−34.8
	Bottom	0.032	0.264	0.029	0.232	0.028	0.244		
5	Top	0.031	0.241	0.021	0.230	0.022	0.243	+22.5	+18.6
	Middle	0.032	0.282	0.034	0.332	0.037	0.331	−30.4	−18.6
	Bottom	0.035	0.351	0.034	0.331	0.030	0.319		

TABLE 5.—*Effect of Tin on Structural Steel, ½-inch Plate*

Ingot No.	Position	Tin, Per Cent	Direction[a]	Hot-rolled					Annealed 1650°F., Furnace-cooled				
				Yield Strength, Lb. per Sq. In.	Tensile Strength, Lb. per Sq. In.	Elongation in 8 In., Per Cent	Reduction of Area, Per Cent	Charpy Impact, Ft-lb.	Yield Strength, Lb. per Sq. In.	Tensile Strength, Lb. per Sq. In.	Elongation in 8 In., Per Cent	Reduction of Area, Per Cent	Charpy Impact, Ft-lb.
2	Top	0.028	L	35,050	60,900	31.2	52.1		29,070	51,920	30.4	58.9	
			T	36,030	60,160	25.0	41.8		27,560	51,610	30.4	55.7	
	Middle	0.030	L	38,010	62,220	25.7	55.0	31.8	28,400	53,610	27.3	53.7	14.5
			T	33,640	62,120	25.7	46.5	18.5	25,020	53,600	28.9	46.4	6.5
	Bottom	0.026	L	33,720	59,900	27.3	52.4		25,830	52,960	28.1	53.7	
			T	35,660	59,390	27.3	47.1		24,940	52,900	29.6	45.8	
3	Top	0.091	L	36,760	60,840	24.2	48.8		30,140	52,180	29.6	60.1	
			T	37,250	60,420	23.4	40.8		27,200	52,080	27.3	55.7	
	Middle	0.103	L	37,640	65,320	24.3	47.7	27.2	32,380	56,360	26.5	49.8	10.0
			T	37,270	65,200	24.3	39.1	18.2	28,810	55,990	25.0	48.0	5.0
	Bottom	0.111	L	34,100	61,620	26.5	54.4		30,700	54,070	30.4	57.4	
			T	34,500	62,200	25.7	47.1		29,030	53,770	26.5	52.0	
4	Top	0.196	L	36,320	63,580	25.0	52.0		29,840	54,910	28.1	57.9	
			T	37,890	63,660	25.0	44.6		30,490	55,760	29.6	37.0	
	Middle	0.229	L	39,250	65,640	23.4	35.2	26.0	31,170	58,650	24.2	49.3	4.2
			T	40,390	66,130	20.1	24.2	17.8	30,450	58,700	26.5	47.7	4.0
	Bottom	0.227	L	39,910	64,150	25.0	45.9		32,270	55,770	27.3	54.9	
			T	38,100	63,540	25.0	48.9		28,420	55,900	26.5	51.6	
5	Middle	0.337	L	41,120	69,200	24.2	40.1	22.2	34,080	60,920	26.5	52.0	2.5
			T	42,280	68,770	21.0	24.7	14.8	32,360	60,550	25.0	40.9	2.8
	Bottom	0.313	L	39,500	65,870	25.0	50.3		34,810	57,820	25.7	50.7	
			T	39,370	66,250	19.5	42.3		34,720	57,420	26.5	48.0	

[a] L stands for longitudinal; T, transverse.

Semikilled Structural Steel

The effect of tin on semikilled structural-grade steel was investigated by adding tin to three ingots of a heat with the following analysis: carbon, 0.21 per cent; manganese, for one ingot, 0.20 for the second and 0.30 for the third. Top, middle and bottom slabs from these ingots and from one ingot with no addition were rolled to ½ × 20-in. universal mill plates. No serious difficulties were encountered in rolling but the two

ingots containing the greatest amount of tin showed checking at the blooming mill. The finished plates all had good surface.

Check analyses were made edge, midway in.; yield strength increased 140 lb. per sq. in.; percentage of elongation in 8 in. decreased 0.07 per cent; Charpy impact resistance decreased 0.26 foot-pounds.

TABLE 6.—*Effect of Tin on Properties of 1040 Steel*

Ingot No.	Tin, Per Cent	Normalized 1600°F.					Water-quenched 1550°F., Drawn 1000°F.				
		Yield Strength, Lb. per Sq. In.	Tensile Strength, Lb. per Sq. In.	Elongation in 2 In., Per Cent	Reduction of Area, Per Cent	Charpy Impact, Ft-lb.	Yield Strength, Lb. per Sq. In.	Tensile Strength, Lb. per Sq. In.	Elongation in 2 In., Per Cent	Reduction of Area, Per Cent	Charpy Impact, Ft-lb.
1	0.020	54,750	91,550	26.5	42.4	15.5	85,010	115,700	19.5	46.0	20.0
2	0.035	56,550	92,400	26.5	48.3	19.5	83,860	117,200	21.5	51.7	25.5
3	0.062	57,600	93,150	26.0	47.7	17.0	88,800	117,300	21.5	51.1	23.0
4	0.104	56,800	94,000	27.5	49.1	17.0	89,100	119,000	22.0	53.8	24.0
5	0.227	55,350	93,900	25.0	37.2	6.5	88,560	120,000	18.5	30.8	15.0

TABLE 7.—*Drop Tests of 112-pound Rails with Increasing Tin Content*

Ingot No.	Rail Letter	Tin, Per Cent	Blows to Break	Total Elongation, In.				
				1st Blow	2nd Blow	3rd Blow	4th Blow	5th Blow
3	A	0.01	5+	0.16	0.31	0.44	0.54	0.63
4	A	0.04	4	0.16	0.28	0.42	0.46	
5	A	0.08	3	0.15	0.37	0.41		
6	A	0.16	3	0.15	0.25	0.29		
3	B	0.01	5+	0.15	0.29	0.39	0.51	0.64
4	B	0.05	5	0.16	0.29	0.43	0.51	0.51
5	B	0.08	5+	0.16	0.26	0.38	0.49	0.51
6	B	0.18	5	0.16	0.28	0.42	0.46	0.58
3	I	0.01	5+	0.16	0.29	0.40	0.43	0.43
4	I	0.04	4	0.16	0.26	0.35	0.39	
5	I	0.07	5	0.17	0.27	0.39	0.46	0.46
6	I	0.12	5	0.16	0.26	0.30	0.38	0.42

and center, of the top, middle and bottom slabs. The analyses for tin and sulphur and degree of segregation are shown in Table 4.

As in the rimmed steel, the tin segregates in the manner of sulphur although less severely.

The physical properties of the plates in the hot-rolled condition and after annealing are shown in Table 5. The longitudinal properties of the middle cuts in the hot-rolled condition are plotted in Fig. 1. Reduction of area is not included because the values were not sufficiently consistent to indicate the slope of the curve. It is evident that the reduction of area is decreased by tin. The effects of 0.01 per cent tin as shown in Fig. 1 are as follows: Tensile strength increased 200 lb. per sq.

The longitudinal properties of the annealed samples are plotted in Fig. 2. Tin has more effect on the properties in the annealed than in the hot-rolled condition. This is particularly true of the impact resistance, which is reduced sharply by tin in the annealed samples. The effects of 0.01 per cent tin, as shown by Fig. 2, are as follows: Tensile strength increased 200 lb. per sq. in.; yield strength increased 150 lb. per sq. in.; percentage elongation in 8 in. decreased 0.09 per cent; Charpy impact resistance decreased 0.40 foot pounds.

Medium-carbon Steel of Forging Quality

The effect of tin on 0.40 per cent carbon steel was investigated on induction-furnace steel. A 300-lb. melt was made and poured

TABLE 8.—*Segregation of Sulphur and Tin in Rail Ingots*
PER CENT

Ingot No.	Rail A Outside		Rail A Midway		Rail A Center		Rail B Outside		Rail B Midway		Rail B Center		Rail I Outside		Rail I Midway		Rail I Center		Degree of Segregation, Per Cent S	Degree of Segregation, Per Cent Sn
	S	Sn	S	Sn	S	Sn	S	Sn	S	Sn	S	Sn	S	Sn	S	Sn	S	Sn		
4	0.026	0.04	0.026	0.04	0.028	0.05	0.025	0.04	0.030	0.05	0.028	0.05	0.026	0.05	0.025	0.04	0.023	0.04	+11.3 / -14.2	+13.6 / -9.1
5	0.026	0.06	0.025	0.08	0.026	0.07	0.026	0.07	0.028	0.08	0.027	0.07	0.025	0.08	0.021	0.07	0.022	0.06	+11.6 / -16.3	+12.6 / -15.5
6	0.025	0.11	0.027	0.16	0.026	0.17	0.023	0.15	0.026	0.18	0.027	0.18	0.025	0.14	0.024	0.12	0.023	0.14	+7.6 / -8.4	+20.0 / -26.6

into five ingots. Tin was added to the furnace after the pouring of each ingot. The heat analysis was as follows: carbon, 0.41 per cent; manganese, 0.63; phosphorus,
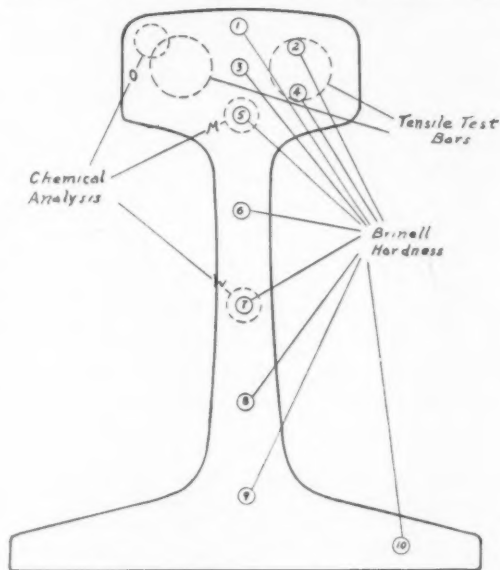
FIG. 3.—POSITIONS OF TESTS ON RAIL SAMPLES.

0.010; sulphur, 0.028; silicon, 0.25. The tin additions aimed at 0.02, 0.04, 0.07, 0.10 and 0.20 per cent in the ingots. The small ingots were forged to 1¼-in. rounds and tested in the normalized and quenched and drawn condition. The quenched and drawn samples were cooled in air from the draw temperature. The physical properties are shown in Table 6. The uniform decrease in ductility and impact resistance found in the lower-carbon steels is not shown by the 0.40 per cent carbon steels. There is a marked drop between 0.104 and 0.227 per cent tin in both the normalized and quenched and drawn samples. The increase in tensile strength and yield strength caused by tin appears to be somewhat greater than in the lower-carbon steels.

McQuaid-Ehn grain size was 2 to 4 on all the ingots, showing that the tin has no effect on the grain-coarsening characteristics of the steel. The ferrite grain size, however, was slightly finer on the steel containing 0.22 per cent tin than on the low-tin sample.

Jominy end-quench tests were made on steel from the five ingots and no difference in hardenability was found.

Rail Steel

Tests on rail steel were made by adding tin to three ingots of a heat of the following analysis: carbon, 0.77 per cent; manganese, 0.82; phosphorus, 0.010; sulphur, 0.027; silicon, 0.18. The tin additions were adjusted to produce ingots with 0.05, 0.08 and 0.11 per cent tin. The heat was rolled to 112 lb. per yard rails. Samples for drop tests and physical tests were cut out at the hot saws from the A, B and I rails (from the top of the ingot next to the top and bottom of the ingot) from the tinned ingots and an adjacent ingot to which no tin had been added.

creased by tin and the stiffness as indicated by elongation is increased.

Analyses for segregation, Brinell hardness surveys and tensile tests were made on the rails. The positions of the various tests are shown in Fig. 3. Table 8 gives the analyses for sulphur and tin and the degree of segregation of the ingots to which tin was added. Ingot No. 3, to which no tin was added, is not included because all positions showed 0.01 per cent tin. Neither element segregated severely. The tin and sulphur showed about the same degree of segregation except in ingot No. 6, in which the tin showed a greater degree of segregation than the sulphur. The tin segregated in the same manner as the sulphur.

The Brinell hardness surveys are shown in Table 9. The tin causes a moderate

TABLE 9.—*Brinell Hardness of 112-pound Rails with Increasing Tin Content*

Ingot No.	Rail Letter	Tin, Per Cent	Brinell Hardness										
			At Position										Average
			1	2	3	4	5	6	7	8	9	10	
3	A	0.01	241	255	248	255	269	269	262	255	255	286	259.5
4	A	0.04	255	262	255	262	262	262	255	255	269	262	259.9
5	A	0.08	269	269	262	269	269	269	262	262	269	269	266.9
6	A	0.16	262	262	269	269	269	269	269	269	255	269	266.2
3	B	0.01	262	255	255	255	255	255	255	286	255	269	260.2
4	B	0.05	255	255	255	255	262	269	269	277	277	286	266.0
5	B	0.08	269	262	262	277	269	269	269	269	255	277	267.8
6	B	0.18	269	262	269	269	269	277	269	293	269	269	267.8
3	I	0.01	255	262	255	255	255	228	228	228	262	269	249.7
4	I	0.04	255	262	255	255	248	241	241	241	241	241	248.0
5	I	0.07	262	262	255	248	241	228	241	241	248	286	251.2
6	I	0.12	269	255	255	.269	255	241	228	228	248	269	251.7

The drop tests were made according to the standard procedure. The rail was supported by centers 4 ft. apart, head up, and a 2000-lb. tup was dropped 20 ft. onto the head midway between the supports. The elongation after each blow was measured on a 6-in. gauge length on the base immediately below the point of impact. The rails were tested to failure, or until they had received five blows. The results of the drop tests are shown in Table 7.

The number of blows to failure is de-

increase in Brinell. The increase does not appear to be uniform, there being a sharp increase in the neighborhood of 0.05 per cent tin.

Two tensile bars were cut from the head of each rail. The results of the two tests were averaged and are shown in Table 10.

The yield strength and tensile strength are increased much more by tin than in the lower-carbon steels. The lack of effect on elongation and reduction of area is probably more apparent than real. These values are

so low for rail steel that a marked reduction in ductility is easily masked by errors in measuring the elongation and reduction of area.

GENERAL OBSERVATIONS

The lack of microscopic evidence of tin was characteristic of all the series. The higher-tin steels were always slightly finer

| a | b |
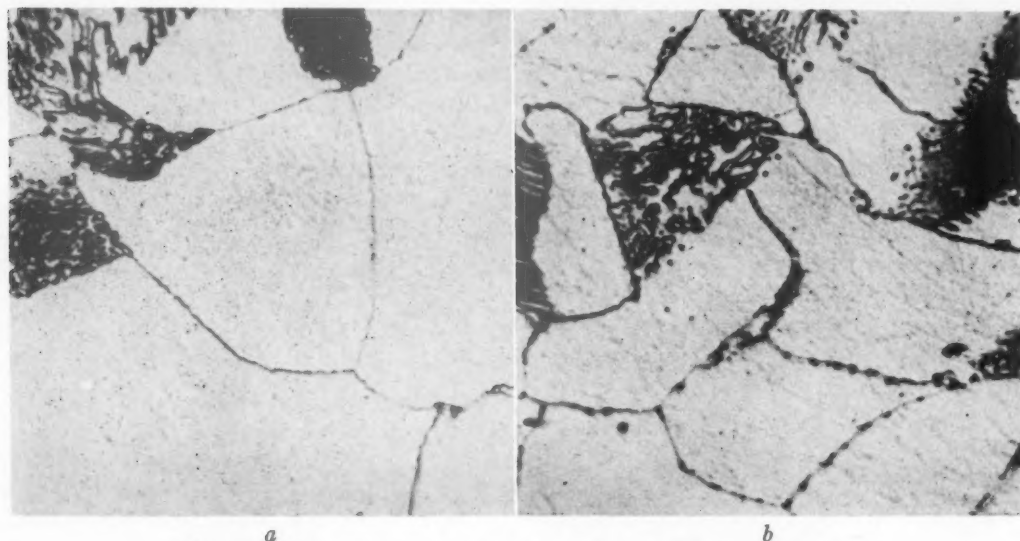
FIG. 4.—GRAIN-BOUNDARY PRECIPITATE FOUND WITH HIGH TIN.
a, 0.27 per cent C; 0.02 per cent Sn. b, 0.28 per cent C; 1.50 per cent Sn.
Original magnification 2500; reduced approximately ⅓ in reproduction.

A further measure of ductility was made in the form of bend tests from the heads of the I rails. Samples ¾ in. thick and 2 in.

TABLE 10.—*Tensile Properties of 112-pound Rails with Increasing Tin Content*

Ingot No.	Rail Letter	Tin, Per Cent	Yield Strength, Lb. per Sq. In.	Tensile Strength, Lb. per Sq. In.	Elongation in 2 In., Per Cent	Reduction of Area, Per Cent
3	A	0.01	66,600	130,400	11.2	12.9
4	A	0.04	77,100	135,300	12.0	13.6
5	A	0.08	64,000	133,900	11.2	12.4
6	A	0.16	67,200	135,600	11.5	14.0
3	B	0.01	63,500	129,300	12.0	13.9
4	B	0.05	63,900	132,000	11.7	12.0
5	B	0.08	64,600	135,800	11.5	12.8
6	B	0.18	66,200	136,200	12.7	14.6
3	I	0.01	64,700	130,000	12.5	14.3
4	I	0.04	64,200	129,300	12.5	15.3
5	I	0.07	64,200	128,000	12.5	16.9
6	I	0.12	66,100	133,100	12.0	14.8

wide were cut from the center of the rail head and bent around a 1½-in. pin. The angle of bend to failure is shown in Table 11; it is decreased uniformly by the addition of tin.

grained than the low-tin steels but the pearlite and ferrite or tempered martensite were unaltered. A number of common etching reagents were tried but none was found

TABLE 11.—*Bend Test of Rail Steel with Increasing Tin Content, I Rails*

Ingot No.	Tin, Per Cent	Angle of Bend
3	0.01	33.3°
4	0.04	26.5°
5	0.07	24.5°
6	0.12	21.5°

that showed any response characteristic of tin. In order to get some idea of the effect of tin on microstructure, a small 2-lb. induction-furnace melt was made and cast into two minute ingots, 1.5 per cent tin being added before the pouring of the second ingot. The chemical analyses of the ingots were as follows:

	C	Mn	P	S	Si	Sn
No. 1	0.27	1.06	0.012	0.028	0.54	0.02
No. 2	0.28	0.90	0.014	0.028	0.47	1.52

The ingots were forged to ½-in. squares. The ingot containing tin cracked up badly during forging. Samples were annealed from 1900°F. (the tin had raised the Ar₃ temperature to over 1850°F.) and examined under the microscope. The high-tin sample was much finer grained than the low-tin sample, and showed a precipitate on the grain boundaries. The structure is shown in Fig. 4. The grain-boundary precipitate is probably carbide. The fact that the high-tin sample decarburized 10 times as deeply during heat-treatment as the low-tin sample indicates a marked tendency to reject carbon. The high-tin steel was extremely brittle and the fracture followed the boundaries between the ferrite grains but passed through the pearlite grains.

Conclusions

The effects of tin are very similar to those of phosphorus. In structural steels 0.01 per cent phosphorus increases the tensile strength by 1000 lb. per sq. in. This same increase in strength would result from 0.05 per cent tin. It is possible to make an estimate of the effect of tin by dividing the tin content by 5 and adding it to the phosphorus. This analogy cannot be carried too far, but it is interesting to note that phosphorus forms a closed gamma loop at 0.40 per cent when alloyed with iron and that tin forms a closed gamma loop at 2.00 per cent. This ratio is also indicated in the rail-steel series, as the addition of 0.030 per cent phosphorus to a heat low in phosphorus (0.010 per cent) would be expected

TABLE 12.—*Effect of Water Quenching versus Furnace Cooling*

Treatment	Yield Strength, Lb. per Sq. In.	Tensile Strength, Lb. per Sq. In.	Elongation in 2 In., Per Cent	Reduction of Area, Per Cent	Charpy Impact, Ft-lb.
Normalized, heated to 1150° and furnace-cooled..	54,930	91,280	24.2	39.0	9.5
Normalized, heated to 1150° and water-quenched.	57,420	92,800	26.8	45.0	12.5

Several investigators have reported that the embrittling effect of tin on quenched and drawn samples was greatly decreased by quenching from the drawing temperature. In order to determine whether or not this phenomenon was peculiar to quenched and drawn steels, two samples of steel containing 0.41 per cent carbon and 0.227 per cent tin were normalized and reheated to 1150°F. One sample was water-quenched from 1150°F. and the other was allowed to cool with the furnace. The physical properties after these treatments were as shown in Table 12.

The ductility and impact resistance of the water-quenched sample is nearly as great as that of the low-tin sample of this series shown in Table 6. It is evident that at least part of the embrittling effect of tin is the result of a subcritical change, and is very similar to temper brittleness.

to reduce the resistance to the drop test but not cause a first blow failure.

References

1. P. J. McKimm: Residual Tin in Steel. *Steel* (1940) **106**, May 6, 64–68; May 13, 60–69.
2. J. H. Andrews and J. B. Peile: The Effect of Tin as an Impurity in Mild Steel. *Jnl.* Iron and Steel Inst. (1933) **128**, 193–202.
3. J. H. Whiteley and A. Braithwaite: Some Observations on the Effect of Small Quantities of Tin in Steel. *Jnl.* Iron and Steel Inst. (1923) **107**, 161–169.
4. G. R. Bolsover and S. Barraclough: The Influence of Tin on Alloy Steels. Iron and Steel Inst. Advance Copy, May 1942.

DISCUSSION

(Frank G. Norris presiding)

T. S. WASHBURN,[*] Indiana Harbor, Ind.— Mr. Halley's review of previous investigations, and his new experimental data, have established more definitely the effect of tin on various grades of carbon steel. For some grades, such as deep-drawing quality strip steel, it is necessary to maintain the tin content at the lowest possible level. For others, such as rail and spring steel, it is permissible to establish higher maximums, but this entails some loss in ductility and consequently necessitates holding the phosphorus to lower limits. For steel used for structural purposes, which is specified to tensile and elongation requirements, Mr. Halley has shown that it is permissible to apply steel containing up to at least 0.15 per cent Sn.

In terms of operating practice, the limits that have been established at our plant for tin on certain representative grades are as follows:

GRADE	MAXIMUM TIN, PER CENT
Extra deep-drawing strip	0.02
Regular deep-drawing strip	0.04
S.A.E.-1020 forging quality	0.08
S.A.E.-1020 structural quality	0.15

The limits set up for forging and structural quality are considerably higher than for the deep-drawing quality grades. The higher limits make it possible to use some tin-bearing scrap in the open-hearth charges for these grades. The scrap charge must be closely controlled, however, as certain types of tin-bearing scrap will introduce excessive amounts of this element even when used in small quantities. An example is bundled tin cans that have not been through the detinning operation. Fig. 5 shows the relation between the percentage of tin-can scrap charged and the tin recovered in the bath. It is apparent from this curve that no scrap of this type can be used in the charge of a heat of extra deep-drawing quality strip, since the average residual tin is only slightly under the 0.02 per cent Sn maximum set up for this grade. For a forging-quality heat with 0.08 per cent Sn maximum specified, it is possible to meet this requirement with approximately 5 per cent tin scrap in the charge, and about 10 per cent can be used for structural grades.

In actual practice it has been found that the

---

[*] Assistant Chief Metallurgist, Inland Steel Company.

use of even small amounts of tin-can scrap is not feasible in an open-hearth shop regularly producing the grades of steel set up for the lower tin maximums. This results from the
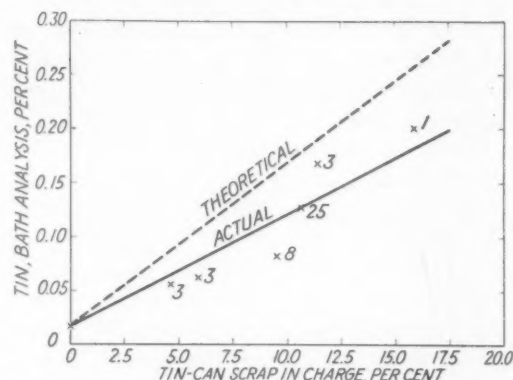
FIG. 5.—RELATION BETWEEN TIN-CAN SCRAP IN CHARGE AND RESIDUAL TIN.

Actual curve based on data from heats on which no terne plate, detinned, bundled scrap (except tin-can) or turnings were charged. Figures in circles indicate number of heats per point.

Theoretical curve based on assumption of 1.5 per cent Sn content of tin-can scrap and on an increment of 0.018 per cent bath Sn from other sources.

difficulty of controlling the amount of tin scrap used in individual charges, and also because of the increase in residual tin from the higher tin scrap returned from the mills. In an open-hearth shop that is scheduled to make most of the heats during certain periods for structural grades, it is possible to utilize tin-can scrap during these periods. This is an unsatisfactory procedure, however, because it places a restriction on providing schedules, and also the scrap with a higher tin content returned from the mills increases the difficulty of producing the grades specified to the lower maximum tin when they are desired.

N. A. ZIEGLER,[*] Chicago, Ill.—Is any information available on the effect of tin on the welding quality of steel?

J. W. HALLEY (author's reply).—I can only make one statement on that. In an article that I did not use as a reference because it was on welding, some one added 0.5 per cent tin and got into trouble welding. We could have said

---

[*] Research Metallurgist, Crane Company.

without trial that probably trouble would occur at 0.5 per cent. We know that a great deal cannot be tolerated, but what the limits are, I have no idea.

S. FEIGENBAUM,* Aliquippa, Pa.—The author said that tin behaves similarly to phosphorus. I wonder if he ever observed any banding.

J. W. HALLEY.—No, the specimens were not particularly banded. An analogy is always dangerous, but the analogy between tin and phosphorus seemed to be one that would help in application of steel high in tin. These steels did show the characteristic of high-phosphorus steels, that the more slowly they were cooled, the more brittle they were.

H. L. WALKER,† Urbana, Ill.—We believe that we have been able to locate lead particles in Ledloy steels by the use of the microradiograph. Would it be any contribution if we were to use some of your tin steels to try to verify precipitation of tin in the grain boundary?

J. W. HALLEY.—That would be interesting, but I would not anticipate much success. According to the equilibrium diagram, 1.5 per cent tin is soluble in iron.

H. L. WALKER.—You thought there was carbide precipitation in the grain boundary.

J. W. HALLEY.—If your microradiograph would show whether it is carbide or tin, that would definitely be a contribution.

H. L. WALKER.—The coefficient of absorption on carbide is so close to that of iron that carbide cannot be detected on a microradiograph, but the difference of density between tin and any tin compound and iron is so great that it would show very nicely.

J. W. HALLEY.—The photomicrograph of Fig. 4 is at 2500 diameters. It took quite a little polishing to show the grain-boundary difference. Your limits of microradiography are considerably below that, I believe.

H. L. WALKER.—Yes, down around 200.

J. W. HALLEY.—I would be very glad to send you some samples of the 1.5 per cent tin steel. I have some small pieces.

C. E. SIMS,* Columbus, Ohio.—You found a relation between the segregation of tin and sulphur. Did you find any other further relations between the effect of the sulphur and of tin? There have been some assertions that tin is more deleterious to the physical property in the presence of high sulphur content. Did you find any evidence of that?

J. W. HALLEY.—As far as physical properties go, we have no information. There is one thing that perhaps should be mentioned: Sulphur and tin combined are very detrimental as far as rolling quality is concerned, particularly if high copper is present. Nearly all steel manufacturers, and we are no exception, have encountered heats with residual copper fairly high, residual sulphur quite high, and tin, and it is practically impossible to roll them. The rolling quality is very poor.

MEMBER.—Does not tin exist in steel as tin oxide?

J. W. HALLEY.—I do not know, but I rather suspect not. Probably you would expect it to be readily reduced by molten iron. I have no direct evidence along that line. I do not know what the relative free energy of tin oxide and iron oxide and tin and iron are, but I would anticipate that tin would be readily reduced by molten iron. For one thing, we would eliminate it in the open hearth if it were not reduced by molten iron, and we eliminate almost none.

R. F. MATHER,† Toledo, Ohio.—The affinity of tin for steel is indicated by the effect of tin content in lead-tin solders on the spreadability of such solders on steel surfaces. The percentage of tin required depends upon the particular application. For example, the lead-silver solders recently developed to meet the shortage

* Jones and Laughlin Steel Corporation.
† Department of Mining and Metallurgical Engineering, University of Illinois.

* Supervising Metallurgist, Battelle Memorial Institute.
† Metallurgical Engineer, Willys-Overland Motors, Inc.

of tin cannot be used for the dip-soldering of iron and steel parts unless these parts are first coated with a more readily soldered metal, such as copper or silver.

Further evidence of the affinity of tin for steel is given by the fact that at least 15 per cent tin must be present in most terne coatings in order to obtain good adhesion. Again, in view of the scarcity of tin, considerable work has recently been done to determine whether this tin content cannot be reduced or eliminated. Electroplating and hot-dipping methods have now been devised for coating iron and steel parts with lead containing little or no tin, although in every case definite precautions must be taken. In one method it is considered essential to deposit a copper strike on the steel before electroplating. In another process steel parts are given a quick and violent oxidizing treatment to remove all surface impurities, including carbon. The surface is left with a coating of gray oxide, which is dissolved in dilute hydrochloric acid. The parts are dipped in flux and finally in a bath of molten lead containing 5 per cent tin plus 5 per cent antimony. The same process was found to be ineffective when applied to gray cast iron because the acid removed some of the metal as well as the oxide, exposing more graphite flakes, to which the coating would not adhere. The difficulty was overcome by using a strong reducing bath after the oxidizing treatment, followed by a quick rinse in weak acid, and finally by dipping in the same flux and molten lead-alloy baths. The fact that the alloy would not dissolve the exposed graphite flakes, and thus give a firm bond, is in line with the supposition that tin in steel exists in the ferrite phase.

The Effect of Silicon on Hardenability

By Walter Crafts,[*] Member A.I.M.E., and John L. Lamont[*]

The principle formulated by Grossmann[1] for calculating hardenability of steel by multiplying the ideal diameter of "pure" iron-carbon alloys by factors for grain size and alloying elements has been confirmed on many steels and has proved useful in designing substitute alloy steels. Grossmann found that the typical behavior of the multiplying factors was to increase directly in proportion to the amount of the alloy present in a steel. However, the multiplying factor for the effect of silicon on hardenability was found by Grossmann to increase to a lesser degree as the amount of silicon was increased. In view of the increasing use of silicon in heat-treating steels, the effect of silicon on hardenability is becoming more important. Calculation of the hardenability of high-silicon steels made at the Union Carbide and Carbon Research Laboratories, Inc., indicated that the multiplying factor for silicon increased directly in proportion to the amount of silicon present. A more extended study of high-silicon steels covering fairly wide ranges of grain size, carbon, manganese, and aluminum has confirmed that up to 2 per cent silicon the multiplying factor is directly proportional to the silicon content. Manganese and aluminum factors have also been determined. The results of the study offer strong confirmation of the general validity of Grossmann's multiplying principle.

Testing Procedure

Steels on which the study of the effect of silicon on hardenability was based were made in high-frequency induction furnaces using Armco iron and standard alloying materials. The ingots were forged to bars, and sections were normalized prior to machining Jominy hardenability test specimens. The Jominy test was carried out under standard conditions.[2] The depth of hardness penetration for determination of ideal diameter at "half hardness" was taken at the hardness level indicated in Fig. 29 in Grossmann's paper by the solid line for 50 per cent martensite in plain carbon steel. The depth of penetration of hardness on the Jominy specimen was converted to ideal diameter by the relation given in Fig. 28 of Grossmann's paper.

Chemical analysis was determined on a sample taken adjacent to the Jominy specimen. Aluminum was determined as "acid-soluble aluminum" rather than as total aluminum, as it is probably more representative of the aluminum that is effective as an alloying agent. In addition to the elements nominally present in the steels, analyses were made for residual phosphorus, sulphur, nickel, copper, molybdenum and chromium on one heat of those made with the same materials during the same period. Actual grain size was determined by microscopic examination of small samples quenched in water after receiving the same thermal cycle as the Jominy hardenability specimens.

Chemical analyses, heat-treatment, grain size, and hardenability are shown in Table 1 representing three ranges of composition.

TABLE 1.—*Chemical Analyses, Heat-treatment, Grain Size and Hardenability*

Heat No.	Chemical Analysis, Per Cent									Acid-soluble Al, Per Cent	Normalizing Temperature, Deg. C.	Quenching Temperature, Deg. C.	Average A.S.T.M. Grain Size	Half Hardness	
	C	Mn	P	S	Si	Ni	Cu	Mo	Cr					Jominy Depth, In.	Ideal Diameter, In.
	RANGE OF COMPOSITION: C, 0.40–0.55 per cent; Mn, 0.50–1.75; Si, 0.20–2.0; Al, <0.10														
1a	0.49	0.58	0.018	0.031	0.27	0.055	0.09	0.006	0.019	0.043	875	850	7½	0.10	1.25
2a	0.46	0.74	0.015	0.035	0.23	0.018	0.086	0.006	0.024	0.025	875	850	8½	0.11	1.30
3a	0.48	1.19	0.018	0.031	0.24	0.055	0.09	0.006	0.019	0.056	875	850	8	0.24	1.89
4a	0.48	1.68	0.010	0.029	0.20	0.023	0.070	0.002	0.025	0.004	875	850	4	0.59	3.29
5	0.51	1.61	0.019	0.031	0.25	0.032	0.084	0.002	0.023	0.052	875	850	9	0.30	2.31
6a	0.49	0.56	0.018	0.031	0.48	0.055	0.09	0.006	0.019	0.037	875	850	7	0.13	1.36
7	0.46	0.82	0.008	0.032	0.49	0.038	0.072	0.003	0.019	0.028	875	850	8	0.14	1.42
8	0.54	1.19	0.013	0.029	0.45	0.026	0.094	0.003	0.06	0.079	875	850	8	0.30	2.13
9a	0.46	1.07	0.010	0.029	0.57	0.023	0.070	0.002	0.025	0.004	875	850	4	0.69	3.62
10	0.56	1.60	0.019	0.031	0.46	0.032	0.084	0.002	0.023	0.053	875	850	9½	0.35	2.38
11	0.48	1.65	0.010	0.029	0.73	0.023	0.070	0.002	0.025	0.004	875	850	4	0.76	3.82
12a	0.47	1.70	0.010	0.028	0.73	0.028	0.052	0.004	0.033	0.066	875	850	8	0.55	3.13
13	0.54	0.56	0.012	0.025	1.04	0.013	0.054	0.004	0.018	0.053	875	850	8	0.16	1.51
14	0.48	0.86	0.011	0.030	1.13	0.037	0.060	0.002	0.021	0.038	875	850	8½	0.18	1.60
15	0.48	1.11	0.010	0.027	1.02	0.022	0.060	0.004	0.033	0.029	875	850	9	0.25	1.92
16a	0.44	1.15	0.013	0.029	1.02	0.026	0.094	0.003	0.06	0.087	875	850	8	0.32	2.26
17a	0.49	1.52	0.010	0.029	0.97	0.023	0.070	0.002	0.025	0.006	875	850	3	1.06	4.68
18a	0.48	1.68	0.010	0.035	0.98	0.022	0.060	0.004	0.033	0.089	875	850	8	0.67	3.57
19a	0.47	0.59	0.018	0.031	1.49	0.055	0.09	0.006	0.019	0.031	900	875	8	0.19	1.70
20a	0.47	1.22	0.018	0.031	1.40	0.055	0.09	0.006	0.019	0.051	900	875	8½	0.48	2.90
21a	0.47	1.68	0.018	0.031	1.46	0.055	0.09	0.006	0.019	0.051	900	875	8½	0.83	4.03
22	0.48	0.57	0.018	0.031	1.97	0.055	0.09	0.006	0.019	0.050	925	900	7½	0.28	2.05
23a	0.46	1.22	0.018	0.031	1.92	0.055	0.09	0.006	0.019	0.051	925	900	8½	0.71	3.67
24a	0.48	1.75	0.018	0.031	1.94	0.055	0.09	0.006	0.019	0.051	925	900	7	1.72	6.02

TABLE 1.—(Continued)

Heat No.	Chemical Analysis, Per Cent										Normalizing Temperature, Deg. C.	Quenching Temperature, Deg. C.	Average A.S.T.M. Grain Size	Half Hardness	
	C	Mn	P	S	Si	Ni	Cu	Mo	Cr	Acid-soluble Al, Per Cent				Jominy Depth, In.	Ideal Diameter, In.
RANGE OF COMPOSITION: C, 0.40–0.55 per cent; Mn, 1.50–1.75; Si, 0.20–1.0; Al, >0.10															
25[a]	0.52	1.59	0.019	0.031	0.21	0.032	0.084	0.002	0.023	0.12	875	850	9	0.34	2.34
26[a]	0.49	1.55	0.019	0.031	0.20	0.032	0.084	0.002	0.023	0.21	875	850	9	0.38	2.48
27[a]	0.52	1.65	0.019	0.031	0.22	0.032	0.085	0.002	0.023	0.36	875	850	8	0.51	3.00
28[a]	0.51	1.66	0.008	0.032	0.48	0.038	0.072	0.003	0.019	0.108	875	850	9	0.41	2.64
29[a]	0.44	1.65	0.010	0.032	0.44	0.020	0.044	0.002	0.057	0.25	875	850	9½	0.36	2.42
30[a]	0.50	1.69	0.008	0.032	0.50	0.038	0.072	0.003	0.019	0.22	875	850	9½	0.46	2.81
31[a]	0.40	1.63	0.010	0.032	0.42	0.020	0.044	0.002	0.057	0.37	875	850	9	0.41	2.64
32[a]	0.49	1.70	0.010	0.028	0.71	0.028	0.052	0.004	0.033	0.181	875	850	7	0.78	3.89
33	0.49	1.66	0.010	0.032	0.59	0.020	0.044	0.002	0.057	0.39	875	850	9	0.63	3.43
34[a]	0.48	1.68	0.010	0.035	0.95	0.022	0.060	0.004	0.033	0.159	875	850	7	0.82	4.02
35[a]	0.50	1.68	0.010	0.035	0.99	0.022	0.060	0.004	0.033	0.33	875	850	7	1.09	4.75
RANGE OF COMPOSITION: C, 0.20–0.30 per cent; Mn, 0.50–1.75; Si, 0.20–1.0; Al, <0.10															
36	0.21	0.85	0.018	0.031	0.27	0.047	0.070	0.007	0.024	0.038	900	871	7	0.09	1.17
37[a]	0.20	1.22	0.018	0.031	0.27	0.047	0.070	0.007	0.024	0.047	900	871	7	0.14	1.43
38[a]	0.22	1.77	0.012	0.025	0.26	0.013	0.054	0.004	0.018	0.047	871	838	8	0.20	1.72
39[a]	0.20	0.89	0.018	0.031	0.47	0.047	0.07	0.007	0.024	0.036	900	871	7	0.09	1.15
40[a]	0.19	1.23	0.018	0.031	0.51	0.047	0.07	0.007	0.024	0.023	900	871	7	0.13	1.37
41	0.28	0.87	0.018	0.031	0.50	0.047	0.07	0.007	0.024	0.024	900	871	7½	0.11	1.27
42[a]	0.30	1.24	0.018	0.031	0.51	0.047	0.07	0.007	0.024	0.016	900	871	7½	0.17	1.59
43[a]	0.20	0.83	0.018	0.031	0.64	0.055	0.09	0.006	0.019	0.043	925	900	7	0.09	1.15
44[a]	0.20	0.88	0.018	0.031	1.02	0.055	0.09	0.006	0.019	0.051	925	900	7	0.13	1.40

[a] P, S, Ni, Cu, Mo, and Cr determined on another steel made during same period.

CALCULATION OF MULTIPLYING FACTORS

The multiplying factor for silicon was first calculated by Grossmann's method and with his factors for other alloys, except

There is also a tendency for high-manganese steels to be above the line and for low-manganese steels to be below the line. These deviations suggested that the multi-
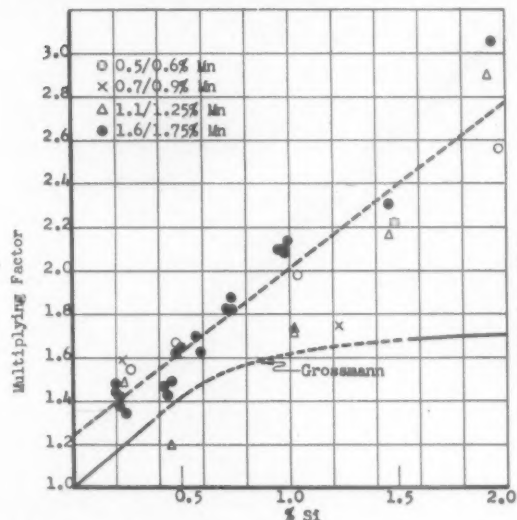
FIG. 1.—MULTIPLYING FACTOR FOR SILICON BASED ON GROSSMANN'S FACTORS (EXCEPT ALUMINUM).

FIG. 2.—MULTIPLYING FACTOR FOR SOLUBLE ALUMINUM.

aluminum, on the 0.40 to 0.55 per cent carbon steels of Table 1. In Fig. 1 are shown plotted against silicon content the ratios of ideal diameter established experimentally to the ideal diameter calculated from Grossmann's ideal diameter for carbon and grain size multiplied by his factors for manganese, phosphorus, sulphur, nickel, copper, molybdenum, chromium and the acid-soluble aluminum factor shown in Fig. 2. The line representing the trend of individual points is straight and does not bend to the right as indicated by Grossmann. Thus it would appear that the multiplying factor for the effect of silicon on hardenability is proportional to the amount present over the range studied from 0.20 to 2.0 per cent silicon.

The trend line in Fig. 1 does not pass through the multiplying factor of 1.0 at zero silicon, as it should do when the increments of hardenability contributed by all of the constituents in the steel are included in the respective multiplying factors.

plying factor for manganese was not sufficiently high to represent the increment of hardenability conferred by manganese. For this reason, a multiplying factor for manganese was determined for these steels.

In calculating the multiplying factor for manganese, it was assumed that Grossmann's values for carbon, grain size, phosphorus, sulphur, nickel, copper, molybdenum and chromium were correct and that, with appropriate factors for manganese, silicon, and acid-soluble aluminum, no other constituents affected the hardenability. With this assumption, the equation for calculation of ideal diameter by Grossmann's principle is as follows (the multiplying function f is the slope of the multiplying factor line):

$$[D_I(\text{C and grain size})][1 + f(\% \text{ Mn})]$$
$$[1 + f(\% \text{ Si})][1 + f(\% \text{ Al})][\text{etc.}] = D_I$$

Because of the difficulties of calculation with three unknown factors, the multiplying factor for acid-soluble aluminum

was determined graphically. Factors for manganese and silicon were first determined roughly for steels of similar aluminum content. The corresponding multiplying multiplying factor for acid-soluble aluminum was found to agree closely with the initially determined value, and is shown in Fig. 2. In the hardenability equation this

FIG. 3.—COMBINED ULTIPLYING FACTORS FOR MANGANESE AND SILICON VS. MANGANESE.
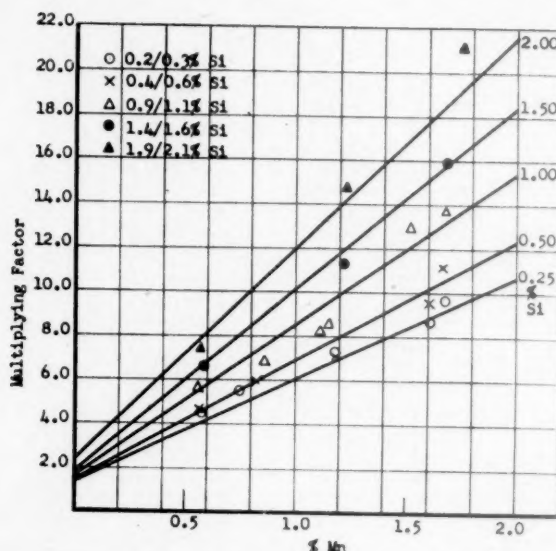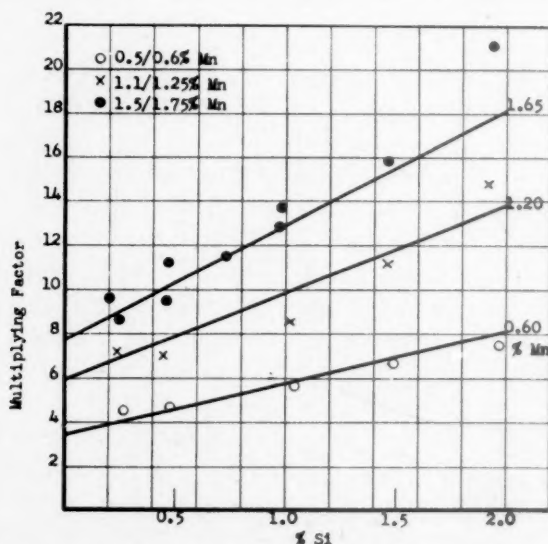
FIG. 4.—COMBINED MULTIPLYING FACTORS FOR MANGANESE AND SILICON VS. SILICON.

factor for aluminum was then determined and introduced into the redetermination of factors for manganese and silicon. These manganese and silicon factors were then calculated more accurately and used to redetermine the aluminum factor. This

factor is represented by the following expression:

$$[1 + (0.93)(\% \text{ Al})]$$

In Figs. 3 and 4 are shown ratios of ideal diameter determined experimentally to

theoretical ideal diameter calculated without manganese and silicon factors. The ratios, therefore, represent the combined product of the multiplying factors for manganese and silicon. Trend lines repre-

The lines are not parallel, as they would be if the multiplying factors were additive, but fan out at higher levels of alloy content because they represent a product of multiplication.
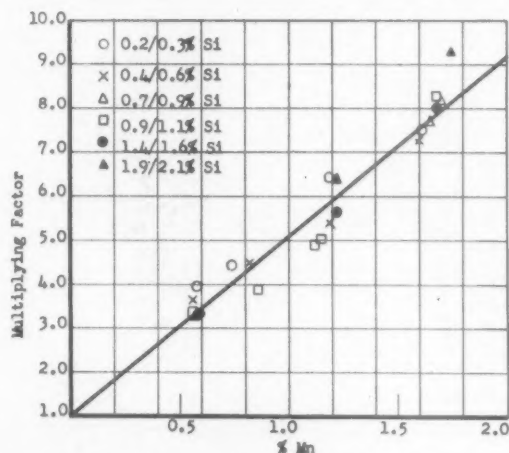
FIG. 5.—MULTIPLYING FACTOR FOR MANGANESE. 0.40 TO 0.55 PER CENT CARBON, < 0.10 PER CENT SOLUBLE ALUMINUM STEEL.
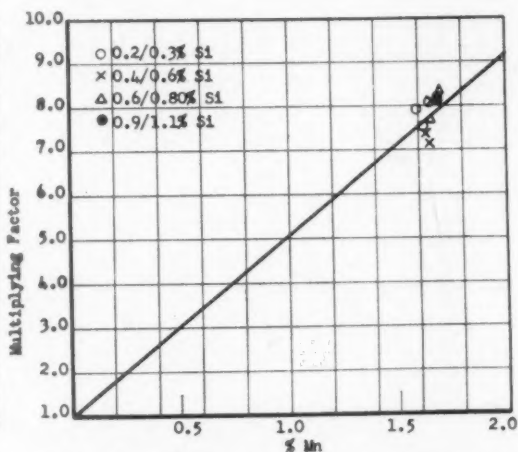
FIG. 6.—MULTIPLYING EACTOR FOR MANGANESE. 0.40 TO 0.55 PER CENT CARBON, > 0.10 PER CENT SOLUBLE ALUMINUM STEEL.
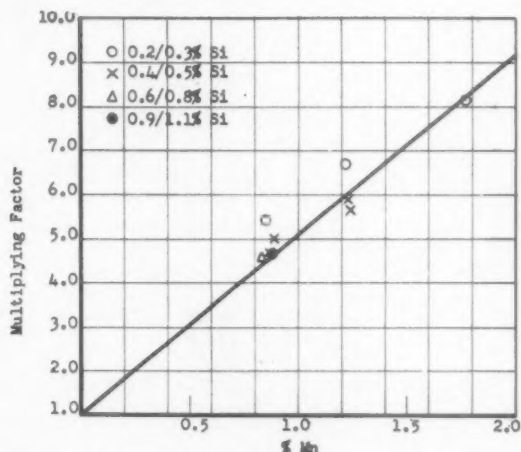
FIG. 7.—MULTIPLYING FACTOR FOR MANGANESE. 0.20 TO 0.30 PER CENT CARBON STEEL.
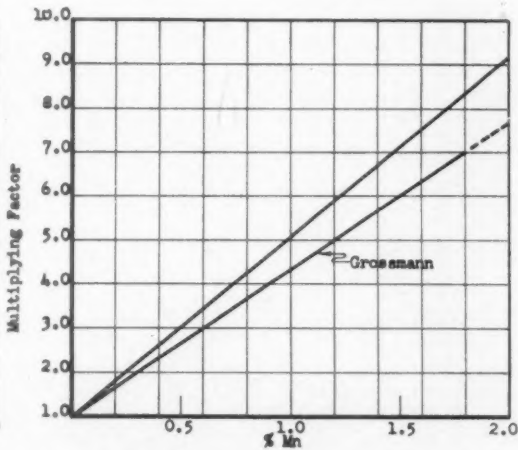
FIG. 8.—COMPARISON OF MULTIPLYING FACTORS FOR MANGANESE.

senting close approximation to the points at graduated levels of manganese and silicon were drawn, and the respective separate multiplying factors were calculated. In the hardenability equation these lines may be represented by the product of the following expressions for the effects of manganese and silicon on hardenability:

$$[1 + (4.08)(\% \text{ Mn})][1 + (0.67)(\% \text{ Si})]$$

The correlation of the multiplying factor for hardenability conferred by manganese alone with the experimentally determined values is shown in Figs. 5, 6 and 7. The points represent the ratio between ideal diameter determined experimentally and ideal diameter calculated from Grossmann's factors except for the acid-soluble aluminum factor given in Fig. 2 and the

silicon factor given in Figs. 9 to 11. As illustrated in Fig. 8, the multiplying factor determined for manganese on these steels is slightly higher than that determined by Grossmann.

through 1.0 at zero alloy content. Thus it is apparent that the higher manganese factor is sufficient to explain the discrepancies of Fig. 1. From this it would seem that, beyond the effects of the elements taken
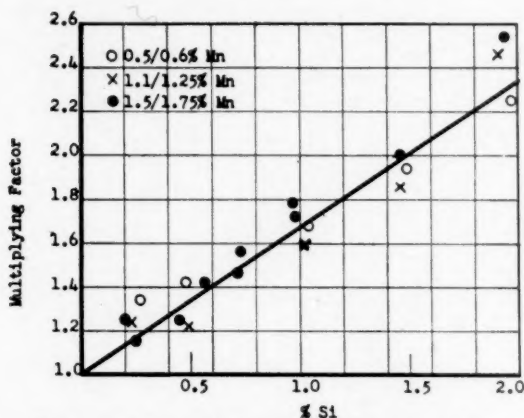
FIG. 9.—MULTIPLYING FACTOR FOR SILICON. 0.40 TO 0.55 PER CENT CARBON, < 0.10 PER CENT SOLUBLE ALUMINUM STEEL.
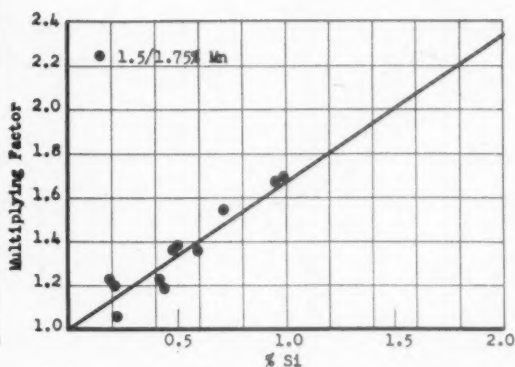
FIG. 10.—MULTIPLYING FACTOR FOR SILICON 0.40 TO 0.55 PER CENT CARBON, > 0.10 PER CENT SOLUBLE ALUMINUM STEEL.
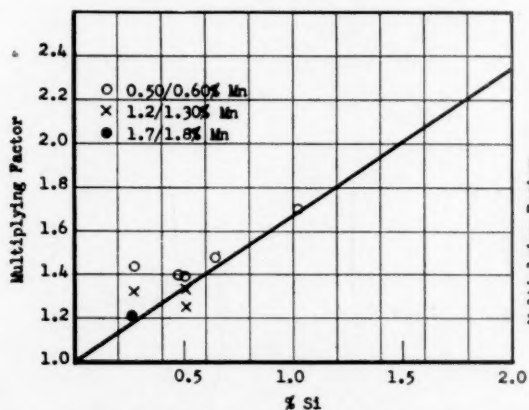
FIG. 11.—MULTIPLYING FACTOR FOR SILICON. 0.20 TO 0.30 PER CENT CARBON STEEL.
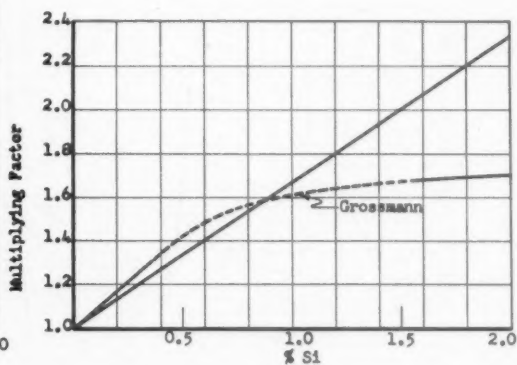
FIG. 12.—COMPARISON OF MULTIPLYING FACTOR FOR SILICON.

The multiplying factor for hardenability conferred by silicon alone is shown in Figs. 9, 10 and 11. The multiplying factor found for silicon in these steels is a straight line from 0.20 to 2.0 per cent silicon and, as shown in Fig. 12, no confirmation was found of the tendency reported by Grossmann for the factor to increase proportionately less at higher silicon contents. It is also notable that, within the limits of error in the data, the multiplying factors for both manganese and silicon appear to pass

into the calculations, there is no other constituent in the steel that exerts a material influence on the hardenability.

CONCLUSIONS

In drawing conclusions from this study of the effect of silicon on hardenability, it should be noted that the steels tested were made in the laboratory and that the results have not been checked against commercial material. The hardenability was measured

by the depth at "half hardness" on Jominy specimens instead of by the direct microscopic examination of quenched bars, therefore the results may not be directly comparable with the multiplying factors determined by Grossmann. With these limitations the following conclusions have been reached:

1. Multiplying factors for the hardenability conferred by silicon, manganese, and acid-soluble aluminum have been determined and found to be applicable within the range of 0.20 to 0.55 per cent carbon, 0.50 to 1.75 per cent manganese, 0.20 to 2.0 per cent silicon and up to 0.40 per cent acid-soluble aluminum. (No test has been made of steel with minimum carbon and manganese and maximum silicon and aluminum contents.)

2. The multiplying factor for silicon has been found to increase directly in proportion to the silicon content up to at least 2 per cent silicon.

3. The steels tested in this investigation have confirmed the Grossmann principle of hardenability calculation by multiplication of factors for each alloy present in the steel.

REFERENCES

1. M. A. Grossmann: *Trans.* A.I.M.E. (1942) 150, 227.
2. S.A.E. Handbook (1942) 315–324.

DISCUSSION

(John S. Marsh presiding)

M. A. GROSSMANN,[*] Chicago, Ill.—The writer was glad to have an opportunity to study the manuscript of this paper, and wishes to express admiration for the care with which the experiments were carried out. Needless to say, we were very pleased to find that the authors were able to confirm the possibility of evaluating hardenability by the use of multiplying factors.

In two respects their values differ somewhat

---

* Director of Research, Carnegie-Illinois Steel Corporation.

from those obtained in our early tests, and we have to admit that their values seem to be reliable.

In the case of manganese, the departure from our results, while not very great, seems nevertheless to be indicated very definitely by their data. With silicon, while their results are not greatly different from ours in the lower range, the values in the higher ranges, from 1 to 2 per cent Si, depart radically from the few data obtained by us. We are inclined to think that some elements unknown to us may have invalidated our earlier factor, especially in view of the continuous linear relationship which they show. We are still at a loss to know why this simple linear relationship apparently holds for so many elements, and we look forward to further work by these authors.

W. CRAFTS AND J. L. LAMONT.—The comments by Dr. Grossmann are greatly appreciated. No explanation for the difference in silicon factors is obvious. For manganese it is believed probable that the minor difference was due to drawing the factor line "through the origin and parallel to the trend" in Grossmann's Figs. 13 and 14. This is equivalent to addition rather than multiplication of factors and would tend to make Grossmann's factor somewhat lower. It is, therefore, believed that there is no real difference between the two manganese factors that cannot be explained by the method of calculation.

J. FIELD, Bethlehem, Pa.—Messrs. Crafts and Lamont have shown that the multiplying factor for silicon, using the Grossmann system, increases in direct proportion to increase in silicon content. This is in contrast to the curve shown by Grossmann in his original paper. The writers have also found that the multiplying factor for manganese is slightly higher than the values shown by Grossmann.

These new values for silicon and manganese were based on Jominy tests made on 44 heats of various silicon and manganese contents shown in Table 1. From these tests, the D_I values were found by noting the distance on the Jominy curve at which the 50 per cent martensite hardness occurred and converting this distance into "ideal critical diameter" (D_I) in accordance with Figs. 28 and 29 of Grossmann's original paper.[1] The D_I values thus obtained

were then used for deriving the new curves for silicon and manganese.

In reversing this process to recalculate the D_I values, using the new values for silicon and manganese, I am at a loss to explain the discrepancy that exists between the calculated values and the values given in Table 1. For example, I have selected several heats shown in Table 1 and calculated the D_I values from the chemical analysis and grain size, using the silicon, manganese, and soluble aluminum factors developed by Crafts and Lamont. The disagreement between the values thus calculated and the values shown in Table 1 is apparent (Table 2).

TABLE 2.—*Comparison of Calculated Values with Values of Table 1*

	Heat No. 18		Heat No. 24		Heat No. 35	
	Table 1	Calculated	Table 1	Calculated	Table 1	Calculated
C	0.48	0.216 (8 gr.)	0.48	0.235 (7 gr.)	0.50	0.240 (7 gr.)
Mn	1.68	7.85	1.75	8.14	1.68	7.85
P	0.010	1.02	0.018	1.05	0.010	1.02
S	0.035	0.98	0.031	0.98	0.035	0.98
Si	0.98	1.67	1.94	2.30	0.99	1.66
Ni	0.022	1.01	0.055	1.02	0.022	1.01
Cu	0.060	1.02	0.09	1.03	0.060	1.02
Mo	0.004	1.01	0.006	1.02	0.004	1.01
Cr	0.033	1.07	0.019	1.04	0.033	1.07
Al	0.089	1.08	0.051	1.05	0.33	1.31
D_I	3.57	3.41	6.02	5.29	4.75	4.56

Work that I have done to date on Jominy tests varying in silicon content from 0.75 to 3.50 per cent substantiates the proportional effect for silicon found by Crafts and Lamont. There is some evidence, however, based on these results, that above 2.00 per cent the curve for the silicon factor is no longer linear. I have not as yet determined the exact silicon content at which the curve ceases to be linear.

I would appreciate the authors' explanation of these apparent discrepancies.

W. CRAFTS AND J. L. LAMONT.—The authors are gratified to learn that Mr. Field's tests confirm the proportional increase in hardenability factor with silicon in the ranges up to 2 per cent Si. It is to be anticipated that this linear relation will be modified by the persistence of ferrite and difficulty of obtaining homogeneous austenite at higher silicon levels. The deviations from the average that were found in individual heats may result from error in analysis, heat-treatment, hardness measurement, grain-size estimation, etc., or from some deficiency in the Grossmann multiplying principle for calculating hardenability. In heats 18 and 35, the deviations from the average are fairly typical and probably are caused by minor errors. Heat 24 is further from the average than most of the other steels, but as it represents the extremes of the manganese and silicon ranges studied, it is not possible to conclude that the deviation is entirely due to an accumulation of small errors, as it might be due in part to a nonlinear tendency of a multiplying factor. However, over the range of compositions studied, the typical and even the extreme deviations from linear proportionality are not considered to justify any modification of Grossmann's multiplying principle for the hardenability factors up to 2 per cent manganese, 2 per cent silicon, and 0.5 per cent aluminum. Mr. Field's question regarding the reasonable degree of deviation is appreciated and emphasizes the need for great care in establishing and utilizing hardenability factors.

Calculated Hardenability and Weldability of Carbon and Low-alloy Steels

By C. E. Jackson,* Member A.I.M.E., and G. G. Luther*

THE relationship between hardenability and weldability has been mentioned many times. The ease of making a hardness survey has led to its wide use as a criterion

FIG. 1.—BEAD WELD SHOWING LOCATION OF V-NOTCH. × 4.

of weldability and with a given class or series of steels for which the ductility under weld heat-treatment is known the test is entirely suitable. However, in studying a new steel the hardness survey is of less value, since it is based on the assumption that there is a correlation between hardness and ductility.

Several attempts have been made to derive indices for weldability[1] and hardenability from the chemical analysis. In most of these proposals the effects of the different elements were considered to be additive, but recently Grossmann[2] proposed a novel method of calculating the hardenability of a steel from its chemical composition. In the method proposed, a steel is considered as having a base hardenability due to its carbon content and grain size, and this base hardenability is multiplied by a factor for each chemical element present. The final product is the hardenability.

The purpose of the present study is to point out the possible relationship between hardenability and the effect of welding on hardness and ductility for a number of plain carbon and low-alloy steels. The composition of the 25 steels reported in this paper as determined by chemical analysis is given in Table 1. To eliminate the effect of variations in finishing temperatures, the ½-in. plates were normalized after heating for one hour at 1650°F. in a controlled-atmosphere furnace.

In making comparative tests, it is essential to hold conditions as constant as possible; hence full automatic welding control was used. The electrodes, all supplied by

[1] References are at the end of the paper.

one manufacturer, were of mild steel, heavy coated, reversed polarity (grade EA, class 1) with $\frac{3}{16}$-in. diameter core.

Single bead welds were deposited trans-

amp. current, an arc voltage of 26 volts, and a speed of travel of 6 in. per min. Knoop and Vickers hardness numbers[3] were determined on sections cut trans-
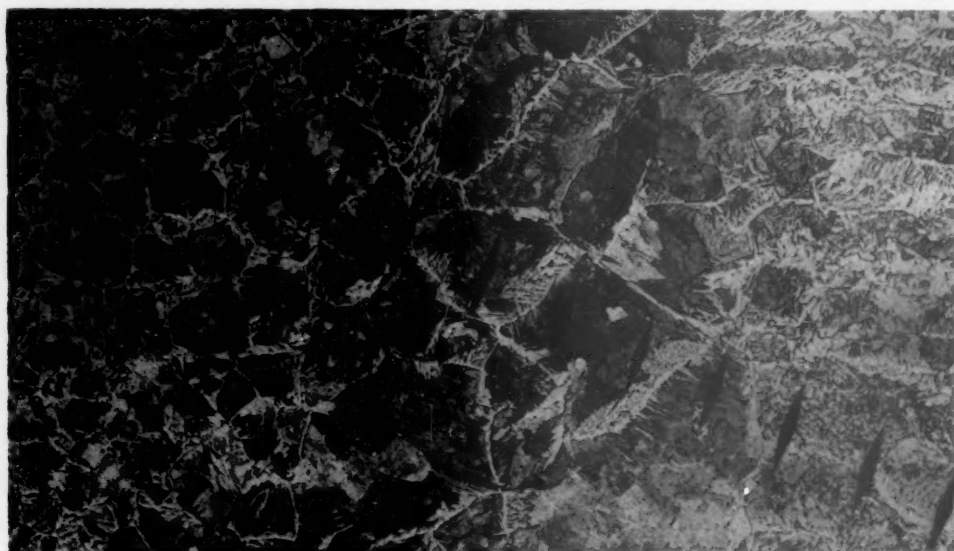
FIG. 2.—MICROSTRUCTURE AT FUSION LINE SHOWING A SERIES OF KNOOP INDENTATIONS. × 100

verse to the direction of rolling on sections of $\frac{1}{2}$-in. plate, 6 in. wide by 7 in. long, by using full automatic welding. A uniform welding technique was used, with 175-

verse to the bead weld (Fig. 1). For the Knoop hardness indents, a load of 0.2 kg. was used. Indentations were made with a separation of not more than 0.1 mm.

TABLE 1.—*Composition of Steels Determined by Chemical Analysis*

Composition, Per Cent								Grain Size at Fusion Line	Calculated Hardenability, In.
C	Mn	Si	S	P	Ni	Cu	Cr		
0.18	0.40	0.002	0.002	0.031				5	0.39
0.25	0.47	0.003	0.003	0.029				3	0.58
0.17[a]	0.40	0.39	0.031	0.012				4	0.66
0.20	0.42	0.05	0.032	0.012		0.05	0.04	3	0.75
0.26	0.45	0.01	0.032	0.008	0.06	0.16	0.05	2	0.77
0.30	0.52	0.01	0.042	0.011	0.08	0.27	0.06	4	0.85
0.23	0.39	0.16	0.037	0.010	0.09	0.22	0.04	2	0.87
0.08[a]	0.55	0.12	0.023	0.010	3.40			5	0.92
0.17	0.46	0.23	0.024	0.016	1.43			3	0.93
0.14[a]	0.52	0.35	0.026	0.010	1.90			5	0.98
0.11	0.46	0.18	0.028	0.007	1.78	0.99		3	1.08
0.31	0.68	0.19	0.037	0.012	0.02	0.15	0.06	3	1.21
0.12[a]	0.51	0.45	0.026	0.010	3.37			4	1.28
0.29	0.78	0.22	0.040	0.023	0.05	0.21	0.06	4	1.30
0.19	0.57	0.22	0.023	0.010	2.34			3	1.31
0.29	1.06	0.25	0.002	0.017				4	1.32
0.23	0.48	0.19	0.022	0.009	3.35			3	1.52
0.28	0.68	0.20	0.019	0.034	2.25			4	1.61
0.18	0.53	0.31	0.024	0.012	3.46			4	1.62
0.34	0.90	0.22	0.032	0.013	0.06	0.21	0.06	3	1.76
0.30	0.95	0.18	0.028	0.012		0.09	0.10	2	1.78
0.14[a]	0.98	0.09	0.017	0.003	2.03	1.06		4	1.90
0.18[a]	0.63	0.48	0.025	0.010	3.38			4	2.00
0.31	1.46	0.25	0.031	0.013	0.09	0.24	0.05	3	2.39
0.26[a]	0.58	0.36	0.023	0.011	3.35			4	2.65

[a] Experimental steels.

(0.004 in.) across the heat-affected zone and particular attention was given to the fusion line. The point of maximum hardness usually occurred 0.1 to 0.2 mm. away from the deposited metal into the base metal.

pearlite grain size is well defined. The A.S.T.M. grain size for the structure that shows the greatest grain growth was determined (Table 1), since it is this grain
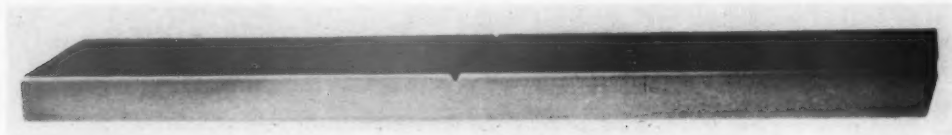
FIG. 3.—V-NOTCHED SLOW-BEND SPECIMEN.
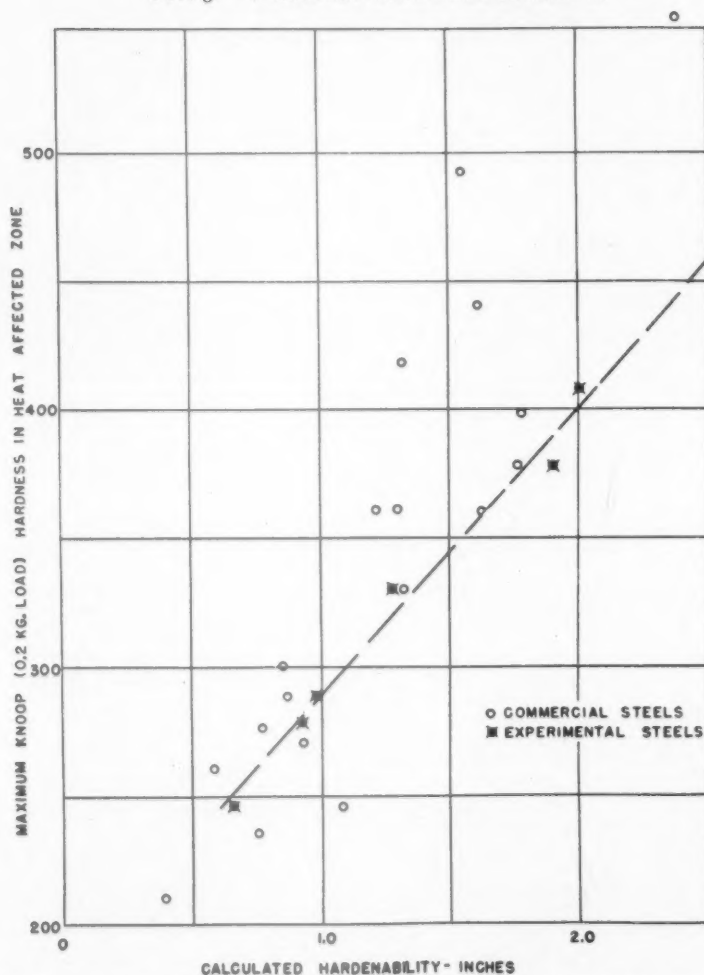
FIG. 4.—RELATION OF MAXIMUM KNOOP HARDNESS AND CALCULATED HARDENABILITY.

the deposited metal into the base metal. The precision of the Knoop method is such that it is possible to detect changes in hardness that cannot be measured by the usual Vickers hardness test methods.

A photograph at 100 times magnification of the microstructure at the fusion line is shown in Fig. 2. The enlarged ferrite-

size that influences the hardenability and mechanical behavior of the fusion zone. The results obtained from calculation of the hardenability of the zone of grain growth, using methods proposed by Grossmann,[2] are also given in Table 1. In some steels that yield an acicular structure in the heat-affected zone, difficulty may be

encountered in determining the ferrite-pearlite grain size at the fusion zone.

As a measure of the effect of welding on ductility, strips 1½ in. wide were cut trans-

For comparison, an identical specimen was prepared and tested from the plate material. The specimens were bent to failure with the notched face in tension in a test jig. The
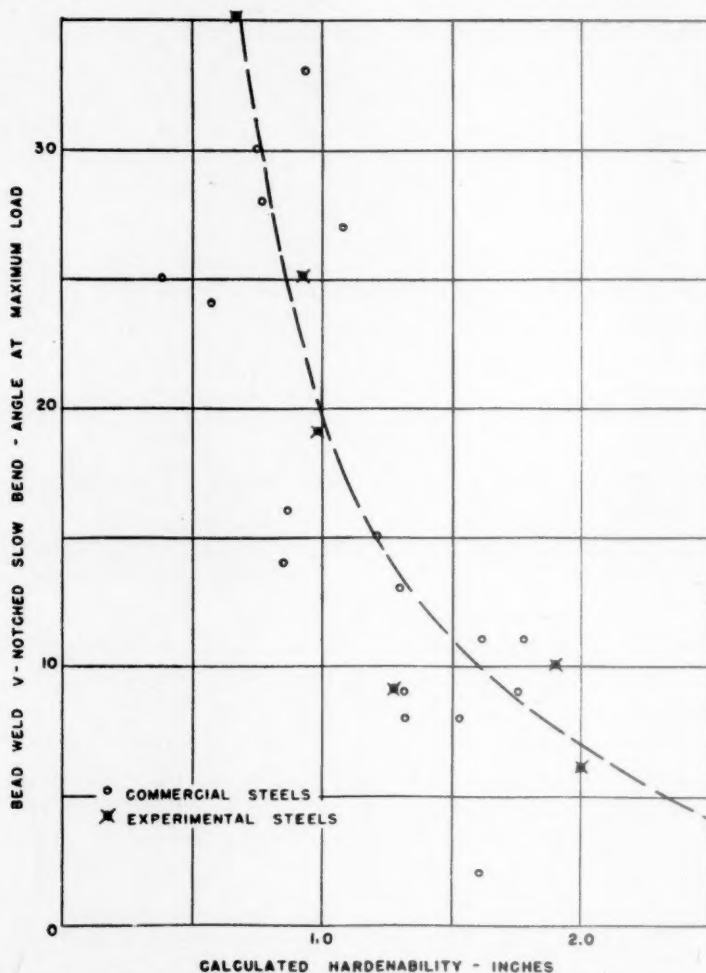
FIG. 5.—RELATION OF ANGLE AT MAXIMUM LOAD FOR SLOW-BEND SPECIMENS AND CALCULATED HARDENABILITY.

verse to the direction of the bead weld. Only sufficient metal was removed from the top surface to eliminate surface irregularities. Material was then machined from the lower surface to obtain a specimen 0.375 in. thick, with a ground finish on both faces. The specimens were etched in a 5 per cent nital solution and the location of the V-notch was determined by scribing a line on the side of the specimen. A standard Izod-type of V-notch was machined with its apex tangent to the fusion line between the weld metal and the plate material (Fig. 3).

angle at maximum load was taken as a measure of ductility for each test specimen.

The relation of hardenability as determined by calculation from the chemical composition to weldability test data is presented in Table 2 and Figs. 4 and 5. The correlation between the calculated hardenability and maximum hardness as determined by the Knoop method is excellent for the experimental steels, in which the minor constituents were held to a minimum. This correlation is by no means as good for the commercial steels in which

there is less control of the minor constituents and for which complete chemical analyses were not made. This will explain the fact that in most cases the maximum hardness reported is higher than that which might be predicted from the calculated hardenability.

TABLE 2.—*Relation of Hardenability to Weldability*

Calculated Hardenability, In.	Maximum Hardness of Bead Weld		V-notched Slow-bend Angle at Maximum Load, Deg.	
	Vickers, 10 Kg.	Knoop, 0.2 Kg.	Plate	Bead Weld
0.39	184	210	25	25
0.58	231	260	31	24
0.66	195	245	56	35
0.75	185	235	58	30
0.77	223	276	25	28
0.85	248	300	22	14
0.87	212	288	25	16
0.92	243	278	40	25
0.93	282	270	33	33
0.98	230	288	31	19
1.08	212	245	32	27
1.21	260	360	21	15
1.28	287	329	25	9
1.30	284	360	25	13
1.31	270	329	11	9
1.32	357	418	19	8
1.53	357	492	38	8
1.61	383	440	15	2
1.62	302	360	27	11
1.76	278	378	16	9
1.78	256	398	14	11
1.90	312	377	26	10
2.00	333	407	22	6
2.39	393	552	13	5
2.65	421	478	19	3

The relationship between the calculated hardenability and weld ductility as measured by the V-notched slow-bend specimen is not as regular as that for the maximum hardness. This is to be expected, as the ductility will also be dependent upon other factors, such as the type and number of nonmetallic inclusions or other segregation present in the steel.

The use of calculated hardenability, or may we say calculated weldability, will increase in its usefulness as additional data for the various welding steels become available. Probably it will be necessary to determine new weldability factors for alloying additions—and it is entirely possible that these factors for the welding thermal cycle will not be in strict agreement

with the factors for full hardening. Care must be taken in applying the calculation to any steel, as the combination of mechanical properties obtained for an alloy steel may show unusually high ductility, although the maximum hardness determined may conform to the general prediction. Additional data should be obtained in order to determine more accurately the limits for the application of calculated hardenability. Actual measurements of hardenability by using a Jominy type specimen or a quenched taper bar will also be useful. Tentatively, a limit of hardenability of a 1.0-in. round in an "ideal quench" (grain size 3) seems to be a limit for straightforward welding in plain carbon and low-alloy steels.

ACKNOWLEDGMENTS

REFERENCES

1. J. Dearden and H. O'Neill: A Guide to the Selection and Welding of Low-alloy Structural Steels. *Trans*. Inst. of Welding (1940) **3**, 203–214.
2. M. A. Grossmann: Hardenability Calculated from Chemical Composition. *Trans*. A.I.M.E. (1942) **150, 227**.
3. C. E. Jackson and G. G. Luther: Weldability Tests of Nickel Steels. Research Supplement, *The Welding Jnl*. (Oct. 1941) **20**, 437s–452s.

DISCUSSION

(*A. B. Kinzel presiding*)

M. A. GROSSMANN,* Chicago, Ill.—Although the authors, in summarizing their results, are properly cautious, nevertheless the correlations they demonstrate constitute a most stimulating advance in the field. Thus they point out that the factors for the welding cycle (absence of full hardening) may not be in agreement with those for full hardening, but that there is some relationship seems indicated strongly by their data.

* Director of Research, Carnegie-Illinois Steel Corporation.

One point may be mentioned in reference to the carbon content. In quenching, the hardness attained is influenced both by the hardenability of the steel and by its carbon content. In this respect their weldability test is again analogous to quenching, since for equal hardenability the hardness is shown to be higher for the higher carbon contents (quite satisfactorily so, considering the difficulties in the microhardness testing).

A. B. KINZEL,* New York, N. Y.—This work by Jackson and Luther maintains their usual standard of excellence and presents a useful method of approximating weldability of steels. The most surprising fact in the results is not some deviation between the calculated and actual values, but rather that these were so close. The Grossmann factor is based on half hardness, generally corresponding to Brinell values appreciably higher than those in question and cited in Table 2. If Jominy curves of the various steels were similar in shape, we would expect the relationship of the higher Brinell to hold for the lower Brinell, but we know that the Jominy curves of various steels that are about the same at high Brinell values may differ markedly at lower levels. This accounts for much of the scatter and probably is even more important than the absence of complete analysis and the effect of very small amounts of residual elements in the steels.

These remarks are not intended in any way to detract from the usefulness of the concept here proposed. It is a qualitative index of weldability and the deviation resulting from any of the causes mentioned above is probably no more than the spread of values for ductility corresponding to identical hardness of different steels. This last factor has been duly emphasized by the authors.

C. M. LOEB, JR.,† New York, N. Y.—In studying Fig. 4, we believe that it is possible that some of the discrepancies between the straight-line relationship of maximum Knoop hardness and calculated hardenability may be due to microscopic heterogeneity. We refer in this term to that discussed recently by Parke and Herzig.[4]

This microscopic heterogeneity could be noted as a result of these new indentation measurements because they are small enough to measure parts of a grain, particularly in the heat-affected zone where the grain size has been greatly increased because of the welding operations. It is possible that where such microscopic heterogeneity is encountered, an average rather than a maximum figure in Knoop hardness would be more indicative of the reaction to welding, and possibly produce a more uniform interpretation of weldability by this method.

A. P. EDSON,* Bayonne, N. J.—This paper is interesting in its implication of the possibility of predicting the weld-hardening of steel from its chemical composition. It is suggested, however, that the choice of Dr. Grossmann's hardenability equation as a basis for relating the results of weld-hardening tests to composition may not have been altogether fortunate. In a recent paper the writer[5] presented an empirical equation for the calculation of maximum weld-zone hardness from the chemical composition of steel welded under specified fixed conditions. The maximum Vickers hardness calculated according to this equation for the analyses of the steels reported here by Jackson and Luther deviates an average amount of less than ± 10 per cent from the reported observed values, although these welds were made under conditions somewhat different from those for which the equation was derived. The order of agreement between observed and calculated hardness values is shown graphically in Fig. 6.

As shown in Fig. 7, there is also a relatively good correlation between ductility in the weld-bead V-notch slow-bend test and the calculated weld-zone hardness; a correlation appreciably better than that shown for ideal critical diameter in the authors' Fig. 5. We should like to suggest, therefore, that maximum hardness in the weld zone may prove a better criterion than the ideal critical diameter for predicting the weldability of steel from its composition.

The weld-zone hardness equation has a distinct advantage over Dr. Grossmann's hardenability expression in that the grain size at the fusion line need not be determined, and calcu-

* Chief Metallurgist, Union Carbide and Carbon Research Laboratories.
† Vice-President, Climax Molybdenum Company.
[4] Parke and Herzig: *Metals and Alloys* (Feb. 1942).

* International Nickel Co., Research Laboratory.
[5] A. P. Edson: Weld Hardening and Steel Composition. *Metals and Alloys* (June 1942).

lations may be made from chemical analysis alone, without regard to silicon content over the normal range. Because of a difference in the nature of the equations, calculations of peak

FIG. 6.—COMPARISON OF OBSERVED AND CALCULATED MAXIMUM WELD-ZONE HARDNESS.

hardness in the weld zone is probably somewhat simpler and more readily amenable to graphical solution than is the ideal critical diameter. The weld-zone hardness equation to which reference has been made is:

$$\log_{10} VHN = 1.957 + 1.141 \times \text{per cent C}$$
$$+ 0.193 \times \text{per cent Mn}$$
$$+ 0.086 \times \text{per cent Ni}$$
$$+ 0.160 \times \text{per cent Cr}$$
$$+ 0.363 \times \text{per cent Mo}$$
$$+ 0.180 \times \text{per cent V}$$
$$+ 0.030 \times \text{per cent Cu}$$

The conditions to which it applies are detailed in the original paper in *Metals and Alloys*.

C. E. JACKSON (author's reply).—The comment by Dr. Grossmann that "in quenching, the hardness attained is influenced both by the hardenability of the steel and by its carbon content" is well taken, since this accounts for much of the variation in Fig. 4. In general the maximum bead-weld hardness for a given hardenability increases with the carbon content. A more complete study of the effect of

grain size is essential in determining the exact relationship of hardenability and weldability.

Dr. Kinzel's discussion of the variations in Jominy curves further substantiates the sug-
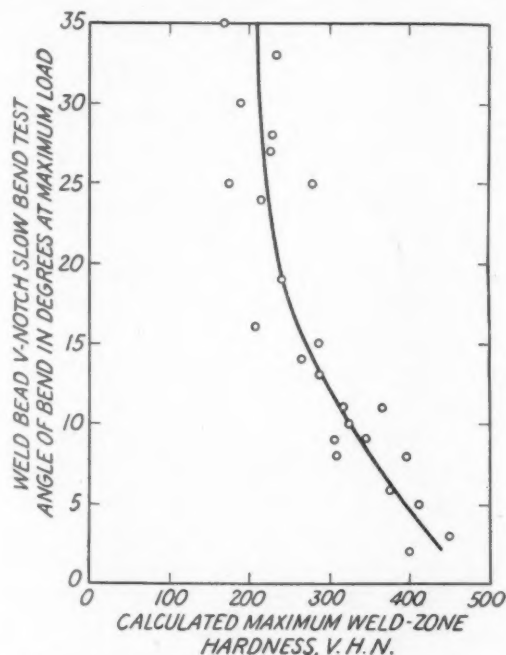
FIG. 7.—RELATION OF ANGLE OF BEND IN DEGREES AT MAXIMUM LOAD TO CALCULATED MAXIMUM WELD-ZONE HARDNESS.

gestion that the use of an end-quench bar for actual measurements of hardenability will be useful in the study of calculated hardenability results.

An attempt to use an average Knoop hardness, as suggested by Mr. Loeb, was disappointing. The precision of the Knoop method is such that it is possible to obtain the maximum hardness in the heat-affected zone; averaging the Knoop hardness values gives a result similar to the Vickers observation.

We appreciate Mr. Edson's discussion, although we definitely feel that the effect of silicon and of grain size on bead-weld hardness cannot be overlooked. There is an ever increasing accumulation of data which points to the fact that the bead-weld hardness is not affected logarithmically by all alloy additions, hence the formula suggested can never furnish more than an approximate result.

Discussion of
Effects of Eight Complex Deoxidizers on Some 0.40 Per Cent Carbon Forging Steels

(Paper by GEORGE F. COMSTOCK, TRANSACTIONS, Vol. 150, p. 408)

BY WALTER CRAFTS,* MEMBER A.I.M.E.

TESTS carried out at the Union Carbide and Carbon Research Laboratories, Inc., on the effects of grain-refining deoxidizers are in substantial agreement with the data presented by Mr. Comstock. Notable is the observation that, although boron and aluminum increased hardenability, the steel was of poor quality in comparison with the other boron-treated steels to which at least two grain refiners were added. The effect of zirconium in improving the ductility of the chromium-nickel steel is in agreement with our experience that zirconium is specifically beneficial to chromium steels. In order to amplify Mr. Comstock's results and to indicate some of the basic principles of special deoxidation, the primary observations of our study have been summarized.

shown that in order to obtain deep hardening without using such large amounts of boron as to result in impairment of ductility, the steel must be thoroughly deoxidized. This may be accomplished by a high silicon content or a grain-refining addition of strong deoxidizers. The degree of grain refinement and hardenability are inclined to be erratic when only one grain-refining element is used, although aluminum, zirconium, titanium, and vanadium have been used singly and resulted in increased, although somewhat erratic, hardenability. The ductility likewise was inclined to be inconsistent when only one grain-refining deoxidizer was added. By combinations of grain-refining elements, it was found possible to combine the specific virtues and

TABLE 1

Deoxidation	Composition, Per Cent			Grain Size	Hardenability J_{50}— $\frac{1}{16}$ In.	Yield Point, Lb. per Sq. In.	Tensile Strength, Lb. per Sq. In.	Elongation in 2 In., Per Cent	Reduction of Area, Per Cent	Izod Ft-lb.
	C	Mn	Si							
Al-B	0.49	1.57	0.22	7–8(6)	12	182,000	208,000	8.0	26.5	7.3
Ti-B	0.43	1.66	0.21	7–8(6)	10	181,000	195,000	12.0	44.0	11.0

The effect of boron in increasing hardenability was described by R. Walther, U. S. Patent No. 1519388, Dec. 16, 1924, but effective amounts in incompletely deoxidized steel are sufficient to harm hot workability and room-temperature ductility. Work at the Union Carbide and Carbon Research Laboratories, Inc., has

counteract some of the defects of each element. In addition, the complex deoxidizers gave more consistent grain refinement and hardenability.

When used in combinations, each element adds its own specific influence as well as modifying the character of the other elements. The function of aluminum is primarily to give consistent results and to minimize abnormalities resulting from too

---

* Research Metallurgist, Union Carbide and Carbon Research Labs. Inc., Niagara Falls, N. Y.

strong additions of other grain refiners. Titanium is of specific value in increasing ductility and, as illustrated by Mr. Comstock, titanium also contributes strongly

TABLE 2

Deoxidation	Grain Size	Hardenability J50—$\frac{1}{16}$ in.	Yield Point Lb. per Sq. In.	Tensile Strength, Lb. per Sq. In.	Elongation in 2 In., Per Cent	Reduction of Area, Per Cent
B-Al-V-Ti	7–8(6)	15	242,500	265,000	6.5	20.9
B-Al-V-Zr	7–8(6)	33	234,000	265,000	8.0	31.2

toward grain refinement. Typical results of high-frequency furnace heats of S.A.E. 1345 steel treated with 0.01 per cent boron and either 0.06 per cent aluminum or 0.075 per cent titanium, follow. The steels had the composition shown in Table 1 and were quenched in oil from 850°C. and drawn at 400°C. in 1-in. diameter bars.

Zirconium produces effects quite similar to titanium and, as observed by Mr. Comstock, is particularly beneficial in maintaining high ductility in chromium steels. The typical results shown in Table 2 were obtained on basic arc furnace steels containing 0.49 per cent C, 1.04 per cent Mn, 0.33 per cent Si, 0.69 per cent Cr that were treated in the ladle with 0.01 per cent boron and 0.05 per cent each of the indicated deoxidizers. The specimens were rough-machined before oil quenching from 850°C. and drawing at 315°C.

Combinations of aluminum, titanium, and zirconium in amounts sufficient to produce grain refinement tend toward the formation of oxide galaxies in the steel. This tendency may be reduced by partial substitution with vanadium or calcium to produce clean steels. Calcium in such combinations is an effective grain-refining element, assists in the development of high ductility, and is believed to balance irregularities in the efficiency of deoxidation to

TABLE 3.—*Properties of Steels Treated with Complex Deoxidizing Alloys*

Steel	Deoxidation	Composition, Per Cent						Grain Size	Hardenability J45 ($\frac{1}{16}$ In.)
		C	Mn	Si	Cr	Mo	Ni		
Cr	Al	0.49	0.91	0.46	0.54			8(6–7)	6
Cr	Silcaz No. 3	0.50	0.75[a]	0.25[a]	0.50[a]			7–8(6)	10
Cr	Silvaz No. 3	0.49	0.75[a]	0.25[a]	0.50[a]			7–8(6)	12
Mn-Cr	Al	0.35	1.19	0.23	0.55			7–8	4
Mn-Cr	Silcaz No. 3	0.37	1.17	0.18	0.54			7–8(6)	11
Mn-Cr	Silvaz No. 3	0.35	1.15	0.20	0.56			7–8(6)	11
Mn-Mo	Al	0.37	1.21	0.18		0.24		7–8(6)	3
Mn-Mo	Silcaz No. 3	0.35	1.19	0.16		0.26		6–8	12
Mn-Mo	Silvaz No. 3	0.36	1.18	0.19		0.27		7–8(6)	9

Steel	Deoxidation	Quenching Temperature, Deg. C.	Medium	Drawing Temperature, Deg. C.	Yield Point, Lb. per Sq. In.	Tensile Strength, Lb. per Sq. In.	Elongation in 2 In., Per Cent	Reduction of Area, Per Cent	Izod Ft-lb.
Cr	Al	850	Oil	550	110,000	136,500	17.5	53.0	46.0
Cr	Silcaz No. 3	850	Oil	550	128,000	147,250	17.0	51.9	31.5
Cr	Silvaz No. 3	850	Oil	550	142,000	156,500	15.0	50.6	30.0
Mn-Cr	Al	850	Oil	400	154,500	170,500	11.0	41.9	14.5
Mn-Cr	Silcaz No. 3	850	Oil	400	189,500	207,000	11.0	42.2	11.5
Mn-Cr	Silvaz No. 3	850	Oil	400	191,000	208,000	11.0	43.4	12.0
Mn-Mo	Al	850	Oil	400	108,000	137,500	14.0	42.2	33.5
Mn-Mo	Silcaz No. 3	850	Oil	400	189,000	203,000	11.0	43.7	14.0
Mn-Mo	Silvaz No. 3	850	Oil	400	193,000	209,500	11.0	44.3	10.8

[a] Nominal analysis.

give more consistent hardenability. Vanadium contributes to hardenability more than the other grain refiners and increases toughness. In order to take advantage of

made in either the high-frequency or arc furnaces. In addition, the ductility of the open-hearth steels is usually superior to that of laboratory heats. In one test an
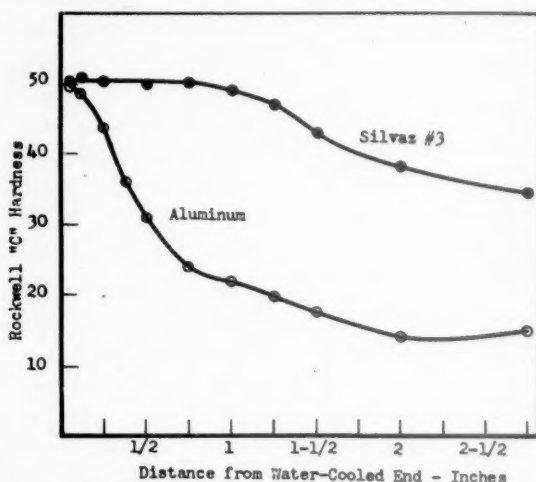
FIG. 1.—HARDENABILITY OF S.A.E. T-1330 STEELS.

the specific properties conferred by individual deoxidizers, combination alloys containing boron, aluminum, zirconium, titanium, and either calcium (Silcaz No. 3) or vanadium (Silvaz No. 3) have been developed. Typical laboratory heats of steels treated with complex deoxidizing alloys of these types have given the properties listed in Table 3.

The results obtained on laboratory heats have been surpassed in the treatment of open-hearth steel. In all cases it has been

aluminum-treated steel containing 0.33 per cent C, 1.69 per cent Mn, 0.23 per cent Si was treated in the mold with 4 lb. per ton of Silvaz No. 3. Jominy hardenability curves of the aluminum-treated and Silvaz-treated bars are shown in Fig. 1. The aluminum-treated steel hardened to R_C 45 at $\frac{4}{16}$-in. whereas the Silvaz-treated steel had a J_{45} depth of $2\frac{2}{16}$ in. After quenching from 850°C. and drawing at the indicated temperatures, the steels had the properties shown in Table 4.

TABLE 4.—*Properties of Aluminum-treated and Silvaz-treated Steels*

Deoxidation	Heat-treated Section, In.	Quenching Medium	Drawing Temperature, Deg. C.	Yield Point, Lb. per Sq. In.	Tensile Strength, Lb. per Sq. In.	Elongation in 2 In., Per Cent	Reduction of Area, Per Cent	Izod Ft-lb.
Al	0.53	Oil	232	207,500	246,000	14.0	48.7	7.3
Silvaz No. 3	0.53	Oil	232	216,000	244,000	14.0	52.1	23.8
Al	1¾	Oil	550	88,150	116,000	22.0	61.2	72.5
Silvaz No. 3	1¾	Oil	550	122,900	137,900	20.0	58.2	55.0
Al	1¾	Water	550	101,250	124,500	21.5	59.4	57.0
Silvaz No. 3	1¾	Water	550	116,500	132,000	21.0	62.8	72.5

found that the hardenability of open-hearth steel treated with special deoxidizers is greater than corresponding compositions

Mr. Comstock concluded that no improvement was conferred by boron-bearing deoxidizers when the specimens were

water-quenched and tempered at high temperatures. It should be pointed out, however, that his tensile tests after tempering at 900°F. were made on small

Cr, Mo, reduce mass effect. The greater hardenability, however, is reflected by the longer time required for transformation of austenite at elevated temperatures.
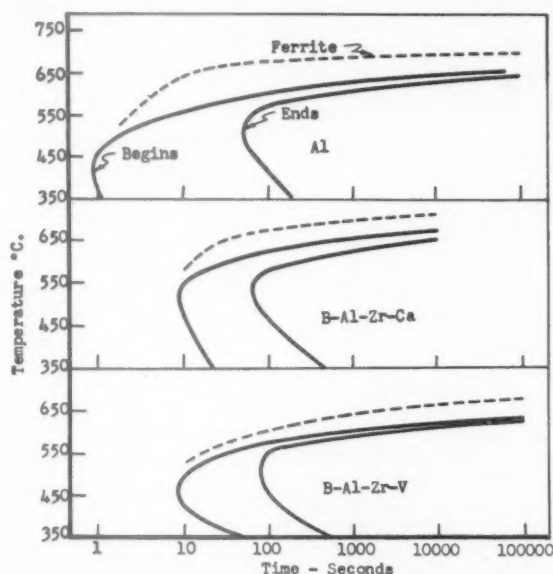
FIG. 2.—ISOTHERMAL TRANSFORMATION OF 1.65 PER CENT MANGANESE STEELS.

specimens quenched in water. The severe quench masked the capacity of special deoxidation to reduce mass effect. As shown above for S.A.E. T1330 steel quenched in 1¾-in. diameter bars, the greater depth of hardening of the steel treated with Silvaz No. 3 resulted in a substantial increase of yield point and tensile strength. Aside from strength alone, the greatest effect of increasing hardenability is to raise the yield point. This is particularly significant in steels that require tempering at a high temperature to a relatively low strength. High alloy contents are usually not necessary to obtain the strength but without alloys the steels are deficient in yield point. Where high yield or proof stress is required at relatively low strength the specially deoxidized steels appear to be eminently suitable.

The mechanism by which deoxidizers and boron increase hardenability is no more readily explained than is the mechanism by which conventional alloys, like Mn, Ni,

This is illustrated by the S-curves of isothermal transformation (Fig. 2) of manganese steels having the following compositions:

Deoxidation	Composition, Per Cent			Grain Size	Hardenability J50—¹⁄₁₆ In.
	C	Mn	Si		
Al	0.51	1.61	0.25	7–8(6)	4
B-Al-Zr-Ca	0.40	1.65	0.28	7–8(6)	11
B-Al-Zr-V	0.52	1.56	0.24	8	14

The interval before ferrite formation is increased sharply by special deoxidation. The tendency toward suppression of ferrite is more evident in the steel treated with the vanadium-bearing deoxidizer. It is also to be noted that the interval before transformation is changed relatively little in the pearlitic range. At lower temperatures, from 550° to 350°C., the beginning of transformation is retarded greatly, but the time required for completion of trans-

formation is increased relatively little. This tendency toward narrowing of the range of transformation has been observed previously as a result of more complete deoxidation.
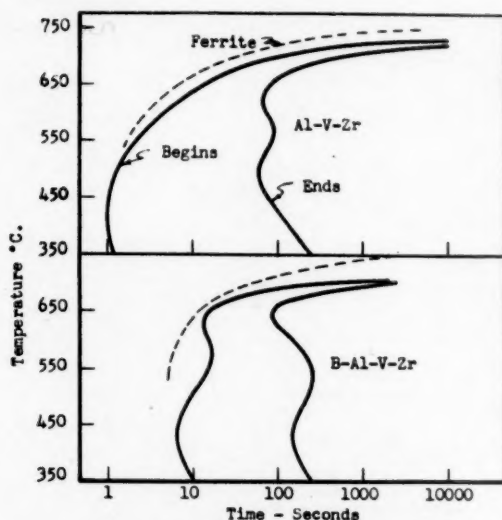
FIG. 3.—ISOTHERMAL TRANSFORMATION OF 0.50 PER CENT CHROMIUM STEELS.

Similar tendencies are shown in Fig. 3, which illustrates S-curves of the following chromium steels:

Deoxida-tion	Composition, Per Cent				Grain Size	Harden-ability J50—$\frac{1}{16}$ In.
	C	Mn	Si	Cr		
Al-V-Zr	0.45	0.79	0.28	0.52	7–8	4
B-Al-V-Zr	0.42	0.80	0.27	0.54	7–8(6)	9

From these examples it appears that the effect of special deoxidation is primarily to condition the austenite against premature transformation. The time required to produce the bulk of the transformation, and therefore the maximum attainable hardenability, is dependent on the alloy composition of the steel. Inasmuch as special deoxidation retards transformation to a greater degree at low temperatures (550 to 350°C.), as do manganese and nickel, it would appear to be most useful in conjunction with chromium and molybdenum, which retard transformation more effectively at higher temperatures.

It is believed to be evident from the work at the Union Carbide and Carbon Research Laboratories, Inc., that strong deoxidation is essential to effective use of boron. In steels of the usual silicon contents the boron-bearing strong deoxidizers must be added in sufficient amount to produce grain refinement in order to produce deep hardenability without harming hot workability and room-temperature ductility. As the amount of deoxidizer controls the depth of hardening, the kind of deoxidizer determines the other characteristics of the steel. Complex deoxidizers, such as Silcaz No. 3 and Silvaz No. 3, produce deep hardenability and high ductility consistently. These observations are implicit in Mr. Comstock's results but are not emphasized to the degree commensurate with their importance. Mr. Comstock is to be highly commended for making available the data on his steels.

Calculation of the Tensile Strength of Normalized Steels from Chemical Composition

By F. M. Walters, Jr.,* Member A.I.M.E.

In order to isolate the effect of an element on some property of an alloy, the effect of the other alloying elements must be elimi-

TABLE 1.—*Tensile Strength of Normalized Manganese Steel (Hypothetical)*

Mn, Per Cent	Percentage of Carbon			
	0.10	0.20	0.30	0.40
	Tensile Strength, Lb. per Sq. In.			
0.50	62,200	72,200	81,200	88,400
1.00	69,800	80,900	91,000	99,200
1.50	79,600	92,400	103,600	113,000
2.00	95,200	110,300	124,000	135,000

TABLE 2.—*Effect of Carbon on Tensile Strength of Normalized Manganese Steels*

Mn, Per Cent	Percentage of Carbon			
	0.10	0.20	0.30	0.40
	Factors that Increase Tensile Strength			
0.50	1.310	1.546	1.736	1.892
1.00	1.329	1.540	1.732	1.888
1.50	1.325	1.540	1.726	1.882
2.00	1.332	1.545	1.736	1.892
Average factors...	1.334	1.543	1.732	1.888

nated, either by reducing their quantity to the extent that they may be neglected or by

determining the specific effect of each. The success of Grossmann[1] in calculating

Fig. 1.—Effect of carbon and phosphorus on tensile strength of normalized steels.

hardenability from chemical composition by means of factors suggested such a

---

* Division of Physical Metallurgy, Naval Research Laboratory, Anacostia Station, Washington, D. C.

[1] References are at the end of the paper.

method for the calculation of the tensile strength of normalized steels. This paper presents an attempt to assess the influence of alloying elements on the tensile strength

are extrapolated to zero carbon, they are found to be 46,700 lb. per sq. in., 52,500 lb., 60,000 and 71,400 lb. per sq. in. for 0.50, 1.00, 1.50 and 2.00 per cent manganese.

TABLE 3.—*Comparison of Observed and Calculated Tensile Strengths*

Specimen No.	Analysis, Per Cent						Treat-ment[a]	Tensile Strength, Lb. per Sq. In.	
	C	Mn	Si	P	Ni	Cu		Observed	Computed
Hot-rolled Carbon Steels									
1B	0.10	0.44	0.032	0.014				55,300	53,800
2B	0.12	0.41	0.030	0.035				57,300	56,300
3B	0.17	0.41	0.17	0.032				61,800	61,800
4B	0.18	0.40	0.002	0.031				61,300	59,200
7B	0.21	0.47	0.24	0.012				67,500	65,500
10B	0.25	0.57	0.006	0.40				67,600	69,400
11B	0.27	0.47	0.002	0.045				69,100	70,000
12B	0.28	0.54	0.058	0.017				77,100	70,200
13B	0.29	1.06	0.25	0.017				86,600	82,900
14B	0.35	0.68	0.23	0.008				83,500	78,800
17B	0.44	0.65	0.24	0.010				104,700	84,700
Nickel Steels									
1C	0.17	0.40	0.39	0.012			N	63,600	62,600
2C	0.17	0.45	0.25	0.022	0.46		HR	67,000	65,100
3C	0.17	0.46	0.23	0.016	1.43		HR	70,500	69,400
4C	0.20	0.70	0.32	0.010	2.31		N	83,400	81,900
5C	0.19	0.57	0.22	0.010	2.34		HR	80,400	77,900
6C	0.18	0.63	0.48	0.010	3.38		N	84,100	84,800
7C	0.18	0.53	0.31	0.012	3.46		HR	79,500	80,300
8C	0.19	0.40	0.18	0.010	3.63		HR	79,600	77,200
9C	0.028	0.19	0.001	0.002	2.08		HR	57,300	51,400
10C	0.04	0.22	0.23	0.010	1.98		N	62,300	56,700
11C	0.06	0.37	0.17	0.008	2.27		N	59,800	60,400
13C	0.14	0.52	0.35	0.010	1.90		N	74,300	70,800
14C	0.28	0.68	0.20	0.034	2.25		HR	93,200	91,200
15C	0.32	0.80	0.34	0.010	2.23		N	101,200	97,600
16C	0.41	0.74	0.40	0.008	2.51		N	118,500	104,700
Normalized Nickel-copper Steels									
85	0.11	0.46	0.18	0.007	1.78	0.99		70,900	74,100
113	0.09	0.52	0.15	0.002	1.99	1.03		70,000	72,400
111	0.14	0.98	0.09	0.003	2.03	1.06		85,000	87,100
83	0.09	0.57	0.05	0.113	0.59	1.12		71,300	74,000

[a] N, normalized; HR, hot-rolled.

of normalized steels, and to provide a basis for its calculation from chemical composition. A study of several hundred steels indicates that each alloying element causes a percentage increase in the tensile strength.

The method for the determination of the factors is simple, requiring only a series of steels in which one alloying element predominates and in which the incidental elements are substantially constant. Such a series is shown in Table 1; it is, however, hypothetical. When the tensile strengths

Dividing the tensile strengths of Table 1 by the strengths without carbon gives Table 2, which shows the factors by which 0.10, 0.20, 0.30 and 0.40 per cent C increase the tensile strength. The factors for the effect of manganese may be determined from these data in a similar manner. When determining factors from actual data, the first attempt results in an approximation, which may be made more accurate as the effect of the other alloying elements present is determined and accounted for. The data that

were used to determine the effect of several elements are not available for publication at this time.

When the assumed base strength of iron of 36,000 lb. per sq. in. is multiplied by all the factors, the product is 81,900. This
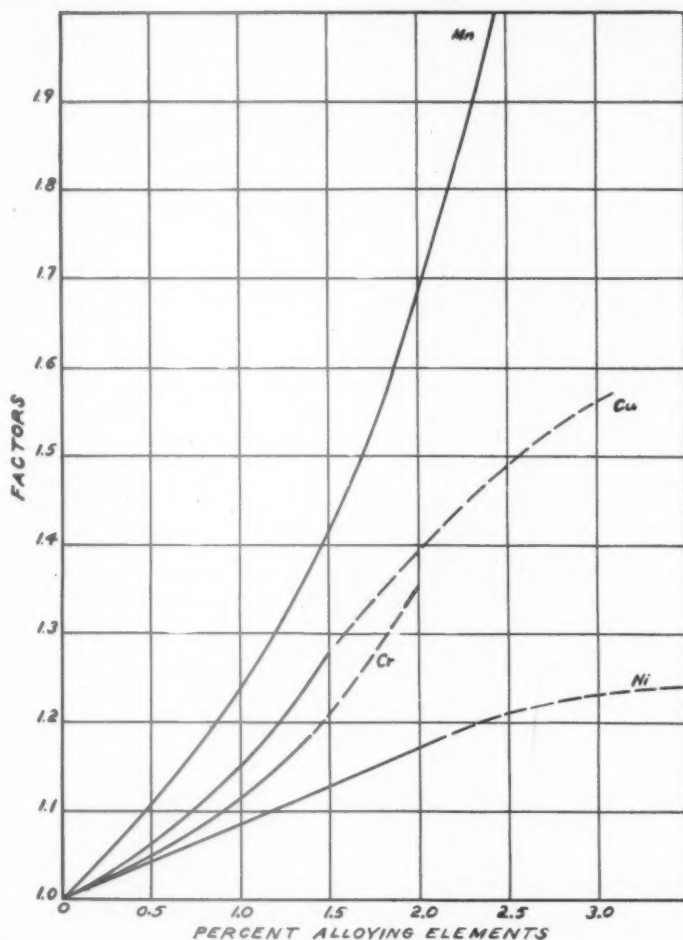
FIG. 2.—EFFECT OF MANGANESE, COPPER, NICKEL AND CHROMIUM.

The method for using the factors given in Figs. 1 to 5 is similar to that used in calculating hardenability by Grossmann's method, except that a base tensile strength is multiplied by factors that are determined by the amounts of the alloying elements present. For example:

ELEMENT	PER CENT	FACTOR	FIGURE
C	0.20	1.528	1
Mn	0.70	1.155	2
Si	0.32	1.060	3
S	0.020		
P	0.010	1.011	1
Ni	2.31	1.203	2

agrees fairly well with observed tensile strength of 83,400 lb. per sq. in., since no account has been taken of residual elements; 0.12 per cent copper, 0.15 per cent chromium or smaller amounts of the two are sufficient to account for the difference between the observed and calculated values. (Whether grain size has an effect on the base strength has not been definitely determined.)

Carbon, manganese. silicon, phosphorus, nickel and copper are uniform in their behavior but elements that form special carbides, molybdenum, chromium, tita-

nium and vanadium do not always show the maximum effect of which they are capable. The curve for molybdenum shown in Fig. 4 was derived from one set of data while the

carbon steels is lower in general than the observed strength, probably because no account was taken of incidental elements. The computed values of the copper-nickel
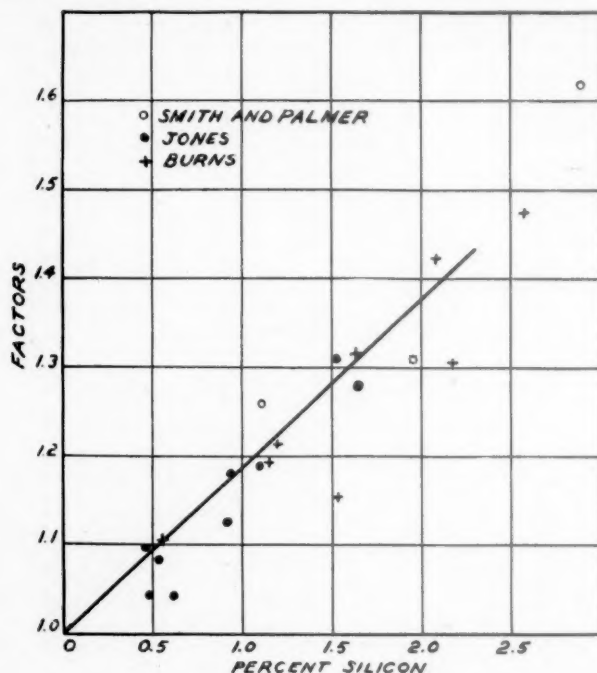
FIG. 3.—EFFECT OF SILICON.

scattered points were obtained from equally reliable sources. The higher-carbon chromium steels are air-hardening and the method of calculation described here does not apply. Vanadium is variable; the data from one investigation[5] show a rather large effect but other observations indicate that the probable factors are those given by the line of Fig. 5. Titanium may have a strong influence on the strength of normalized steels, but so far no sufficiently consistent data have been found to establish its effect.

Aluminum and sulphur in the amounts usual in steel appear to have no direct effect on the tensile strength, although it may be presumed that high sulphur decreases the effect of manganese.

A comparison of observed and calculated tensile strengths of some steels of which the weldability[6,7] has been studied is given in Table 3. The calculated strength of the

steels are all higher, which may mean that a base tensile strength of 36,000 lb. per sq. in. is too high if copper and nickel (the most frequent residual elements) are included in the chemical analysis.

The factor method for calculating the tensile strength of normalized steels appears to account for the combined effect of alloying elements. There are, however, certain restrictions: The hardenability of the steel must be low enough so that little or no martensite is formed on normalizing. The factors given here were derived for the most part from tests made on steels normalized as ¾-in. rounds, and will not apply without correction to steels air-cooled in larger or smaller sections.

The method promises to be useful in working out new steel compositions of a particular tensile strength, since the number of heats necessary to determine the
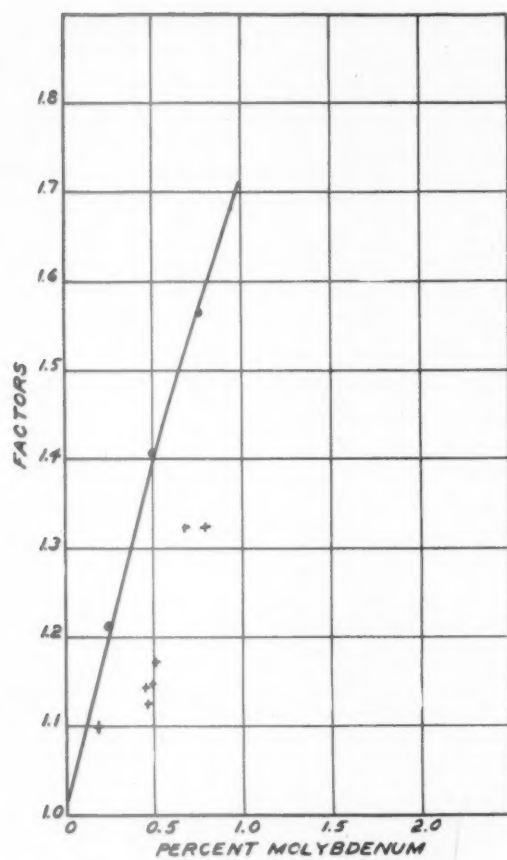
FIG. 4.—EFFECT OF MOLYBDENUM.
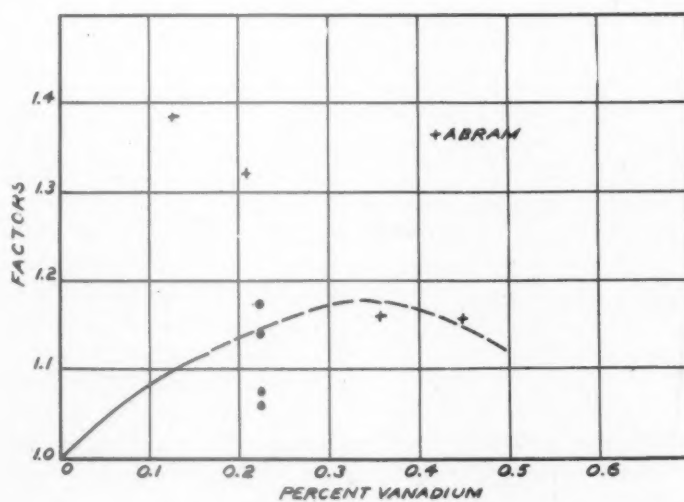
FIG. 5.—EFFECT OF VANADIUM.

optimum composition may be reduced. Also, the effect of variations in the amounts of minor elements can be accounted for and the effect of the principal alloying elements may be evaluated with greater certainty.

When the calculated values do not agree with the observed values of the tensile strength, certain inferences may be drawn. If the computed strength is too low, the chemical analysis is incomplete, or if the steel is tested as rolled, it may have been finished cold. Too high a calculated strength may indicate that the full value of the alloying elements has not been realized.

REFERENCES

1. M. A. Grossmann: Hardenability Calculated from Chemical Composition. *Trans.* A.I.M.E. (1942) **150,** 227.
2. E. C. Wright and P. F. Mumma: Properties of Low-carbon Medium-chromium Steels of the Air-hardening Type. *Trans.* A.I.M.E. (1933) **105,** 77–87.
3. W. Craft: Chromium in Structural Steel. *Trans.* A.I.M.E. (1939) **135,** 473–485.
4. J. A. Jones: Chromium-Copper Structural Steels. *Jnl.* Iron and Steel Inst. (1930) **121,** 209–224.
5. H. H. Abrams: The Influence of Vanadium on Nickel-Chromium and Nickel Chromium-Vanadium Steels. *Jnl.* Iron and Steel Inst. (1936) **134,** 241–249.
6. C. E. Jackson and G. G. Luther: A Comparison of Tests for Weldability of Twenty Low-Carbon Steels. *Welding Jnl.* (1940) **19,** 351s–364s.
7. C. E. Jackson and G. G. Luther: Weldability Tests of Nickel Steels. *Welding Jnl.* (1941) **20,** 437s–452s.
8. C. S. Smith and E. W. Palmer: Precipitation-hardening of Copper Steels. *Trans.* A.I.M.E. (1933) **105,** 133–168.
9. J. A. Jones: High Elastic Limit Structural Steels. *Jnl.* Iron and Steel Inst. (1929) **120,** 127–140.
10. G. Burns: Properties of Some Silico-Manganese Steels. *Jnl.* Iron and Steel Inst. (1932) **125,** 363–384.

DISCUSSION

(J. W. Halley presiding)

M. TENENBAUM,* East Chicago, Ind.—The curves in Dr. Walters' paper present a novel method of calculating the tensile strength of steel from its chemical composition. The method suggested for this calculation departs markedly from the equations that heretofore

* Metallurgist, Inland Steel Company.

have been used for this purpose. Using a method similar to that employed by Dr. Walters, we have developed an equation relating tensile strength of plain carbon hot-rolled steel with analyses in which the various multiplying factors are expressed algebraically rather than graphically. Most of the data on which this equation is based were accumulated over a period of years at the Inland Steel Co. The equation has proved reasonably accurate in the ranges from 0.10 to 0.40 per cent carbon and from 0.30 to 1.50 per cent manganese. The equation can be expressed in the form

$$T.S. = 38,000(1 + 0.024 \text{ C})(1 + 0.0009 \text{ Mn} + 0.00001 \text{ Mn}^2)(1 + 0.015 \text{ P}) (1 + 0.004 \text{ Si})(1.07 - 0.22G + 0.10G^2)$$

where C, Mn, P, and Si represent the concentration of those elements in units of 0.01 per cent. G represents the gauge of the test piece in inches. The gauge correction is valid only in the range between $\frac{1}{8}$ in. and 1 in. For gauges heavier than 1 in. there is no significant further change in this factor. The example of multiplying factors given in Dr. Walters' paper has been extended to compare with corresponding values derived from the preceding equation:

Element	Per Cent	Multiplying Factor	
		Curves	Equation
C	0.20	1.528	1.480
Mn	0.70	1.155	1.112
Si	0.32	1.060	1.128
P	0.01	1.011	1.015

Several discrepancies are evident between the two sets of values, but owing to the lack of information concerning analyses, gauge, and cooling rate of the samples used as a basis for Dr. Walters' curves, it was not possible to determine the source of these differences.

The effects of the four common elements considered in the foregoing equation were evaluated in the following manner: A value of 38,000 lb. per sq. in. was accepted for the tensile strength of pure iron. This includes the effect of the small percentages of residual elements (excluding C, Mn, P, and S) that normally are present in steel.

In the manganese range between 0.25 and 1.50 per cent, considerable data are available concerning the effect of carbon and manganese on tensile strength. In steels containing less than 0.80 per cent manganese there is little variation in the slope of the line relating tensile strength with carbon content. Accordingly, the slight extrapolation necessary to obtain the effect of carbon, alone, does not introduce any appreciable error into the equation. The resultant relation between tensile strength and carbon can be expressed by the equation

$$T.S. = 38,000(1 + 0.024\ C).$$

The effect of manganese was studied in four carbon ranges. The differences in the multiplying factor noted in these ranges were of a minor nature. It was necessary to resort to a parabolic type of function to express the relation between manganese and tensile strength.

Studies of the effect of phosphorus in the two tensile ranges, 50,000 to 70,000 and 75,000 to 85,000 lb. per sq. in., have indicated that the multiplying factor for this element can be expressed by a linear equation. In the former range each point of phosphorus increased the tensile strength about 900 lb. per sq. in., while the corresponding value in the latter range was 1200 lb. per sq. in.

For steels having tensile strengths around 85,000 lb. per sq. in. each point of silicon was found to increase the tensile strength about 340 lb. per sq. in. No other data were available on the effect of silicon in lower tensile ranges. The expression for the multiplying factor was assumed to be linear. While this assumption is not necessarily true, any error introduced would be of a minor nature as long as the use of the equation is restricted to plain carbon steels.

Until more data become available the multiplying factor type of relation, whether graphical or algebraic, must be considered as a tentative method of calculating tensile strength from chemical composition. This method of calculation should be checked to improve the accuracy of the results and to extend its application to a wider range of steel analyses.

M. A. GROSSMANN,* Chicago, Ill.—Dr.

Walters' stimulating paper, compressed into a modest six pages, passes over lightly what must have been a really very extensive mass of calculations. The result, as embodied in part, for example, in his Fig. 2, makes a very persuasive case for itself: thus the results listed in his Table 3 show astonishingly good correlation between prediction and actuality.

Several points seem worthy of note. Dr. Walters points out that these numbers apply only to ¾-in. rounds, but it should not be too difficult to develop bands of values for various sizes of bars and plates, now that the broad behavior has been established, and these would have great additional value.

Another point mentioned by him refers to alloy carbides. In our work on hardenability calculation, this has similarly proved a stumbling block when the carbides fail to dissolve, and indeed it seems hopeless at this time to do more than estimate broad boundaries, until a way is devised to estimate undissolved alloy carbides.

W. CRAFTS,* Niagara Falls, N. Y.—This is a very interesting and stimulating paper. The character of the results is remarkable in view of the complex microstructures of low-carbon steels. As Dr. Walters pointed out, carbide-forming elements do not always exert the same effects on tensile strength; in fact, in some steels chromium acts as a softening and toughening agent rather than as a strengthener.

In view of recent work on the influence of hardenability on weldability, it is notable that the ratios between multiplying factors for increase of strength and Grossmann's factors for hardenability vary widely. Manganese confers a high degree of hardenability in relation to its effect on the increase of strength. Chromium and molybdenum are intermediate, while silicon, nickel, and copper increase strength at a high rate in comparison with the increase in hardenability that they confer. This comparison is outside of the scope of the paper, as are the other benefits conferred by alloys, but these factors for tensile strength will be of great help in evaluating other valuable properties.

* Director of Research, Carnegie-Illinois Steel Corporation.

* Union Carbide and Carbon Research Laboratories.

F. M. WALTERS, JR. (author's reply).—The validity of the factor method for the calculation of tensile strength is nicely confirmed by Mr. Tenenbaum's discussion. That there are differences in the values for the factors is not at all surprising, and it is to be hoped that a compromise satisfactory to all may be reached. Whether the effect of the alloying elements is expressed as an equation or by curves is to some extent a matter of personal convenience in computation. The graphical method has the advantage of expressing empirical observations as they are found without forcing them into the straitjacket of an algebraic equation.

Chromizing of Steel

By Irvin R. Kramer,* Junior Member A.I.M.E., and Robert H. Hafner*

(Cleveland Meeting, October 1942)

In recent years considerable interest has been shown in surface-alloyed metals, particularly those of chromium (chromized steels), which have excellent corrosion

FIG. 1.—DEPTH-CONCENTRATION CURVE.

peratures of 1200° to 1400°C. (2200° to 2550°F.) caused excessive grain growth and warpage. Louenstein and Ulmer[2] packed iron castings in ferrochromium and com-

resistance under a variety of severe conditions, and may undergo bending and flanging operations without spalling.
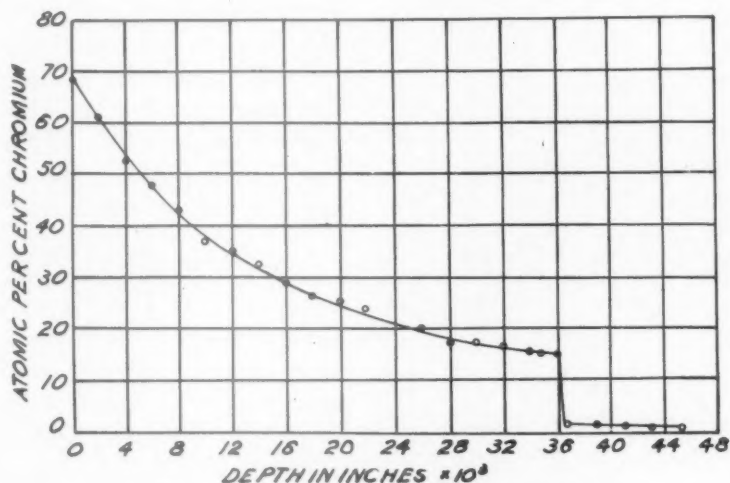
An early method[1] employed to produce a high-chromium case on steel was developed by Kelley in 1921. It consisted of heating a low-carbon steel in intimate contact with powdered chromium in the presence of hydrogen at temperatures sufficiently high to permit diffusion of chromium into the steel. The usefulness of this process was limited because the extremely high tem-

mon salt, and heated for approximately three hours at 930° to 1040°C. (1700° to 1900°F.).

A recent and more practical method of depositing chromium on steel surfaces has been developed in Germany by Daeves, Becker and Steinberg[3-8] and in Russia by Izgaryshev and Sarkisov.[9] This process consists of passing gaseous chromium chloride over the steel to be chromized at temperatures of 900° to 1000°C., or packing them in a porous, ceramic material that previously had been saturated with chromium chloride. They reported obtaining a chromized layer, 0.004 in. thick, on low-carbon steels. Later, Daeves[4] established a relationship between the carbon content

and specimen dimensions after finding difficulty in chromizing steels of carbon content higher than 0.10 per cent. He found that when the product $H = Cd$ (where
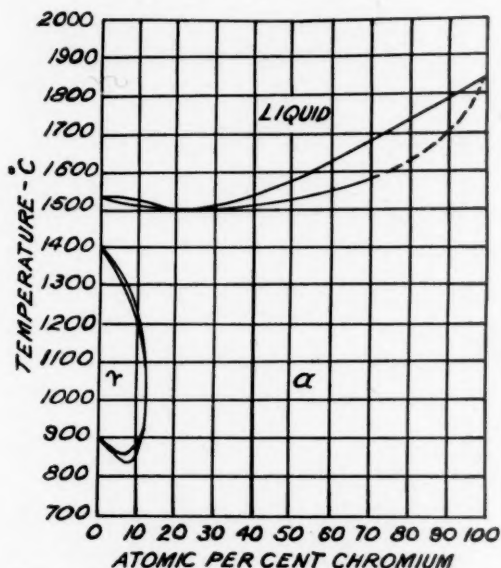
FIG. 2.—IRON-CHROMIUM CONSTITUTIONAL DIA-GRAM ACCORDING TO ADCOCK.

C = carbon content in per cent and d = thickness in millimeters) exceeds 0.12, diffusion will not take place satisfactorily.

A chromized case differs from an electro-plated coat in that it is a diffused layer, integral with the base metal; thus no difficulty is encountered with cracking or peeling. Because of this, "chromizing" appeared to have definite commercial applications and it seemed desirable to determine whether an effective coating could be secured in a reasonable time at a temperature low enough to be harmless to the steel.

The purpose of this investigation was to determine the time-temperature relationships as well as other factors pertinent to the process, since this information was not published by previous investigators.

The reaction involved in this method proceeds according to the equation

$$CrCl_2 + Fe \rightleftarrows Cr + FeCl_2$$
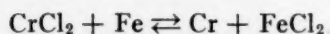
Chromium atoms are deposited on the surface and diffuse in as the iron atoms diffuse out, forming a layer high in chromium.

Of the two mechanisms, chemical reaction and diffusion, the one operating at the slower rate will determine the rate of formation of the layer. In this case, diffusion will be slower, therefore any factors influencing its rate will similarly affect the process.

The rate of diffusion is influenced by the crystal structure of the base metal as well as by temperature.[10,11] A depth-concentration curve for the diffusion of chromium[10] at 1200°C. (Fig. 1) shows that the concentration falls off gradually for a considerable distance and then drops sharply at 13 per cent chromium, the point coincident with the gamma loop (Fig. 2). The percentage of chromium at the surface will vary from 35 to 70 per cent, depending upon the temperature and time of treatment.

EXPERIMENTAL PROCEDURE

Three types of alloys were used in this study: a plain carbon steel, a chromium-molybdenum steel, and an experimental steel with 0.5 per cent molybdenum and 0.06 per cent carbon (Table 1). These steels were chromized by chromium chloride produced by passing hydrogen chloride over 95 per cent ferrochromium. A diagrammatic sketch of the chromizing apparatus is shown in Fig. 3. Tank hydrogen was passed over copper gauze at 700°C. to remove oxygen and then through two sulphuric acid bubbling towers to remove water vapor. A mercury pressure regulator and flow gauge were placed in the line to control and measure the flow. The purified dry hydrogen was then passed into a chamber filled with glass beads, where it mixed with hydrogen chloride. Anhydrous hydrogen chloride was introduced directly into the system, since further purification was not necessary. The mixture of the two gases passed through a quartz tube into a furnace containing ferrochromium in porcelain boats at a temperature of 760°C., then into the furnace containing the specimen to

be chromized. At the exit end of the apparatus a sulphuric acid bottle was placed to prevent back diffusion of water vapor.

Another method[12] that was used successfully was to pack the steel in a mixture of $BaCl_2.2H_2O$ and ferrochromium and to heat in an atmosphere of hydrogen. The
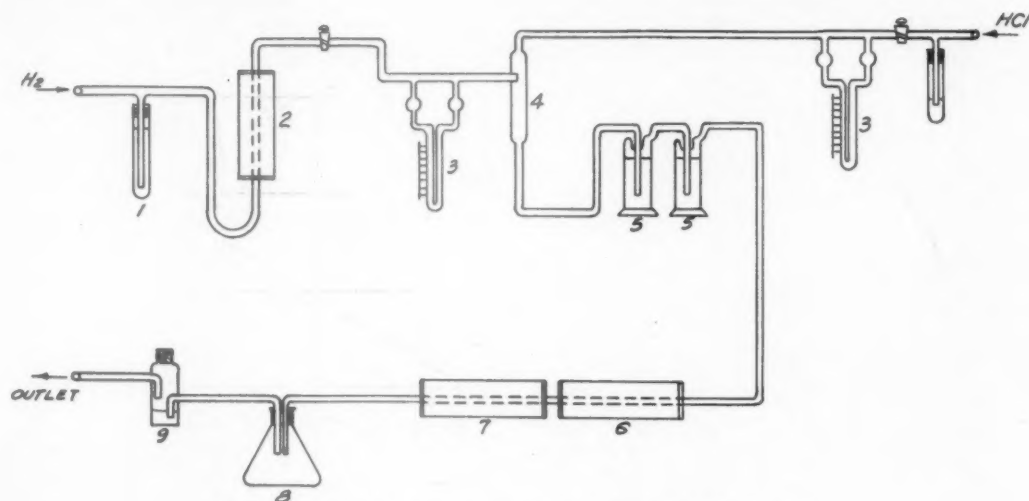
FIG. 3.—SCHEMATIC DIAGRAM OF CHROMIZING ASSEMBLY.

1. Mercury constant-pressure regulators.
2. Copper-gauze deoxidizing furnace.
3. Flowmeter.
4. Mixing tube.
5. Milligan bubbling towers.

6. Furnace for production of C_rCl_2
7. Chromizing furnace.
8. Erlenmyer flask.
9. Sulphuric acid valve.

The temperature of the chromizing furnace was automatically controlled and any fluctuations in temperature were held to a minimum by inserting the thermocouple in the furnace windings. As it was not convenient to measure the temperature of the specimen during a run, because of the contamination of the thermocouple by chromium, the temperature was determined by measuring the temperature just before the run was started.

After preliminary trials, it was found that 2.5 c.c. of hydrogen chloride and 12 c.c. of hydrogen per minute gave good results. The depth of the chromized layer was determined by polishing a cross section of the specimen and etching it in 2 per cent Nital, which attacked only the regions that contained less than 13 per cent chromium and sharply delineated the higher-chromium regions. The diffusion zones were measured at 400 magnifications.

$BaCl_2.2H_2O$ partially decomposes, forming HCl, which reacts with the chromium to form chromium chloride.

TABLE 1.—*Chemical Analysis of Alloys*
PER CENT

Alloy	C	Si	Mn	Cr	Mo
A	0.06				0.50
B	0.18	0.43	0.20		
C	0.14	0.49	0.49	1.81	0.70

The chromizing results of the steels studied (Table 1) are given in Table 2 and the time-penetration relationship at 1000°C. in Fig. 4. Figs. 5 to 8 show the cross section of the chromized layer. The columnar structure of the chromized layer may be revealed by a ferric chloride-hydrochloric acid etchant (Fig. 5).

The presence of carbon greatly influences the chromizing process. Fig. 6 shows the structure of steel B when subjected to the

chromizing treatment for 8 hr. at 1000°C. Instead of a clearly defined chromized layer, a carbide layer was formed, which inhibited the diffusion of chromium into

combined with strong carbide-forming elements such as chromium or molybdenum, which decrease the diffusion rate of carbon. If this is not done, the carbon will
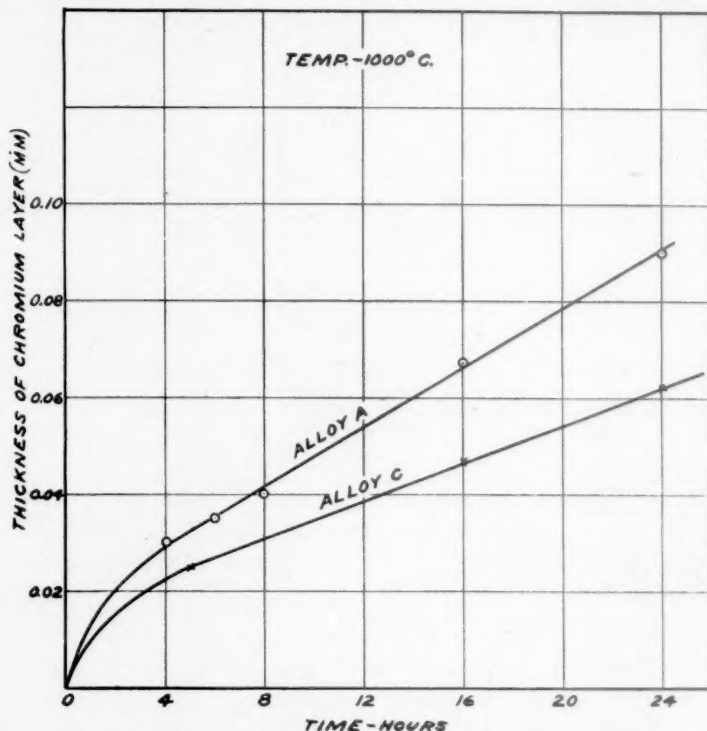
FIG. 4.—TIME-PENETRATION RELATIONSHIP.

the base metal. On the other hand, the chromium-molybdenum steel C chromized without difficulty. It appears that in order to chromize successfully the carbon must be

diffuse from the interior of the steel faster than the chromium can diffuse inward, thus forming a carbide barrier. The manner in which the diffusion takes place may be seen in Fig. 7. Here a specimen of steel C was exposed to hydrogen for a sufficient time to remove the carbon from the grain boundaries only. Upon subsequent treatment with chromium chloride, the chromium penetrated into the grain boundaries only, and did not enter into the grains.

The corrosion resistance of the chromized layer is indicated by the effect of a drastic acid treatment. Specimens of steels A and C were held in boiling 25 per cent nitric acid until the original base metal was completely dissolved, leaving the chromized layers unaffected (Fig. 8).

It is of interest to note that the hardness of the chromized layer as measured by the

TABLE 2.—Chromizing Results

Alloy	Temperature, Deg. C.	Time, Hr.	Depth of Layer, Mm.	Comments
C	813	16	nil	
C	813	24	nil	
C	909	4	nil	
C	909	6	0.008	
A	1000	4	0.030	
A	1000	6	0.035	
A	1000	8	0.040	
A	1000	16	0.068	
A	1000	24	0.090	
C	1000	5	0.025	
C	1000	16	0.048	
C	1000	24	0.062	
B	1000	4	nil	
B	1000	8	nil	Formed carbide layer
A	1000	16	0.068	BaCl₂ method
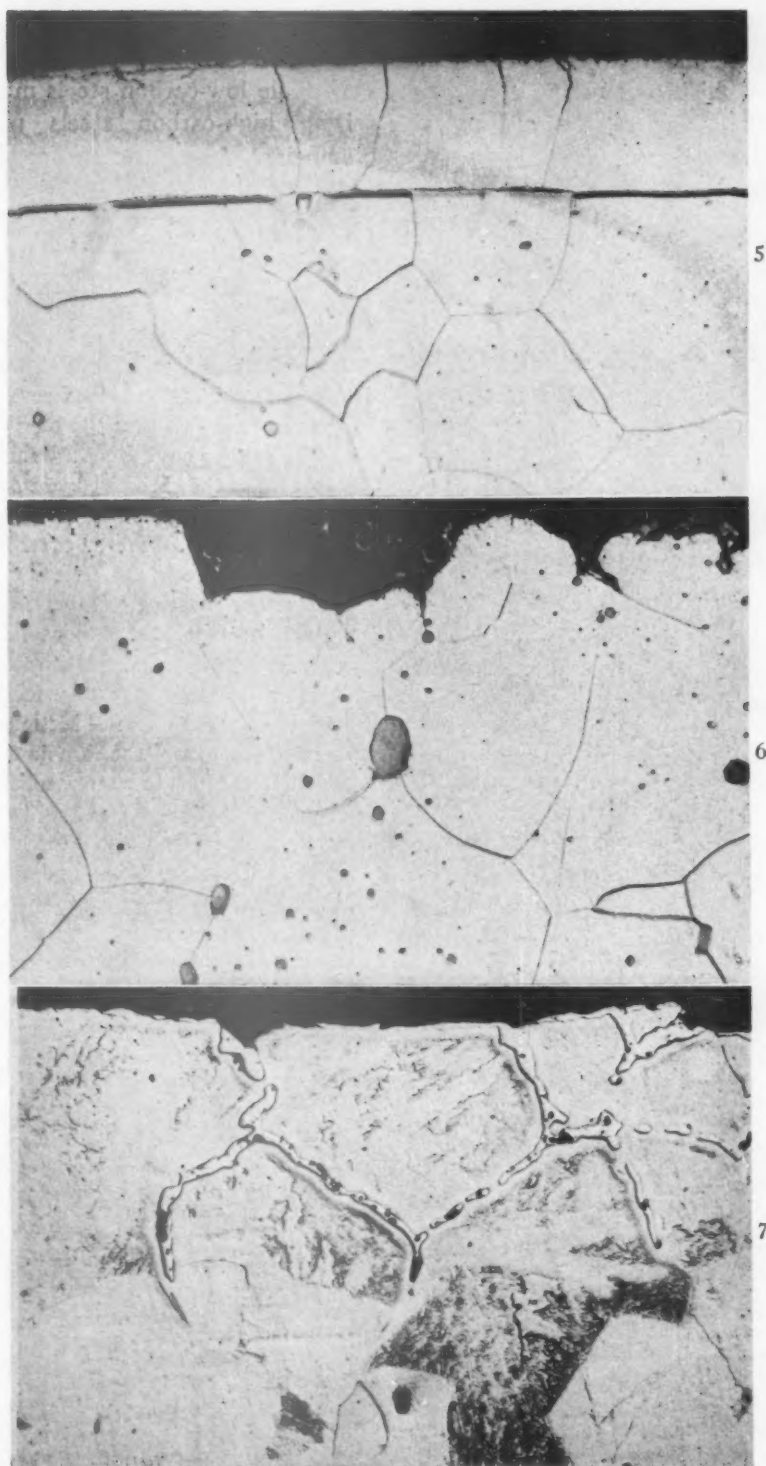
FIG. 5.—CHROMIZED LAYER OF ALLOY A ETCHED WITH $FeCl_3.HCl$ TO SHOW COLUMNAR STRUCTURE. $\times 250$.

FIG. 6.—MICROSTRUCTURE OF ALLOY B SHOWING FORMATION OF CARBIDE BARRIER AFTER AN ATTEMPT TO CHROMIZE. $\times 250$.

FIG. 7.—MICROSTRUCTURE OF ALLOY C SHOWING DIFFUSION ALONG GRAIN BOUNDARIES. $\times 250$.

Knoop indentor was 267 (240 Brinell), which is in the magnitude of the hardness expected in high-chromium iron alloys. This low hardness of the coating aids
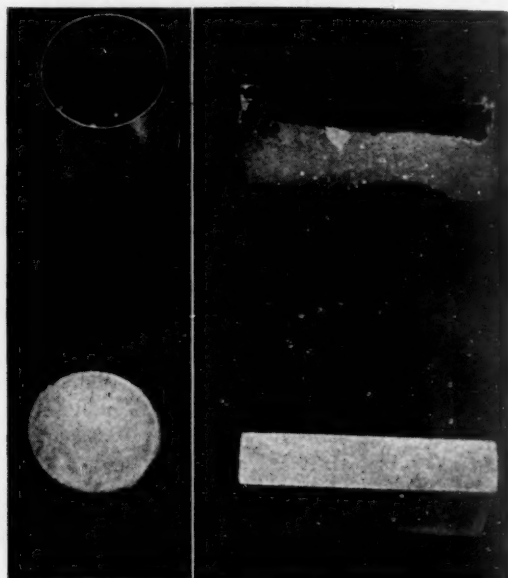
FIG. 8.—RESULT OF BOILING CHROMIZED SPECIMENS IN 25 PER CENT NITRIC ACID.
Left, alloy A; right, alloy C.

greatly in the manufacture of parts requiring close tolerances or fitting.

REFERENCES

1. F. C. Kelley: U. S. Patent 1365494 (1921).
2. Louenstein and Ulmer: U. S. Patent 2046638 (1936).
3. Daeves, Becker and Steinberg: U. S. Patent 2219004 (1940).
4. Daeves, Becker and Steinberg: U. S. Patent 2255482 (1941).
5. Daeves, Becker and Steinberg: U. S. Patent 2257668 (1941).
6. Daeves, Becker and Steinberg: French Patent 840975.
7. Becker and Steinberg: British Patent 492521.
8. Hertel and Becker: British Patent 440641.
9. I. Zgaryshev and E. E. Sarkisov: Compt. rend. Acad. U.S.S.R. (1938) 18, 437–440.
10. Hicks: Trans. A.I.M.E. (1934) 113, 163–172.
11. G. Grube: Ztsch. Metallkunde (1927) 19, 38.
12. French Patent 844283 (July 21, 1939).

SUMMARY

A high-chromium corrosion-resistant coating may be produced at 1000°C. through the medium of chromium chloride, produced either from the reaction of hydrogen chloride or barium chloride on ferrochromium.

While low-carbon steels may be chromized, high-carbon steels must contain sufficient strong carbide-forming elements to fix the carbon.

DISCUSSION

(A. B. Kinzel presiding)

F. C. KELLEY,* Schenectady, N. Y.— Messrs. Kramer and Hafner have confirmed the work of Daeves, Becker and Steinberg. They have shown that the process is workable and in Table 2 have given valuable data on the thickness of the chromized layers. Their photomicrographs, Figs. 5 to 7, also confirm the claims made by Daeves, Becker and Steinberg, that special steels are necessary to obtain a satisfactory coating; namely, steels of low carbon content, those containing titanium, molybdenum or manganese to fix the carbon or limit its diffusion to the surface. Low-carbon steel parts with thin steel sections are the most desirable because the amount of available carbon in the part to be treated is the important factor.

This process has also been checked in our laboratory using previously decarburized cold-rolled iron by passing a mixture of $H_2 + HCl$ over ferrochromium at 900°C. for 3 hr. The sample to be chromized was contained in the same furnace. The ferrochromium was placed on the gas-inlet end of the quartz tube furnace. The furnace was automatically controlled and the drop in temperature through the wall of the tube was measured with hydrogen gas passing through the quartz tube. This allowed us to control the temperature inside the tube by placing a thermocouple on the outside. Fig. 9 shows the high-chromium layer, 0.5 mil thick, obtained after 3 hr. at 900°C. Fig. 10 shows the chromium layer etched to bring out its grain structure. This layer varied in thickness from 0.5 to 1.0 mil.

We noticed that there was a variation in the thickness of the chromized layer where the gas was passed over the sample in the horizontal furnace. These layers are naturally thin because the rate of diffusion of Fe through the chrome

* Research Laboratory, General Electric Company.

coating is fairly slow, and I should like to ask the authors about the behavior of their iron samples when subjected to corrosion. Did the thickness of the coating vary in spots enough to cause local breakdown?

A. S. HENDERSON,* Columbus, Ohio.—During the past few years, we have been interested in the general field and have found a number of factors to be of primary interest in depositing metal from the vapor phase. For the most part,
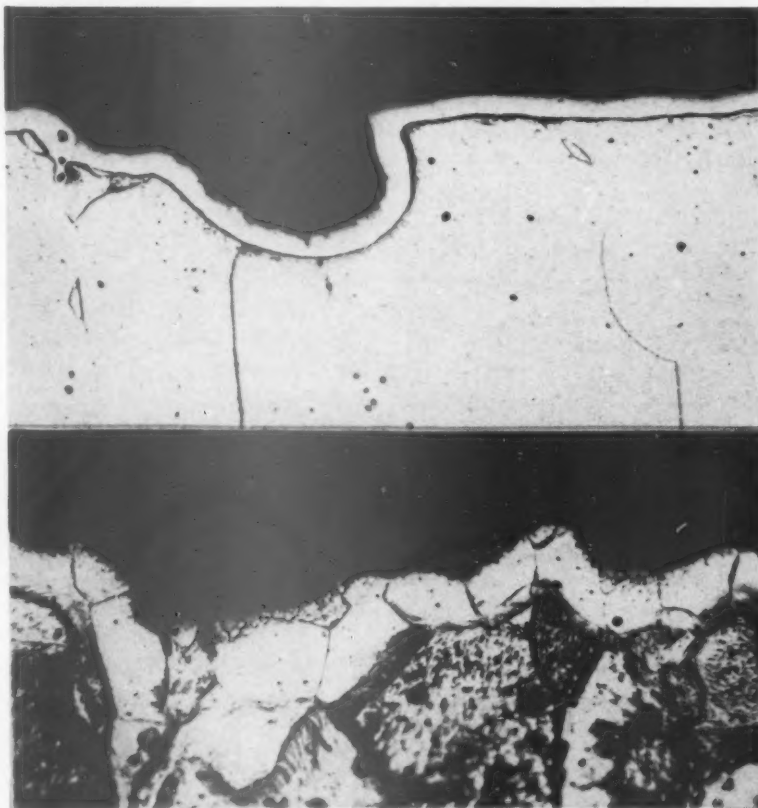
FIG. 9.—CHROMIZED BY PASSING H_2 + Hcl OVER FERROCHROME AND HEATING IRON SAMPLE TO 900°C. FOR 3 HOURS.
Chromium layer 0.5 mil. 2 per cent nital etch.
FIG. 10.—CHROMIZED BY PASSING H_2 + Hcl OVER FERROCHROME AND HEATING IRON SAMPLE TO 900°C. FOR 3 HOURS.
Chromium layer 0.5 to 1.0 mil. Ferric chloride etch.

Which of the two methods employed by them gave the better results?

Did the authors attempt to impregnate any ceramic materials with $CrCl_2$ as did the Germans and, if so, how did the results compare with the two processes described by them?

C. E. SIMS,* Columbus, Ohio.—In the molybdenum steels, what becomes of the molybdenum during chromizing? Does it stay uniformly disposed or does it retreat before the advance of the chromium?

these have not been treated by the authors, and so have been proposed as a basis for this discussion.

When a heavy reacting gas such as $CrCl_2$ is used in the vapor reaction, considerable difficulty is experienced in providing a uniform concentration over the cross section of the object to be coated. In the German patents, this was obtained by using a suitable packing medium that had been saturated with solid $CrCl_2$. By this process, $CrCl_2$ vapors were generated at or near the surface on which chromium was deposited and no attempt was

* Supervising Metallurgist, Battelle Memorial Institute.

* Battelle Memorial Institute.

made to obtain a uniform chloride concentration in the gas stream.

Purity of the gas is of the utmost importance in this type of reaction and the authors have not discussed the purity of the hydrogen obtained by their purification apparatus or the effect upon the reaction of other gases. A misstatement was made on the function of copper gauze, as it does not remove the oxygen but acts as a contact surface to burn the oxygen to water, which was afterward removed in the drying towers.

In previous work with the formation of the reacting chloride from the action of anhydrous HCl, etching of the object to be coated has often resulted, and this phenomenon has been difficult to overcome. As shown by Becker and others, the best results have been obtained by using $CrCl_2$ direct rather than by producing it from the reaction between chromium and anhydrous HCl.

I. R. KRAMER AND R. H. HAFNER (authors' reply).—In regard to the discussion by Mr. Kelley, no work was done on the effect of variations in thickness upon corrosion except to subject the specimens to boiling 25 per cent nitric acid. In these cases, no differential attack was noticed. No attempt was made by the authors to impregnate ceramic materials with chromium. Of the two methods described in this paper, the barium chloride ferrochromium gave very uniform chromized layers whereas some difficulty was encountered with the hydrogen chloride method.

In answer to Mr. Sims' question, 0.49 per cent molybdenum was found in the chromized layer of alloy A after the base metal had been dissolved with boiling 25 per cent nitric acid.

Apparently the molybdenum does not diffuse away during the chromizing process.

In regard to Mr. Henderson's comments, no measurements were made to determine the purity of the hydrogen employed in the system. Since no evidence of chromyl chloride was found, it may be assumed that the oxygen and water contents were very low. The water content must have been reduced at least to its partial pressure over concentrated sulphuric acid.

Mr. Henderson is correct in his statement that the copper does not remove the oxygen in the presence of hydrogen by the formation of cuprous oxide. In fact, the mechanism of the reaction is autocatalytic in nature. However, the authors made no attempt to explain the mechanism since it was not an essential part of the paper. The reactions of other gases with chromium chloride has been given in many standard chemistry textbooks. Chromium chloride will react with oxygen and water to form chromyl chloride (CrO_2Cl_2). The presence of hydrocarbon and carbon oxides leads to similar results. Chromyl chloride, CrO_2Cl_2, is a yellowish red vapor resembling nitrogen peroxide. When heated above 300°C. it decomposes according to the following equation

$$4CrO_2Cl_2 \rightarrow 2Cr_2O_3 + O_2$$
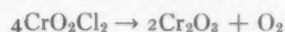
If chromyl chloride is heated with dry hydrogen it reacts as follows:

$$3CrO_2Cl_2 + 3H_2 \rightarrow 6HCl + Cr_2O_3 \cdot CrO_3$$
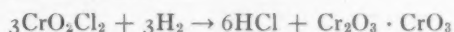
It is obvious that if such reactions occur chromizing would not result.

The etching effect was found when free hydrogen chloride was present. This was easily eliminated by decreasing its flow rate and increasing the flow rate of the hydrogen.

True Stress-strain Relations at High Temperatures by the Two-load Method

By C. W. MacGregor,* Member A.I.M.E., and L. E. Welch†

(Cleveland Meeting, October 1942)

The past 20 years has seen a revolutionary change in the testing of materials at elevated temperatures. This has largely been brought about by the practical importance of the creep problem in the design of equipment for operation at high temperatures. The short-time tension test carried out at elevated temperatures has consequently assumed in many cases only a secondary role compared with the long-time creep test.

In many problems, however, a knowledge of the short-time high-temperature properties of a metal is essential. To mention a few cases in which this is so, we might include all hot-forming operations such as rolling, forging, etc., the welding problem if residual stresses are to be computed, the development of new alloys for high-temperature service where, in the initial stages, time does not permit of long duration creep tests, and others. Usually a knowledge of the short-time properties is desired, if only to serve as a background against which to compare creep behavior.

In conducting short-time high-temperature tests, it has been almost the universal practice to determine stresses based on the original area and strains referred to the original gauge length which is usually chosen as 2 in. It has been pointed out[1,2] that one of the reasons that the true significance of certain tensile properties is not understood, which perhaps curtails their usefulness, especially when the material is applied
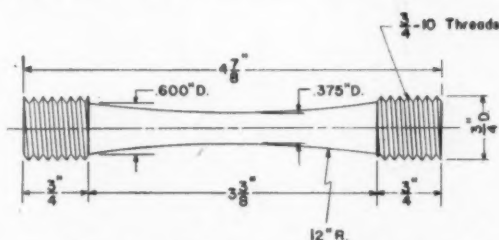
FIG. 1.—CURVED TAPER SPECIMEN.
Polished with No. ooo emery paper.

under conditions differing considerably from the test conditions, is that true physical stresses and strains are not determined. It is essential to have a knowledge of true stresses and strains in order to correlate the values present in the tension test with those existing, for example, in hot metal-forming operations and in the general problem of the yielding and failure of metals under combined stress conditions. Stress and strain values based on the original dimensions of the test piece do not exist physically except in the early stages of the test.

Since at the present time there is very little information in the literature on true stress-strain relations in the short-time high-temperature tension test it is proposed in the following pages to describe a

[1] P. Ludwik: Elemente der Technologischen Mechanik. Berlin, 1909. Julius Springer.

[2] C. W. MacGregor: The Tension Test. Proc. Amer. Soc. Test. Mat. (1940) 40, 508–534. Also, "Relations between Stress and Reduction in Area for Tensile Tests of Metals." Trans. A.I.M.E. (1937) 124, 208, and Differential Area Relations in the Plastic State for Uniaxial Stress. S. Timoshenko Anniversary Volume. New York. Macmillan Co.
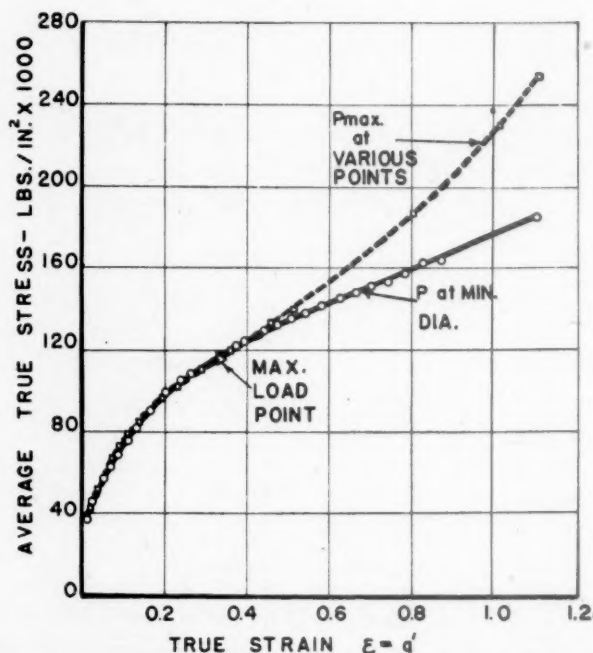
FIG. 2.—TRUE STRESS-STRAIN CURVE FOR MONEL-METAL SPECIMEN 1B AT 750°F., INDICATING TWO-LOAD CONSTRUCTION METHOD.

series of such experiments made on various metals at elevated temperatures, in which
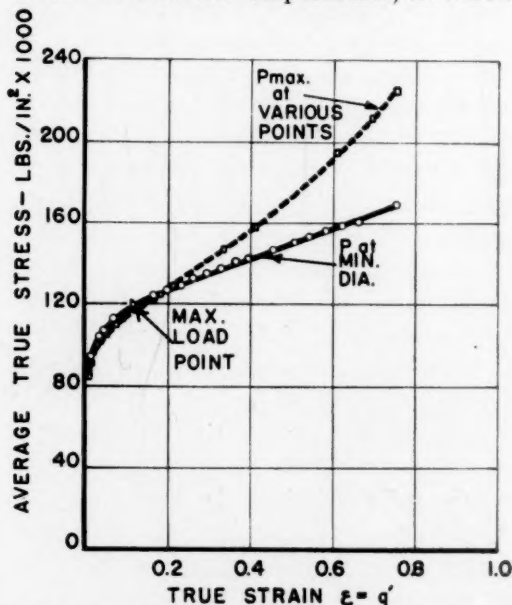
FIG. 3.—TRUE STRESS-STRAIN CURVES FOR TUNGSTEN-NICKEL-CHROMIUM IRON SPECIMEN 3B AT 950°F. TWO-LOAD METHOD INDICATED.

both true stresses and strains are determined from the beginning of yielding to fracture. In order to facilitate the deter-

mination of true stress-strain relations in the short-time high-temperature test, a two-load method[3] was suggested some time ago by one of the authors whereby this could be accomplished without the necessity of measuring any deformations during the test. In this case only the maximum and fracture loads need be noted during the experiment, which is made on a tapered specimen. If this method can be used in the tension test at high temperatures, the testing procedure is considerably simplified.

The principal objects of the paper are to investigate the application of the two-load method to the short-time high-temperature tension test and at the same time to report true stress-strain results for various materials at different temperatures. The definition of true stress and strain will be given first, followed by a description of the two-load method. A discussion will then be included of the experimental

[3] C. W. MacGregor: A Two-Load Method of Determining the Average True Stress-Strain Curve in Tension. *Jnl. Applied Mechanics* (Dec. 1939) **6**, A-156–158.
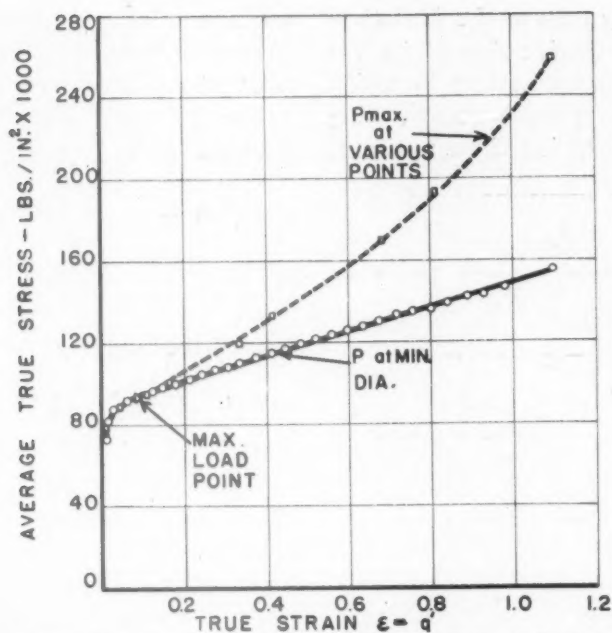
FIG. 4.—TRUE STRESS-STRAIN CURVE FOR CHROME-IRON SPECIMEN 4B AT 950°F. SHOWING TWO-LOAD CONSTRUCTION METHOD.
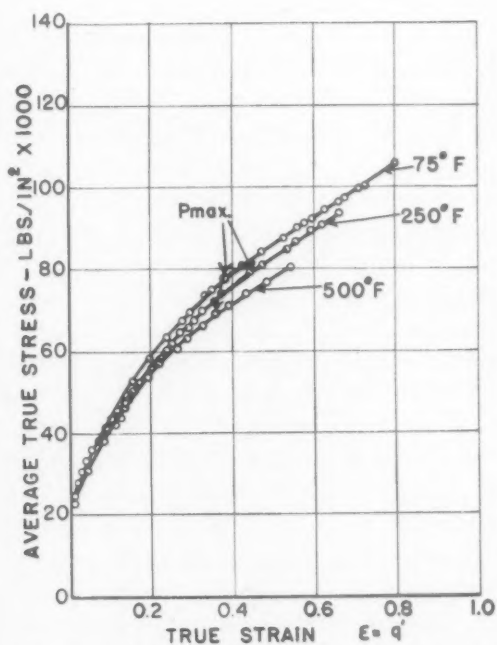
FIG. 5.—TRUE STRESS-STRAIN CURVES FOR BRASS AT VARIOUS TEMPERATURES.
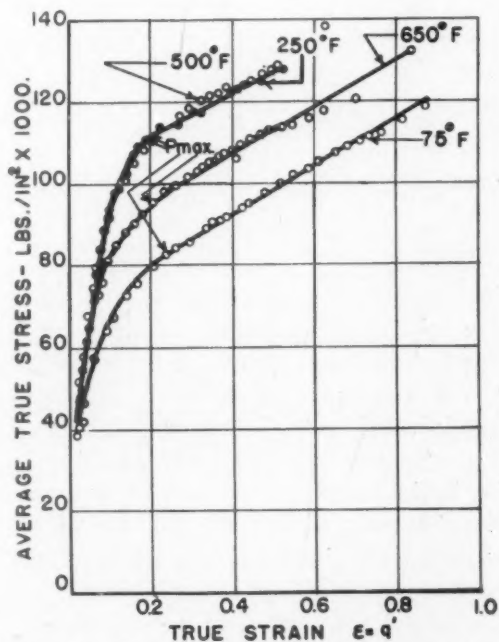
FIG. 6.—TRUE STRESS-STRAIN CURVES FOR S.A.E.-1112 STEEL AT VARIOUS TEMPERATURES.

results obtained by the use of this method together with the verification of its use within the temperature range in which appreciable creep does not occur during the relatively short period of the test.
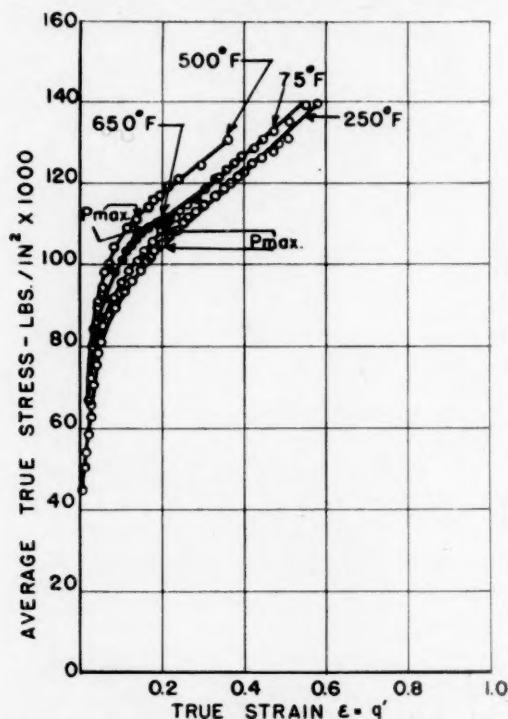
FIG. 7.—TRUE STRESS-STRAIN CURVES FOR S.A.E.-1045 STEEL AT VARIOUS TEMPERATURES.

TRUE STRESS-STRAIN CURVES AT NORMAL TEMPERATURES

Wherever the term *true stress* appears in the following discussion, this refers to the axial load present at any time during the test divided by the actual cross-sectional area present when this load is applied. This value is correct theoretically up to the maximum load where local necking begins. During necking, a three-dimensional stress system is set up in the locally constricted region with an axial stress that varies somewhat over the cross section. To be strictly correct, after local necking starts the load divided by the actual area of cross section determines the *average of the axial stresses*. On the curves to be described later on the latter designation is used. In order to conserve space, however, the word "average" will be omitted in most places in the text.

The true strain or true reduction of area is defined (ref. 2) as

$$\epsilon = q' = -\int_{A_o}^{A} \frac{dA}{A} = \log \frac{A_o}{A}$$
$$= \int_{L_o}^{L} \frac{dL}{L} = \log \frac{L}{L_o} \quad [1]$$

The above equality between $\epsilon = \log \frac{L}{L_o}$ and $q' = \log \frac{A_o}{A}$ holds if the volume of the material remains constant, which is true for the ductile metals. In Eq. 1, ϵ, q', A, A_o, L and L_o are the true axial strain, the true reduction of area, the actual area present, the original area of cross section of the bar, the actual gauge length, and the original gauge length, respectively. For very small strains these definitions are equivalent to the more commonly used $\epsilon_o = \frac{\Delta L_o}{L_o}$. As has been discussed earlier,[2] the strain definitions given in Eq. 1 relate the change in cross-sectional area or change in the gauge length to the area or length, respectively, from which that change is produced, and not to the original dimension. In such a definition no ambiguity exists in the choice of the proper reference dimension, which is apparent if the older strain definition is used. While it is not the intention to discuss the detailed advantages of this strain definition here, since this has been covered elsewhere, it should be mentioned that Eq. 1 permits the determination of the true axial strain throughout the test and even during the local necking of the bar by simple diameter measurements.

In the testing of materials at ordinary temperatures, it has been found convenient to measure the diameter of a uniform standard test bar of 0.505-in. diameter throughout the test by the use of a dial gauge and clamp. From the load-diameter data so obtained $S - q'$ or $S - \epsilon$ curves

can be constructed where $S = \dfrac{P}{A}$. If this procedure is followed, it will be found that the $S - q'$ curve becomes a straight line between the true stress corresponding to

curve. Before the final $S - q'$ or $S - \epsilon$ curve is constructed, a preliminary curve of $\dfrac{P_{max}}{A}$ vs. q' is determined by dividing the maximum load P_{max} by the final areas
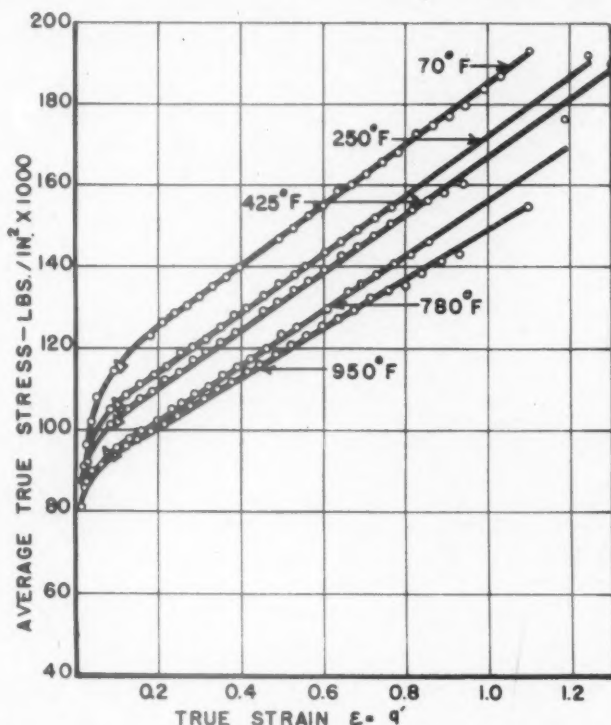
FIG. 8.—TRUE STRESS-STRAIN CURVES FOR CHROME IRON AT VARIOUS TEMPERATURES.

the maximum load and fracture. While the linear relation so obtained in this region has many advantages in itself, it provides the possibility to determine the complete $S - q'$ curve by noting only two loads during the test, and forms a basis for the two-load method.

THE TWO-LOAD METHOD[3]

The method consists in using a properly tapered tensile specimen, which is scribed by means of a diamond tool with uniformly spaced light circumferential scratches, measuring the diameters of the bar at these positions before and after the test with a dial gauge and clamp mounted on a lathe comparator; noting only the maximum and fracture loads during the test, and constructing the true stress-strain

of cross section successively from the large ends of the tapered portion of the bar to the fracture position, and plotting these as a function of the corresponding q' values given by Eq. 1 for these same positions. The portion of this curve from the beginning of yielding to the point of inflection will be found to correspond to the $S - q'$ curve from initial yielding to the point corresponding to the maximum load. The remainder of the $\dfrac{P_{max}}{A}$ vs. q' curve is fictitious and is used only to facilitate the construction of the remaining portion of the $S - q'$ or $S - \epsilon$ curve. This is accomplished by dividing the fracture load by the fractured area, plotting this on the diagram with the corresponding fracture value of q' and drawing a straight line from

this point tangent to the $\frac{P_{max}}{A}$ vs. q' curve at the point of inflection. Previous tests at normal temperatures have shown that the curve so constructed is identical with one obtained by using a uniform bar and measuring its diameter throughout the test.

bine installations. The testing temperatures varied from 70° to 970°F. in the different cases. Fig. 1 shows the type of curved tapered test piece used. It has been found in the past that this test piece, while perhaps not as free from restraint as some having a short uniform gauge

TABLE 1.—*Materials Tested*

Material No.	Material	Heat-treatment	Test Temperatures, Deg. F.
1	S.A.E.-1112 steel	Annealed 1 hour at 1650°F. and slowly cooled	75, 250, 500, 650
2	S.A.E.-1045 steel	Annealed 1 hour at 1470°F. and slowly cooled	75,250,500,650
3	A.T.V.-1 steel as rolled (Ni, 36; Cr, 11; Mn, 1.30; C, 0.30; P, 0.03 max.; S, 0.03 max.; Si, 0.20; Fe remainder)	As rolled condition; no heat-treatment	70, 250, 450, 600, 750
4	W-Ni-Cr iron (Cr, 12–14; Ni, 1.8–2.2; W, 2.5–3.5; C, 0.12 max.; Si, 0.50 max.; P, 0.025 max.; S, 0.025 max.; Mn, 0.50 max.; Fe remainder)	Heat-treated to 60,000 lb. per sq. in. proof stress by heating to 1800°F. for 30 min., air quenching, and drawing between 1230° and 1240°F. for 2 hours	70, 300, 580, 780, 950
5	Chrome iron (Cr, 11.5–13.0; Ni, 0.50 max.; Cr and Ni, 13.0 max.; C, 0.06–13 max.; Mn, 0.25–0.80; Si, 0.50 max.; P, 0.03 max.; S, 0.03 max.; Fe remainder)	Heat-treated to 60,000 lb. per sq. in. min. proof stress, by heating to 1725°F. for ½ hour, air quenching, and drawing at 1240°F. for 2 hours	70, 250, 425, 780, 950
6	Turbine-bolt stock (Cr, 0.80–1.10; Mo, 0.45–0.65; V, 0.25–0.35; Mn, 0.40–0.70; C, 0.50 max.; P, 0.04 max.; S, 0.045 max.; Si, 0.20–0.35; Fe remainder)	Heat-treated to 100,000 lb. per sq. in. min. proof stress by heating to 1650°F., holding for 8 hours, oil quenching, and drawing between 1250° and 1260°F. for 8 hours, 1180°F. for 4 hours, furnace cool	70, 250, 400, 650, 970
7	Brass, ½ hard drawn (Cu, 62; Zn, 35; Pb, 3.0)	Annealed 2 hours at 800°F. and slowly cooled	75, 250, 500
8	Monel metal (Ni, 67–70; Cu, 26–30; Mn, 1.5 max.; Fe, 3.0 max.; Si, 0.25 max.; C, 0.25 max.)	As rolled condition, no heat-treatment	70, 250, 400, 600, 750

The two-load method thus lends itself particularly well to cases where it is either inconvenient or not feasible to measure the diameter of the bar continuously throughout the experiment as in the short-time high-temperature test.

EXPERIMENTAL PROCEDURE

Eight different materials were tested in the conditions shown in Table 1.* Certain of these materials are representative of steels used today in high-temperature tur-

length, gave fairly satisfactory results. It was used here because the check measurements made during the test could be made at a single cross section throughout.

The general procedure followed was to scribe each test bar with light circumferential scratches at close intervals along the axis, to measure the diameter at these positions both before and after the test, to take continuous readings of load and minimum diameters throughout the test (to be used only as a check on the two-load method at high temperatures—this would not be necessary under the two-load method alone), and to construct the true

* The experimental results were submitted as two separate M. S. theses under the direction of the senior author by L. E. Welch in 1941 and R. E. Christie in 1940 at the Massachusetts Institute of Technology.

stress-strain curve as described under the previous headings: (1) by the two-load method and (2) from the continuous readings at the minimum diameter position.

During each experiment, the test specimen was surrounded by a tube furnace mounted on a 60,000-lb. Southwark-Emery hydraulic testing machine, which was used to apply the load. The temperature was controlled throughout each run by means of a Brown potentiometer pyrometer temperature-control unit with the thermocouple mounted at the center of the test bar. While the diameters of the tapered specimens were measured before and after the test in a converted bench lathe comparator equipped with a special dial-gauge clamp and an "electric eye" tube to establish proper contact pressure, the minimum test-piece diameters were measured continuously during the experiment by means of a special dial-gauge extensometer, which extended from the bottom of the furnace to the cross section of minimum diameter. This extensometer merely consisted of a frame of Invar metal constructed in the form of a lever system with knife-edges on one end for the measurement of the minimum diameter of the specimen, and an attachment at the other end for holding an Ames dial indicator. A calibration was made of this instrument before the experiments were undertaken and it was found to give very reliable results. The expansions of the gauge and of the specimens themselves were found to be very small in the temperature ranges used.

True Stress-strain Curves at High Temperatures

Figs. 2, 3 and 4 show the method of construction of the true stress-strain curves by the two-load procedure for Monel metal at 750°F., tungsten-nickel-chromium iron at 950°F. and chrome iron at 950°F., respectively. In each the upper dashed curve was determined by dividing the load P_{max} by the final areas along the fractured test

bar and by plotting these values as a function of the true strains determined from the initial and final diameter readings measured along the test bar. The lower
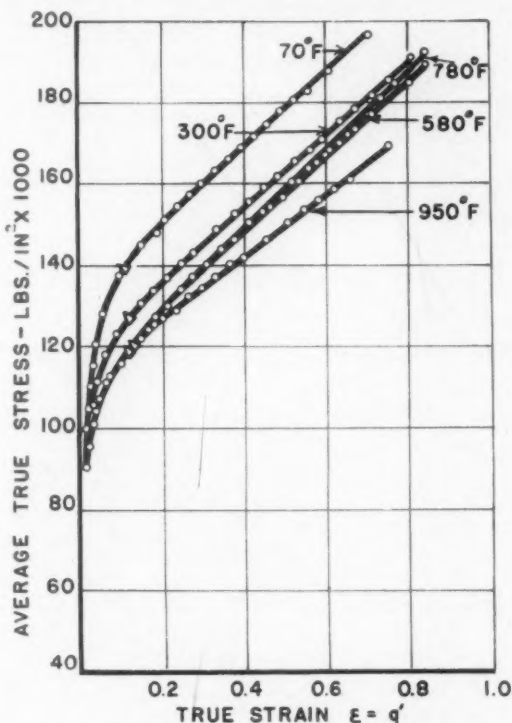
FIG. 9.—True stress-strain curves for tungsten-nickel-chrome iron at various temperatures.

curves were constructed from load and diameter readings taken during the test, the diameter being read at the smallest cross section. The latter curve was plotted only to check the two-load method. It is seen that if a straight line is drawn from the final fracture point on the lower curve tangent to the upper curve at its inflection point, a final curve is obtained made up of this straight line and the portion of the upper curve from initial yielding to the maximum load, which checks the lower curve very closely, as shown in the figures. This shows, then, that for these tests it would not have been necessary to take diameter readings during the test. The upper curve could have been determined from the initial and final diameter readings

along the test bar and the maximum load, obtaining in this way the true stress-strain curve to the maximum load point. The remainder of the curve could then have

would still determine the correct $S - \epsilon$ curve up to the maximum load. This phenomenon occurs in only a very small number of the tests conducted and its
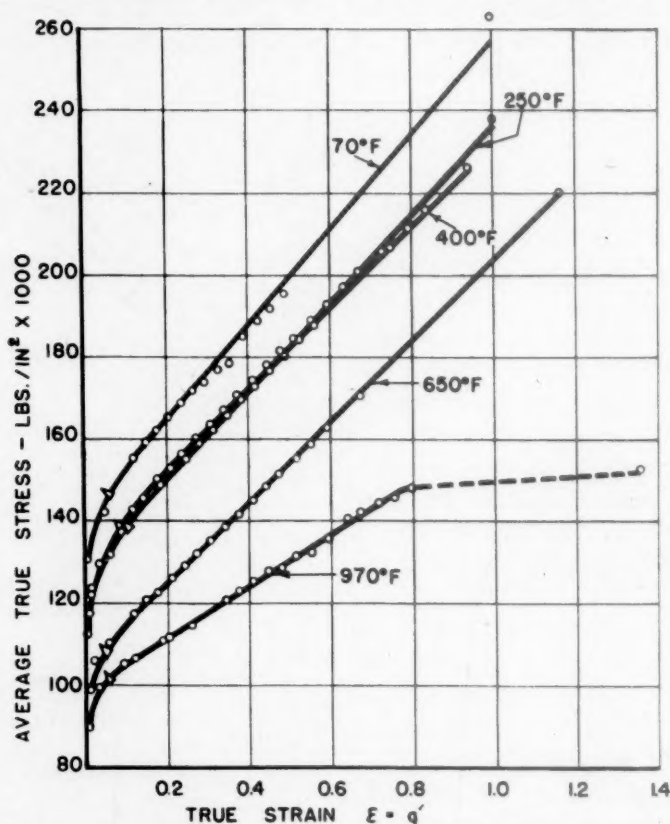
Fig. 10.—True Stress-Strain Curves for Turbine-Bolt Steel.

been determined by drawing the straight line from the fracture point, using the fracture load, tangent to the upper curve at the inflection point. These results are typical of most of the materials tested and show that the two-load method can be used at elevated temperatures in most cases, and that strain readings during the test are not usually necessary. It will be noted later on, however, that if an internal fissure forms during necking some time before complete fracture the load on the specimen drops rapidly, which will cause a departure from linearity of the $S - \epsilon$ curve before fracture. In such cases the two-load method would not be applicable in the necking region of the curve but

presence can usually be detected by the impossibility of drawing a straight line from the fracture point tangent to the $\frac{P_{max}}{A}$ vs. ϵ curve at its point of inflection.

This same procedure of checking the application of the two-load method at high temperatures was carried out for each of the other tests to be discussed and a similar check was found. Instead of including the upper construction curve for each material, however, only the final true stress-strain curve will be shown, since it is felt that the three tests discussed above are sufficient to illustrate the method.

Figs. 5, 6 and 7 show the final true stress-strain curves for a brass, an S.A.E.-1112 and an S.A.E.-1045 steel tested at temperatures in the range 75° to 650°F. Since these materials are not particularly resistant to creep, somewhat lower temperatures were chosen than for the alloy steels to be discussed later. These curves show a linear relation between true stress and strain after the maximum load has been reached. While the curves for the brass show a gradual but progressive lowering with increasing testing temperatures, Figs. 6 and 7 indicate no such continuous effect for the S.A.E.-1112 and S.A.E.-1045 steels. In these, owing to "blue brittleness," an initial increase in the height of the curves is first obtained, followed by a lowering as higher testing temperatures are used. The increase in the height of the true stress-strain curve for the S.A.E.-1112 is also accompanied by a shortening along the strain axis, indicating less ductility as measured by the true fracture strain. This embrittling tendency for these materials has been known for some time although generally it has not been pictured through true stress-strain values.

The true stress-strain curves for the alloy steels included in Figs. 8, 9, and 10 give evidence of a continuous lowering with increased testing temperatures. It will be noted that straight lines are obtained between the maximum load points and fracture for each test, with the exception of the experiment at 970°F. with the turbine-bolt steel. For the latter, a linear relation is obtained for a major portion of the necking region, followed by a drop. The rather anomalous behavior of this steel is probably due to the formation of an incipient crack in the center of the test bar at the position in the test indicated by the departure from the straight line. X-ray tests made previously on aluminum test bars that showed this same unusual behavior proved definitely that the drop in the $S - q'$ curve, when received, was due

to the formation of such a crack. The peculiar double cup and cone fracture received in the aluminum was also disclosed by the turbine-bolt steel.
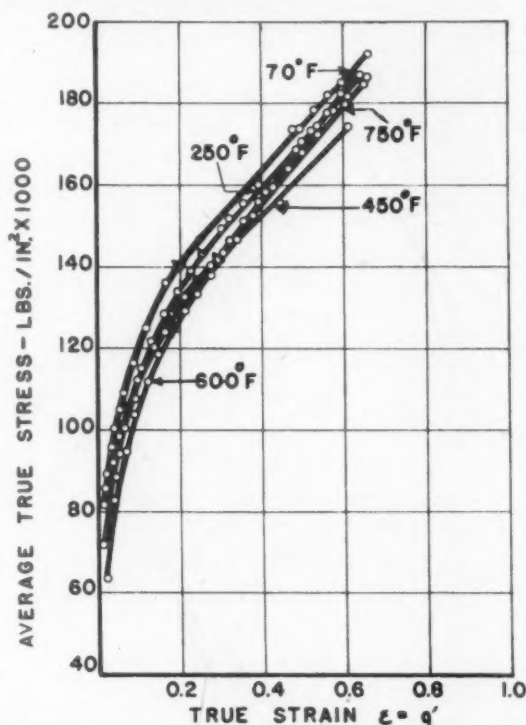
FIG. 11.—TRUE STRESS-STRAIN CURVES FOR A.T.V.-1 STEEL.

While a continuous lowering of the $S - \epsilon$ curves was shown by the three alloy steels discussed above, the A.T.V.-1 steel and the Monel metal, as indicated in Figs. 11 and 12, not only showed a relatively small effect of the testing temperatures in the range investigated but also revealed no continuous behavior with increasing temperature. Straight-lined $S - \epsilon$ curves were obtained, however, in the necking regions.

The general effect of the testing temperature on the modulus of strain-hardening $\frac{\partial S}{\partial \epsilon}$ in the necking region for five of these materials is given by Fig. 13. From this it can be seen that the three alloy steels showing the greatest temperature sensitivity as regards the lowering of the curves

for a given ϵ value—namely, the tungsten-nickel-chromium iron, the chrome iron, and the turbine-bolt steel—also possess negative slopes in Fig. 13, which become larger with increasing temperature. The Monel metal and the A.T.V.-1 steel, on

of the strain-hardening coefficient is important.

Summary of Test Results

The true stress-strain data obtained in the various experiments are summarized
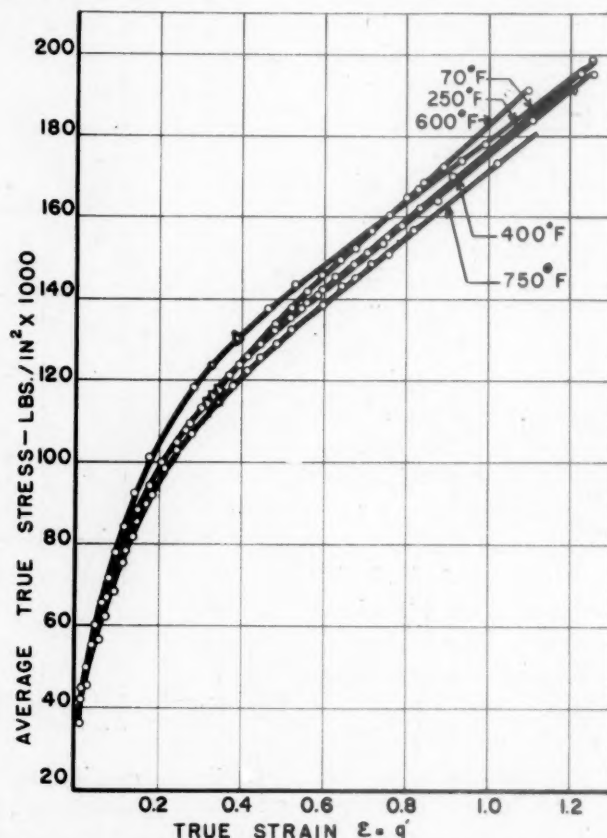
Fig. 12.—True stress-strain curves for Monel metal at different temperatures.

the other hand, which are not so temperature sensitive in this respect, both indicate positive slopes which decrease with the higher temperatures. Materials that have the latter type of variation of $\dfrac{\partial S}{\partial \epsilon}$ with temperature may show $S - \epsilon$ curves at temperatures higher than room temperature, which cross over those at the lower temperatures even though the true stresses at the maximum loads are lower. Information like that given in Fig. 13 may prove useful later on if used in connection with the analysis of the creep problem in which a knowledge of the functional variation

in Table 2. This table reveals that the true stresses at the maximum load for the brass, the chrome iron, the tungsten-nickel-chromium iron, and the turbine-bolt steel all decrease continuously with increasing temperatures. The S.A.E.-1112, on the other hand, shows a rapid increase with temperature in the true stresses at the maximum load followed by a rapid decrease. The remaining materials exhibit an "S" effect, in that the true stresses at the peak load initially decrease with an increase in temperature, then increase, followed by an additional decrease.

The fourth column of Table 2 shows the effect of temperature on the true stresses at fracture. A comparison of these values with the true stresses at the maximum loads indicates that temperature does not always affect the latter values in the same

true stresses at fracture than on the true stresses at the maximum load.

The effect of testing temperature on the ductility of the materials is pictured in Table 2 through the use of three different strain values; namely, the true fracture

TABLE 2.—*Summary of Test Results*

Material	Testing Temperature, Deg. F.	True Stress at Maximum Load, Lb. per Sq. In.	Average True Stress at Fracture, Lb. per Sq. In.	$q'_u = \epsilon_u$ True Uniform Strain at Maximum Load	$q'_b = \epsilon_b$ or True Fracture Strain	$q'_n = \epsilon_n$ or True Local Necking Strain
1	2	3	4	5	6	7
S.A.E.-1112 steel	75[a]	83,800	117,800	0.243	0.871	0.628
	250[a]	112,000	127,800	0.183	0.525	0.342
	500[a]	110,000	140,800	0.194	0.631	0.437
	650[a]	93,200	131,400	0.180	0.817	0.637
S.A.E.-1045 steel	75[a]	109,700	142,700	0.197	0.571	0.374
	250[a]	101,900	136,000	0.168	0.547	0.379
	500[a]	114,100	131,500	0.136	0.343	0.207
	650[a]	107,100	120,100	0.147	0.313	0.166
A.T.V.-1 steel	70	140,600	192,000	0.195	0.663	0.468
	250	141,500	178,500	0.244	0.620	0.376
	450[a]	132,200	176,700	0.203	0.625	0.422
	600[a]	140,000	173,600	0.272	0.587	0.315
	750	137,800	185,500	0.263	0.631	0.368
W-Ni-Cr iron	70	139,000	198,000	0.103	0.718	0.615
	300	127,400	192,000	0.119	0.806	0.687
	580[a]	122,000	191,500	0.129	0.849	0.720
	780	118,200	194,000	0.121	0.845	0.724
	950	118,800	167,000	0.123	0.739	0.616
Chrome iron	70	114,900	192,800	0.094	1.150	1.056
	250	105,200	193,200	0.081	1.245	1.164
	425	101,700	190,200	0.0843	1.2553	1.171
	780	93,400	178,000	0.0695	1.1875	1.118
	950	93,600	157,000	0.0825	1.1115	1.029
Turbine-bolt steel	70	147,200	263,000	0.0649	1.0049	0.939
	250[a]	138,200	239,000	0.1025	1.0044	0.9022
	400[a]	138,500	226,500	0.0990	0.9460	0.8470
	650	107,500	220,000	0.0583	1.1643	1.106
	970	102,000	153,500	0.0469	1.359	1.312
Brass	75[a]	78,000	101,900	0.388	0.738	0.350
	250	77,800	93,800	0.429	0.660	0.231
	500	69,500	81,000	0.358	0.543	0.185
Monel metal	75	131,400	189,000	0.384	1.231	0.847
	250	117,000	199,000	0.330	1.252	0.922
	400[a]	112,200	196,200	0.315	1.262	0.947
	600[a]	120,000	191,400	0.369	1.099	0.730
	750	118,600	183,000	0.347	1.098	0.751

[a] Average of two or more specimens.

way that it does the true fracture stresses. An S effect is revealed in some cases for the one and not for the other, and vice versa. It is apparent, for instance, that temperature affects the true stresses at maximum load much more than the true stresses at fracture for the S.A.E.-1112. In other words, the "blue brittleness" effect is less pronounced on the average

strain ϵ_b, the true uniform strain ϵ_u, and the true local necking strain ϵ_n.[2] These are related as follows:

$$\epsilon_b = \epsilon_u + \epsilon_n = \log \frac{A_o}{A_u} + \log \frac{A_u}{A_b} =$$

$$\log \frac{A_o}{A_b} \quad [2]$$

where A_o is the original cross-sectional

area, A_u the area at the maximum load, and A_b the fracture area. When defined in this way a direct addition of the uniform and local strains is possible. As discussed

FIG. 13.—MODULUS OF STRAIN-HARDENING FOR VARIOUS TEMPERATURES IN THE NECKED-DOWN REGION.

before, these two quantities have a greater physical significance than the ordinary strain $\epsilon_o = \dfrac{\Delta L_o}{L_o}$ and the ordinary reduction in area $q_o = \dfrac{\Delta A_o}{A_o}$ which are the more commonly used expressions for ductility.

Column 6 of Table 2 shows the effect of testing temperature on the true fracture strain ϵ_b. The "blue brittleness" effect is again depicted here for the S.A.E.-1112 by a decrease in ϵ_b values in this temperature range. These tests show that there is a wide difference in the character of the effect of temperature on fracture ductility properties with the different materials. Some show a continuously drooping characteristic with increasing temperature, as in the brass; others an increase followed by a decrease as portrayed by the tungsten-nickel-chromium iron, the chrome iron,

and the Monel metal; and still others exhibit a decrease followed by an increase as for the S.A.E.-1112, the A.T.V.-1 steel, and the turbine-bolt stock.

The variation of the true uniform strain ϵ_u with temperature is depicted in column 5 of Table 2. It is evident again that the testing temperatures affect the uniform strains quite differently from the fracture strains. However, in comparing column 7 with column 6, it is again clear that the testing temperatures affect the local necking strains ϵ_n in much the same way as they do the fracture strains ϵ_b. In view of the fact that the determinations of ϵ_u and ϵ_b were quite separate, with ϵ_n obtained from these, the consistency of the relationship between ϵ_b and ϵ_n as affected by temperature acts as a check on the results.

It is interesting to note that the testing temperatures in general affect both the strength and ductility at the maximum loads in a different manner than at fracture. This fact points to the importance of recording the true strength and ductility values at fracture when assessing the properties of materials. These properties usually are neglected in tension tests.

CONCLUSIONS

It may be concluded from the data submitted that: (1) the two-load method can be used in the short-time high-temperature test provided appreciable creep does not occur during the test; (2) the true stress-strain curves are linear from the maximum load point to incipient fracture; (3) the effect of testing temperature on the true stress at the maximum load and on the average true stress at fracture is different for most of the materials tested (summarized in Table 2); (4) the ductility of metals at high temperature may best be pictured by the true uniform and true local necking strains upon which the testing temperature usually has a different effect, as revealed in Table 2; (5) that, while the testing temperature affects the true uniform and frac-

ture strains differently, the true fracture and local necking strains are affected by temperature in a similar manner.

ACKNOWLEDGMENT

The experimental work described in this paper was carried out in the laboratories of the Department of Mechanical Engineering at the Massachusetts Institute of Technology, and the authors wish to acknowledge the interest and support given to the work by Dr. Compton and Dean Moreland of the Administration and by Dr. Hunsaker, Head of the Mechanical Engineering Department. Further acknowledgment is due Mr. R. E. Christie for the initial work carried out on the brass and the two carbon steels.

DISCUSSION

(J. W. Halley presiding)

N. METCALF,* Hamilton, Ont.—As a point of interest, what is the object of preparing that specimen down to such a fine finish if the effect of a little circle going down half a thousandth does not produce a notch effect?

L. E. WELCH (author's reply).—The principal function of the high finish is that it aids in the measurement of the diameters. You see, there is not much of a scribe line. It is made by a small diamond. It is a fine line, pretty difficult to see, and the finish aids in the visual observation in being able to pick up and measure the same diameter both before and after the test. We found that the best policy is to polish the specimen axially, and then to scribe the lines circumferentially.

N. METCALF.—In other words, it is just a question of contrast?

L. E. WELCH.—Yes, because the notches must not be very deep. One that is a thousandth or a thousandth and a half down in the minimum section will break there every time. It is just enough notch sensitivity to break.

* Burlington Steel Company.

S. L. HOYT,* Columbus, Ohio.—The theory underlying the paper is entirely sound, I believe, and I think we are fortunate to have a better method for handling this type of subject matter.

I wonder about a few points. For instance, the designation of a material as "chrome iron."

L. E. WELCH.—Rather lengthy compositions are given in the paper.

S. L. HOYT.—And the structure and treatments?

L. E. WELCH.—The structures are named, but pictures are not shown. The heat-treatments are given also.

S. L. HOYT.—The data show for Monel metal that the work-hardening characteristics or the strength characteristics increase rather than decrease with temperature. It seems to me that would call for some explanation if the authors have any to offer. Possibly it is due to precipitation-hardening occurring during the test.

L. E. WELCH.—I guess that is just about the way we feel about it. It is rather difficult. I would say that that was about the most promising theory. Some of the other effects can be explained by such phenomena as blue brittleness, which we know occurs. But for the Monel metal and the special tungsten steel, the A.T.V.-1, it probably is just a case of precipitation-hardening. I would not say definitely.

S. L. HOYT.—In that case, I would expect the rate of applying the load to affect the shape of the curves.

L. E. WELCH.—That is entirely possible. That is why I say we have just begun the work, and all these tests were made at about the same rate except when we got up into the plastic region. In order to obtain good data, it is necessary to slow down the machine, because it will neck down pretty fast; it is questionable whether there will be a satisfactory technique until we get a recorder that will actually do the work for us. We were not able to do much about controlling the rate. That was all done

* Technical Adviser, Battelle Memorial Institute.

manually, and the recorder will have to be a fairly complicated thing to do it automatically.

S. L. HOYT.—My last question has to do with the change from, let us say, low-temperature behavior to high-temperature or creep behavior. There seems to be sort of a twilight zone where there is at least some uncertainty as to the proper handling of materials, whether they should be handled as materials that creep or as materials that respond elastically. You mentioned that point. It would be interesting if you would expand on that a bit, to let us know what the possibilities are of developing criteria to give the temperature range over which this change occurs.

L. E. WELCH.—The companies that make stills have made a considerable number of creep tests on them for their own information, because they are used in creep applications. I think that the temperature at which creep becomes important can be established best from the long-time creep curve because in design in industry a certain allowable creep limit is specified. With a given material, the lowest temperature that gives that creep limit is probably the one to use in determining whether an application will involve creep or not, using that material.

I do not know how it could be done with a short-time tensile test. These tests took 15 to 20 min., and as you know, creep tests run anywhere from six months to a number of years. It seems to me the best way to determine that temperature for a given material is by actual long-time creep tests.

C. R. SODERBERG,* Cambridge, Mass.—The rationalization of the stress-strain curve, which was made some time ago by Professor Mac-Gregor, and which is now extended to experiments at high temperature, is a noteworthy contribution to the subject. The obscurity of the conventional representation of the tension test is shown to be more apparent than real. The plastic region of our metals seems to be remarkably simple, in that there is proportionality between stress and strain, at least for increasing strain.

In view of the body of knowledge already

* Department of Mechanical Engineering, Massachusetts Institute of Technology.

existing on the plastic properties of metals at high temperature, it is somewhat surprising to find in this paper no reference to the strain velocities with which the tests were conducted. At first sight, one would expect very considerable differences in results if high-temperature tension tests were conducted at widely different strain or stress rates. If the strain rate varied during each test, which it certainly must do during the necking of the specimen, a departure from the straight-line relation should be expected. The absence of any pronounced departure from the straight-line relation might mean that the strain-hardening characteristics are less dependent upon the strain rate than was formerly suspected, or, which is much more likely, that the strain rates in these particular tests were relatively constant.

Just what the dependence between the modulus of strain-hardening and the strain rate is likely to be is a matter of conjecture at the present time. Analysis of creep tests at constant stress suggests that the modulus of strain-hardening ought to increase with the strain rate. The behavior in impact loading gives the same indication. In either case there is a suggestion that the factor of proportionality between the modulus of strain-hardening and the strain rate is in some way related to the stress. This makes the straight-line relation between stress and strain, clearly demonstrated in this paper, quite remarkable, and its true significance is yet to be revealed.

Tests of the type described in this paper, but with controlled strain rates, should do much to clear up this question, and it is hoped that the authors may find it possible to extend their valuable results in this direction.

C. W. MACGREGOR (author's reply).—The question of the effect of the strain rate on the results was mentioned by Mr. Hoyt and Professor Soderberg. Early in the development of this method, we conducted experiments to study the general effect of the strain velocity on the true stress-strain curve. Rather wide ranges of strain velocity showed no appreciable effect on the shape of this curve when the tests were made at room temperature and on metals that showed no appreciable creep at this temperature. This, of course, excludes the low-melting alloys of lead, tin, etc., which show excessive creep at room temperature. Subse-

quent tests reported previously[4] confirmed these early experiments and showed on S.A.E.-1045 steel, for example, that an increase in the testing speed by a ratio of 8.65×10^5 to 1 increased the true stress at the maximum load only 6.9 per cent, the true strain at fracture 3.1 per cent, and the true fracture stress 11.3 per cent. Similar results were found for other metals.

In tapered test pieces such as those used here, it is clear that, because the cross-sectional area varies along the length, the true strain rates $v = d\epsilon/dt = -1/A \cdot dA/dt$ also vary along the length. This variation in strain rates would be very important if creep were a problem and the use of the two-load method under creep conditions would be questionable. This is not true here, however. The temperatures of test were not sufficiently high for any appreciable creep to occur, and in a sense these materials behaved at these temperatures not unlike weaker materials at room temperature, for which former tests showed no appreciable velocity effect.

As a matter of fact, the test results at elevated temperatures included in the paper show definite confirmation that strain velocities were of no practical importance here. Figs. 2, 3 and 4 demonstrate this. True stress-strain curves are included in these figures, constructed both by the two-load method utilizing measurements on cross sections of different areas and consequently of different strain rates, and also by taking continuous measurements throughout the test at the smallest cross section, as a check. If strain velocity had any important effect, it would not be possible to obtain identical results from measurements on cross sections of different areas, and consequently of different strain rates. As these figures show, however, identical results, were obtained by these two methods, thus revealing no appreciable velocity effect.

Further work on true stress-strain relations is in progress.

[4] A. V. de Forest, C. W. MacGregor and A. R. Anderson: Rapid Tension Tests Using the Two-load Method. *Trans*. A.I.M.E. (1942) **150**, 301.

INDEX

Institute of Metals Division
Volume 152, Transactions A.I.M.E., 1943

CONTENTS

Institute of Metals Division Lecture

Physical Metallurgy

Copper and Brass

Alloys of Aluminum and Magnesium

Miscellaneous Heavy Metals and Alloys

Nonferrous Reduction Metallurgy